Project No. 10-872

Corrosion in Supercritical Carbon Dioxide: Materials, Environmental Purity, Surface Treatments, and Flow Issues

Reactor Concepts RD&D

Dr. Kumar Sridharan
University of Wisconsin-Madison

Sue Lesica, Federal POC
Jeremy Busby, Technical POC

NEUP Nuclear Energy University Programs
U.S. Department of Energy

Final Report for Project:

Corrosion in Supercritical Carbon Dioxide: Materials, Environmental Purity, Surface Treatments, and Flow Issues

Funded By: U.S. Department of Energy in cooperation with Battelle Energy Alliance, LLC under their Prime Contract No. DE-AC07-05ID14517
(US Department of Energy, Nuclear Energy University Program)

Project Investigators: Dr. Kumar Sridharan (Principal Investigator), Dr. Mark Anderson, Dr. Todd Allen (University of Wisconsin-Madison)

Project Contact: Dr. Kumar Sridharan
kumar@engr.wisc.edu

Date: December 10th, 2013

Preface

This body of work reports research that was carried out in the Department of Engineering Physics at the University of Wisconsin – Madison under the direction and supervision of Dr. Todd R. Allen, Dr. Kumar Sridharan, and Dr. Mark H. Anderson. The work described in this report was undertaken by graduate students Jacob Jelinek and his predecessor, Paul Roman, under Funding Opportunity Announcement (FOA) DE-FOA-0000998 and RPA Identification Number RPA-10-318, Project Number 10-872, and Contract Number 102081 for the United States Department of Energy's Office of Nuclear Energy (DOE-NE).

Part of the work contained herein has been published, and at the time of completing this project, some work was undergoing publication efforts. The publications were as follows:

1. Jelinek, J.J., Sridharan, K., Allen, T.R., Anderson, M., Firouzdor, V., and Cao, G. (2012). "*Corrosion Behavior of Alloys in High Temperature Supercritical Carbon Dioxide"*, NACE International.

2. Roman, P., Jelinek, J., Sridharan, K. Allen, T.R., Anderson, M., and Cao, G. (2013). "*Corrosion Study of Alloys in High Temperature, High Pressure Supercritical Carbon Dioxide for Brayton Cycle Applications"*, NACE International.

3. Roman, P., Sridharan, K., Allen, T.R., Anderson, M., He, L., and Leng, B. (2013). "*Effect of Aluminum and Yttrium PVD Coatings and Surface Modification by Shot Peening on Oxidation-Corrosion Resistance"*, Surface and Coatings Technology, to be published.

4. He, L., Sridharan, K., Allen, T.R., Anderson, M., Leng, B., and Roman, P. (2013). "*Corrosion Behavior of Alumina-Forming Austenitic Steels in Supercritical Carbon Dioxide"*, Corrosion Science, to be published.

5. Leng, B., Sridharan, K., Allen, T.R., Anderson, M., He, L., and Roman, P. (2013). "*Corrosion Behavior of 316L and 347SS in Supercritical Carbon Dioxide of Different Purity"*, Corrosion Science, to be published.

Executive Summary

The supercritical CO_2 Brayton cycle is gaining importance for power conversion in the Generation IV Fast Reactor system because of its high power conversion efficiencies. When used in conjunction with a Sodium Fast Reactor for example, the supercritical CO_2 cycle offers additional safety advantages, by eliminating potential sodium-water interactions that may occur in a steam cycle. In power conversion systems for Generation IV Fast Reactors, supercritical CO_2 temperatures could be in the range of 30oC to 650oC or higher, depending on the specific component in the system. Materials corrosion particularly at the higher temperatures will be an important issue. Therefore, the corrosion performance limits for materials at various temperatures in supercritical CO_2 must be established. Additionally, it is also important to gain a fundamental understanding of mechanisms of materials corrosion in this environment that can guide the selection of alloys for supercritical CO_2 Brayton cycle applications and aid the development of models for long-term corrosion prediction.

In this project, the corrosion behavior of various candidate alloys was investigated in supercritical CO_2 at temperatures ranging from 450oC to 650oC for exposure durations of up to 1000 hours (in some cases up to 1500 hours). Most tests were performed at a pressure of 20MPa, although select tests were also performed at 8.27MPa to investigate the role of pressure on corrosion. Alloys investigated included ferritic steels NF616 (Grade T92) and HCM12A (Grade T122), and austenitic alloys IN800H, 347 stainless steel, and three grades of AFA alloys (alumina forming austenitics). AFA alloys, that contain small amounts of aluminum to promote alumina surface layer formation, were developed at Oak Ridge National Laboratory (ORNL) for high temperature oxidation resistance. Tests were performed in research grade (very high purity) and industrial grade CO_2. Three types of surface treatments, namely, deposition of thin films (~500nm) of aluminum and yttrium, and shot peening were also investigated with the goal of enhancing corrosion resistance.

Evaluation of corrosion was performed using weight change measurements, scanning electron microscopy in conjunction with energy dispersive spectroscopy (SEM-EDS), x-ray diffraction (XRD), and for select samples by transmission electron microscopy (TEM). These results are discussed in great detail in the report and in technical papers that have been written or being written on this work. In general ferritic steels exhibited the least corrosion resistance and at best suitable for the lower temperature regime of the temperature range investigated. AFA alloys exhibited better corrosion resistance and in general suitable for the intermediate temperature range, although there was a notable difference in the performance of the three AFA alloys tested. 347 stainless steel and alloy 800H were superior to the other alloys tested with alloy 800H exhibiting the best corrosion resistance. All three surface treatments resulted in notable improvements in corrosion resistance and warrant further investigation. Surprisingly, in many cases the alloys exhibited lower corrosion in industrial grade CO_2 compared to research grade CO_2. We are tentatively attributing this improvement to the presence of small quantities of hydrocarbons in industrial grade CO_2 but this observation too warrants further investigation. In all evaluations of weight change and oxide thickness measurements statistical variations as well as other physical effects such as oxide layer spallation and carbon film deposition have been taken into account.

The findings of this research are being disseminated quite extensively in scientific journals, and conferences including National Association of Corrosion Engineers (NACE) Conference and National Supercritical CO_2 Power Cycle Conference. The project has also spawned collaborations with the supercritical CO_2 Brayton Cycle research programs at Sandia National Laboratories and Argonne National Laboratory, and U.S. industries working in this area. The project has provided a rich scientific environment for training and educating students. Over the three-year term of the project, two Master's Thesis degrees were awarded on this subject, and at least five undergraduate students were actively involved in various phases of this project. Three post-doctoral research associates were also involved in this project.

We thank the U.S. Department of Energy – NEUP program for providing the funding for this project.

Table of Contents

Table of Tables

Table of Figures

1. Literature Review

1.1 High Temperature Corrosion of Alloys

While the mechanism of low temperature corrosion was being investigated, the physical-chemist Gustav Tammann wrote in 1920 [1] what is popularly considered to be the first paper that expressly addressed high temperature oxidation in metals. It is the earliest mentioning of the length proportionality to square root of time relationship for the corrosion rate of a metal, a simple growth law or rate equation we refer to as the parabolic oxidation law equation. In 1922, Tammann deduced an exponential relationship from observations of color changes with the oxidation of various metals in air at relatively low temperatures [2]. A more accurate optical method was employed by Constable several years later. The classical work of Pilling and Bedworth [3] in 1923 led to the development of the well-known volume ratio or Pilling-Bedworth ratio, which states that if the ratio of the molar volume of the reaction product to that of the metal is greater than 1, the thick oxide (scale) layers which form on the metal during oxidation are adherent and pore-free. If the volume ratio is less than 1, the linear time law has been found to apply for the obvious reason that the oxide is not able to form a coherent layer, and thus fresh metal surface is continuously exposed [4]. The P-B ratio is defined as

$$\boldsymbol{PB = \frac{V_o}{V_m} = \frac{m_o \rho_m}{n m_m \rho_o}} \quad \textbf{(1)}$$

where V_o is the molar volume of the oxide, V_m is the molar volume of the metal, m_o and ρ_o are the molecular mass and density of the oxide, m_m and ρ_m are the molecular mass and

density of the metal, and n is the number of atoms of metal per one molecule of the oxide. Following the experimental approach of Pilling and Bedworth, Dunn attempted to formulate a more fundamental theory of oxidation and diffusion. In 1926, Dunn was able to show analytically from reaction kinetics, agreement with the Arrhenius law equation [5]. This result may be stated as

$$\frac{d\log_e k}{dT} = -\frac{Q}{RT^2} \quad \rightarrow \quad k = k_o \mathrm{e}^{(-\frac{Q}{RT})} \tag{2}$$

The rearranged Arrhenius equation to resemble a straight line equation is given below as

$$\ln k = \ln k_o - \frac{Q}{R} * \frac{1}{T} \tag{3}$$

Many oxidation reactions involving metals and alloys seem to show a linear temperature dependence of oxidation rate constants that obey the Arrhenius equation. Both Q and k_o are supposedly very useful physical quantities to know because the rate constant k can be calculated for any temperature once these two parameters are known. Using (3), the apparent activation energy Q can be determined from the slope of the best-fit line by plotting $\log_{10}$ k as a function of 1/T. In terms put forth by Kubaschewski, the activation energy refers to the concept that only those atoms having energies of oscillation exceeding Q/6.02 x 10^{23} at a certain moment are able to leave their crystallographic positions [4]. The rate constant k is most commonly determined at different temperatures from isothermal measurements.

In 1933 Wagner published a theory on the high temperature oxidation of metals by the parabolic rate law, which was observed by Tammann, and which indicates that a diffusion process is rate-determining. However, details of the lattice defect phenomena at diffusion processes are not discussed here (i.e., Wagner-Schottky theory of lattice defects). To distinguish between the two oxidation regions, Hauffe delineates high temperature oxidation processes into those oxide layers which are thin (tarnishing process) and those oxide layers which are thick (scaling processes), and goes on to describe that for thick layers, the effects of the electric field transport region are negligible (but not for thin layers), since their contribution under these conditions are no longer detectable, and that the migration processes in thick layers are beyond the field transport region, and are diffusion processes involving two types of lattice defects; interstitial cations or anion vacancies and free electrons in the conduction band or cation vacancies with holes in the valence band [6].

To give some background on the use of ferritics and ferritic-martensitic steels, one can turn to Klueh. According to Klueh, Fe-Cr alloys, in particular 9-12Cr ferritic-martensitic steels, were developed during the first half of the last century and have a long history of use in the power-generation industry as boiler and turbine materials. Such steels were selected for use in steam generators of nuclear power plants during the 1960's, and steels with addition of V, Nb, and/or W and with oxide dispersions were subsequently chosen and evaluated as fuel element core component (duct and cladding) materials in sodium-cooled fast breeder reactors. Even though austenitics and nickel based alloys are potential candidates, they are more expensive, have higher coefficients of thermal expansion and show lower heat conductivity, which are significant drawbacks for their use as heat exchanger tubes [7]. The

fission (in core) and fusion reactor applications require steels that are resistant to radiation damage induced by bombardment from high energy neutrons, and in part has led to the development of reduced-activation steels, containing W, V, Mn, Ta, and Ti and without Mo, Nb, and Ni [8]. Advancement in alloys have been undertaken primarily for the sole intention of performing under extreme conditions, particularly at elevated pressures and temperatures. Specialty alloys have been either developed or tailored as modified versions to serve a specific application or to compete with an alloy already in use for another application in terms of corrosion resistance and creep-rupture resistance. *Fig. 1* below shows a timeline related to gains made in high temperature corrosion and power generation relative to the Brayton cycle.

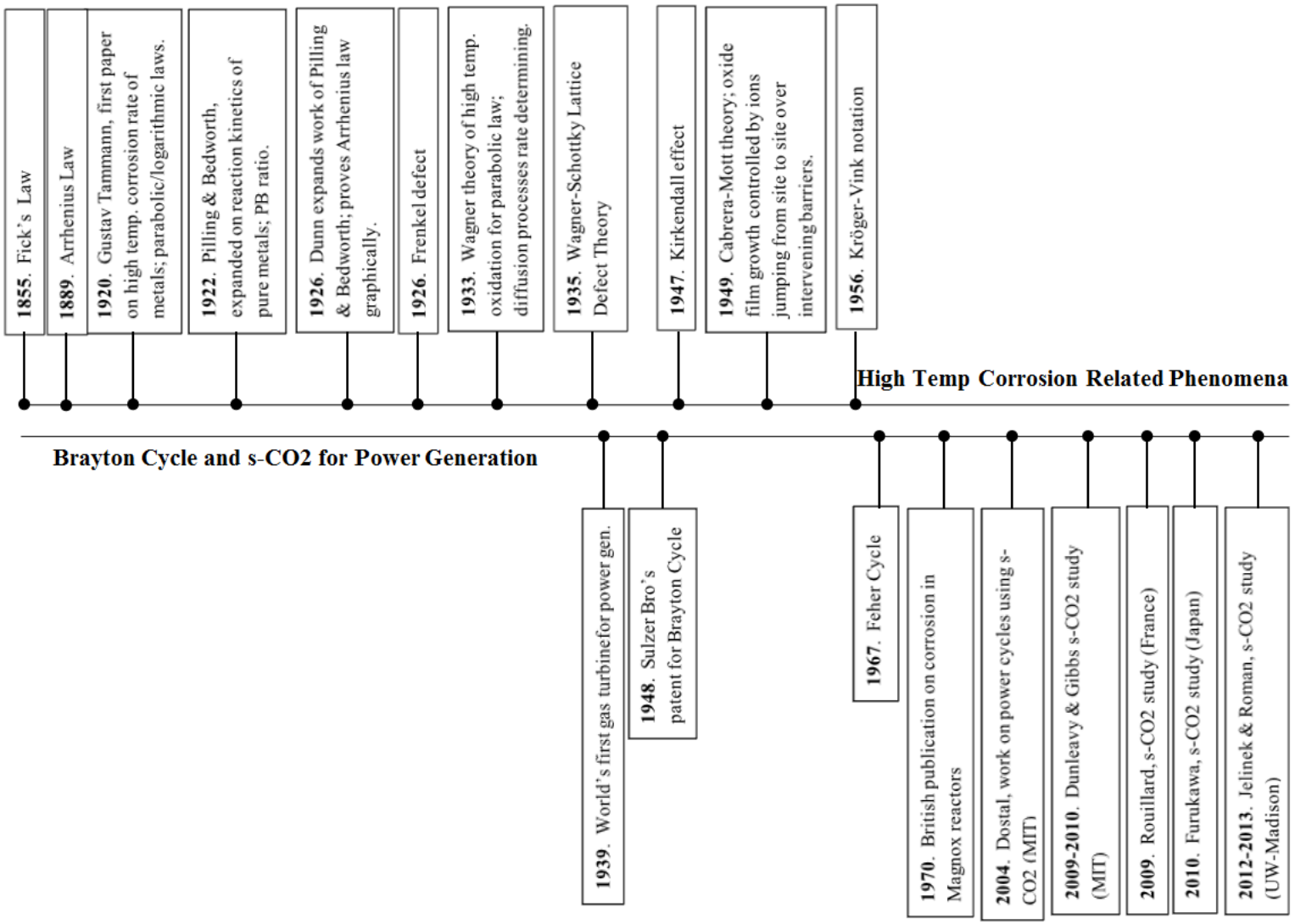

Fig. 1: Timeline of Phenomena

1.2 Supercritical Carbon Dioxide

1.2.1 Brayton Cycle Application

The working fluid is very important for the power conversion system of the next generation nuclear power plant. The cycle efficiency, the size of all the components such as turbine, compressor, recuperator, intermediate heat exchanger, and other components will depend on the fluid because each different fluid has different heat transfer and transport properties. Due to the different properties of the fluids, the balance of plant will have varying energy and mass balances [9]. Several heat transfer fluids (HTF) being considered for next generation power plants are supercritical CO_2 ($SCCO_2$), liquid metal alloys, and molten salts. This body of work focuses on $SCCO_2$ and mimics the high temperatures and pressures anticipated for turbomachinery components as it would be in-plant for a $SCCO_2$ Brayton Cycle.

The supercritical carbon dioxide (SC-CO2) Brayton cycle system originally proposed by Sulzer (1950) [10] and later by Feher (1967) [11] was introduced as a means to provide high energy conversion system efficiency at moderate temperatures. Further development of the system from its initial intent was for many years neglected. The lack of interest was mainly due to the much wider use of Rankine cycle technology. However, there has been renewed interest in Brayton cycle technology stemming in part from the advanced nuclear reactor initiative (Generation IV) and the Global Nuclear Energy Partnership (GNEP). Although now that development is under way, applications are being made to a much wider array of power generating technologies including solar, geothermal, and fossil/bio fuel systems.

The most advantageous aspect of the supercritical Brayton cycle is its reduced compression work compared to that of an ideal gas Brayton cycle; improving efficiency by performing

compression close to the critical point. The critical point of carbon dioxide is 7.38MPa at 31.1^{o}C. The $SCCO_2$ Brayton cycle utilizes CO_2 as a coolant above its critical point to reduce compression work, which in turn results in higher efficiency. The reduced volumetric flowrate of CO2 due to higher density compared to helium will reduce compression work, which will eventually increase turbine work enhancing the plant net efficiency [9]. This translates into the simplification of the compressor, often down to a single unit without intercooling stages. Full inlet conditions at the turbine inlet are anticipated to be 550^{o}C and 20MPa with the high side of the cycle possibly seeing 650^{o}C. The high pressure necessary for efficiency also becomes beneficial allowing the use of more compact turbines and heat exchangers. Even when compared to Helium (the most viable contender in the nuclear field), CO_2 requires far fewer turbine and compressor stages. The SC-CO_2 Brayton cycle is therefore under consideration for power conversion systems for fast reactors as well as high temperature gas reactors [12] [13] [14]. Additionally, using CO_2 in conjunction with Sodium Fast Reactors (SFR) eliminates the possibility of sodium water interactions that would be present with a more traditional steam cycle. According to Dostal [15], above 20 MPa the efficiency of the cycle is not significantly improved. However, operating at high temperature and high pressure necessitates the use of a high strength material whose mechanical properties and corrosion performance are well suited for a $SCCO_2$ environment for an intended temperature and power output. The corrosion performance of low alloy/mild steels in sub-critical CO_2 have been studied and characterized, but only at medium temperatures and relatively low pressures (0.1 MPa to 4 MPa) for the British MAGNOX and AGR program, wherein ferritic steels made up most of the structural support [16].

1.2.2 Concentrating Solar Power (CSP) Application

The basic concept behind a concentrated solar power-plant (CSPP) is to translate solar thermal energy into production of electricity. This type of power plant is similar in terms of an energy production rationale to other competing technologies such as the coal-fired power plant (CFPP), nuclear power plant (NPP), etc., but is different in applied thermodynamic cycle and machinery, and more notably its fuel source. The CSPP uses a parabolic trough of mirrors or central power tower to tune the sunlight. Current, or for namesake 'conventional' CSPP's, utilize oil or steam to transfer the solar energy at peak temperatures ~ 400^{o}C [17] to a turbine for generating electricity. Conventional CSPP's use either a Rankine thermodynamic cycle or an organic Rankine thermodynamic cycle (ORC) [18]. The majority of large coal-fired power plants (CFPP) used to be operated at sub-critical steam conditions (pressures $\leq$ 22.1 MPa) prior to about 1990; the main steam temperature was standardized at 540^{o}C worldwide, although 565^{o}C was the standard in the U.K., with the steam pressure being typically 18 MPa. However, the need to develop CFPP's with reduced generating costs and acid rain and greenhouse gas productions was widely recognized in the late 1970's and early 1980's and subsequently led to the design and construction of supercritical water (SCW) or ultra-supercritical water (USCW) and combined cycle power plants with improved thermal efficiencies [19]. Today, the most advanced CFPP's operate at steam conditions of 593^{o}C, and new plants are being commissioned that operate up to 620^{o}C [20]. To be competitive in the field of electric power generation, the solar and nuclear power plant industry is performing R&D efforts to qualify structural materials for a new generation of power plants that operate at higher temperatures. The underlying ongoing efforts behind this

temperature increase are analogous to those of a CFPP, to achieve higher power conversion efficiencies by raising the operating temperature along with the additional thermodynamic property benefits of operating above the fluids critical point. Such R&D efforts by Dostal [15] and Gong [21] have renewed interest in supercritical carbon dioxide ($SCCO_2$) as a heat transfer or working fluid (HTF) in a Brayton thermodynamic cycle. This cycle yields significant benefit with respect to the turbo machinery size and allows increased efficiency at temperatures above 650^oC. Experimental work at Sandia National Lab on low pressure closed Brayton cycles [27] has led to the construction of high pressure $SCCO_2$ Brayton flow loops and has added momentum for the advocacy of $SCCO_2$. Currently, these cycles hold significant promise for any high temperature energy source, including fossil systems if sequestration of carbon dioxide is anticipated.

1.3 Carburization and Metal Dusting

Carburization is a high temperature phenomena caused by carbon ingress (diffusion of carbon containing molecules through the pores of the scale), leading to internal carbide formation or "metal dusting" and changes the mechanical properties of the materials [28]. Metal dusting, a catastrophic form of carburization that can occur in high carbon activity environments, produces pit or crevice corrosion where metal is disintegrated into a powdery mixture of carbon, metal, oxides and carbides which can easily detach from the surface. According to Grabke, the material is considered to be carburized if its carbon content exceeds the original carbon content when it was first place in service. Carburization generally is problematic at 800-1200^oC with carbon activities $a_c \leq 1$. Metal dusting is a

lesser degree form of carburization that precedes it and is generally observed between 350-900^{o}C. This phenomenon leads to material decomposition, i.e., pitting or general metal wastage in Fe, Ni, and Co based alloys into fine metal or carbide particles and carbon (coke) in carbonaceous gases ($a_c > 1$).

1.4 High Temperature Oxidation- Test Methods & Models

Discontinuous measurements are widely used to assess corrosion kinetics at high temperatures and over long exposure times, and this method has been applied in recent years by $SCCO_2$ investigators Ballinger and McKrell at MIT [24,25,26] , Furukawa in Japan [27], Rouillard in France [28,29] and previously by Anderson and Sridharan [30,31]. The discontinuous method consists of stopping the experiment after some chosen duration of exposure time to allow removal of specimens for examination and weighing. *Thermogravimetry* is used to measure the weight at temperature after each interval of removal, and the difference between the weight after and the weight before exposure is termed weight change. High temperature oxidation of metals and alloys by this process tends to lead to a weight gain by the growth of an oxide layer or layers, whether external or internal does not matter. These measurements are typically made in an environment under isobaric and isothermal conditions. This method appears to be suitable for rank ordering of different alloys, and can be extended to evaluate not just flat coupon samples, but samples having a geometry or weld condition as it would be in industrial application. It is interesting to note that little effort has been aimed at developing appropriate guidelines and standards agreed upon as best practice [32, 33]. Therefore, interpretation and comparison of weight gain data

from different studies should be evaluated with caution. Many other methods and techniques can and have been applied at high temperatures. Kofstad as well as Grabke have used the continuous thermogravimetric technique in the past through automatic recording microbalances in their laboratories, but done typically with a reaction chamber and furnace. Kofstad has even stated that the continuous method can be applied and the temperature linearly increased for determining the activation energy from a single oxidation run [34, 35]. Cyclic oxidation, which was a method more frequently encountered in literature during review, is devised solely to introduce thermal cycling with a higher frequency interval with rapid cooling, which imposes a thermal shock or stress on the coupons causing a protective oxide layer to crack and spall, rendering the base alloy unprotective and susceptible to accelerated corrosion attack, thereby naturally leading to higher metal wastage rate and witnessing of a weight loss earlier rather than a weight gain. Such measurements are said to be more representative of the cycling conditions seen by materials in an industrial application. For example, Pint et al [36] used 10hr thermal cycles in order to simulate the CSP duty cycle for a heat exchanger application at a high temperature, and to force rapid Al depletion for purposes of lifetime prediction. Nesbitt [37] also used cyclic oxidation of 1hr cycles and with a 20min cooling period to assist development of a numerical model (COSIM) to simulate coating degradation by simultaneous oxidation and coating-substrate interdiffusion, namely by measuring the initial Al and Cr contents of the coating and substrate and their concentration – depth profiles.

3. Test Setup and Procedure

3.1. Thermogravimetry

For this study, the discontinuous thermogravimetric measurement method was used to determine the weight gain. Details on the method and procedure used to determine weight gain at discrete points is described below in subsequent sections.

3.1.1. Test Setup and Shakedown

The SC-CO_2 test facility was designed and constructed based on the requirements for the experimental testing. The corrosion test facility needed to sustain a maximum temperature of 650°C as well as a pressure of 20MPa. Components were therefore selected to exceed these defined maximum testing parameters, providing a margin of safety.

The supercritical carbon dioxide corrosion test facility consisted of the following basic features; namely, Gas Source, Autoclave, GCMS, and Automation Equipment. These basic aspects can be broken down into more specific components outlined as follows:

Gas Source:

1. Gas cylinders
2. High resolution scale
3. Bottle side pressure transducer
4. High pressure CO2 pumping system

Autoclave:

1. Resistive heaters
2. Two inch diameter (SCH 160) 25 inch in length Inconel 625 pipe
3. High pressure high temperature hubs and seals (Grayloc)
4. Alumina sample holder with Inconel mounting bracket
5. Exit gas chiller

GCMS:

1. Pressure and flow control system
2. Gas analyzer

Automation:

1. Thermocouples and test section pressure transducer
2. Acquisition system
3. Computer controller (automation)

Components for each section were selected based on both the aspects of the supercritical fluid as well as cost constraints at the time of the build. A photograph of the experimental equipment and a process flow diagram of the test setup are shown below in *Fig. 2* and *Fig. 3*.

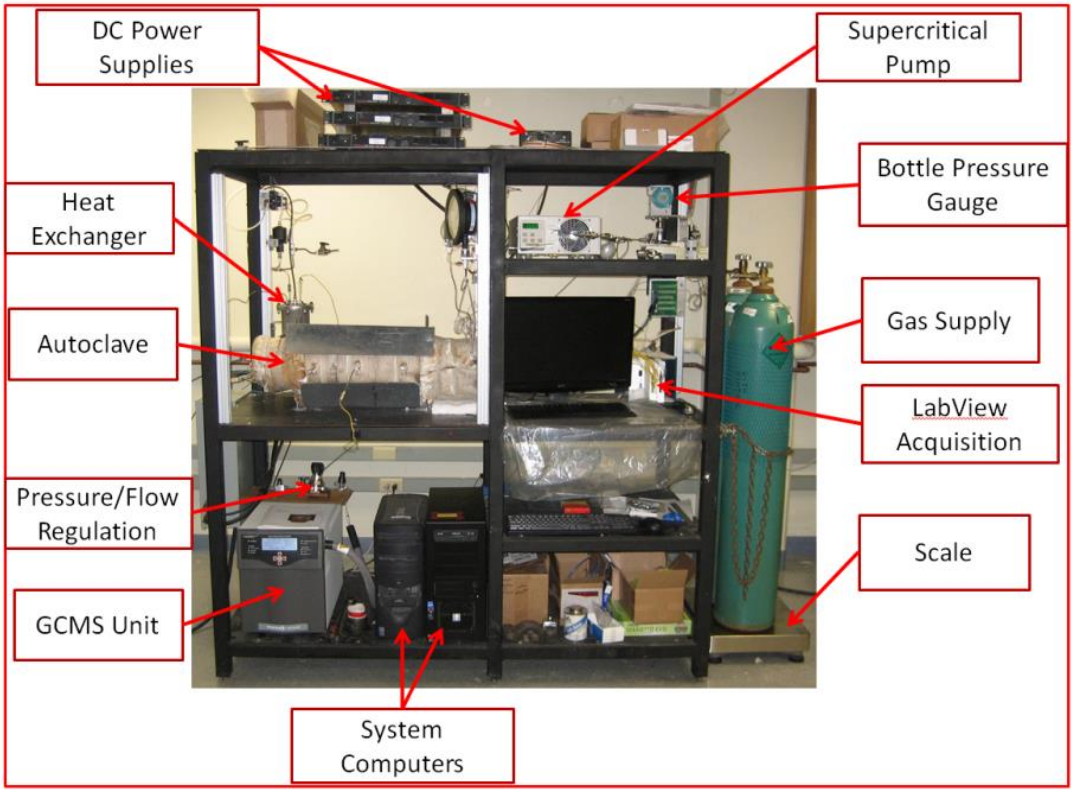

Fig. 2: Photograph of $SCCO_2$ Equipment and Experimental Test Setup

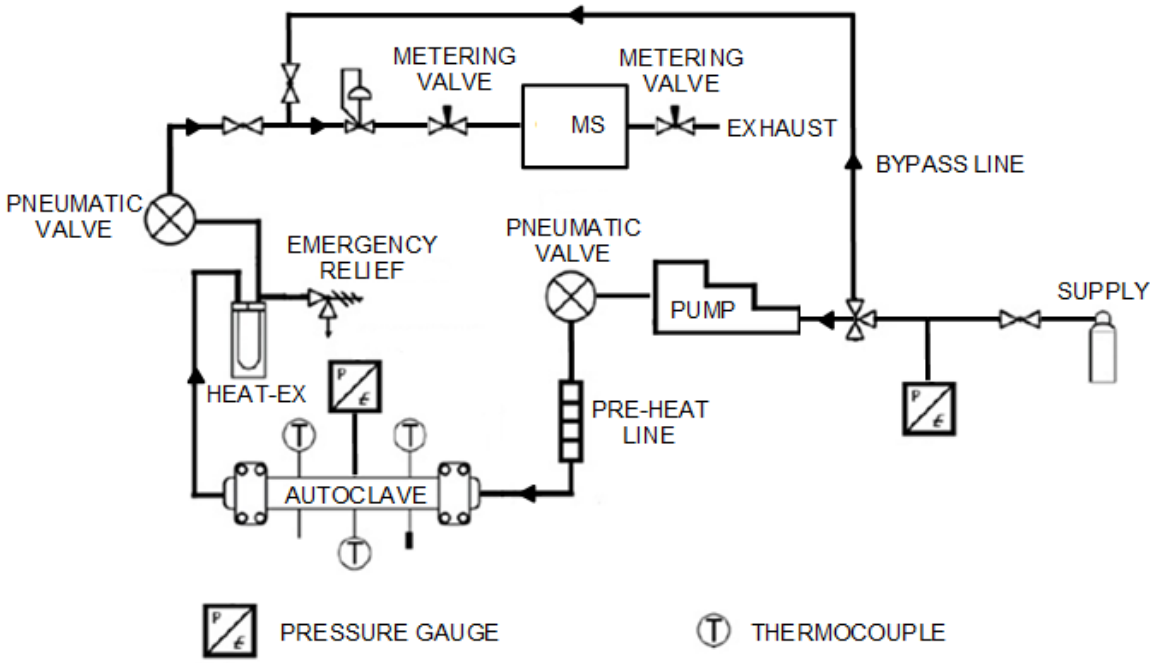

Fig. 3: Process Flow Diagram of $SCCO_2$ Experimental Test Setup

After the system was reconstructed, it was necessary to perform “shakedown” tests designed to establish reliability and to identify potential weakness in the system prior to experimental testing. The first few shakedown tests were performed using CO_2 at a pressure of approximately 800 psi (cylinder pressure). These tests isolated the autoclave test section at room temperature and monitored system pressure for signs of leakage. Leaks that were identified were marked and sealed after the conclusion of the test. This process was repeated until it was shown that the system could retain consistent pressure for 200 hours.

The second stage of shakedown testing involved ramping the temperature up in 50 degree intervals to a maximum temperature of 650°C then allowing the system to cool. This procedure established ramping ability, temperature stability during ramping (consistency across all three sections of the autoclave), as well as the cool down characteristics. It was found that the automated temperature ramping algorithm could consistently and evenly ramp the system without overshooting, and without the need to use manual stepped temperature intervals. The automated temperature ramping algorithm was therefore used for all system startups in lieu of manual temperature ramping. Pressurized CO_2 at ~800 psi was added to this test regime to observe the extent of pressurization during temperature ramping. It was found that pressures typically reached 1000-1800 psi depending on the flow settings. A small pumping study followed one of the pressurization tests to determine approximately how quickly the system could be pressurized, and the results indicated that pressurization could be achieved within tens of minutes. Therefore, based on these results, it was decided that pumping would not be initiated until the temperature was about 50°C from the set point.

Having established system integrity as well as temperature and pressure ramping characteristics, the final shakedown tests were conducted for real experimental conditions. Three tests were conducted at 450°C, 550°C, and 650°C with a testing pressure of 20 MPa (2900.75 psi) for all three tests. These final shakedown tests not only established system reliably, but also provided baselines for system startup and cool down times.

Fig. 4 and *Fig. 5* show examples of temperature and pressure ramping for 650°C conducted during the shakedown tests. As can be seen in the temperature profile, heating across the three sections was fairly uniform. Temperature in the middle section (TC9) corrects itself as pressure ramping is initiated. *Fig. 6* and *Fig. 7* show examples of temperature and pressure trends during a cool down from 650°C. The figures show temperature and pressure information just before the termination command is executed indicating a stable temperature of 650°C and pressure of 2900.75psi (20MPa). The termination command then immediately stops the heaters as well as the pump. As can be seen, temperature and pressure quickly drop once the termination command is given. While the system is cooling, the pump is stopped but gas is still allowed to flow through the system to promote cooling. Therefore, *Fig. 7* shows a plateau at about 800psi indicating bottle pressure. It takes the system approximately 10 hours to cool below 100°C at which point the flowing gas is completely stopped. Temperature and pressure continue to drop until levels are reached allowing for safe sample removal.

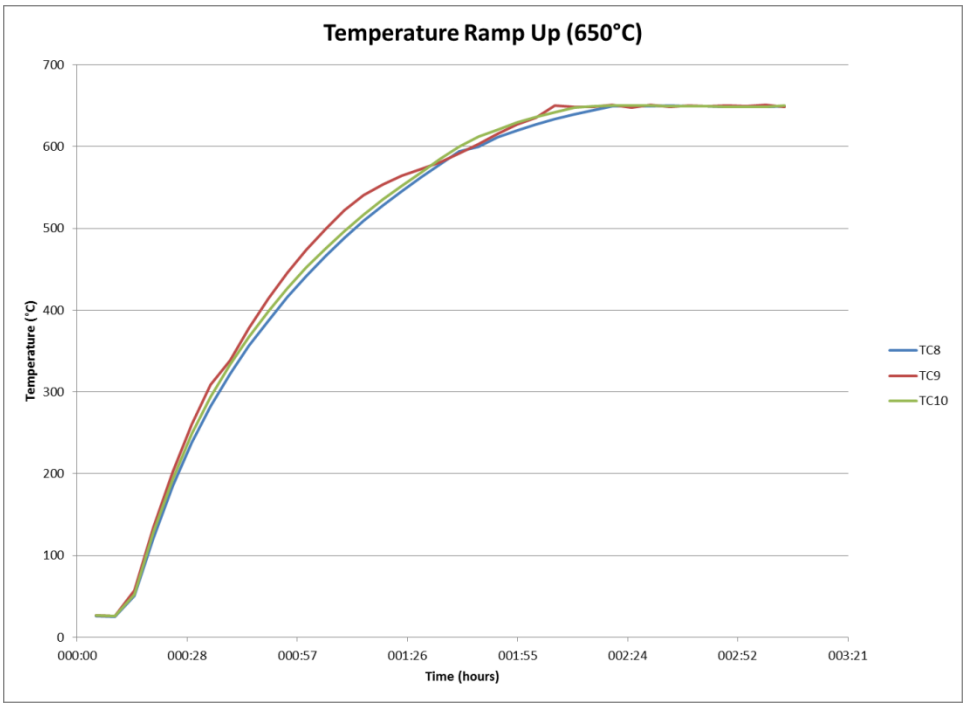

Fig. 4: Example of a temperature ramp up trend to 650°C

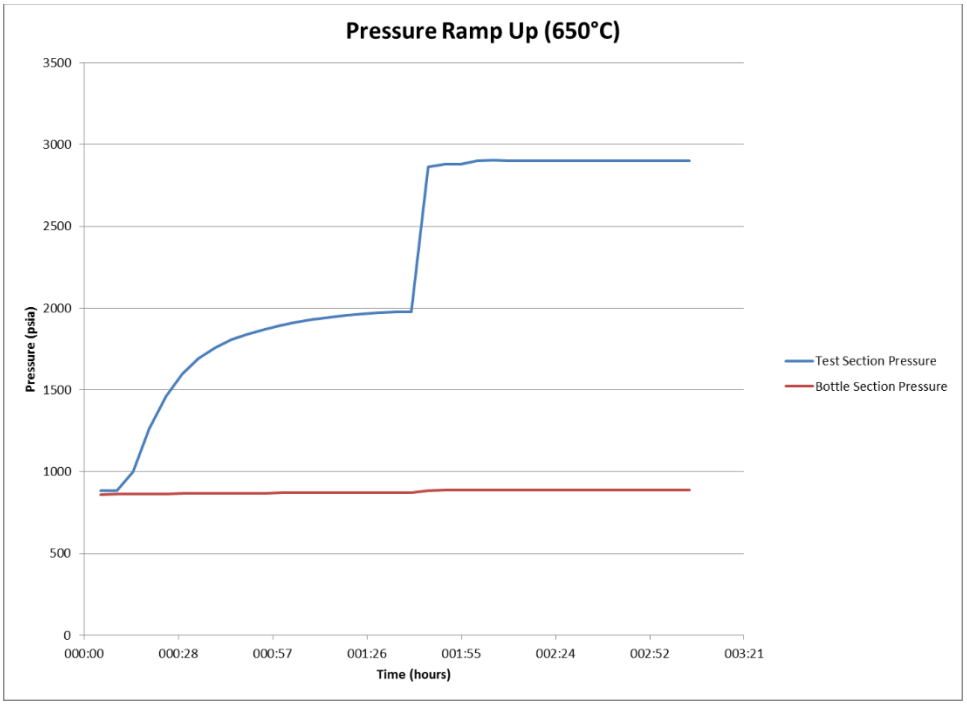

Fig. 5: Example of a pressure ramp up trend to 650°C

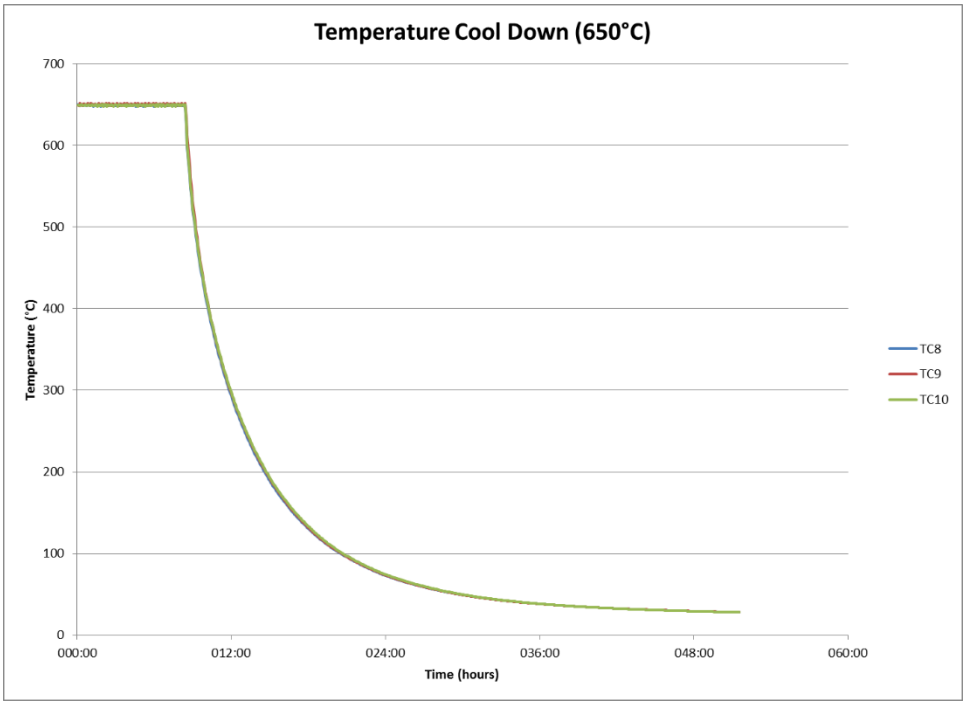

Fig. 6: Example of a temperature cool down trend from 650°C

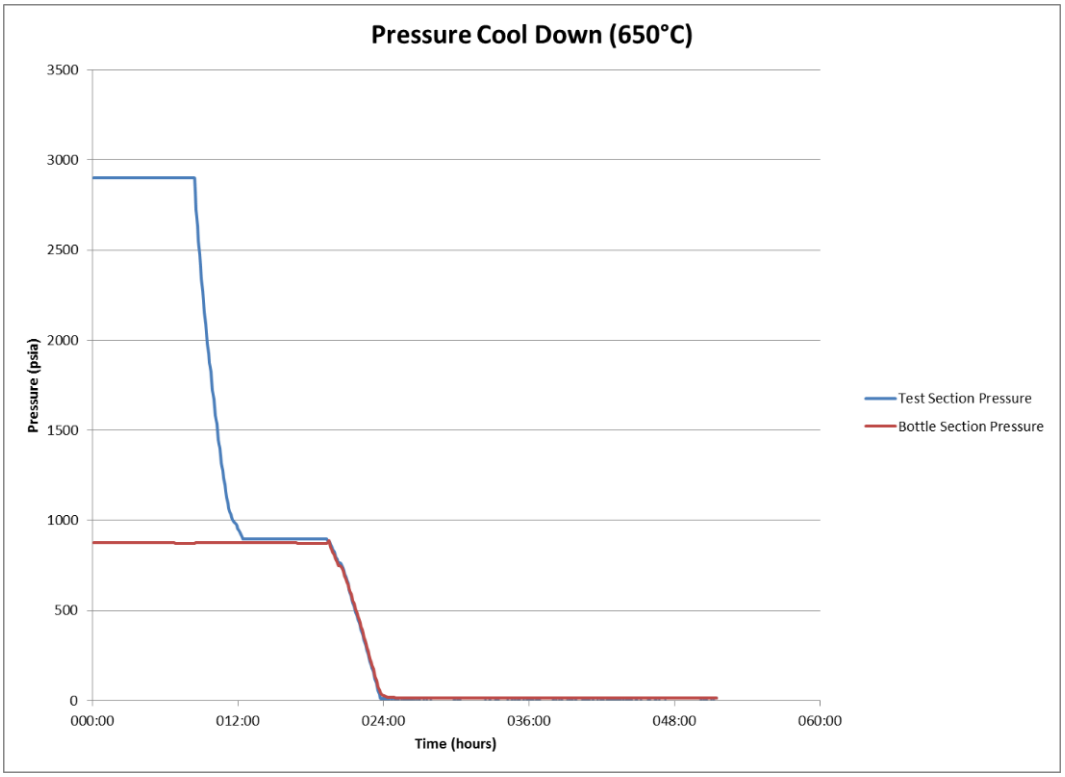

Fig. 7: Pressure profiles during temperature cool down from 650°C

Fig. 8, *Fig. 9*, and *Fig. 10* are examples of the stability of the system observed during the shakedown testing. As can be seen, temperatures are very stable fluctuating only as much as 3°C under all three conditions. Considering the temperature sections, thermocouple placement is illustrated in *Fig. 17*. Thermocouples TC8, TC9, and TC10 are inserted into the autoclave taking direct measurements in the middle of each of the three heating segments.

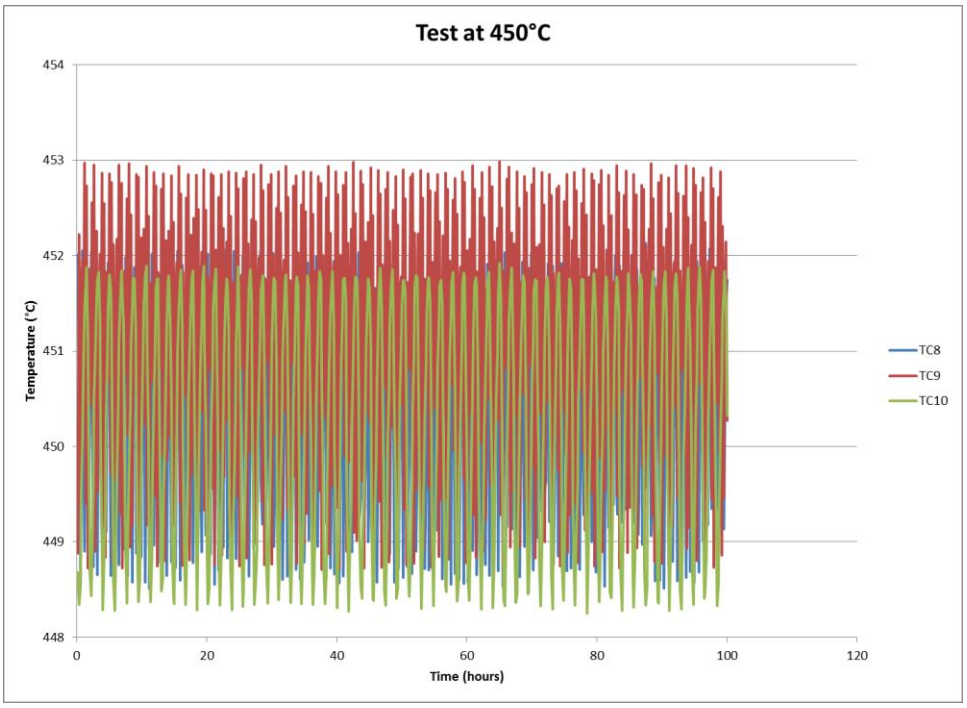

Fig. 8: Temperature stability trend for 450°C

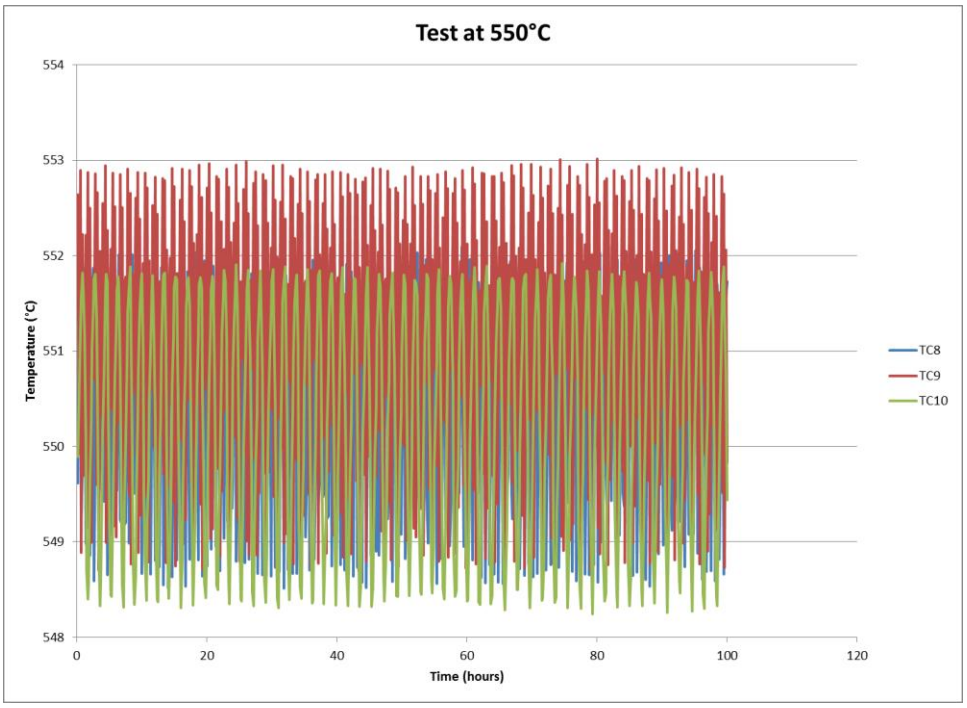

Fig. 9: Temperature stability trend for 550°C

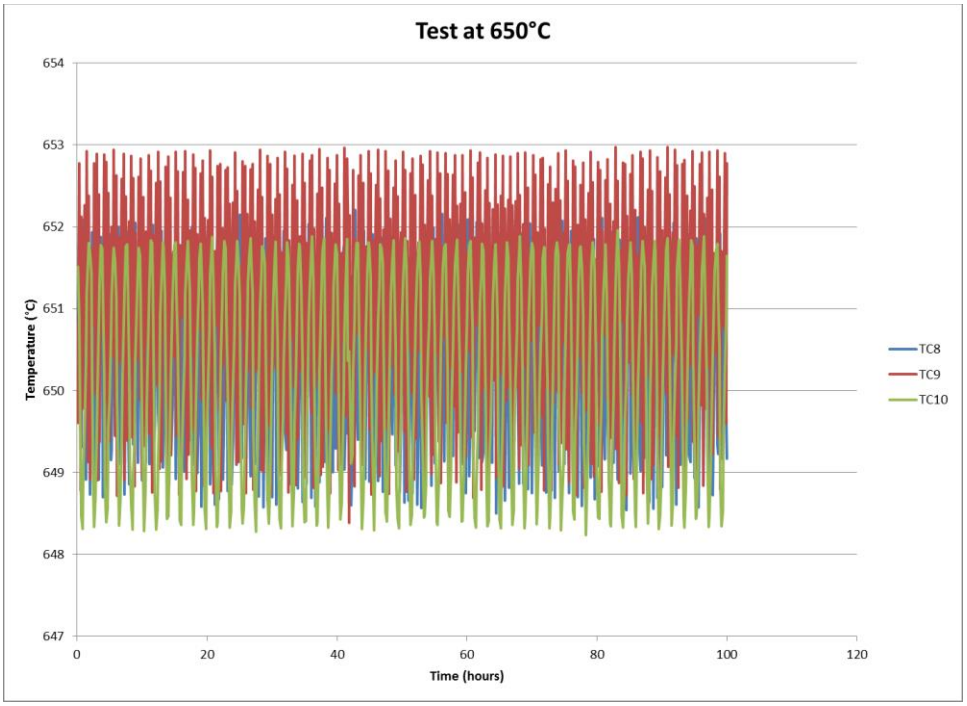

Fig. 10: Temperature stability trend for 650°C

3.1.2 Gas Source

Gas originated from vender supplied gas cylinders. For the experiments described herein, research grade CO_2 was provided by Airgas Inc. and certified at 99.9998% CO_2 per gas cylinder. During operation only one gas cylinder was in use at any given time. Two gas cylinders were connected to the system at all times to ensure redundancy. Gas cylinders were placed on an Adam GFK 330aH scale with a resolution of ±2 grams so that the change in mass could be accurately determined during testing. The change in mass from the cylinders determined both the mass flow rate, and whether or not the cylinder was nearing empty. With only one gas cylinder used in process at a time, separate ball valves were installed to isolate the reserve cylinder. This feature also made it possible to switch from a spent cylinder to a new cylinder during testing. *Fig. 11* illustrates the gas supply setup with cylinders set atop the scale, and an enhanced view of the control valves.

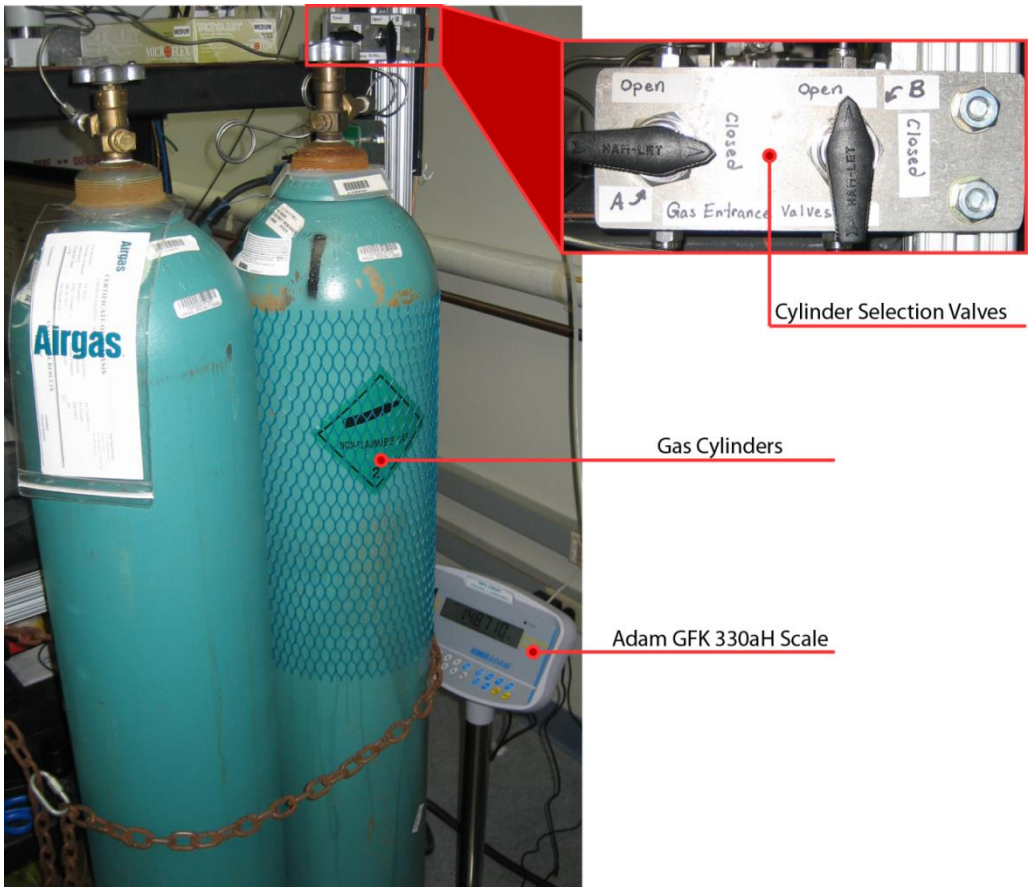

Fig. 11: Photograph of Gas Supply Cylinders, Scale, and Process Control

All the process connections for the test facility, except where specifically described, were made using 316 stainless steel. This included tubing, as well as Swagelok fittings. Additionally, all tubing in the system was rated for 6000 psi or greater, providing a large pressure margin for safe operation, as the expected operating pressure was not to exceed 3000 psi. Because the gas was at approximately room temperature outside of the autoclave, corrosion in the process lines was considered negligible.

Directly after the cylinder switching valves a Siemans Sitrans pressure transducer (*Fig. 12*) was connected to provide accurate (±0.25% FS) pressure information about the process gas

before it entered the supercritical pump. The full scale range for this transducer was 0.63 bar to 63 bar. The supercritical pump provided the pressure for the autoclave, maintaining the critical pressure as well as inducing a flow large enough to ensure fresh fluid to the samples (avoiding stagnation) and small enough so that fluid flow effect could be considered negligible. Approximately, the flow was set to refresh the 9.18x10-4 cubic meter autoclave volume once in two hours' time. The supercritical pump (*Fig. 13*), a Chrom Tech SFC-24, consisted of two sapphire pistons and a pulse dampener for a smooth fluid flow, and was capable of pumping at 24 ml/min to pressures up to 10,000 psi.

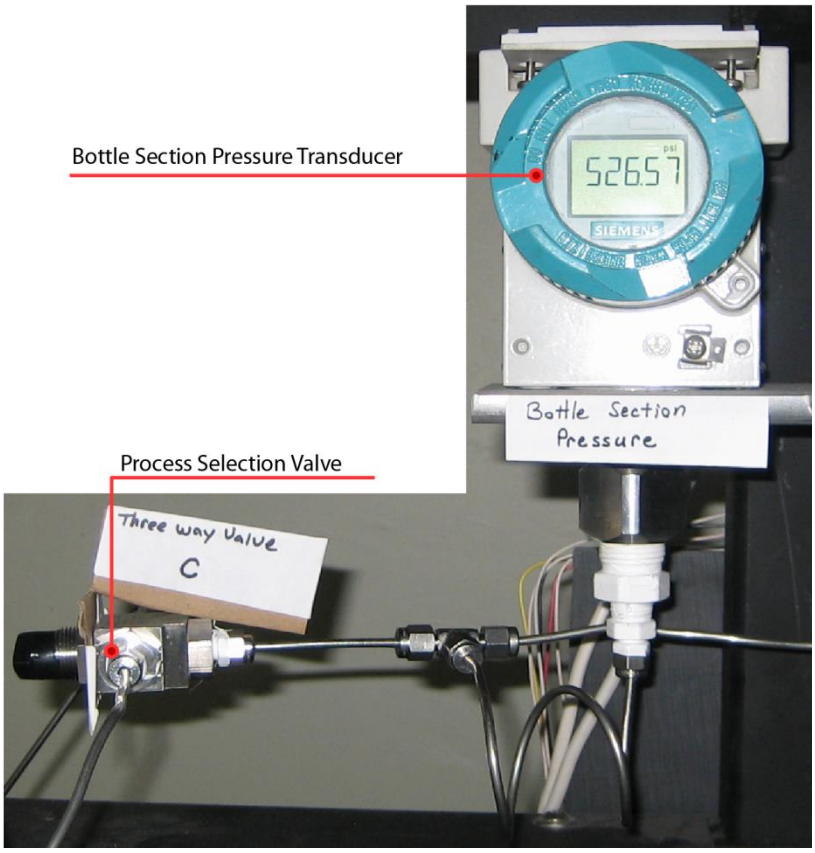

Fig. 12: Photograph of Bottle Section Pressure Transducer and 3-Way Process Valve

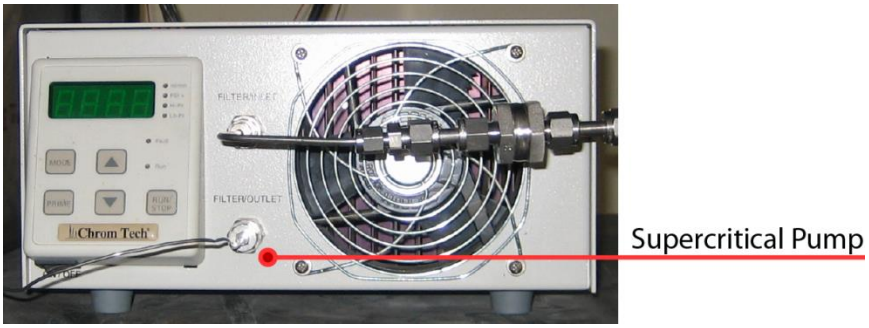

Fig. 13: Photograph of ChromTech Supercritical CO_2 Pump

3.1.3 Autoclave

After leaving the pump and before entering the autoclave tube, the supercritical CO_2 was heated to test temperature by a coil of Ni-chrome wire wrapped around a 1/8 inch (outer diameter) coil of Hastelloy C-276 tube (~ 3 linear feet). The resistive heating was accurately controlled using a thermocouple and a variable DC power supply. The autoclave itself consisted of a ~25 inch long NPS 2 Schedule160 Inconel 625 pipe that had Grayloc pressure fittings attached at both ends. Six ¼ inch Hastelloy C-276 tubes were welded into holes in the body of the tube, and allowed access for three Omega K-type thermocouples and two pressure sensors used to monitor the testing environment. The remaining port was used for a positioning rod (described later). *Fig. 14* shows part of the autoclave pipe with a Grayloc hub and clamps sealing the end. Seen in the figure protruding from the autoclave are two of the six tube ports.

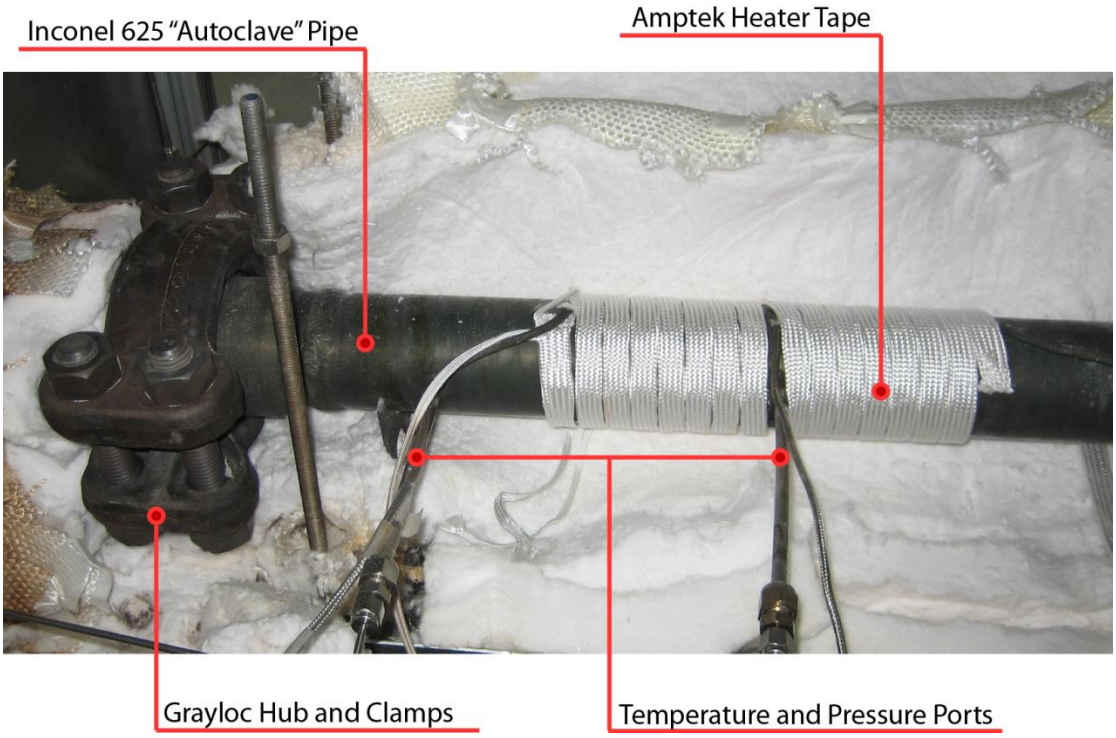

Fig. 14: Photograph of IN625 Pipe, Grayloc Hub and Clamps, Amptek Heater Tape, and Kaowool Insulation

Test gas entered and exited through the end caps which had 1/8 inch Hastelloy C-276 tube inlets welded into them. The body of the Autoclave was maintained at the test temperature by the use of three independent HTS/Amptek AMOX-covered heater tapes. *Fig. 14* also depicts the Amptek heater wrapped for the middle heating section. The heater tapes had a maximum operation temperature of 760°C and were controlled via three Control Concepts model 1032 power controllers. Five additional K-type thermocouples were attached to the outer body of the autoclave tube for system monitoring. The end caps were maintained at temperature by small coils of Ni-chrome wire; with resistive heating controlled via DC supply and thermocouples.

While the Grayloc fitting on the exit gas end of the autoclave was repeatedly used as the sample exchange port, the Grayloc hub on the inlet gas side remained sealed. This limited the possibility of seal ring failure for the inlet gas end. The Grayloc seals worked very well, but there were concerns about the integrity of the seal ring after multiple removals from the higher temperature tests. This held especially true for testing at 650°C where the seal ring coating did not hold up past three uses. The Grayloc seal rings were Inconel 625 material coated with silver, and after multiple exposures, the silver started to separate from the seal ring creating breaches into the system from which CO_2 could leak. Therefore, seal rings were inspected after each test interval and replaced when they showed signs of wear.

Fig. 15 shows the location for thermocouples, the thermocouple number, the location for pressure transducers, and the heating zones. The entire body of the autoclave was wrapped with refractory insulation (Kaowool in two 1” thick layers) and an alumina fiber blanket to maintain the temperature, and limit heat loss. Two, approximately crescent shaped, polished aluminum reflectors were added above and below the autoclave to reflect thermal radiation back into the autoclave.

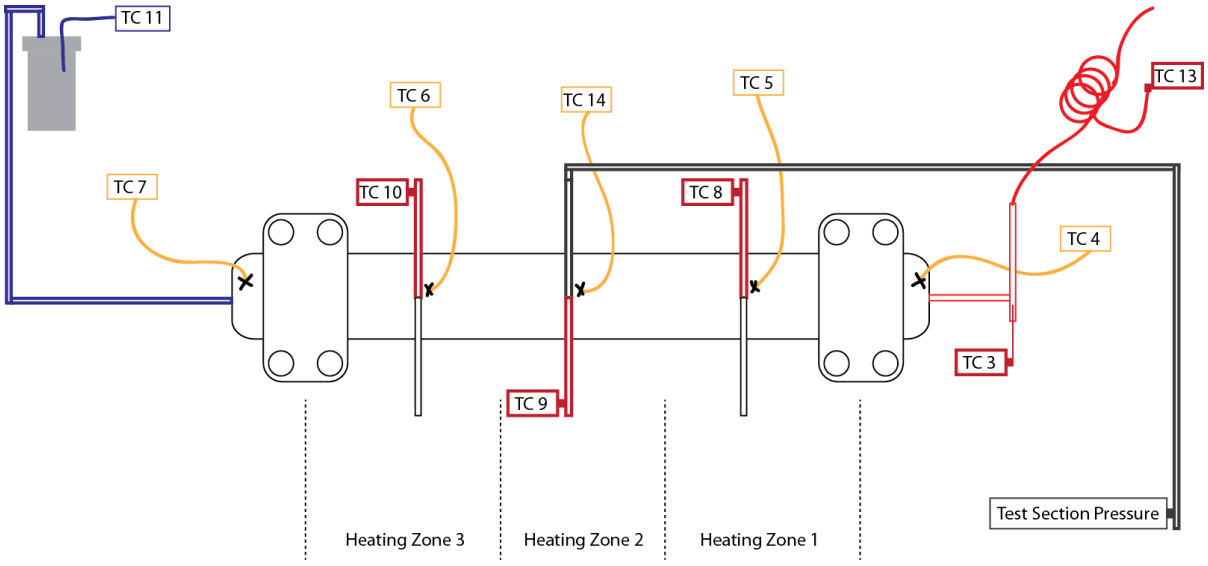

Fig. 15: Diagram of the Autoclave Showing Thermocouple Placement and Heating Zones

After leaving the autoclave test section, the CO_2 needed to be cooled considerably. A simple counter flow heat exchanger was used for this purpose (*Fig. 16*). The "chiller" consisted of a "can" (stainless steel container) that was filled and circulated with building cooling water. A 20 foot piece of 1/8" Hastelloy tube was coiled inside the can through which the hot CO_2 could pass. A thermocouple attached to the chiller monitored the exit temperature of the CO_2 to make certain it reached a safe temperature.

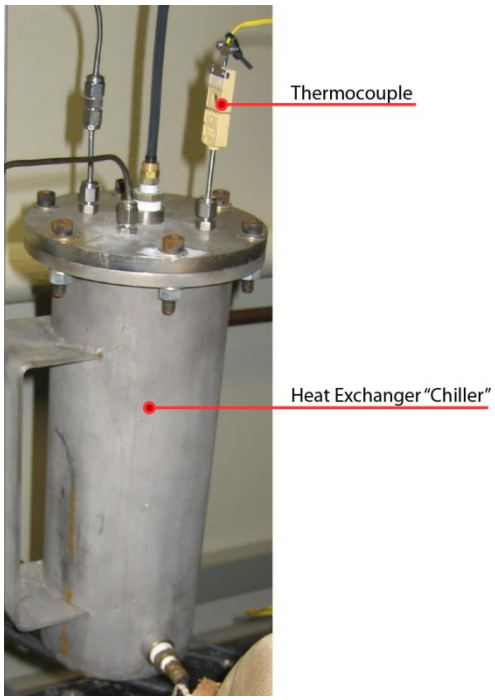

Fig. 16: Photograph of Gas Cooler (Heat Exchanger)

3.1.4. Sample Mounting Hardware

The test coupons were mounted in a sample holder consisting of components capable of withstanding the elements of a high temperature, high pressure environment, and that could be entirely removed from the autoclave at regular intervals for examination. The one additional component of the corrosion testing facility not strictly associated with maintaining the high pressure high temperature environment was the sample holder. The sample holder, used to hold the test material during testing, was made out of alumina owing to its benign interaction with CO_2 and its high temperature capabilities. The outer framework of the sample holder acted as a chassis and was constructed of IN625. An alumina ceramic "boat" was precision machined and inserted into the IN625 frame and pinned into position within

the frame at both ends by 3.0 mm Ø alumina pins. Alumina inserts with a slot were machined and placed at the end of the boat so that a 3.0 mm Ø alumina rod could be freely suspended and traverse the length of the boat. This enabled the freedom to remove and install coupons. This design also served the purpose to gauge and retain spalled oxide particles from suspended test coupons, which could later be collected from the boat for further chemical analysis if necessary. To mitigate the effect of galvanic corrosion and catalytic effects between coupons and coupons of different materials, a 1.0 mm thick alumina ceramic washer (spacer) was inserted between each coupon on the sample boat holder. *Fig. 17* and *Fig. 18* below show the layout of the sample holder and its components and the alumina spacer.

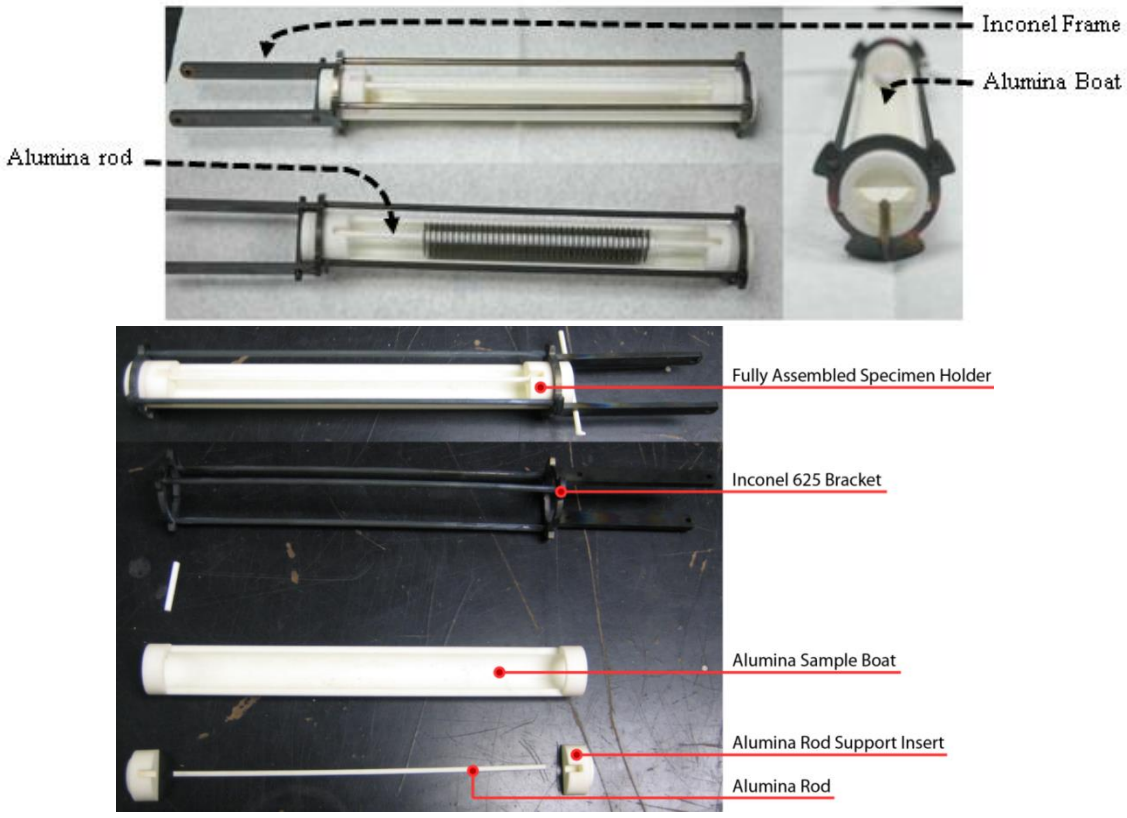

Fig. 17: Different Views of Test Sample Holder

Fig. 18: Image of Alumina Spacer.

ID = 0.120-0.133”, OD = 0.370-0.383”, thickness = 0.036-0.045”.

3.1.5 Automation

The SC-CO_2 Corrosion Test facility was completely automated. Automation was accomplished through the use of National Instruments (NI) hardware, and software (LabView). Specifically, acquisition signals were gathered from the thermocouples and pressure transducers wired into an NI SCXI data acquisition device connected to a custom built computer. *Fig. 19* depicts the National Instruments hardware acquisition device wired to all the thermocouples and pressure transducers. LabView software running on the computer executed code specifically written for the system to read in values from the data acquisition device. Data driven events were then used to execute commands to the hardware. System readings were simultaneously compiled into a report format for data logging so that an accurate history of the testing conditions for the duration of the experiment could be maintained.

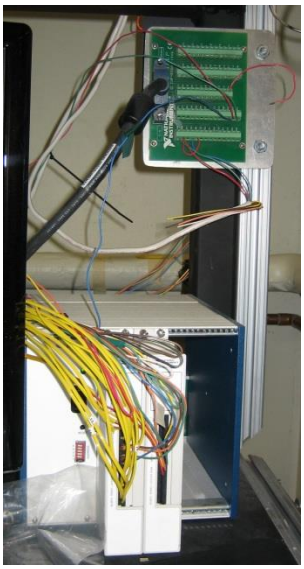

Fig. 19: National Instruments hardware with temperature, sensors, heater control, DC power supply triggering, and valve signaling

Heating was executed using the data from thermocouples ported in the autoclave. Thermocouple signals were processed and interpreted with respect to calibrations, and the resulting temperatures were further processed with a proportional-integral-derivative (PID) algorithm to determine the appropriate heating response. Commands from LabView based on the temperature readings were output to analog channels on the NI SCXI device which then were used to control the Model 1032 power controllers. The power controllers dictated the power to the heater tape; controlling the temperature. Pressure readings taken from the pressure transducer in the autoclave section were likewise used to determine control commands sent via com port to the SC-CO_2 pump.

Although the Adam scale was not directly wired into the NI SCXI data acquisition module, its connection via com port allowed LabView to record periodic measurements. These

measurements were then graphically displayed within the program interface, and recorded with the temperature and pressure measurements.

Possibility of the failure of the SC-CO_2 pump necessitated the ability to isolate the autoclave to maintain pressure. Between the pump and the "preheat" section as well as just after the cooler, pneumatic LabView controlled valves were inserted so that the autoclave could be automatically isolated in the event of a malfunction mid test. The settings to the valves were made such that in the event of power failure the valves would close isolating the autoclave section. *Fig. 20* shows the pneumatic valves attached to the testing facility and individual close ups.

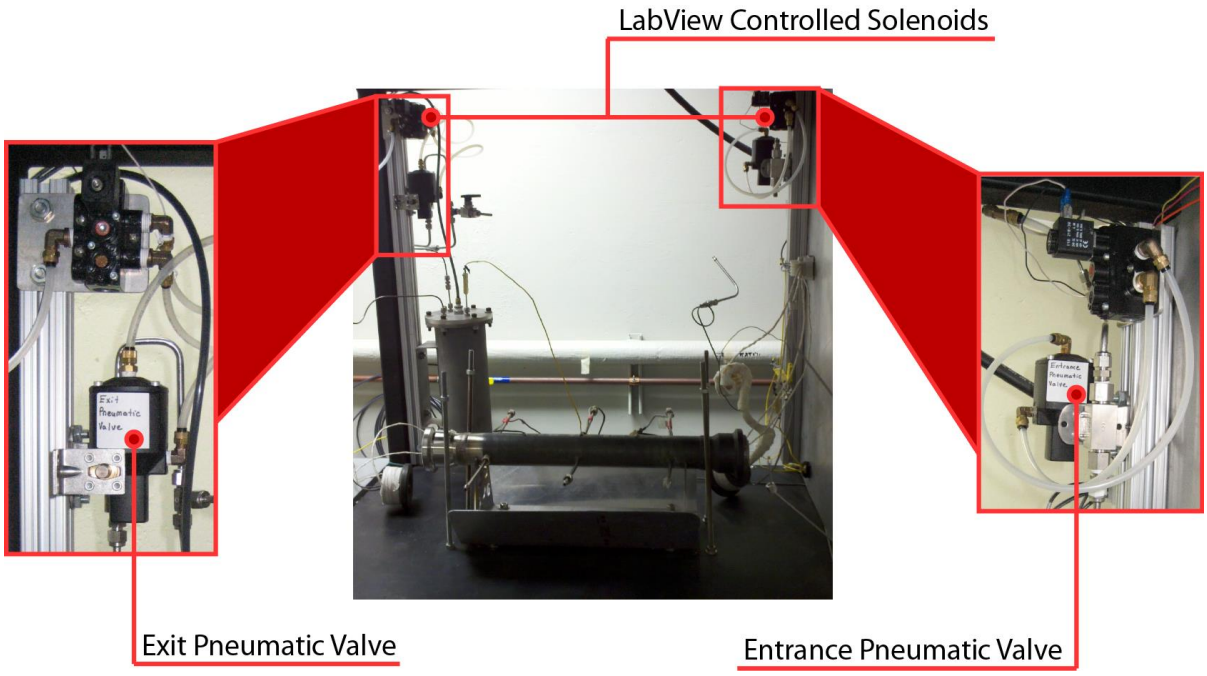

Fig. 20: Photographs of the Automated Entrance and Exit Valves

Additional items were added to the system for safety and ease of monitoring. These items included a manual pressure vent (hand operated purge valve), an automatic pressure release valve, an easily visible pressure gauge, polycarbonate blast shields, inline filters, and a calibration-check gas-bypass. The bypass was inserted into the process line after the bottle section pressure transducer using a three way ball valve, and ran directly to the GCMS (including pressure regulation). This bypass allowed easier access to the gas directly from the cylinder for calibration and monitoring purposes. To address the potential for power fluctuations an uninterruptable power source (UPS) was added to the system. The Tripp Lite SU3000XL on-line double conversion 2400 watt UPS system not only provided backup power to the system in the event of power failure, but also actively conditioned the supplied power.

3.1.6. Mass Spectrometer

A Pfeiffer Vacuum Thermo Star quadrupole mass spectrometer (MS) was selected as the device to measure both the inlet gas composition and outlet reaction products. Denoted by MS in *Fig. 3*, and also shown in *Fig. 22*, the MS operates with feed gas at atmospheric pressure and was attached downstream from the two-stage pressure regulator. With the exit gas at room temperature after leaving the heat exchanger, a pressure and flow regulation system was implemented to simultaneously maintain a set backpressure and allow a small flow of gas to exit at atmospheric pressure. A two-step system was devised using a high pressure regulator in conjunction with a precision needle valve to manage flow and provide proper backpressure. The pressure regulator selected was a Conoflow HP 700 rated specifically for use up to 6000 psi. This particular regulator used two stages to provide

constant outlet pressure regardless of fluctuations on the inlet side. Using the HP700 to bring the pressure down to a manageable level (approximately 25 psi), a high precision Parker needle valve was used to set the flow. *Fig. 21* depicts the pressure/flow regulation setup.

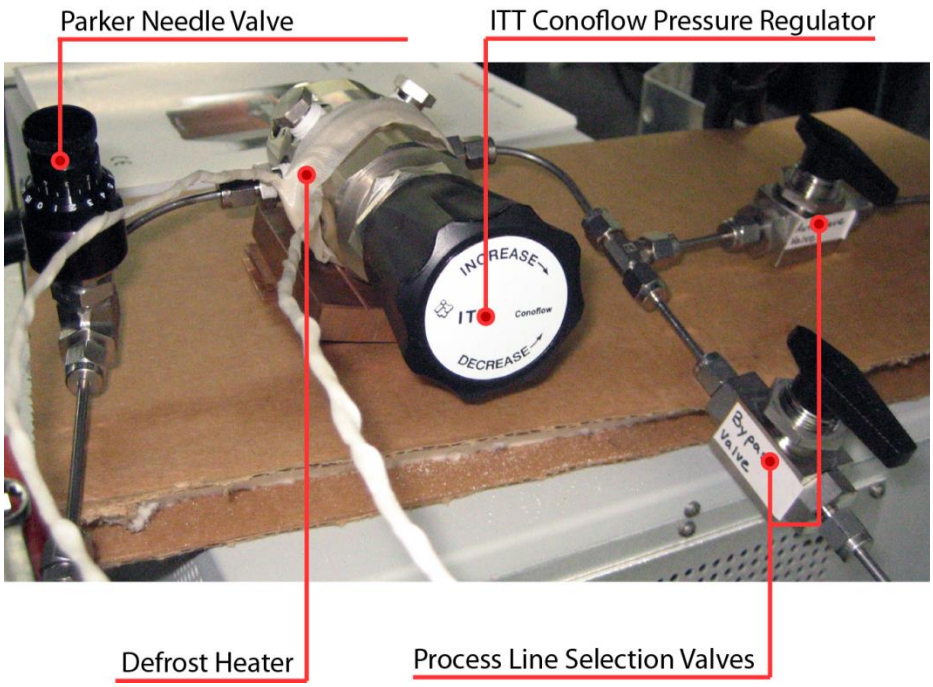

Fig. 21: Photograph of Pressure Regulation Setup

In order to investigate any chemical reactions possibly taking place during the corrosion process, the use of gas chromatography was implemented in the facility. Cylinder gas would be initially characterized using a process line that bypassed the autoclave, and exit gas from the autoclave could be monitored through the duration of the experiment. Because this unit could be operated with gas at atmospheric pressure, it was attached at the end of the process line. A "T" fitting, a small length of stainless steel capillary tube, and another Parker needle valve were used to set the flow of gas as well as prevent any backflow of air into the GCMS unit.

Fig. 22: Photograph of Pfeiffer Vacuum Thermostar MS

A mass spectrum will usually be presented as a vertical bar graph, in which each bar represents an ion having a specific mass to charge ratio (m/z) and the length of the bar indicates the relative abundance of the ion. The most intense ion is assigned an abundance of 100, and it is referred to as the base peak. Most of the ions formed in a MS have a single charge and the m/z value is equivalent to mass itself. Modern day MS's can distinguish ions by only a single atomic mass unit (amu), and can provide measurement of a molecular species of differing mass. But if one seeks after the elemental isotopes, these are not measurable directly and must be determined by calculations based on the observed molecular spectrum [38]. A carbon dioxide molecule is composed of only three atoms, and has a reasonably simple mass spectrum. The base peak or ion current is at m/z 44 ($^{12}C^{16}O_2$), and the only fragment ions are CO (m/z 28) and O (m/z 16). Table 1 below lists the amu peaks of different gaseous species.

Table 1: List of amu Peaks for Different Gaseous Species

Species	Atomic Mass Unit
CO_2	12,13,16,22,28,29,**44**,45,46
CO	12,14,16,**28**,29,30
O_2	16,**32**,33,34
Air	14,16,17,18,20,28,29,32,34,40,44
H_2O	16,17,**18**,19,20
N_2	14,**28**,29
NO_2	14,16,**30**,31,46
SO_2	16,24,32,34,48,49,50,**64**,65,66

Note: Bold value indicates base (principal) peak

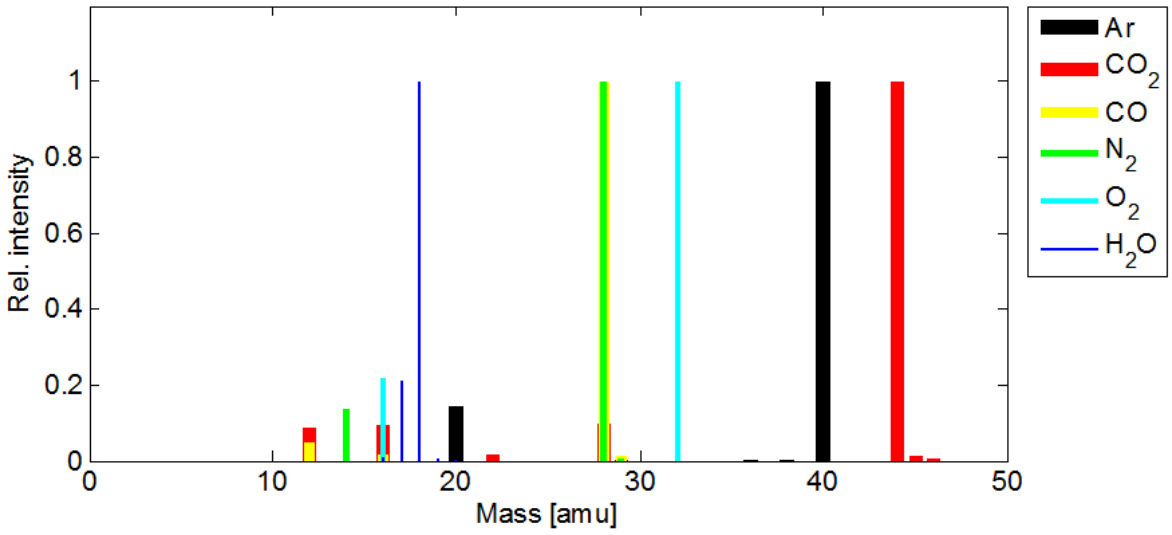

Fig. 23: Mass Spectra of Different Species from NIST
Courtesy of David Grierson

The mass spectra for RG-CO_2, IG-CO_2 and BDG-CO_2 from their respective supply cylinders are provided below in *Fig. 24*, *Fig. 25*, and *Fig. 26*, respectively. Measurements were made for each CO_2 concentration through the bypass line (see *Fig. 3*). Kane and Goodell have observed that mass spectrometers require far more attention than a gas chromatograph, whereas they have been able to setup, install, operate, and serviced their gas chromatograph with only casual assistance from colleagues, the mass spectrometer was very demanding of professional services [39].

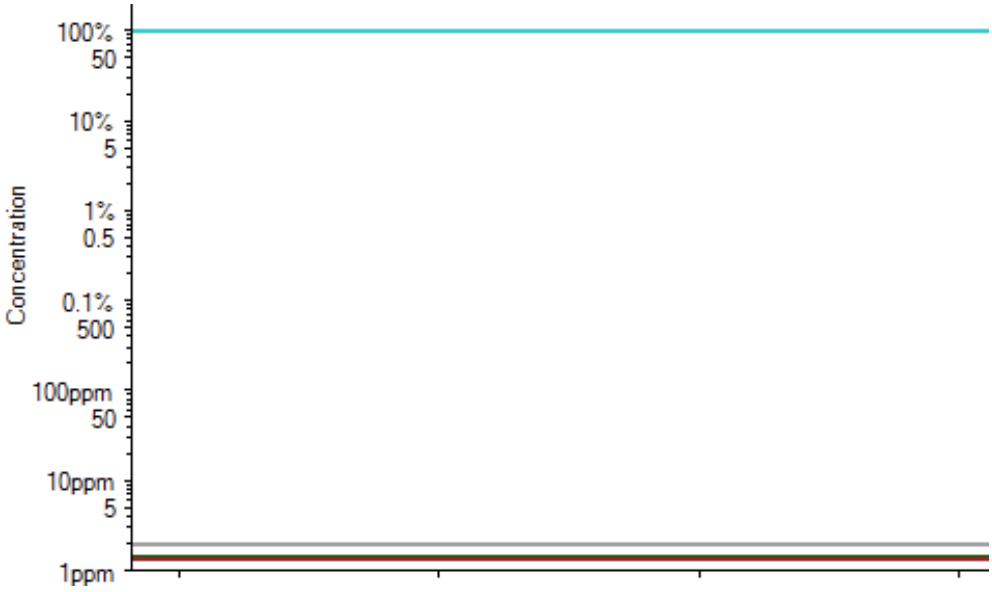

Fig. 24: Measured Gas Composition of RG-CO_2 at Outlet
CO_2 = 99.999%, CO < 2ppm, O2 < 2ppm, H_2 < 2ppm, H_2O < 1ppm

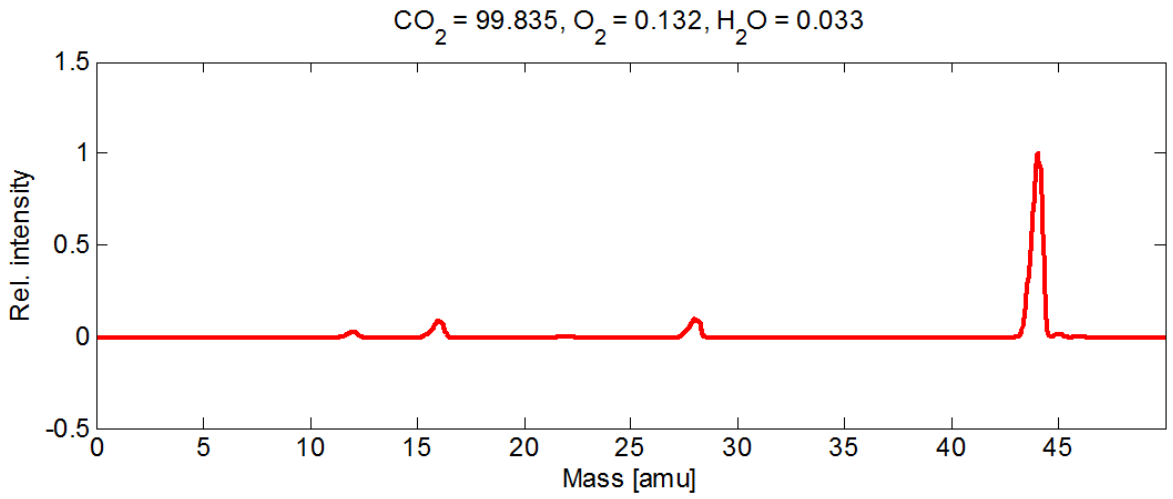

Fig. 25: Mass Spectra of BDG-CO_2 at Inlet (from Cylinder)

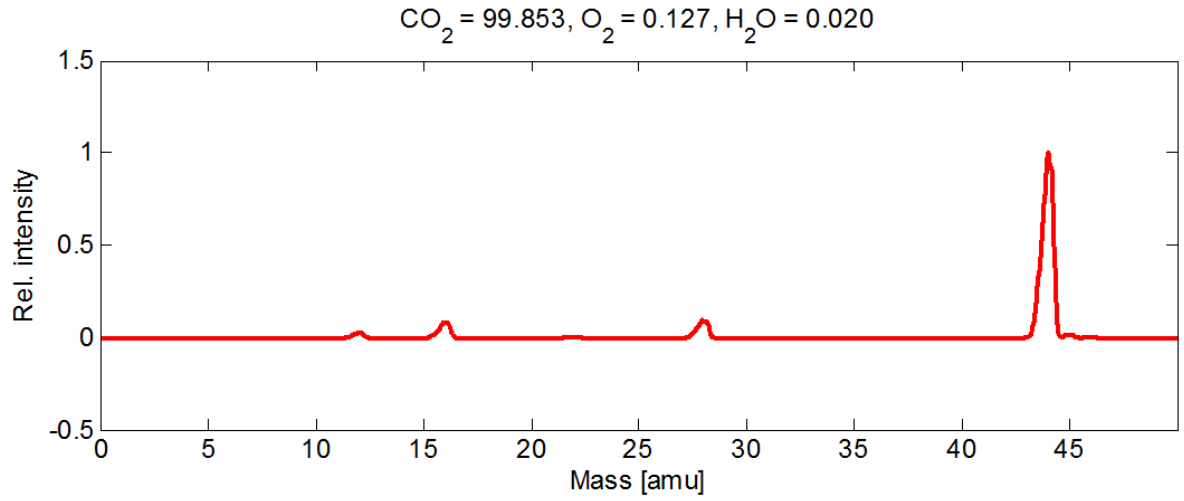

Fig. 26: Mass Spectra of IG-CO_2 at Inlet (from Cylinder)

3.1.7. Test Procedure

After the sample holder has been installed in the autoclave, the sample holder is set into the same repeating position by a locating pin that penetrates through both extending arms at the front of the sample holder and into a hole inset. The coupons, which are suspended on an alumina sample holder, are positioned approximately in the center of the autoclave. A silver-coated ribbed seal ring with two lips is installed onto the end of the autoclave pipe, followed by a blind end hub. These components make up the Grayloc connector system typically used for high pressure piping and vessel connections. The Grayloc end hub is then wrapped with a ceramic fiberglass insulation blanket and a protective alumina fiber blanket cover. First, the autoclave temperature is raised from atmospheric STP conditions to the desired temperature (i.e., 450^{o}C, 550^{o}C, 650^{o}C). The rate of temperature increase was approximately 605K/hr at 550^{o}C. The CO_2 is fed in a liquid state from a commercial cylinder (70^{o}F, ~ 835 psia, ~ 450 hours life) to a constant flow, dual-piston supercritical CO_2 pump, which displaces the liquid at a constant rate beyond it's critical pressure (7.39 MPa) to 20 MPa. A pre-heat line, just after the pump outlet, heats the gas to within close proximity of the desired temperature to minimize thermal disparity prior to entering the conductively heated autoclave above its critical temperature (31^{o}C). The coupons, which are suspended on an alumina sample holder, were positioned approximately in the center of the autoclave. The flow rate of $SCCO_2$ was about 0.02 kg/hr, sufficient to refresh the autoclave every two hours, and can be considered as low flow or quasi-static. The $SCCO_2$ is then returned to STP conditions after 200 hours of exposure to enable removal of coupons for weighing and determination of weight change. A total of 10 coupons were tested, with two coupons removed every 200

hours of exposure for surface analysis examination using optical methods. *Fig. 27* shows the sequence used for removing coupons. Gas composition from the cylinder and the autoclave outlet were monitored using the MS system.

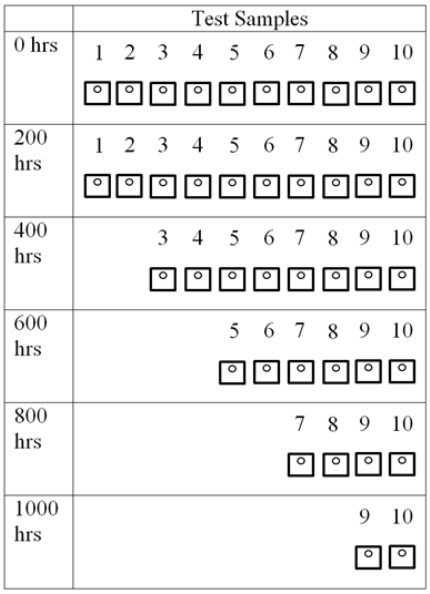

Fig. 27: Sequence for Coupon Removal

3.2. Metallic Coatings

From the weight gain results of alloys in tested in research grade CO_2, the 9-12Cr ferritic-martensitic steels T92 and T122 exhibited the highest weight gains. Therefore, these two materials were selected to see if corrosion resistance could be enhanced by a suitable coating. Previous works by Ren [40] and Allen and Sridharan et al [41, 42] have shown improvement in corrosion resistance at high temperature for ferritics in supercritical water environment, and Tang et al [43] have shown improvement in corrosion resistance in air at high temperature. For this study, the surface treatments selected were as follows:

- Single Element Aluminum Coating (5.000 kÅ, both sides)
- Single Element Yttrium Coating (5.000 kÅ, both sides)
- Shot Peening (SS shot, 60psi/6secs, both sides)

3.2.6. Sputterer

Deposition of the thin film aluminum and yttrium coating were conducted using a Denton Discovery 24 RF/FC physical vapor deposition (PVD) system at the Wisconsin Center for Applied Microelectronics (WCAM). This system was chosen for its capability to achieve high vacuum pressures and its wide diameter palette, enabling the radial distribution of a uniform sputtered coating on as many as 25 samples simultaneously, all within 1-2% of 5.000 kÅ. Given the range of variation observed in weight gain amongst individual samples, it is beneficial to minimize this variation any further by depositing on all the samples under the same conditions at one time if possible.

Fig. 28: Photograph of RF/DC Multi-Cathode PVD Sputterer

3.2.7. Coating Procedure

For each coating, the coupons were installed on a palette along the inside of a copper ring guide. *Fig. 29* below shows a photograph of this installation. Several additional coupons were added to allow for SEM/EDS/XRD and thickness check of coated samples.

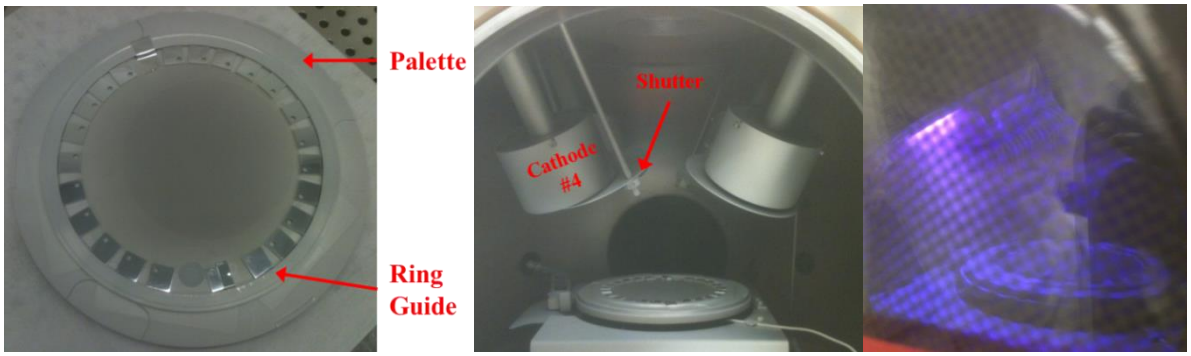

Fig. 29: Photograph of Sample Mounting, Chamber, and Coating Deposition

The chamber was then allowed to pump down to a pressure of about 1.1-1.8e^{-6} torr. The deposition was then started and deposited a 5.000 kÅ at a rate of about 3.3-3.5 Å/s for about 24-25 minutes. The deposition was then manually stopped and the cathode allowed to cool before removing the samples. After the cathode cooled down, the palette was removed from the chamber and each coupon was gently flipped over to allow for coating of the other side by repeating the above process. This process was essentially the same for both coatings using aluminum and yttrium. Table 2 below shows the deposition parameters used in this study. The Yttrium target, which had not been used before in this sputterer chamber, was "broken-in" (out-gassed) and ramped-up in power for about 60 minutes to determine the cathode power setpoint and deposition rate.

Table 2: PVD Sputtering Parameters for Al and Y Coatings

Parameter	**Aluminum (2.70 g/cc, 1.080 Z)**		**Yttrium (4.34 g/cc, 0.835 Z)**	
Side	Front	Back	Front	Back
No. of Coupons	23	23	23	23
HCM12A	10	10	10	10
NF616	13	13	13	13
Purge Gas	Argon	Argon	Argon	Argon
Gas Flow Setpt	20 sccm	20 sccm	20 sccm	20 sccm
Cathode #	4	4	4	4
Rotational Speed	13rev/min	13rev/min	13rev/min	13rev/min
Dep. Screen Thk.	4.996 kÅ	5.011 kÅ	5.000 kÅ	5.000 kÅ
Dep. Time	00:25:07	00:24:57	00:23:41	00:23:39
Dep. Rate	3.3 Å/s	3.4 Å/s	3.5 Å/s	3.5 Å/s
Dep. Pressure	$1.8e^{-6}$ torr	$1.7e^{-6}$ torr	$1.1e^{-6}$ torr	$1.5e^{-6}$ torr
Sputter Press Setpt	6 mtorr	6 mtorr	12 mtorr	12 mtorr
Sputter Power Setpt	45%	45%	17.5%	17.5%

3.3. Shot Peening

Shot peening is the process of cold working the surface of a structural or machine part by means of a propelled stream of spherical shot. The process is used to improve the fatigue properties of the part, and to retard stress corrosion cracking, by the introduction of compressive stresses in the surface layer. The presence of this layer of compressive stresses serves as a retardant to initiation and growth of failure cracks. Shot peening causes local plastic flow in the surface of the object, stressing the material beyond its yield strength, which results in a residual compressive stress [44]. Stress corrosion is failure by cracking under a combination of corrosion and tensile stresses. Peening inhibits stress corrosion by virtue of the associated surface compressive residual stress state. It is generally applied to increase resistance to fatigue and stress corrosion failure and is widely used on springs and gears [44, 45]. In regards to other surface deformation methods, Grabke et al [45, 46] have

shown the effect of grain size, cold working, and surface finish on the metal dusting resistance of steels in a carburizing environment. Cast steel shot is the most widely used media. Despite carbon steel shot being the most widely used and least expensive media, to avoid imparting carbon onto the alloy sample surface with carbon-bearing particles and to do away with having to further clean the surface, an Ervin AMACAST ES-300 (S110) stainless steel shot was selected. Pricing of three different shot media considered is provided below in Table 3.

Table 3: Shot Media and Pricing

Blast Media	Pail/Drum Wt.	Density	Total Costs	Piece Price
Stainless Steel (S110 size)	50 lbs	7.0 g/cc	$213	$4.25/lb
Glass Bead (Potter's Product "AA" Size)	50 lbs	2.5 g/cc	$33	$0.66/lb
Ceramic (Zirblast B-40)	55 lbs	-	$262	$4.75/lb
Carbon Steel (S110)	50 lbs	7.0 g/cc	$50	$1.00/lb

3.3.6. Peen Machine

For this study, a Media Blast & Abrasives Powerpeen 2000™ pneumatic shot machine was selected. The nozzle size was chosen based on the shot size, flow volume, intensity, and area (pattern) to be peened. Media already present in the machine was evacuated through the abrasive mixing valve located below the mixing pot and blasted down with an air hose completely from the inside of the cabinet. This action was performed to prepare for install of the stainless steel shot. The blast nozzle was a ¼" venturi boron carbide nozzle and was positioned 6.5" normal from the almen sample holder.

3.3.7. Mounting Hardware

Fig. 30 below shows a schematic of the shot peening process and related hardware. *Fig. 31* below shows how the ferritic samples were mounted for shot peening.

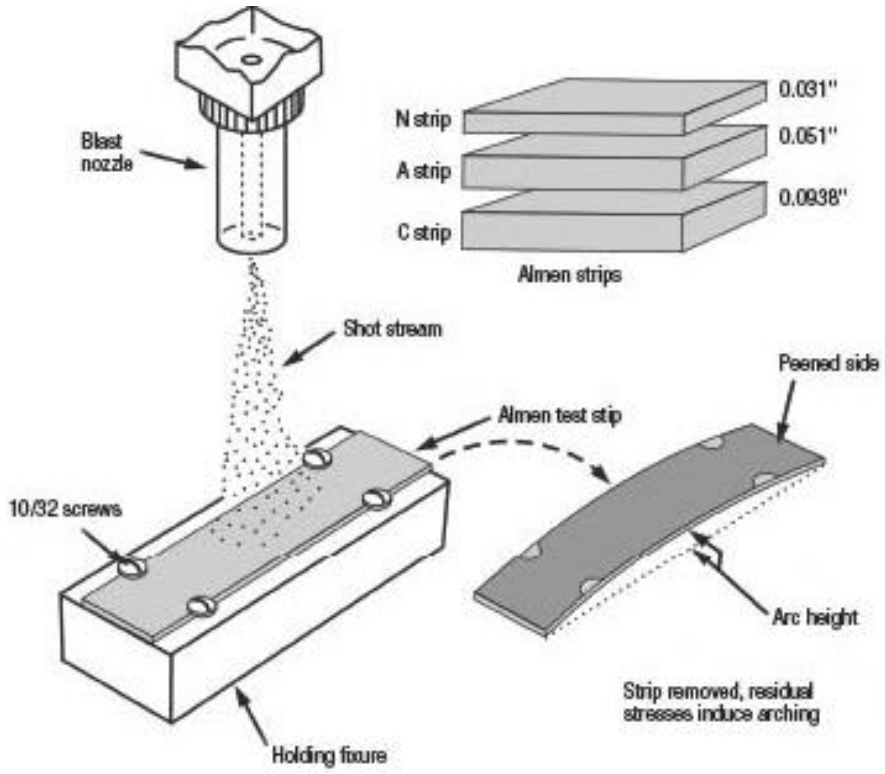

Fig. 30: Schematic of Shot Peening Process and Hardware

Fig. 31: Mounting of (a) Almen Strips and (b) Coupons for Shot Peening

3.3.8. Peening Procedure

Prior to determining the intensity curve, the newly installed virgin stainless steel shot was pre-blasted against a SS plate to work harden the dead soft 20 HRC shot to as much as 50+ HRC.

To ensure that shot peening operating conditions were similar from coupon to coupon, the procedures followed for shot peening and determining the peening intensity saturation curve were in general accordance with SAE J443 [48]. *Fig. 32* below shows a typical intensity curve.

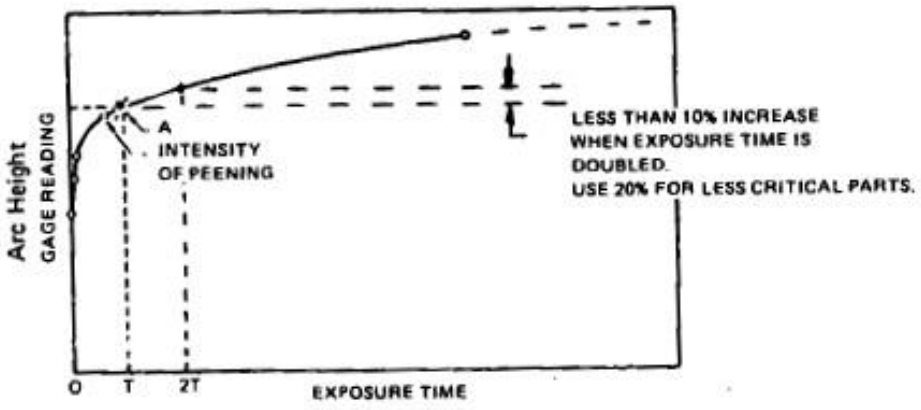

Fig. 32: Typical Intensity/Saturation Curve Determination

The peening intensity is expressed as the arc height of a shot peened test strip. By peening a series of test strips with increasing exposure time, a curve can be fit to the resulting data. Saturation is defined as the "knee" in the curve since increasingly longer periods of time are required to impose a significant increase in arc height. To determine the intensity curve for this study, almen "A" strips were mounted on an almen holder and blasted at 60 psi under a

side-to-side sweeping motion for times of 6, 12, 20, 30, and 60 seconds. This sweeping motion was implemented to ensure full coverage of the test strip due to the flow pattern generated from the blast nozzle. The difference between the flat height and peened height is the arc height, measured at the center of the strip where maximum deflection has occurred. *Fig. 33* below shows the peening intensity curve for this study.

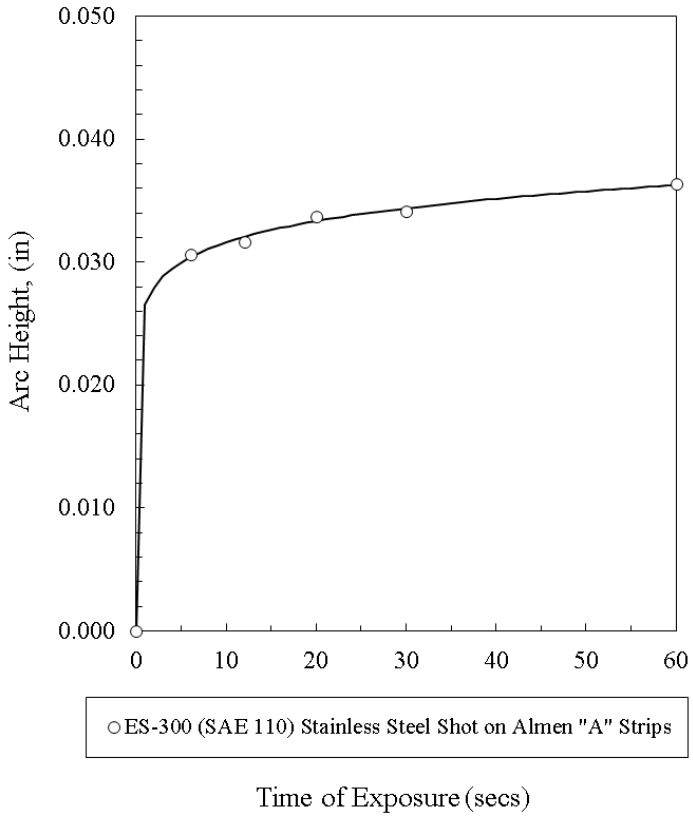

Fig. 33: Shot Peen Intensity/Saturation Curve

The FM steels, NF616 and HCM12A, were shot peened at 60 psi for 6 seconds on both sides. This time was chosen for all coupons since it was at the saturation point of the intensity curve. This time was also beneficial in the sense that it did not produce a bow in the sample after peening both sides, keeping the sample relatively flat with zero arch, which is crucial to

maximize the coupon capacity of the sample boat holder. Interestingly enough, corrosion tests to evaluate stresses in the oxide layer have been performed on arched coupons by Huntz. Table 4 below provides the shot peening parameters for this study.

Table 4: Shot Peen Parameters for Determining Intensity/Saturation Curve

Parameter	**Strip #1**	**Strip #2**	**Strip #3**	**Strip #4**	**Strip #5**
Pressure (psi)	60	60	60	60	60
Nozzle Size	¼"	¼"	¼"	¼"	¼"
Nozzle Angle	90^{o}	90^{o}	90^{o}	90^{o}	90^{o}
Nozzle Distance (in)	6.5	6.5	6.5	6.5	6.5
Holder Type	Almen	Almen	Almen	Almen	Almen
Shot Media	SAE 110	SAE 110	SAE 110	SAE 110	SAE 110
Shot Type	SS	SS	SS	SS	SS
Shot Density (g/cc)	7.0	7.0	7.0	7.0	7.0
No. of Passes	3	3	3	3	3
Peen Time (sec)	6	12	20	30	60
Flat Ht. (in)	0.05010	0.05045	0.05010	0.05040	0.05000
Peened Ht. (in)	0.08070	0.08210	0.08380	0.08455	0.08635
Arc Ht. (in)	0.03060	0.03165	0.03370	0.03415	0.03635

4. Test Materials and Sample Preparation

4.1. Tested Alloys

A test matrix of the experiments conducted and alloys tested is provided below in Table 5. Experiments 2 through 5 were spear-headed by former graduate student, Jacob Jelinek, with whom the current author was assisting in material preparation and data analysis during that time.

The alloys tested in this study represent different families of stainless steels as defined by crystallographic structure. Those families are:

- **Ferritic-Martensitic** (Fe-Cr), b.c.c
- **Austenitic** (Fe-Cr-Al), f.c.c
- **Advanced Austenitic** (Fe-Cr-Ni-Al), f.c.c
- **Superalloy** (Fe-Ni-Cr), f.c.c.
- **High Ni-based** (Ni-Cr-Co), f.c.c

Other alloys such as IN617, Haynes 182, Duplex 2205, and MA 754 were considered but set aside for potential future testing. PM2000, an oxide-dispersion strengthened (ODS) alloy, performed very well in a $SCCO_2$ environment along with several other alloys by Anderson et al [31] that are not discussed here. IN617 is receiving considerable attention for high temperature applications in next generation nuclear power plants. MA 754 (UNS N07754), an oxide dispersion strengthened superalloy, which was used for jet engine applications and made by Specialty Metals Corporation for GE many years ago, has not been made in the past 5 years or so with the equipment being mothballed [49]. Therefore, acquisition of this material for $SCCO_2$ corrosion screening has proven challenging. Initial screening by Idaho National Laboratory (INL) appears to promote the high creep resistance and corrosion resistance of MA 754 in $SCCO_2$ [9]. The mechanical pretreatment of the alloys is provided below in Table 6. Elemental compositions of alloys are provided below in Table 7.

Table 5: Test Matrix

Expt. #	Phase	Gas	Gas Purity	Temp.	Pressure	Hours	Alloys
1	I	RG-CO_2	99.9998%	450°C	8.274 MPa	400	NF616, HCM12A, 347SS, OC-6
2	I	RG-CO_2	99.9998%	450°C	20 MPa	400	NF616, HCM12A, 347SS, OC-6
3	I	RG-CO_2	99.9998%	450°C	20MPa	1000	[a] NF616, [a] HCM12A, 347SS, 800H, OC-6, OC-7, OC-10
4	I	RG-CO_2	99.9998%	550°C	20MPa	1000	[b] NF616, [b] HCM12A, 347SS, 800H, OC-6, OC-7, OC-10
5	I	RG-CO_2	99.9998%	650°C	20MPa	1000	[c] NF616, [c] HCM12A, 347SS, 800H, OC-6, OC-7, OC-10
6	II	IG-CO_2	99.85%	550°C	20MPa	1000	NF616, HCM12A, 347SS, 800H, OC-6, OC-7, OC-10
7	II	IG-CO_2	99.85%	650°C	20MPa	200	[d] 316L, 347SS, 800H, OC-6, [d] Haynes 230
8	II	BDG-CO_2	99.9%	650°C	20MPa	200	[d] 316L, 347SS, [d] IN740H, 800H, [d] Haynes 230, AFA-OC6
9	III	RG-CO_2	99.9998%	550°C	20MPa	1000	NF616 (Al, Y Coat, Peen), HCM12A (Al, Y Coat, Peen)

Note: [a] removed after 800 hours, [b] removed after 400 hours, [c] removed after 400 hours, in all cases due to excessive weight gain and/or spallation, and to prevent contaminating other samples. [d] added to study at a later time, but tested together.

Table 6: Pretreatment of Tested Alloys

Mat'l ID	UNS	Mfr./Supplier	Mfr. Heat No.	Pretreatment
NF616 (T92/P92)	K92460	Nippon Steel	N/A	[1] Normalized @ 1070°C/2hrs/AC, tempered @ 770°C/2hrs/AC
HCM12A (T122/P122)	K91271	Sumitomo Metal	N/A	[1] Normalized @ 1070°C/2hrs/AC, tempered @ 770°C/2hrs/AC
316L	S31603	N/A	N/A	N/A
347SS	S34700	Crucible Specialty Metals	A19926	[2] SA @ 1950°F, followed by WQ
IN740H	N/A	Specialty Metals Corp.	HT313OJY	[2] SA @ 2075°F, followed by WQ and aging @ 1472°F/4 hrs and AC
IN800H	N08810	Specialty Metals Corp.	HH925AG	N/A
Haynes 230	N06230	Haynes International	8-7828	[3] SA @ 2150-2275°F, followed by WQ or AC
Haynes 282	N07208	Haynes International	5-8355	[3] SA @ 2050-2100°F, followed by WQ, aging @ 1850°F/2 hrs/AC + 1450°F/8 hrs/AC
AFA-OC6	N/A	Oak Ridge National Lab	001919	[4] SA @ 1200°C, followed by WQ
AFA-OC7	N/A	Oak Ridge National Lab	001920	[4] SA @ 1200°C, followed by WQ
AFA-OC10	N/A	Oak Ridge National Lab	001923	[4] SA @ 1200°C, followed by WQ

Note: [1] Allen et al [50]. [2] Mfr. certificate. [3] Mfr. tech. brochure. [4] ORNL. **SA** = Solution Annealed, **WQ** = Water Quenched, **AC** = Air Cool.

Table 7: Elemental Composition (wt %) of Tested Alloys

	NF616 (T92)	**HCM12A** (T122)	**316L**	**347SS**	**AFA-OC6**	**AFA-OC7**	**AFA-OC10**	**IN740H**	**IN800H**	**Haynes 230**	**Haynes 282**
Fe	Bal.	Bal.	Bal.	Bal.	Bal.	Bal.	Bal.	0.1491	Bal.	3.0 **	1.5**
Cr	8.82	10.83	17.09	17.85	13.84	13.80	13.85	24.57	19.63	22.0	19.0
Ni	0.17	0.39	10.12	9.53	25.04	25.08	12.18	Bal.	33.17	Bal.	Bal.
Al	0.005	0.001	-	-	3.56	3.59	2.54	1.33	0.46	0.3	1.5
Mn	0.45	0.64	1.56	1.72	1.99	1.92	6.96	0.245	0.77	0.5	0.3**
Nb	0.06	0.05	< 0.01	0.67	2.51	2.50	1.02	1.46	-	-	0.2**
Cu	-	1.02	0.45	0.38	0.51	0.52	3.10	0.015	0.20	-	0.1**
Mo	0.46	0.30	2.01	0.35	0.18	1.98	0.15	0.35	-	2.0	8.5
Si	0.10	0.27	0.29	0.76	0.13	0.13	0.13	0.17	0.29	0.4	0.15**
C	0.11	0.11	0.03	0.06	0.114	0.112	0.114	0.023	0.06	0.10	0.06
W	1.87	1.89	-	-	0.16	0.96	0.15	0.022	-	14.0	0.5**
Ti	-	-	< 0.01	< 0.01	0.05	0.05	0.05	1.33	0.53	-	2.1
V	0.19	0.19	-	-	0.05	0.05	0.05	0.012	-	-	-
P	-	-	0.032	0.026	0.022	0.02	0.01	0.0023	-	-	-
N	-	0.06	0.050	0.049	0.001	0.001	0.0017	0.0038	-	-	-
B	-	-	-	-	0.008	0.0085	0.0086	0.0013	-	-	0.005
Zr	-	-	-	-	-	0.16	-	0.021	-	-	-
Co	-	-	0.31	0.27	-	-	-	20.09	-	5.0 **	10.0
Ta	-	-	< 0.01	< 0.01	-	-	-	0.004	-	-	-
S	-	-	< 0.001	0.02	-	-	-	0.003	-	-	-
Other	-	-	-	-	-	-	-	-	-	B, La	-
Note	3	3	2	2	3	3	3	3	3	1	1

Note: [1] Nominal Composition, [2] Chemical Analysis Testing at Anderson Labs, Inc., [3] Mfr. Certificate

4.2. Sample Geometry

Rectangular, square, disc, arc, and even rod/tube shaped samples have been tested in high temperature corrosion environments [33]. For this study, each raw material was cut to size using the electrical discharge machining (EDM) technique to yield a square geometry of 12.7 mm (1/2”), approximately 1.59 mm (1/16”) thick. Alloys 316L and Haynes 230 came in sheet form at a stock gauge thickness thinner (~1.00 mm) and slightly thicker (~2.00 mm) than the specified thickness, yielding a surface-to-volume ratio (of which the effect is not known) different from the other materials. A 3.18 mm (1/8”) Ø hole was drilled through the upper corner of each specimen to allow the samples to be suspended along a free-free cantilevered and removable alumina rod. A drawing of the coupon geometry is given in *Fig. 34*. The term coupon will be used from here forward in place of sample or specimen.

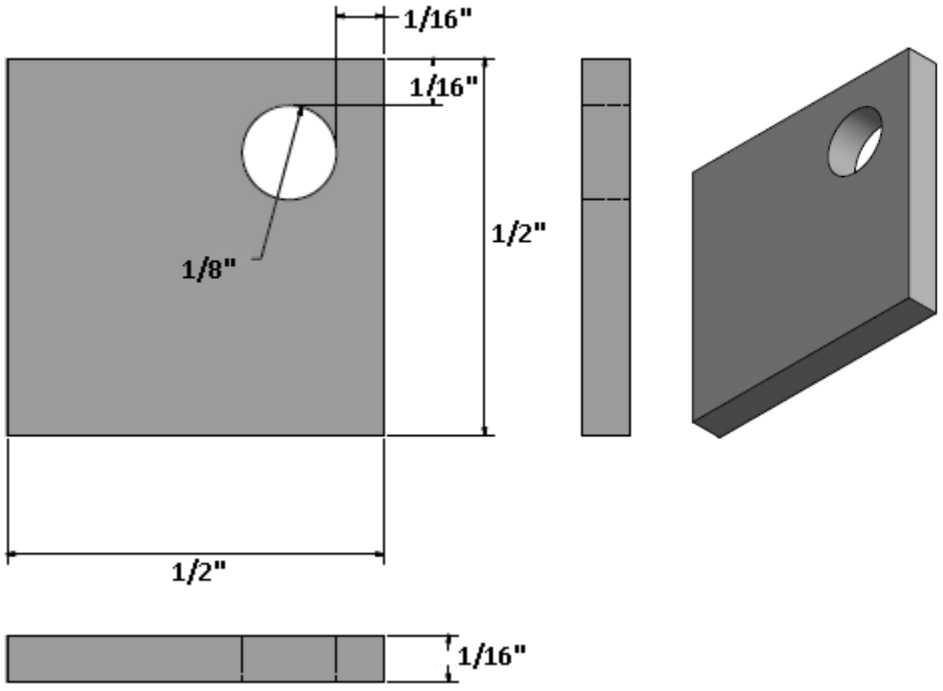

Fig. 34: Drawing for Test Coupon

4.3. Surface Finish for Thermogravimetry

Prior to corrosion testing, all surfaces of the coupons were carefully finished by hand to 800 grit, using SiC abrasive papers (*Fig. 35*). In this study, all samples were polished by the same operator

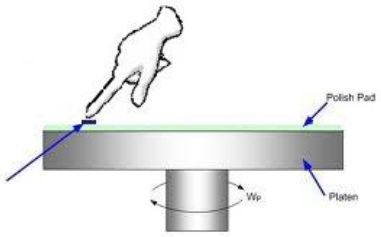

Fig. 35: Schematic of Polishing

for experiments 4 through 9. This was done to cast-out any possible variation that could occur by using more than one operator. The polishing rate was also carefully controlled. A coupon face was polished for approximately 30-45 seconds and then rotated 90 degrees for another 30-45 seconds, and so on and so on, until a full rotation was completed. This was done for both sides. The edges were polished after both faces were completed for about 60 seconds on each edge, rotating again every 90 degrees and repeating until a full rotation is completed. This process was repeated for each increment in SiC paper, which was 320 grit, 400 grit, 600 grit, and finally with 800 grit. Using this method, a polishing rate of 5 coupons (both sides) per SiC paper was found to produce consistent results. Despite the added consumption of SiC paper, the purpose of this method was to keep the dimensional variation between samples to a minimum. To minimize the possibility of preferential attack at the edges, the edges were rounded off slightly using 600 grit SiC paper. This was done since corrosion rates at corners and edges may be significantly greater than on flat surfaces [33].

The final surface finish was 800 grit on the faces and 600 grit on the edges. In experiments 4 through 9, this was done to maintain consistency in final surface finish with that chosen by the author's predecessor. After obtaining the desired surface finish, each coupon geometry was measured using a digital micrometer (± 0.001 mm) and weighed (± 2μg) to determine relevant property information for computing weight change. The term bare coupon will be used hereafter to denote the surface prior to exposure or without oxidation. Following all dimensioning, all coupons were cleaned in an ethanol solution using an ultrasonic agitator prior to testing.

4.4. Surface Finish for Treatments

The surface finish for coupons that were coated or shot peened was the same as that done for thermogravimetry testing. However, additional coupons were prepared for each treatment to have extra samples that could be characterized via SEM, EDS, XRD, surface topography (thickness), Vickers hardness, and adhesion testing by ASTM D3359 tape test. However, the nature of the films being so thin applied in this study may call for deviation from standard practices to properly measure adhesion.

5. Reaction Kinetics and Surface Morphology

5.1. Oxidation Rate Equations

The reaction kinetics of a pure metal or alloy and corresponding rate equation depend on a number of factors such as temperature, pressure, exposure time, surface finish, and

mechanical pretreatment to name a few. Such rate equations can be utilized to classify the oxidation behavior of metals, but need to be accompanied by additional information from other optical studies such as SEM/EDS, XRD, AES, etc., to elucidate the proper mechanism or mechanisms taking place. Some of the commonly observed rate equations in oxidation studies are shown below in *Fig. 36*. Not always can rate data be fitted to a single rate equation, but on occasion, oxidation reactions can be found to fit a combination of rate equations. In rare instances, an unusual S-shaped curve has even been observed in thermogravimetric oxidation studies. *Fig. 37* below gives an example of such an oxidation curve from one of these studies.

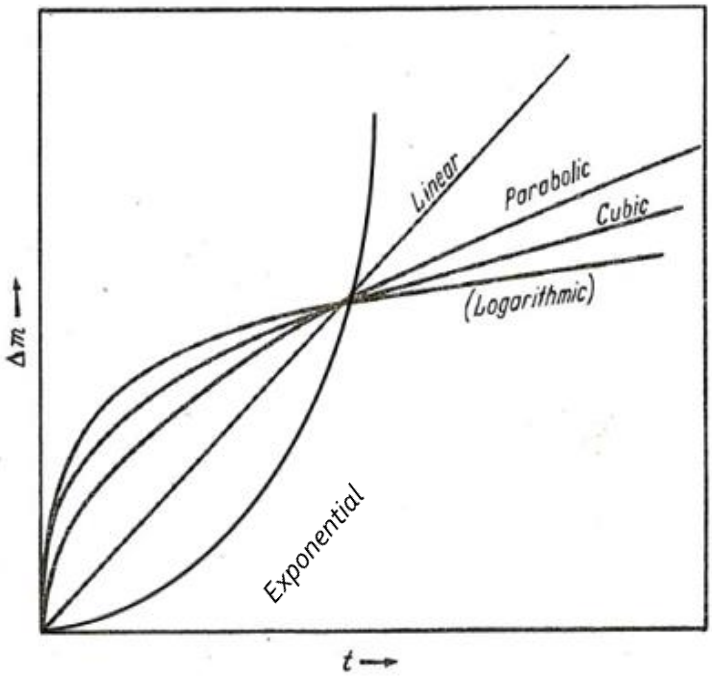

Fig. 36: Typical Oxidation Curves [4]

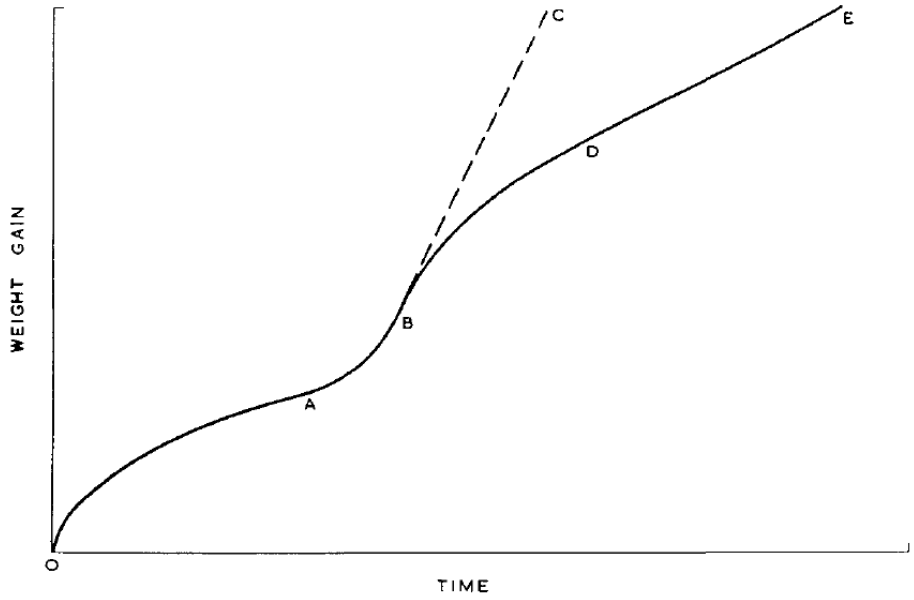

Fig. 37: Example of an S-Shaped Oxidation Curve by Cox and Johnston [51].

General oxidation curve for pure niobium in oxygen, showing the pretransition region (OA), the transition region (AB) up to the maximum oxidation rate (BC), and a period of decelerating oxidation (BD) ending in the linear post-transition rate (DE).

Focusing on oxidation in a carbonaceous environment, oxidation curves in sub-critical CO_2 at medium temperatures and low pressures for the British MAGNOX and AGR program were characterized by regions or regimes to explain the protection afforded by the oxide layer and the breakdown of its protection. *Fig. 38* below shows the oxidation curve trend associated with these regimes.

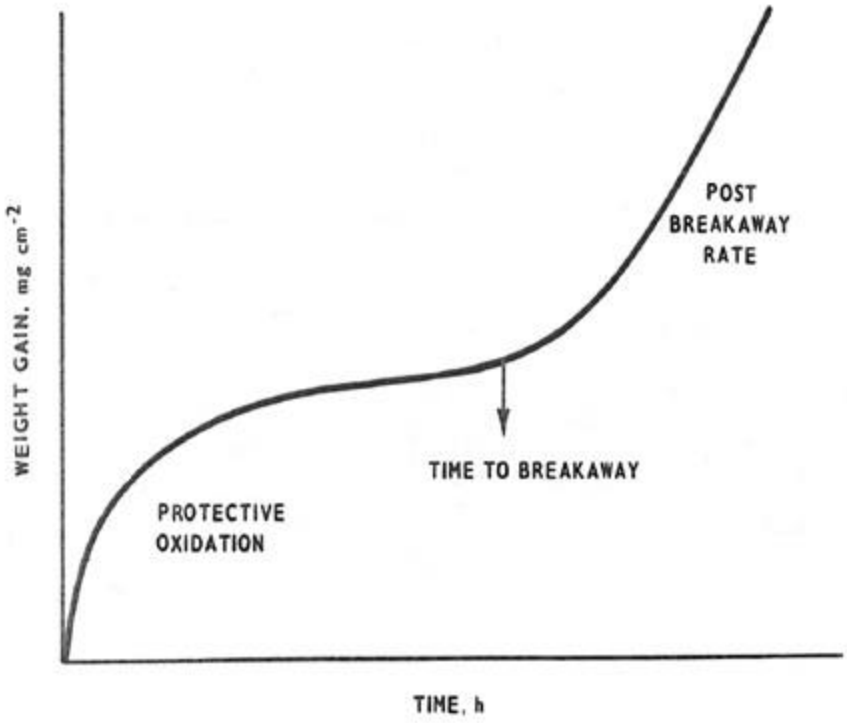

Fig. 38: Schematic Representation of Oxidation Regimes [16]

Going one step further, another explanation given in more recent years of associating oxidation mechanisms to such similar regimes was done by Kofstad. However, this was for oxidation of pure iron in CO_2 and CO_2+CO gas mixtures at high temperature and low pressure. *Fig. 39* below shows this curve.

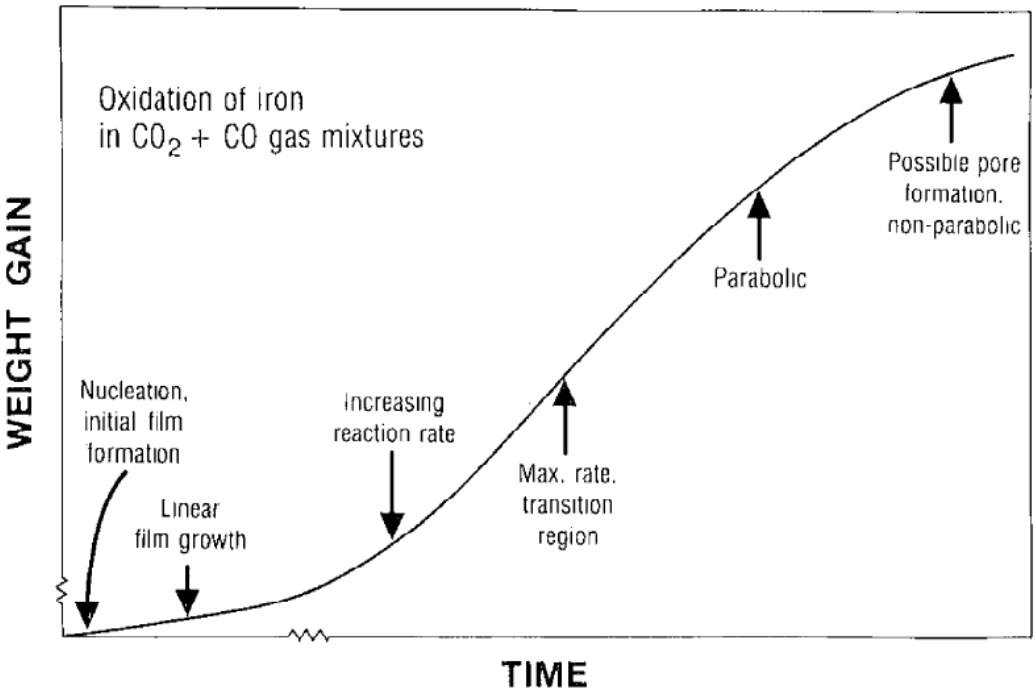

Fig. 39: Another Schematic Representation of Oxidation Regimes [52]

The many types of rate equations that can be encountered in oxidation studies are expressed below. Reference is made to books by Kofstad [35], Kubaschewski and Hopkins [4], and Grabke [33].

Linear $$\frac{d(\frac{\Delta m}{A})}{dt} = k \quad (4)$$

Parabolic $$\left(\frac{\Delta m}{A}\right)\frac{d(\frac{\Delta m}{A})}{dt} = k \quad (5)$$

Cubic $$\left(\frac{\Delta m}{A}\right)^2 \frac{d\left(\frac{\Delta m}{A}\right)}{dt} = k \quad (6)$$

Quadratic $$\left(\frac{\Delta m}{A}\right)^2 + k_1\left(\frac{\Delta m}{A}\right) = k_2 \quad (7)$$

Direct Logarithmic $$\frac{\Delta m}{A} = klog(t + t_o) + C \quad (8)$$

Inverse Logarithmic $$\frac{A}{\Delta m} = C - klog(t) \quad (9)$$

Paralinear (Kofstad) $$x = \frac{k_p}{k_l} ln\left[\frac{k_p}{k_p - k_l(x - k_l t)}\right] \quad (10)$$

Paralinear (Grabke) $$\frac{\Delta m}{A} = {k_1}^{1/2} t^{1/2} + k_2 t \quad (11)$$

Log-Parabolic $$x = k_{log}(t + t_o) + k_p t^{0.5} + C \quad (12)$$

where $\frac{\Delta m}{A}$ is the weight gain (mg/cm^2), t is the exposure time (hrs), k is the oxidation rate constant, and n is the oxidation exponent.

5.2. Effect of Pressure – Experiment 2

The effect of pressure on oxidation-corrosion in s-CO_2 was investigated not as a pre-defined objective, but out of the opportunity at the onset of the study to capture a short-term glimpse of whether or not there are such effects in s-CO_2, and to what degree. A representative alloy from each grade or type of metal matrix was selected for testing at 450°C. *Fig. 40* below shows the difference in weight gain for several alloys at both 8.274 MPa and 20 MPa.

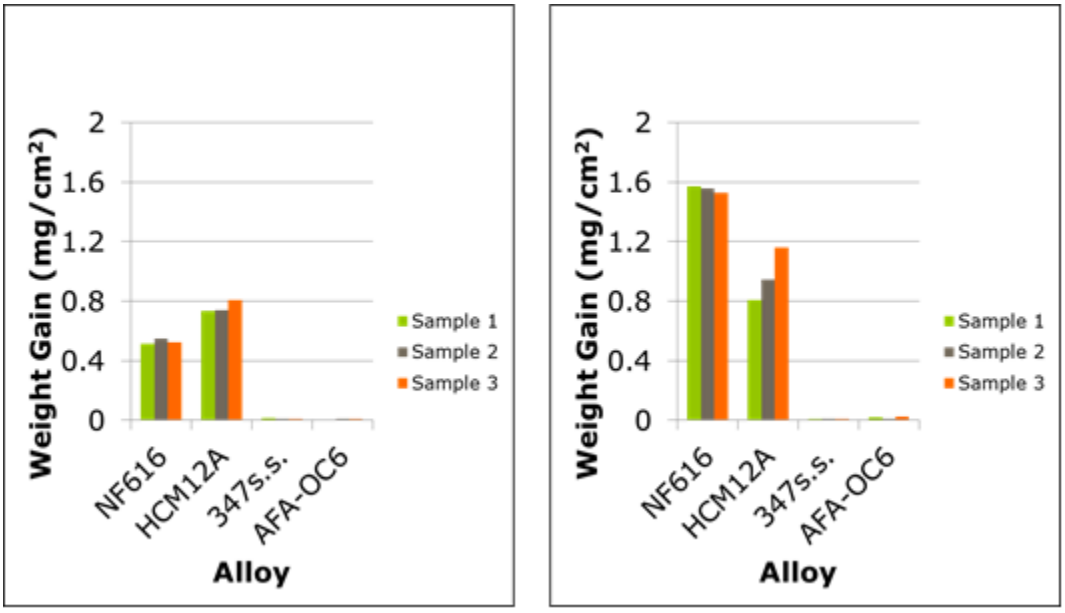

(a) (b)

Fig. 40: Weight Gains at Different Pressures after 400 hours at 450°C in RG-CO_2 (a) 8.274 MPa and (b) 20 MPa

The magnitude of the weight gain increases with increasing pressure. For the 9-12%Cr FM alloys, the rate of oxide growth from the lower to higher pressure for T92 supersedes that of the higher chromium T122. Although this seems counterintuitive since it is generally considered that added Cr improves corrosion resistance, Jelinek suggests that this is likely

due to sporadic spallation of the oxide layer formed on T122 [30]. A somewhat similar counterintuitive finding was observed by Dunlevy for 316L with increase in temperature, attributing the increase in temperature to an increase in the diffusion rate within the alloy, facilitating a faster growth of an inner healing layer, rich in chromium-oxide, which may have restricted the outward diffusion of cations and inward diffusion of anions [25]. Ballinger et al also showed that the magnitude of the weight gain increases with increasing pressure for several alloys, except for 316L which decreased [26]. Perhaps this phenomenon can be explained by the growth of stresses causing the oxide to spall. Coincidently, this phenomenon occurs again for T122 after short exposure times at 550^{o}C, when comparing its weight gain in RG-CO_2 to that in IG-CO_2. The physical nature of the oxide changes in content, color, and texture, which could be described as a thick powdery fur coat, and could easily be rubbed off. For several coupons, the alumina spacer adhered to the scale and required a slight force to separate, and resulted in detached scale on the spacer. An image of this thick fur coat can be seen in *Fig. 122*.

Alloys 347ss and AFA-OC6 showed very low weight gains with no significant difference between the two exposure pressures. SEM images of 347SS and AFA-OC6 after exposure to Experiment 1 conditions (*Fig. 41*) showed what looked like the early stages of oxide formation. Samples did not appear to display a fully developed oxide layer at either pressure. It is clear that neither the AFA-OC6 nor the 347SS material formed an oxide layer of any significant thickness, indicating superior corrosion resistance of these two alloys compared to the two ferritic alloys.

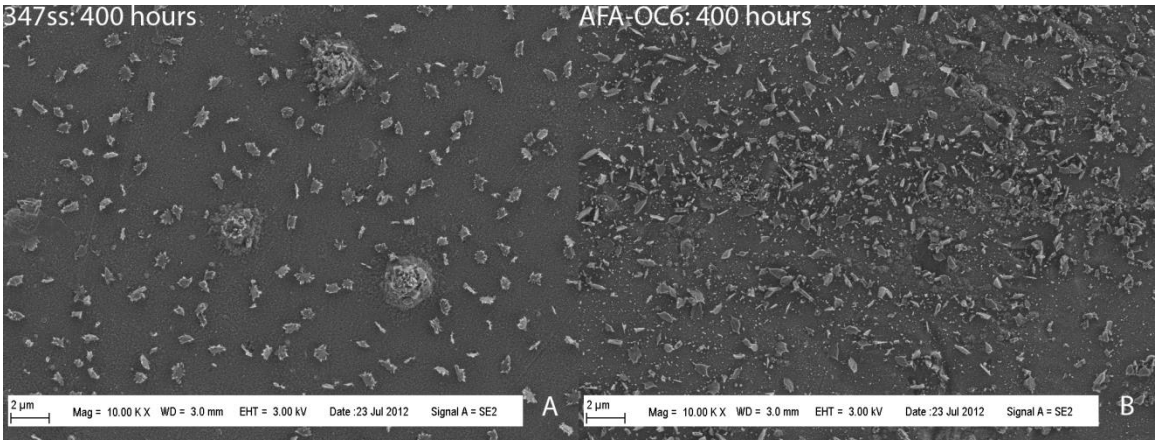

Fig. 41: Experiment 01 SEM 10000x images of (a) 347SS and (b) AFA-OC6 showing what looks like the early stages of oxide formation

Surface analysis using SEM was performed on the ferritic steel samples. *Fig. 42* and *Fig. 43* show images taken of NF616 and HCM12A respectively after exposure to each test condition. *Fig. 42a* shows larger sized grain growth when compared to *Fig. 42b*. Both images display a continuous oxide structure that formed on NF616 after exposure. *Fig. 44a* and *Fig. 44b* show how this oxide layer had further developed into a thick and uniform and adherent structure. *Fig. 43* shows similar results for the HCM12A material as compared to NF616 under the same conditions. *Fig. 44d* however shows disparate areas of oxidation indicative of material loss or at least breakdown of the oxide layer.

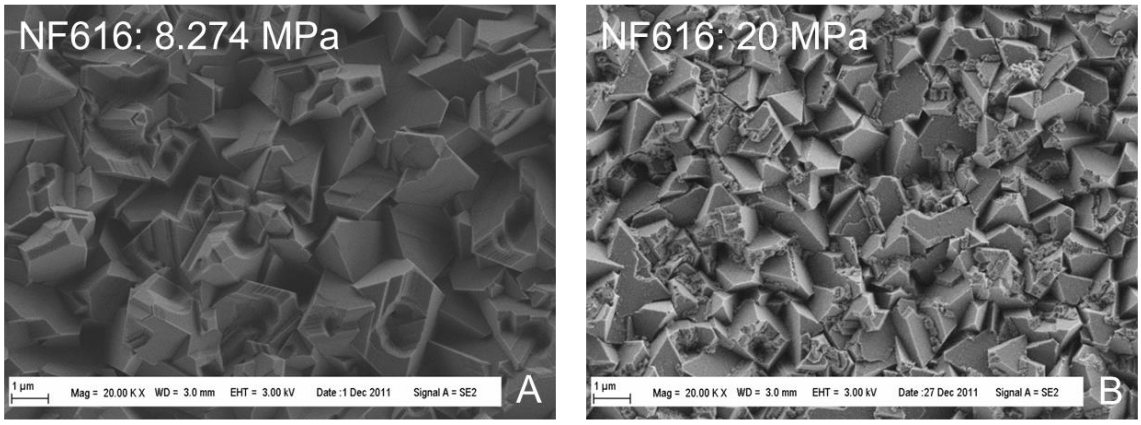

Fig. 42: SEM micrographs of NF616 exposed to 450°C for 400 hours at (a) 8.274 MPa and (b) 20 MPa

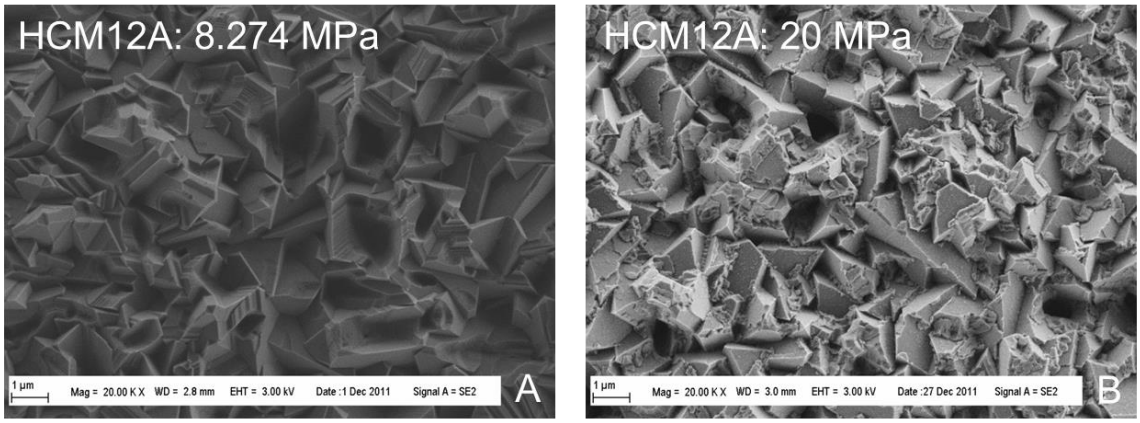

Fig. 43: SEM micrographs of HCM12A exposed to 450°C for 400 hours at (a) 8.274 MPa and (b) 20 MPa

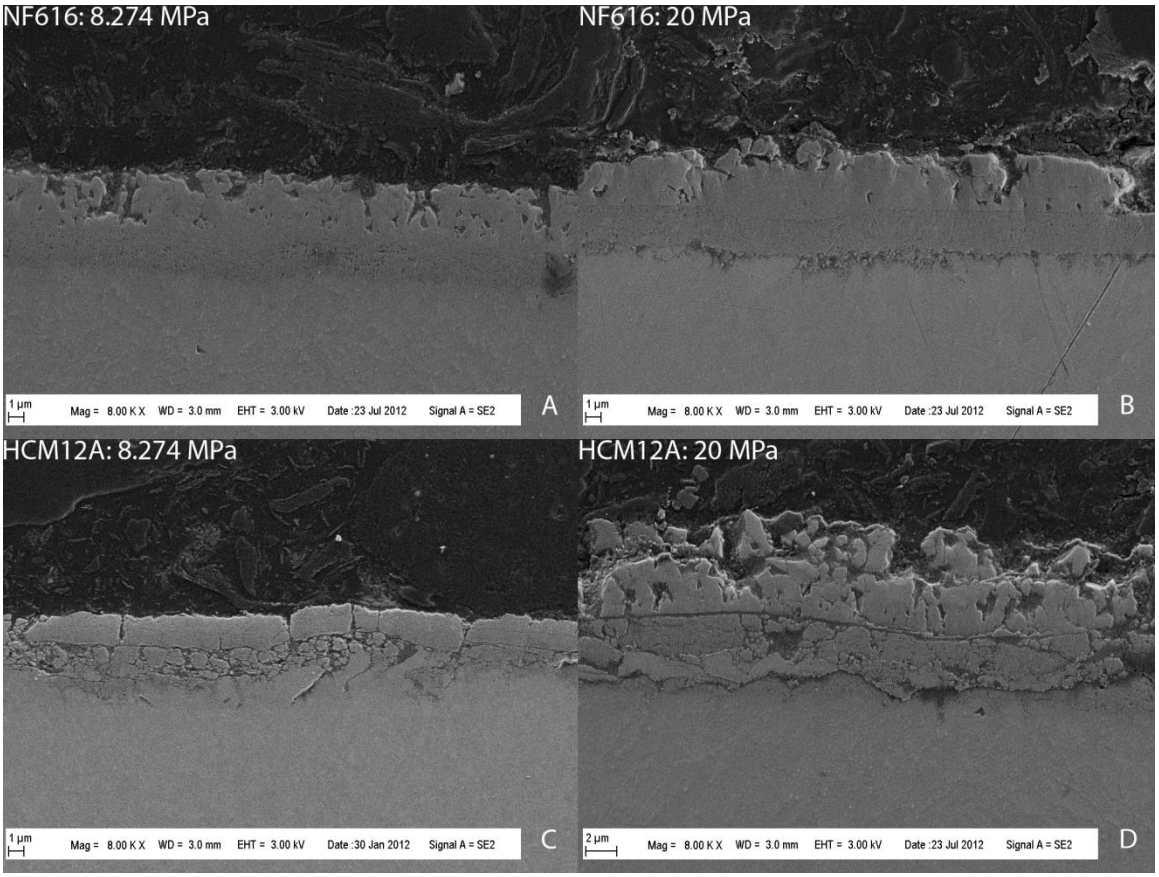

Fig. 44: SEM cross section 8000x micrographs of (a) NF616 after Experiment 1 exposure, (b) NF616 after Experiment 02 exposure, (c) HCM12A after Experiment 01 exposure, and (d) HCM12A after Experiment 2 exposure

The main conclusion drawn from the pressure study was that the higher pressure environment produced increased oxidation to the ferritic materials. Considering the extent of oxide formation after only 400 hours, ferritic material was anticipated to perform poorly for longer exposures and increased temperatures. For higher corrosion resistant materials such as 347ss and AFA-OC6, there was no observed change in performance. However, the possibility of increased corrosion with pressure could not be precluded without further testing. Given that very little oxidation was observed on the 347SS and AFA-OC6 samples

exposed to 20MPa, it was decided that a longer testing duration could be necessary to observe meaningful results.

5.3. Effect of Temperature – Experiments 3 through 5

The results of the measured weight gains for the alloys tested at 450^{o}C (Expt. 3), 550^{o}C (Expt. 4), and 650^{o}C (Expt. 5) are shown below in *Fig. 45* through *Fig. 53*. For ease of comparison, an appropriate magnitude for the weight gain and scale size for the plot in each of the figures was held fixed where possible, mindful of future overlay of results chosen by the reader if desired. A Matlab code was written to accommodate the commonly encountered, singularly described rate equations in Sec. 5.1 denoted as equations (4-9) using discrete weight gain values as input data to generate the oxidation curves, which are displayed in all the weight gain figures that follow. Oxidation curves fitted to the measured data points describing the reaction kinetics are also shown.

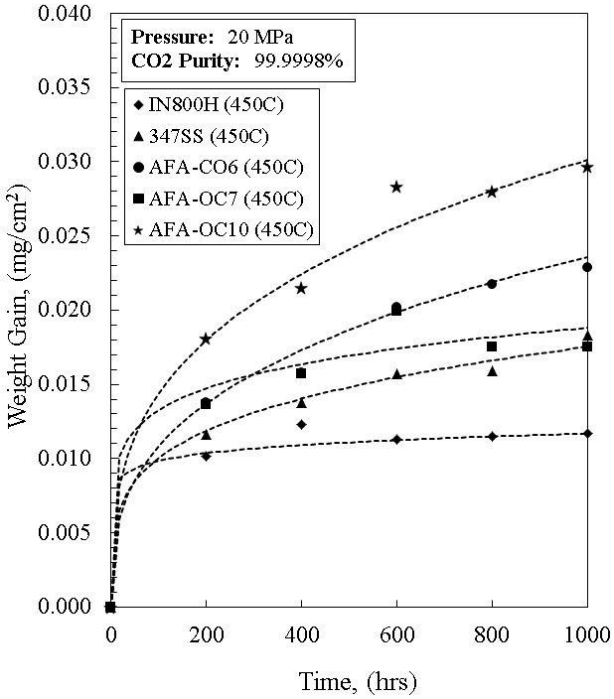

Fig. 45: Weight Gain Curves of Tested Alloys at 450°C, 20MPa.

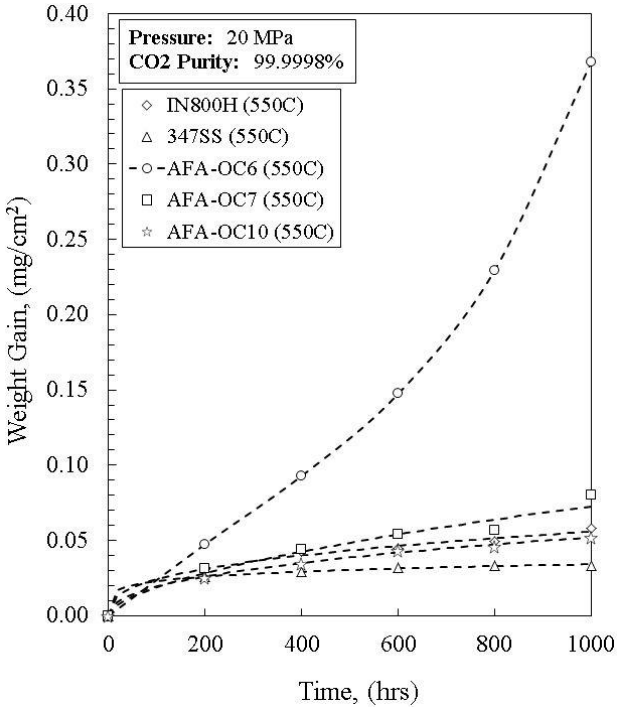

Fig. 46: Weight Gain Curves of Tested Alloys at 550°C, 20MPa.

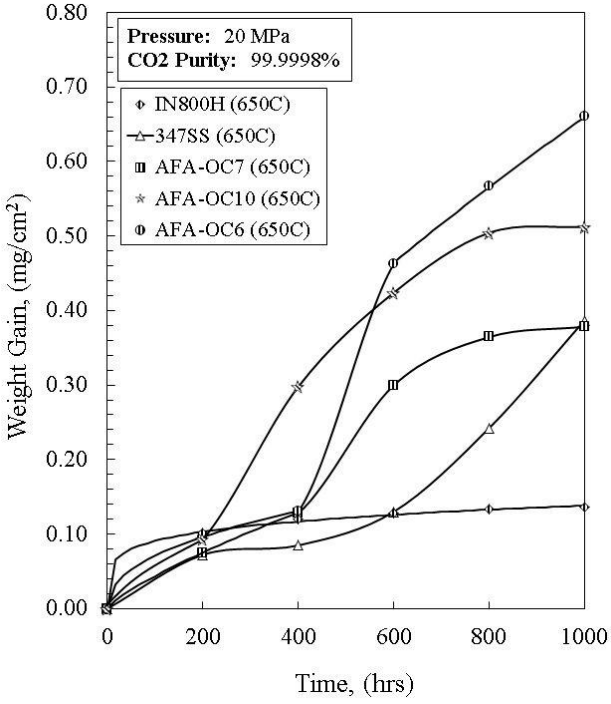

Fig. 47: Weight Gain Curves of Tested Alloys at 650°C.

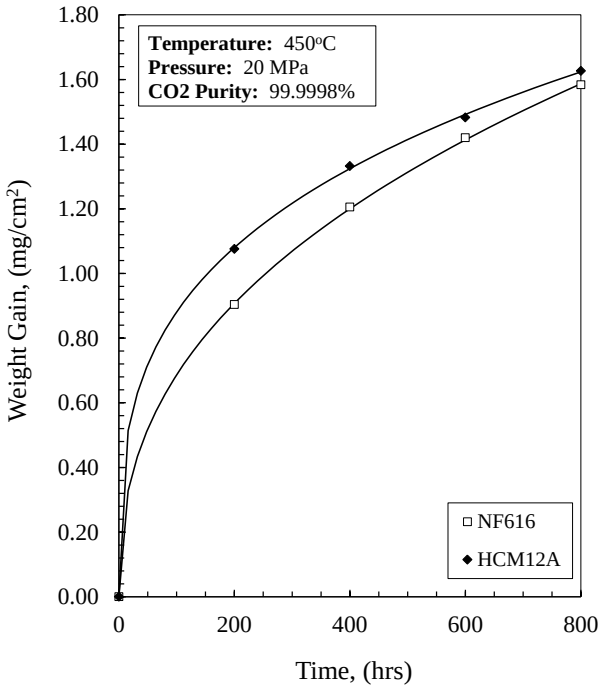

Fig. 48: Weight Gain Curves of 9-12%Cr Ferritic-Martensitics at 450°C.

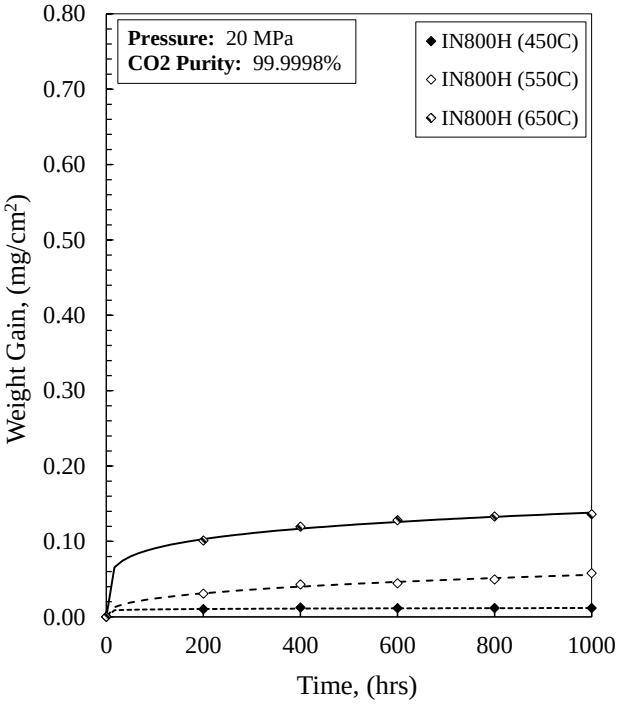

Fig. 49: Weight Gain Curves of IN800H at 450°C, 550°C, and 650°C.

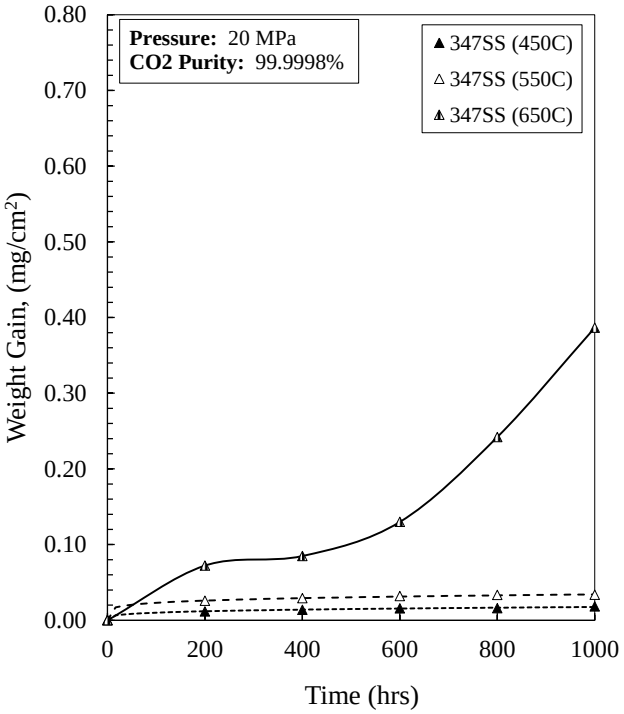

Fig. 50: Weight Gain Curves of 347SS at 450°C, 550°C, and 650°C.

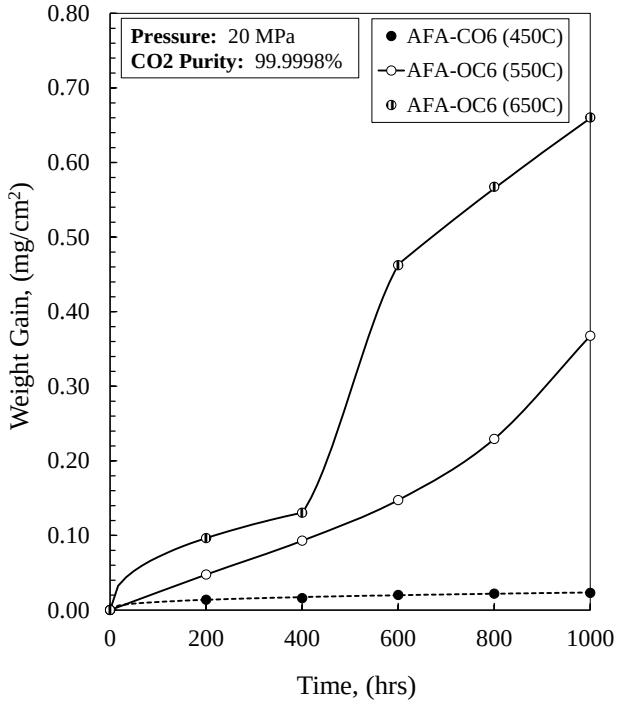

Fig. 51: Weight Gain Curves of AFA-OC6 at 450°C, 550°C, and 650°C.

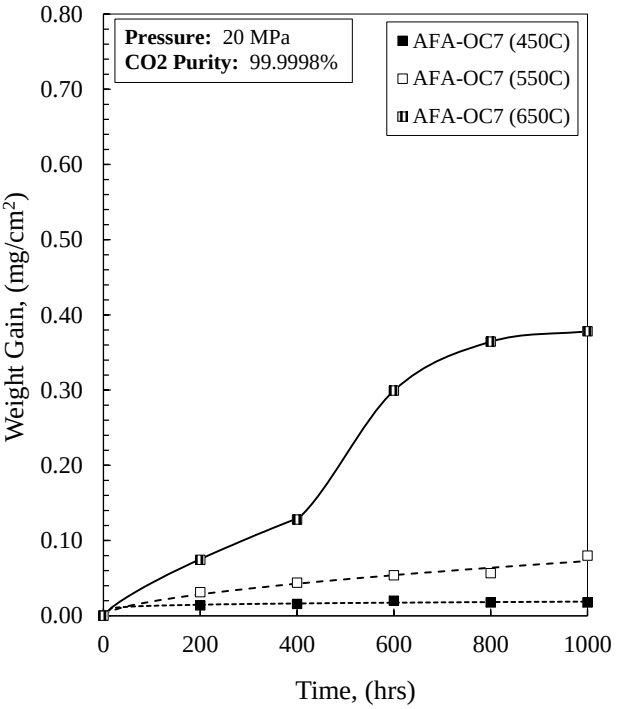

Fig. 52: Weight Gain Curves of AFA-OC7 at 450°C, 550°C, and 650°C.

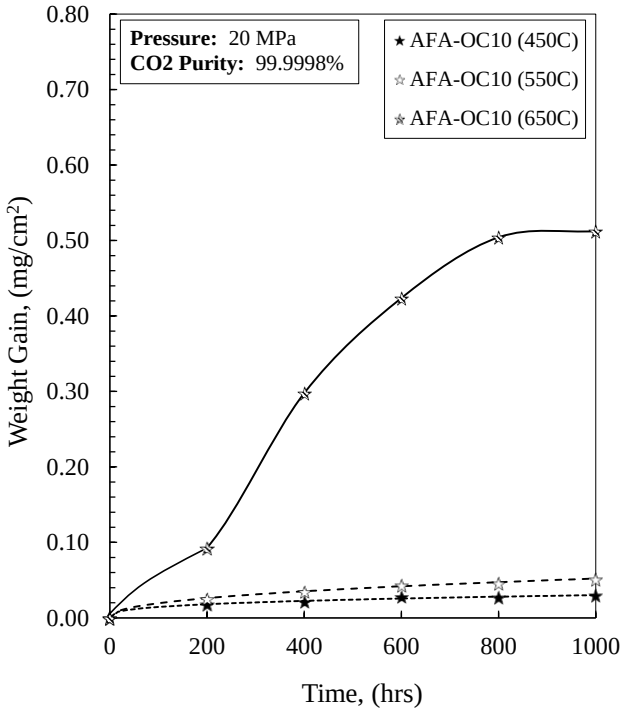

Fig. 53: Weight Gain Curves of AFA-OC10 at 450°C, 550°C, and 650°C.

Supplementing the weight gain data and kinetics evaluation, surface analysis was performed on the alloys. *Fig. 54* shows an SEM image of NF616 after 800 hours of exposure to SC-CO_2 at 450°C and 20 MPa. Similar to the image taken at 400 hours in Experiment 2 (*Fig. 44*b), the oxide was fully developed and covered the entirety of the sample. This image also displayed pit like areas where sample oxide material has likely been lost. This material loss is more consistent with dusting than spallation, as the areas tend to be small and pit-like rather than large and plate-like, and SC-CO_2 is a strongly carburizing environment [53]. The same phenomenon was observed for HCM12A, but covering more surface area per sample (Fig. *55*), indicating greater material loss and less corrosion resistance than NF616. While this may seem counterintuitive, as HCM12A contains more Cr than NF616, similar results have been observed in steam. Below approximately 600°C in steam, studies have concluded that

NF616, HCM12A, and other ferritic material in the range of 2 – 11 wt% Cr display corrosion behavior independent of Cr content [54, 55, 56].

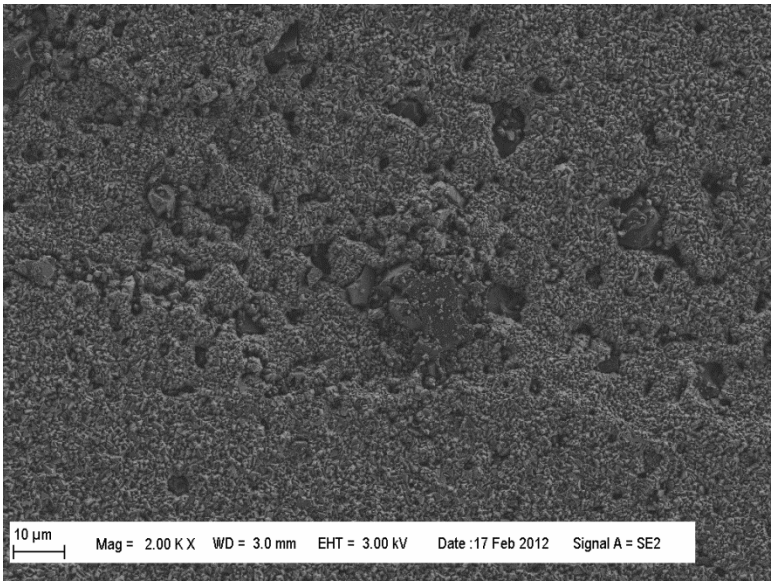

Fig. 54: SEM image of NF616 after exposure to 450°C and 20 MPa for 800 hours

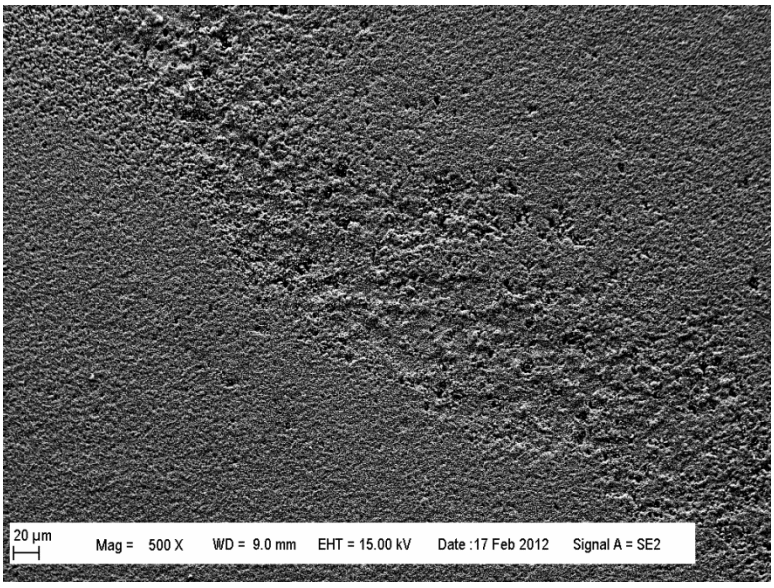

Fig. 55: SEM image of NF616 after exposure to 450°C and 20 MPa for 800 hours

In addition to the observation of material loss, both NF616 and HCM12A displayed areas thought to be carbon deposits (*Fig. 56*); also consistent with metal dusting. These areas tended to increase in frequency and magnitude with longer exposure. However, at the time of this writing there is no apparent explanation for the position of the deposits. Occurrence was not uniform over the surface, and location was apparently random, with some patches occurring near the edges, while others were found near the center of the sample. The composition was qualitatively confirmed as carbon using EDS mapping. Further analysis is necessary to provide quantitative results.

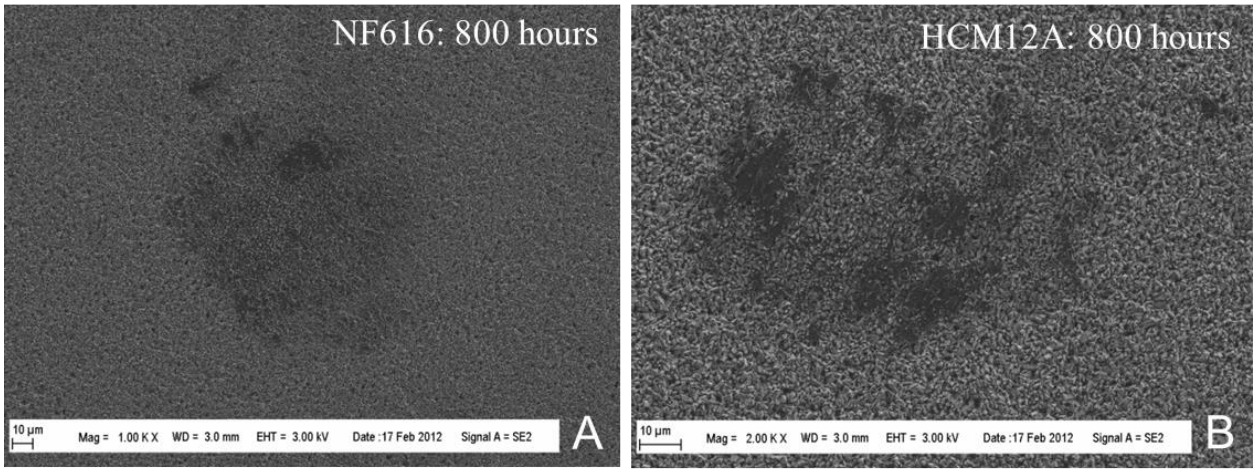

Fig. 56: Experiment 3 SEM images of (A) NF616, and (B) HCM12A displaying possible carbon deposits

To gain better insight into the development of the oxide through the oxide layer, cross sectional analysis was performed using an ion milling technique. FIB (Focused Ion Beam) was used to mill, or remove a microscopic area of the sample surface, penetrating through the thickness of the oxide. This technique is relatively non-destructive because it does not

necessitate sample mounting (resin, phenolic, etc.), or the deposit of films (for conductivity or preservation of the surface). This technique therefore allows specific accurate selection of positions of interest on the sample surface to perform analysis.

Fig. 57 and *Fig. 58* show SEM images of FIB milled cross sections. EDS line scans were made through the thickness of the oxide layer to determine the general composition. Both oxides display a fairly dense, thick oxide, which can visibly be seen to consist of two distinct layers. EDS lines scans confirm that there are indeed two distinct layers, consisting of an outer iron oxide layer (magnetite), and inner Cr-spinel layer.

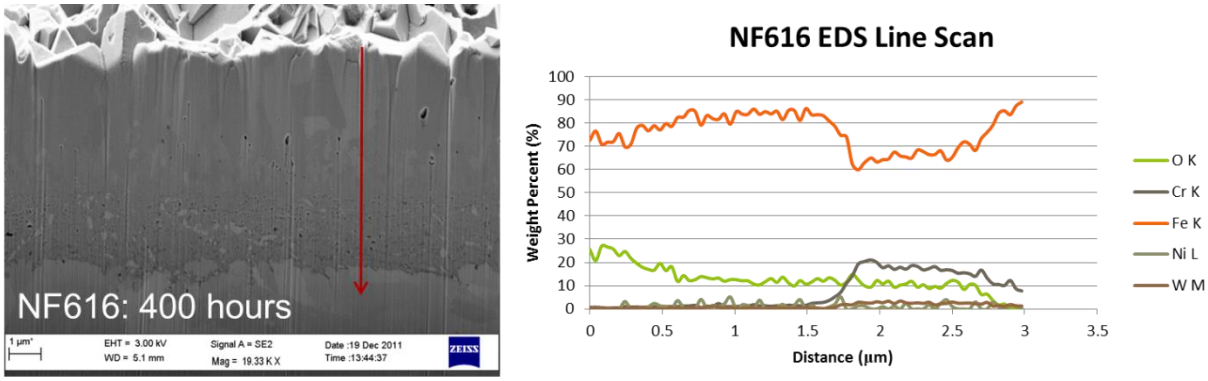

Fig. 57: NF616 SEM image of a FIB milled cross section and corresponding EDS line scan through the oxide layer with the scan position and direction indicated by the arrow

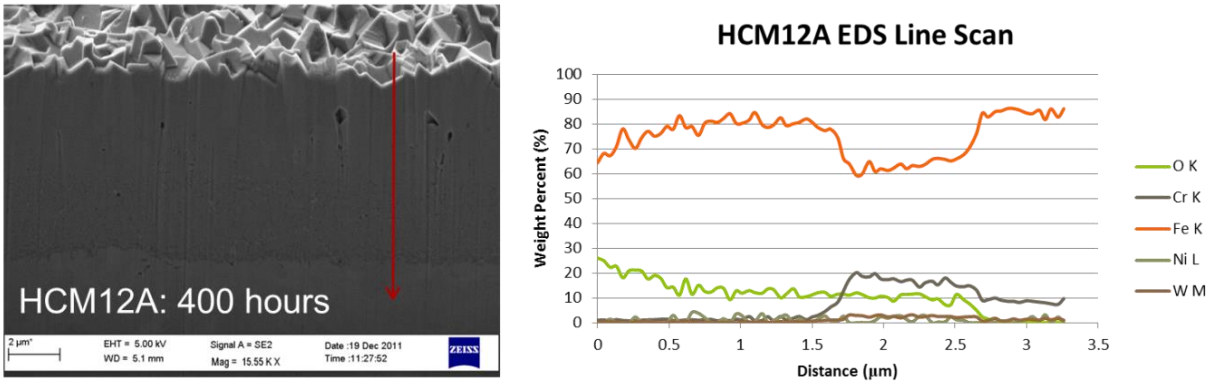

Fig. 58: HCM12A SEM image of a FIB milled cross section and corresponding EDS line scan through the oxide layer with the scan position and direction indicated by the arrow

SEM observation of the other test matrix alloys (IN 800H, 347ss, and AFAs) indicated overall excellent performance. Oxide layers were observed to be uniform, fine grained, and fully adherent. *Fig. 59* shows both 347ss and IN 800H after 600 and 1200 hours of exposure. As can be seen, the oxide remained very consistent through the duration of the test. EDS analysis performed on 347ss indicated that the nodules of larger oxide growth (oxide islands) tended to show signs of increased carbon (*Fig. 60*). EDS point analysis further indicated oxide islands on 347ss tended to be high in niobium (*Fig. 61*). This was expected, as niobium is added to the 347ss composition to prevent sensitization, and will readily form carbides before chromium. It is hypothesized that carbide formation (e.g. niobium/titanium carbide) on the surface of the sample prevented complete oxide coverage, creating a pathway for either matrix metal or oxygen to diffuse, circumventing the developed protective layer [57]. This then becomes a nucleation point for further oxidation.

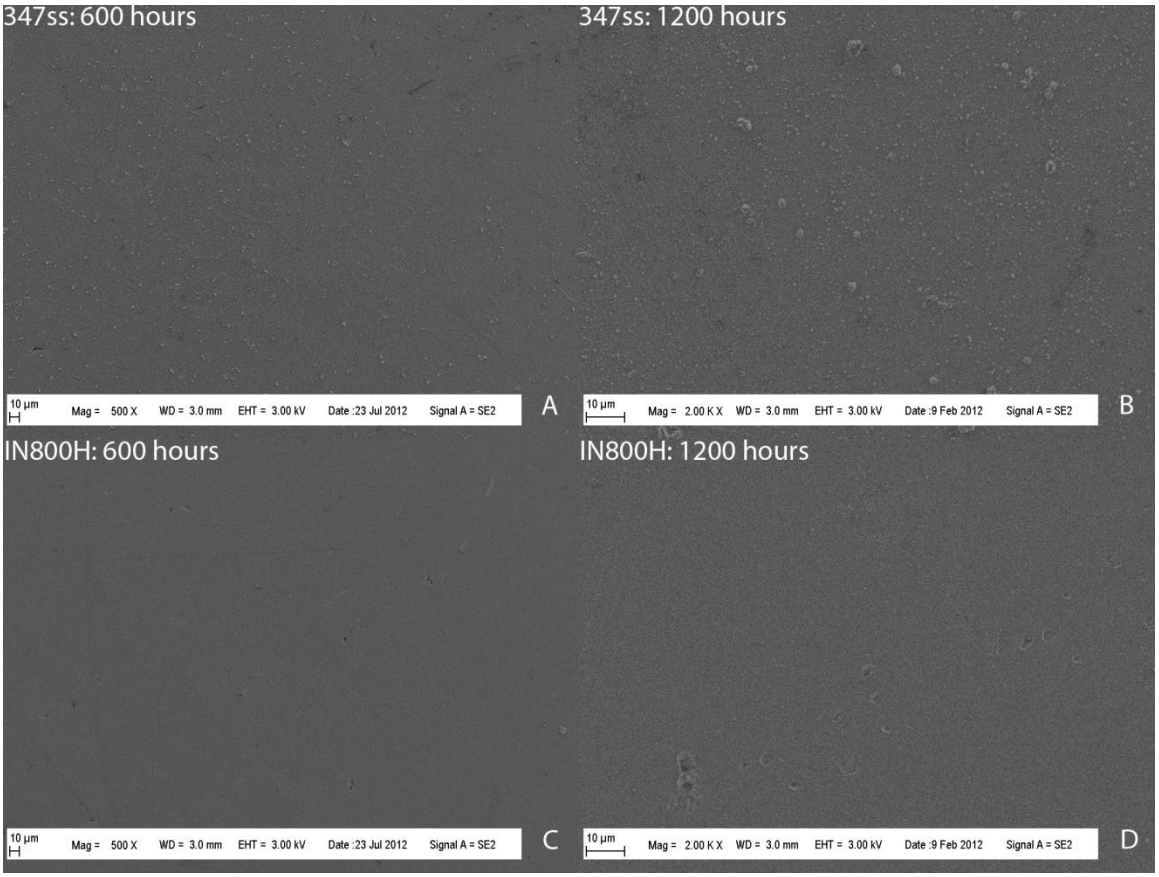

Fig. 59: Experiment 3 500x SEM images showing (A) 347SS after 600 hours, (B) 347SS after 1200 hours, (C) IN 800H after 600 hours, and (D) IN 800H after 1200 hours

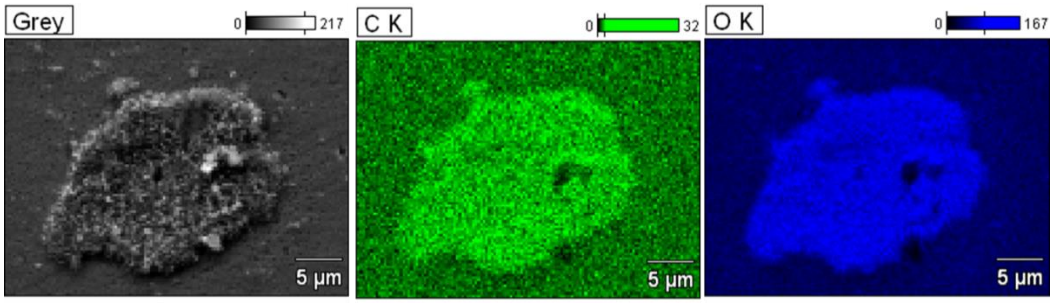

Fig. 60: EDS maps of 347SS indicating a correlation between increased oxide growth and increased carbon

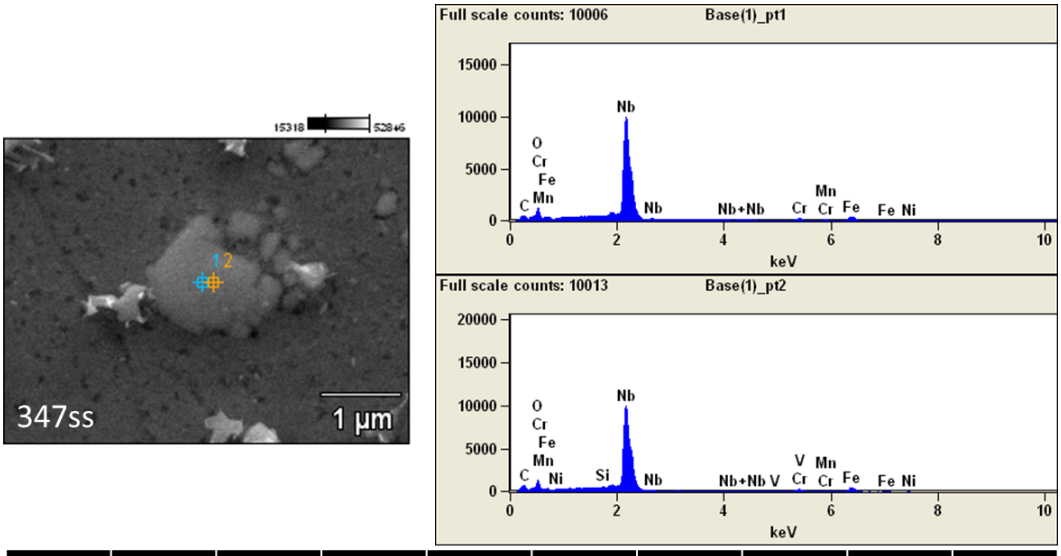

Wt%	C	O	Si	V	Cr	Mn	Fe	Ni	Nb
Pt 1	5.0	11.1			2.9	1.3	7.7	0.7	71.4
Pt 2	6.9	10.7	0.3	0.3	3.3	1.3	8.8	1.2	67.3

Fig. 61: EDS point analysis of an oxide island on 347SS indicating observed peaks and compositional analysis in weight percent

The AFA material tended to show signs of complex oxide growth in islands uniformly distributed across the surface of the sample. *Fig. 62* typifies all three AFA compositions after 600 and 1200 hours displaying relative oxide development. Considering the oxide formations on the AFA material and similarity to oxides observed on 347SS, it was likely that the AFA oxide islands formed at locations containing precipitates of niobium, titanium, and/or manganese depending upon the specific AFA composition. *Fig. 63* shows EDS mapping of AFA-OC7 which illustrated a strong correlation between niobium and the oxide structures. The EDS observations made on AFA-OC6 were essentially the same as AFA-OC7, which was not surprising considering the major differences between the two materials are AFA-OC7 has 1.8 wt% more Mo, and 0.8 wt% more W. The EDS maps also indicated higher

concentrations of carbon in each of the oxide islands, supporting the notion that niobium carbides formed at these locations. *Fig. 64* depicts EDS maps for AFA-OC10 indicating that increased oxidation tended to occur with manganese. This was consistent with general findings indicating that increasing manganese content decreases the oxidation resistance of Fe-Mn-Al alloys [58]. AFA-OC10 contained nearly 7 wt% Mn as an austenite stabilizer, supplementing a reduction in Ni.

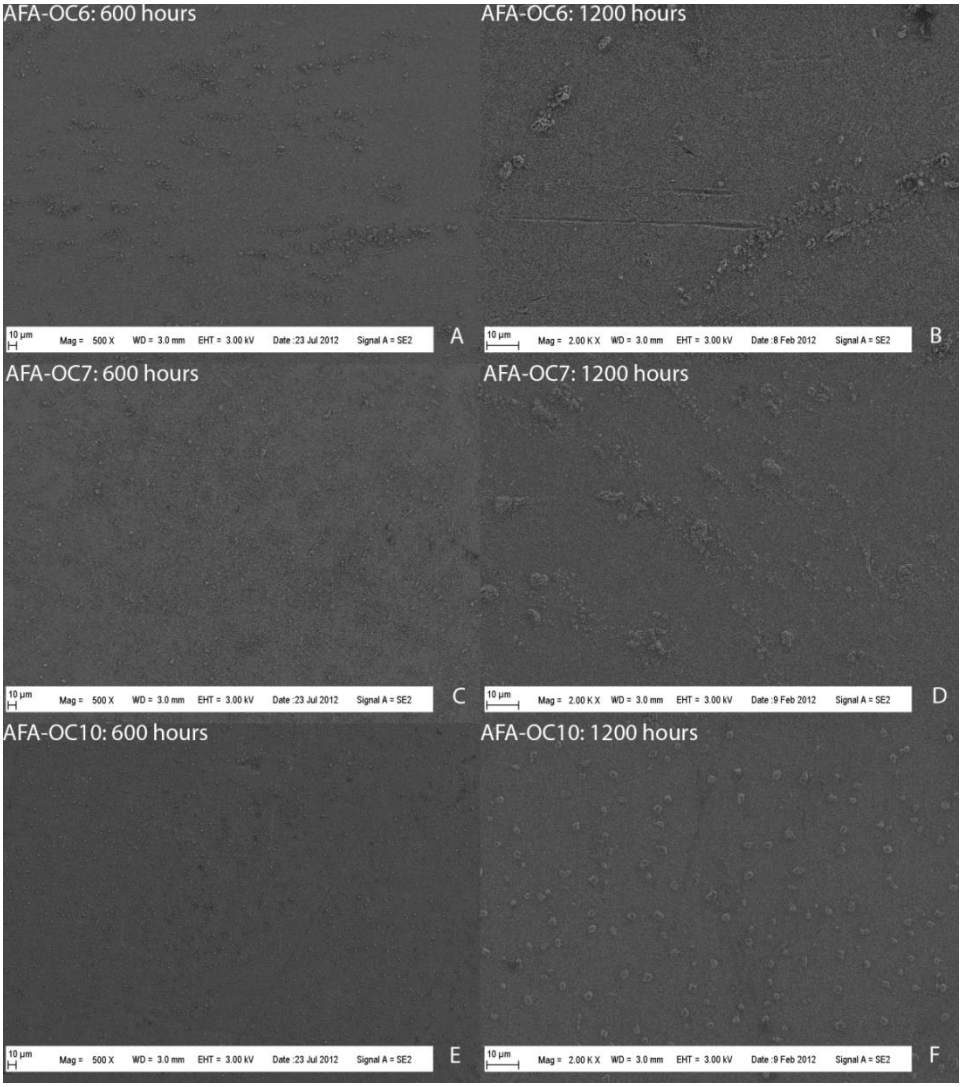

Fig. 62: Experiment 3 500x SEM images showing (A) AFA-OC6 after 600 hours, (B) AFA-OC6 after 1200 hours, (C) AFA-OC7 after 600 hours, (D) AFA-OC7 after 1200 hours, (E) AFA-OC10 after 600 hours, and (F) AFA-OC10 after 1200 hours

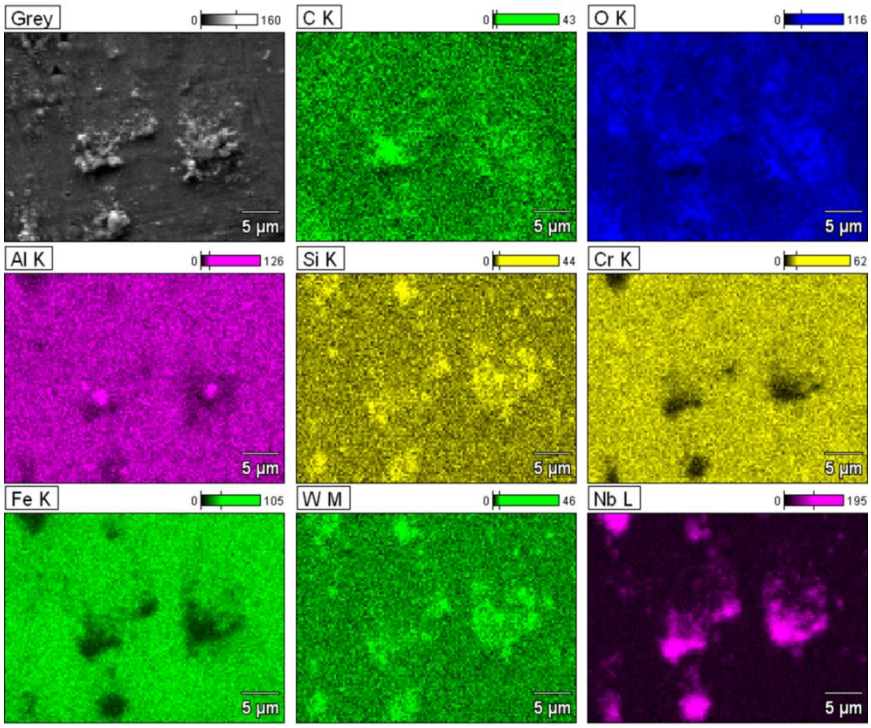

Fig. 63: EDS maps taken of AFA-OC7 indicating correlation between strong carbide formers (e.g. Nb) and islands of increased oxidation

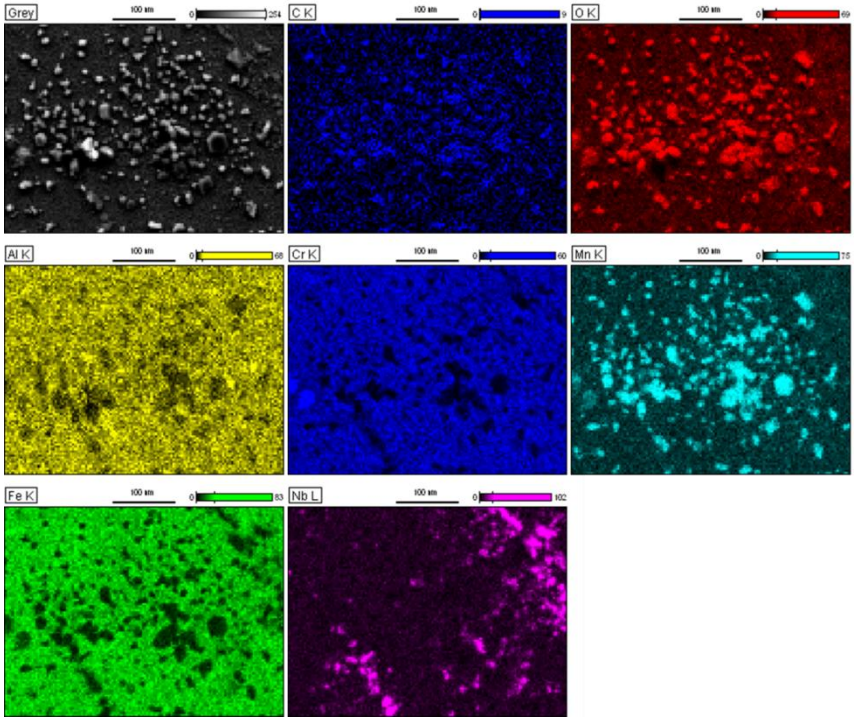

Fig. 64: EDS maps taken of AFA-OC10 after exposure to Experiment 3 conditions indicating islands of increased oxidation are mainly Mn

Further surface analysis was performed using optical microscopy. The broader scope granted by lower magnification provided a more complete understanding of the oxide development across the full surface of a sample. Illustrated in *Fig. 65*, the surface of 347SS after 1000 hours of exposure to SC-CO_2 at 450°C and 20 MPa displayed a largely continuous oxide layer (blue) interrupted by one large oxide island (yellow/gold). The thin nature of the protective oxide can further be inferred by the visibility of the polishing marks crosshatching the sample. When compared to images taken of the polished and etched sample (*Fig. 66*), it can be seen that the black spots on the exposed sample (B) correspond to carbides (black spots) on the etched sample (A), which were qualitatively confirmed using EDS.

Indication of a thin protective oxide via clearly visible polishing marks is also true of observations of IN 800H after 1000 hours exposure at the conditions of Experiment 3 (*Fig. 67a*). What is even more interesting to note, was clear indication of preferential oxidation of the grain boundaries, most likely due to sensitization. *Fig. 67* also shows the polished and etched surface of IN 800H (B) for comparison, displaying both titanium carbides and titanium nitrides (confirmed using EDS). Observation of the AFA materials using the optical microscope found increased levels of oxidation as was expected given the weight gain data and observations made using the SEM. Like the weight gain ranking, AFA-OC10 showed the most oxidation, AFA-OC6 the second most, and AFA-OC7 showed the least oxide development of the three AFA materials (*Fig. 68*).

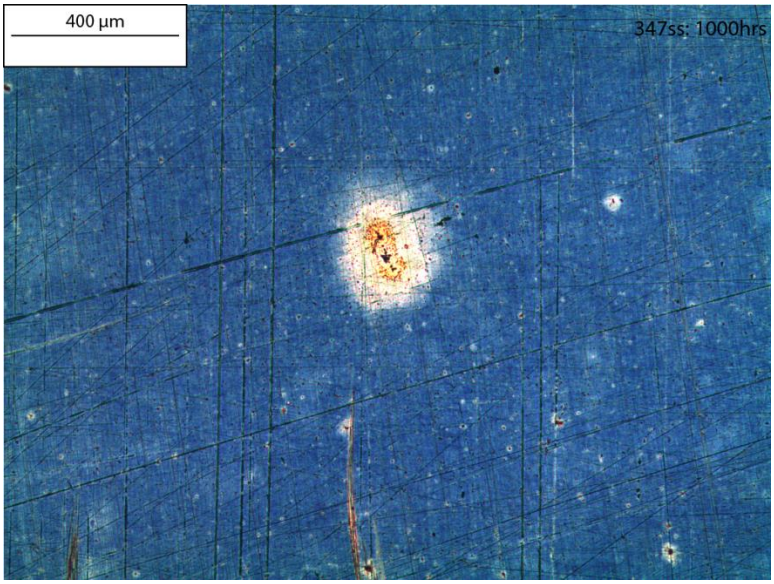

Fig. 65: Image of 347SS after 1000 hours exposure to SC-CO_2 at 450°C and 20 MPa

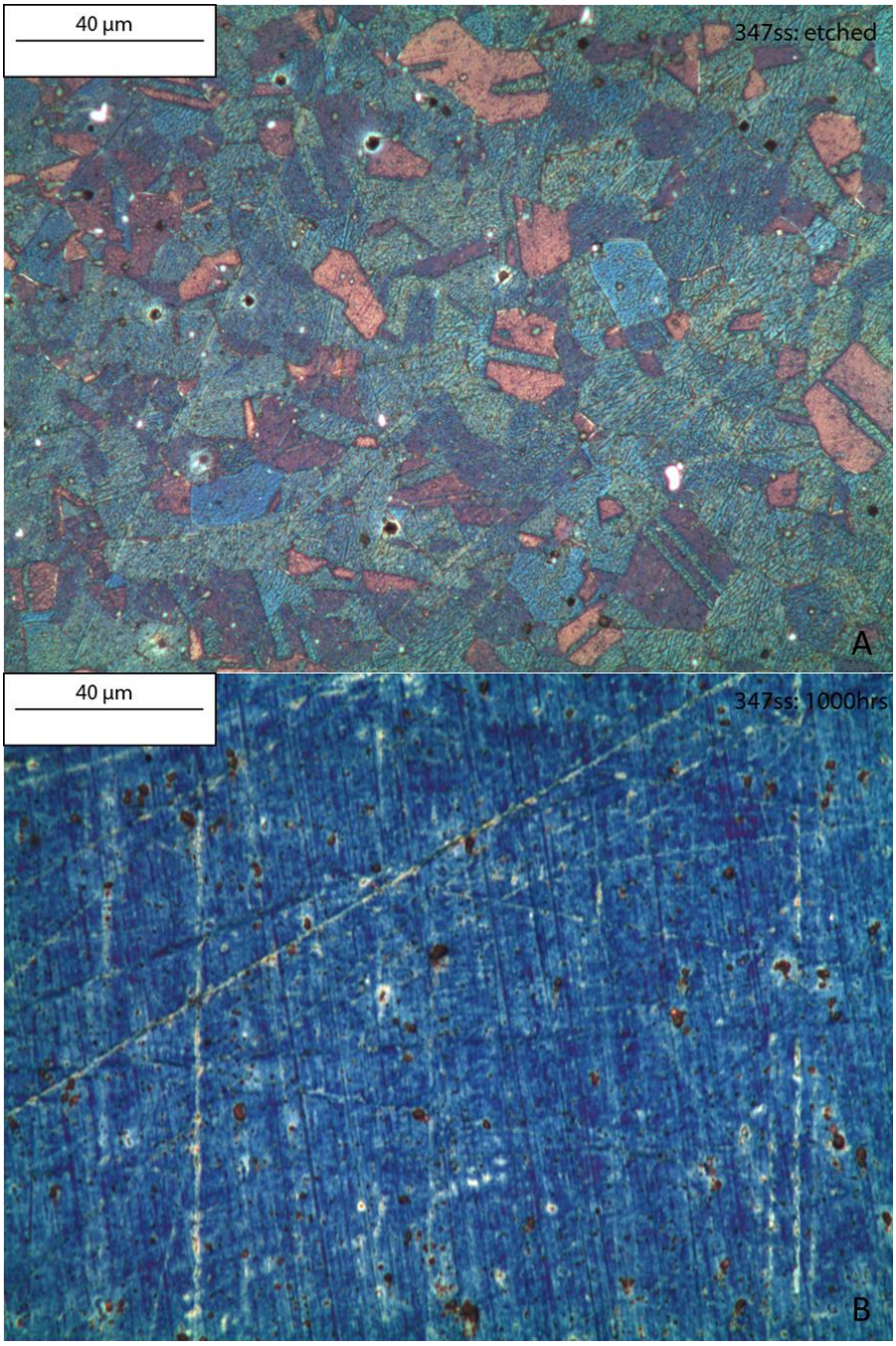

Fig. 66: Optical microscope images of 347ss with (A) etched using Beraha's Reagent, and (B) exposed to Experiment 3 test conditions for 1000 hours

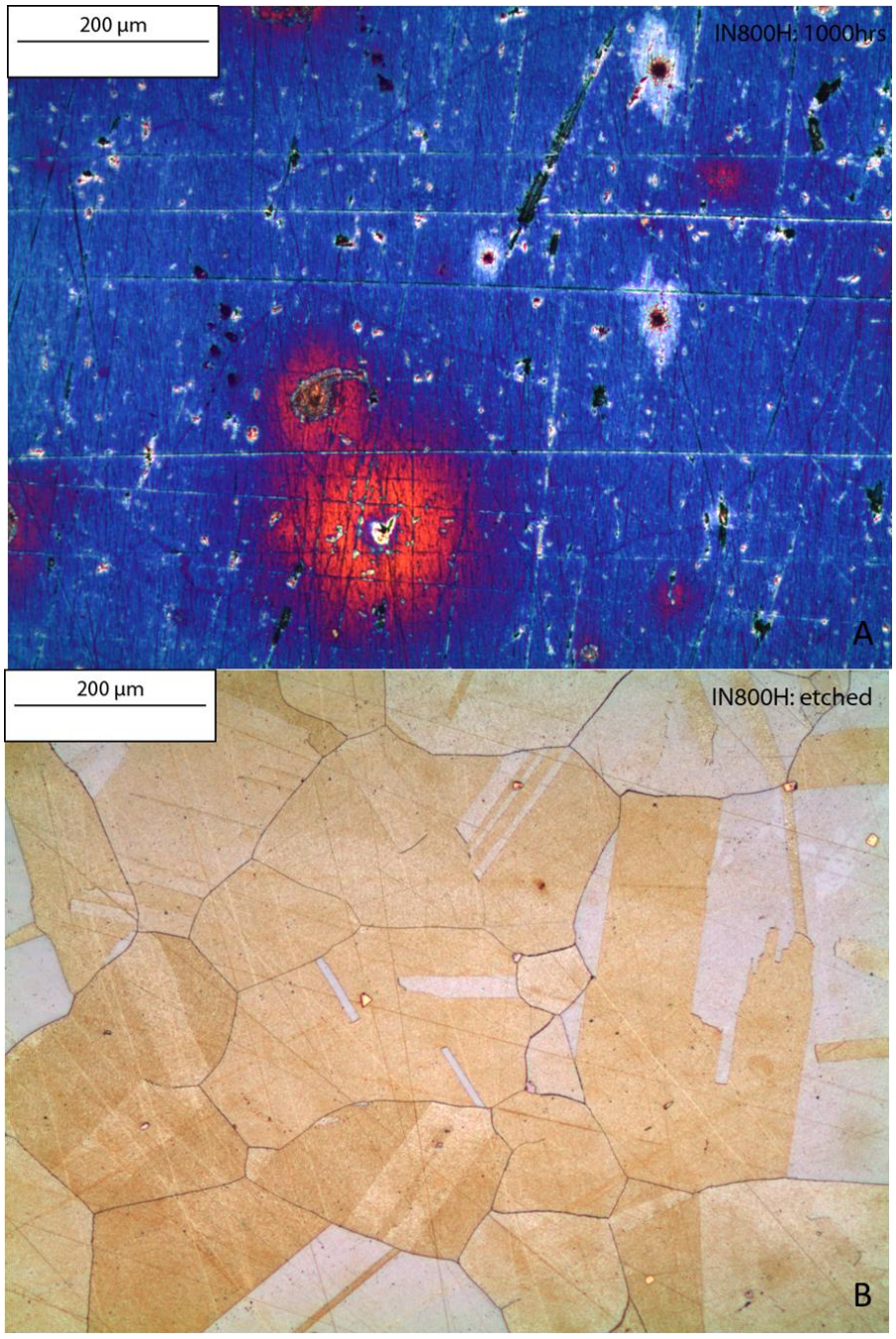

Fig. 67: Optical microscope images of IN 800H with (A) exposed to Experiment 3 test conditions for 1000 hours, and (B) etched using Beraha's Reagent

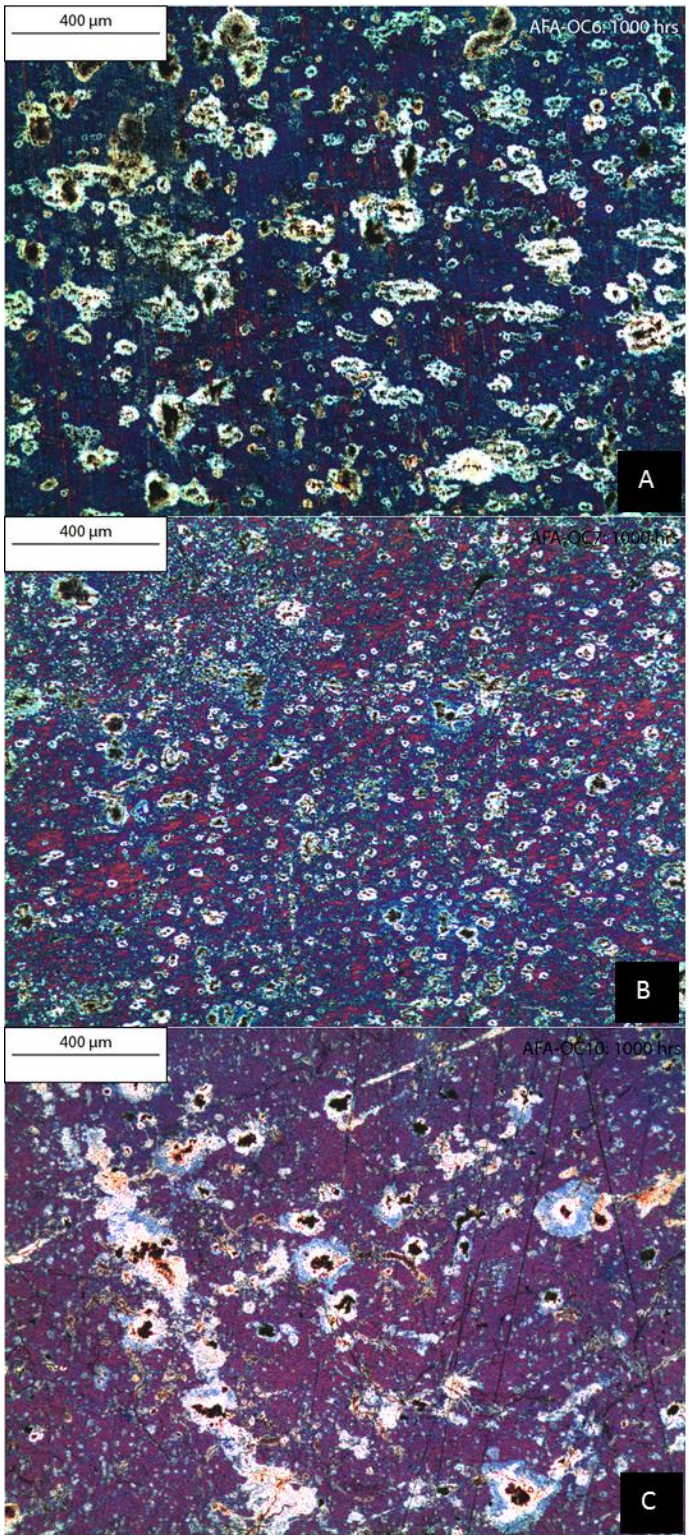

Fig. 68: Optical microscope images of (A) AFA-OC6, (B) AFA-OC7, and (C) AFA-OC10 after 1000 hours exposure to Experiment 3 condition

Cross-sections of the samples after 1000 hours of testing at Experiment 3 conditions were analyzed using EDS. The oxide layers that were found on 347ss and the three AFA materials were generally very thin (*Fig. 70*) and did not exceed approximately 1 μm. Inspection of IN 800H found some evidence of an oxide layer, but it was very thin and did not register well using EDS. *Fig. 71* illustrates the distribution of niobium in each of the AFA materials. While it was found that oxide islands on the surface correlated with Nb, it was hard to identify the oxide island structures in the cross-sections that were performed. Further analysis using FIB milling would be more beneficial, as these oxide islands could be specifically targeted for cross-sectional analysis. However, as *Fig. 69* would suggest, increased oxidation does occur above Nb concentrations that penetrate to the surface.

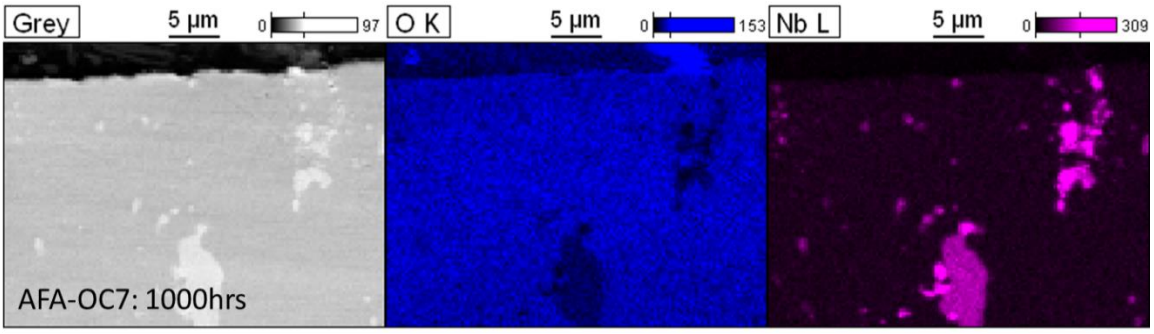

Fig. 69: Experiment 3 EDS map of AFA-OC7 displaying increased oxidation above concentrated Nb

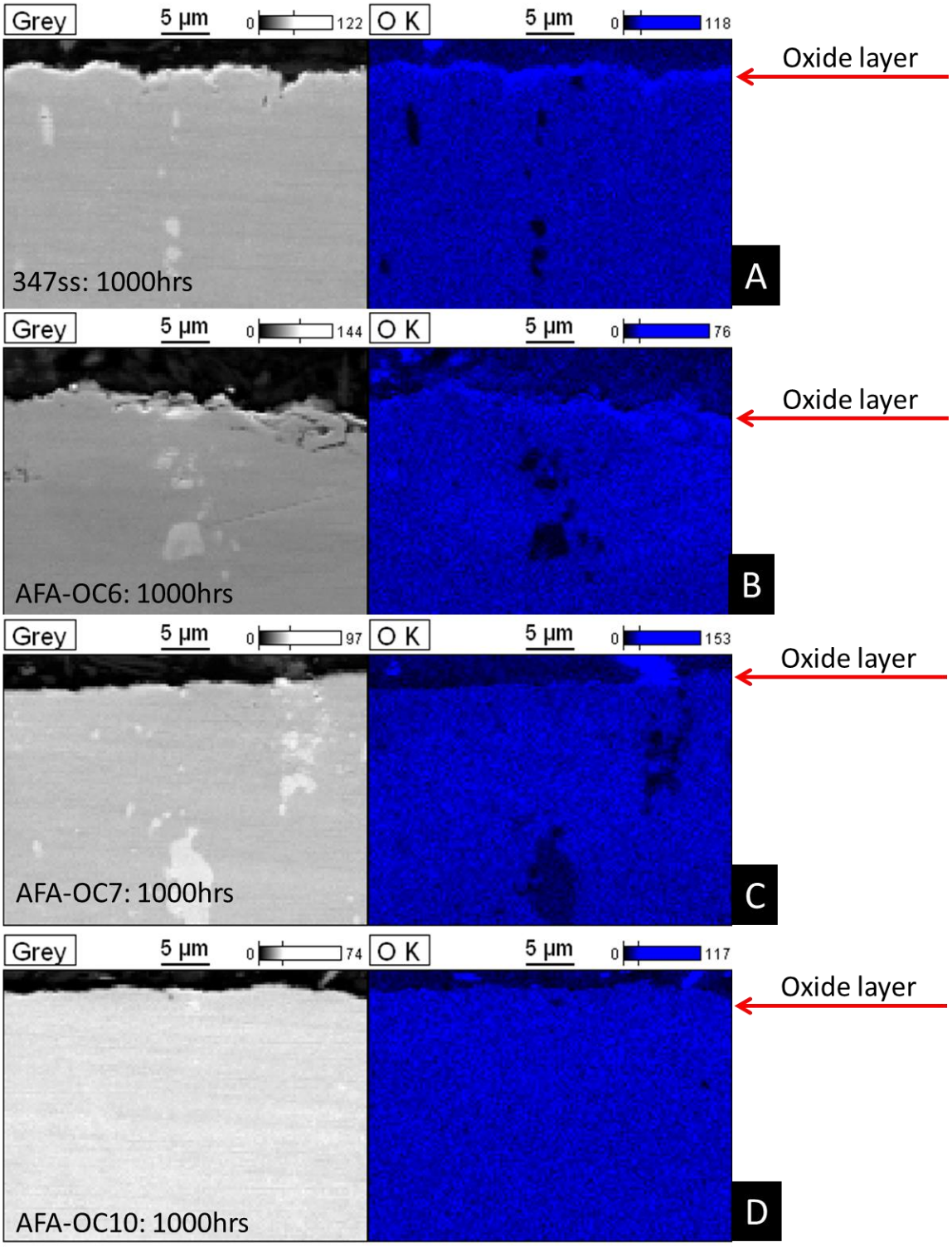

Fig. 70: EDS cross-section maps of (A) 347ss, (B) AFA-OC6, (C) AFA-OC7, and (D) AFA-OC10 after 1000 hours exposure to Experiment 3 conditions showing very thin oxide layers

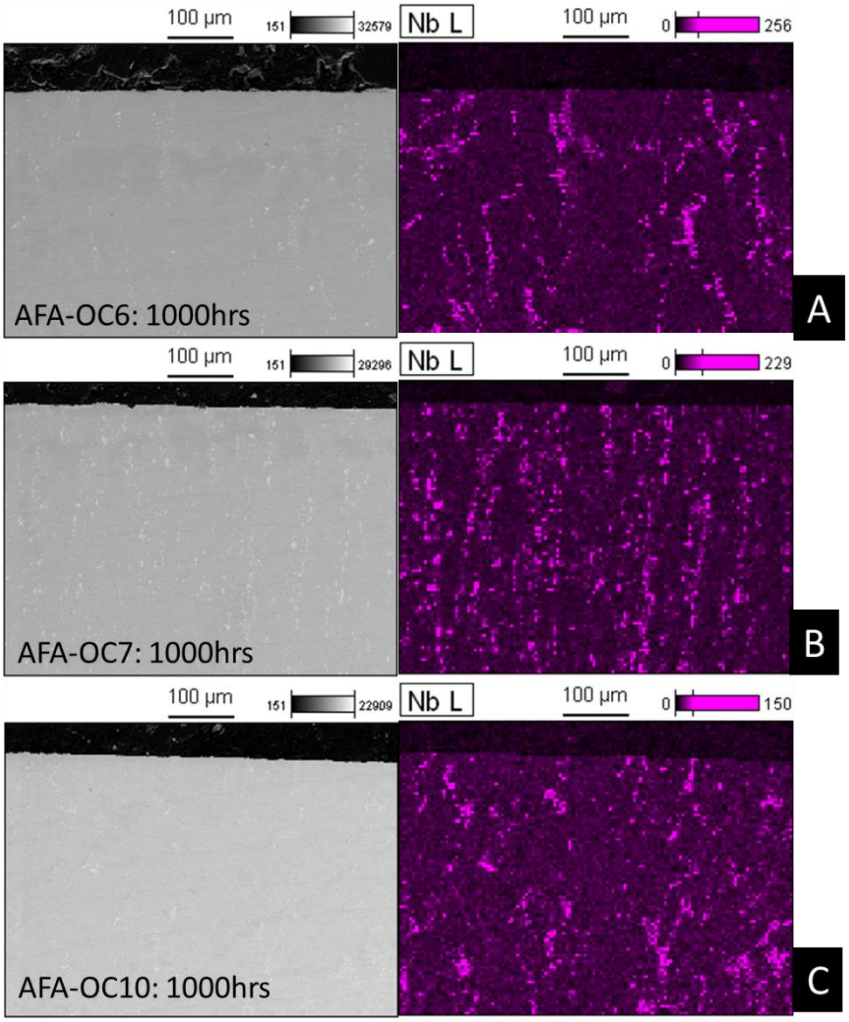

Fig. 71: EDS cross-section maps of (A) AFA-OC6, (B) AFA-OC7, and (C) AFA-OC10 after 1000 hours exposure to Experiment 03 conditions showing Nb distribution

Testing for Experiment 4 was conducted at 550°C and 20MPa. The total duration of testing was to be 1000 hours based on the performance observed at 450°C and the expectation that higher temperatures would produce a more aggressive oxidizing environment. Because of the low performance observed in the ferritic material at 450°C it was anticipated that the ferritic material would once again need to be removed from the test, potentially sooner than 800

hours. This proved to be true, and the two ferritic steels showed signs of significant material loss after only 200 hours. In an effort to gain one more data set at 400 hours, two samples each for NF616 and HCM12A were returned for further testing. To limit the potential for cross contamination, the ferritic samples were further separated from each other and the other alloys using additional alumina washers. At the completion of 400 hours, both ferritic materials were removed from further testing.

Surface analysis of NF616 and HCM12A confirmed material was being lost from the samples. SEM images in Fig. *72* of NF616 and HCM12A exhibit large scale material loss, or spallation. Areas that displayed the pit like dusting material loss mechanism were also visible on the surface of both ferritic materials. Observation of large scale spallation after only 200 hours was unexpected; therefore, it was theorized that carbon buildup near the oxide/metal interface provided low oxide adherence and an initiation point for spallation.

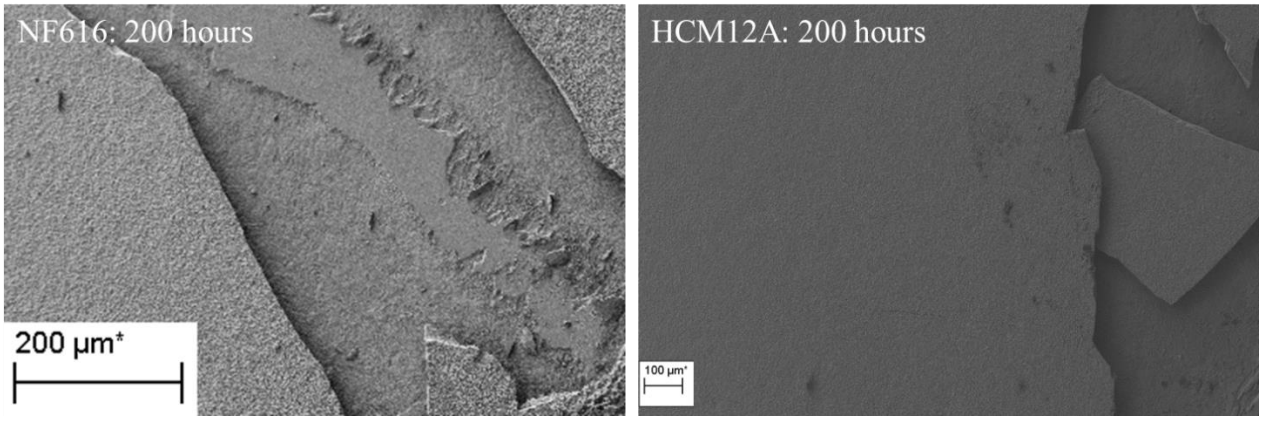

Fig. 72: SEM images of NF616 (left) and HCM12A (right) showing signs of material loss (spallation)

FIB cross sections were again performed on the HCM12A and NF616 material to observe the oxide through the thickness. EDS line scans accompanied SEM imaging, and provided insight into compositional changes through the oxide. *Fig. 73* shows a cross sectional SEM image of NF616 on the left, with definite layers visible through the thickness. To the right in *Fig. 73*, an EDS line scan confirmed that there were at least two definite layers (magnetite outer, Cr-spinel inner). There also appeared to be a layer slightly enriched in Cr, directly before returning to the bulk matrix composition. *Fig. 74* illustrates the same general findings in HCM12A that were observed in NF616; being, a definite duplex oxide structure consistent with a magnetite outer and Cr-spinel inner, along with some indication of Cr enrichment at the bulk matrix boundary. Although EDS does not provide a true quantitative measure of carbon, EDS line scans qualitatively indicated that carbon did occur within the inner oxide. This was congruent with the hypothesis that carbon layer formation within the inner oxide layer could develop and reduce oxide adherence.

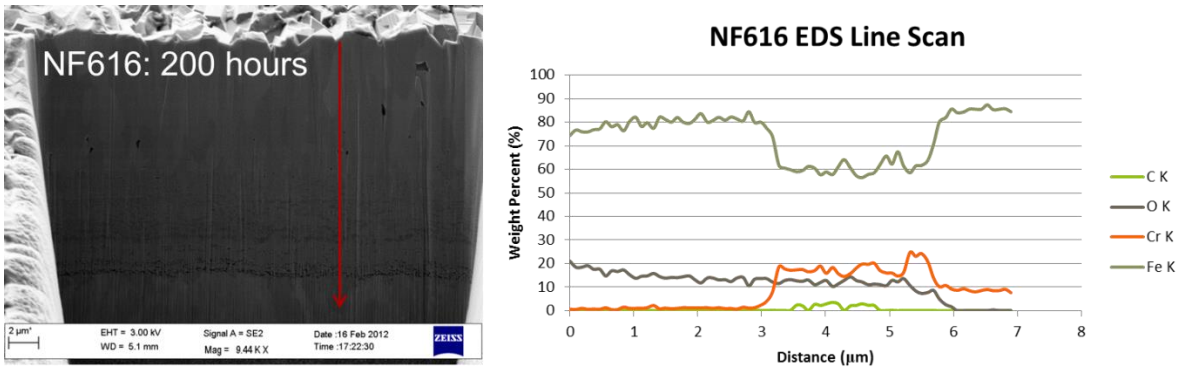

Fig. 73: NF616 SEM image of a FIB milled cross section and corresponding EDS line scan through the oxide layer with the scan position and direction indicated by the arrow

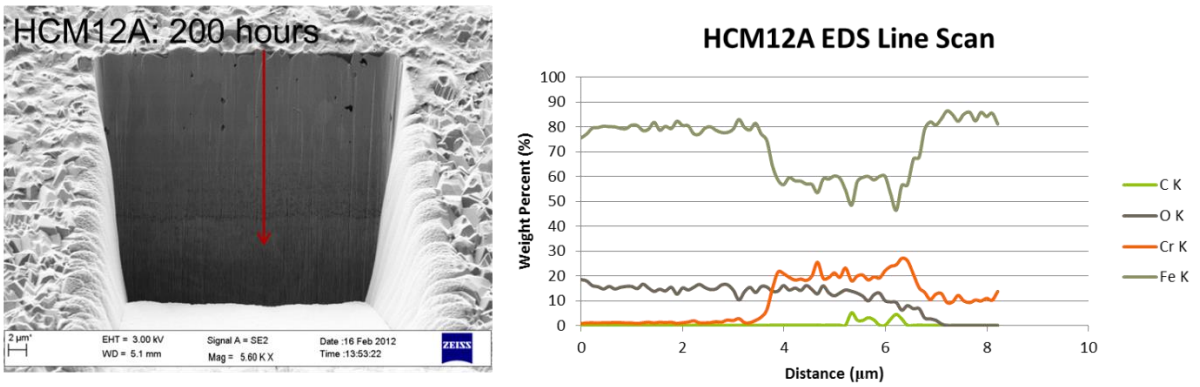

Fig. 74: HCM12A SEM image of a FIB milled cross section and corresponding EDS line scan through the oxide layer with the scan position and direction indicated by the arrow

Surface analysis of 347ss and IN800H after exposure to Experiment 4 test conditions, conducted using SEM, found similar results to Experiment 3. Oxide layers were very uniform and fully adherent, with no signs of material loss. Islands of increased oxide growth observed on 374ss were similar to Experiment 3. Higher magnification imaging (*Fig. 75*) further ascertained that these oxide islands were generally twice the circumferential size after 1000 hours at 550°C than they were after 1200 hours at 450°C, consistent with the idea that higher temperatures are more readily oxidizing. Observation of increased oxide growth between Experiment 3 and Experiment 4 was less apparent in IN 800H. Only at increased magnifications (*Fig. 76*) was it apparent that the oxide covering IN 800H had developed.

Further investigation using optical microscopy found some development of the 347SS oxide islands along with a color change of the surface from generally blue to yellow/magenta (*Fig. 77*). Likewise, IN 800H displayed a color change from generally blue to magenta/yellow with exposure to Experiment 04 test conditions (*Fig. 78*). Oxide development on IN 800H was not as readily apparent from the micrographs as was 347SS when compared to

corresponding optical images taken after Experiment 3 exposure (*Fig. 66* and *Fig. 67*). Observation of preferential attack on grain boundaries was not observed.

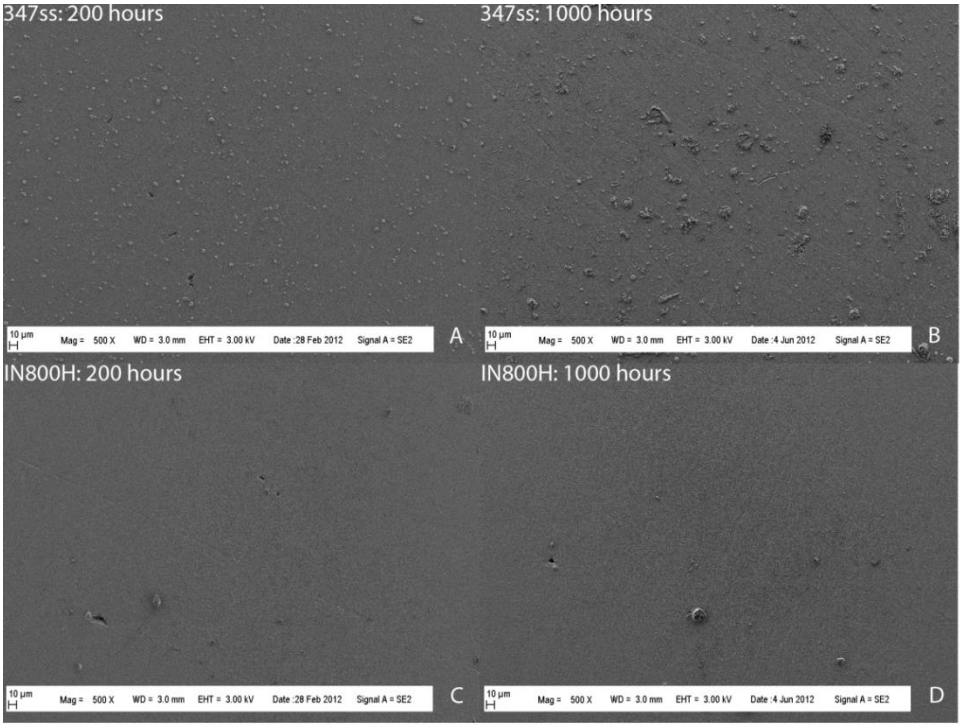

Fig. 75: Experiment 4 500x SEM images showing (A) 347SS after 200 hours, (B) 347SS after 1000 hours, (C) IN 800H after 200 hours, and (D) IN 800H after 1000 hours

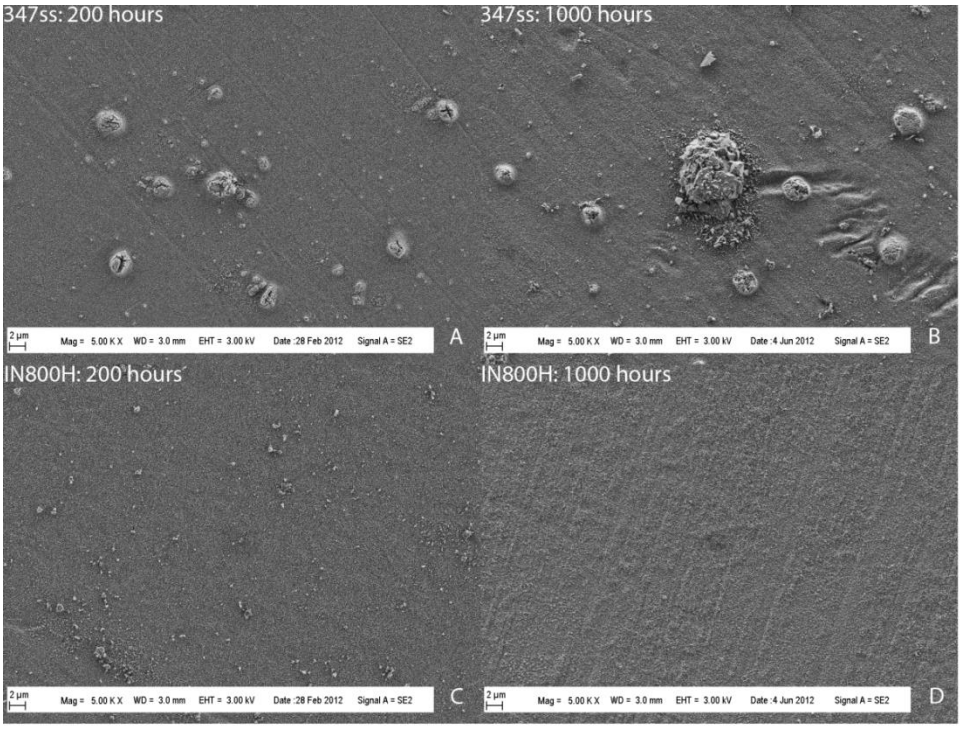

Fig. 76: Experiment 4 5000x SEM images showing (A) 347ss after 200 hours, (B) 347SS after 1000 hours, (C) IN 800H after 200 hours, and (D) IN 800H after 1000 hours

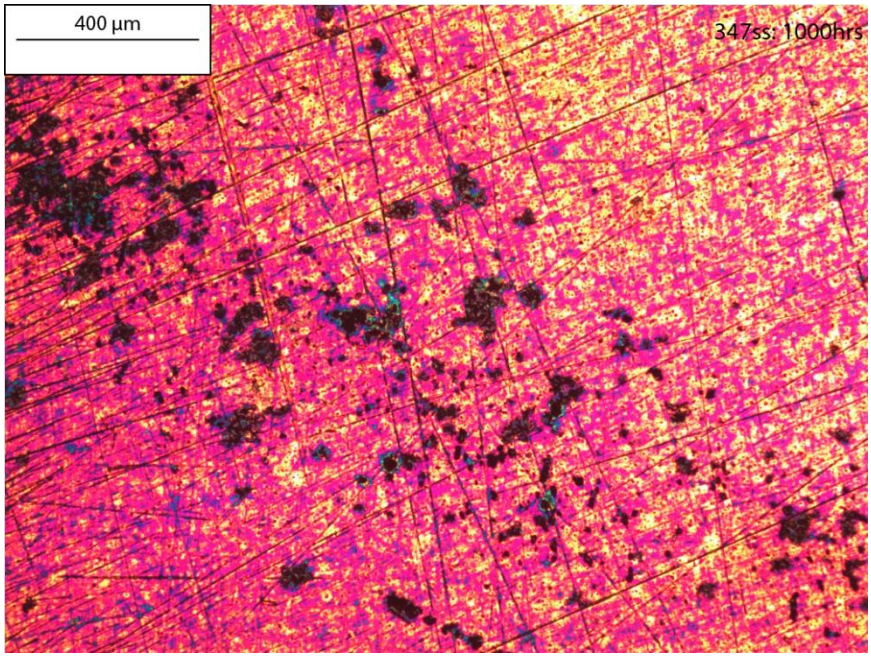

Fig. 77: Optical microscope image of 347SS exposed to Experiment 4 test conditions for 1000 hours

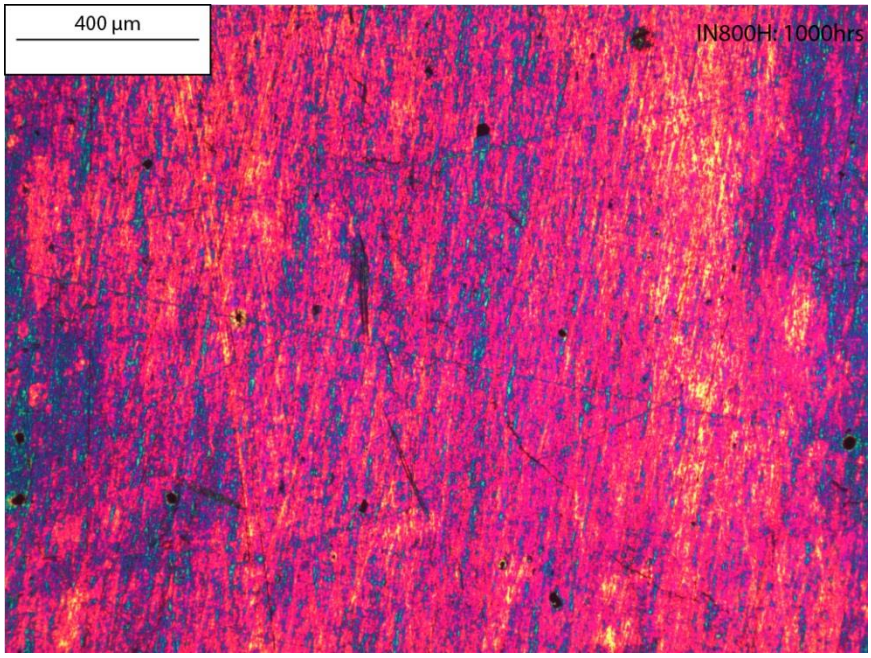

Fig. 78: Optical microscope image of IN 800H exposed to Experiment 4 test conditions for 1000 hours

SEM surface analysis of the three AFA materials was performed, and select images are shown in *Fig. 79*. As can be seen from the images, oxide islands on AFA-OC6 grew considerably from 200 to 1000 hours, whereas oxide growth for AFA-OC7 and AFA-OC10 was apparent, but not as pronounced. Areas of carbon were again visible after 200 hours, and generally increased in magnitude and quantity with increasing exposure. Imaging at increased magnification (*Fig. 80*) better illustrates the nucleation and growth of complex oxides on the AFA material.

Images taken with the optical microscope (*Fig. 81*) depicted the extent of oxidation across the surface of the AFA materials. Like 347ss and IN 800H, color changes were observed on

the AFA samples: AFA-OC6 transitioned from generally blue to gold, AFA-OC7 went from darker blue to lighter blue with gold accents, and AFA-OC10 developed from a violet/blue hue to gold with red accents. The dark black/brown patches on the surface were areas where thick oxide developed.

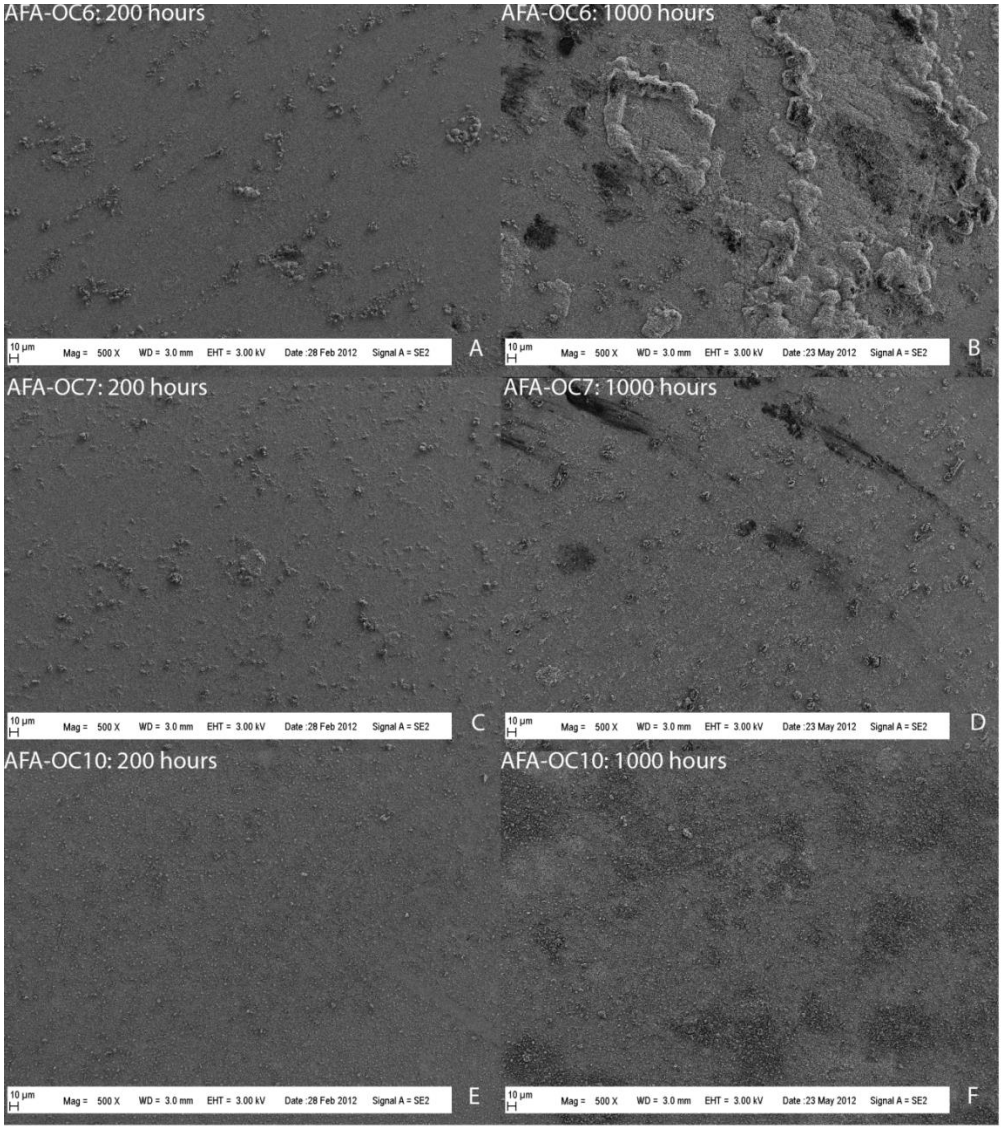

Fig. 79: Experiment 4 500x SEM images showing (A) AFA-OC6 after 200 hours, (B) AFA-OC6 after 1000 hours, (C) AFA-OC7 after 200 hours, (D) AFA-OC7 after 1000 hours, (E) AFA-OC10 after 200 hours, and (F) AFA-OC10 after 1000 hours

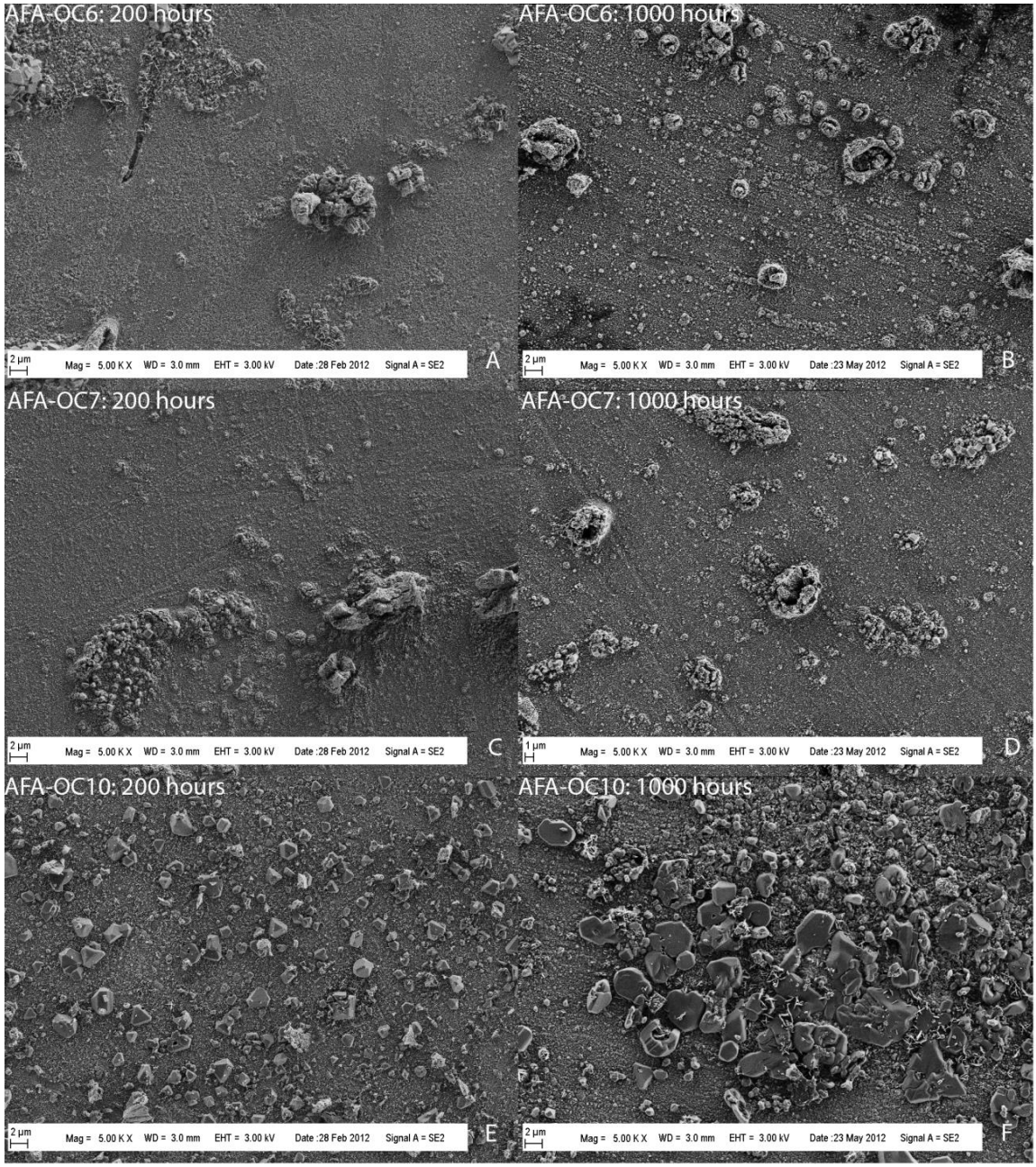

Fig. 80: Experiment 4 5000x SEM images showing (A) AFA-OC6 after 200 hours, (B) AFA-OC6 after 1000 hours, (C) AFA-OC7 after 200 hours, (D) AFA-OC7 after 1000 hours, (E) AFA-OC10 after 200 hours, and (F) AFA-OC10 after 1000 hours

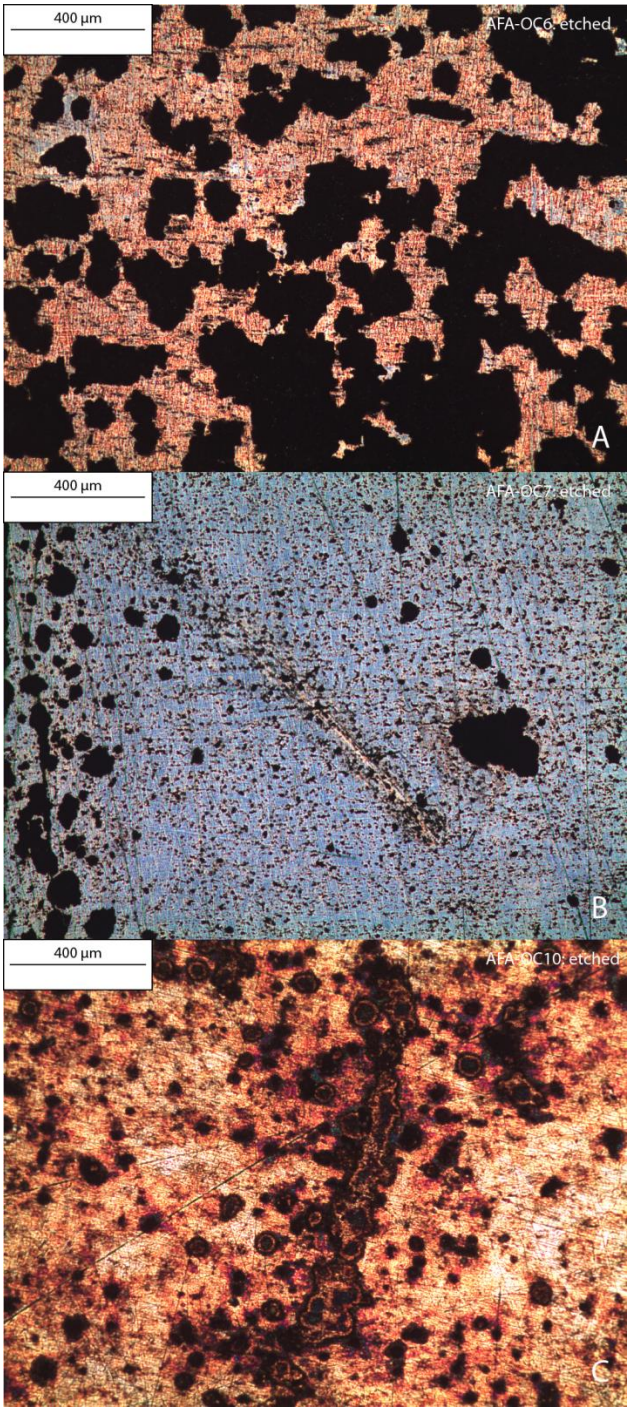

Fig. 81: Optical microscope images of (A) AFA-OC6, (B) AFA-OC7, and (C) AFA-OC10 after 1000 hours exposure to Experiment 4 conditions

EDS analysis of the oxide islands on the AFA materials was performed. As can be seen from the EDS maps in *Fig. 82* and *Fig. 83*, AFA-OC6 and AFA-OC7 developed oxide islands with very similar compositions. Both displayed oxide islands which correlated to areas of higher niobium and carbon. EDS point analysis of characteristic oxide islands on both AFA-OC6 and AFA-OC7 (*Fig. 84*) reveal that oxide islands on AFA-OC7 generally had higher levels of Cr and Ni, and lower levels of Mn and Nb which indicate a more protective, slower growing oxide than those of AFA-OC6. While there is some indication that Mo is detrimental in the formation of protective oxide due in part to MoO_3 volatilization at high temperatures, below approximately 875°C Mo can act like Si to prevent the diffusion of cations, slowing overall oxide development [59, 60].

EDS maps of AFA-OC10 (*Fig. 85*), indicated oxide islands were mostly developments of Mn oxide, with some additional oxide development that can be correlated to Nb. EDS point analysis confirms the nucleation of separate oxide islands with either high concentration of Nb or Mn (*Fig. 86*). Development of the oxide structure from that observed on samples exposed to the Experiment 03 test conditions would indicate that manganese oxide appeared to grow outward in a plate like structure (also seen from *Fig. 80e* to *Fig. 80f*).

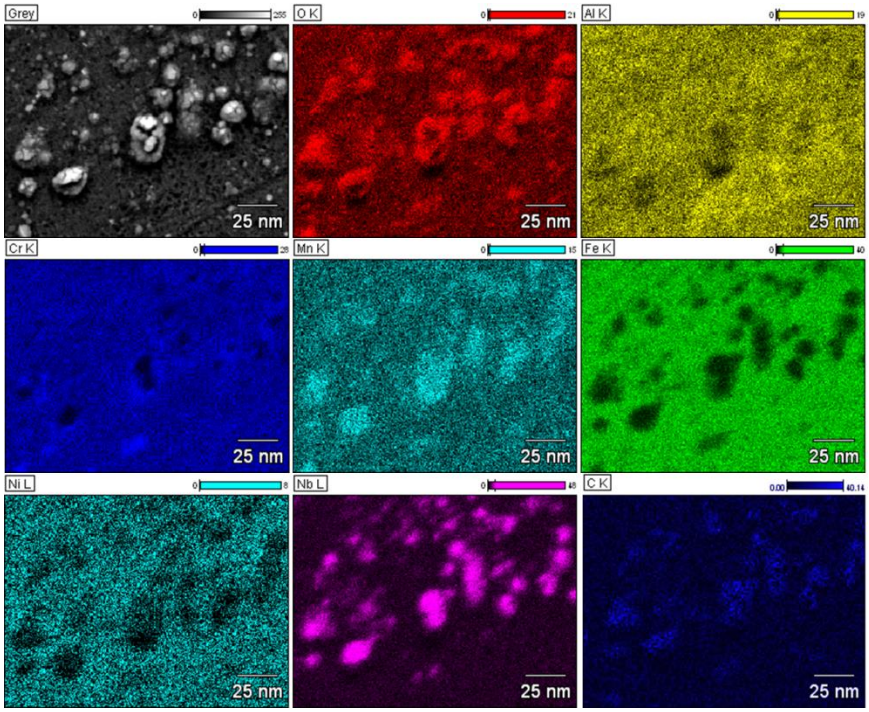

Fig. 82: EDS maps taken of AFA-OC6 after exposure to Experiment 4 conditions indicating islands of increased oxidation correlate to areas of niobium and carbon

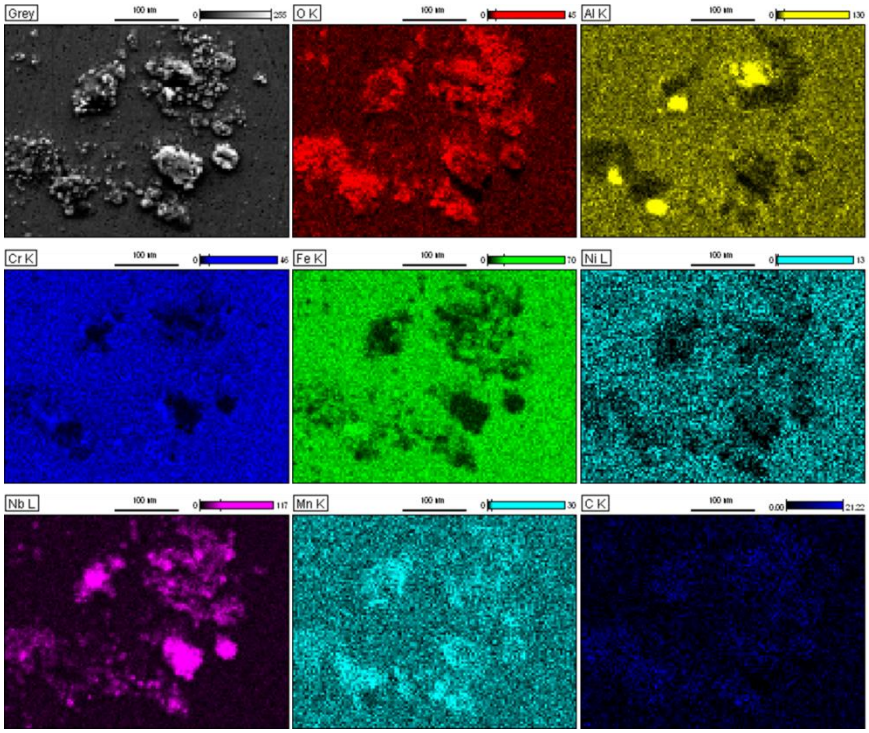

Fig. 83: EDS maps taken of AFA-OC7 after exposure to Experiment 4 conditions indicating islands of increased oxidation correlate to areas of niobium and carbon

AFA-OC6

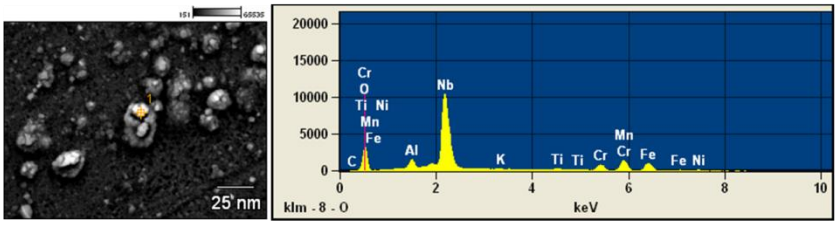

Wt%	C	O	Al	Ti	Cr	Mn	Fe	Ni	Nb
Pt 1	1.45	26.46	1.01	0.87	4.47	12.95	9.40	1.31	42.08

AFA-OC7

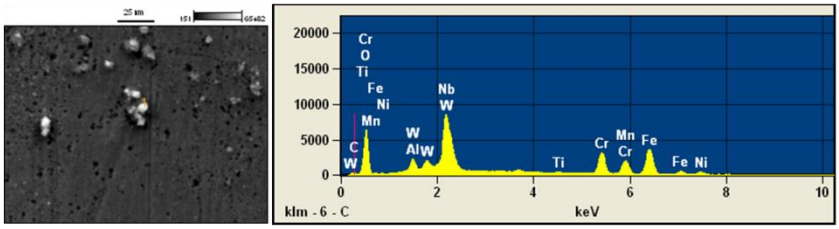

Wt%	C	O	Al	Ti	Cr	Mn	Fe	Ni	Nb	W
Pt 1	3.98	21.73	1.76	0.34	12.25	8.69	22.74	4.37	20.91	3.24

Fig. 84: EDS point analysis of (top) AFA-OC6, and (bottom) AFA-OC7 after exposure to Experiment 4 conditions

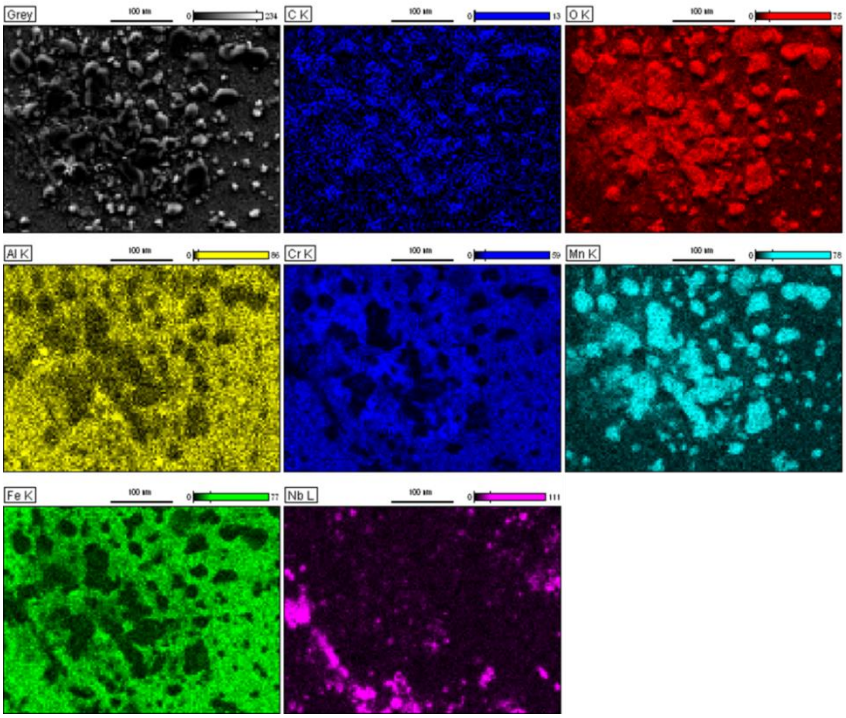

Fig. 85: EDS maps taken of AFA-OC10 after exposure to Experiment 4 conditions indicating islands of increased oxidation are mainly Mn

AFA-OC10: Oxide island with increased Nb

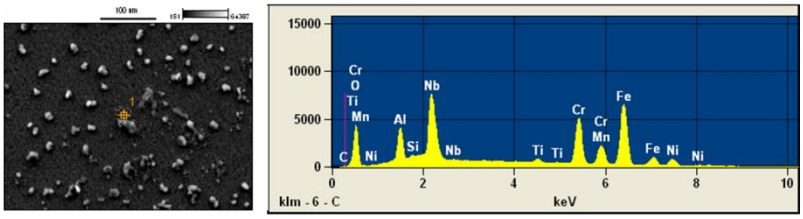

Wt%	C	O	Al	Si	Ti	Cr	Mn	Fe	Ni	Nb
Pt 1	1.23	11.45	3.63	0.31	0.84	16.87	7.08	35.83	6.31	16.47

AFA-OC10: Oxide island with increased Mn

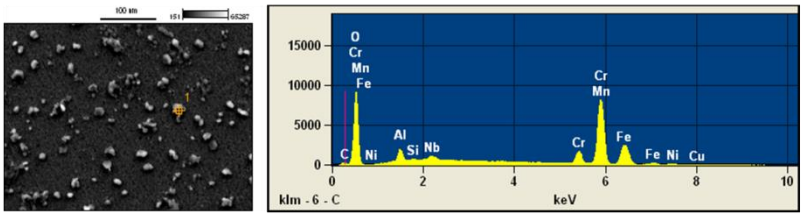

Wt%	C	O	Al	Si	Cr	Mn	Fe	Ni	Cu	Nb
Pt 1	2.53	23.90	1.86	0.15	6.41	47.67	13.67	1.66	0.55	1.58

Fig. 86: EDS point analysis of AFA-OC10 after exposure to Experiment 4 conditions indicating (top) oxide islands with high concentrations of Nb, and (bottom) oxide islands with high concentrations of Mn

Cross-sections of the Experiment 4 AFA material after 1000 hours exposure found oxide layers to be thicker than those observed after 1000 hours exposure to Experiment 3 test conditions. An example of the increased oxidation is shown using AFA-OC7 in *Fig. 87*, along with more evidence of increased oxide growth above areas concentrated in Nb. Region of interest analysis (*Fig. 88*) would also seem to suggest that oxygen moved into the sample (point 1) and aluminum enriched near the surface, exhibiting an internal oxidation zone consistent with alumina formation. Furthermore, EDS profiles in the Nb rich vicinity illustrated in *Fig. 88* (point 3) indicated that there was no oxygen and less aluminum present along with the Nb, which may suggest that oxygen is not penetrating the surface and diffusing inward, but rather metal is diffusing out. These regions are also likely to be grain

boundaries, as niobium in general precipitates out along grain boundaries (*Fig. 89*). Oxide layers on 347ss and IN 800H did not appear to greatly differ from those observed after 1000 hours exposure to Experiment 3.

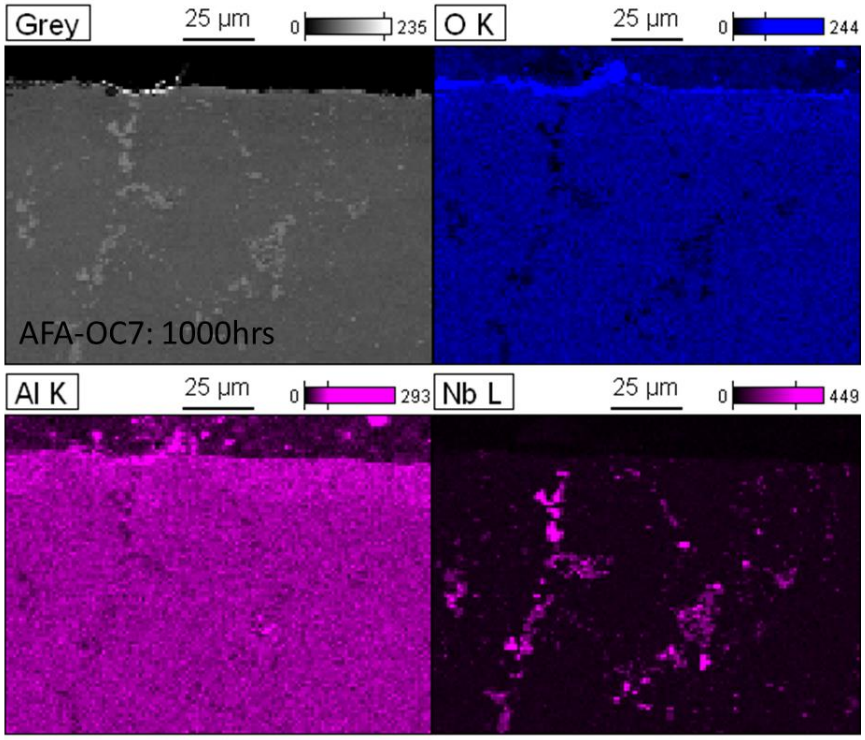

Fig. 87: EDS maps of AFA-OC7 after 1000 hours exposure to Experiment 4 conditions indicating defined oxide layer and apparent increased surface oxidation above Nb concentrations

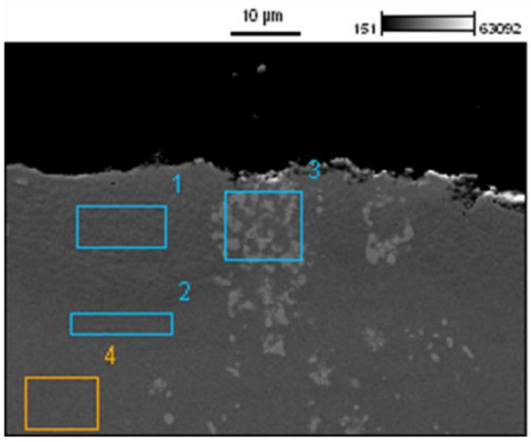

Wt%	O	Al	Si	Cr	Mn	Fe	Ni	Nb	Mo	W
Pt 1	3.5	4.7	0.5	13.8	2.0	48.4	24.6		1.4	
Pt 2		3.6	0.4	14.6	2.1	50.8	25.8		1.2	
Pt 3		3.0		12.7	1.8	43.1	20.1	14.5		3.3
Pt 4		3.5	0.4	14.6	2.2	50.9	25.9		1.3	

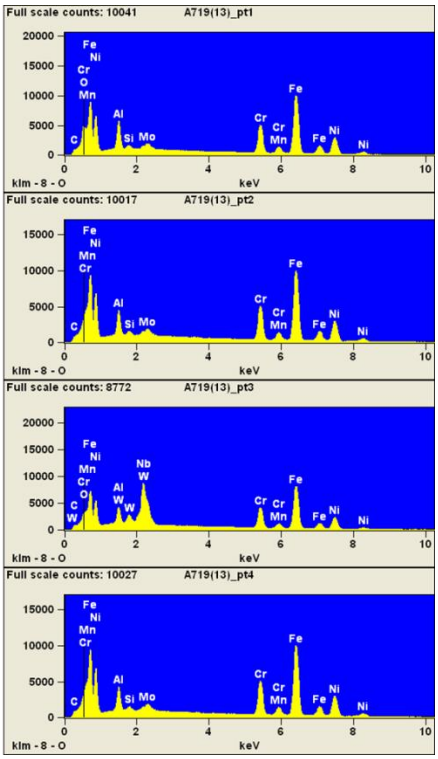

Fig. 88: EDS region of interest analysis of AFA-OC7 after 1000 hours exposure to Experiment 4 conditions

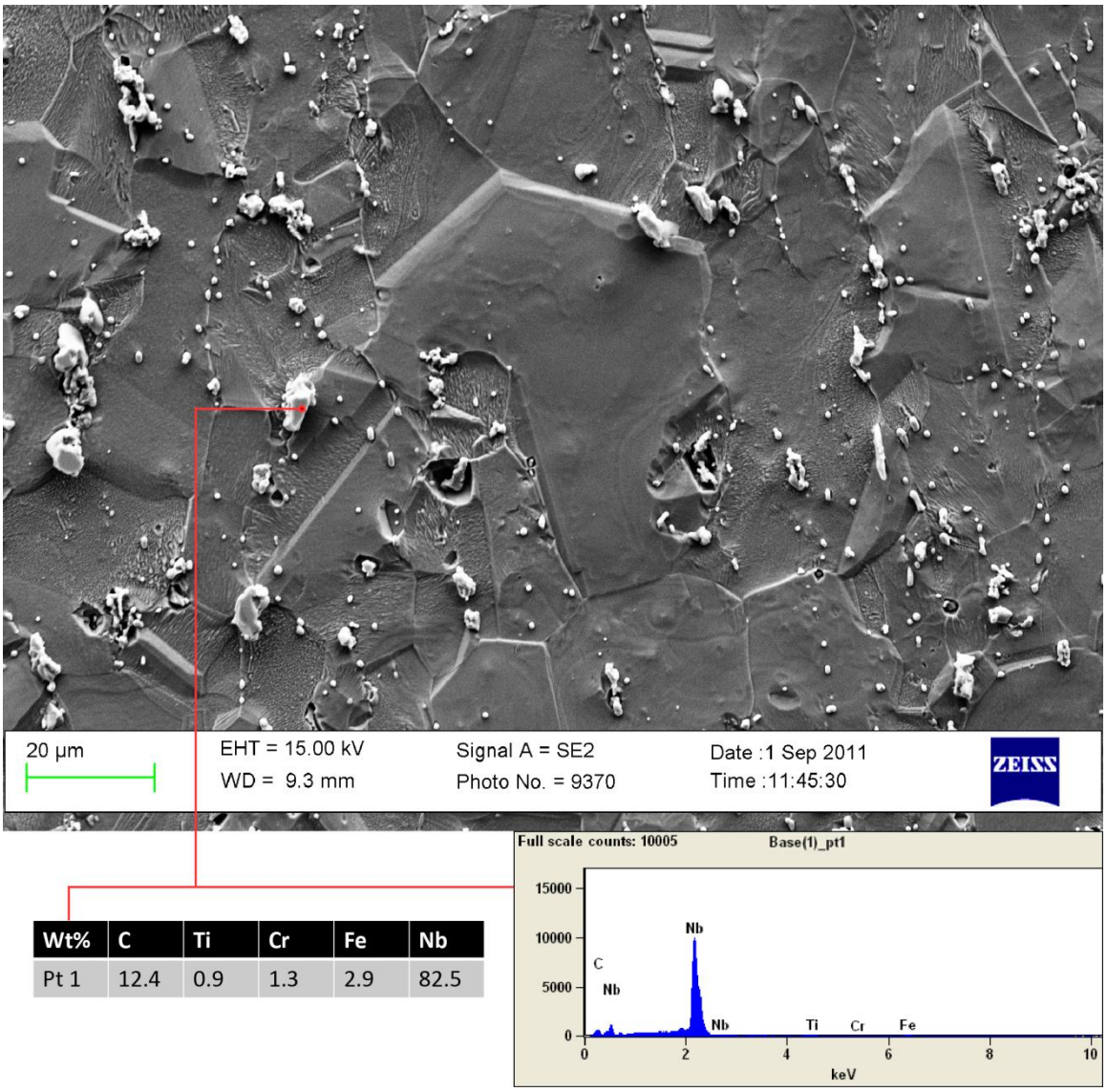

Fig. 89: SEM image of as-received AFA-OC7 etched with aqua regia revealing niobium carbide precipitation to grain boundaries

Testing for Experiment 5 was conducted at 650°C and 20MPa. The total duration of testing was chosen to be 1000 hours based on the performance observed at 550°C. Because of the poor performance observed in the ferritic material at 550°C it was anticipated that testing at

650°C would produce even worse results; however, two samples each of NF616 and HCM12A were tested for 200 hours to provide a data point for comparison.

Surface analysis of the ferritic materials revealed a definite difference in the oxide scale formed on NF616 compared to HCM12A. After 200 hours of exposure at 650°C and 20 MPa, NF616 displayed a relatively consistent outer layer of Magnetite (*Fig. 90*). By contrast, definite areas of chromia formed on the HCM12A material, which lead to a reduction in overall oxide development and subsequent lower weight gain than NF616 (*Fig. 91*). Further investigation of the ferritic materials was not conducted due to their poor performance. With the purpose of this investigation being to determine suitable material for use in the SC-CO_2 Brayton cycle, it can be concluded that ferritic materials produce an unacceptable level of oxidation at 650°C, 550°C, and even 450°C to be considered useful in high temperature long service life sections. Furthermore, thick oxide layers, like the ones that were observed to develop on the ferritic steels can detrimentally affect heat transfer properties, limiting the performance of ferritic material in heat exchanger components.

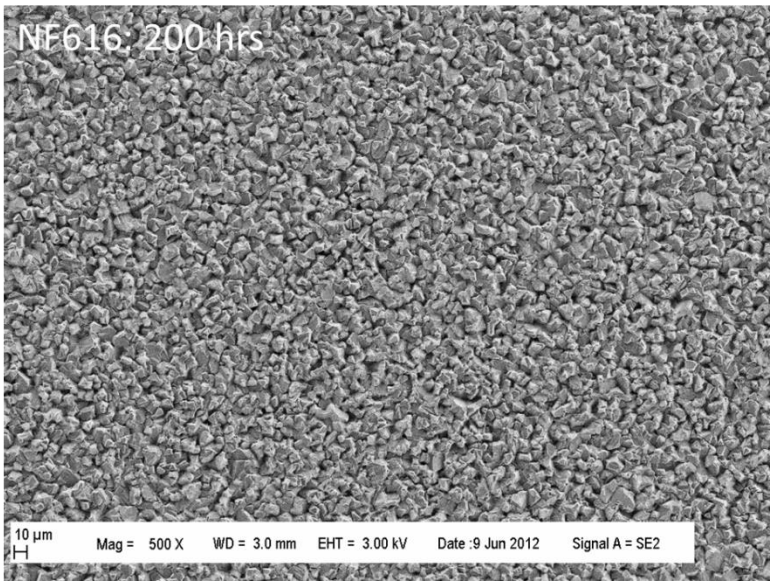

Fig. 90: Experiment 5 500x SEM image of NF616 showing general structure of the outer oxide layer consisting of iron oxide

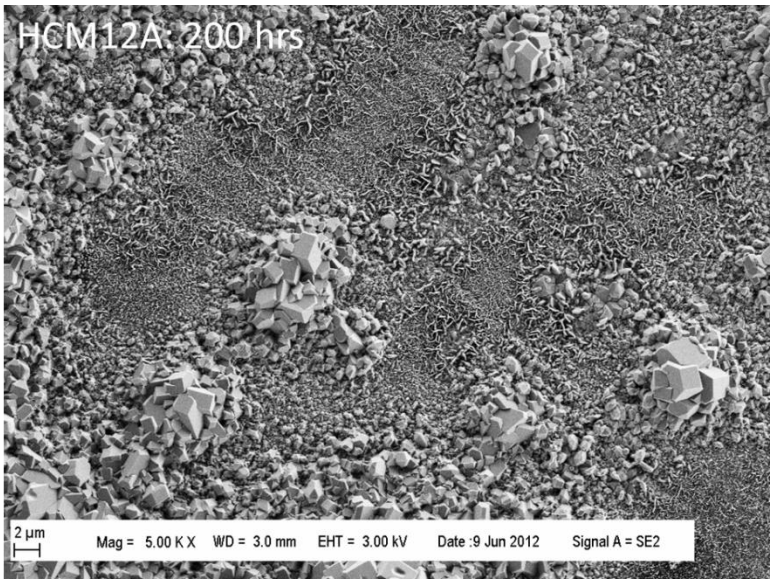

Fig. 91: Experiment 5 5000x SEM image of HCM12A showing areas of chromium oxide formation in addition to the typical iron oxide

Select images from the surface analysis of 374ss and IN 800H, exposed to the conditions of Experiment 5, conducted using SEM are shown in *Fig. 92*. After 200 hours both samples

exhibited a fully adherent chromia layer; additionally, the oxide layer covering 347SS showed a more pronounced development compared to 347SS samples exposed to 200 hours in Experiment 3 or Experiment 4. Failure of the 347SS oxide layer became apparent after 400 hours as seen in *Fig. 93*. Chromia scale from 347SS after 1000 hours was observed to be detached from the surface of the sample (spallation), as illustrated in *Fig. 94b;* the exposed base material was then susceptible to further oxidation. This is consistent with the oxidation kinetics trend which exhibited exponential growth, indicating breakaway oxidation.

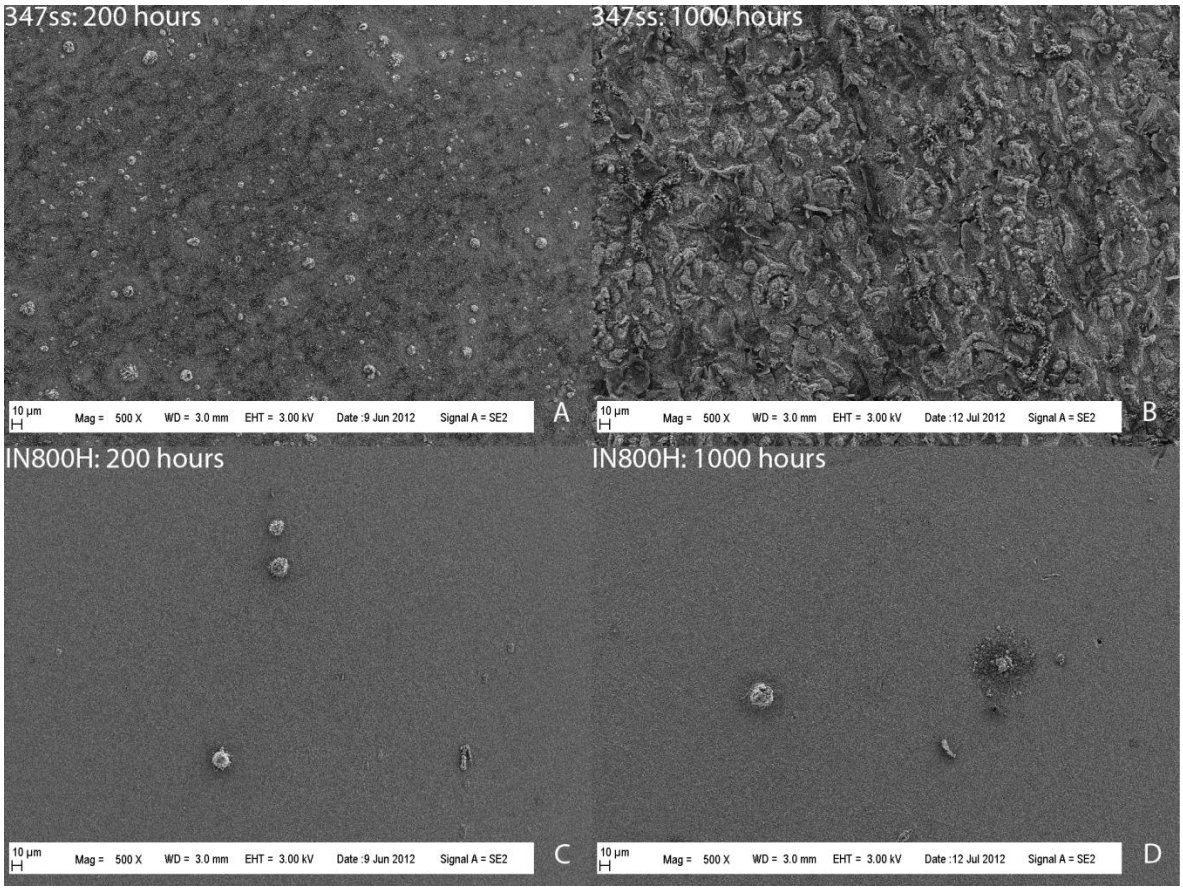

Fig. 92: Experiment 5 500x SEM images showing (A) 347ss after 200 hours, (B) 347ss after 1000 hours, (C) IN 800H after 200 hours, and (D) IN 800H after 1000 hours

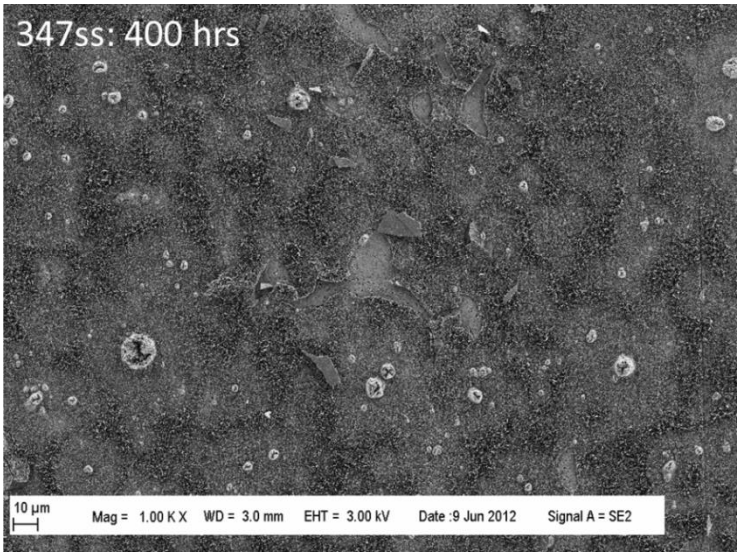

Fig. 93: Experiment 5 1000x SEM image of 347ss showing areas of chromia breaking free from the sample surface

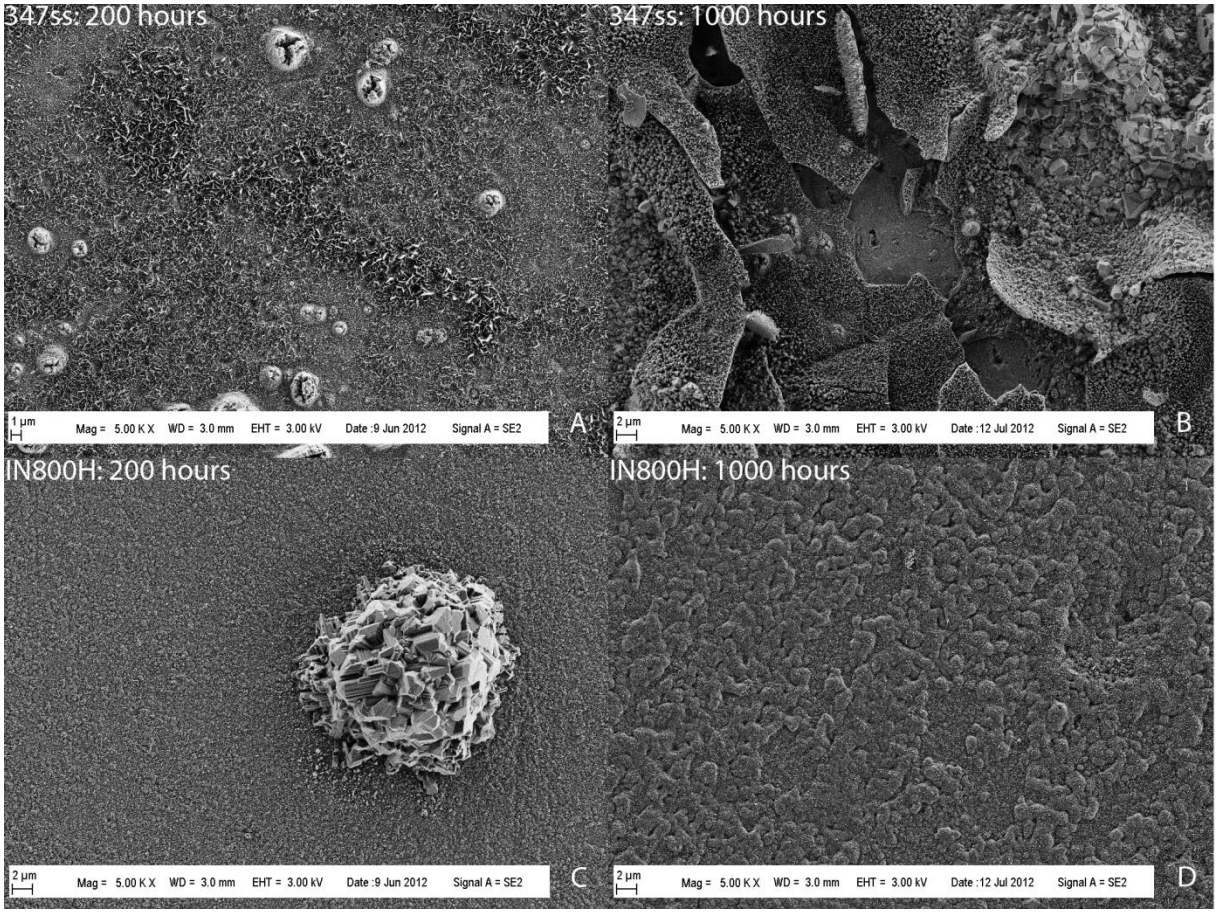

Fig. 94: Experiment 5 5000x SEM images showing (A) 347ss after 200 hours, (B) 347ss after 1000 hours, (C) IN 800H after 200 hours, and (D) IN 800H after 1000 hours

EDS analysis was performed on a number of the oxide fragments that had spalled from the surface of 347SS and overturned, allowing examination of the interface (*Fig. 95*). These overturned chromia fragments all displayed increased levels of carbon (*Fig. 95b*). EDS analysis performed on the exposed areas indicated no significant increase in carbon (*Fig. 95c*). The presence of carbon does not necessarily produce the observed spallation of the chromia layer, but it would certainly seem to be an influencing factor. If chromium carbides were formed as levels of carbon increased in the oxide layer, chromium available for protective oxide formation would be reduced. Both carbide formation and reduced protective oxide formation would lead to a greater ingress of oxygen into the metal, to the point where chromium would be consumed beyond the minimum concentration necessary for protective oxide formation. Voids formed beneath the oxide layer (visible in *Fig. 95a*) reduce adhesion of the outer oxide layer. Spallation of the outer chromia oxide occurs potentially aided by thermal expansion/contraction as the material was cycled from room temperature to testing conditions every 200 hours. Iron oxide would rapidly form and grow from the newly exposed sites.

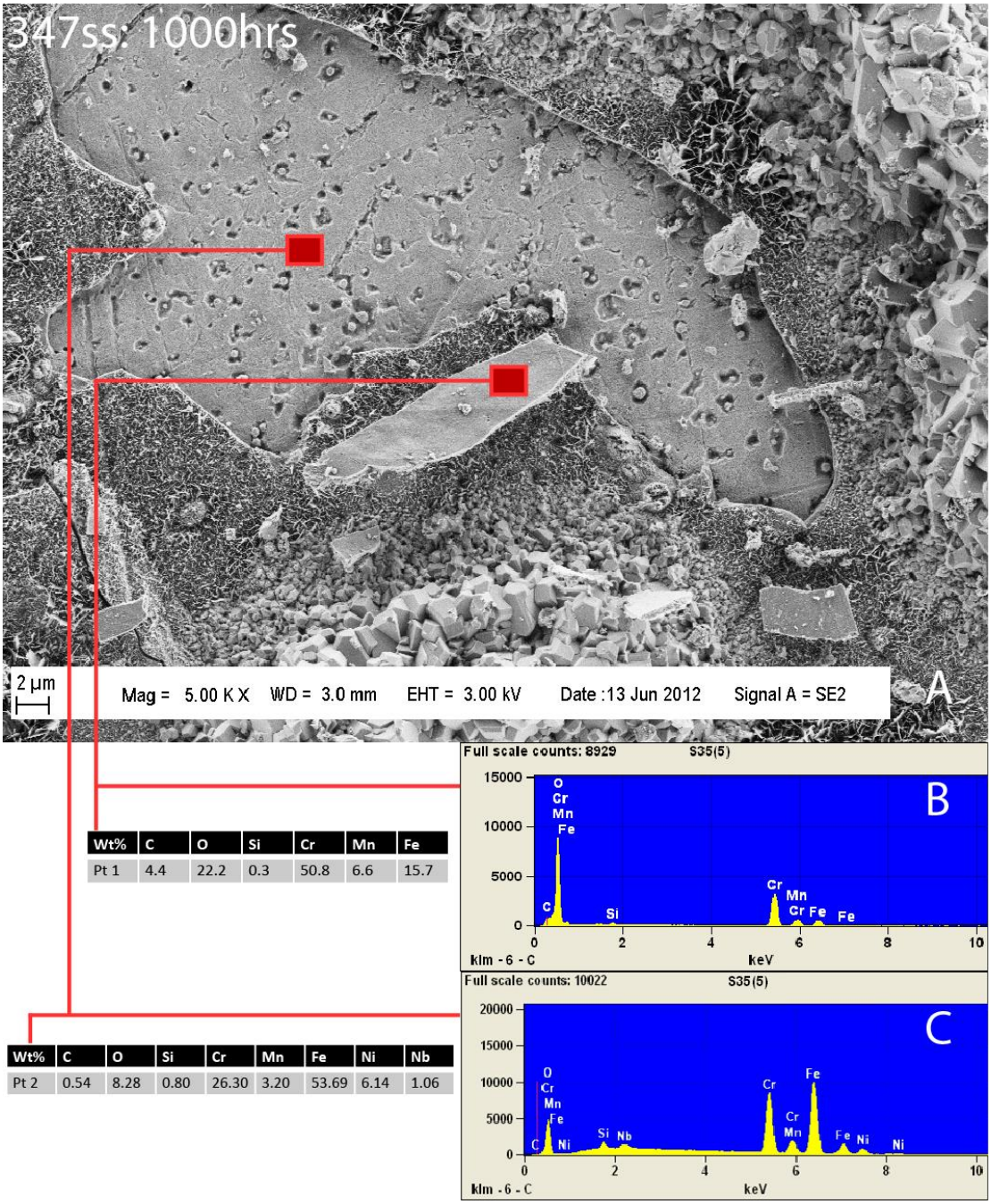

Wt%	C	O	Si	Cr	Mn	Fe
Pt 1	4.4	22.2	0.3	50.8	6.6	15.7

Wt%	C	O	Si	Cr	Mn	Fe	Ni	Nb
Pt 2	0.54	8.28	0.80	26.30	3.20	53.69	6.14	1.06

Fig. 95: 347SS after exposure to Experiment 5 conditions: (A) SEM image showing oxide spallation site with (B) EDS analysis performed on the overturned oxide layer that had broken free of the surface indicating increased carbon present at the interface, and (C) EDS analysis of the newly exposed surface.

Surface analysis of the AFA materials found surprisingly large amounts of oxide growth on AFA-OC10 after only 200 hours (*Fig. 96*), which continued to grow and develop into even larger oxide structures after 1000 hours. Optical imaging performed on AFA-OC10 after 1000 hours of exposure to Experiment 5 conditions, seen in *Fig. 97c*, found a highly oxidized surface, which would easily deteriorate upon the most delicate handling (manipulation with tweezers gave a crunchy sensation). Similarly, SEM and optical images of AFA-OC6 depicted large scale non-protective oxide growth (*Fig. 96* and *Fig. 97*). As the weight gain analysis would indicate, AFA-OC7 did not oxidize to the same extent as either AFA-OC6 or AFA-OC10, and the plateau in weight gain of AFA-OC7 after 600 hours could possibly indicate a stabilization of the protective oxide. Congruent to the idea of protective oxide stabilization, *Fig. 97b* indicated that while AFA-OC7 did develop large oxide islands, they did not coalesce into a single layer as was observed on AFA-OC6 and AFA-OC10 after 1000 hours. Further testing to longer durations would prove to be more conclusive in determining whether or not the oxide would continue to exhibit a low growth trend, or more rapidly oxidize like the other two AFA materials.

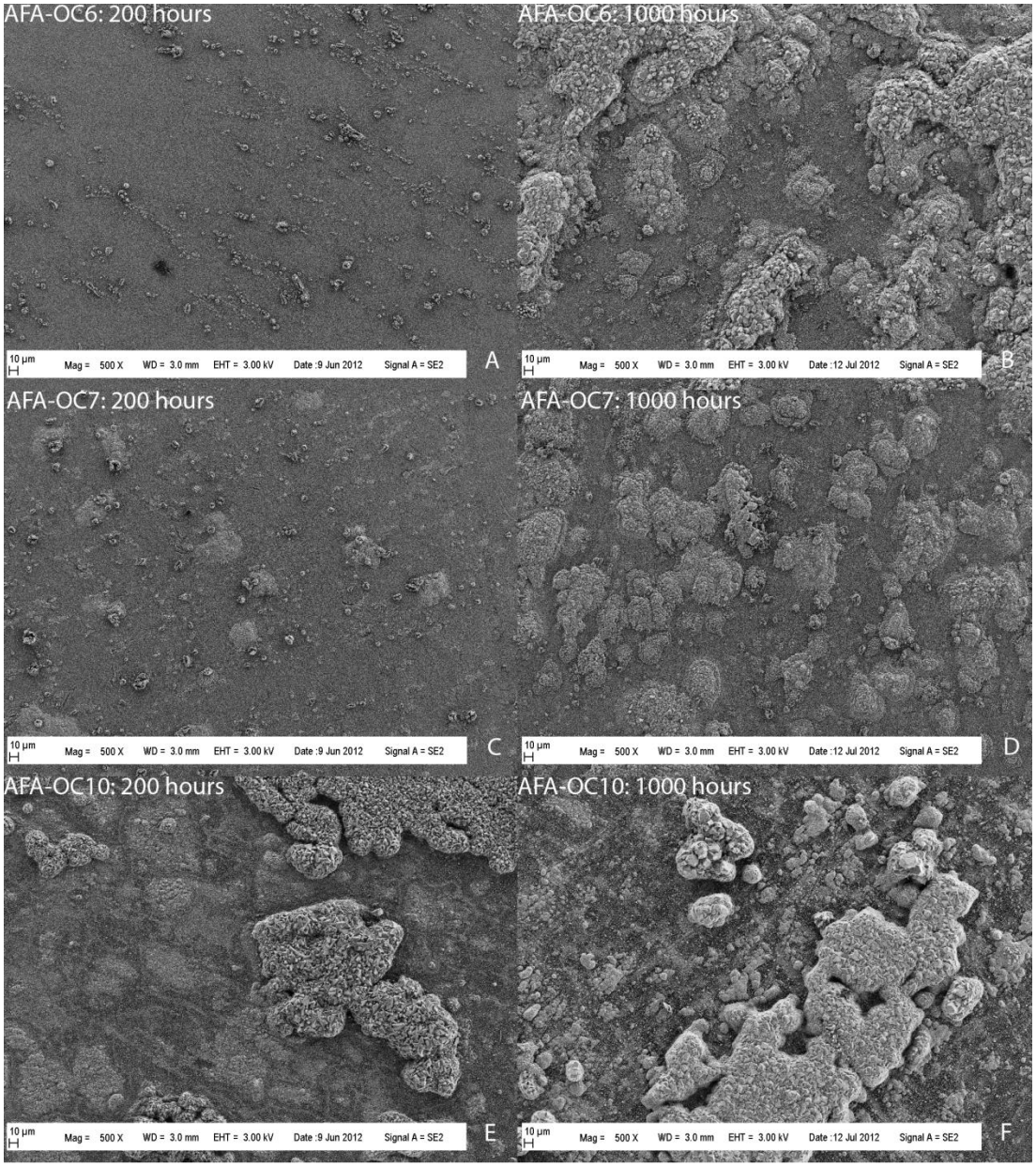

Fig. 96: Experiment 5 500x SEM images showing (A) AFA-OC6 after 200 hours, (B) AFA-OC6 after 1000 hours, (C) AFA-OC7 after 200 hours, (D) AFA-OC7 after 1000 hours, (E) AFA-OC10 after 200 hours, and (F) AFA-OC10 after 1000 hours

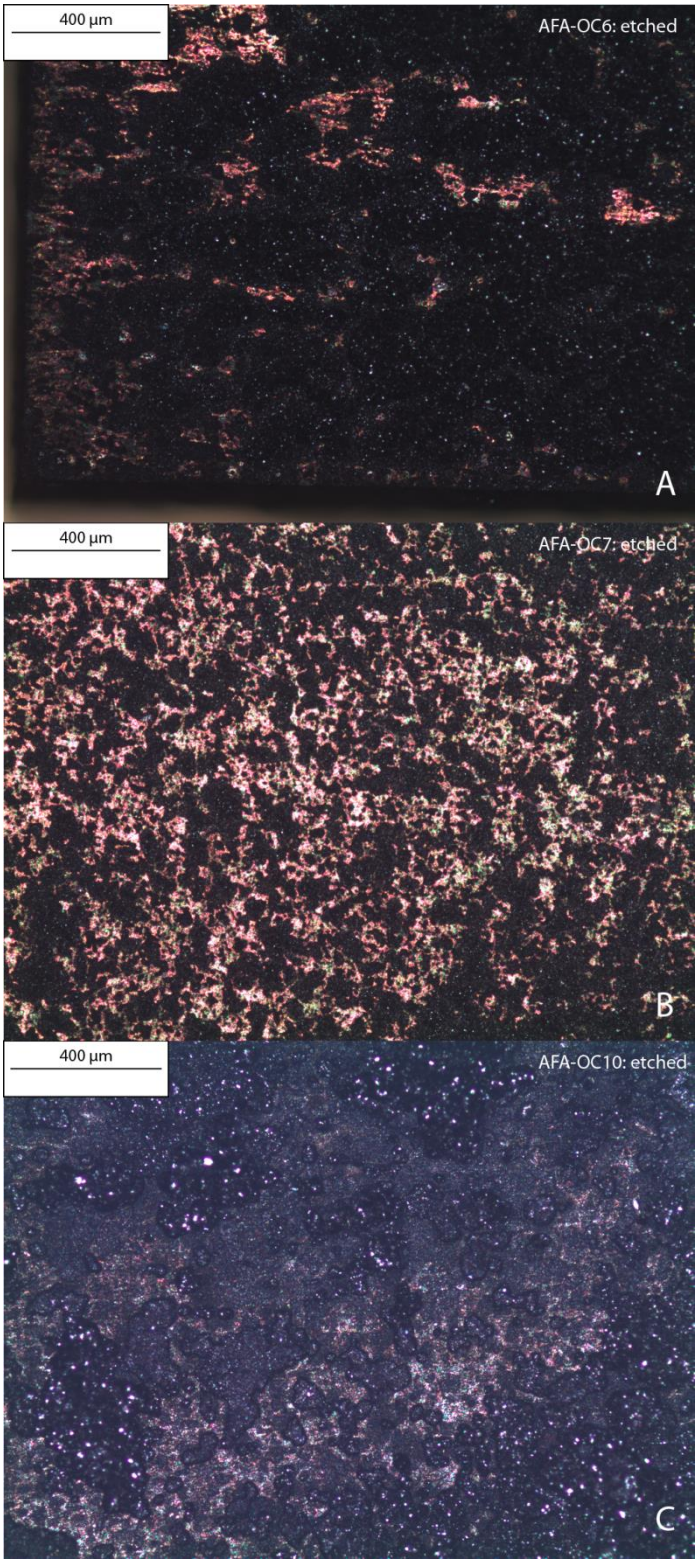

Fig. 97: Optical microscope images of (A) AFA-OC6, (B) AFA-OC7, and (C) AFA-OC10 after 1000 hours exposure to Experiment 5 conditions

Analysis of the heavily oxidized areas present on the three AFA materials by EDS found generally high concentrations of iron. Heavily oxidized regions on AFA-OC10 were also found to contain areas of manganese. Both iron and manganese are poorly protective oxide layers; in particular, the formation and substantial outgrowth of iron points to the general failure of any protective oxide layer that may have formed on the material.

Area specific EDS analyses on AFA-OC6 and AFA-OC7 were performed in areas displaying increased oxide growth and areas displaying protective thin oxide. This investigation found that larger oxide growths were similar in composition on AFA-OC6 and AFA-OC7. The difference in the two materials came by increased levels of molybdenum found in the protective (thin) oxide on AFA-OC7. The protective oxide areas on AFA-OC6 which accounted for less surface area than AFA-OC7 contained no measurable amounts of Mo. By comparison of AFA-OC6 and AFA-OC7 both in composition and performance, it would seem that increased molybdenum could be correlated to increased corrosion resistance. More in-depth study of the exact composition of the protective oxides on AFA-OC7 is recommended to determine if molybdenum oxides are entirely responsible for the observed improvement in corrosion resistance.

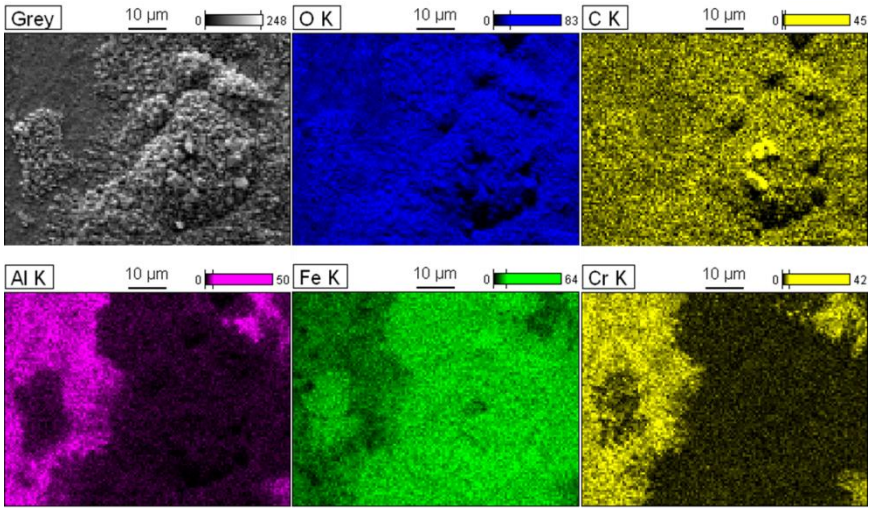

Fig. 98: EDS maps taken of AFA-OC6 after exposure to Experiment 5 conditions identify heavily oxidized areas as mostly iron oxide with some indication of increased carbon

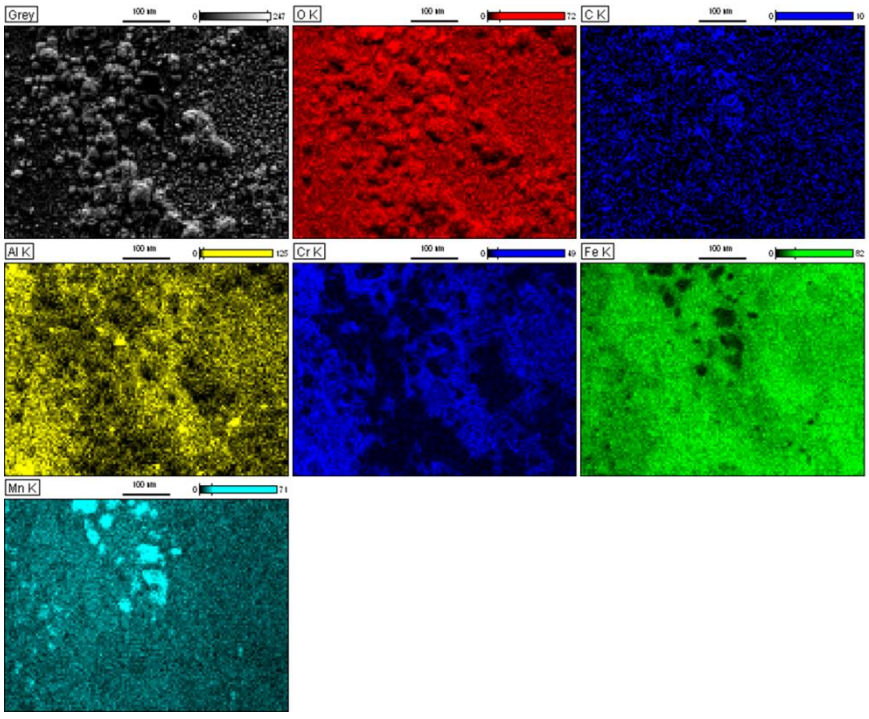

Fig. 99: EDS maps taken of AFA-OC10 after exposure to Experiment 5 conditions find heavily oxidized areas contain manganese in addition to iron as well as some indication of increased carbon

Cross-sectional analysis for IN 800H has not been shown up to this point because no considerable oxide layer developed on the surface. After exposure to 1000 hours at Experiment 5 conditions, IN 800H was observed to develop a consistently thin adherent outer chromium oxide layer (*Fig. 100*), which was observed to range in thickness from approximately 0.3 to 1 micron. An inner chromium depleted zone formed as a result of chromium moving outward to form the oxide layer. The observed inner chromium depleted zone ranged in thickness from approximately 1 to 3 microns.

Islands of increased oxidation on IN 800H, depicted in the surface analysis, were found to develop from titanium carbides or nitrides which protruded through the surface. These precipitates were not very numerous since IN 800H only contained 0.53 wt% Ti (*Fig. 102*). Luckily one such titanium particle was caught in the cross-section, affording EDS analysis (*Fig. 101*). Analysis indicated there was some oxidation of the titanium, as well as penetration of oxygen beneath the metal surface, where a chromium rich oxide layer developed. Iron oxide was observed to form around the outside of the titanium particle.

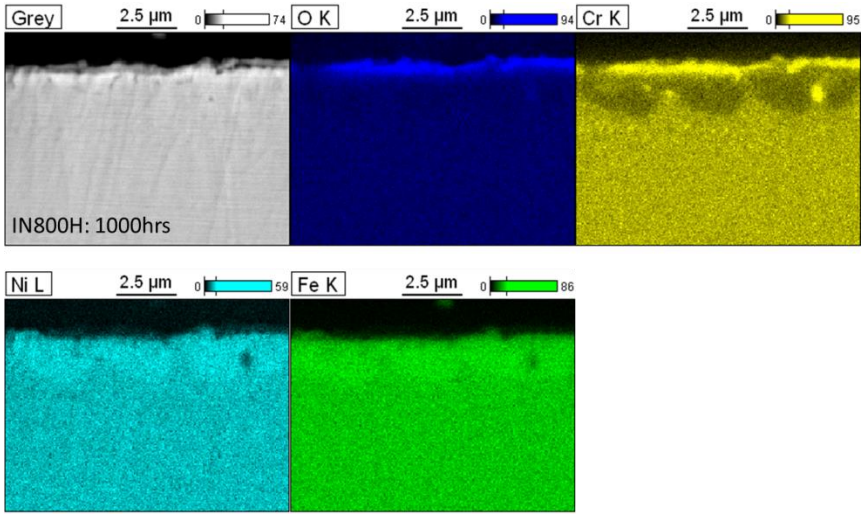

Fig. 100: EDS maps of IN 800H exposed to Experiment 5 conditions displaying protective outer chromia layer

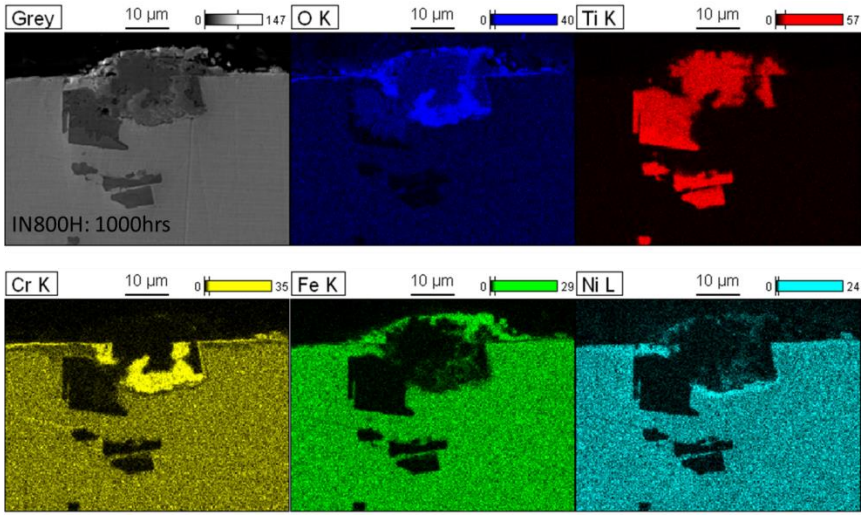

Fig. 101: EDS maps of cross-sectioned titanium particle protruding to the surface of IN 800H after exposure to Experiment 5 conditions

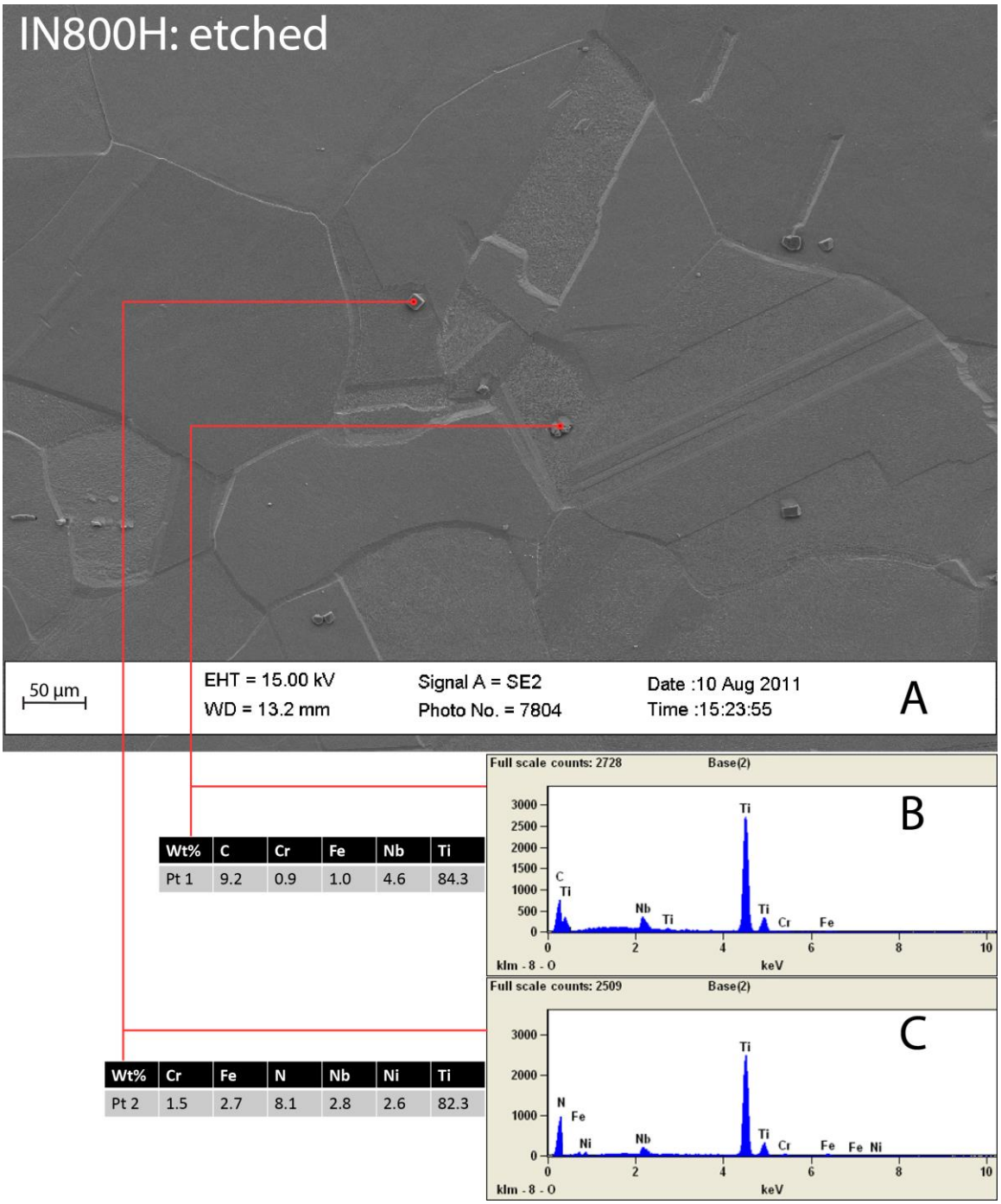

Fig. 102: (A) SEM image of as-received IN 800H etched with aqua regia revealing (B) titanium carbide and (C) titanium nitride precipitates

From cross-sections of 347SS material exposed to 1000 hours at Experiment 5 test conditions, chromium oxide thickness was found to exist in the range of 3 to 5 microns. Larger outgrowths of iron oxide were observed to occur where the protective chromia layer had apparently failed. EDS analysis of 347SS in cross-section (*Fig. 103*) found an outer chromium rich oxide layer (chromia), and a corresponding inner layer that was depleted of chromium (iron enriched). Chromium therefore diffused outward to form the protective chromia layer, leaving the adjacent bulk metal matrix depleted. As was previously described, failure of the outer oxide layer occurred in part because chromium was no longer available for protective oxide formation. Where the chromia layer failed, oxidation of iron was allowed to occur. Because of iron oxide's poor protective nature, it readily oxidized and grew. Given time, it is expected that an inner chromium rich protective oxide layer will form, and the outer iron oxide layer will break away, thus the observed oxidation process will likely reoccur.

Subsequent EDS line scans (*Fig. 104*) of the larger oxide formations starting in the chromium depleted zone indicated iron oxide had mostly developed as the outer layer. Increased levels of carbon were also found to occur in the outer oxide layer, consistent with the analyses performed on the interfacial size of the spalled outer chromia layers observed on the surface of the 347SS samples.

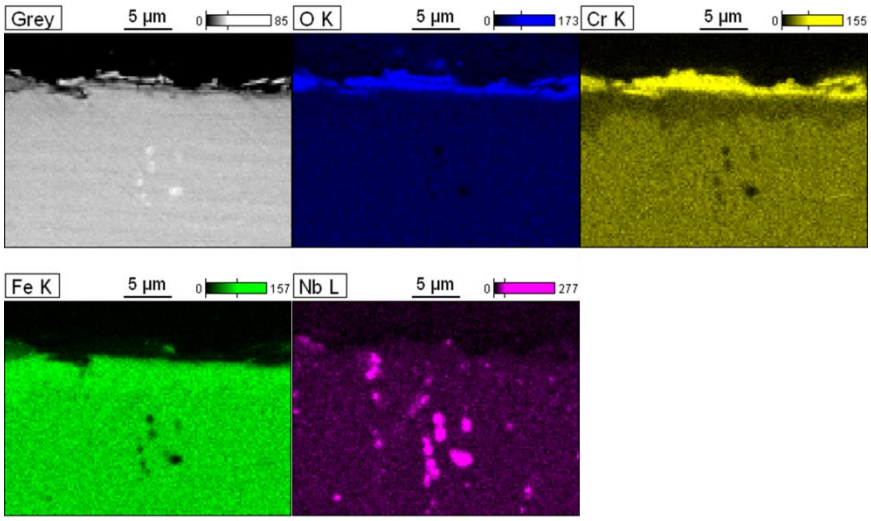

Fig. 103: EDS maps of 347SS after exposure to Experiment 5 conditions reveal outer chromia layer and corresponding inner layer deplete in chromium

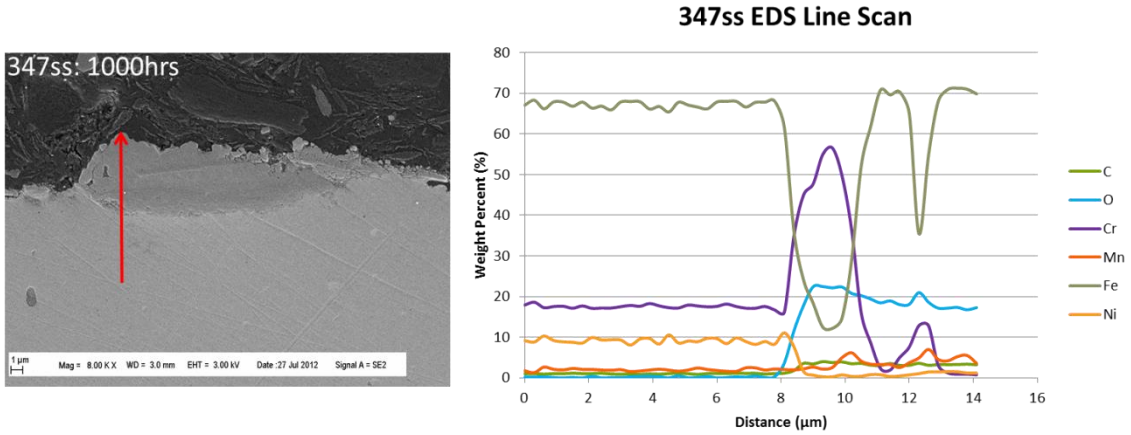

Fig. 104: EDS line scan through large oxide outgrowth on 347SS after 1000 hours exposure to Experiment 5 conditions

Cross-sectional analysis of the AFA materials corroborated the results of surface analysis representing notable oxide development nucleated at sites containing increased concentrations of niobium (*Fig. 105*, *Fig. 106*, and *Fig. 107*). These cross-sectional EDS maps also revealed outer layers of iron rich oxide, and inner oxide layers consisting of

aluminum and chromium. AFA-OC10 additionally contained a noticeable presence of manganese, consistent with manganese oxide development.

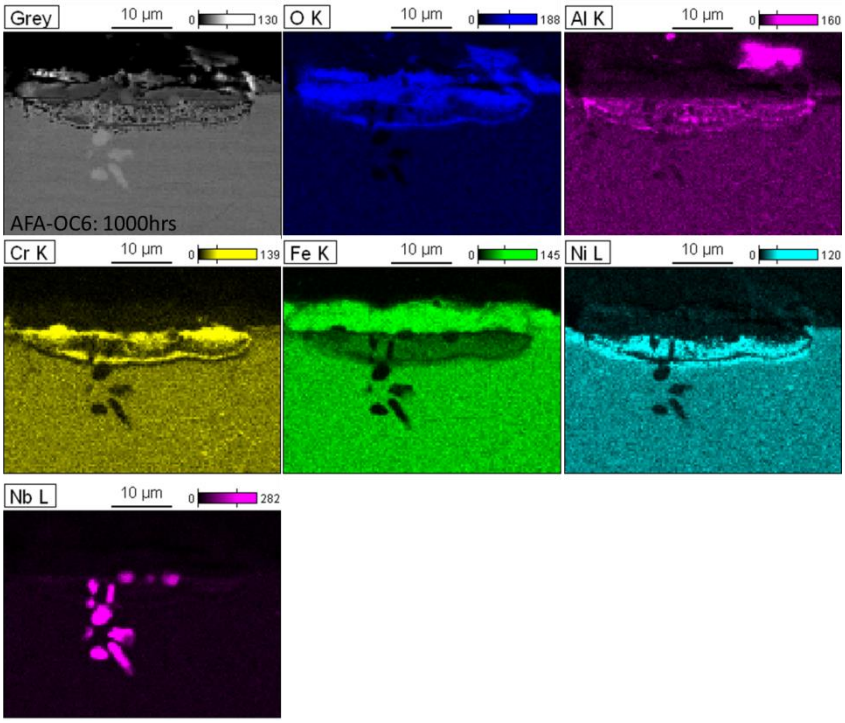

Fig. 105: EDS maps of AFA-OC6 after exposure to Experiment 5 conditions reveal large oxide growth to be associated with niobium

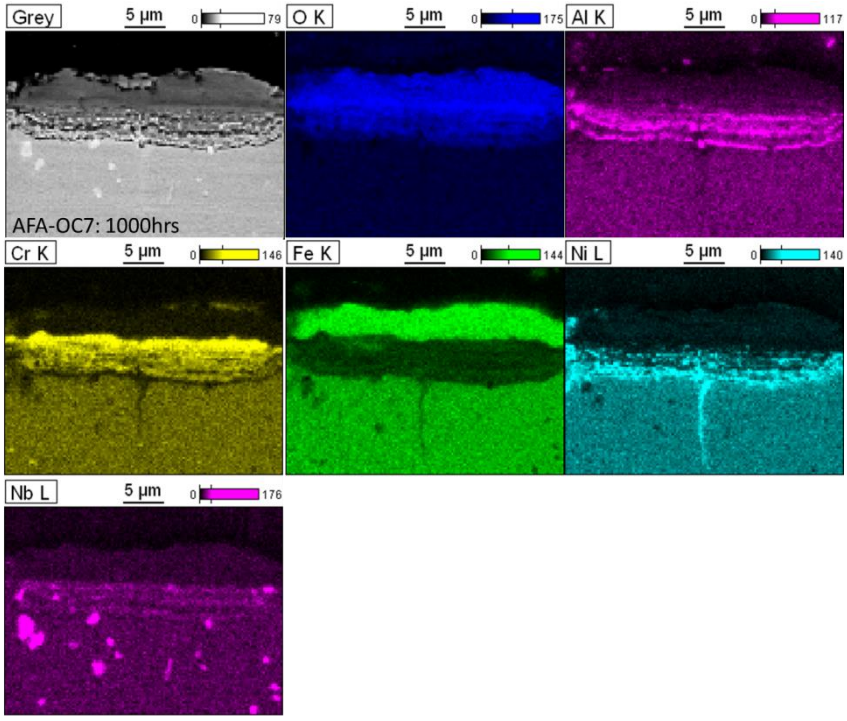

Fig. 106: EDS maps of AFA-OC7 after exposure to Experiment 5 conditions reveal large oxide growth to be associated with niobium

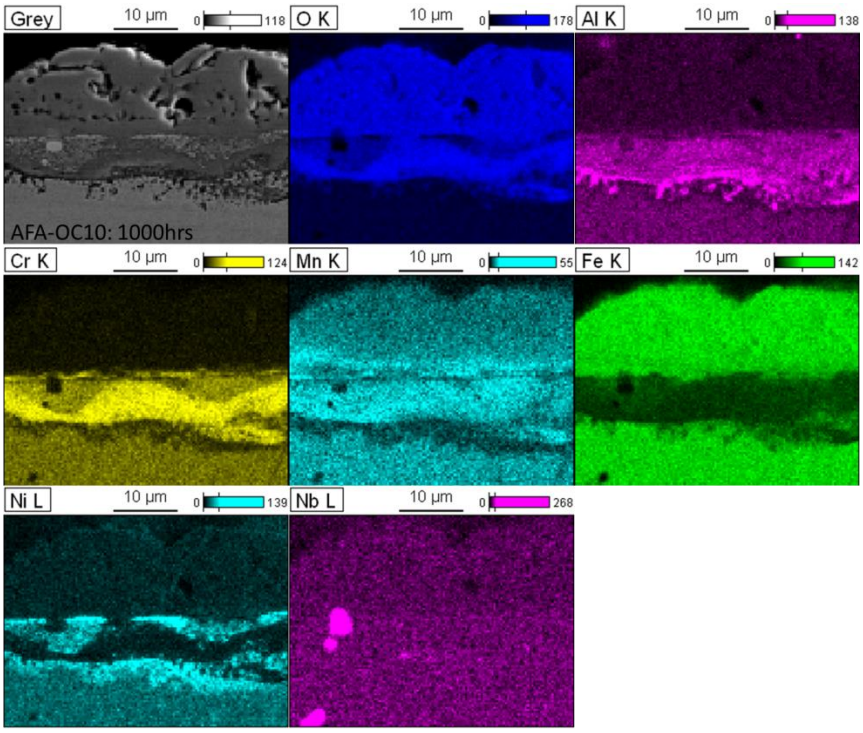

Fig. 107: EDS maps of AFA-OC10 after exposure to Experiment 5 conditions reveal large oxide growth to be associated with niobium

5.3.1 Temperature Dependence and Activation Energy

Many oxidation reactions have shown empirically that the temperature dependence of oxidation rate constants obey the Arrhenius law, enabling determination of activation energies (Q). Thus, the Matlab code described in Sec. 5.3 was also written to output correlation coefficients (R^2) and oxidation rate constants (k) for each respective rate equation. For the reasonable generated curves that described the reaction kinetics, R^2 and k values are shown below in Table 8. In many instances, the R^2 value was deemed unreasonable as a fit to the data and those rate equations were discarded for consideration. Careful analysis revealed that the oxidation kinetic rate could be most aptly described by either the parabolic, direct logarithmic, and indirect logarithmic equations which are shown in Table 8 for comparison. Using (2) and (3), the k value calculated at each temperature for each of the reasonable equations was plotted on the same curve to assess which rate equation might illustrate occurrence of linear temperature dependence. Arrhenius plots for alloys tested in phase I are shown below in *Fig. 108* through *Fig. 112*.

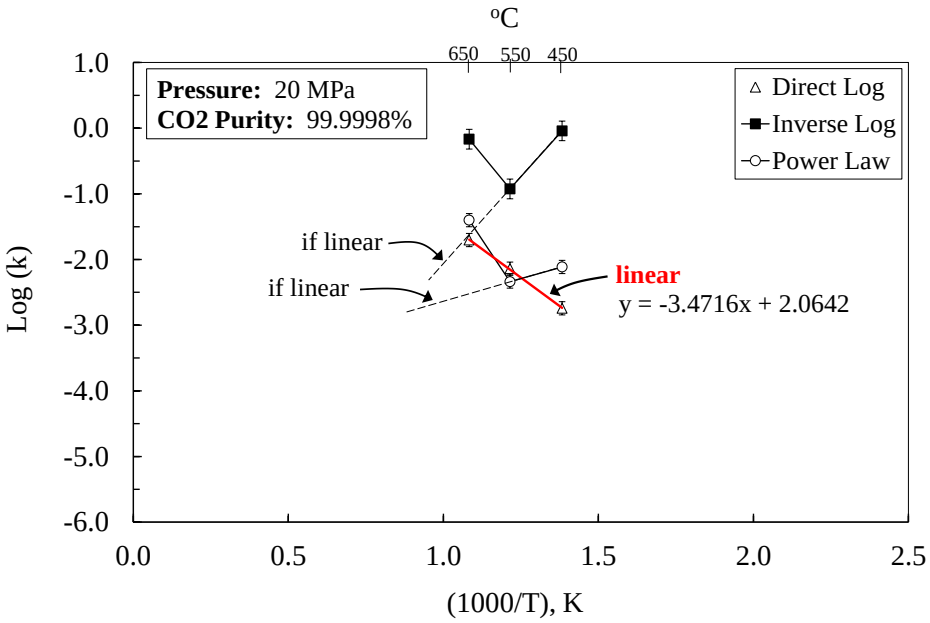

Fig. 108: Oxidation Constants of IN800H in RG-CO_2

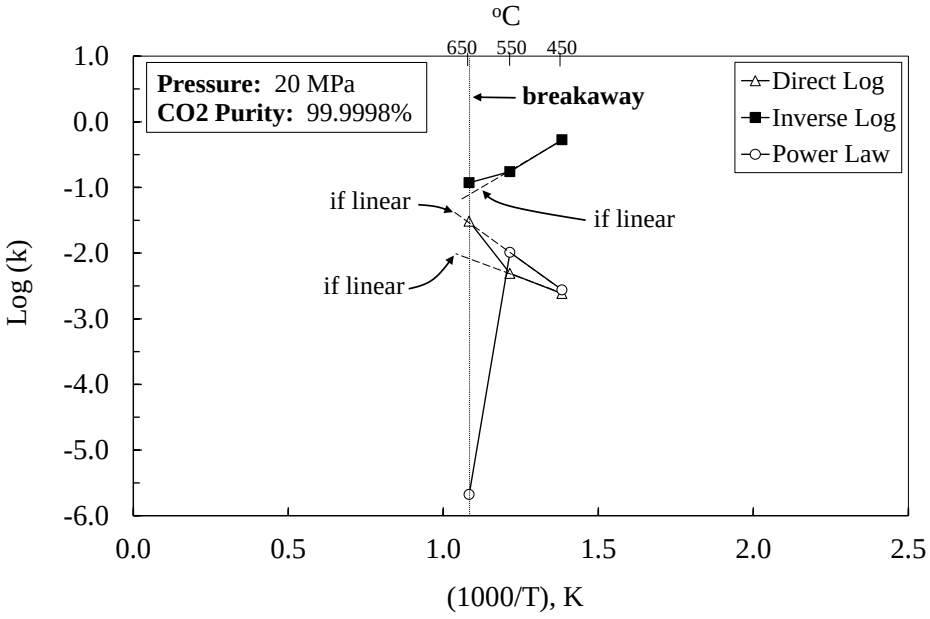

Fig. 109: Oxidation Constants of 347SS in RG-CO_2

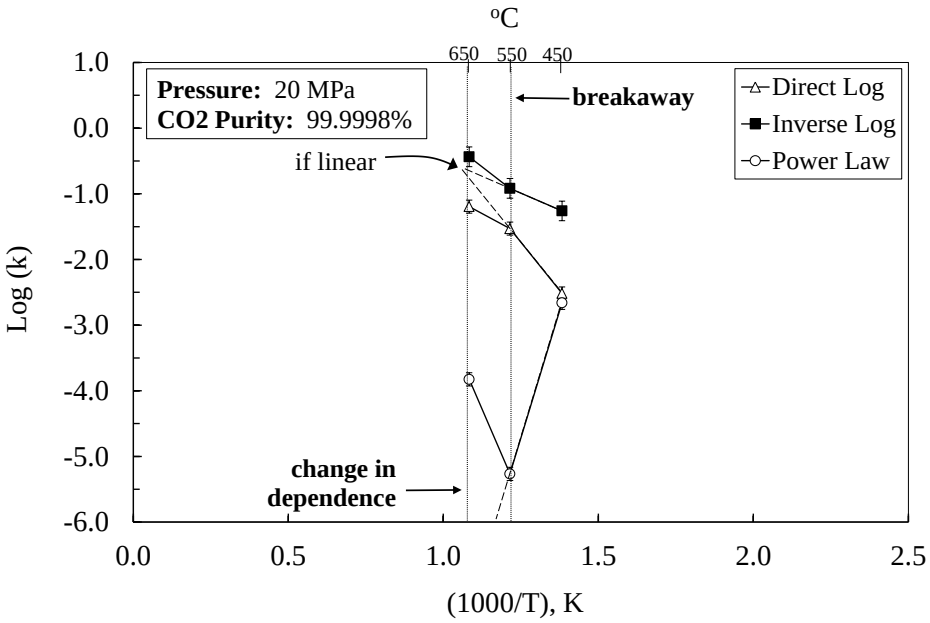

Fig. 110: Oxidation Constants of AFA-OC6 in RG-CO_2

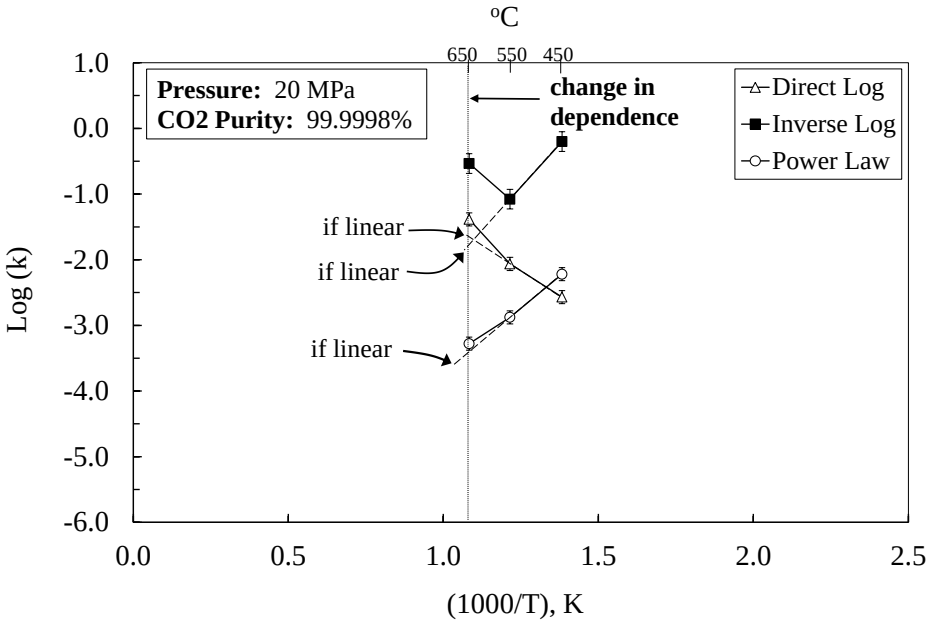

Fig. 111: Oxidation Constants of AFA-OC7 in RG-CO_2

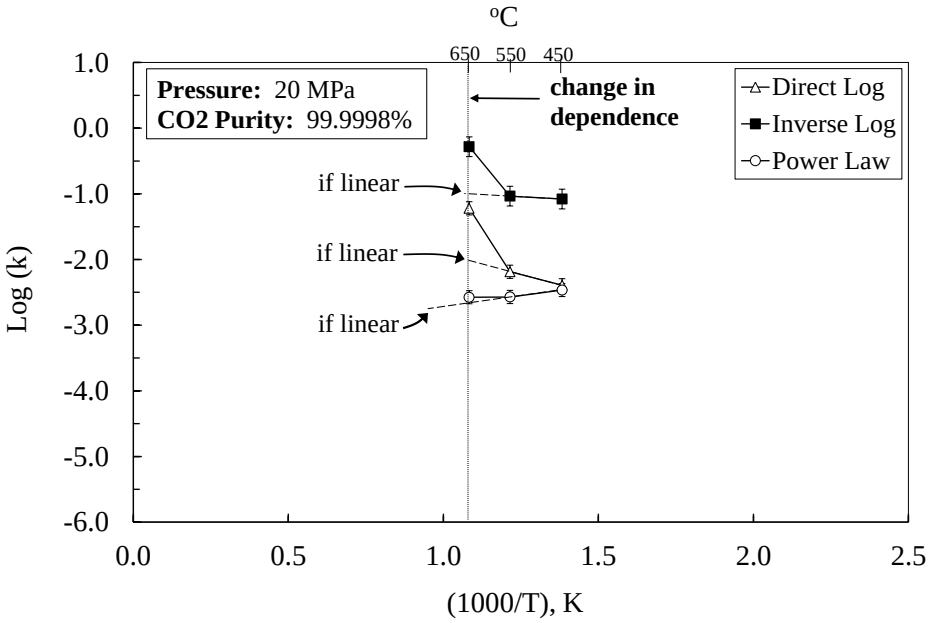

Fig. 112: Oxidation Constants of AFA-OC10 in RG-CO_2

It is noteworthy to mention that oxidation curves were singularly fit to the data at 450°C and 550°C. However, only IN800H had oxidation curves that singularly fit the data through 650°C (*Fig. 49*). All other alloys tested in RG-CO_2 at 650°C could best be described by a combination of rate equations. This is not all too surprising since even pure and binary metals have shown a deviation in temperature dependence at high temperature, resulting in two lines of differing slopes. According to Kofstad , over the temperatures where there is a linear dependence, the activation energy remains constant as long as the same rate-determining (single diffusion) mechanism prevails, and changes in temperature dependence may therefore signify changes in the oxidation (diffusion) mechanism. Also, if the oxidation follows different rate equations but has the same activation energy, the same basic mechanism is not operative in both [35]. It is also possible that two or more diffusion mechanisms may operate simultaneously, known as the two-mechanism hypothesis,

postulated thermodynamically by Gibbs [62, 63]. In the Arrhenius plots above, only IN800H demonstrated linear temperature dependence, and it did so by a direct logarithmic fit. From the slope of the best fit line, IN800H was found to have an activation energy of 28.8 kJ/mol. In other supercritical environments, such as supercritical water (SCW), Was and Teysseyre have mentioned that virtually no free radical reaction rates follow an Arrhenius law [64].

Table 8: Calculated Rate Constants of Alloys at 450°C, 550°C, and 650°C in RG-CO_2

		Power-law			Direct Log			Inverse Log			Combination
Material	**Temp.**	**k_p ($mg^2\ cm^{-4}\ hr^{-1}$)**	**n**	**R^2**	**k_{log} ($mg^2\ cm^{-4}\ hr^{-1}$)**	**n**	**R^2**	**k_{ilog} ($mg^2\ cm^{-4}\ hr^{-1}$)**	**n**	**R^2**	
HCM12A	450°C	2.26E-01	0.29	1.000	-	-	-	-	-	-	-
NF616	450°C	1.07E-01	0.40	1.000	-	-	-	-	-	-	-
347SS	450°C	2.76E-03	0.27	0.995	2.42E-03	1.00	0.98	5.32E-01	77	0.91	-
AFA-OC6	450°C	2.19E-03	0.34	0.994	3.04E-03	1.00	0.95	5.49E-02	169	0.99	-
AFA-OC7	450°C	6.03E-03	0.16	0.962	2.69E-03	1.00	0.96	6.29E-01	69	0.93	-
AFA-OC10	450°C	3.43E-03	0.32	0.987	4.05E-03	1.00	0.95	8.33E-02	115	0.98	-
IN800H	450°C	7.69E-03	0.29	1.000	1.81E-03	1.00	0.97	9.09E-01	95	0.98	-
347SS	550°C	1.03E-02	0.17	0.999	4.91E-03	1.00	1.00	1.74E-01	69	1.00	-
AFA-OC6	550°C	5.43E-06	1.61	0.987	2.95E-02	0.98	0.46	1.21E-01	60	1.00	-
AFA-OC7	550°C	1.32E-03	0.58	0.969	8.63E-03	0.99	0.81	8.36E-02	96	0.98	-
AFA-OC10	550°C	2.68E-03	0.43	0.997	6.51E-03	0.99	0.91	9.21E-02	94	0.99	-
IN800H	550°C	4.60E-03	0.36	0.990	7.26E-03	1.00	0.94	1.19E-01	76	0.99	-
347SS	650°C	-	-	-	-	-	-	-	-	-	Yes
AFA-OC6	650°C	-	-	-	-	-	-	-	-	-	Yes
AFA-OC7	650°C	-	-	-	-	-	-	-	-	-	Yes
AFA-OC10	650°C	-	-	-	-	-	-	-	-	-	Yes
IN800H	650°C	3.97E-02	0.18	0.999	1.98E-02	1.00	1.00	6.78E-01	17	1.00	-

Note: Calculated values based on 1000 hours of exposure, except for HCM12A and NF616 at 450°C, which were tested up to 800 hours.

The oxide layer of AFA-OC6 at 450^{o}C was mainly composed of continuous and protective Al_2O_3 and Cr_2O_3 layers, whereas at 550^{o}C the oxide layer exhibited non-protective oxidation at a linear to exponential rate, characterized by definition as breakaway oxidation. The mechanism of breakaway oxidation relates to the depletion of Al and Cr arising from their selective oxidation. Intrinsic chemical failure develops when the Al and Cr concentration within the alloy at the oxide/metal interface is less than those in equilibrium with Al_2O_3 and Cr_2O_3. The oxides will change to the less protective $FeCr_2O_.$ At 650^{o}C, the oxidation curve was more S-shaped with a rapid growth (ballooning effect) shown by weight gain and thickness of the oxide layer up to 600 hour, after which some healing of the oxide layer took effect, but to a degree that left it still in an unprotective state. Investigation into the surface morphology of the tarnishing (thin) layer on AFA-OC6 at 650^{o}C revealed several individual layers, comprising a multilayer series of $M/FeCr_2O_4/Fe_2O_3/CO_2$. Considering the identification of Al_2O_3 and Ni-Fe particles, a more detailed arrangement of the layers is given below as (see also *Fig. 113*):

$$\underline{\mathbf{I}} \quad \underline{\mathbf{II}} \quad \underline{\mathbf{III}} \quad \underline{\mathbf{IV}} \quad \underline{\mathbf{V}} \quad \underline{\mathbf{VI}}$$

$$\boldsymbol{M(metal) \mid Fe_2Cr_2O_4, Al_2O_3 \mid Fe_2Cr_2O_4 \mid Fe_2Cr_2O_4, Al_2O_3 \mid Fe_2O_3 \mid CO_2(gas)} \qquad (13)$$

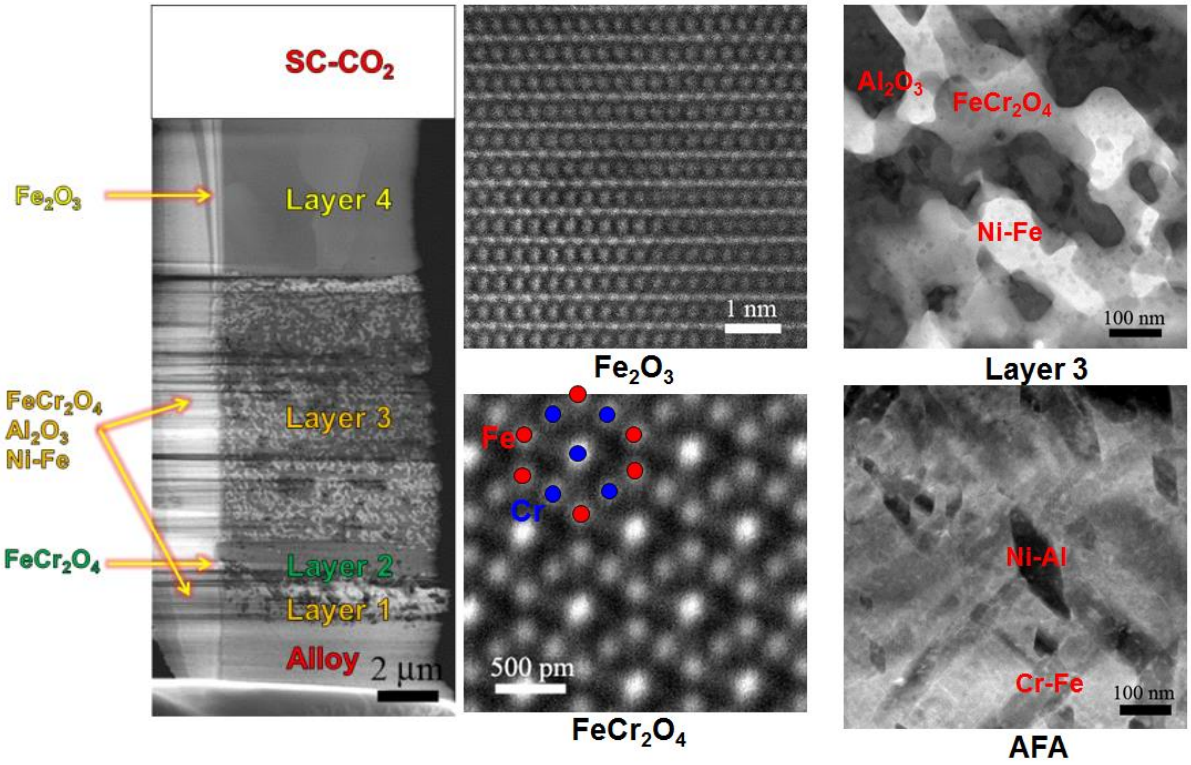

Fig. 113: STEM Cross-Section showing multi-oxide layers on AFA-OC6.
Surface after 600 hours in RG-CO_2 at 650°C, 20 MPa.

5.4. Effect of Gas Purity – Experiments 6 through 8

The purpose of this phase is to study the effect of different bulk supplied commercial CO_2 purity grades on corrosion performance. Industrial CO_2 (99.85%) and Bone Dry CO_2 were selected since these compositions can be supplied in bulk and are closer to what could be anticipated for use in plant operation. *Fig. 114* through *Fig. 118* below show weight gain results in IG-CO_2 compared to RG-CO_2 for each alloy. This is referenced as Expt. 6 in Table 5.

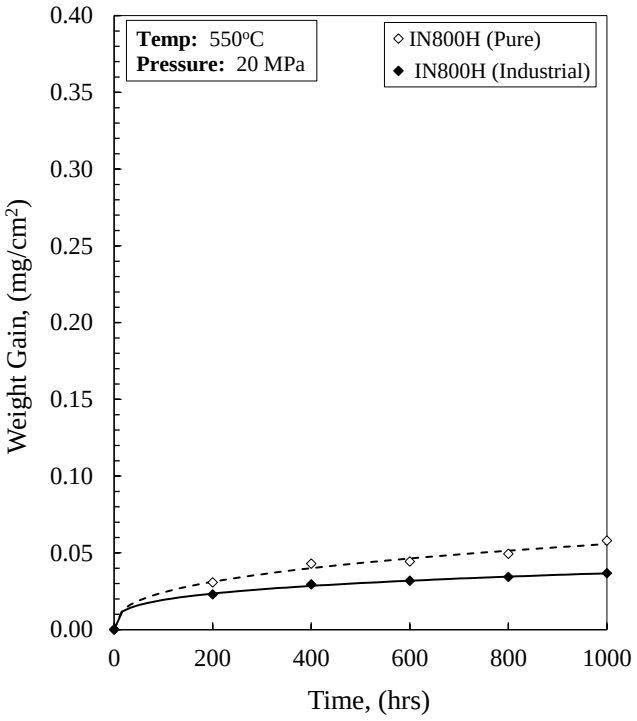

Fig. 114: Comparison of IN800H in RG-CO_2 and IG-CO_2 at 550^{o}C, 20MPa

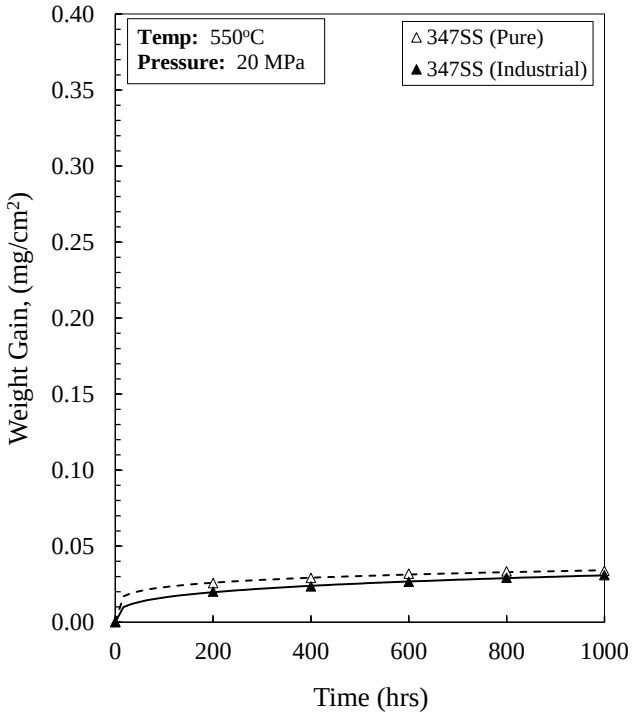

***Fig. 115*:** Comparison of 347SS in RG-CO_2 and IG-CO_2 at 550^{o}C, 20MPa

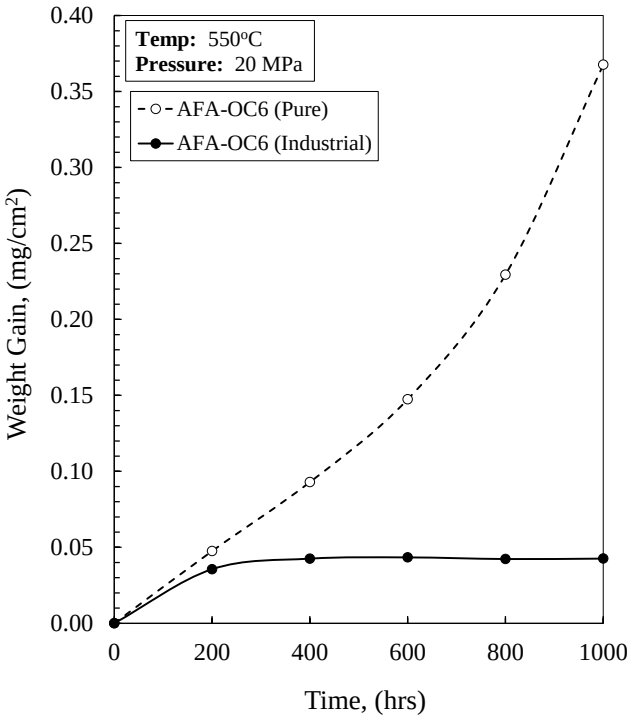

Fig. 116: Comparison of AFA-OC6 in RG-CO_2 and IG-CO_2 at 550°C, 20MPa

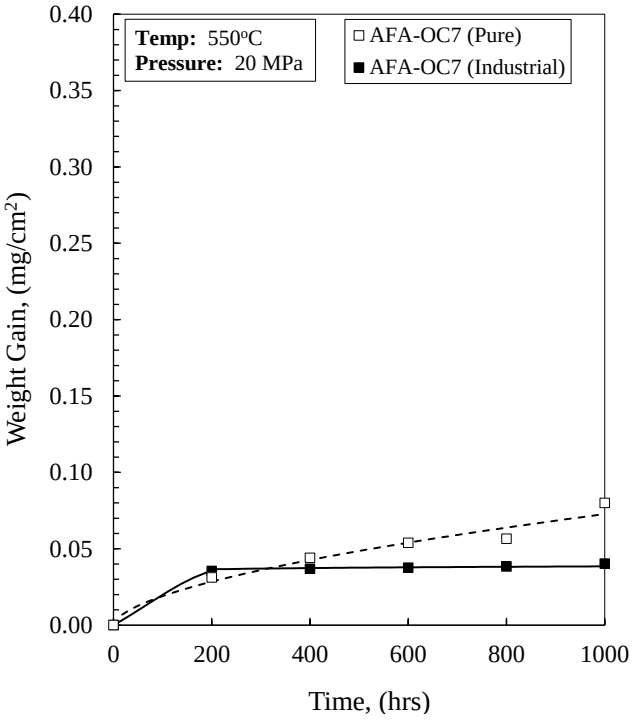

Fig. 117: Comparison of AFA-OC7 in RG-CO_2 and IG-CO_2 at 550°C, 20MPa

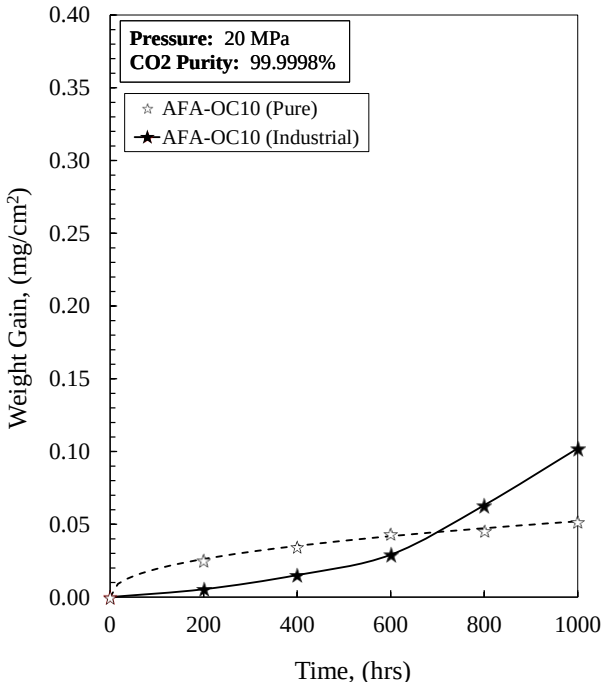

Fig. 118: Comparison of AFA-OC10 in RG-CO_2 and IG-CO_2 at 550^{o}C, 20MPa

Results generally indicate lower weight gains, which may imply that of the competing species, the oxygen content is rate determining and helps suppress oxide growth by formation of a thin protective layer. Further testing is needed to ascertain reaction products at the outlet compared to RG-CO_2 to verify this. This was not the case for AFA-OC6, which appears to have an inflection point at 600 hours and is experiencing breakaway oxidation with the inability to form a protective layer at earlier exposures. A marked improvement in weight gain is observed for AFA-OC6 (*Fig. 116*). But the biggest change in oxidation was observed by the FM steels. T92 (9%Cr) had a much larger weight gain than T122 (12%Cr) and the nature of the oxide scale formed in IG-CO_2 was significantly different than that formed in RG-CO_2. In IG-CO_2, the scale was a dark burgundy, lightly adherent, thick powdery textured scale which did not spall off (*Fig. 122*g). However, T122 showed the beginnings

on the surface of oxide spots similar in color to T92, but the formation of thick oxide scale was either suppressed or merely spalled off, owing to its much lower weight gain. It is plausible that in this particular case, the surface finish characteristics of T122 were more ground (may have been 600 grit opposed to 800 grit) than T92 which enhanced the Cr-diffusion, enabling faster formation of Cr_2O_3 to form a protective layer. Grabke has described how different surface finishes affect Cr-diffusion on ferritics and austenitics in synthesis gas [65]. SEM micrographs of T122 in *Fig. 123* clearly show how oxide has preferentially formed along polishing lines.

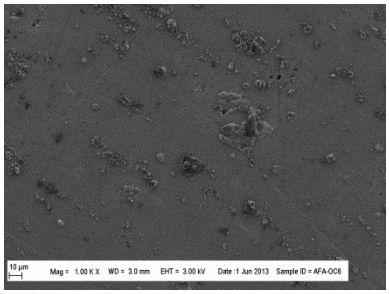

(a)

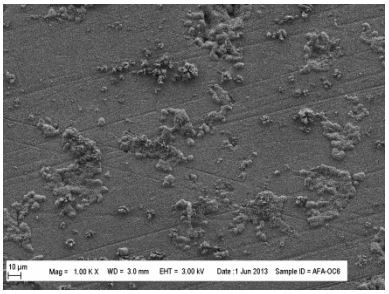

(b)

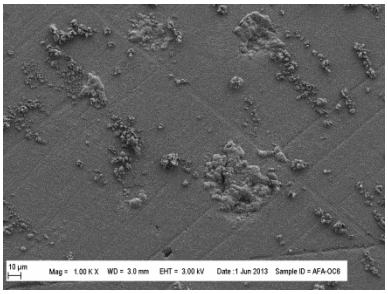

(c)

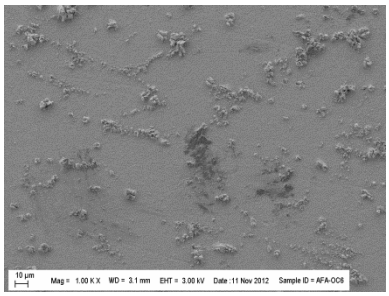

(d)

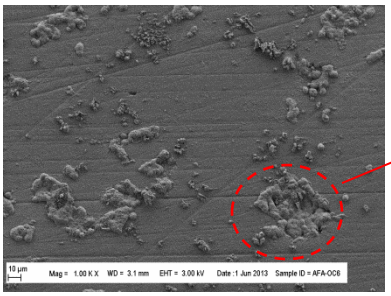

(e)

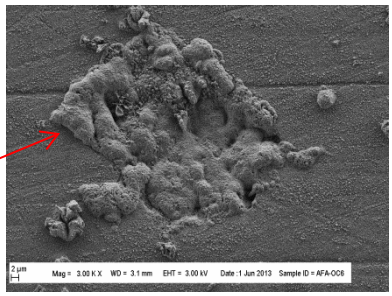

(f)

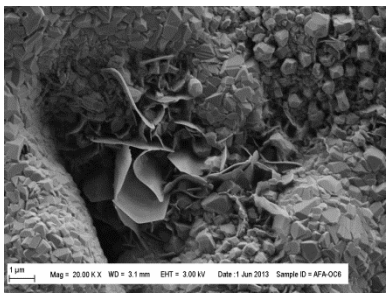

(g)

Fig. 119: SEM micrographs of AFA-OC6 in IG-CO_2 at 550^{o}C, 20 MPa.

After exposure of (a) 200 hrs, (b) 400 hrs, (c) 600 hrs, (d) 800 hrs, and (e) 1000 hrs at 1000X. (f) *Smooth textured oxide island*, prevalent at all exposure times, and (g) closeup of this oxide island at 20,000X showing a nestled, plate-like feature.

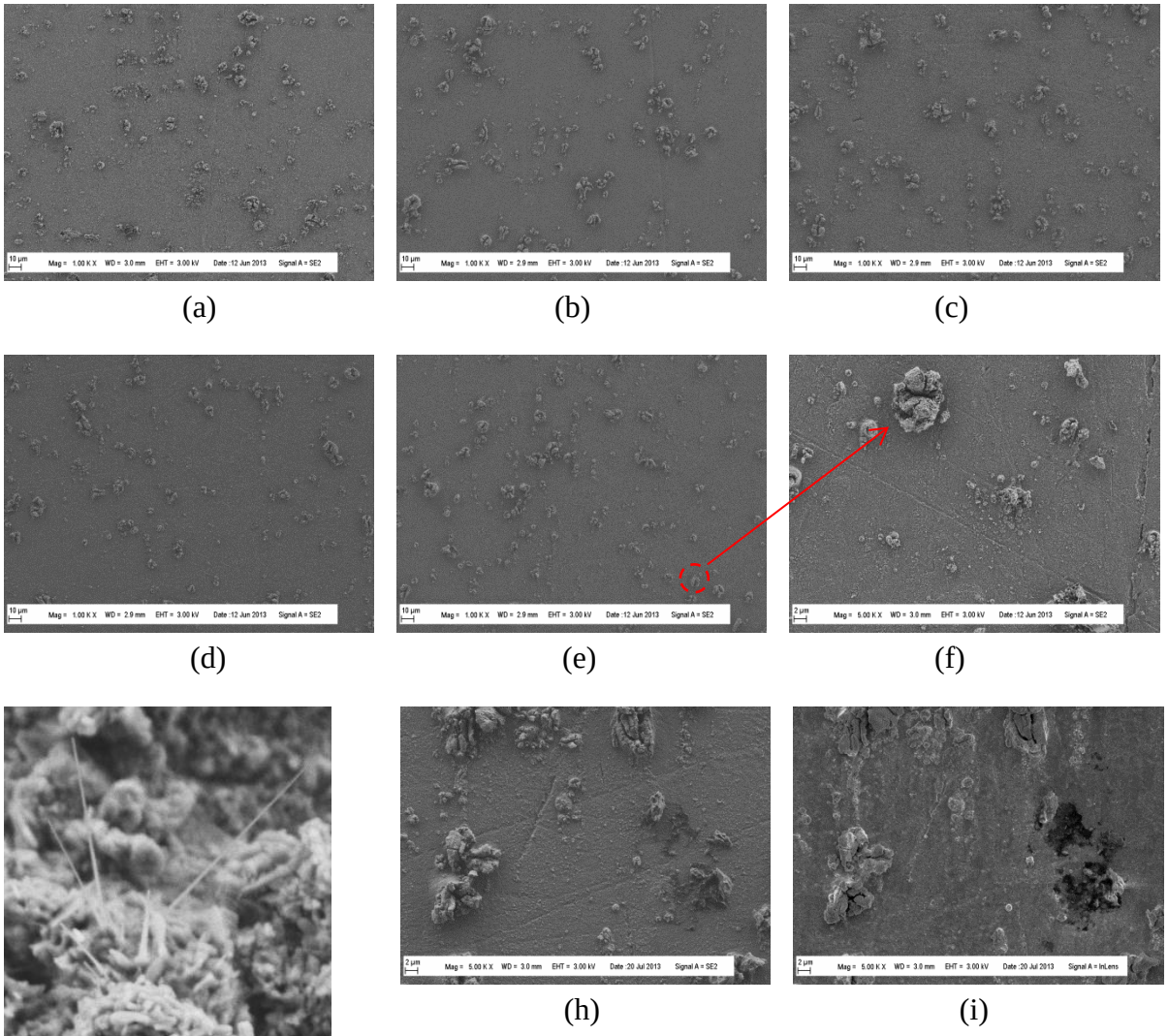

(a) (b) (c)

(d) (e) (f)

(g) (h) (i)

Fig. 120: SEM micrographs of AFA-OC7 in IG-CO_2 at 550^{o}C, 20 MPa

After exposure of (a) 200 hrs, (b) 400 hrs, (c) 600 hrs, (d) 800 hrs, and (e) 1000 hrs at 1000X. (f) *Butterfly popcorn shaped* growths, prevalent at all exposure times, and (g) closeup of this popcorn-like feature at 50,000X showing whiskers. Sparse showing of (h) carbon deposits and (i) an InLens view accentuating presence of carbon deposited on the surface.

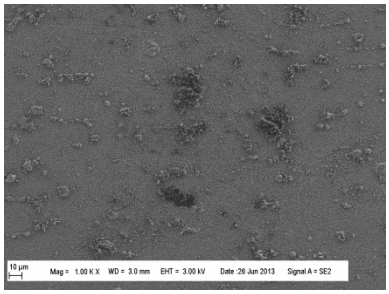

(a)

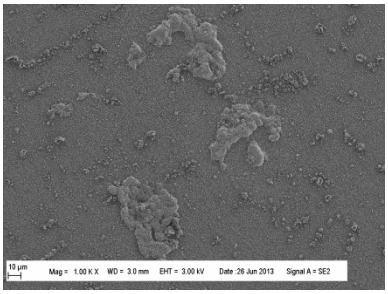

(b)

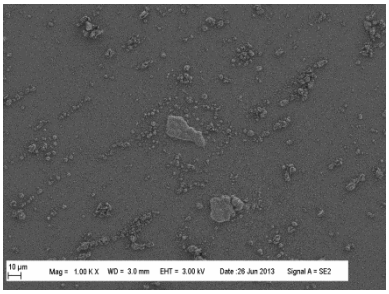

(c)

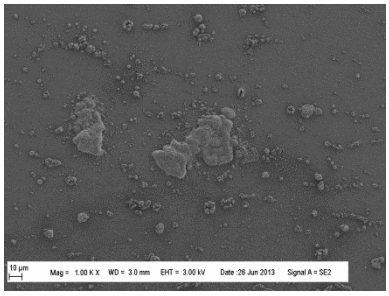

(d)

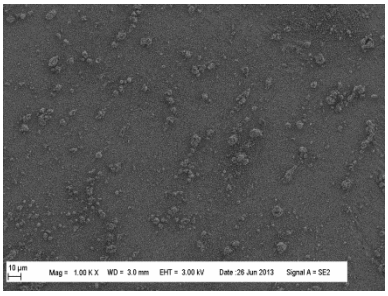

(e)

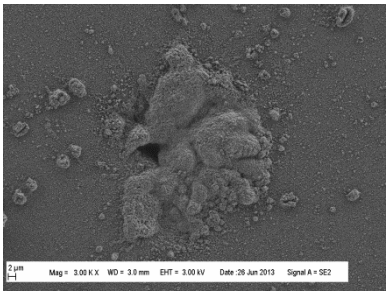

(f)

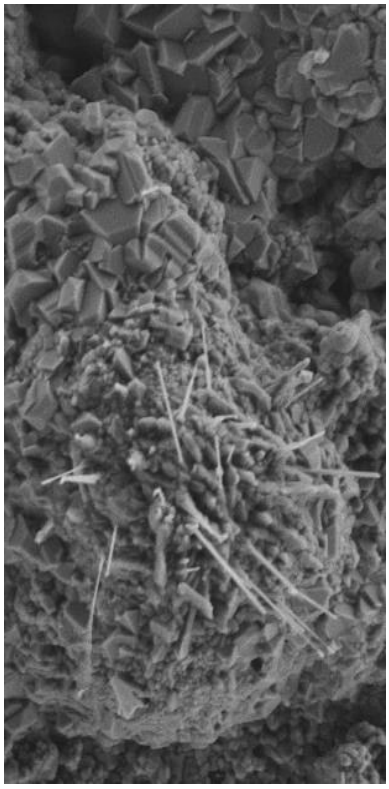

(g)

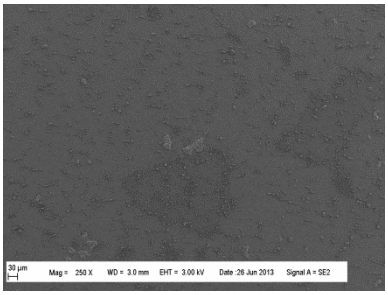

(h)

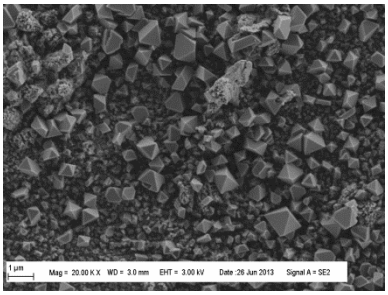

(i)

Fig. 121: SEM micrographs of AFA-OC10 in IG-CO_2 at 550^{o}C, 20MPa

After exposure of (a) 200 hrs, (b) 400 hrs, (c) 600 hrs, (d) 800 hrs, and (e) 1000 hrs at 1000X. (f) Smooth textured oxide island (same as in AFA-OC6), prevalent at all exposure times, and (g) closeup of this oxide island showing whiskers. (h) Preferential accumulation of particles resembling shape of grains and (i) closeup of polyhedral shaped particles

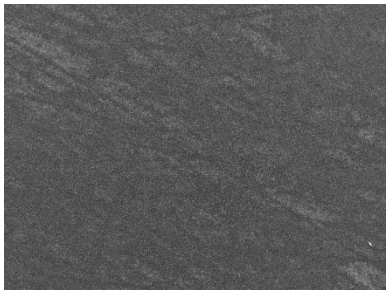

(b)

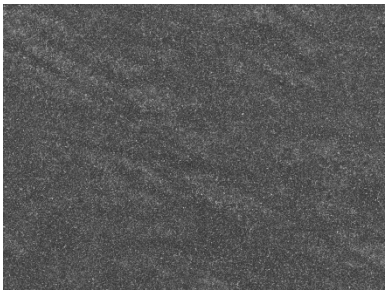

(b)

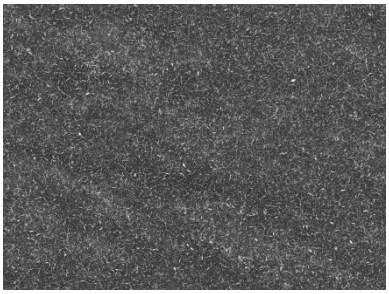

(c)

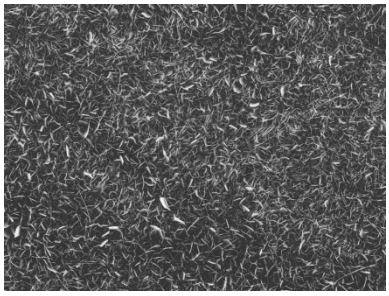

(e)

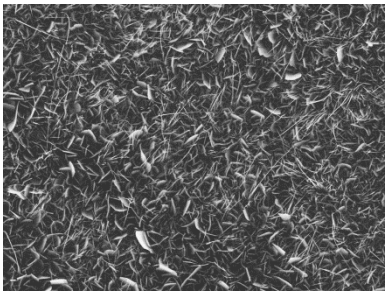

(e)

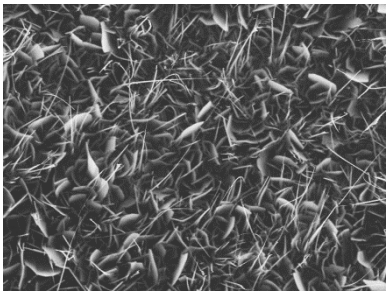

(f)

(g)

Fig. 122: SEM micrographs of NF616 in IG-CO_2 at 550^{o}C, 20 MPa

After 200 hrs exposure at (a) 125X, (b) 250, (c) 500X, (d) 1,000X, (e) 3000X, and (f) 8,000X. Oxide consisting of tight packed plate-like features with whiskers and covered entire surface. (g) Digital photograph of lightly adhered, dark burgundy, powdery-textured scale.

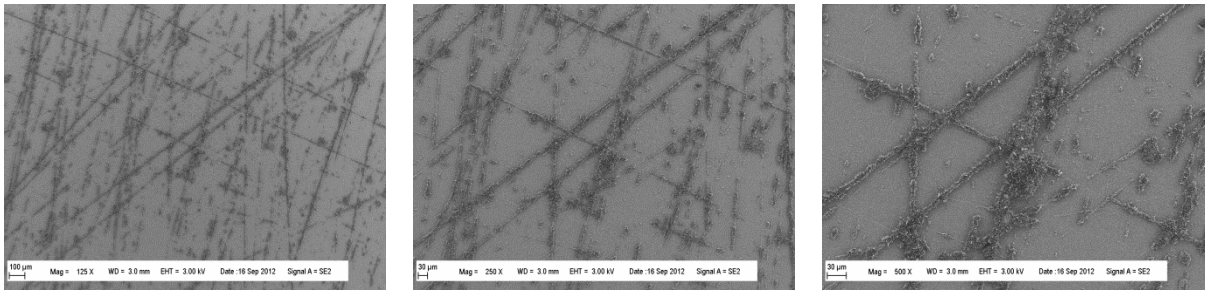

(a) (b) (c)

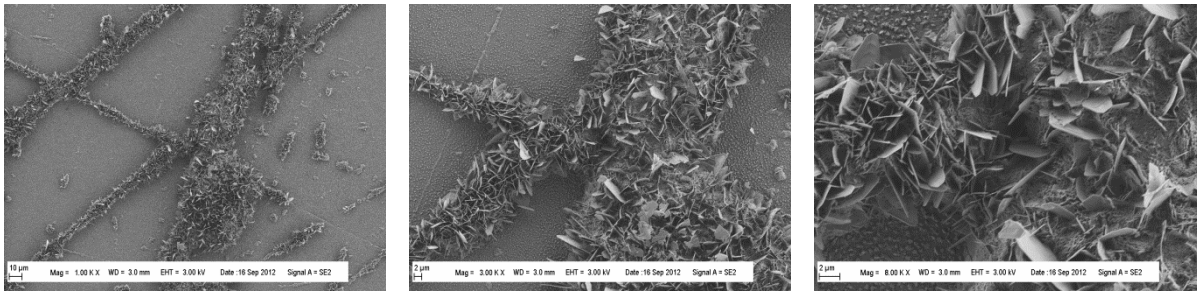

(d) (e) (f)

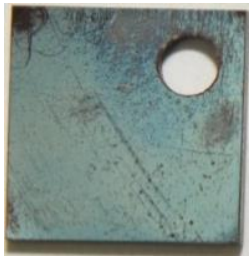

(g)

Fig. 123: SEM micrographs of HCM12A in IG-CO_2 at 550^{o}C, 20 MPa

After 200 hrs exposure at (a) 125X, (b) 250, (c) 500X, (d) 1,000X, (e) 3000X, and (f) 8,000X. Plate-like oxide with whiskers formed along polishing lines, dark burgundy in color. (g) Digital photograph showing slight sign of dark burgundy, powdery spots on surface.

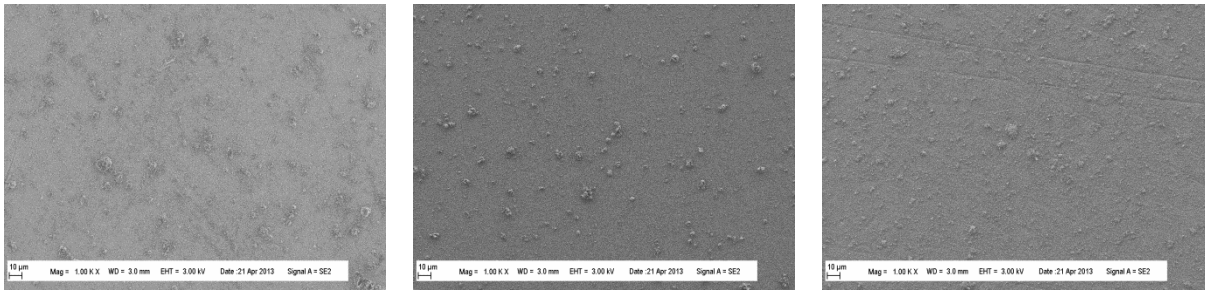

(a) (b) (c)

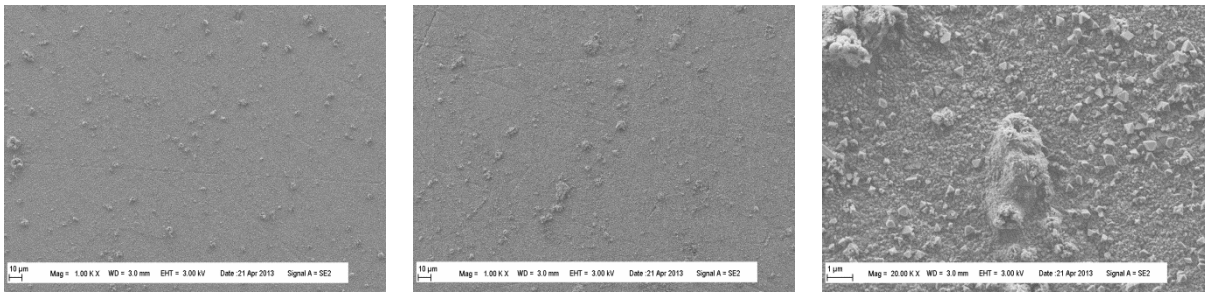

(d) (e) (f)

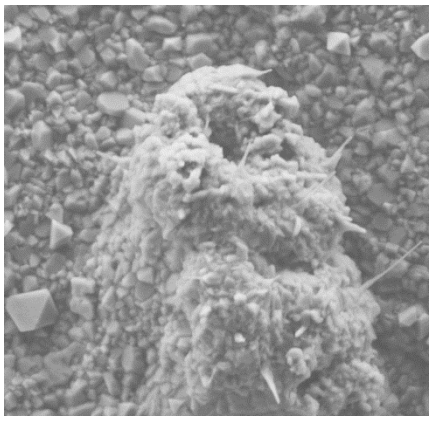

(g)

Fig. 124: SEM micrographs of 347SS in IG-CO_2 at 550^{o}C, 20 MPa

After exposure of (a) 200 hrs, (b) 400 hrs, (c) 600 hrs, (d) 800 hrs, and (e) 1000 hrs at 1,000X. (f) *Mushroom popcorn shaped* growth, prevalent at all exposure times, and (g) closeup of this popcorn-like feature at 60,000X showing small whiskers.

Cross-sections were evaluated for 316L and IN800H after 200 hours exposure, and are provided below in *Fig. 125* and *Fig. 126*. The cross-sections show a very thin oxide layer with display of little other discernible activity beneath in the substrate. Consequently, cross-sections were not evaluated at higher exposure times due to reaction kinetics demonstrating protective oxidation.

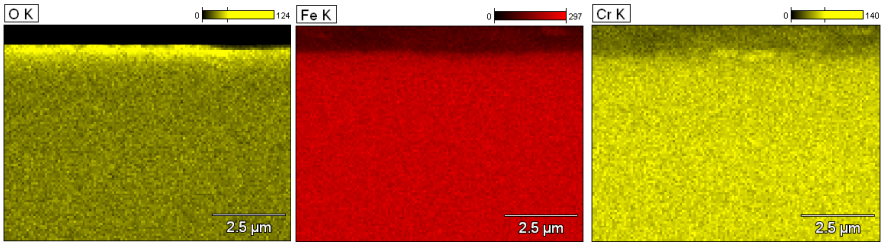

Fig. 125: Cross-Section of 316L at 550°C after 200 hours in IG-CO_2 (30,000X)

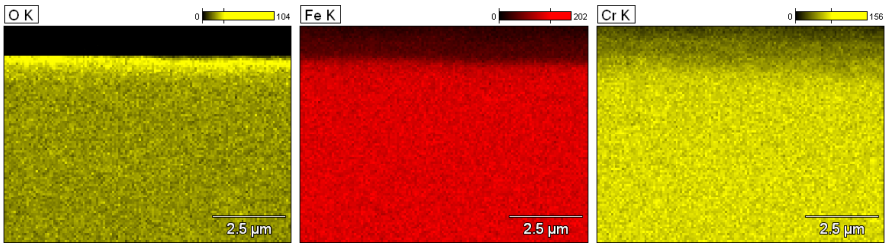

Fig. 126: Cross-Section of IN800H at 550°C after 200 hours in IG-CO_2 (30,000X)

The different morphological features observed on alloys tested in IG-CO_2 are shown below in *Fig. 127*.

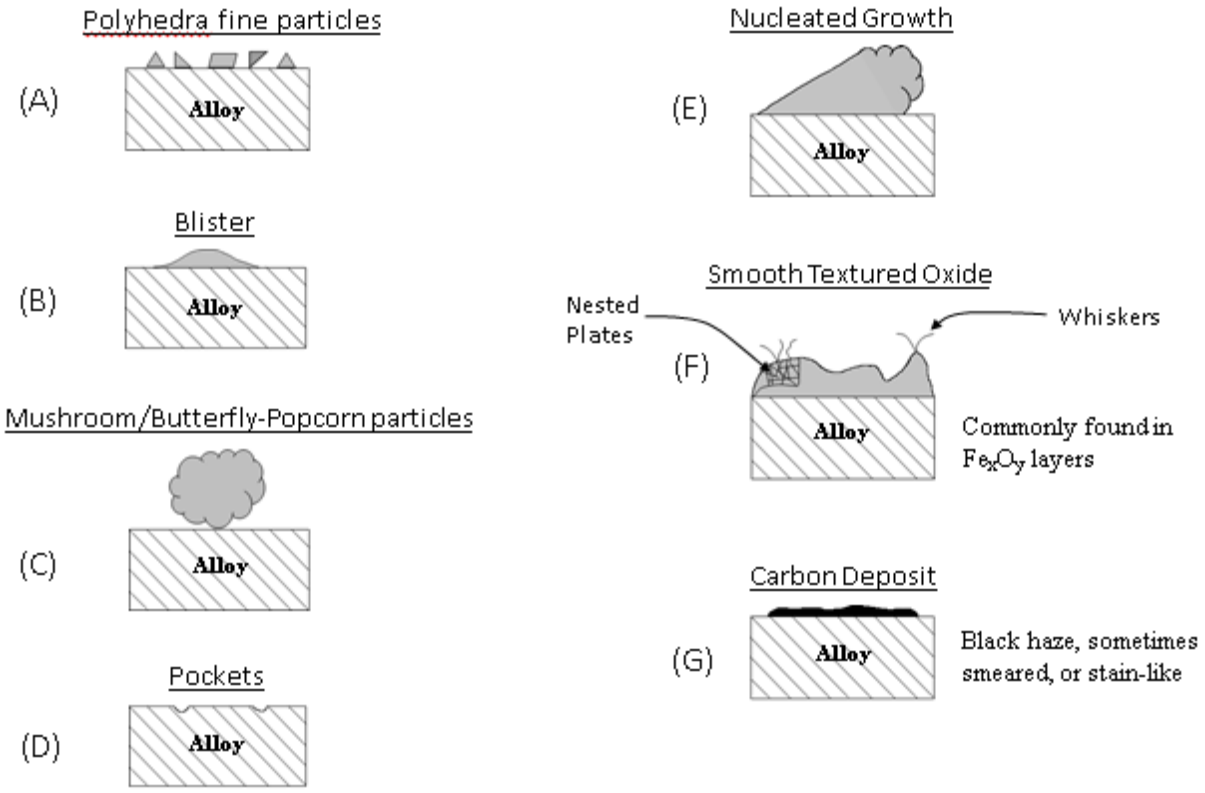

Fig. 127: Salient Morphological Features in IG-CO_2 at 550°C, 20MPa

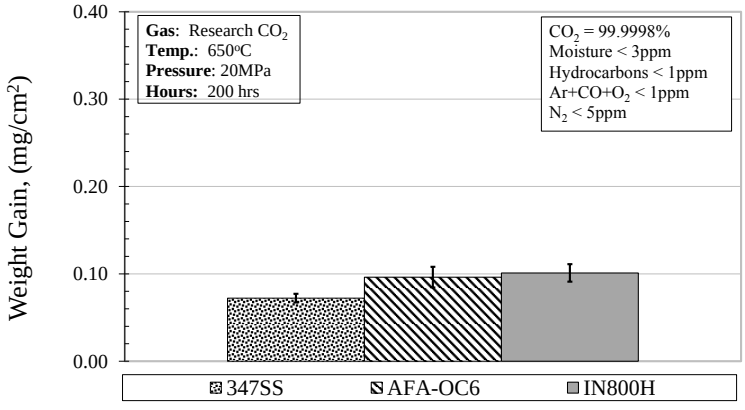

Fig. 128: Weight Gain of Alloys after 200 hours in RG-CO_2 at 650°C, 20MPa

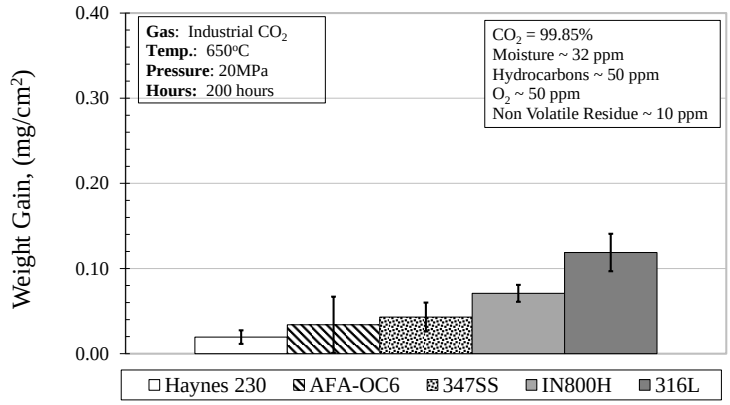

Fig. 129: Weight Gain of Alloys after 200 hours in IG-CO_2 at 650°C, 20MPa

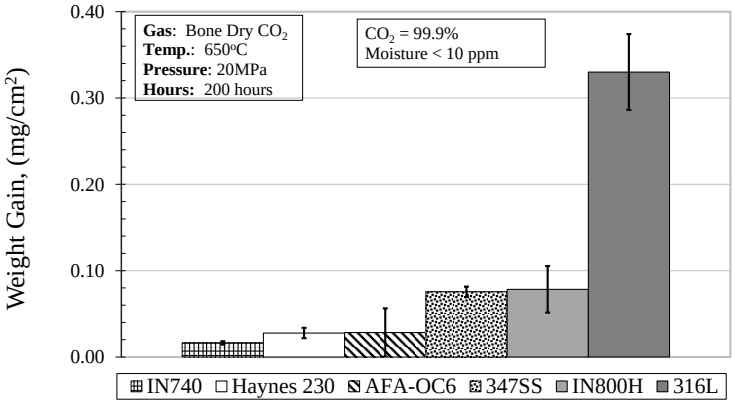

Fig. 130: Weight Gain of Alloys after 200 hours in BDG-CO_2 at 650°C, 20MPa

For Expt. 7 and Expt. 8 at the upper limit temperature of 650°C, formations of different kinds of oxides were confirmed by SEM/EDS. The evidence of carburization of alloys in these experiments at 650°C after 200 hours in different purity CO_2 levels has not been fully clarified. The summary of oxide types, approximate size, and number density in all tested alloys after corrosion in $SCCO_2$ of different impurity level are listed in Table 9.

Table 9: Assessment of Oxide Morphological Features in Different CO_2 Grades

	Research CO2 (650C, 200hr)		Bone Dry CO2 (650C, 200hr)		Industrial CO2 (650C, 200hr)	
Alloys	Oxide	Number Density	Oxide	Number Density	Oxide	Number Density
IN740	To be tested		Elongated Nb-Ti rich oxide cluster (50um)	Low	To be tested	
			Cr rich oxide (<1um)	High		
Haynes230	To be tested		Elongated W rich oxide cluster (30um)	Medium	Elongated W rich oxide cluster (30um)	Medium
			Cr rich oxide (<1um)	High	Cr rich oxide (<1um)	High
AFA-OC6	To be analyzed		Nb oxide (<10um)	High	Nb oxide (<5um)	High
			Cr-Mn rich oxide (<1um)	Very high	Cr-Mn rich oxide (<1um)	Very high
			Fe oxide (<10um)	Low	Fe oxide(<10um)	Medium
347SS	Nb oxide (<1um)	Medium	Nb oxide (5um)	Low	Nb oxide (5um)	Low
	Needle Cr-Mn rich oxide scale	Whole surface with some spallation	Polyhedral Cr-Mn rich oxide scale	Whole surface with a few spallation	Cr-Mn rich oxide (<1um)	Very high
	Polyhedral Fe oxide cluster (20um)	High	Porous polyhedral Fe oxide cluster (20um)	Medium		
IN800H	Ti oxide cluster (20um)	Low	Ti oxide cluster (20um)	Low	Ti oxide cluster (20um)	Low
	Cr-Mn rich oxide (<1um)	High	Cr-Mn rich oxide (<1um)	High	Cr-Mn rich oxide (<1um)	High

Alloys are ranked from top to bottom in the sequence of increasing weight gain (only exception is that in RG-CO_2, AFA-OC6 has a slightly higher weight gain than 347SS).

Since only plan views were examined in most of the samples, the results are represented in a qualitative way. It should also be pointed out that by looking at SEM plan view, it is difficult to distinguish whether continuous oxide layers are being formed or just distributions of high number density nano-sized oxides are forming on sample surfaces, especially due to the short

exposure time of 200 hours. Therefore, only oxide scale in samples that showed strong evidence of existing scales are listed and there could also be thin oxide scales existing in other samples, which require further investigation. Table 9 provides us a fundamental understanding of oxidation behavior of the tested alloys and seems to be consistent with the weight change data. Cr-rich oxides always showed very small size or form stable scales and are considered to be beneficial for corrosion resistance. Fe-oxides tended to have the largest size, which greatly increases the weight gain when forming, indicating poor corrosion resistance. From Table 9, it can be seen that 316L has the largest amount of Fe-oxide clusters and weight change data. It also shows that it has the highest weight gain of the austenitic stainless steels. Results of 347SS, IN800H, and 316L, clearly show that formation of Fe-oxides is greatly affected by the impurity level of $SCCO_2$. In alloys containing Nb and Ti, their oxides were clearly detected, however owing to their lower concentrations of these elements, their oxidation does not contribute significantly to weight gain.

Generally speaking, Cr and Ni are good for corrosion resistance, and alloys with higher Cr and Ni content showed lower weight gain, as mentioned in the above section. One exception is IN800H, which has higher content of both Cr and Ni than 347SS, but shows higher weight gain. This may be attributable to the short exposure time used in this experiment. Further experiments at longer exposure times are needed to confirm this conclusion.

In this experiment, the composition diversity in tested alloys was very large, such that the effect of specific elements is hard to be obtained by directly comparing two alloys. Additionally, alloy microstructure will also affect the corrosion behavior. 316L and 347SS were selected for detailed comparison because they have very close chemical composition

and similar as-received microstructure, but showed notable differences in weight gain. 347SS has niobium additions which may reduce any sensitization effects by scavenging any residual carbon.

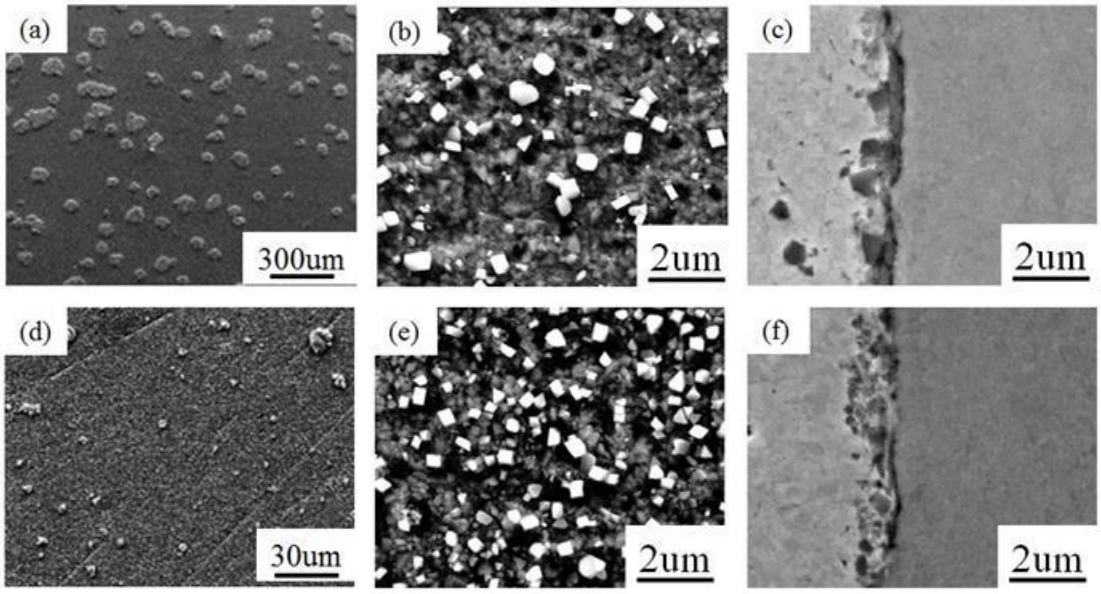

Fig. 131: Surface Morphology of 316L and 347SS at 650^{o}C after 200 hours in IG-CO_2

(a) plan view distribution of oxide nuclei, (b) magnified view of particles dispersed between and amongst those nuclei, and (c) cross-sectional view of oxide scale. Similarly, surface morphology of **347SS** showing (d) plan view distribution of oxide nuclei, (e) magnified view of particles dispersed between and amongst those nuclei, and (f) cross-sectional view of oxide scale.

As it is shown in Fig. 131a, oxide clusters with a size of about 100um were uniformly distributed on 316L stainless steel surface after exposure in IG-CO_2, and EDS results confirmed that those were Fe-oxide clusters. On the contrary, no Fe-oxide was found in 347SS, but rather Nb-oxide smaller than 10um was found to be the major oxide in this alloy (*Fig. 131*d). Higher magnification plan-view (*Fig. 131*b, *Fig. 131*e) show that in both alloys, Cr-Mn rich oxide grains with size less than 1um (bright dot in figures) were uniformly

distributed, and in the initial stages of formation of a Cr-Mn oxide scale. The size of these clusters in 316L was larger than that in 347SS, whereas their number density was lower. From the cross-section photos (*Fig. 131*c, *Fig. 131*f) it can be seen that the oxide scale in both has not yet completely formed, and the scale in 347SS was denser than in 316L. It can be concluded that, the higher weight gain of 316L was mainly caused by forming these large Fe-oxide clusters.

Fig. 132 shows a grazing incidence x-ray diffraction (GIXRD) pattern for 316L showing phases comprising the oxide. Developing a Cr-Mn rich oxide scale is effective suppressing the formation of Fe-oxide, and because 347SS has a slightly higher Cr and Mn content than 316L (~1wt% higher in Cr and ~0.4wt% in Mn), it formed a denser protective scale, thus preventing the Fe-oxide formation. 347SS contains 0.7wt% Nb (not contained in 316L), which combines with oxygen readily to form stable Nb-oxide and and precludes Fe-oxide formation. This also improves corrosion resistance of 347SS.

SEM and EDS analysis of cross-sections revealed what could be classified as thin oxide layers on many of the samples from IG-CO_2 and BDG-CO_2. It is difficult to say at which point the film thickness may be considered thin or thick, and Mott and Cabrera [66] had attempted to give description on thin layers in his theory and a critical thickness. Since the thickness of the oxide was thin, conventional XRD measurements of thin films (< 1000 nm) using a $2\theta/\omega$ scan method over the coupon surface produced weak signals from the film, significantly masked by the level of the background. Thus, grazing incidence X-ray diffraction (GIXRD) measurements were performed with a fixed low-incident angle ($\omega=1^{o}$) to maximize the signal from the thin film layer. Thin films are sometimes very difficult to

analyze due to their small diffracting volumes, which result in low diffracted intensities compared to the substrate and background. For this study, conventional XRD measurements were conducted using a scan from 10-105^{o} and a step size of 0.04 and time of 10 seconds. GIXRD measurements were made using a scan from 20-105^{o} and a step size of 0.04 and *minimum* time of 12 seconds. The yttrium coated samples however required a longer measurement time (15-20sec) to resolve identifiable peaks from the thin oxide layer and aid in comparison to other GIXRD patterns. The orientation of the coupon was kept consistent and the same for all tests. *Fig. 132* below shows a GIXRD pattern of 316L in both IG-CO_2 and BDG-CO_2. *Fig. 133* shows a GIXRD pattern for 347SS in all three different grades of CO_2.

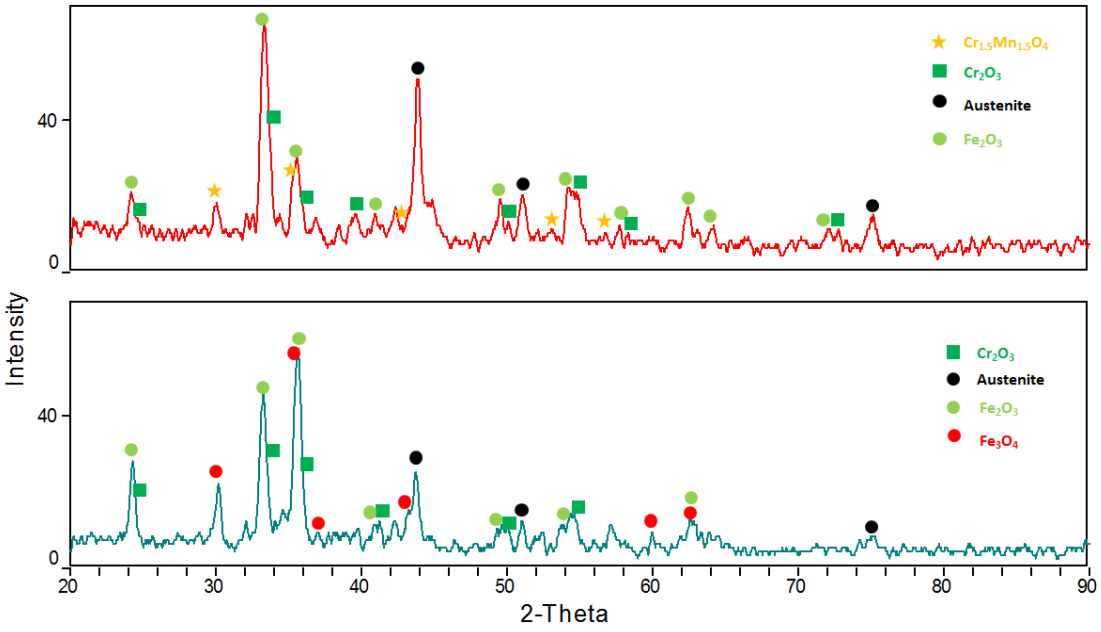

Fig. 132: GIXRD Patterns of 316L.
(a) IG-CO_2 and (b) BDG-CO_2 after 200 hours at 650^{o}C, 20MPa

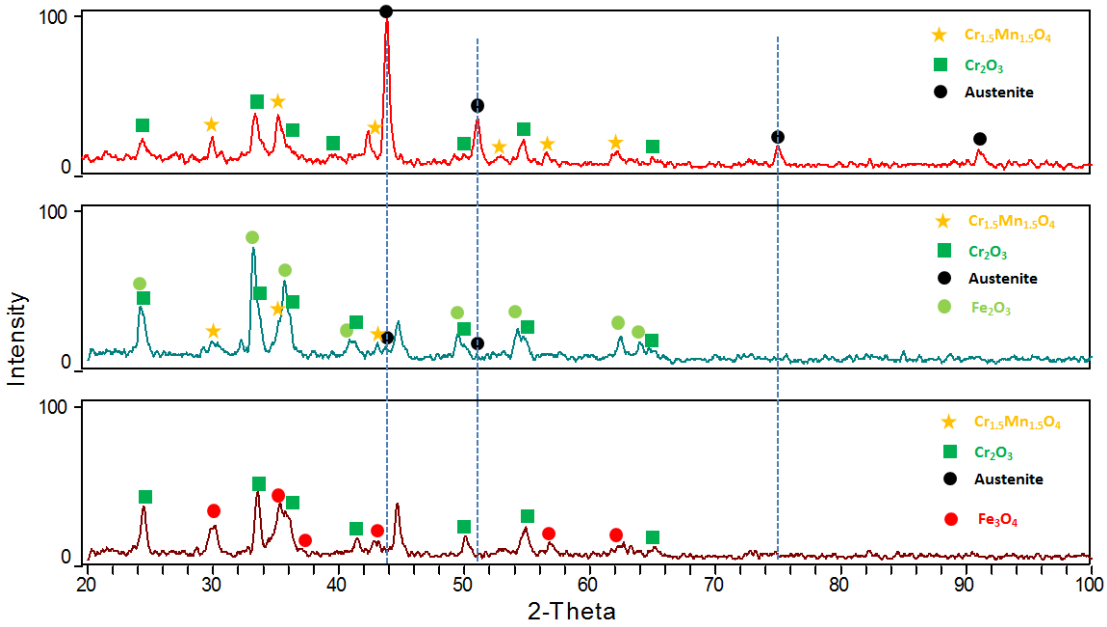

Fig. 133: GIXRD Patterns of 347SS.
(a) IG-CO_2, (b) BDG-CO_2, and (c) RG-CO_2 after 200 hours at 650°C, 20MPa

5.5. Effect of Surface Treatment – Experiment 9

5.5.1. Single Element Al Coating on 9-12%Cr Ferritic-Martensitics

Coated coupons were examined after sputtering to evaluate the deposition of aluminum onto the substrate. *Fig. 134* below shows a SEM/EDS analysis on the aluminum coated substrate after deposition and before testing.

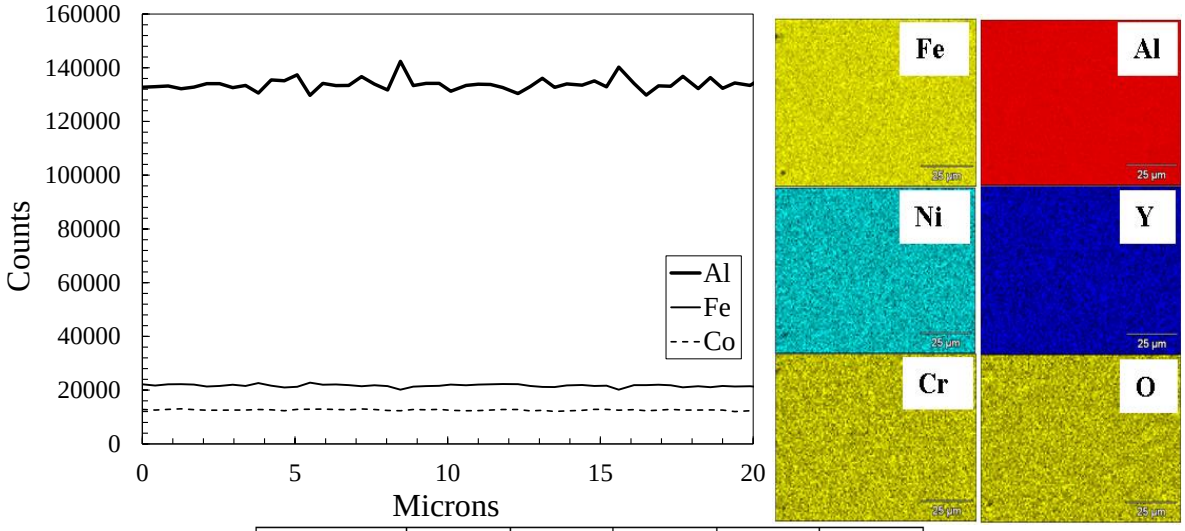

	Al	Fe	C	O	Y
Atom %	63.6	24.6	2.83	1.39	0.00

Fig. 134: SEM/EDS of **Al Coated NF616** before exposure

The metallic Al coating nominal thickness was about 500 nm. A strong signal for aluminum was detected for the aluminum coating. Aluminum is highly conductive (2.37 W/cm-K at room temperature). Aluminum coated samples were also found to be slightly magnetic. SEM cross-sections seem to suggest that the coating itself is quite irregular in thickness, which is likely due to compressive stresses exerted on the coating surface during specimen mounting in Cu for examination. SEM micrographs shown later on for heavily oxidized coated samples at 1000 hours show a more uniform layer, suggesting the coating layer was also uniform. This is discussed in more detail for the 1000 hours cross-sections. Measurements made after coating deposition on half-coated coupons to determine thickness were performed using a Tencor AlphaStep 200 surface profilometer (± 5nm resolution), which uses a contacting stylus scanned across the surface to acquire step height. Measured

thickness is provided in Table 10. The coating surface weight was determined by taking the difference in measured weight of the samples before and after coating deposition, assuming the surface area to be constant since the film applied is thin.

Coating porosity and adhesion were not measured, but the total porosity can be measured using the Archimedes technique referenced in ASTM C373-88 as done by Su et al [67], and the adhesion can be measured by the tape peel test in ASTM D3359. Results from Alvarez et al [68] suggest that the quality of the coatings, particularly their density and adhesion, are more important than the thickness of the layer deposited for effective protection against metal dusting.

The morphology of the oxide structure of aluminum coated coupons after 200 hours exposure in RG-CO_2 as seen by SEM micrographs (*Fig. 135*) formed differently in shape. Donut-shaped oxide rings formed during the initial rapid stage and were observed across much of the surface with a high number density, and were approximately 75-350um in diameter. It is presumed that the growth initiates with polyhedral shaped nuclei that rapidly grow preferentially by a flat annular shape until the entire inside is covered with additional oxide, and proceeds in this fashion migrating outward.

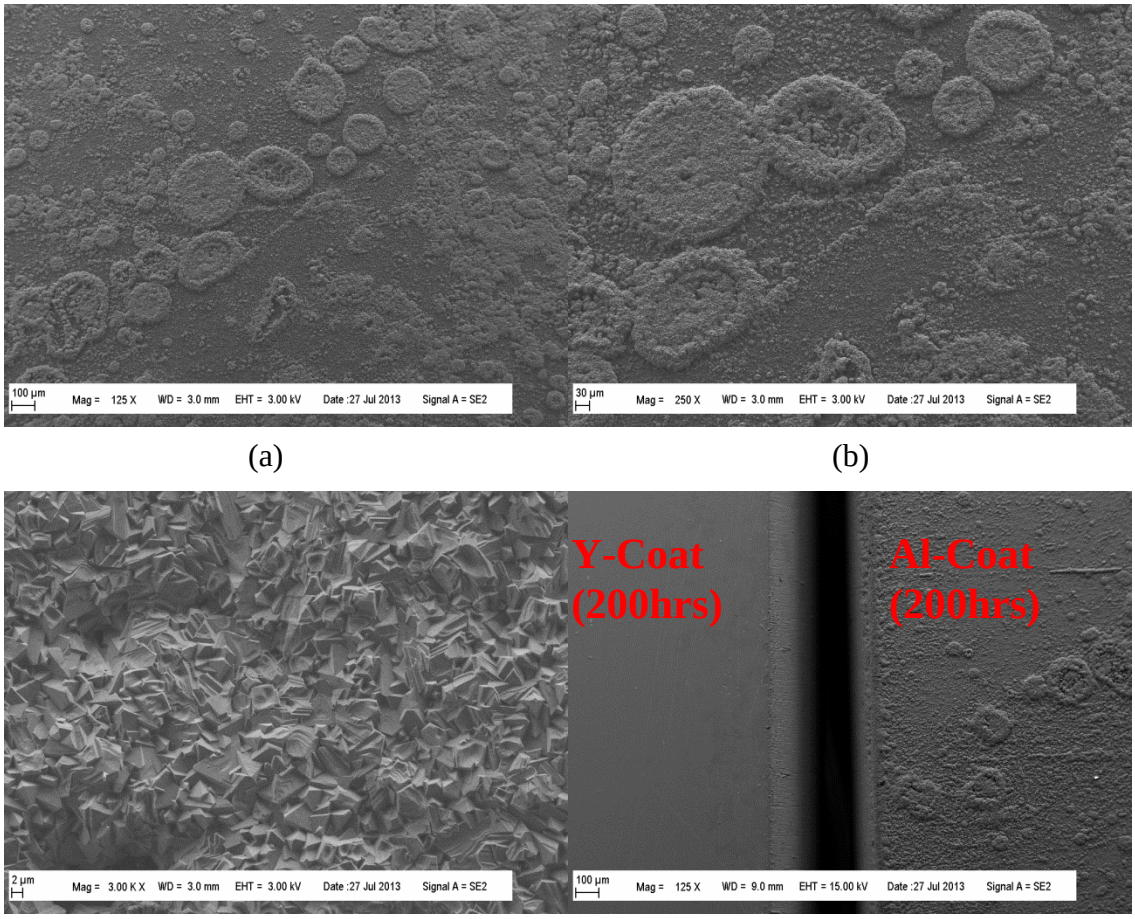

Fig. 135: SEM micrographs of **Al Coated NF616** in Research CO_2 at 550^{o}C, 20 MPa. After 200 hrs exposure at (a) 125X, (b) 250, (c) 3,000X, and (d) 125X.

After 1000 hours of exposure, a significant amount of the surface appears entirely covered with a thick oxide scale about 20-30µm in thickness and about 35 µm at the edges. *Fig. 136* show SEM micrographs of the developed oxide observed at low magnifications. *Fig. 136*c was taken of an area not exhibiting large oxide growth and shows blistering of the aluminum coating and its eventual cracking.

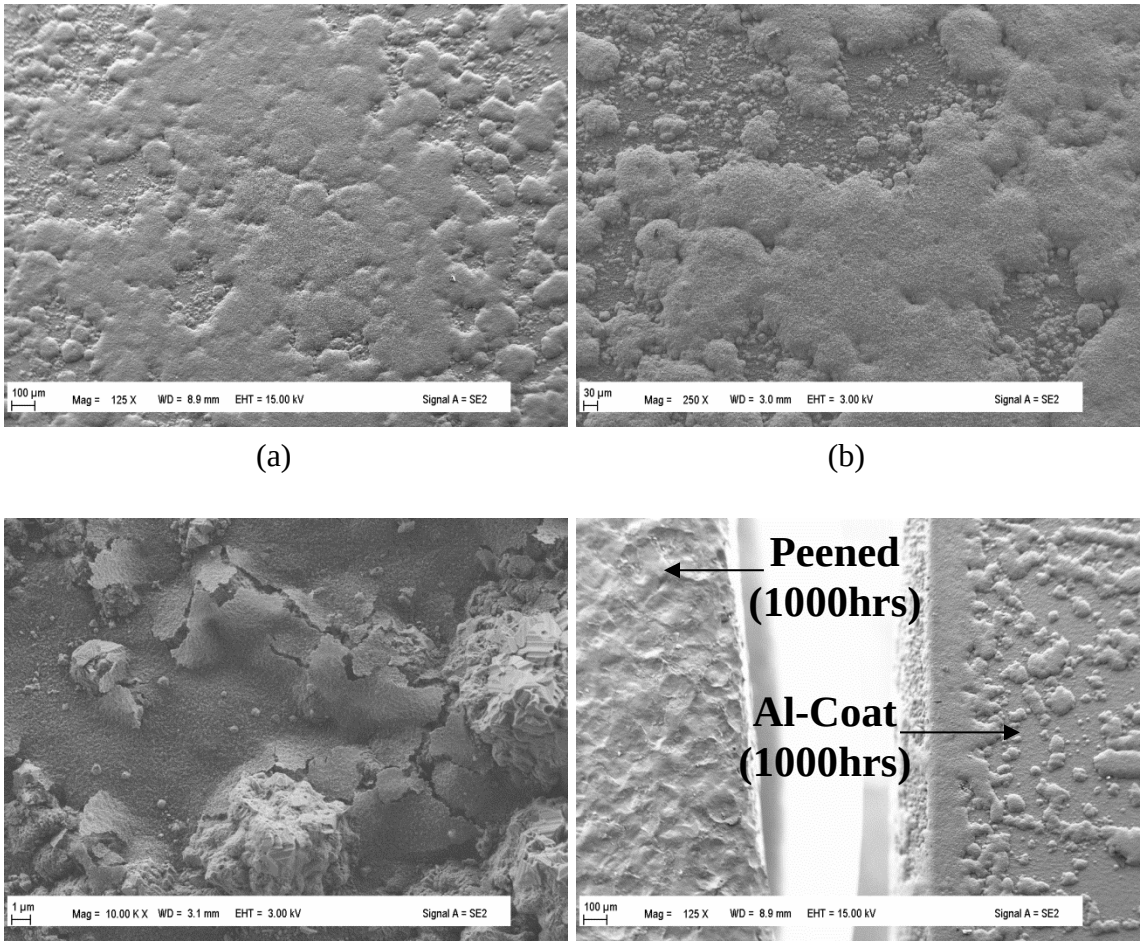

Fig. 136: SEM micrographs of Al-Coated T92 in Research CO_2 at 550^{o}C, 20 MPa. After 1000 hrs exposure at (a) 125X, (b) 250, (c) 10,000X, and (d) 125X.

Exposed coupons were electroplated with Cu to retain the features of the oxide and provide a visual contrast between possible differing features when mounted for cross-section. Cross-sections for Al-coated T92 and T122 after 1000 hours exposure are shown below in *Fig. 138* and *Fig. 141*, respectively. EDS concentration profiles of the cross-sections how two different oxide phases containing Fe and O in the outer layer and Fe, Cr, and O in the bottom layer, with a higher concentration of Fe in the outer layer. Selective analysis was performed by choosing 3 points in each differing contrasted layer and taking the atomic fraction average in each layer, respectively. EDS provided quant results of the atomic fraction (%) where the outer layer (II) displays the right stoichiometry for Fe_2O_3 (hematite), an n-type semiconductor. The bottom layer appears to have a stoichiometry not quite equivalent to that of $FeCr_2O_4$ spinel, but it's non-stoichiometry of $Fe_xCr_yO_z$ is similar in structure to that spinel, which perhaps is changing at a non-linear rate. Raman analysis was not performed, but could be performed to support these findings, similar to what Roulliard did for T91 [69]. *Fig. 145* shows a schematic of the duplex oxide scale formation on the Al-coated samples. *Fig. 143* shows the GIXRD patterns of Al-coated T92 and T122, confirming the oxide scale characterized by SEM/EDS cross-sections. It is difficult to say for certain, but closer examination shows what one could interpret to be a higher density of holes or pores in the bottom layer than in the top layer. Rouillard referred to these holes at the oxide-metal interface as voids. Also, the bottom layer texture differs from the top, where the top appears to be more solid and dense and the bottom more loose and porous. Based on weight gain data, it may be that initially through 200 hours the rate of oxidation is parabolic but becomes linear and essentially remains linear, a combined reaction rate termed paralinear oxidation. Kofstad describes such a system and proposes a model, whereby a compact scale growing at

a parabolic rate transforms at a linear rate to an outer porous and non-protective oxide layer if a diffusion layer is depleted by sublimation of oxide (*Fig. 137*). Supposedly, the inner layer approaches a stationary thickness such that it grows at the same rate at which it is consumed by the linear depletion. But the stoichiometry and surface features when evaluated together seem to favor what may be in this case a compact dense outer layer and a more loose and porous bottom layer.

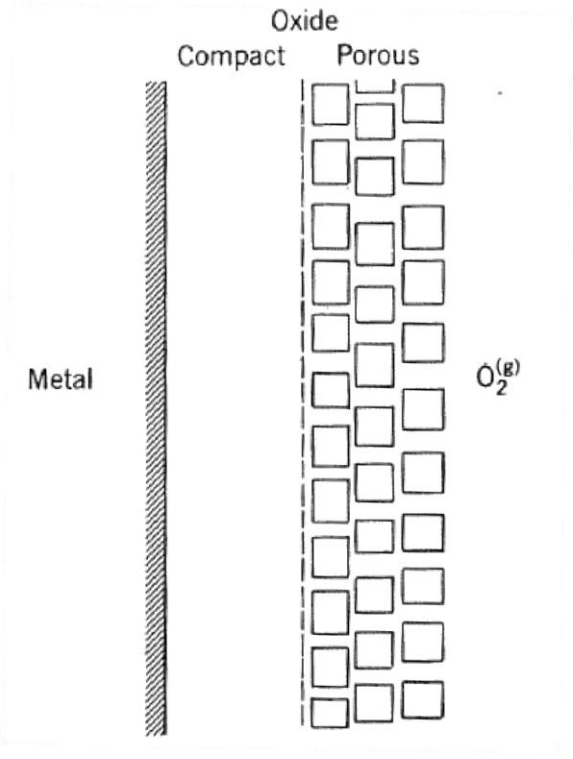

Fig. 137: Model for paralinear oxidation growth of duplex scale [35].

An inner compact scale (parabolic) which at a linear rate is converted to an outer, porous, nonprotective scale.

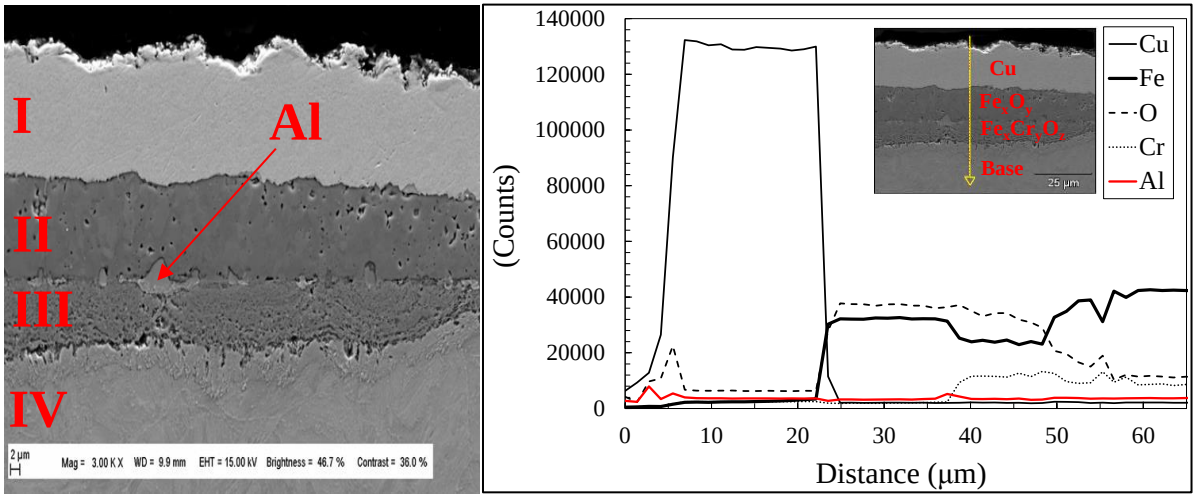

Layer	Cu	Fe	Cr	O
I	95%	-	-	-
II	-	49%	0.25%	48%
III	-	39%	13%	45%
IV	-	88%	9%	0%

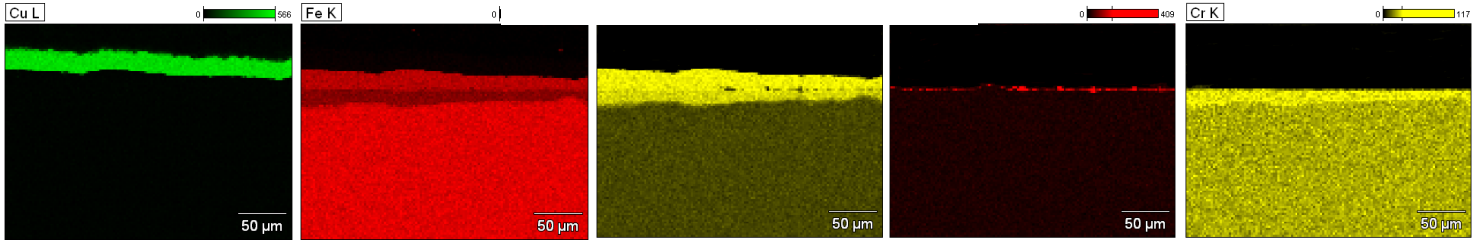

Fig. 138: Cross-Section of Al-Coated T92 after **1000** hours in RG-CO_2/550°C/20MPa. Electroplated with Cu for enhanced characterization. **Top Left**: Atom % of layers hinting dual density Fe-Oxide layer formation (taken at 3000X). **Top Right**: EDS linescan through layers showing lower Fe, higher Cr content in bottom layer. **Bottom**: Spectral maps of key elements.

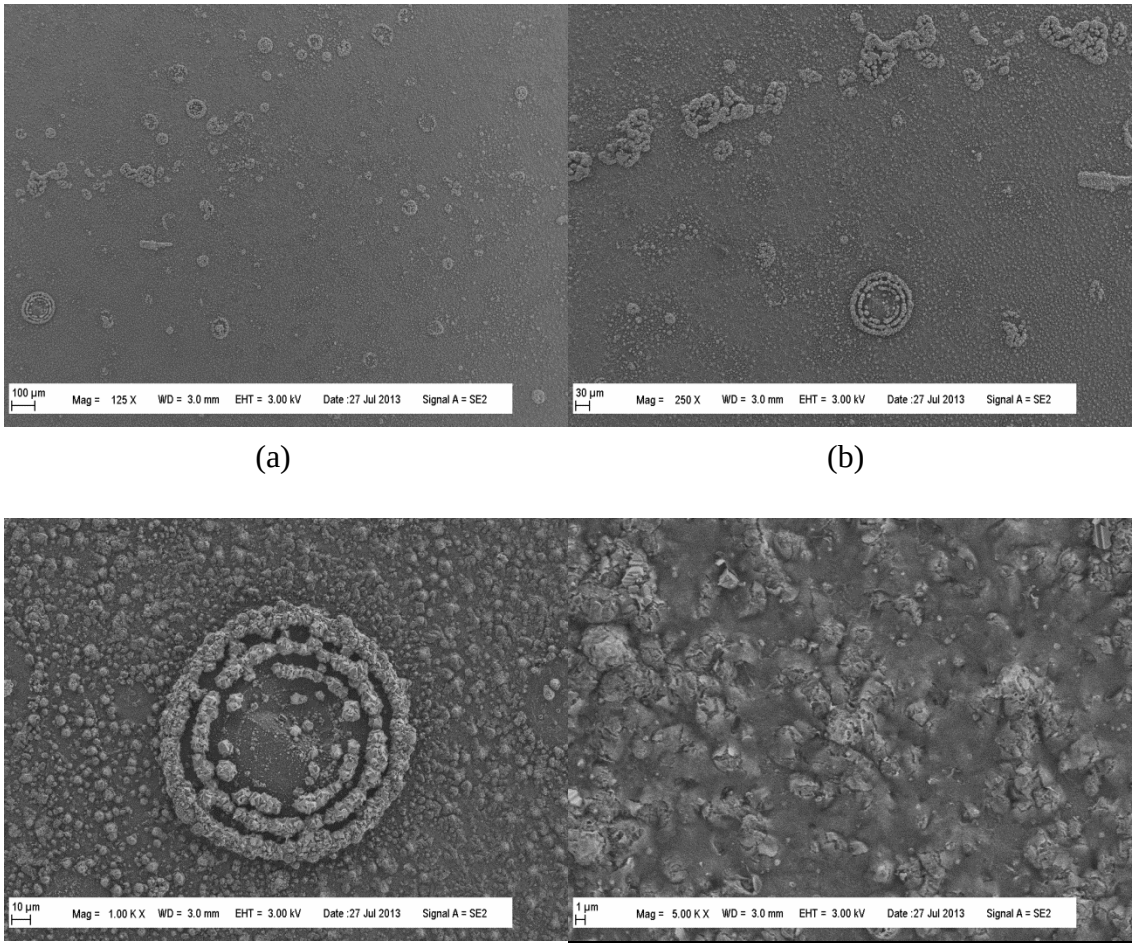

Fig. 139: SEM micrographs of **Al Coated HCM12A** in Research CO_2 at 550^{o}C, 20 MPa After **200** hrs exposure at (a) 125X, (b) 250, (c) 1,000X, and (d) 5,000X.

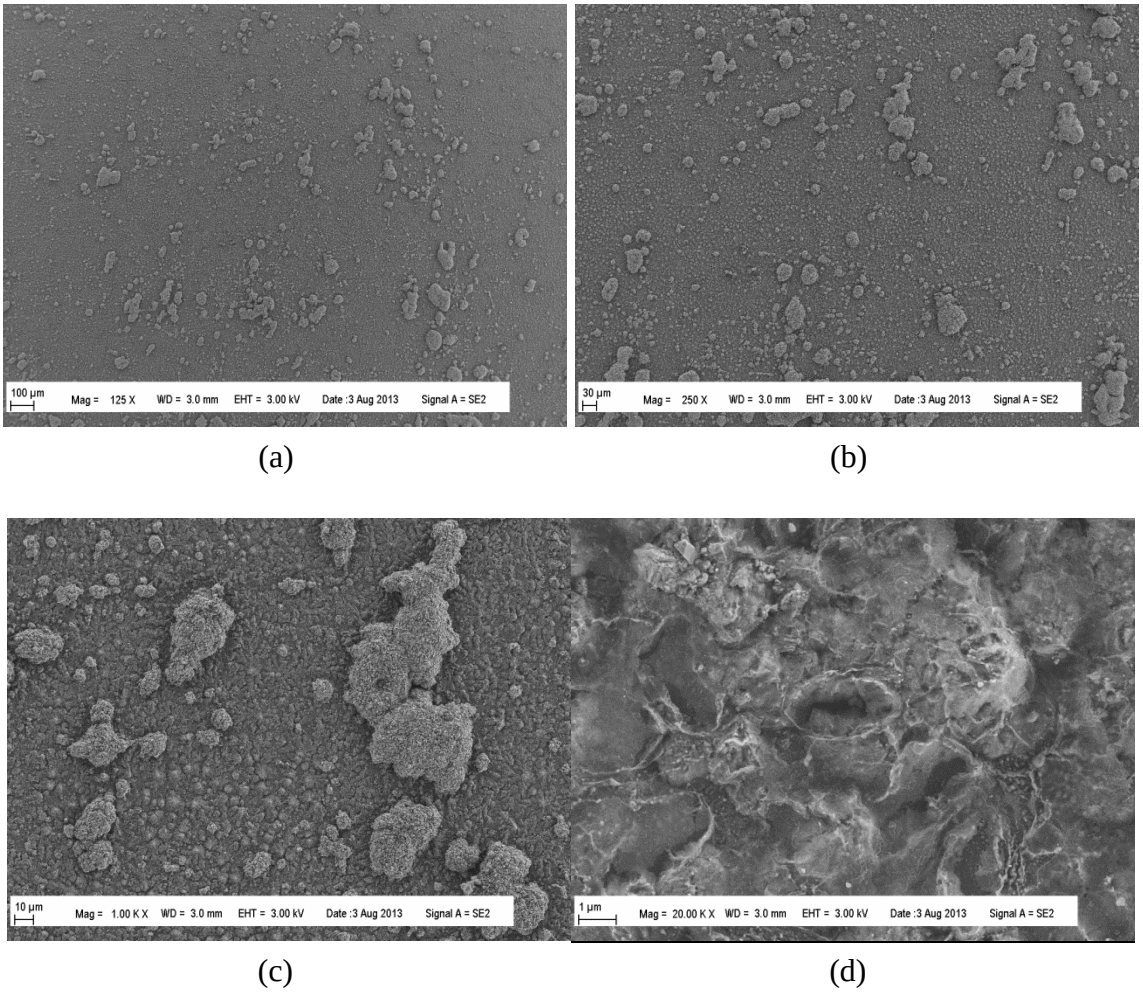

Fig. 140: SEM micrographs of Al-Coated T122 in Research CO_2 at 550^{o}C, 20 MPa After **1000** hrs exposure at (a) 125X, (b) 250, (c) 1,000X, and (d) 20,000X.

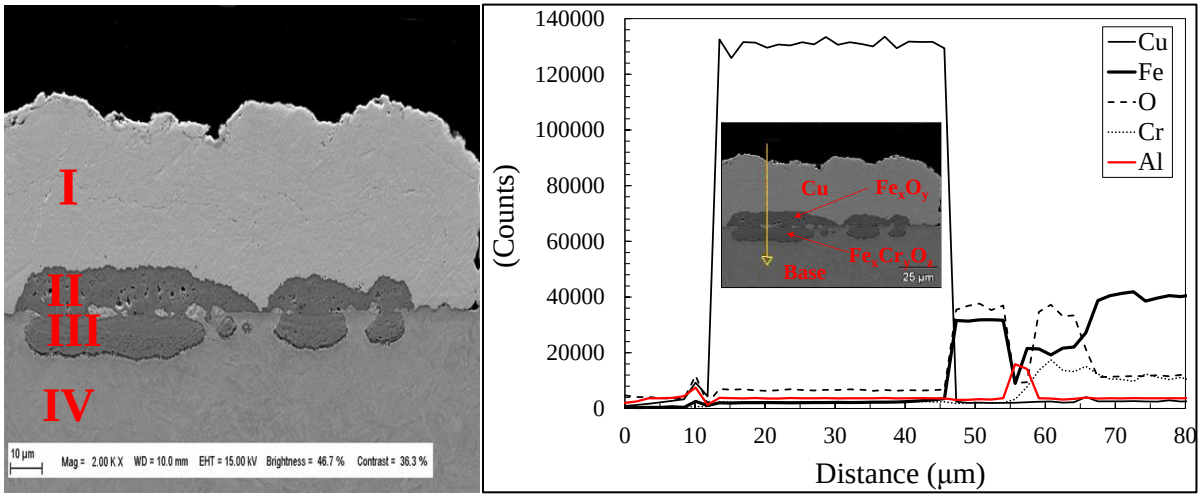

Layer	Cu	Fe	Cr	O
I	98%	-	-	-
II	-	60%	0.50%	35%
III	-	35%	16%	45%
IV	-	85%	11%	0%

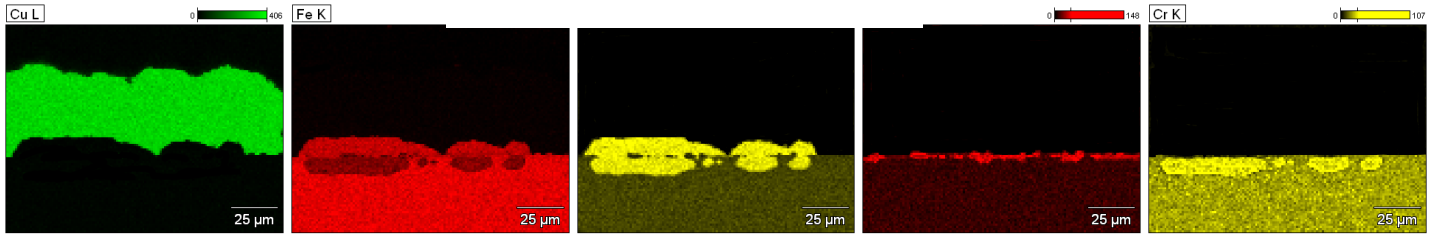

Fig. 141: Cross-Section of Al-Coated T122 after 1000 hours in RG-CO_2 at 550°C, 20MPa. Electroplated with Cu for enhanced characterization. **Top Left**: Atom % of layers hinting dual density Fe-Oxide layer formation (taken at 3000X). **Top Right**: EDS linescan through layers showing lower Fe, higher Cr content in bottom layer. **Bottom**: Spectral maps of key elements.

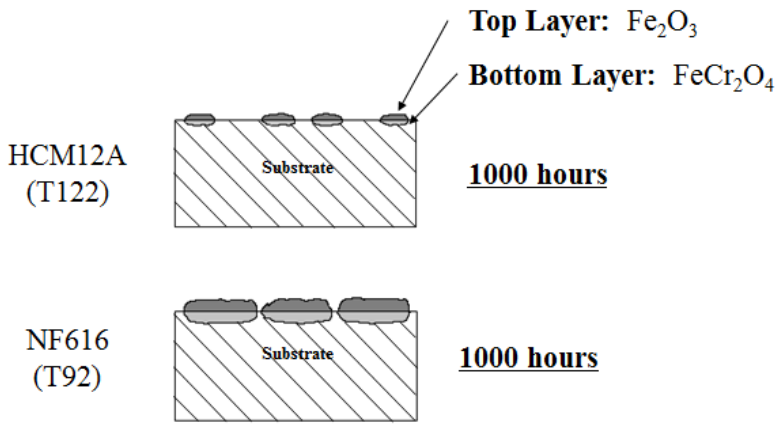

Fig. 142: Schematic Representation of Duplex Oxide Formation on Al-Coated FM Steels

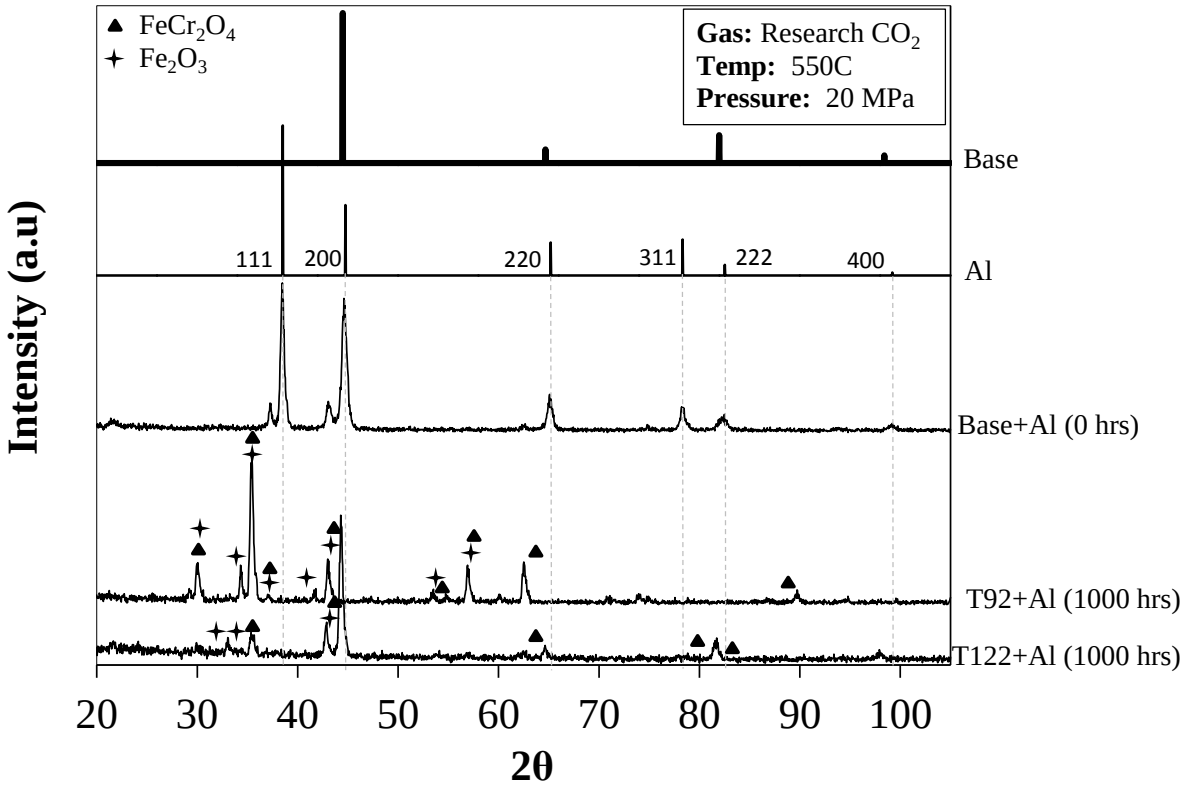

Fig. 143: GIXRD patterns of Al-Coated NF616 (T92) and HCM12A (T122)
After 1000 hours exposure.

5.5.2. Single Element Y Coating on 9-12%Cr Ferritic-Martensitics

Coated coupons were examined after sputtering to evaluate the deposition of yttrium onto the substrate. *Fig. 144* below shows a SEM/EDS analysis on the yttrium coated substrate after deposition and before testing. The linescan shows high levels of P and Zr in addition to yttrium, and are likely detected due to the nature of the inner workings of the EDS system. This is confirmed by point and shoot analysis, where the atomic fraction (%) points toward a balanced content of yttrium and oxygen.

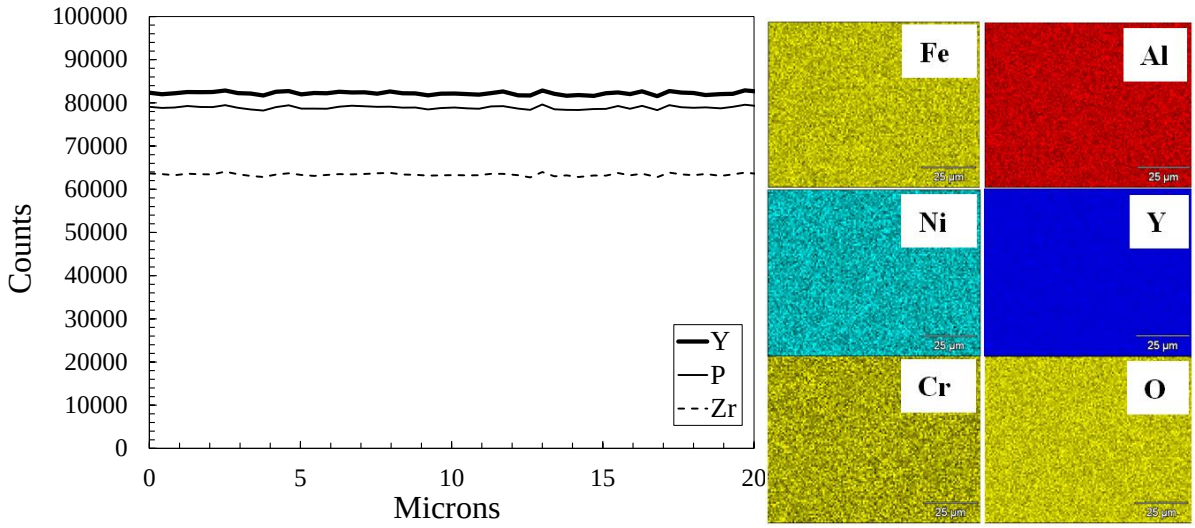

	Al	Fe	C	O	Y
Atom %	0.0	11.5	9.96	33.9	34.0

Fig. 144: SEM/EDS of Y Coated NF616 FM Steel (0hrs)

SEM micrographs of Y-coated NF616 (*Fig. 145*, *Fig. 146*) and HCM12A (*Fig. 147*, *Fig. 148*) both displayed preferential lifting of the coating near the edges, as well as significant oxide growth at a few sparse areas small in size., not to be confused for occurrence around the entire edge for this was not the case. Images also show small pockets toward the center of the coupon the experienced cracks and pockets of missing coating that were also scarce and few and number. Small oxide islands were observed and found to be rich in Fe and O, depleted in Cr and Y.

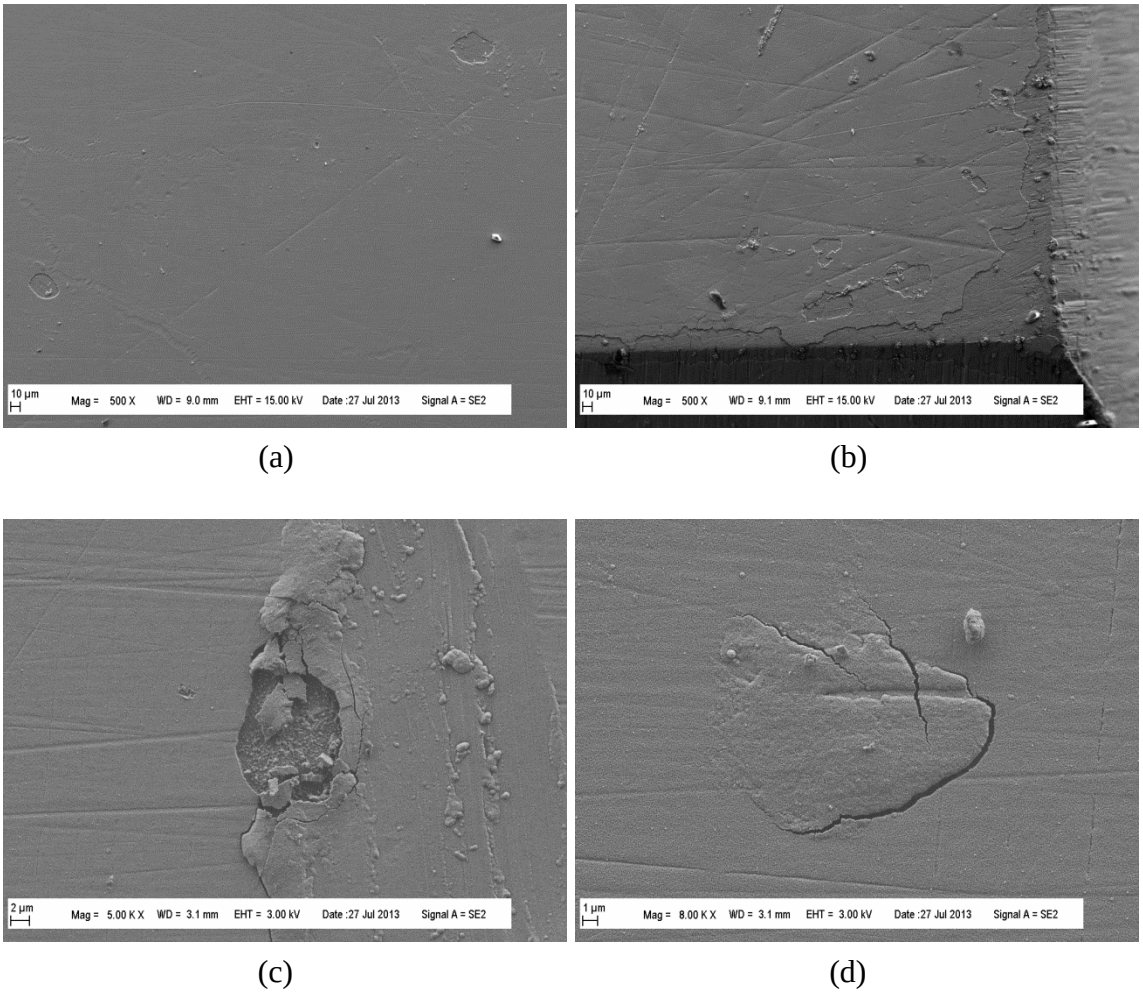

Fig. 145: SEM micrographs of **Y-Coated NF616** in Research CO_2 at 550^{o}C, 20 MPa After **200** hrs exposure at (a) 500X, (b) 500X near the corner edge, (c) 5,000X, and (d) 8,000X.

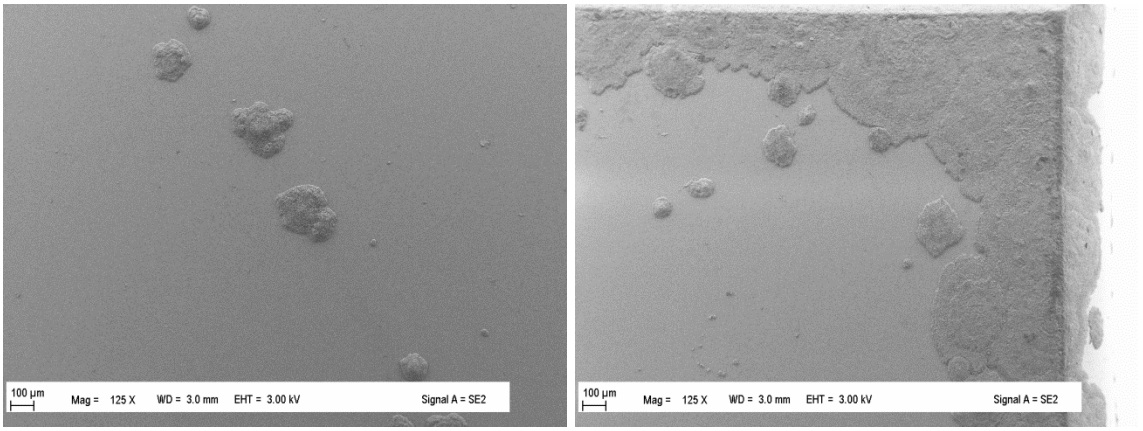

(a) (b)

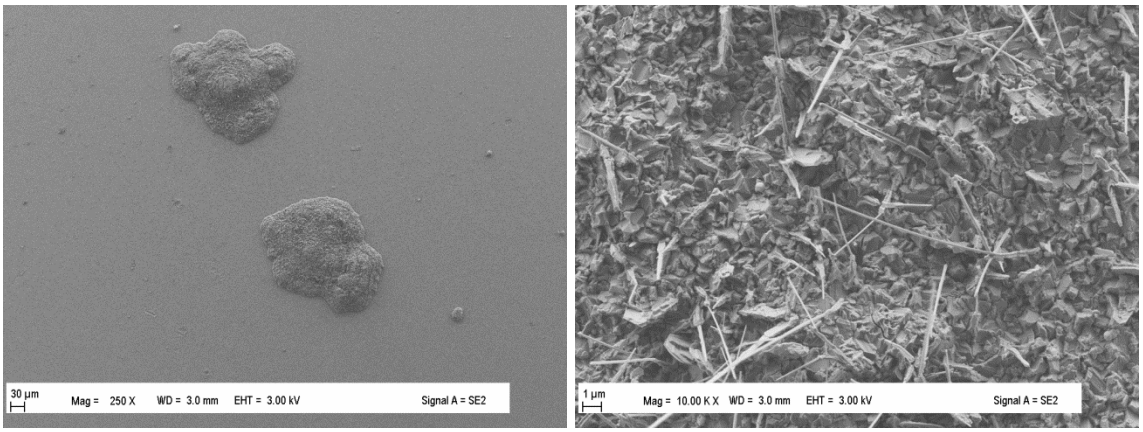

(c) (d)

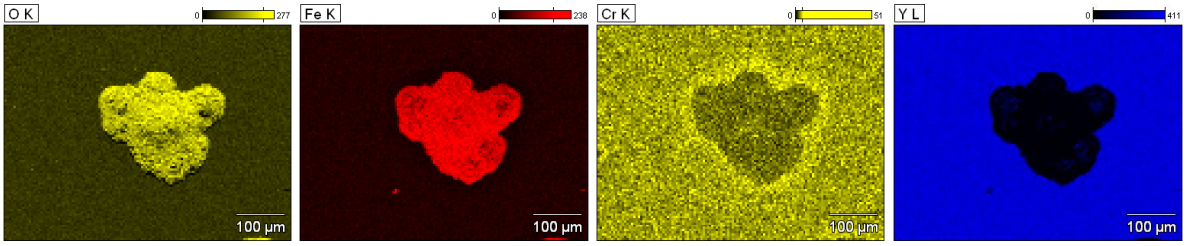

(e)

Fig. 146: SEM micrographs of **Y-Coated NF616** in Research CO_2 at 550^{o}C, 20 MPa After **1000** hrs exposure at (a) 125X, (b) 125X near the corner edge, (c) 500X, (d) 10,000X, and (e) spectral maps of nucleated oxide growths on surface rich in Fe and O.

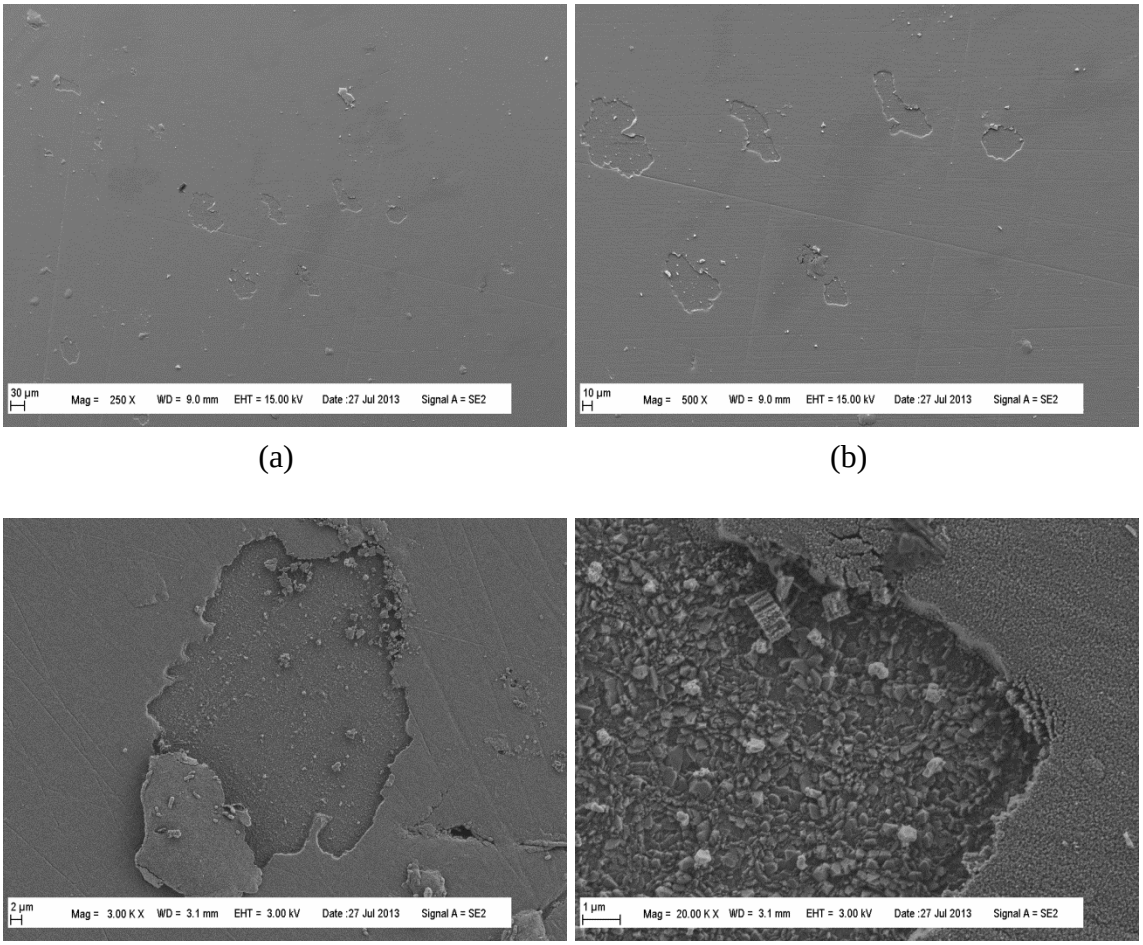

Fig. 147: SEM micrographs of **Y-Coated HCM12A** in Research CO_2 at 550^{o}C, 20 MPa After **200** hrs exposure at (a) 250X, (b) 500X, (c) 3,000X, and (d) 20,000X.

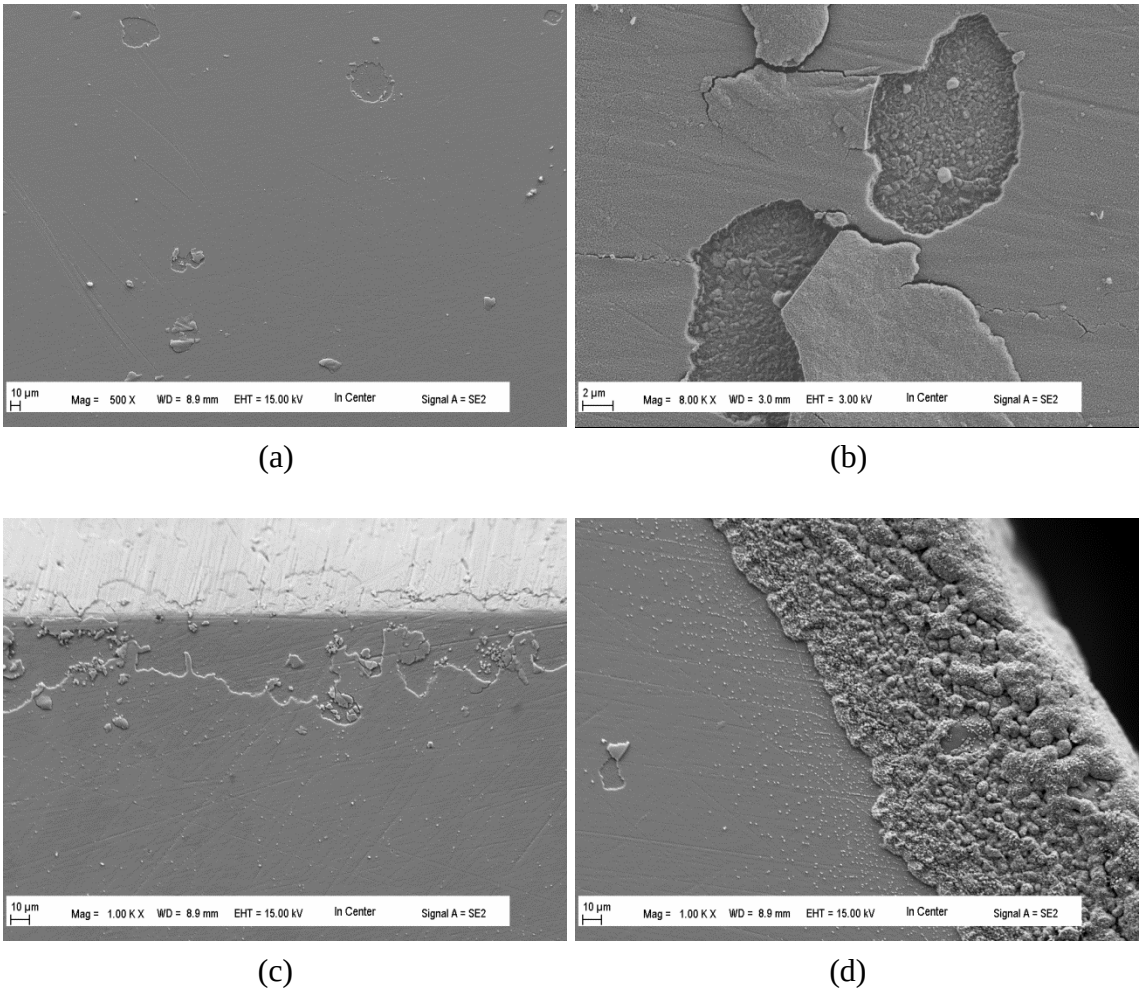

Fig. 148: SEM micrographs of Y-Coated T122 in Research CO_2 at 550^{o}C, 20 MPa After **1000** hrs exposure at (a) 500X, (b) 5,000X, (c) 1,000X near the edge, and (d) 1,000X at a different location on the edge.

The yttrium coated coupons proved resistive to electroplating with Cu. *Fig. 149* below shows photographs of electroplated coupons for purposes of retaining the coating prior to sectioning and mounting for examination. This obstacle explains why cross-sections for Y-coated samples are not provided above in this work, but will be provided for future publication as described in the preface. Options are to investigate putting down a seed layer using Ti and then electroplate with Cu. It seems the microstructure of Cu is highly

dependent on the characteristic of the underlying layer, with perhaps yttrium having a poor affinity for bonding to Cu.

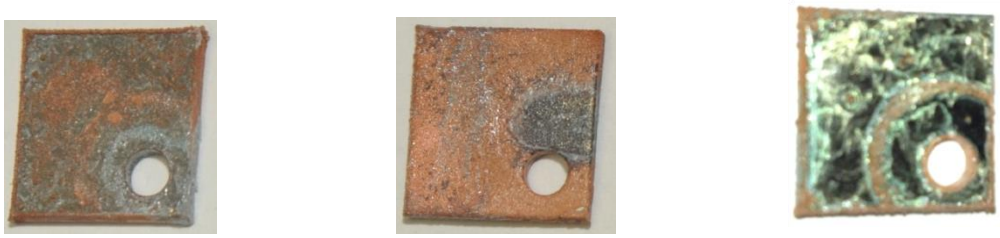

(a) (b) (c)

Fig. 149: Photographs of Electroplated Coupons for Examining Cross-Sections

Measured properties of the applied coatings are provided below in Table 10. Steps were taken to prepare the surface and weigh the coupons and then coat the samples and weigh them again. The difference between these weights is the coating weight and is shown in the table. Again, all surface treated samples were slightly magnetic.

Table 10: Measured Properties of Applied Coatings

	Coating	Meas. Weight (μg)	Meas. Area (mm^2)	Meas. Thickness (Å)	Meas. Surf. Wt. (mg/cm^2)	Nominal Density (g/cm^3)
T92	Al	468	380.25	4996	0.13	2.70
T122	Al	499	384.91	4996	0.13	2.70
T92	Y	931	383.73	5042	0.24	4.34
T122	Y	964	380.16	5042	0.25	4.34

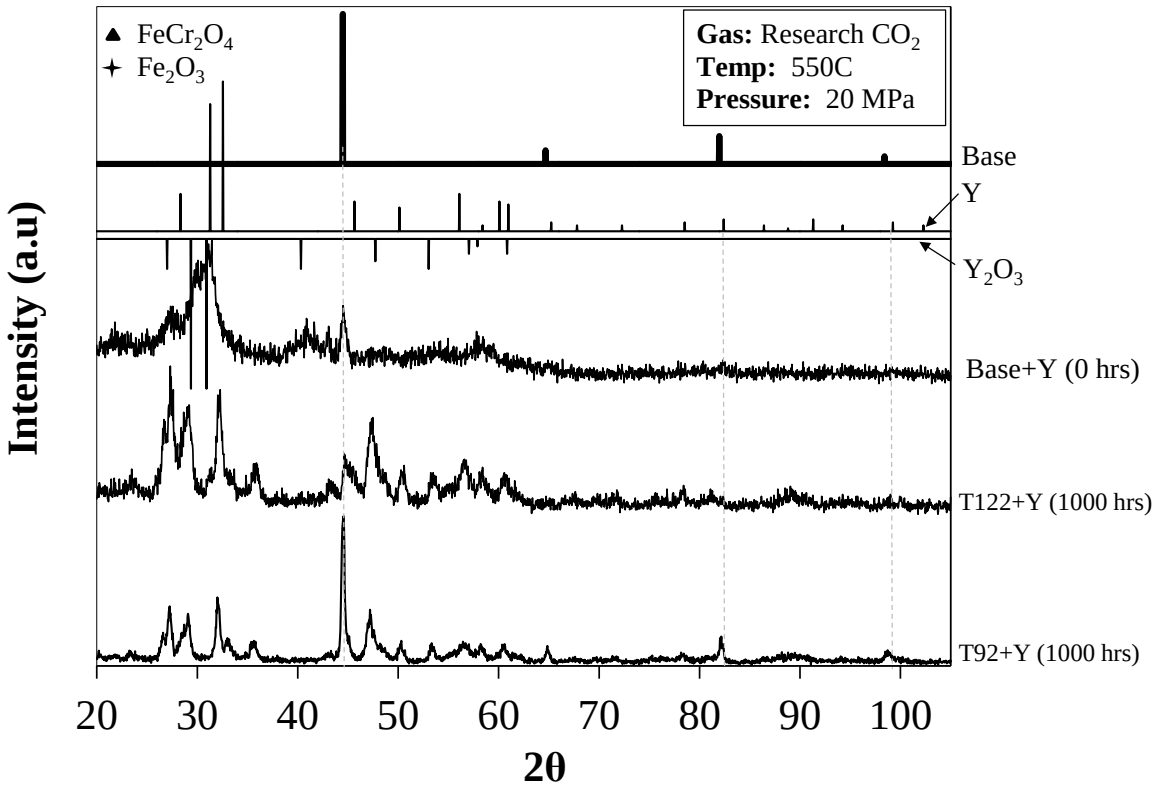

Fig. 150: GIXRD patterns of Y-Coated NF616 (T92) and HCM12A (T122) After 1000 hours exposure.

5.5.3. *Shot Peening on 9-12%Cr Ferritic-Martensitics*

SEM and EDS surface analysis of NF616 after shot peening is shown below in *Fig. 151*. EDS quant results show an atomic fraction (%) of chromium consistent with that of the actual composition.

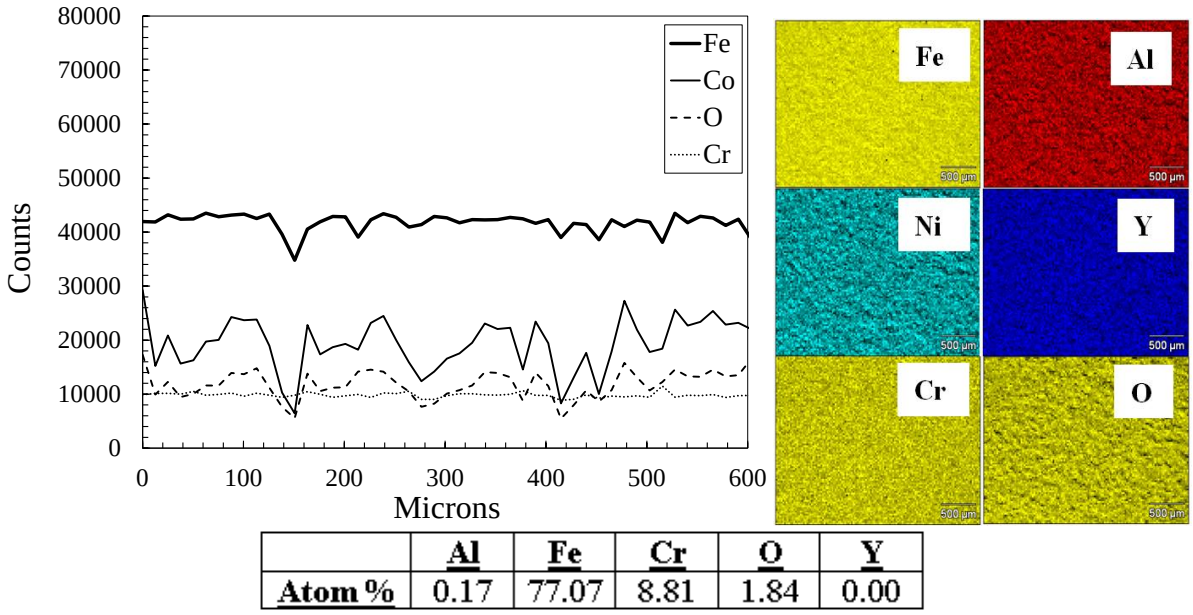

	Al	Fe	Cr	O	Y
Atom %	0.17	77.07	8.81	1.84	0.00

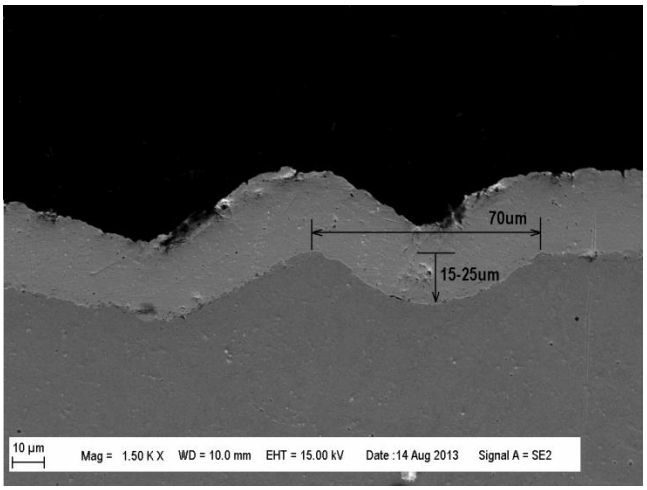

Fig. 151: SEM/EDS of Shot Peened T92 before exposure

SEM micrographs of peened T92 are shown below for 400 hours (*Fig. 152*) and 1000 hours (*Fig. 153*).

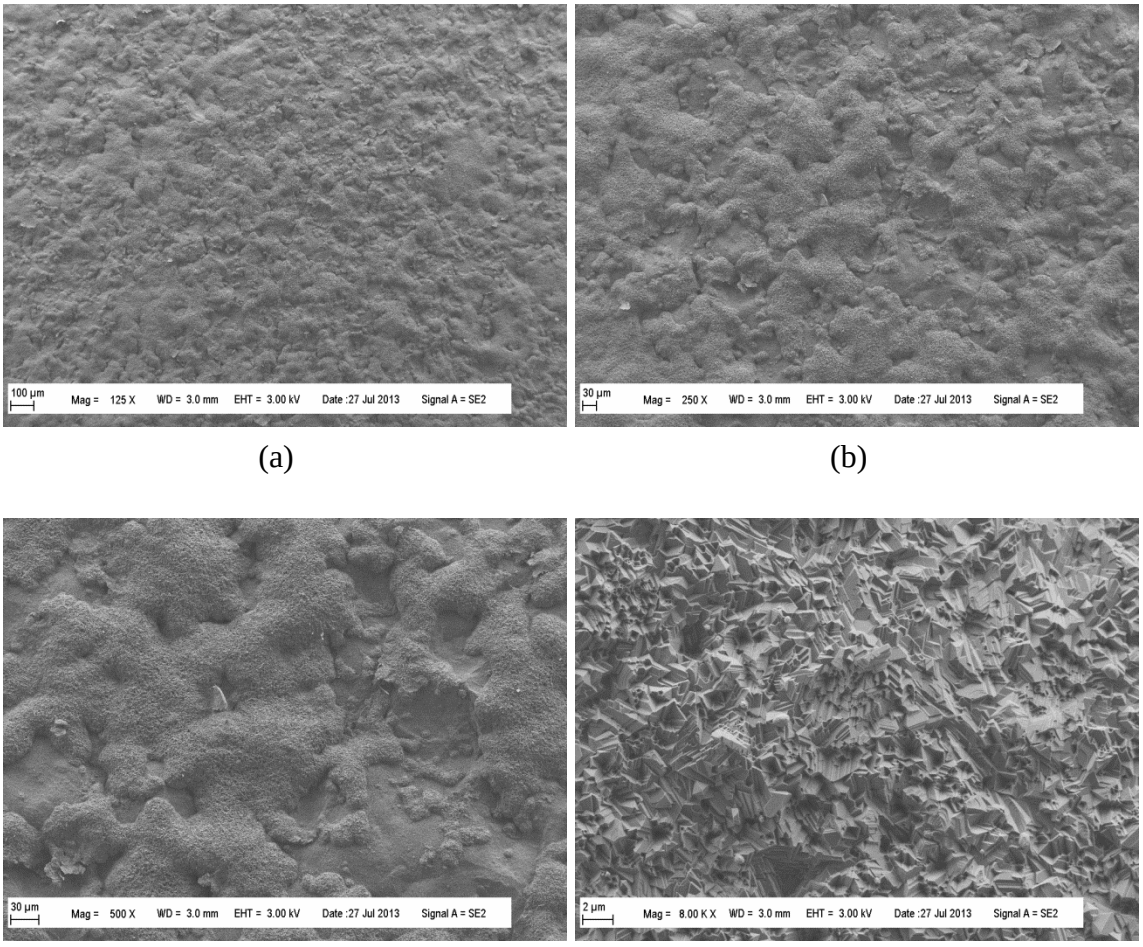

Fig. 152: SEM micrographs of Shot Peened T92 in RG-CO_2 at 550^{o}C, 20 MPa After 400 hrs exposure at (a) 125X, (b) 250X, (c) 500X, and (d) 8,000X.

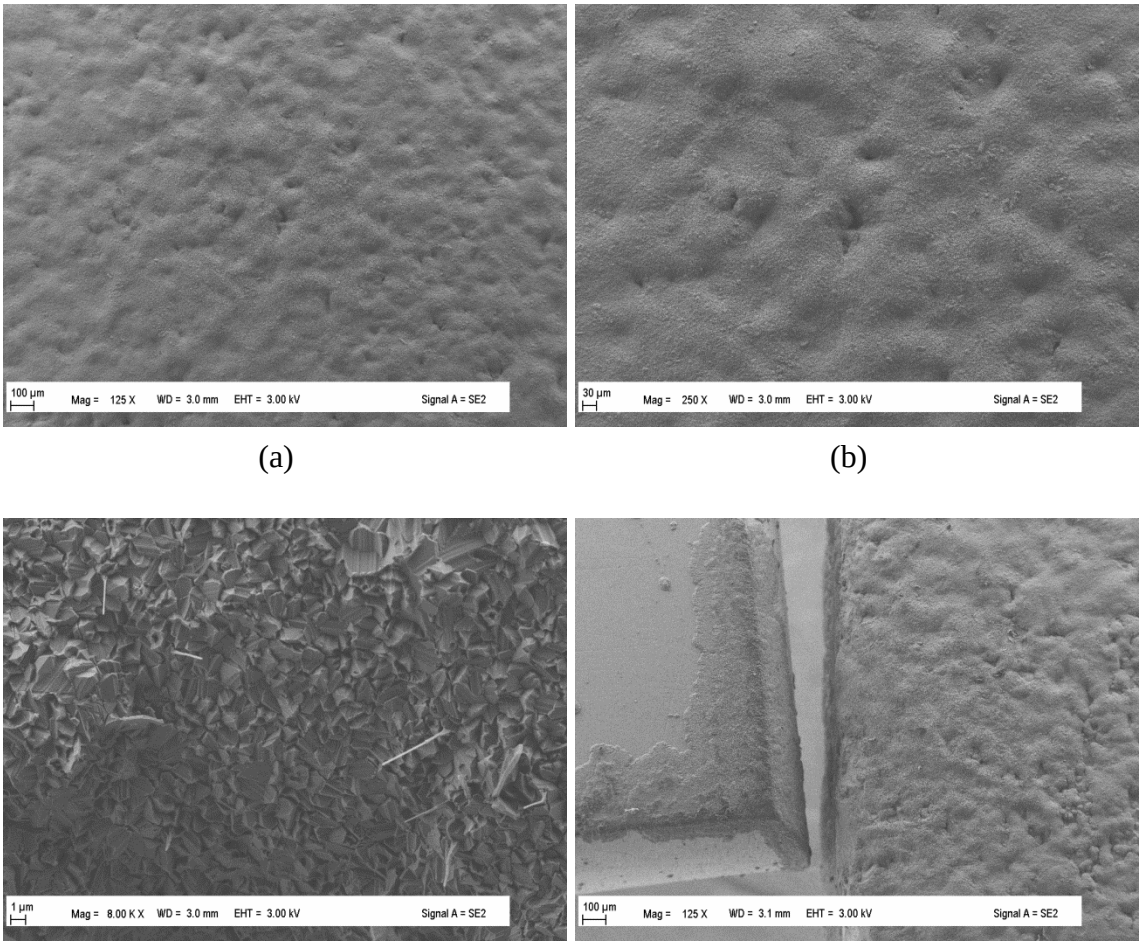

Fig. 153: SEM micrographs of Shot Peened T92 in RG-CO_2 at 550^{o}C, 20 MPa After **1000** hrs exposure at (a) 125X, (b) 250X, (c) 8,000X showing needles, and (d) 125X toward the edge to compare edge of peened surface to Y-coated.

EDS cross-section maps of peened T122 before exposure are shown below in *Fig. 154.* The top lightly contrasted layer is the protective Cu layer that helps distinguish between the features of the base alloy. Atomic fraction (%) is also provided in the figure, and should be used as reference for comparison to atomic fraction in other figures that follow to quantify changes in stoichiometry of observed layer(s).

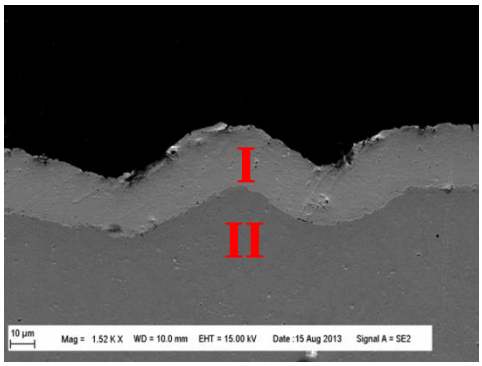

Layer	Cu	Fe	Cr	O
I	97%	-	-	-
II	-	87%	9.5%	-

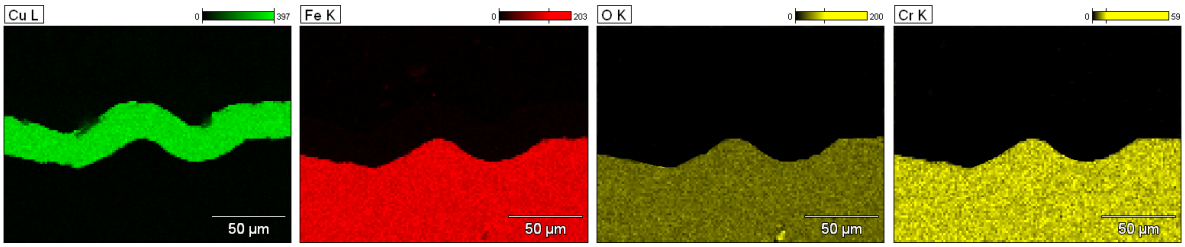

Fig. 154: Cross-sections of Shot Peened T122 Before Exposure. Electroplated with Cu for enhanced characterization. **Top Right**: Atomic fraction (%) of base material (taken at 1500X). **Bottom**: Spectral maps of key elements.

Cross-section of peened T92 after 1000 hours exposure is shown below in *Fig. 155*. Both the atomic fraction taken at different points in the oxide layers and the linescan correlate well to suggest existence of a rich Fe and O top layer thicker than the Fe, Cr, and O layer beneath it. Intensity difference in, as well as between Fe, Cr, and O in the layers highlighted by EDS spectral maps are clear and distinguishable, however the line of reference to where the base surface was originally and is now is not entirely clear. The changes in the spectral map for oxygen show a migration direction of oxygen from the base to the top layer. The atomic fractions and surface features both suggest a dual density or duplex oxide layer forming on the peened surface. The stoichiometry of the top layer (II) is very closely aligned with the Fe_2O_3 (5.24 g/cc) oxide (hematite) and the bottom layer (III) a non-stoichiometric iron-

chromium oxide $Fe_xCr_yO_z$ that is likely the spinel $FeCr_2O_4$, as observed in phase I and on AFA-OC6.

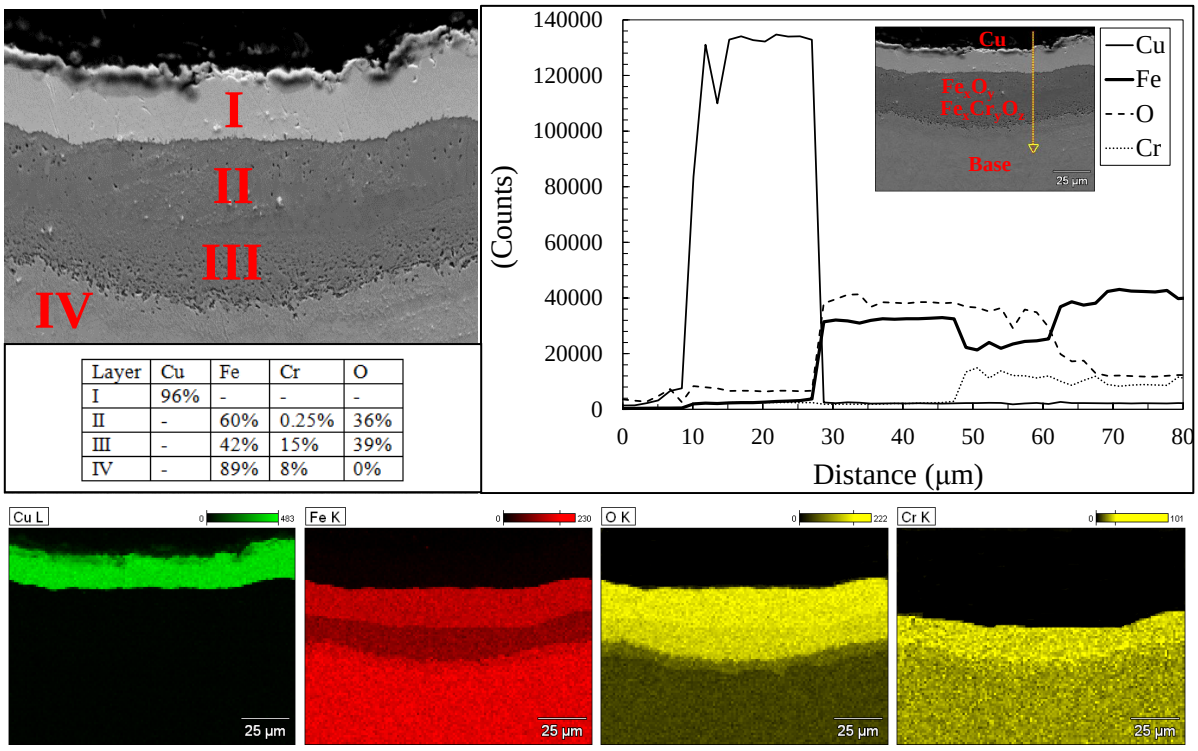

Fig. 155: Cross-Section of Shot Peened T92 after 1000 hours in RG-CO_2/550°C/20MPa. Electroplated with Cu for enhanced characterization. **Top Left**: Atom % of layers hinting dual density Fe-Oxide layer formation (taken at 2000X). **Top Right**: EDS linescan through layers showing lower Fe, higher Cr content in bottom layer. **Bottom**: Spectral maps of key elements.

SEM micrographs of peened T122 are shown below for 200 hours (*Fig. 156*) and below for 1000 hours exposure (*Fig. 157*).

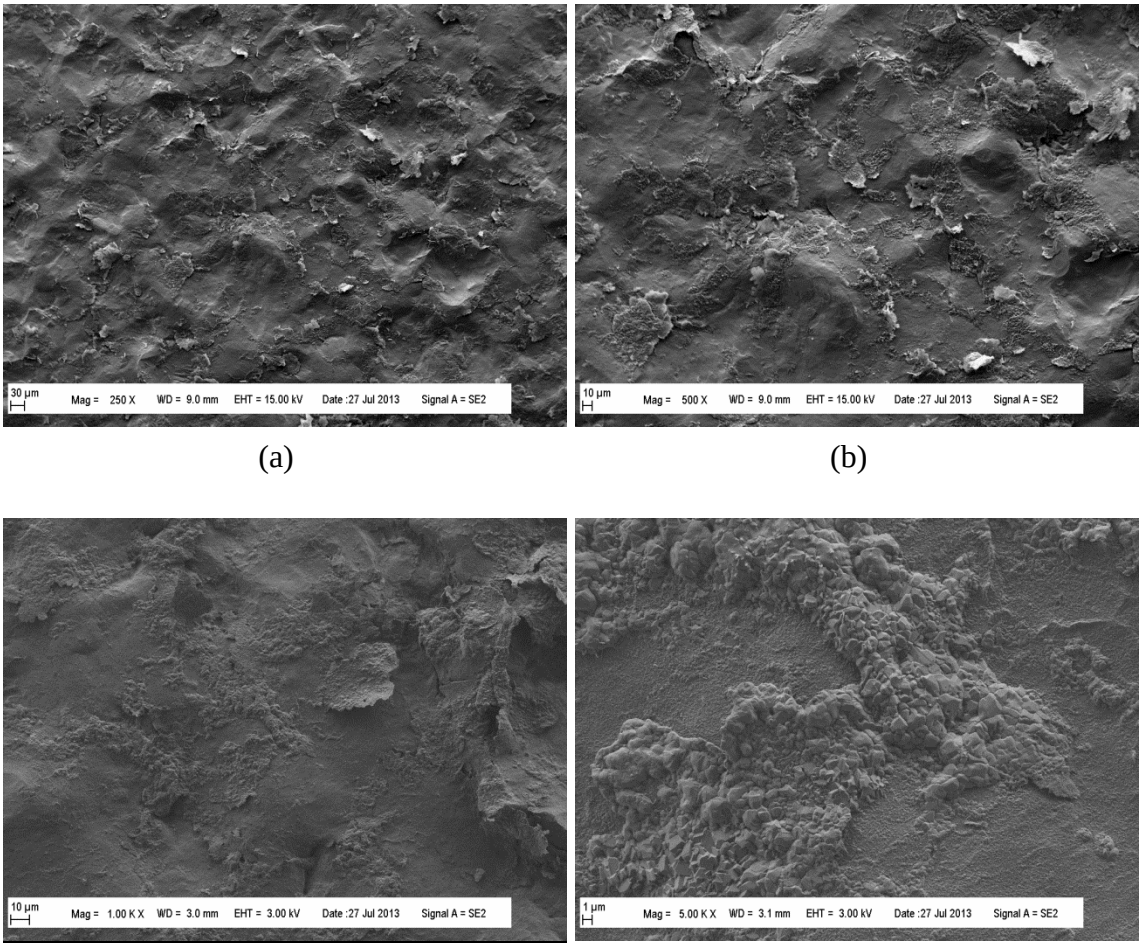

Fig. 156: SEM micrographs of Shot Peened T122 in RG-CO_2 at 550^{o}C, 20 MPa After **200** hrs exposure at (a) 250X, (b) 500X, (c) 1,000X and (d) 5,000X.

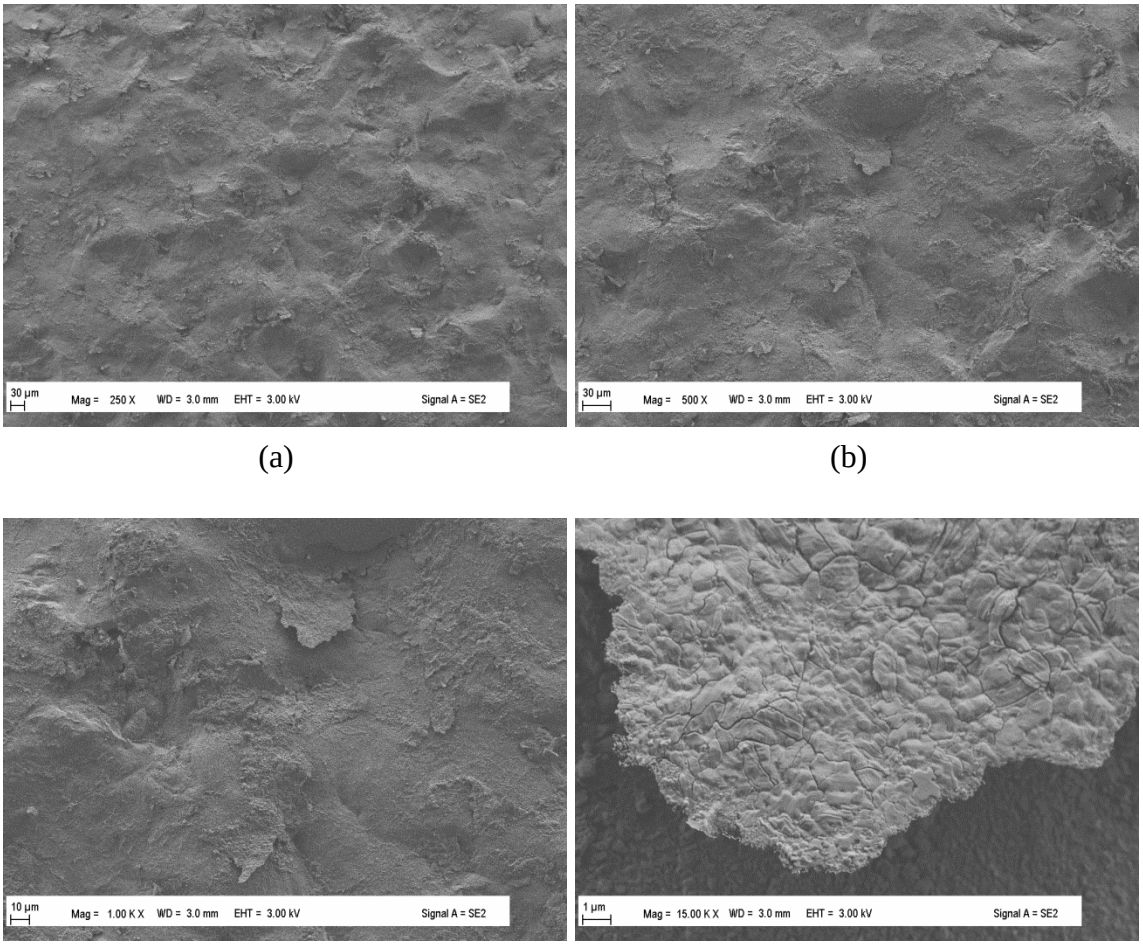

Fig. 157: SEM micrographs of Shot Peened T122 in RG-CO_2 at 550^{o}C, 20 MPa After **1000** hrs exposure at (a) 250X, (b) 500X, (c) 1,000X and (d) 15,000X.

Cross-section of peened T122 after 1000 hours exposure is shown below in *Fig. 158*. The oxide structure still appears duplex in nature, but is much thinner than that seen on T92. Also it is important to mention the oxide features shown in *Fig. 158* were discrete and far between, whereas the oxide layer for T92 was fairly uniform and quite continuous. Once again, stoichiometries of the layers coincide with that obtained also by T92, a Fe_2O_3 top layer followed by a $FeCr_2O_4$ bottom layer. A schematic representation of the nature of the oxide

formed as observed through cross-sections is shown below in *Fig. 159*. A GIXRD pattern taken for T92 and T122 after 1000 hours is shown in *Fig. 160*. The suspected oxide layers observed and ascertained stoichiometrically from cross-sections are identified as phases and confirmed for T92 and T122. Similar observations described here for shot peened samples were also observed for Al-coated samples (Sec 5.1).

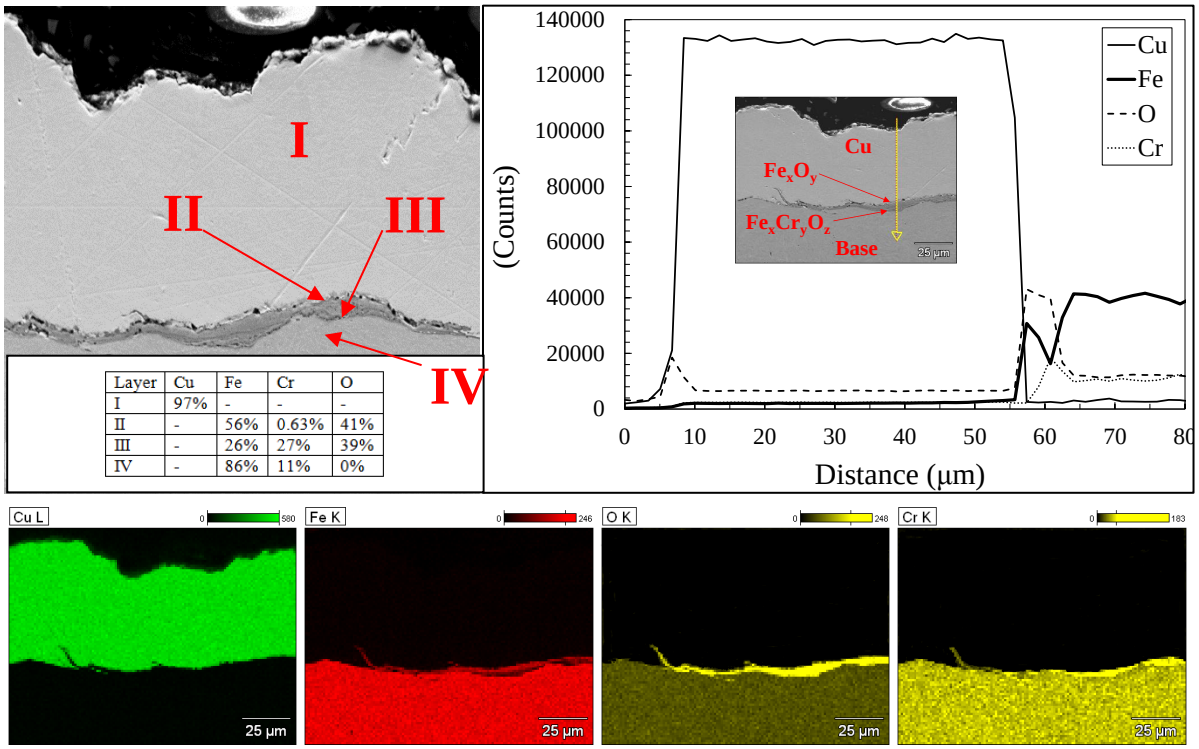

Fig. 158: Cross-Section of Shot Peened T122 after 1000 hours in RG-CO_2/550^oC/20MPa. Electroplated with Cu for enhanced characterization. **Top Left**: Atom % of layers hinting thin dual density Fe-Oxide layer formation (taken at 2000X). **Top Right**: EDS linescan through layers showing lower Fe, higher Cr content in bottom layer. **Bottom**: Spectral maps of key elements.

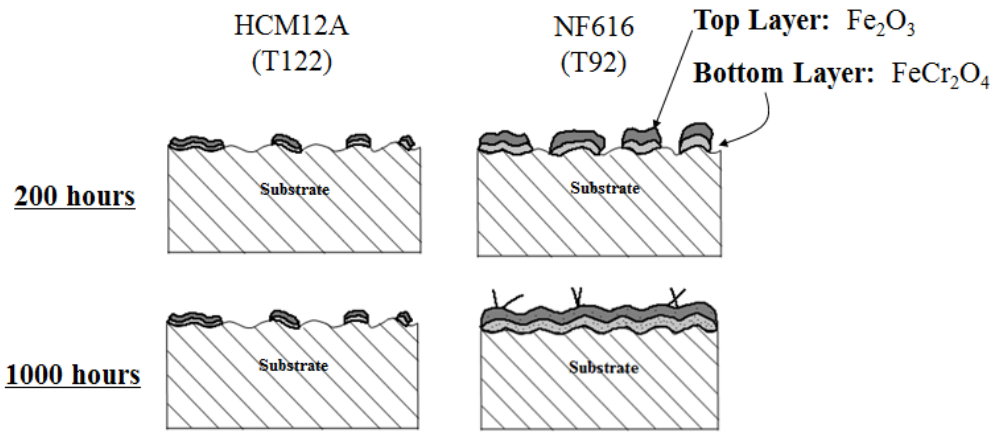

Fig. 159: Schematic Representation of Duplex Oxide Formation on Peened FM Steels

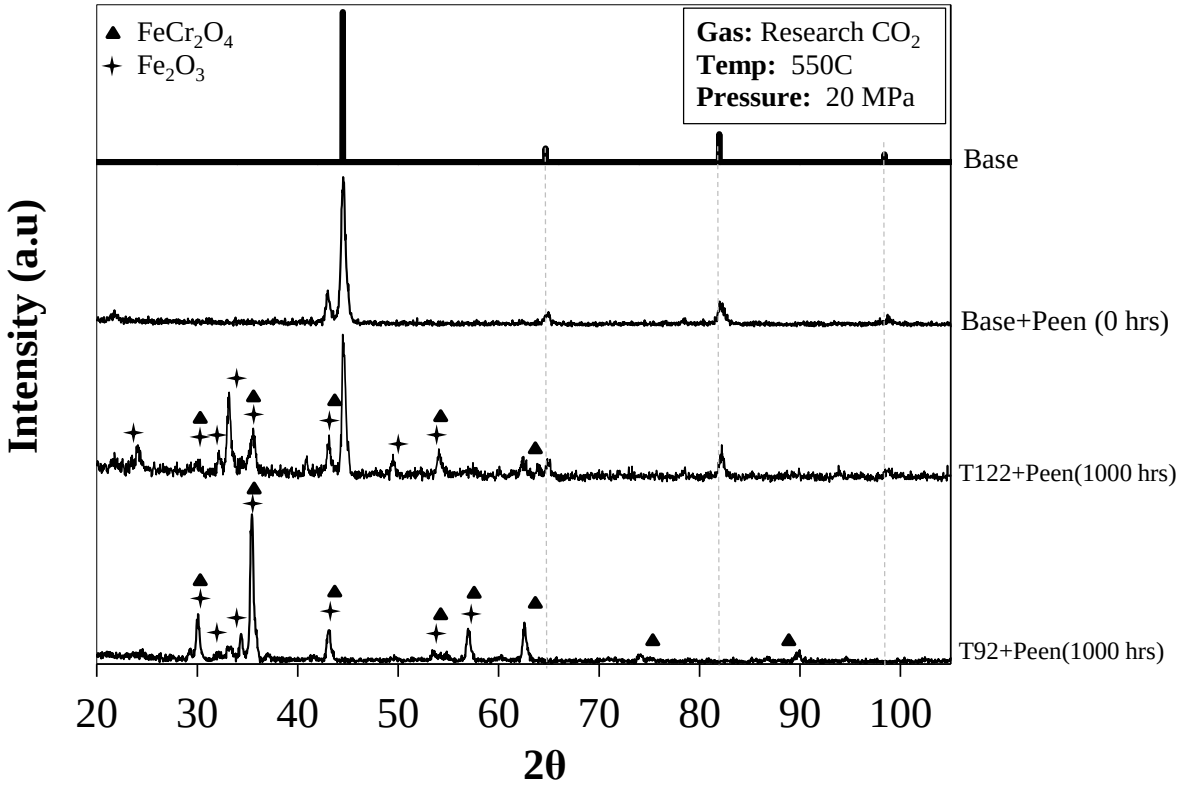

Fig. 160: GIXRD patterns of Shot Peened T92 and T122 after 1000 hours exposure.

Hardness measurements were made on unpeened and shot-peened FM steels and are provided below in Table 11. Measurements were made on both superficial and Rockwell scales for comparison.

Table 11**:** Measured Hardness of Unpeened and Shot Peened Samples

	Condition	**15N (15 kgf) Superficial**	**30N (30 kgf) Superficial**	**HRC (150kgf) Rockwell**
NF616	Unpeened	83.32	68.78	34.20
	Peened	83.74	69.70	35.25
HCM12A	Unpeened	83.76	69.44	37.74
	Peened	84.52	70.0	35.34

Note: Unpeened values based on average of 5 measurements, peened values based on average of 10 measurements. Shot peened sample only peened on one side; all samples polished to 800 grit finish. All meas. made using 135^{o} diamond tipped pointer.

The superficial scales were selected for several reasons; they can be used for coatings by applying a lighter load, and the indenter is more likely to give a more representative hardness value that can be converted to Vickers micro hardness. Measuring directly using Vickers micro hardness was initially thought to produce values that may not be truly representative of the surface due to the unevenness and propensity of surface irregularities. Vickers micro hardness of shot peened samples was performed by Naraparaju et al [70] to illustrate increase in fatigue strength and associate the increase in hardness to the presence of dislocations on the peened surface. According to Grabke [65], surface working such as grinding, sand-

blasting, machining, shot-peening, etc. introduces near surface deformation, i.e. many dislocations, and upon heating to the process temperature a partially recrystallized microstructure results with many grain boundaries and sub-boundaries, which can act as fast diffusion paths for supply of (say in this instance from this paper, Cr) to the surface. It is like a cold working effect, and has been shown to be favorable in protection against metal dusting.

5.5.4. Comparison of Surface Treatments on 9-12%Cr Ferritic-Martensitics

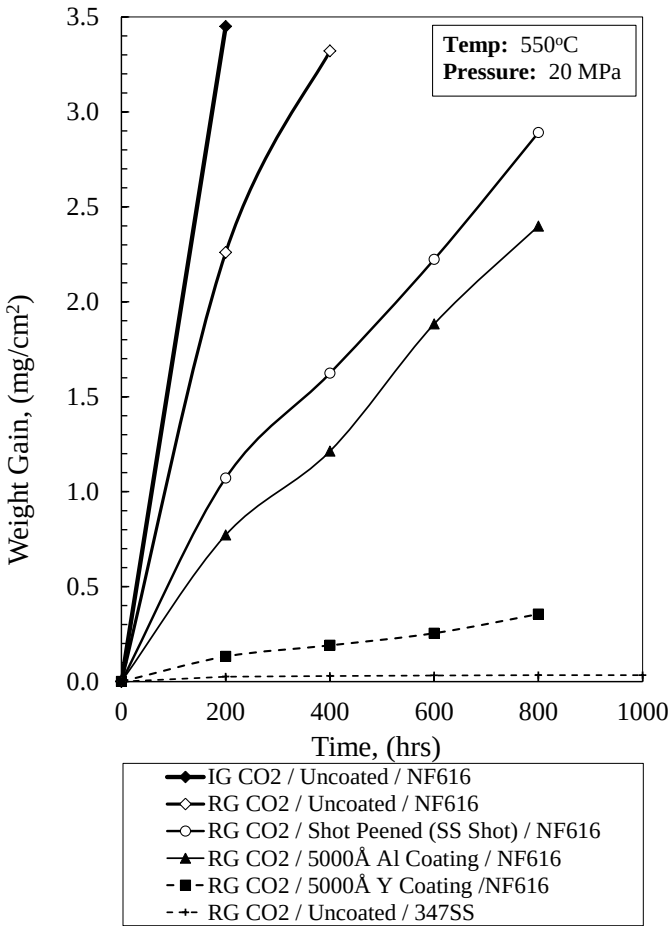

Fig. 161: Effect of Al, Y Coatings and Shot Peening on NF616 at 550°C, 20 MPa

Results from Alvarez et al [68] indicate that the quality of the coatings, particularly their density and adhesion, are more important than the thickness of the layer deposited for effective protection against metal dusting. Reactive elements (rare earth) like yttrium significantly increase the adhesion and spalling resistance of the oxide layers, thereby further enhancing the high temperature corrosion resistant behavior [71]. Delaunay and Huntz have showed that growth rate can be decreased and spalling reduced by additions of Y, Ce, or La [72, 73].

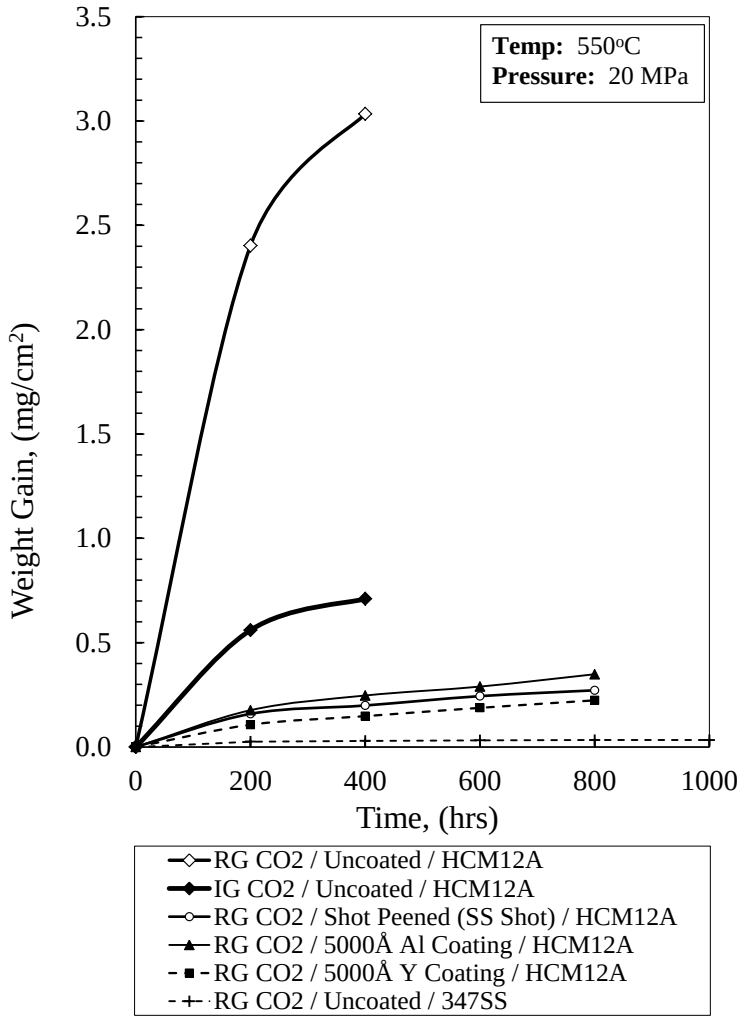

Fig. 162: Effect of Al, Y Coatings and Shot Peening on HCM12A at 550°C, 20 MPa

5.5. Analysis of Interference Colors

According to Vander Voort [74], interference colors and their relationship to film thickness have been observed for pure iron, steel, nickel, and copper. The colors produced by a film of suitable thickness are caused by interference between light rays reflected from the inner and outer film surfaces. Recombination of two waves with a phase difference of 180^{o} causes light of a certain wavelength to disappear, and the reflected light exhibits the complimentary color. In this study, interference colors were observed on the austenitic and alumina forming alloys in the temperature range of 450-650^{o}C. Images were taken with a high resolution digital camera at an angle off-normal to the coupon to capture the proper hue of colors. These images can be located in Sec. 8.1 of the appendices. The progression of observed colors with increasing temperature was generally fairly consistent between the austenitic alloy group, and likewise with the alumina forming alloy group. The only clearly evident distinction between surface oxidation and exposure time witnessed in the austenitic group was for the 347SS alloy. The surface oxidation appears as closely grouped spot-like black particles. Between 400 and 600 hours, this physical distinction manifests itself and continues to grow thereafter. It's interesting to note that the manifestation of this physical distinction also happens to occur around the inflection point on the oxidation curve from linear to parabolic, a transition commonly referred to as break-away oxidation. According to Kofstad [35], during transition to the accelerated oxidation of niobium in oxygen, the first nuclei of Nb_2O_5 are detected as spots on the surface, and the breakaway oxidation itself is associated with Nb_2O_5 formation. The Nb_2O_5 scale is porous and offers no or little resistance to the oxidation. This oxide scale phenomena with interference colors during transition was also

observed and reported by Hurlen [75], Blackburn [76], Cox and Johnston [77], which may similarly be taking place here in this study for 347SS and the AFA's, but obviously with a different oxide layer given the metal/alloy composition and test conditions. As for oxidation colors observed for the ferritic alloys, this was not the case. Their color remained strictly between a dull and dark grey with evidence of spallation at 450°C, leading to their removal from the study at higher temperatures. *Fig. 163* below illustrates the observed progression of interference colors after 200 hours in each of the different CO_2 gas grades.

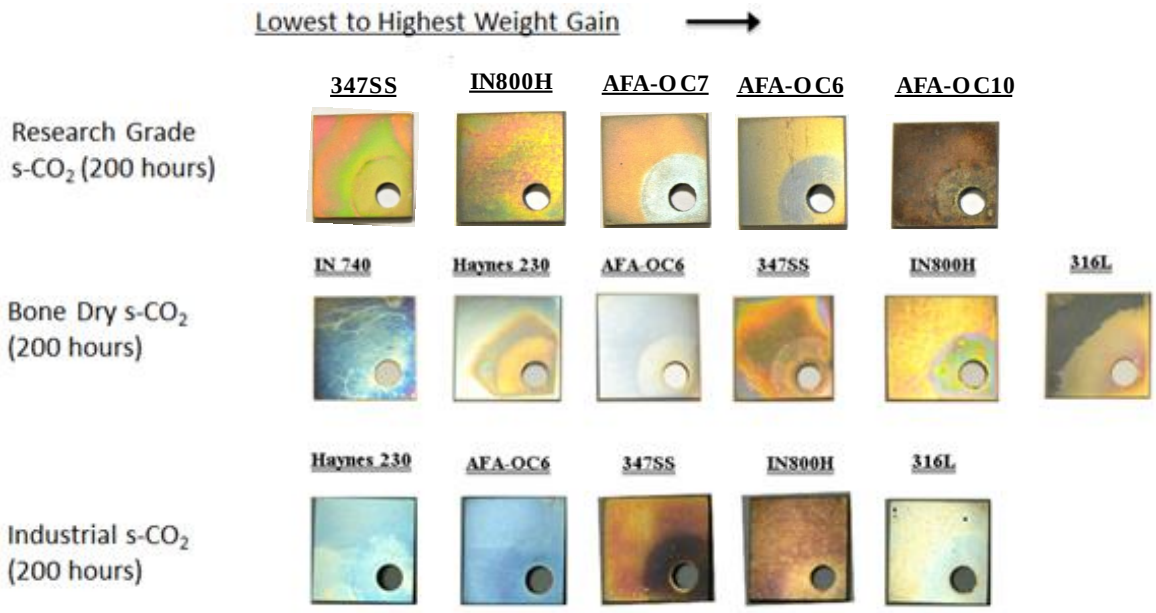

***Fig. 163*:** Progression of Interference Colors with Magnitude of Weight Gain at 650°C

Is there a relationship between interference color and magnitude of weight gain/film thickness under supercritical conditions? Techniques such as imaging spectrophotometry, ellipsometry, and multi-wavelength interferometry are a few approaches that might be used for determining film thickness as provided by Kitagawa [78].

5.6. Statistical Analysis Techniques

5.6.1. Monitoring Individual Weight Gains using Control Charts

In this study, ASTM control charts [79] were used as a statistical quality control method to monitor the variation of individual weight gains with respect to the average reported weight gain. A control chart always has a central line for the average, a line for the upper control limit (UCL) and a line for the lower control limit (LCL). The mentioning of this bears particular importance for alloys AFA-OC6 and AFA-OC10. The individual weight gains of these coupons at 650^{o}C consisted of several peculiar outlying values that were outside of set control limits. For example, *Fig. 164* below shows control charts for the individual weight gains of AFA-OC10 at 650^{o}C. A few outliers are detected outside of control limits at 200 hours, but notice how coupon A129 becomes an outlier at 400 hours and its impact on the average continues to propagate through 1000 hours. These outliers have the potential to significantly alter the average weight gain and possibly even the type of oxidation curve that is generally taking place. Such removal of individual outliers from the computed average weight gain is a principle that was applied by Brush [80] in his study in superheated steam. *Fig. 165* below shows the "as is" average weight gain curve versus the 'adjusted' for outliers average weight gain curve. The procedure for determining the adjusted curve consisted of removing the highest outlier from the average and repeating until individual weight gains fell within ASTM control limits. It should also be noted that at 650^{o}C, the AFA materials appear to be susceptible to a large amount of variation and they exhibited the largest deviation amongst individuals. This can be seen in *Fig. 168*. The adjusted values for AFA-OC6 and

AFA-OC10 at 650^{o}C are plotted in *Fig. 51* and *Fig. 52*. Freeman [81] has shown that the weight measurement is the dominating contributor to the standard error and that the longer the test, the smaller the error. Quesenberry [82] emphasizes the effect of sample size on control limits for $\overline{X}$ charts and recommends a number of samples and sample size for establishing individual measurement control limits.

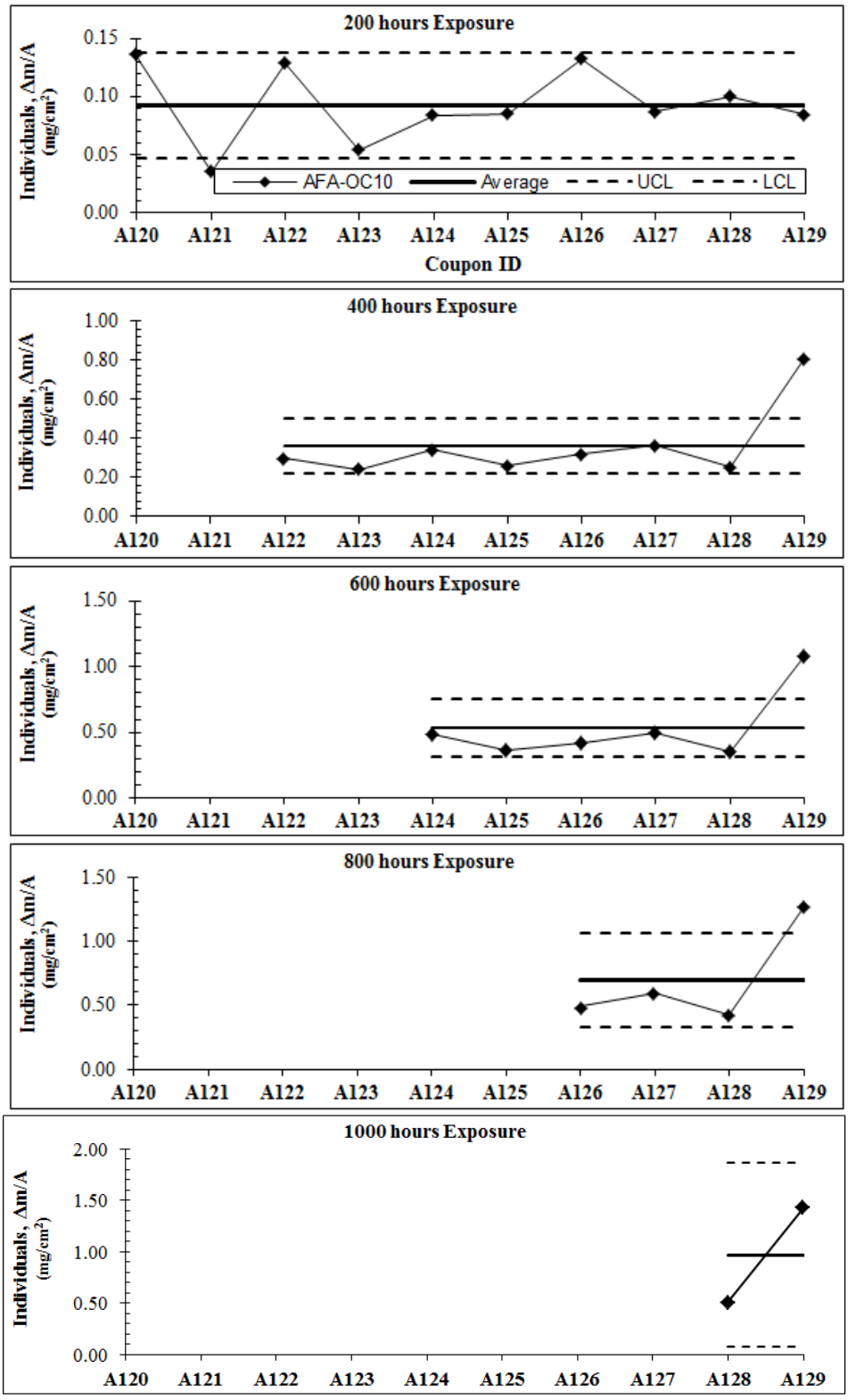

Fig. 164: Control Chart for Individual Weight Gains of AFA-OC10 (Expt. 5)

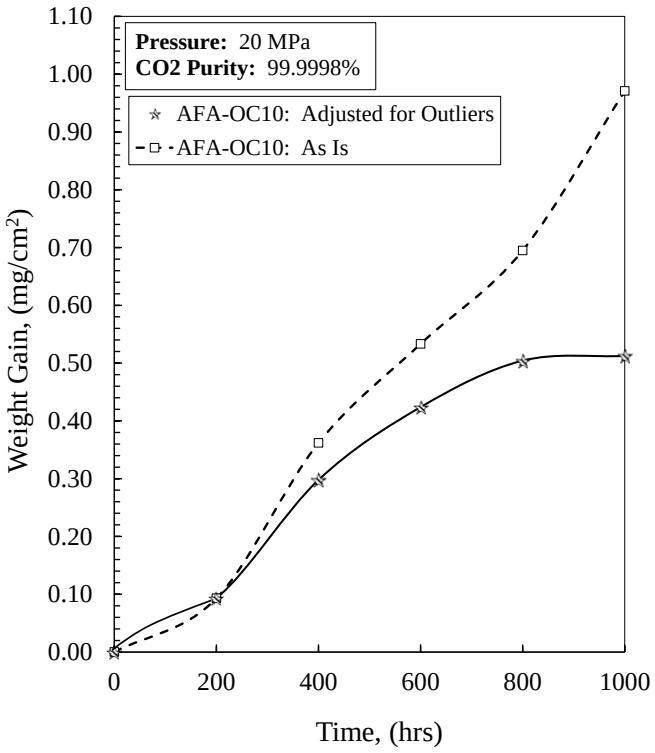

Fig. 165: Effect of Outliers on Weight Gain Oxidation Curve.

5.6.2. Effect of Individuals on Average Weight Gain

As a part of exploratory data analysis, it was observed that on occasion, outliers existed in what could mistakenly be the same frequent position. To expand on this, there was concern that perhaps outliers were occurring with a greater frequency at the same locations between different materials when arranged on the sample holder. Therefore, individual weight gains were plotted in the same arrangement coupons were arranged on the sample holder according to material, to evaluate where these outliers were occurring. This is shown in *Fig. 166* through *Fig. 170*.

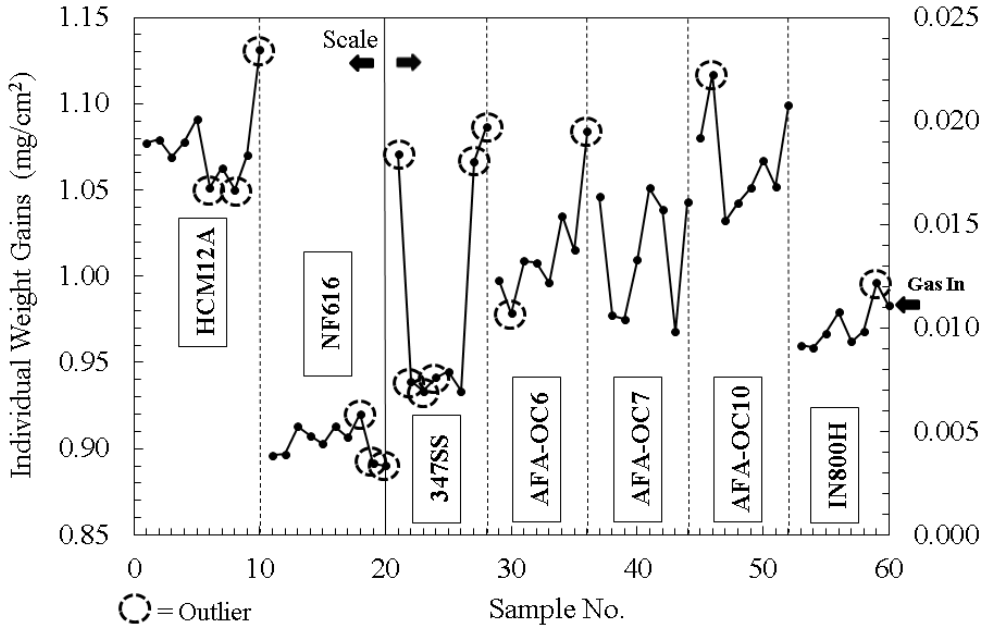

Fig. 166: Individual Weight Gains at 450°C, 20MPa in RG-CO_2 after 200hrs (Expt. #3)

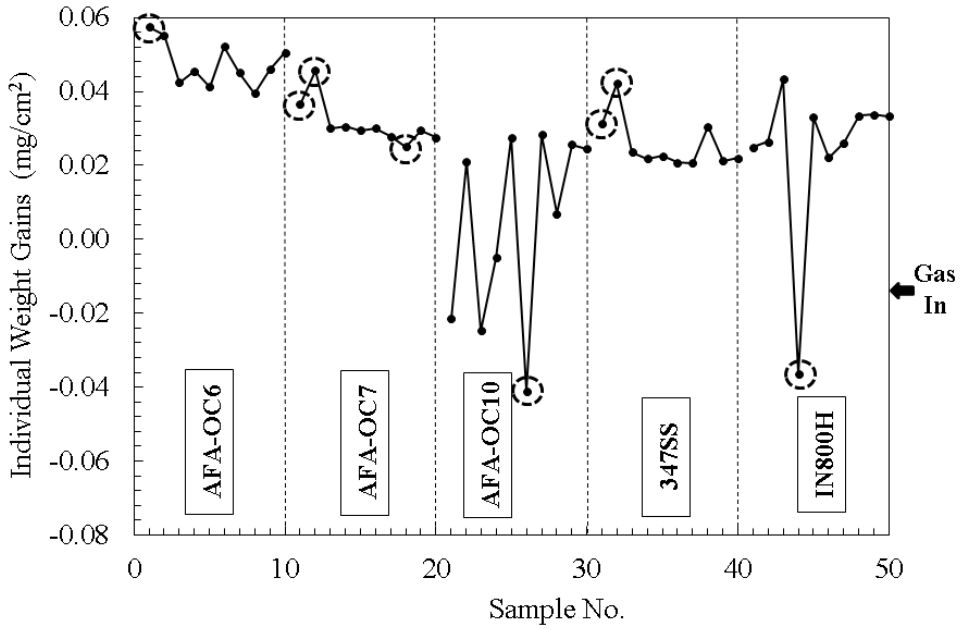

Fig. 167: Individual Weight Gains at 550°C, 20MPa in RG-CO_2 after 200hrs (Expt. #4)

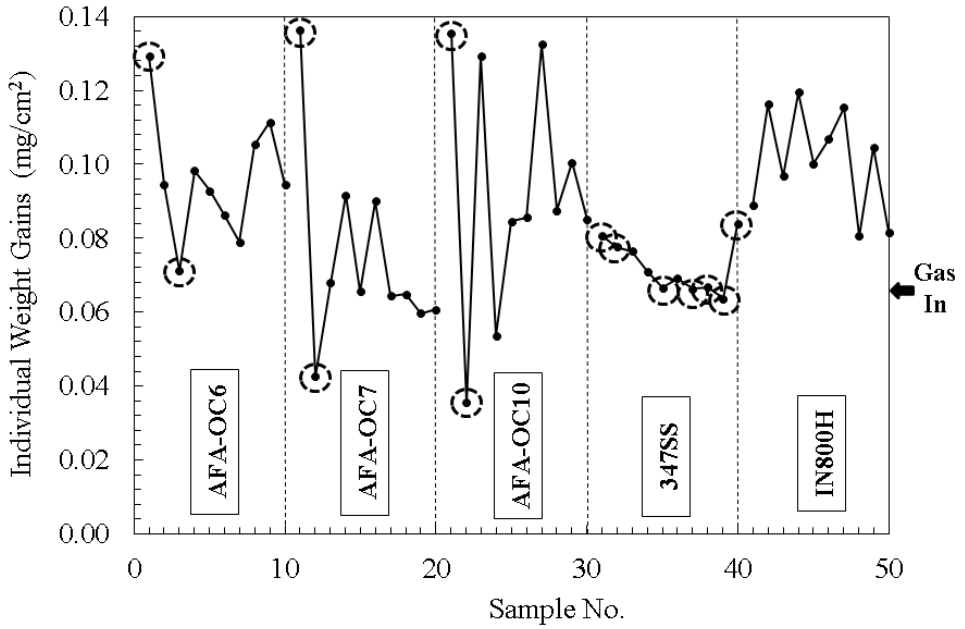

Fig. 168: Individual Weight Gains at 650°C, 20MPa in RG-CO_2 after 200hrs (Expt. #5)

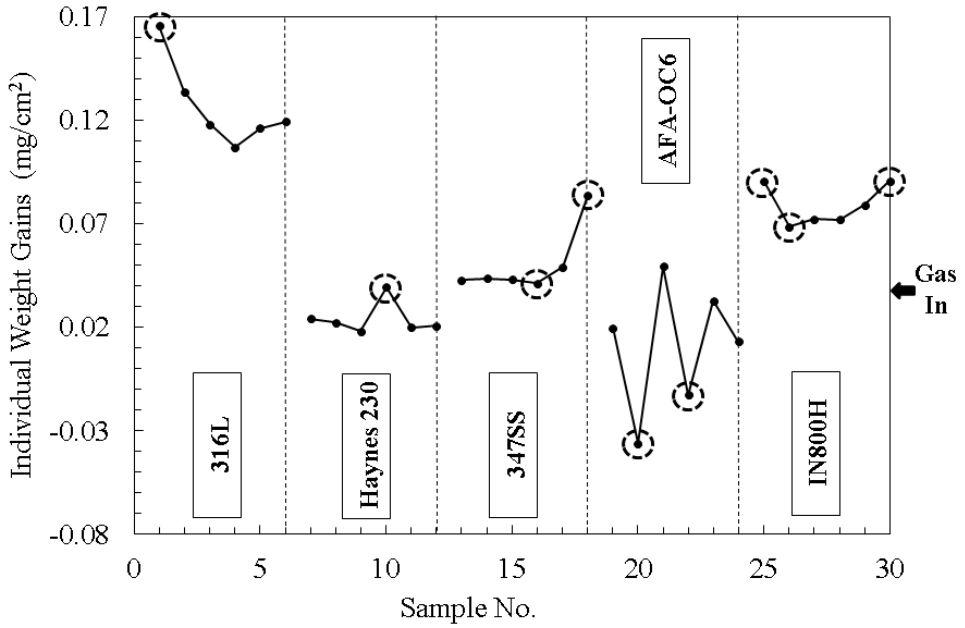

Fig. 169: Individual Weight Gains at 650°C, 20MPa in IG-CO_2 after 200hrs (Expt. #7)

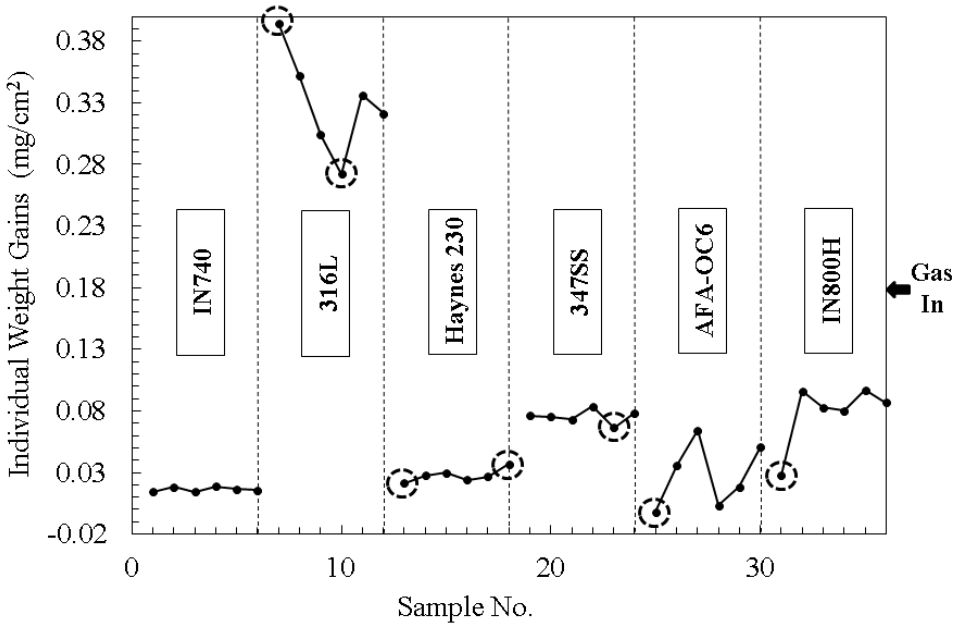

Fig. 170: Individual Weight Gains at 650°C, 20MPa in IG-CO_2 after 200hrs (Expt. #8)

In *Fig. 166* it is interesting to note that 347SS (austenitic) is the only alloy sandwiched between two different alloys (either ferritic, AFA, or a superalloy) in RG-CO_2 experiments 3 through 5. However, outliers appear not only at the ends, but also near the center for 347SS, where the individual data points resemble somewhat a U/V-shaped valley. Such location of outliers may be purely random or just chance, or could present insight into a phenomena taking place that is not clearly known. According to Grabke, care should be taken over the positioning of specimens and in particular the possibility of catalytic effects between multiple specimens of different alloys, whereby volatile corrosion products from one sample may trigger corrosion on a neighbor. To minimize this possibility, duplicate sample positions should be randomized in the autoclave, avoiding like specimen configurations [33]. In *Fig. 166* through *Fig. 168*, the range in difference between individual weight gains for RG-CO_2 is larger than in IG-CO_2 (*Fig. 169*) and BDG-CO_2 (*Fig. 170*), especially for the AFA's which

have significant scattering amongst their individuals. In RG-CO_2, the weight gains were higher, and in turn the growth rates occurred faster at early exposure times. This large range of difference between individuals in RG-CO_2 may be related to the growth rate observed. This could imply that for environments where coupons experience high growth rates, large deviations may be expected between individuals, and a sufficient number of samples should be selected to overcome such an effect and to assist in obtaining a weight gain value that is well-averaged and meaningful.

6. Summary

6.1. Results and Conclusions

- An experimental system for performing oxidation tests of various grades of alloys in $SCCO_2$ up to 650^{o}C and 20 MPa has been constructed and is capable of rank ordering alloy oxidation-corrosion performance.
- An effect of operating pressure (8.274MPa vs. 20 MPa) at 450^{o}C was found to increase the magnitude of weight gain and oxide growth for both T92 and T122, but the austenitics exhibited comparatively low weight gain at either pressure.
- Both ferritic materials at 450^{o}C developed a thick duplex oxide layer consisting of an outer magnetite (Fe_3O_4) layer and a chromium rich inner spinel layer, despite simultaneous material loss via pitting and carbon deposition. These effects, fitting in

definition to metal dusting, together with large magnitude weight gains compared to the other test alloys, warranted their removal from study at temperatures > 450^{o}C.

- The austenitic and AFA alloys at 450^{o}C displayed low weight gains and near parabolic oxidation curves and were exempt from metal dusting or material loss, suggesting protective oxidation and good corrosion resistance.
- The austenitic and AFA alloys at 650^{o}C are best portrayed by a combination of rate laws to describe their behavior as transition in stages of oxidation occur, fitting the type of regimes experienced in earlier works and denoted by an S-shaped curve, unseen before in this particular environment. This was not the case for IN800H, which demonstrated good corrosion resistance at all three test temperatures. 347SS began to show signs of spallation after 400 hours, while none of the AFA materials appeared to show such signs.
- Preferential attack was observed at the flat edges and corners of coupons, and contributed largely to the measured weight gains. This may be an important consideration for in-plant application of materials for components where joining and welds are present.
- Weight gains were lower in IG-CO_2 than in RG-CO_2 likely owing to the extra oxygen content helping suppress oxidation by forming a protective oxygen-rich oxide layer. More mass spectrometer analysis is needed at the outlet to ascertain the reaction products with respect to higher contents of moisture, hydrocarbons, and oxygen as provided by the gas certificate. The austenitics were generally unaffected by this change in environment, similarly as it was seen in changes of pressures. However

AFA-OC6 showed marked improvement while NF616 experienced a much larger weight gain than in RG-CO_2.

- Very thin oxide scales were observed in IG-CO_2. TEM analysis may help describe the nature of the thin oxide layer(s) formed.
- All surface treatments (Al, Y, and Shot Peen) showed improvement to oxidation resistance on the 9-12%Cr FM steels. The integrity or adherence of the aluminum layer rapidly diminished and continued to diminish at a linear rate. Y-coating added significant benefit for both FM steels, slowing down the rate of oxide but at a much lower continued linear rate. Peening proved effective as a cold working tool, and was similar in performance to Y-coating for T122.

6.2. Future Work

Testing was still being performed at the conclusion of this work to evaluate the oxidation-corrosion performance of alloys at high temperature.

- In the near future, efforts will be made by my predecessor, Jacob Mahaffey, to gain more insight and understanding into the effects of impurities in controlled doses such as H_2O, CO, O_2, hydrocarbons, etc., but primarily moisture at the onset. Several doses are anticipated to be trialed at 50, 75, 100, and 1000ppm of H_2O at 650^oC.
- In addition, measurements will be made in collaboration with Sandia National Laboratory using the same concentration as that employed in their $SCCO_2$ flow loops to simulate an in-plant condition. The difference between the measurements made in

this study with the aforementioned in-plant condition may help to provide some explanation of the byproducts to be expected (dumped) downstream in other machinery components. Many measurements have been made on iron-based alloys using CO_2/CO mixtures, as well as different concentrations of CO in the gas [16], but at sub-critical pressures.

- Use will be made of a mass spectrometer system running simultaneously with LabVIEW acquisition to capture mass spectra of inlet moisture and concentrations of reaction products at the outlet of the autoclave apparatus. Such measurements will be made in a similar fashion to that of Quadakkers et al [83], but who used gas chromatography and an electrolytic-type H_2O monitor for impurities in impure helium.
- Future testing also includes measurements made at lower temperatures and/or pressures for lower temperature components in the Brayton cycle that do not experience full turbine inlet conditions, as well as those expected for the precooler.

7. References

[1] Tammann, G. (1920). *Über Anlauffarben von Metallen*, Z. Anorg. Allg. Chem. III, pp. 78-89.

[2] Tammann, G. and Koster, W. (1922). Z. Anorg. Chem., 123.

[3] Pilling, N.B. and Bedworth, R.E. (1923). *The Oxidation of Metals at High Temperature*, Journal of the Institute of Metals, Vol. 29, pp. 529-582.

[4] Kubaschewski, B.E. and Hopkins, O. (1962). *Oxidation of Metals and Alloys*, Butterworths Publishing.

[5] Dunn, J.S. (1926). *The High Temperature Oxidation of Metals*, Proc. R. Soc. Lond. A. 111, pp. 203-209.

[6] Hauffe, K. (1965). *Oxidation of Metals*, Plenum Press, New York.

[7] Rohr, V., Schutze, M., Fortuna, E., Tsipas, D.N., Milewska, A., and Perez, F.J. (2005). *Development of Novel Diffusion Coatings for 9-12% Cr Ferritic-Martensitic Steels*, Materials And Corrosion, Vol. 56, No. 12, pp. 874-881.

[8] Klueh, R.L., and Harries, D.R. (2001). *High Chromium Ferritic and Martensitic Steels for Nuclear Applications*, ASTM International.

[9] Oh, C., Lillo, T., Windes, W., Totemeier, T., and Moore, R. (2004). *Development of a Supercritical Carbon Dioxide Brayton Cycle: Improving PBR Efficiency and Testing Material Compatability*, Nuclear Energy Research Initiative, pp. 1-28.

[10] G. Sulzer, "Verfahren zur Erzeugung von Arbeit aus Warme," 269599, July 15, 1950.

[11] E. G. Feher, "*The Supercritical Thermodynamic Power Cycle*," in Intersociety Energy Conversion Engineering Conference, Miami Beach, 1967, Paper No. 4348.

[12] "Conference Proceedings from the Supercritical CO2 Power Cycle Symposium," in Supercritical CO2 Power Cycle Symposium, Troy, NY, 2009.

[13] Y Kato, T Nitawaki, and Y Muto, "*Medium Temperature Carbon Dioxide Gas Turbine Reactor*," Nuclear Engineering and Design, p. Vol. 230 pp. 195, 2004.

[14] Chang H. Oh, "*Development of a Supercritical Carbon Dioxide Brayton Cycle: Improving VHTR Efficiency and Testing Material Compatibility*," Idaho Falls, 2006.

[15] Dostal, V, Driscoll, M.J., and Hezjlar, P. (2004). *A Supercritical Carbon Dioxide Cycle for Next Generation Nuclear Reactors*, Advanced Nuclear Power Technology Program, pp. 1-307.

[16] Holmes, D.R. and Hill, R.B. (1974). *Corrosion of Steels in CO_2*, British Nuclear Energy Society (BNES), Reading University.

[17] Ma, Z., and Turchi, C.S. (2011). *Advanced Supercritical Carbon Dioxide Power Cycle Configurations for Use in Concentrating Solar Power Systems*, Supercritical CO2 Power Cycle Symposium: NREL/CP-5500-50787, pp. 1-5.

[18] Chapman, D.J., and Arias, D.A. (2009). *An Assessment of the Supercritical Carbon Dioxide Cycle for Use in a Solar Parabolic Trough Power Plant*, Proceedings of SCCO2 Power Cycle Symposium, April 29-30, Troy NY.

[19] Klueh, R.L., and Nelson, A.T. (2007). *Ferritic-Martensitic Steels for Next Generation Reactors*, Journal of Nuclear Materials, pp.37-52.

[20] Sridhar, S., Rozzelle, P., Morreale, B., and Alman, D. (2011). *Materials Challenges for Advanced Combustion and Gasification Fossil Energy Systems*, Metallurgical and Materials Transactions A, Vol. 42A, pp. 871-877.

[21] Gong, Y, et al. *Analysis of Radial Compressor Options for Supercritical CO2 Power Conversion Cycles*, MIT-GFR-034, June 2006

[22] Wright, S.A., Radel, R.F., Vernon, M.E., Rochau, G.E., and Pickard, P.S. (2010). *Operation and Analysis of a Supercritical CO2 Brayton Cycle*, Sandia National Laboratories-SAND2010-0171, pp. 1-101.

[23] Grabke, H.J.(1998). *Carburization: A High Temperature Corrosion Phenomenon*, Materials Technology Institute of the Chemical Process Industries, Inc., MTI Publication No. 52

[24] Gibbs, J.P. (2010). *Corrosion of Various Engineering Alloys in Supercritical Carbon Dioxide*, M.S. Thesis, MIT.

[25] Dunlevy, M.W. (2009). *An Exploration of the Effect of Temperature on Different Alloys in a Supercritical Carbon Dioxide Environment*, A Dissertation submitted to the Massachusetts Institute of Technology, pp. 1-176.

[26] Lim, J.Y., McKrell, T.J., Eastwick, G., and Ballinger, R.G. (2008). *Corrosion of Materials in Supercritical Carbon Dioxide Environments*, NACE International, Paper No. 08430.

[27] Furukawa, T., Inagaki, Y., and Aritomi, M. (2010). *Corrosion Behavior of FBR Structural Materials in High Temperature Supercritical Carbon Dioxide*, Journal of Power and Energy Systems, Vol. 4, No. 1, pp. 252-261.

[28] Rouillard, F., Charton, F., and Moine, G. (2009). *Corrosion Behavior of Different Metallic Materials in Supercritical CO2 at 550^{o}C and 250 Bars*, Proceedings of the SCCO2 Power Cycle Symposium, Troy, NY, April 29-30.

[29] Rouillard, F., Moine, G., Tabarant, M., and Ruiz, J.C. (2012). *Corrosion of 9Cr Steel in CO2 at Intermediate Temperature II: Mechanism of Carburization*, Oxidation of Metals, Vol. 77, pp. 57-70.

[30] Jelinek, J. (2012). *Corrosion Behavior of Alloys in High Temperature High Pressure Supercritical Carbon Dioxide*, M.S. Thesis, UW-Madison

[31] Anderson, M., Cao, G., Tan, L., Sridharan, K., and Allen, T. (2009). *High Pressure and Temperatures S-CO2 Alloy Testing*, University of Wisconsin-Madison: Thermal Hydraulics Laboratory, pp. 1-52.

[32] Baxter, D.J., Fordham, R.J., and Norton, J.F. (1993). *The Need for Standard Test Methodologies for High Temperature Corrosion: Simulating Gaseous Corrosion Processes*, Materials at High Temperature, 11, 1-4, pp. 70-74.

[33] Grabke, H.J., and Meadowcraft, D.B. (1995). *Guidelines for Methods of Testing and Research in High Temperature Corrosion*, Institute of Metals, European Federation of Corrosion Publications, No. 14.

[34] Kofstad, P. (1958). *Oxidation of Metals: Determination of Activation Energies*, Acta Chemica Scandinavica, Vol. 12, No. 4, pp. 701-707.

[35] Kofstad, Per (1966). *High Temperature Oxidation of Metals*, John Wiley & Sons Inc.

[36] Pint, B.A., Anderson, B.N., Matthews, W.J., Waldhelm, C.M., and Treece, W. (2013). *Evaluation of a NiCrAl Foil for a Concentrated Solar Power Application*, Proceedings of the ASME Turbo Expo, June 3-7, San Antonio, TX.

[37] Nesbitt, J.A., and Heckel, R.W. (1984). *Modeling Degradation and Failure of Ni-Cr-Al Overlay Coatings*, Thin Solid Films, Vol. 119, pp. 281-290.

[38] Santrock, J., Studley, S.A., and Hayes, J.M. (1985). *Isotopic Analyses Based on the Mass Spectrum of Carbon Dioxide*, Anal. Chem., Vol. 57, pp. 1444-1448.

[39] Kane, R.H., and Goodell, P.D. (1982). *Gas Analysis Techniques for High Temperature Corrosion Testing*, Journal of Testing and Evaluation, JTEVA, Vol. 10, No. 6, pp. 286-291.

[40] Ren, X. (2008). *Corrosion of Ferritic-Martensitic Steels and Ni-Based Alloys in Supercritical Water*, M.S. Thesis, UW-Madison.

[41] Tan, L., Ren, X., Sridharan, K., and Allen, T. (2008). *Effect of Shot-Peening on the Oxidation of Alloy 800H Exposed to Supercritical Water and Cyclic Oxidation*, Corrosion Science, Vol. 50, pp. 2040-2046.

[42] Allen, T.R., Chen, Y., Ren, X., Sridharan, K., Tan, L., Was, G.S., West, E., and Guzonas, D. (2012). *Material Performance in Supercritical Water*, pp. 279-326.

[43] Tang, Z., Wang, F., Wu, W., Wang, Q., and Li, D. (1998). *Effect of Coatings on Oxidation Resistance and Mechanical Performance of Ti60 Alloy*, Materials Science & Engineering, Vol. A255, pp. 133-138.

[44] SAE (1991). *SAE Manual on Shot Peening*, SAE HS-84, 3rd Edition, Sep. 1991.

[45] Garibay, R.P., and Chang, N.S. (1989). *Improved Fatigue Life of a Carburized Gear by Shot Peening Parameter Optimization*, International Conference on Carburizing: Processing & Performance, July, pp. 283-289.

[46] Grabke, H.J., Muller-Lorenz, E.M., Strauss, S., Pippel, E., and Woltersdorf, J. (1997). *Effects of Grain Size, Cold Working, and Surface Finish on the Metal Dusting Resistance of Steels*, Oxidation of Metals, Vol. 50, Nos. 3/4, pp. 241-254.

[47] Piehl, C., Tokei, Z., and Grabke, H.J. (2001). *Surface Treatment and Cold Workings as Tools to Improve Oxidation Behaviour of Chromium Steels*, Materials Science Forum, Vol. 369-372, pp. 319-326.

[48] SAE J443 (1984). *Procedures for using Standard Shot Peening Test Strip*, Warrendale, PA.

[49] Personal communication with Lue Schumaker at SMC

[50] Allen, T.R., Chen, Y., Ren, X., and Sridharan, K. (2005). *Corrosion of Candidate Materials for Supercritical Water-Cooled Reactors*, Proc. of 12th Inter. Conf. on Env. Deg. Of Matls in Nuclear Power System - Water Reactors, pp. 1397-1407.

[51] Cox, B., and Johnston, T. (1963). *The Oxidation and Corrosion of Niobium*, Trans. Met. Soc. AIME, Vol. 227, pp. 36-47.

[52] Kofstad, P., and Bredesen, R. (1991). *On the Oxidation of Iron in CO2 + CO Gas Mixtures II: Reaction Mechanisms During Initial Oxidation*, Oxidation of Metals, Vol. 35, Nos. 1/2, pp. 107-137.

[53] Abdulaziz I. Al-Meshari, *Metal Dusting of Heat-Resistant Alloys*, 2008, Ph. D. Dissertation, University of Cambridge.

[54] J. C. Griess, J. H. DeVan, and W. A. Maxwell, "*Long-Term Corrosion of Cr-Ni Steels in Superheated Steam at 482 and 538C*," in NACE Corrosion 81, Houston, TX, 1981.

[55] F. Eberle and J. H. Kitterman, "*Behavior of Superheater Alloys in High Temperature, High Pressure Steam*," American Society of Mechanical Engineers, p. 67, 1968.

[56] Y. Watanabe et al., Proceedings of the 9th International Conference on Pressure Vessel Technology, April 9-14, 2000.

[57] J. Litz, A. Rahmel, and M. Schorr, "*Selective Carbide Oxidation and Internal Nitridation of the Ni-base Superalloys IN 738 LC and IN 939 in Air*," Oxidation of Metals, vol. 30, no. 1-2, pp. 95-105, 1988.

[58] A. A. Krishnan and V. Prakash, "*High Temperature Oxidation Characteristics of Some Manganese-Aluminum Steels Part I*," Journal of Scientific and Industrial Research , vol. 13B, pp. 444-449, June 1954.

[59] H. Buscail et al., "*Characterization of the Oxides Formed at 1000C on the AISI 316L Stainless Steel- Role of Molybdenum*," Materials Chemistry and Physics, vol. 111, pp. 491-496, April 2008.

[60] G. D. Smith, *High Temperature, Corrosion Tests and Standards* -- Application and Interpretation, R. Baboian, Ed.: American Society of Testing and Materials, 1995.

[61] Zhang, J., Spech, P., Young, D. (2012). *Metal Dusting of Alumina-Forming Creep-Resistant Austenitic Stainless Steels*, Oxidation of Metals, Vol. 77, No. 3-4, pp. 167-187.

[62] Gibbs, G.B. (1965). *On the Temperature Dependence of the Activation Energy for Diffusion, Acta Metallurgica*, Vol. 13, pp. 926-927.

[63] Gibbs, G.B. (1968). *The Analysis of Curved Arrhenius Plots*, Scripta Metallurgica, Vol. 2, pp. 65-68.

[64] Was, G.S., and Teysseyre, S. (2005). *Challenges and Recent Progress in Corrosion and Stress Corrosion Cracking of Alloys for Supercritical Water Reactor Core*

Components, Proceedings of the 12th International Conference on Environmental Degradation of Materials in Nuclear Power System – Water Reactors.

[65] Grabke, H.J., Muller-Lorenz, E.M., Alcester, B., and Lucas, M. (2000). *Formation of chromium rich oxide scales for protection against metal dusting*, Materials at High Temperatures, Vol. 17, pp. 339-346.

[66] Cabrera, N., and Mott, N.F. (1949). *Theory of the Oxidation of Metals*, Rep. Prig. Phys. 12, pp. 163-184.

[67] Su, Y.J., Trice, R.W., Faber, K.T., Wang, H., and Porter, W.D. (2004). *Thermal Conductivity, Phase Stability, and Oxidation Resistance of YSZ Thermal Barrier Coatings*, Oxidation of Metals, Vol. 61, Nos. 3/4, pp. 253-271.

[68] Alvarez, J., Melon, D., Salas, O., Oseguera, J., and Lopez, V. (2008). *Protective Coatings Against Metal Dusting*, Surface & Coatings Technology, Vol. 203, pp.422-426.

[69] Rouillard, F., Moine, G., Martinelli, L., and Ruiz, J.C. (2012). *Corrosion of 9Cr Steel in CO2 at Intermediate Temperature I: Mechanism of Void-Induced Duplex Oxide Formation*, Oxidation of Metals, Vol. 77, pp. 27-55.

[70] Naraparaju, R., Christ, H.J., Renner, F.U., and Kostka, A. (2011). *Effect of Shot-Peening on the Oxidation Behaviour of Boiler Steels*, Oxidation of Metals, Vol. 76, pp. 233-245

[71] Agarwal, D.C., Kloewer, J., and Brill, U. (2001). *Recent Results on Metal Dusting of Nickel Base Alloys and Some Applications*, NACE International, Paper No. 01382

[72] LaGrange, M.H., Huntz, A.M., and Davidson, J.H. (1984). *The Influence of Y, Zr, or Ti Additions on the High Temperature Oxidation Resistance of Fe-Ni-Cr-Al Alloys of Variable Purity*, Corrosion Science, Vol. 24, No. 7, pp. 613-627.

[73] Delaunay, D., Huntz, A.M., and Lacombe, P. (1980). *Mechanical Stresses Developed in High Temperature Resistant Alloys During Isothermal and Cyclic Oxidation Treatments: The Influence of Yttrium Additions on Oxide Scale Adherence*, Corrosion Science, Vol. 20, pp. 1109-1117.

[74] Vander Voort, G.F. (1984). *Metallography, Principles, and Practice*, ASM International.

[75] Hurlen, Tor. (1961). *Oxidation of Niobium*, Journal of Institute of Metals, Vol. 89, 1960-61, pp. 273-280.

[76] Blackburn, P.E. (1962). *The Mechanisms of the Niobium Reaction with Water Vapor and with Oxygen*, Journal of Electrochemical Society, Vol. 109, pp. 1142-1150.

[77] Cox, B., and Johnston, T. (1963). *The Oxidation and Corrosion of Niobium*, Trans. Met. Soc. AIME, Vol. 227, pp. 36-47.

[78] Kitagawa, K. (2013). *Thin-Film Thickness Profile Measurement by Three-Wavelength Interference Color Analysis*, Applied Optics, Vol. 52, No. 10, pp. 1998-2007.

[79] ASTM (1990). *Manual on Presentation of Data and Control Chart Analysis: 6th Edition*, Committee E-11 on Quality and Statistics, ASTM Manual 7.

[80] Brush, E.G. (1965). *Corrosion Rate Law Considerations in Superheated Steam*, Nuclear Applications, Vol. 1, pp. 246-251.

[81] Freeman, R.A., and Silverman, D.C. (1992). *Technical Note: Error Propagation in Coupon Immersion Tests*, NACE Corrosion, Vol. 48, No. 6, pp. 463-466.

[82] Quesenberry, C.P. (1993). *The Effect of Sample Size on Estimated Limits for X-bar and X Control Charts*, Journal of Quality Technology, Vol. 25, No. 4, pp. 237-247.

[83] Quadakkers, W.J., Schuster, H., and Shindo, M. (1986). *Corrosion Behaviour of High Temperature Alloys in Impure Helium Environments*, Jour. of Nuclear Materials 140, pp. 94-105.

8. Appendices

The appendices contained herein include those too large to include in the main body of this work, but have relevant reference to discussion made within, and will serve to aid in the future for quick reference of measured values, and also for which additional exploratory statistical analyses may be carried out.

8.1. Interference Colors

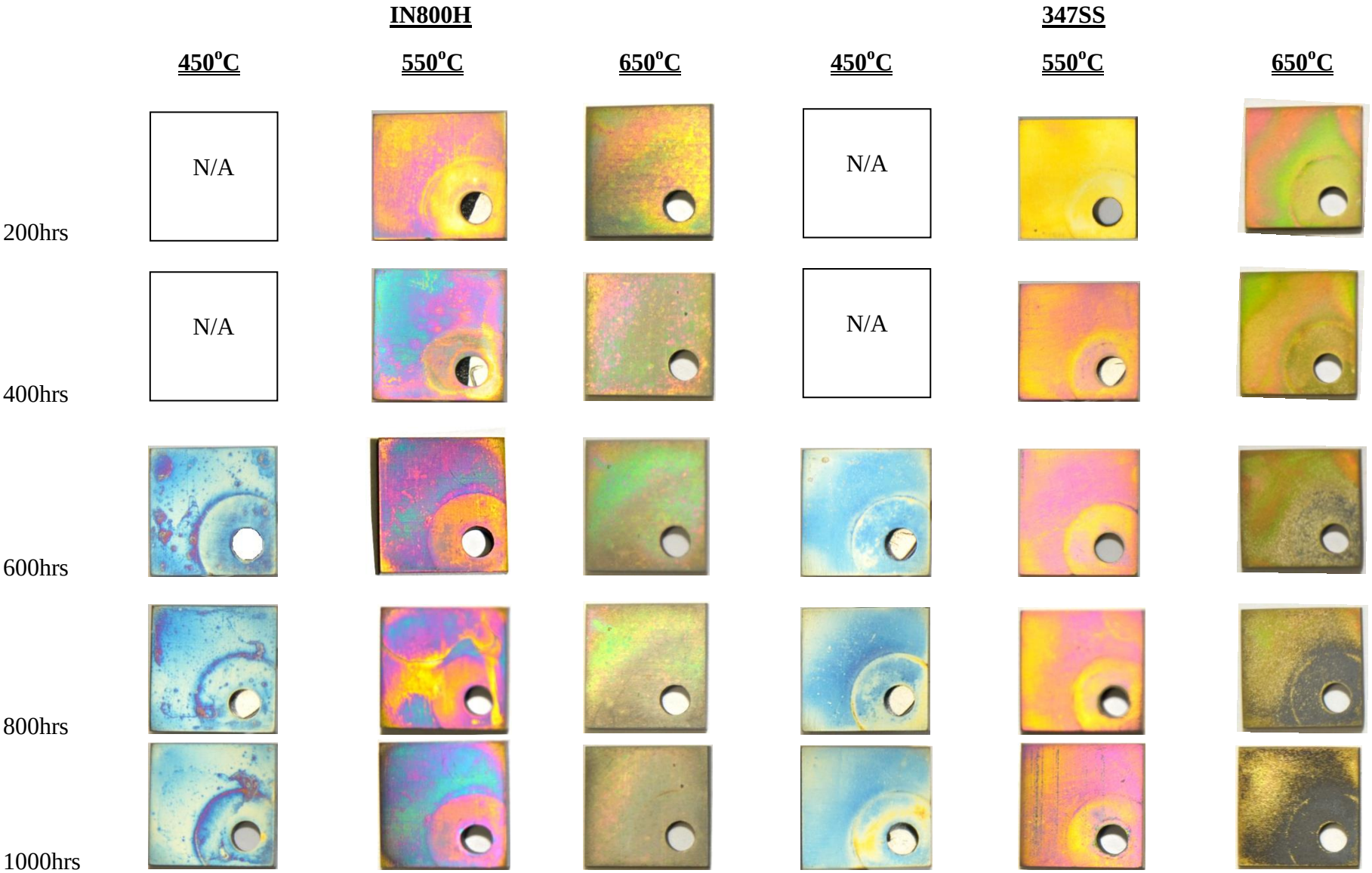

Fig. 171: Interference Colors of Coupons for **Expt. #3 through #5**

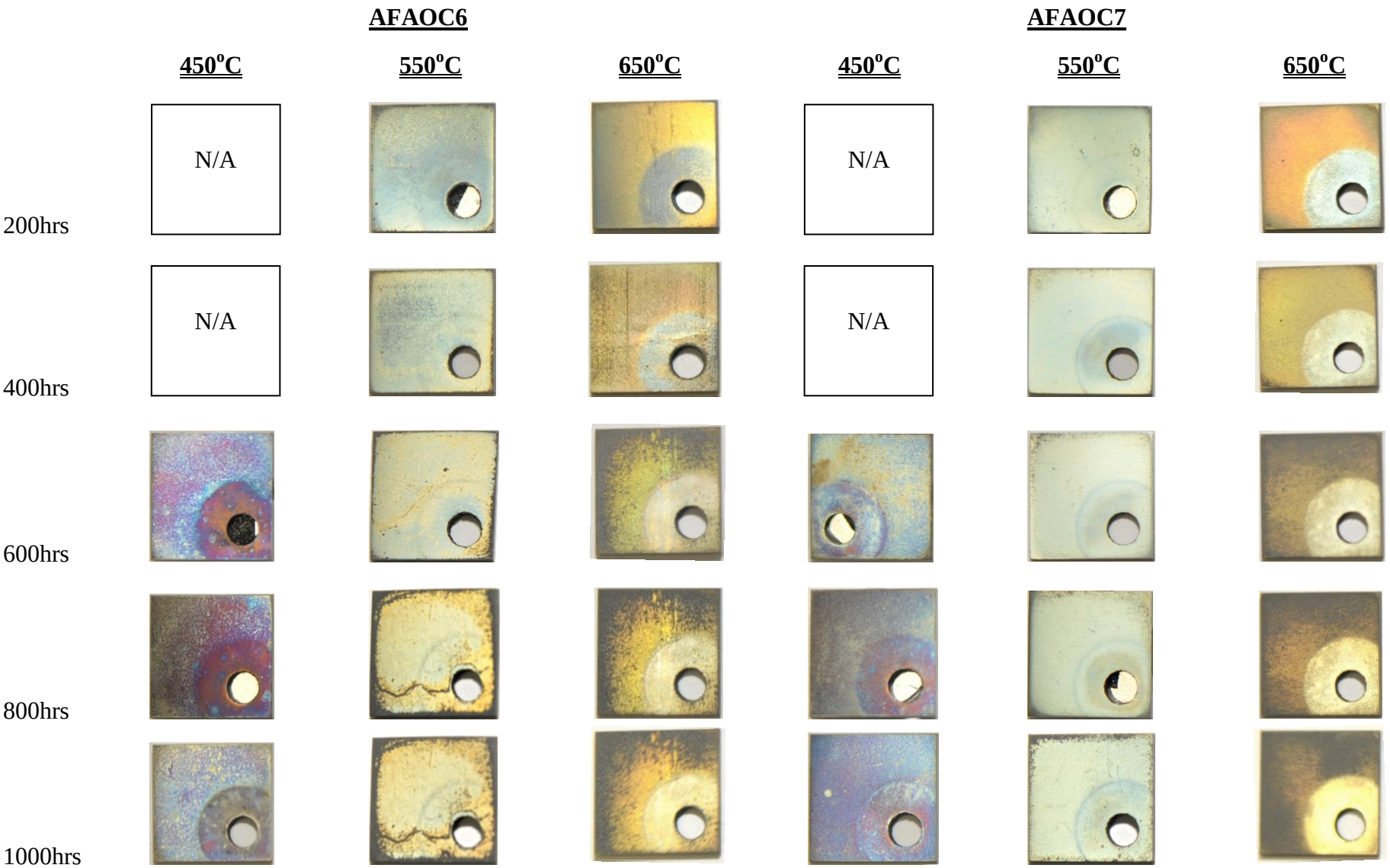

***Fig. 172*:** Interference Colors of Coupons for **Expt. #3 through #5** (Cont.')

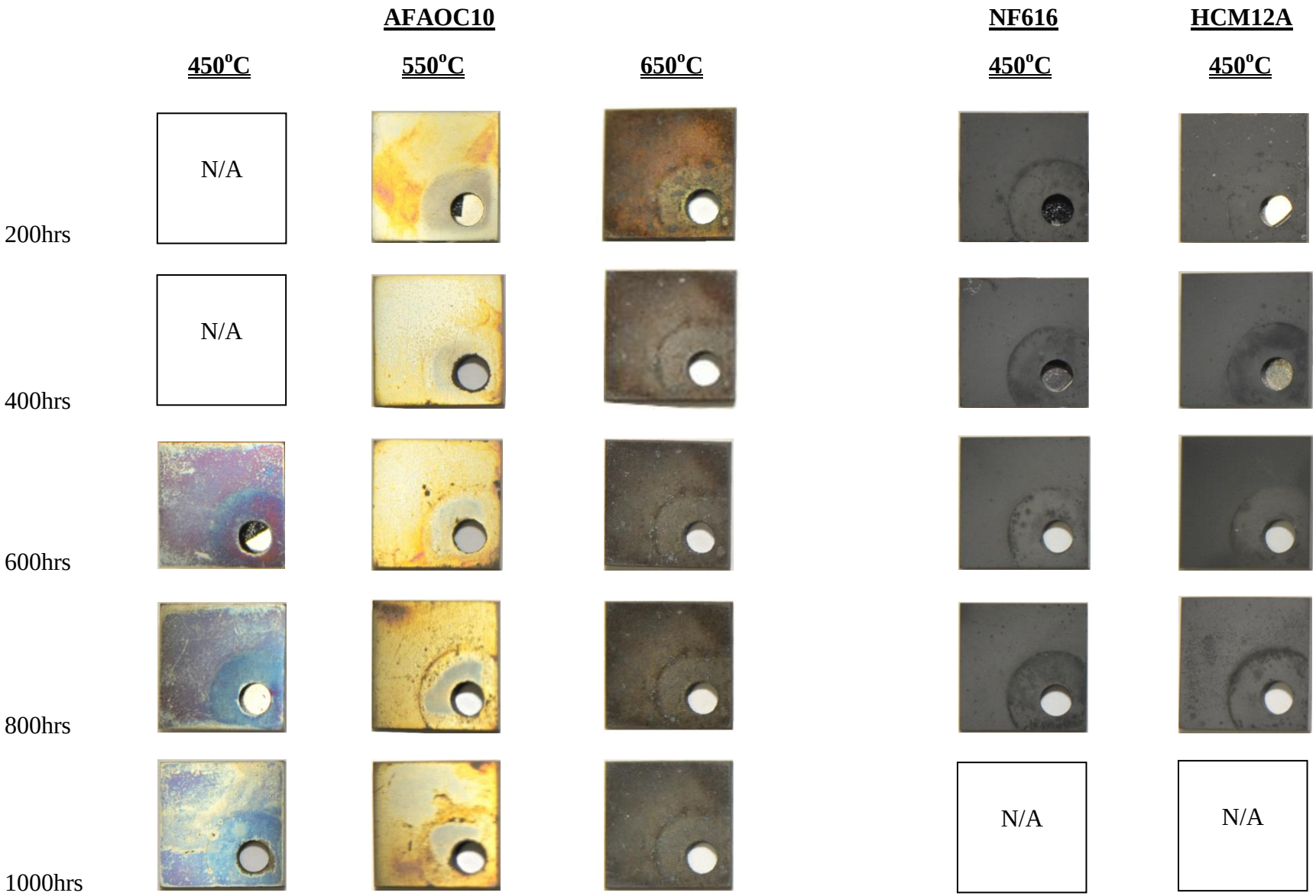

Fig. 173: Interference Colors of Coupons for **Expt. #3 through #5** (Cont.')

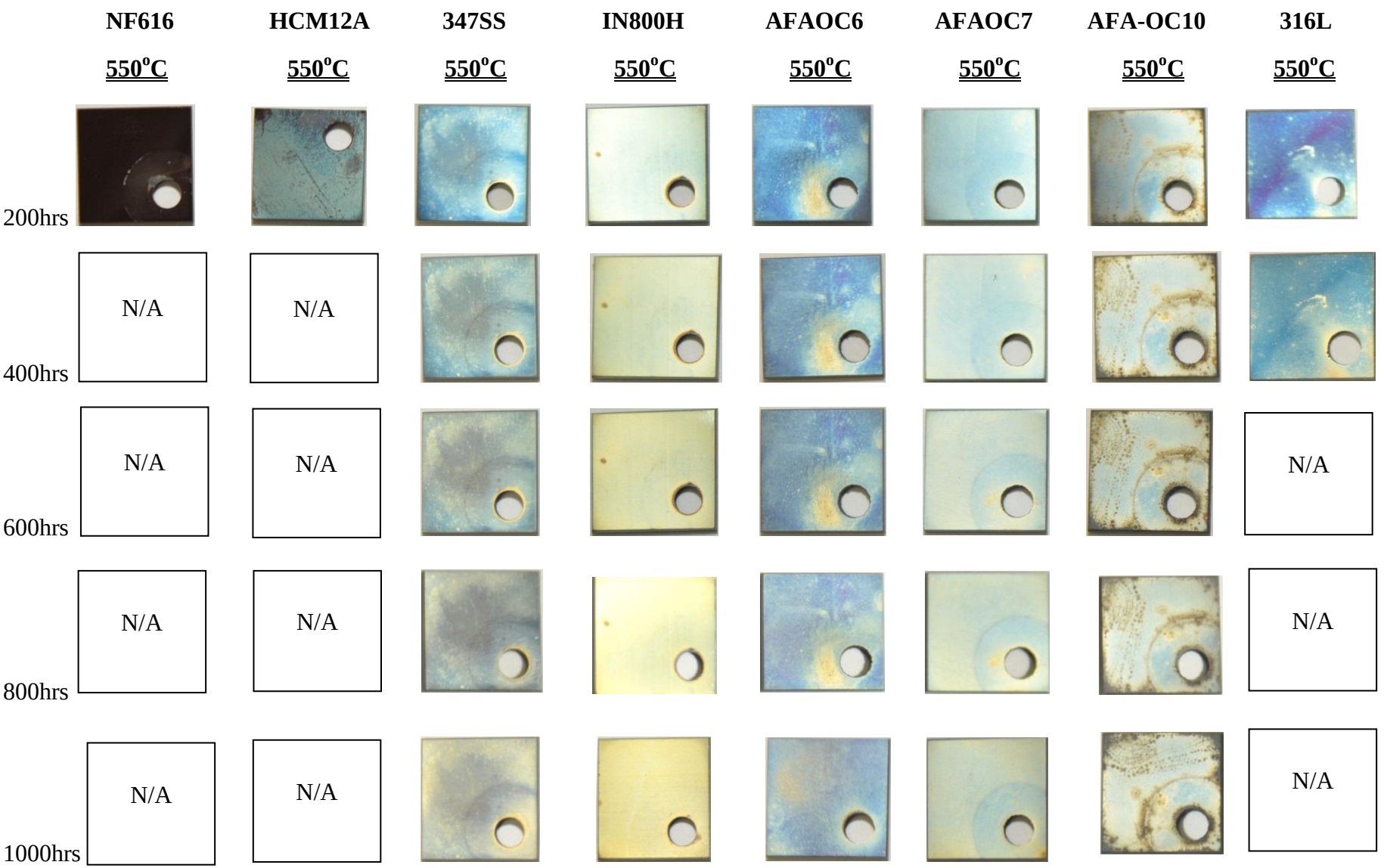

Fig. 174: Interference Colors of Coupons for **Expt. #6**

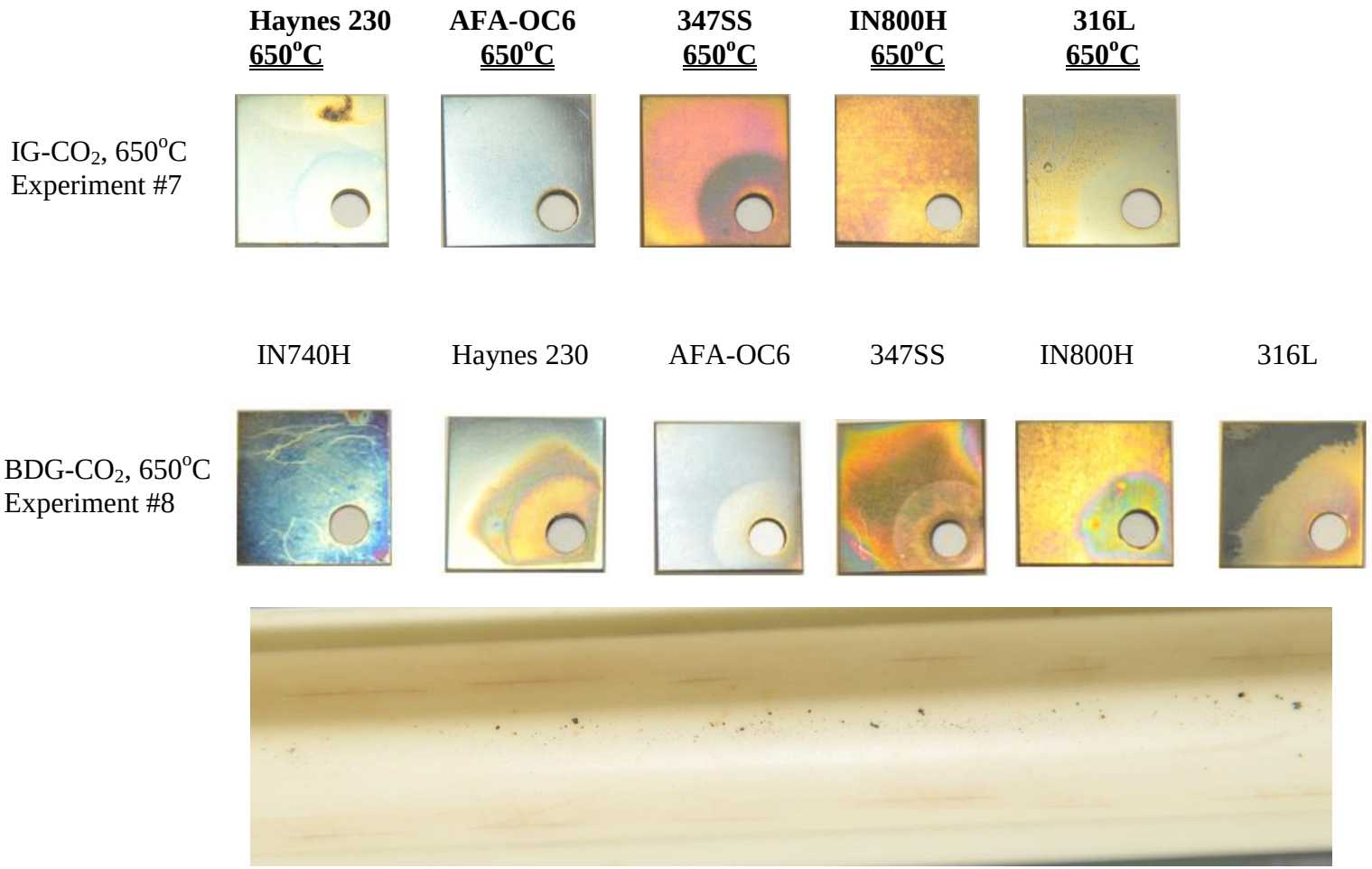

Fig. 175: Interference Colors of Coupons for Expt. #7 and #8.
Bottom: Metal particles collected on alumina boat at 1000 hour interval.

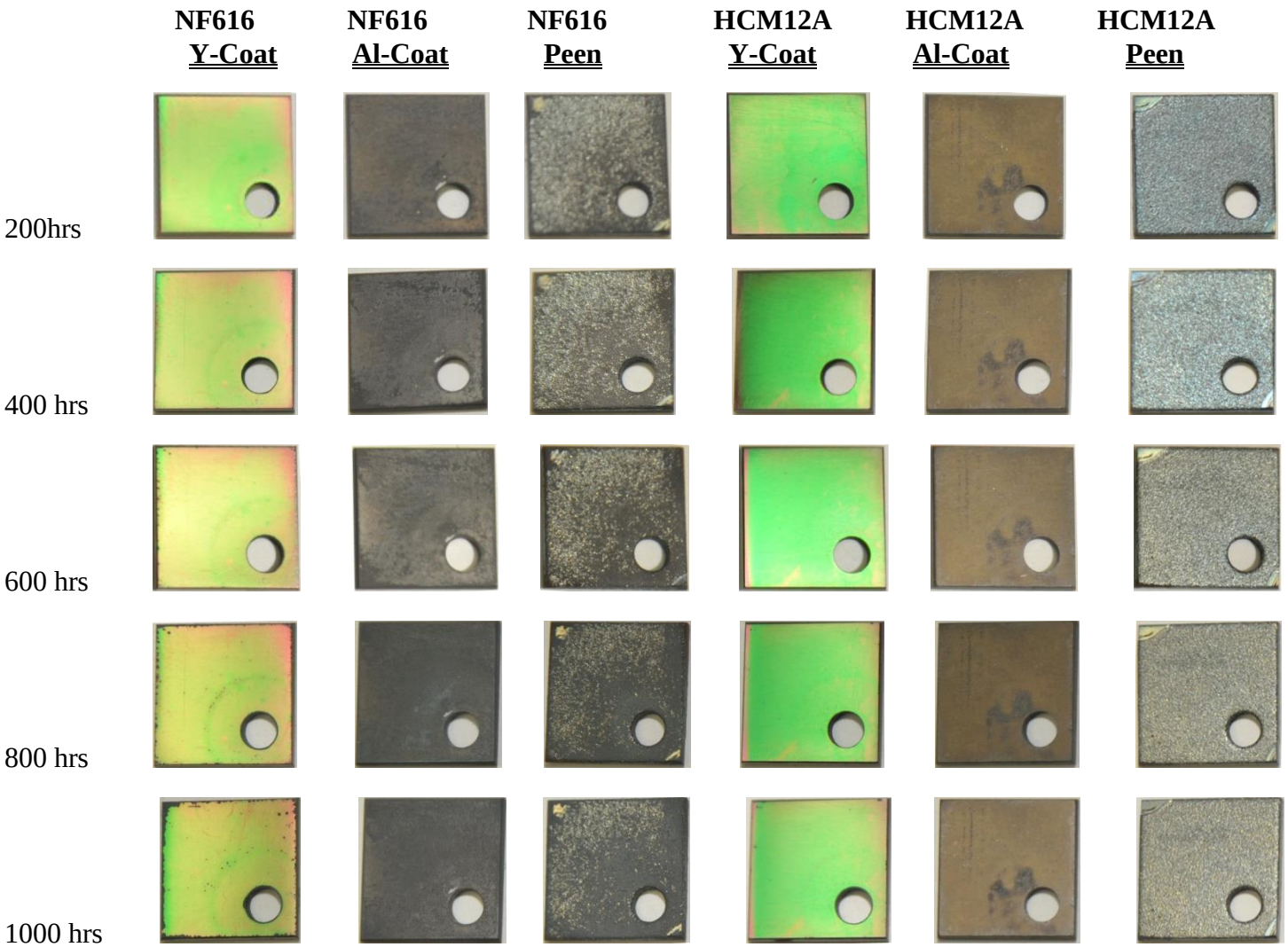

Fig. 176: Interference Colors of Coupons for Expt. #9

8.2. Average Weight Gains with 95% Confidence Limits

Table 12: Expt. #3- #5 Avg. Weight Gain Values using Research Grade CO_2 (mg/cm^2)

Sample ID	Temp./Press.	200 hours	400 hours	600 hours	800 hours	1000 hours
IN800H	450°C/20MPa	0.010149 ± 0.000916	0.012275 ± 0.000928	0.011288 ± 0.000951	0.011481 ± 0.001576	0.011666 ± 0.001923
	550°C/20MPa	0.030700 ± 0.015767	0.042900 ± 0.022789	0.044327 ± 0.010191	0.049395 ± 0.015482	0.057889 ± 0.004741
	650°C/20MPa	0.101062 ± 0.010043	0.119500 ± 0.009595	0.127967 ± 0.012225	0.132887 ± 0.018915	0.136063 ± 0.010324
347SS	450°C/20MPa	0.011625 ± 0.004933	0.013791 ± 0.005725	0.015682 ± 0.006018	0.015918 ± 0.008509	0.018299 ± 0.010146
	550°C/20MPa	0.025660 ± 0.004981	0.029093 ± 0.002862	0.031872 ± 0.004060	0.033359 ± 0.007320	0.033617 ± 0.001243
	650°C/20MPa	0.072201 ± 0.004957	0.084852 ± 0.007165	0.129877 ± 0.048710	0.242039 ± 0.142072	0.386471 ± 0.141390
AFA-OC6	450°C/20MPa	0.013782 ± 0.002237	0.015784 ± 0.002496	0.020170 ± 0.002687	0.021745 ± 0.003143	0.022846 ± 0.004112
	550°C/20MPa	0.047509 ± 0.004331	0.092908 ± 0.010342	0.147400 ± 0.027605	0.229400 ± 0.058298	0.367599 ± 0.044455
	650°C/20MPa	0.096249 ± 0.011774	0.130344 ± 0.011777	0.799084 ± 0.355170	0.787897 ± 0.466297	0.660381 ± 0.070337
	* 650°C/20MPa	0.096249 ± 0.011774	0.130344 ± 0.011777	0.462216 ± 0.028905	0.567428 ± 0.052324	0.660381 ± 0.070337
AFA-OC7	450°C/20MPa	0.013637 ± 0.002484	0.015724 ± 0.002360	0.019903 ± 0.002765	0.017488 ± 0.002254	0.017506 ± 0.003916
	550°C/20MPa	0.031197 ± 0.004182	0.043984 ± 0.003738	0.053847 ± 0.011360	0.056479 ± 0.013860	0.079962 ± 0.007977
	650°C/20MPa	0.074386 ± 0.018628	0.127827 ± 0.024785	0.299352 ± 0.064107	0.364361 ± 0.111194	0.378229 ± 0.086913
AFA-OC10	450°C/20MPa	0.018141 ± 0.002039	0.021551 ± 0.003203	0.028363 ± 0.002662	0.028042 ± 0.002014	0.029676 ± 0.003402
	550°C/20MPa	0.025400 ± 0.018319	0.034900 ± 0.023401	0.043500 ± 0.033613	0.045700 ± 0.026440	0.051800 ± 0.006199
	650°C/20MPa	0.092972 ± 0.023582	0.361957 ± 0.156000	0.533214 ± 0.288466	0.694914 ± 0.616866	0.970907 ± 0.898627
	* 650°C/20MPa	0.092972 ± 0.023582	0.297815 ± 0.043638	0.423829 ± 0.084247	0.504246 ± 0.147183	0.512423 ± 0.260711
HCM12A	450°C/20MPa	1.076044 ± 0.016615	1.332318 ± 0.031026	1.482732 ± 0.028265	1.626375 ± 0.051709	**Not tested**
	550°C/20MPa	2.402450 ± 0.130907	3.034332 ± 0.010793	**Not tested**	**Not tested**	**Not tested**
NF616	450°C/20MPa	0.903723 ± 0.007139	1.205530 ± 0.009868	1.419824 ± 0.025574	1.583505 ± 0.042408	**Not tested**
	550°C/20MPa	2.259518 ± 0.592245	3.321001 ± 0.520771	**Not tested**	**Not tested**	**Not tested**

Uncertainty values computed based on 95% confidence limits (Student t table) provided in ASTM Manual 7 [55].

* Average weight gain value computed with "outliers" outside of ASTM control limits removed. Applied by Brush [75], but done here if outside controls.

Table 13: Expt. #6 Avg. Weight Gain Values using Industrial Grade CO_2 (mg/cm^2)

Sample ID	Temp./Press.	200 hours	400 hours	600 hours	800 hours	1000 hours
IN800H	550°C/20MPa	0.022911 ± 0.003289	0.029466 ± 0.004099	0.031747 ± 0.007013	0.034211 ± 0.003182	0.036681 ± 0.003882
347SS	550°C/20MPa	0.020013 ±0.003379	0.023499 ± 0.003482	0.026439 ± 0.004939	0.029212 ± 0.003611	0.030870 ± 0.001228
AFA-OC6	550°C/20MPa	0.035580 ± 0.008855	0.042456 ± 0.013026	0.043357 ± 0.012275	0.042283 ± 0.007623	0.042563 ± 0.007870
AFA-OC7	550°C/20MPa	0.035475 ±0.004461	0.036784 ± 0.006030	0.037620 ± 0.009801	0.038362 ± 0.011343	0.040204 ± 0.008353
AFA-OC10	550°C/20MPa	0.005381 ±0.005412	0.015098 ± 0.004786	0.029096 ± 0.003484	0.063138 ± 0.005279	0.102197 ± 0.002252
HCM12A	550°C/20MPa	0.558454 ± 0.176256	0.774983 ± 0.164184	**Not tested**	**Not tested**	**Not tested**
NF616	550°C/20MPa	3.450994 ± 0.162144	**Not tested**	**Not tested**	**Not tested**	**Not tested**
316L	550°C/20MPa	0.016933 ± 0.001596	0.022841 ± 0.004029	**Not tested**	**Not tested**	**Not tested**

Uncertainty values computed based on 95% confidence limits (Student t table) provided in ASTM Manual 7. [55]

Table 14: Expt. #9 Avg. Weight Gain Values using Research Grade CO_2 (mg/cm^2)

Sample ID	Temp./Press.	200 hours	400 hours	600 hours	800 hours	1000 hours
HCM12A (Al Coat)	550°C/20MPa	0.176429 ± 0.021598	0.246831 ± 0.033288	0.289554 ± 0.021331	0.348784 ± 0.027073	0.396836 ± 0.031427
HCM12A (Y Coat)	550°C/20MPa	0.106714 ± 0.005452	0.147899 ± 0.007409	0.187766 ± 0.011835	0.223650 ± 0.054191	0.266629 ± 0.052443
HCM12A (Shot Peen)	550°C/20MPa	0.158822 ± 0.010585	0.199023 ± 0.014730	0.243791 ± 0.037619	0.273148 ± 0.009971	0.293403 ± 0.009980
NF616 (Al Coat)	550°C/20MPa	0.771573 ± 0.095404	1.212986 ± 0.169118	1.882982 ± 0.215472	2.398347 ± 0.276442	2.917167 ± 0.350244
NF616 (Y Coat)	550°C/20MPa	0.131762 ± 0.003889	0.190560 ± 0.010339	0.254493 ± 0.035196	0.355282 ± 0.086095	0.479291 ± 0.126023
NF616 (Shot Peen)	550°C/20MPa	1.071789 ± 0.205456	1.623505 ± 0.281161	2.223219 ± 0.529005	2.791231 ± 0.633449	3.339116 ± 0.695360

Uncertainty values computed based on 95% confidence limits (Student t table) provided in ASTM Manual 7. [55]

8.3. Raw Data Tables

Table 15: Raw Data, Expt. #3, RG-CO_2/450^{o}C/20MPa, Coupon Arrangement

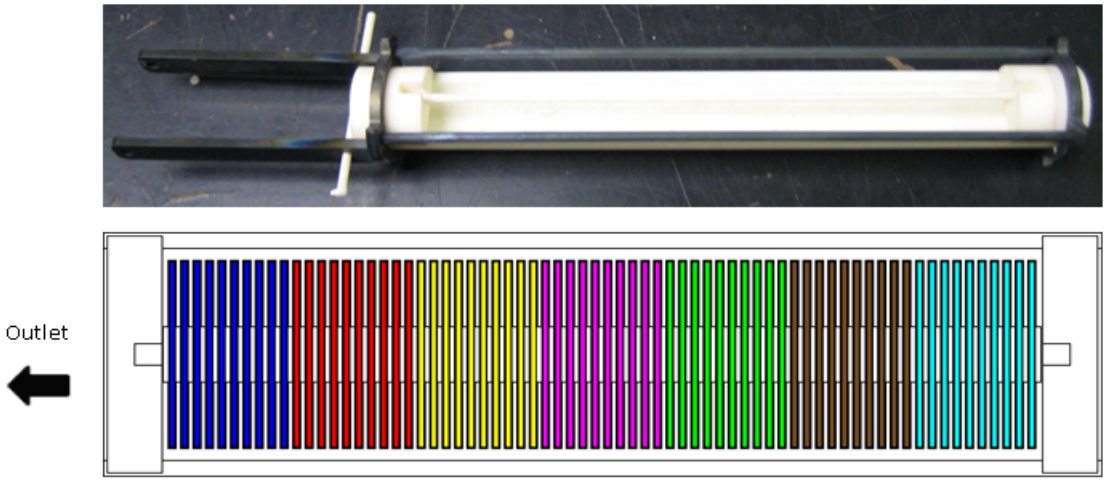

Sample	Blue HCM12A	Red NF616	Yellow 347ss	Magenta AFA-OC6	Green AFA-OC7	Brown AFA-OC10	Cyan IN800H
1	H08	N08	S08	A608	A702	A102	I02
2	H09	N09	S09	A609	A703	A103	I03
3	H10	N10	S10	A610	A704	A104	I04
4	H11	N11	S11	A611	A705	A105	I05
5	H12	N12	S12	A612	A706	A106	I06
6	H13	N13	S13	A613	A707	A107	I07
7	H14	N14	S14	A614	A708	A108	I08
8	H15	N15	S15	A615	A709	A109	I09
9	H16	N16					
10	H17	N17					

Table 16: Raw Data, Expt. #3, RG-CO_2/450°C/20MPa, HCM12A

Project:	**SCCO2**
Grant #:	PRJ39TC
MDS:	MD24386
Expt. #:	**3**
Phase:	1 of 4
Phase Type:	Pure CO2
Temp. (°C):	450
Pressure:	2900psi
Sample ID:	**HCM12A**
Notes:	

Rel. Uncertainty in Meas. Mass:	Δm = ± 0.000002 g
Rel. Uncertainty in Meas. Length:	Δl = ± 0.001 mm
Rel. Uncertainty in Meas. Width:	Δw = ± 0.001 mm
Uncertainty in Meas. Area:	

Supplier/UNS ID:	K91271
Metal Type:	Ferritic-Martensitic
Color Designation:	Blue
Hole Diameter in Sample (mm):	3

		Sample # / Description									
	Meas #	**H08**	**H09**	**H10**	**H11**	**H12**	**H13**	**H14**	**H15**	**H16**	**H17**
BARE WEIGHT (gm)	**1**	1.866788	1.872840	1.867796	1.854164	1.889370	1.874356	1.886408	1.880476	1.870132	1.881146
	2	1.866794	1.872846	1.867794	1.854164	1.889368	1.874358	1.886414	1.880480	1.870138	1.881146
	3	1.866792	1.872842	1.867796	1.854166	1.889368	1.874356	1.886408	1.880478	1.870136	1.881146
	4	1.866788	1.872840	1.867792	1.854166	1.889366	1.874360	1.886408	1.880476	1.870136	1.881148
	5	1.866788	1.872844	1.867794	1.854166	1.889368	1.874360	1.886410	1.880478	1.870134	1.881146
	6	1.866790	1.872840	1.867798	1.854164	1.889370	1.874358	1.886406	1.880478	1.870138	1.881148
	7	1.866794	1.872846	1.867796	1.854168	1.889372	1.874356	1.886408	1.880476	1.870138	1.881144
	8	1.866788	1.872844	1.867796	1.854168	1.889374	1.874356	1.886406	1.880478	1.870136	1.881144
	9	1.866792	1.872842	1.867794	1.854164	1.889368	1.874360	1.886408	1.880480	1.870138	1.881148
	10	1.866786	1.872846	1.867796	1.854166	1.889368	1.874358	1.886410	1.880476	1.870140	1.881146
BARE AREA (mm2)	**1_L**	12.738	12.745	12.741	12.740	12.729	12.733	12.722	12.716	12.715	12.720
	2_L	12.740	12.746	12.742	12.738	12.735	12.745	12.718	12.723	12.716	12.738
	3_L	12.741	12.744	12.740	12.737	12.743	12.731	12.718	12.726	12.711	12.739
	4_W	12.701	12.709	12.711	12.707	12.695	12.666	12.680	12.667	12.686	12.669
	5_W	12.702	12.708	12.711	12.704	12.693	12.664	12.688	12.666	12.683	12.669
	6_W	12.705	12.708	12.713	12.703	12.685	12.665	12.679	12.665	12.664	12.671
BARE THICKNESS (mm)	**1**	1.578	1.559	1.554	1.559	1.561	1.557	1.565	1.567	1.559	1.561
	2	1.576	1.563	1.560	1.560	1.570	1.558	1.569	1.570	1.565	1.569
	3	1.563	1.565	1.561	1.561	1.573	1.557	1.568	1.572	1.567	1.570
	4	1.574	1.562	1.553	1.541	1.567	1.551	1.562	1.564	1.559	1.561
	5	1.576	1.564	1.562	1.572	1.572	1.558	1.569	1.574	1.565	1.576

Table 17: Raw Data, Expt. #3, RG-CO_2/450^{o}C/20MPa, HCM12A

		Measured Weight (g)									
	Meas #	H08	H09	H10	H11	H12	H13	H14	H15	H16	H17
200 hrs	1	1.870988	1.877044	1.871958	1.858354	1.893612	1.878432	1.890532	1.884550	1.874282	1.885538
	2	1.870986	1.877048	1.871956	1.858356	1.893612	1.878438	1.890534	1.884548	1.874286	1.885536
	3	1.870988	1.877044	1.871954	1.858356	1.893610	1.878436	1.890534	1.884550	1.874286	1.885540
	4	1.870984	1.877044	1.871956	1.858358	1.893612	1.878432	1.890532	1.884550	1.874282	1.885542
	5	1.870986	1.877042	1.871954	1.858354	1.893610	1.878430	1.890530	1.884552	1.874284	1.885538
	6	1.870988	1.877040	1.871958	1.858356	1.893610	1.878432	1.890534	1.884552	1.874284	1.885538
	7	1.870986	1.877044	1.871956	1.858354	1.893612	1.878432	1.890530	1.884550	1.874282	1.885540
	8	1.870990	1.877048	1.871956	1.858358	1.893614	1.878434	1.890532	1.884548	1.874286	1.885536
	9	1.870988	1.877046	1.871954	1.858358	1.893616	1.878432	1.890536	1.884550	1.874288	1.885538
	10	1.870988	1.877044	1.871952	1.858356	1.893614	1.878430	1.890534	1.884550	1.874284	1.885536
400 hrs	1			1.872870	1.859332	1.894682	1.879348	1.891658	1.885468	1.875332	1.886534
	2			1.872882	1.859336	1.894682	1.879350	1.891652	1.885468	1.875330	1.886534
	3			1.872882	1.859340	1.894688	1.879348	1.891656	1.885468	1.875332	1.886538
	4			1.872884	1.859340	1.894684	1.879346	1.891658	1.885464	1.875332	1.886534
	5			1.872874	1.859338	1.894688	1.879344	1.891658	1.885468	1.875332	1.886540
	6			1.872874	1.859340	1.894684	1.879344	1.891652	1.885460	1.875334	1.886540
	7			1.872884	1.859332	1.894688	1.879346	1.891658	1.885466	1.875336	1.886538
	8			1.872886	1.859338	1.894682	1.879348	1.891654	1.885464	1.875334	1.886536
	9			1.872886	1.859338	1.894682	1.879346	1.891650	1.885462	1.875334	1.886536
	10			1.872886	1.859332	1.894682	1.879350	1.891654	1.885462	1.875336	1.886538
600 hrs	1					1.895232	1.879968	1.892166	1.886138	1.875876	1.887036
	2					1.895228	1.879968	1.892164	1.886134	1.875878	1.887036
	3					1.895230	1.879970	1.892164	1.886134	1.875878	1.887038
	4					1.895232	1.879966	1.892168	1.886136	1.875880	1.887038
	5					1.895232	1.879972	1.892166	1.886134	1.875878	1.887036
	6					1.895228	1.879970	1.892166	1.886132	1.875876	1.887034
	7					1.895232	1.879968	1.892168	1.886136	1.875878	1.887034
	8					1.895230	1.879966	1.892164	1.886134	1.875880	1.887038
	9					1.895234	1.879966	1.892166	1.886136	1.875882	1.887036
	10					1.895232	1.879968	1.892166	1.886136	1.875880	1.887038

		Measured Weight (g)									
	Meas #	H08	H09	H10	H11	H12	H13	H14	H15	H16	H17
800 hrs	1							1.892714	1.886640	1.876436	1.887620
	2							1.892712	1.886638	1.876436	1.887616
	3							1.892712	1.886638	1.876434	1.887618
	4							1.892710	1.886640	1.876432	1.887620
	5							1.892712	1.886636	1.876434	1.887620
	6							1.892710	1.886638	1.876436	1.887618
	7							1.892714	1.886636	1.876436	1.887620
	8							1.892714	1.886636	1.876434	1.887622
	9							1.892712	1.886638	1.876432	1.887622
	10							1.892710	1.886640	1.876434	1.887622
1000 hrs	1										
	2										
	3										
	4										
	5										
	6										
	7										
	8										
	9										
	10										
1200 hrs	1										
	2										
	3										
	4										
	5										
	6										
	7										
	8										
	9										
	10										

Table 18: Raw Data, Expt. #3, RG-CO_2/450°C/20MPa, NF616

Project:	**SCCO2**
Grant #:	PRJ39TC
MDS:	MD24386
Expt. #:	**3**
Phase:	1 of 4
Phase Type:	Pure CO2
Temp. (°C):	450
Pressure:	2900psi
Sample ID:	**NF616**
Notes:	

Rel. Uncertainty in Meas. Mass:	Δm = ± 0.000002 g
Rel. Uncertainty in Meas. Length:	Δl = ± 0.001 mm
Rel. Uncertainty in Meas. Width:	Δw = ± 0.001 mm
Uncertainty in Meas. Area:	

Supplier/UNS ID:	K92460
Metal Type:	Ferritic-Martensitic
Color Designation:	Red
Hole Diameter in Sample (mm):	3

		Sample # / Description									
	Meas #	**N08**	**N09**	**N10**	**N11**	**N12**	**N13**	**N14**	**N15**	**N16**	**N17**
BARE WEIGHT (gm)	**1**	1.838592	1.830504	1.862160	1.858502	1.812018	1.830518	1.846152	1.848064	1.840752	1.815008
	2	1.838594	1.830502	1.862160	1.858504	1.812016	1.830516	1.846156	1.848060	1.840752	1.815010
	3	1.838592	1.830500	1.862162	1.858504	1.812016	1.830518	1.846150	1.848062	1.840754	1.815008
	4	1.838590	1.830504	1.862158	1.858506	1.812018	1.830514	1.846150	1.848064	1.840752	1.815006
	5	1.838588	1.830500	1.862158	1.858500	1.812014	1.830516	1.846152	1.848068	1.840758	1.815010
	6	1.838594	1.830504	1.862156	1.858502	1.812018	1.830518	1.846154	1.848062	1.840756	1.815012
	7	1.838596	1.830502	1.862160	1.858506	1.812016	1.830518	1.846154	1.848064	1.840758	1.815010
	8	1.838594	1.830506	1.862162	1.858506	1.812018	1.830520	1.846156	1.848062	1.840758	1.815008
	9	1.838594	1.830504	1.862160	1.858508	1.812018	1.830518	1.846156	1.848066	1.840756	1.815008
	10	1.838592	1.830506	1.862158	1.858508	1.812020	1.830516	1.846156	1.848064	1.840760	1.815010
BARE AREA (mm2)	**1_L**	12.699	12.676	12.681	12.681	12.699	12.672	12.687	12.670	12.655	12.659
	2_L	12.696	12.675	12.682	12.682	12.698	12.674	12.682	12.670	12.660	12.665
	3_L	12.699	12.678	12.684	12.686	12.695	12.666	12.681	12.675	12.662	12.652
	4_W	12.680	12.657	12.649	12.669	12.679	12.649	12.656	12.637	12.637	12.632
	5_W	12.680	12.656	12.650	12.669	12.677	12.649	12.650	12.648	12.641	12.633
	6_W	12.678	12.657	12.652	12.669	12.677	12.648	12.641	12.644	12.642	12.634
BARE THICKNESS (mm)	**1**	1.521	1.545	1.554	1.547	1.508	1.524	1.535	1.546	1.542	1.505
	2	1.547	1.546	1.569	1.556	1.507	1.540	1.539	1.548	1.542	1.532
	3	1.554	1.540	1.571	1.560	1.502	1.539	1.540	1.545	1.537	1.548
	4	1.544	1.512	1.563	1.556	1.510	1.536	1.536	1.554	1.548	1.539
	5	1.542	1.561	1.569	1.553	1.504	1.530	1.539	1.536	1.534	1.519

Table 19: Raw Data, Expt. #3, RG-CO_2/450^{o}C/20MPa, NF616

		Measured Weight (g)									
	Meas #	N08	N09	N10	N11	N12	N13	N14	N15	N16	N17
200 hrs	1	1.84205	1.833956	1.865686	1.862010	1.815482	1.834022	1.849640	1.851602	1.844180	1.818416
	2	1.842052	1.833954	1.865682	1.862010	1.815488	1.834020	1.849640	1.851602	1.844176	1.818420
	3	1.842054	1.833954	1.865684	1.862008	1.815484	1.834026	1.849642	1.851604	1.844178	1.818418
	4	1.842052	1.833950	1.865686	1.862008	1.815486	1.834022	1.849640	1.851602	1.844176	1.818418
	5	1.842054	1.833954	1.865686	1.862010	1.815482	1.834024	1.849644	1.851600	1.844176	1.818422
	6	1.842052	1.833956	1.865684	1.862010	1.815486	1.834026	1.849642	1.851600	1.844178	1.818420
	7	1.842050	1.833954	1.865682	1.862006	1.815488	1.834022	1.849640	1.851602	1.844174	1.818418
	8	1.842052	1.833952	1.865680	1.862008	1.815488	1.834020	1.849638	1.851604	1.844178	1.818418
	9	1.842054	1.833956	1.865684	1.862008	1.815490	1.834024	1.849640	1.851600	1.844180	1.818420
	10	1.842056	1.833954	1.865680	1.862006	1.815488	1.834022	1.849642	1.851600	1.844176	1.818416
400 hrs	1			1.866836	1.863152	1.816614	1.835176	1.850806	1.852768	1.845376	1.819538
	2			1.866838	1.863154	1.816618	1.835172	1.850800	1.852764	1.845380	1.819540
	3			1.866838	1.863150	1.816618	1.835174	1.850808	1.852762	1.845378	1.819540
	4			1.866840	1.863152	1.816612	1.835176	1.850806	1.852764	1.845380	1.819544
	5			1.866842	1.863150	1.816616	1.835176	1.850802	1.852766	1.845380	1.819542
	6			1.866838	1.863154	1.816616	1.835172	1.850802	1.852764	1.845378	1.819540
	7			1.866836	1.863156	1.816618	1.835172	1.850804	1.852766	1.845380	1.819544
	8			1.866838	1.863152	1.816614	1.835174	1.850806	1.852768	1.845376	1.819540
	9			1.866836	1.863154	1.816616	1.835170	1.850802	1.852762	1.845376	1.819538
	10			1.866840	1.863150	1.816614	1.835176	1.850806	1.852764	1.845378	1.819540
600 hrs	1					1.817412	1.836022	1.851618	1.853680	1.846096	1.820408
	2					1.817410	1.836020	1.851620	1.853680	1.846098	1.820406
	3					1.817408	1.836024	1.851620	1.853678	1.846096	1.820408
	4					1.817410	1.836022	1.851622	1.853678	1.846100	1.820408
	5					1.817412	1.836020	1.851618	1.853680	1.846098	1.820410
	6					1.817410	1.836020	1.851616	1.853678	1.846100	1.820406
	7					1.817410	1.836022	1.851616	1.853676	1.846096	1.820406
	8					1.817408	1.836020	1.851618	1.853678	1.846096	1.820408
	9					1.817412	1.836022	1.851620	1.853678	1.846098	1.820406
	10					1.817410	1.836024	1.851616	1.853680	1.846100	1.820410

		Measured Weight (g)									
	Meas #	N08	N09	N10	N11	N12	N13	N14	N15	N16	N17
800 hrs	1							1.852186	1.854286	1.846734	1.821100
	2							1.852184	1.854286	1.846734	1.821098
	3							1.852184	1.854284	1.846732	1.821102
	4							1.852188	1.854286	1.846736	1.821104
	5							1.852186	1.854282	1.846734	1.821102
	6							1.852186	1.854282	1.846732	1.821100
	7							1.852188	1.854286	1.846732	1.821098
	8							1.852184	1.854284	1.846736	1.821100
	9							1.852186	1.854286	1.846734	1.821100
	10							1.852188	1.854286	1.846734	1.821100
1000 hrs	1										
	2										
	3										
	4										
	5										
	6										
	7										
	8										
	9										
	10										
1200 hrs	1										
	2										
	3										
	4										
	5										
	6										
	7										
	8										
	9										
	10										

Table 20: Raw Data, Expt. #3, RG-CO_2/450^{o}C/20MPa, 347SS

Project:	**SCCO2**
Grant #:	PRJ39TC
MDS:	MD24386
Expt. #:	**3**
Phase:	1 of 4
Phase Type:	Pure CO2
Temp. (^{o}C):	450
Pressure:	2900psi
Sample ID:	**347SS**
Notes:	

Rel. Uncertainty in Meas. Mass:	Δm = ± 0.000002 g
Rel. Uncertainty in Meas. Length:	Δl = ± 0.001 mm
Rel. Uncertainty in Meas. Width:	Δw = ± 0.001 mm
Uncertainty in Meas. Area:	ΔA = ± 0.000182 cm^2

Supplier/UNS ID:	S34700
Metal Type:	Austenitic
Color Designation:	Yellow
Hole Diameter in Sample (mm):	3

		Sample # / Description									
	Meas #	**S08**	**S09**	**S10**	**S11**	**S12**	**S13**	**S14**	**S15**		
BARE WEIGHT (gm)	**1**	1.940586	1.946918	1.944050	1.952448	1.934344	1.830346	1.837530	1.834796		
	2	1.940582	1.946914	1.944046	1.952448	1.934342	1.830346	1.837528	1.834798		
	3	1.940582	1.946916	1.944048	1.952448	1.934344	1.830342	1.837530	1.834796		
	4	1.940584	1.946914	1.944046	1.952446	1.934348	1.830346	1.837530	1.834796		
	5	1.940582	1.946914	1.944048	1.952446	1.934348	1.830344	1.837532	1.834798		
	6	1.940586	1.946918	1.944050	1.952450	1.934344	1.830344	1.837530	1.834796		
	7	1.940586	1.946920	1.944050	1.952448	1.934346	1.830346	1.837528	1.834794		
	8	1.940580	1.946918	1.944048	1.952450	1.934342	1.830348	1.837526	1.834796		
	9	1.940582	1.946916	1.944046	1.952450	1.934346	1.830346	1.837526	1.834796		
	10	1.940584	1.946914	1.944050	1.952450	1.934346	1.830348	1.837528	1.834800		
BARE AREA (mm2)	**1_L**	13.217	13.237	13.194	13.236	13.210	13.009	12.912	12.904		
	2_L	13.212	13.219	13.199	13.225	13.204	13.004	12.926	12.947		
	3_L	13.203	13.204	13.200	13.218	13.188	13.001	12.935	12.992		
	4_W	12.656	12.654	12.651	12.653	12.659	12.536	12.434	12.362		
	5_W	12.658	12.655	12.653	12.655	12.660	12.537	12.508	12.351		
	6_W	12.660	12.660	12.657	12.660	12.658	12.542	12.530	12.305		
BARE THICKNESS (mm)	**1**	1.559	1.561	1.558	1.562	1.530	1.499	1.541	1.544		
	2	1.560	1.563	1.563	1.564	1.538	1.498	1.541	1.545		
	3	1.564	1.565	1.566	1.566	1.540	1.491	1.537	1.546		
	4	1.558	1.562	1.563	1.560	1.530	1.492	1.539	1.539		
	5	1.563	1.563	1.560	1.566	1.540	1.495	1.537	1.549		

Table 21: Raw Data, Expt. #3, RG-CO_2/450^{o}C/20MPa, 347SS

		Measured Weight (g)									
	Meas #	S08	S09	S10	S11	S12	S13	S14	S15		
200 hrs	1	1.940656	1.946948	1.944076	1.952480	1.934376	1.830374	1.837598	1.834878		
	2	1.940656	1.946946	1.944078	1.952478	1.934374	1.830376	1.837598	1.834872		
	3	1.940658	1.946944	1.944078	1.952478	1.934378	1.830374	1.837600	1.834874		
	4	1.940656	1.946946	1.944074	1.952480	1.934376	1.830374	1.837598	1.834872		
	5	1.940656	1.946948	1.944078	1.952478	1.934374	1.830372	1.837600	1.834872		
	6	1.940658	1.946948	1.944076	1.952476	1.934376	1.830376	1.837602	1.834870		
	7	1.940660	1.946944	1.944074	1.952478	1.934378	1.830372	1.837598	1.834874		
	8	1.940658	1.946948	1.944072	1.952480	1.934380	1.830370	1.837596	1.834870		
	9	1.940656	1.946946	1.944076	1.952482	1.934378	1.830370	1.837600	1.834872		
	10	1.940658	1.946942	1.944078	1.952480	1.934376	1.830368	1.837596	1.834868		
400 hrs	1	1.940666	1.946946	1.944084	1.952492	1.934382	1.830372	1.837610	1.834888		
	2	1.940668	1.946948	1.944090	1.952492	1.934382	1.830374	1.837612	1.834888		
	3	1.940670	1.946950	1.944088	1.952490	1.934384	1.830376	1.837614	1.834882		
	4	1.940668	1.946948	1.944084	1.952488	1.934384	1.830376	1.837610	1.834880		
	5	1.940672	1.946954	1.944086	1.952496	1.934386	1.830376	1.837612	1.834884		
	6	1.940670	1.946948	1.944082	1.952488	1.934386	1.830370	1.837614	1.834886		
	7	1.940666	1.946950	1.944086	1.952492	1.934384	1.830372	1.837616	1.834890		
	8	1.940668	1.946944	1.944086	1.952490	1.934382	1.830372	1.837612	1.834882		
	9	1.940666	1.946952	1.944084	1.952488	1.934380	1.830368	1.837610	1.834884		
	10	1.940672	1.946946	1.944088	1.952486	1.934382	1.830374	1.837612	1.834886		
600 hrs	1	1.940676	1.946956	1.944090	1.952496	1.934386	1.830384	1.837618	1.834896		
	2	1.940678	1.946958	1.944090	1.952496	1.934390	1.830382	1.837620	1.834894		
	3	1.940678	1.946956	1.944092	1.952498	1.934388	1.830382	1.837618	1.834898		
	4	1.940680	1.946956	1.944090	1.952498	1.934388	1.830380	1.837622	1.834898		
	5	1.940676	1.946958	1.944094	1.952496	1.934386	1.830382	1.837620	1.834896		
	6	1.940678	1.946954	1.944092	1.952496	1.934384	1.830380	1.837618	1.834894		
	7	1.940676	1.946956	1.944092	1.952494	1.934388	1.830380	1.837616	1.834896		
	8	1.940680	1.946958	1.944094	1.952496	1.934388	1.830384	1.837618	1.834898		
	9	1.940680	1.946956	1.944090	1.952494	1.934390	1.830382	1.837616	1.834898		
	10	1.940678	1.946954	1.944094	1.952496	1.934388	1.830380	1.837620	1.834896		

		Measured Weight (g)									
	Meas #	S08	S09	S10	S11	S12	S13	S14	S15		
800 hrs	1			1.944090	1.952498	1.934390	1.830380	1.837628	1.834902		
	2			1.944088	1.952494	1.934390	1.830382	1.837626	1.834904		
	3			1.944092	1.952496	1.934392	1.830380	1.837622	1.834902		
	4			1.944092	1.952494	1.934388	1.830380	1.837626	1.834902		
	5			1.944094	1.952496	1.934390	1.830380	1.837624	1.834900		
	6			1.944092	1.952496	1.934388	1.830382	1.837626	1.834904		
	7			1.944090	1.952500	1.934388	1.830382	1.837626	1.834900		
	8			1.944092	1.952500	1.934390	1.830378	1.837624	1.834902		
	9			1.944088	1.952498	1.934392	1.830380	1.837626	1.834902		
	10			1.944090	1.952498	1.934392	1.830382	1.837628	1.834902		
1000 hrs	1					1.934390	1.830380	1.837626	1.834904		
	2					1.934386	1.830380	1.837624	1.834906		
	3					1.934388	1.830376	1.837624	1.834904		
	4					1.934388	1.830382	1.837626	1.834906		
	5					1.934390	1.830378	1.837628	1.834904		
	6					1.934392	1.830380	1.837626	1.834904		
	7					1.934390	1.830382	1.837626	1.834902		
	8					1.934390	1.830380	1.837628	1.834904		
	9					1.934392	1.830382	1.837624	1.834904		
	10					1.934390	1.830382	1.837626	1.834904		
1200 hrs	1										
	2										
	3										
	4										
	5										
	6										
	7										
	8										
	9										
	10										

Table 22: Raw Data, Expt. #3, RG-CO_2/450°C/20MPa, AFA-OC6

Project:	**SCCO2**
Grant #:	PRJ39TC
MDS:	MD24386
Expt. #:	**3**
Phase:	1 of 4
Phase Type:	Pure CO2
Temp. (°C):	450
Pressure:	2900psi
Sample ID:	**AFA-OC6**
Notes:	

Rel. Uncertainty in Meas. Mass:	Δm = ± 0.000002 g
Rel. Uncertainty in Meas. Length:	Δl = ± 0.001 mm
Rel. Uncertainty in Meas. Width:	Δw = ± 0.001 mm
Uncertainty in Meas. Area:	ΔA = ± 0.00018 cm^2

Supplier/UNS ID:	Heat # 001919 (CRADA RPT)
Metal Type:	Alumina-Forming-Austenitic
Color Designation:	Magenta
Hole Diameter in Sample (mm):	3

		Sample # / Description									
	Meas #	**A608**	**A609**	**A610**	**A611**	**A612**	**A613**	**A614**	**A615**		
BARE WEIGHT (gm)	**1**	1.833206	1.828396	1.797156	1.831640	1.841900	1.849838	1.784030	1.832356		
	2	1.833210	1.828396	1.797154	1.831644	1.841896	1.849842	1.784030	1.832352		
	3	1.833208	1.828394	1.797158	1.831644	1.841898	1.849840	1.784030	1.832358		
	4	1.833206	1.828394	1.797160	1.831644	1.841898	1.849842	1.784032	1.832356		
	5	1.833208	1.828396	1.797158	1.831642	1.841900	1.849838	1.784032	1.832356		
	6	1.833208	1.828396	1.797154	1.831646	1.841902	1.849838	1.784034	1.832358		
	7	1.833206	1.828398	1.797154	1.831642	1.841898	1.849836	1.784032	1.832360		
	8	1.833204	1.828396	1.797156	1.831642	1.841896	1.849838	1.784034	1.832358		
	9	1.833208	1.828400	1.797154	1.831644	1.841898	1.849838	1.784032	1.832362		
	10	1.833210	1.828398	1.797154	1.831642	1.841898	1.849840	1.784036	1.832356		
BARE AREA (mm2)	**1_L**	12.957	12.972	12.960	12.948	12.865	12.924	12.797	12.834		
	2_L	12.955	12.971	12.958	12.950	12.873	12.940	12.671	12.819		
	3_L	12.956	12.970	12.955	12.952	12.874	12.944	12.622	12.800		
	4_W	12.670	12.663	12.684	12.653	12.565	12.582	12.590	12.571		
	5_W	12.668	12.667	12.685	12.661	12.567	12.583	12.590	12.588		
	6_W	12.667	12.673	12.685	12.667	12.573	12.587	12.563	12.597		
BARE THICKNESS (mm)	**1**	1.544	1.560	1.524	1.558	1.572	1.569	1.549	1.563		
	2	1.550	1.556	1.523	1.559	1.572	1.574	1.555	1.566		
	3	1.551	1.550	1.519	1.556	1.568	1.570	1.549	1.565		
	4	1.541	1.533	1.512	1.545	1.573	1.574	1.547	1.563		
	5	1.558	1.570	1.532	1.571	1.573	1.571	1.554	1.567		

Table 23: Raw Data, Expt. #3, RG-CO_2/450^{o}C/20MPa, AFA-OC6

		Measured Weight (g)									
	Meas #	A608	A609	A610	A611	A612	A613	A614	A615		
200 hrs	1	1.833254	1.828440	1.797208	1.831698	1.841948	1.849898	1.784086	1.832432		
	2	1.833254	1.828436	1.797206	1.831694	1.841944	1.849898	1.784086	1.832436		
	3	1.833256	1.828436	1.797208	1.831694	1.841946	1.849900	1.784084	1.832430		
	4	1.833256	1.828438	1.797206	1.831696	1.841948	1.849902	1.784086	1.832432		
	5	1.833258	1.828440	1.797210	1.831694	1.841944	1.849900	1.784088	1.832436		
	6	1.833256	1.828440	1.797208	1.831698	1.841946	1.849898	1.784084	1.832434		
	7	1.833258	1.828438	1.797210	1.831692	1.841944	1.849900	1.784086	1.832436		
	8	1.833254	1.828436	1.797208	1.831694	1.841946	1.849900	1.784082	1.832430		
	9	1.833256	1.828440	1.797208	1.831692	1.841944	1.849898	1.784084	1.832430		
	10	1.833256	1.828442	1.797206	1.831696	1.841948	1.849900	1.784084	1.832432		
400 hrs	1	1.833266	1.828444	1.797216	1.831698	1.841958	1.849902	1.784100	1.832438		
	2	1.833260	1.828440	1.797214	1.831702	1.841956	1.849904	1.784098	1.832442		
	3	1.833264	1.828442	1.797218	1.831700	1.841958	1.849900	1.784096	1.832440		
	4	1.833264	1.828442	1.797218	1.831700	1.841958	1.849902	1.784102	1.832442		
	5	1.833266	1.828440	1.797216	1.831698	1.841960	1.849900	1.784100	1.832438		
	6	1.833262	1.828444	1.797218	1.831702	1.841958	1.849904	1.784098	1.832444		
	7	1.833264	1.828438	1.797214	1.831704	1.841956	1.849906	1.784098	1.832440		
	8	1.833262	1.828440	1.797220	1.831700	1.841958	1.849904	1.784100	1.832444		
	9	1.833260	1.828442	1.797218	1.831704	1.841956	1.849906	1.784096	1.832442		
	10	1.833260	1.828438	1.797216	1.831702	1.841956	1.849902	1.784102	1.832444		
600 hrs	1	1.833276	1.828462	1.797232	1.831724	1.841976	1.849908	1.784122	1.832458		
	2	1.833278	1.828460	1.797234	1.831718	1.841978	1.849912	1.784124	1.832462		
	3	1.833280	1.828464	1.797236	1.831720	1.841978	1.849912	1.784122	1.832458		
	4	1.833274	1.828458	1.797230	1.831720	1.841980	1.849910	1.784122	1.832460		
	5	1.833278	1.828460	1.797232	1.831718	1.841976	1.849908	1.784120	1.832460		
	6	1.833276	1.828460	1.797234	1.831720	1.841976	1.849910	1.784122	1.832458		
	7	1.833280	1.828462	1.797232	1.831722	1.841978	1.849912	1.784124	1.832456		
	8	1.833276	1.828458	1.797232	1.831718	1.841976	1.849912	1.784126	1.832458		
	9	1.833274	1.828460	1.797234	1.831720	1.841978	1.849910	1.784124	1.832456		
	10	1.833278	1.828462	1.797230	1.831724	1.841980	1.849908	1.784120	1.832458		

		Measured Weight (g)									
	Meas #	A608	A609	A610	A611	A612	A613	A614	A615		
800 hrs	1			1.797238	1.831726	1.841980	1.849910	1.784126	1.832458		
	2			1.797232	1.831726	1.841982	1.849908	1.784126	1.832456		
	3			1.797236	1.831728	1.841978	1.849904	1.784130	1.832456		
	4			1.797236	1.831726	1.841978	1.849906	1.784126	1.832454		
	5			1.797234	1.831730	1.841980	1.849910	1.784132	1.832456		
	6			1.797238	1.831728	1.841980	1.849906	1.784128	1.832454		
	7			1.797234	1.831726	1.841978	1.849906	1.784128	1.832456		
	8			1.797236	1.831728	1.841980	1.849908	1.784132	1.832454		
	9			1.797232	1.831726	1.841982	1.849910	1.784130	1.832454		
	10			1.797236	1.831728	1.841978	1.849910	1.784130	1.832454		
1000 hrs	1					1.841982	1.849912	1.784136	1.832462		
	2					1.841980	1.849910	1.784132	1.832462		
	3					1.841978	1.849910	1.784134	1.832458		
	4					1.841978	1.849910	1.784132	1.832454		
	5					1.841980	1.849910	1.784134	1.832458		
	6					1.841978	1.849912	1.784130	1.832456		
	7					1.841980	1.849912	1.784132	1.832456		
	8					1.841982	1.849910	1.784132	1.832458		
	9					1.841982	1.849908	1.784130	1.832460		
	10					1.841980	1.849910	1.784132	1.832460		
1200 hrs	1										
	2										
	3										
	4										
	5										
	6										
	7										
	8										
	9										
	10										

Table 24: Raw Data, Expt. #3, RG-CO_2/450°C/20MPa, AFA-OC7

Project:	**SCCO2**
Grant #:	PRJ39TC
MDS:	MD24386
Expt. #:	**3**
Phase:	1 of 4
Phase Type:	Pure CO2
Temp. (°C):	450
Pressure:	2900psi
Sample ID:	**AFA-OC7**
Notes:	

Rel. Uncertainty in Meas. Mass:	Δm = ± 0.000002 g
Rel. Uncertainty in Meas. Length:	Δl = ± 0.001 mm
Rel. Uncertainty in Meas. Width:	Δw = ± 0.001 mm
Uncertainty in Meas. Area:	ΔA = ± 0.000181 cm^2

Supplier/UNS ID:	Heat # 001920 (CRADA RPT)
Metal Type:	Alumina-Forming-Austenitic
Color Designation:	Green
Hole Diameter in Sample (mm):	3

		Sample # / Description									
	Meas #	**A702**	**A703**	**A704**	**A705**	**A706**	**A707**	**A708**	**A709**		
BARE WEIGHT (gm)	**1**	1.860566	1.844168	1.841398	1.844678	1.825728	1.849198	1.844340	1.834756		
	2	1.860574	1.844166	1.841396	1.844676	1.825726	1.849192	1.844342	1.834762		
	3	1.860568	1.844172	1.841396	1.844674	1.825728	1.849200	1.844344	1.834766		
	4	1.860568	1.844170	1.841396	1.844676	1.825722	1.849198	1.844348	1.834756		
	5	1.860568	1.844168	1.841398	1.844682	1.825724	1.849200	1.844348	1.834758		
	6	1.860566	1.844168	1.841394	1.844678	1.825726	1.849204	1.844340	1.834762		
	7	1.860568	1.844170	1.841396	1.844684	1.825728	1.849208	1.844346	1.834762		
	8	1.860570	1.844174	1.841392	1.844680	1.825726	1.849202	1.844342	1.834766		
	9	1.860570	1.844172	1.841394	1.844684	1.825722	1.849200	1.844342	1.834766		
	10	1.860568	1.844170	1.841392	1.844680	1.825728	1.849204	1.844344	1.834766		
BARE AREA (mm2)	**1_L**	12.860	12.852	12.856	12.852	12.866	12.866	12.853	12.862		
	2_L	12.865	12.860	12.858	12.851	12.866	12.870	12.855	12.862		
	3_L	12.868	12.863	12.858	12.851	12.868	12.873	12.857	12.864		
	4_W	12.704	12.687	12.691	12.687	12.670	12.696	12.673	12.680		
	5_W	12.706	12.689	12.692	12.685	12.678	12.699	12.670	12.681		
	6_W	12.707	12.688	12.693	12.684	12.679	12.695	12.669	12.686		
BARE THICKNESS (mm)	**1**	1.564	1.548	1.552	1.549	1.547	1.551	1.553	1.542		
	2	1.569	1.559	1.554	1.554	1.550	1.566	1.562	1.555		
	3	1.568	1.564	1.557	1.555	1.548	1.572	1.564	1.561		
	4	1.555	1.557	1.552	1.550	1.544	1.563	1.551	1.543		
	5	1.574	1.559	1.556	1.554	1.552	1.568	1.564	1.560		

Table 25: Raw Data, Expt. #3, RG-CO_2/450^{o}C/20MPa, AFA-OC7

		Measured Weight (g)									
	Meas #	A702	A703	A704	A705	A706	A707	A708	A709		
200 hrs	1	1.860634	1.844214	1.841434	1.844730	1.825790	1.849262	1.844382	1.834828		
	2	1.860634	1.844212	1.841432	1.844732	1.825792	1.849262	1.844380	1.834826		
	3	1.860636	1.844214	1.841438	1.844728	1.825790	1.849264	1.844380	1.834824		
	4	1.860632	1.844214	1.841438	1.844730	1.825790	1.849266	1.844380	1.834824		
	5	1.860634	1.844210	1.841434	1.844734	1.825792	1.849264	1.844382	1.834826		
	6	1.860630	1.844208	1.841436	1.844732	1.825794	1.849260	1.844384	1.834824		
	7	1.860632	1.844208	1.841438	1.844732	1.825794	1.849260	1.844382	1.834828		
	8	1.860632	1.844210	1.841434	1.844730	1.825790	1.849262	1.844384	1.834824		
	9	1.860634	1.844212	1.841440	1.844730	1.825790	1.849264	1.844384	1.834824		
	10	1.860630	1.844212	1.841436	1.844734	1.825792	1.849260	1.844382	1.834822		
400 hrs	1	1.860638	1.844228	1.841444	1.844738	1.825798	1.849270	1.844388	1.834834		
	2	1.860638	1.844226	1.841444	1.844740	1.825798	1.849268	1.844386	1.834834		
	3	1.860636	1.844230	1.841442	1.844742	1.825796	1.849272	1.844388	1.834832		
	4	1.860640	1.844228	1.841440	1.844740	1.825798	1.849270	1.844388	1.834836		
	5	1.860638	1.844226	1.841442	1.844736	1.825796	1.849270	1.844390	1.834836		
	6	1.860636	1.844226	1.841444	1.844738	1.825800	1.849268	1.844386	1.834834		
	7	1.860638	1.844228	1.841440	1.844742	1.825798	1.849272	1.844386	1.834836		
	8	1.860640	1.844224	1.841446	1.844740	1.825800	1.849266	1.844388	1.834832		
	9	1.860642	1.844226	1.841444	1.844744	1.825796	1.849270	1.844390	1.834834		
	10	1.860638	1.844224	1.841444	1.844742	1.825800	1.849268	1.844388	1.834834		
600 hrs	1	1.860670	1.844248	1.841456	1.844746	1.825814	1.849282	1.844406	1.834844		
	2	1.860670	1.844246	1.841454	1.844746	1.825816	1.849278	1.844406	1.834844		
	3	1.860668	1.844248	1.841458	1.844748	1.825814	1.849278	1.844408	1.834848		
	4	1.860666	1.844248	1.841456	1.844750	1.825816	1.849280	1.844408	1.834848		
	5	1.860668	1.844244	1.841454	1.844748	1.825812	1.849282	1.844404	1.834846		
	6	1.860666	1.844246	1.841458	1.844748	1.825814	1.849282	1.844406	1.834844		
	7	1.860670	1.844246	1.841460	1.844750	1.825816	1.849280	1.844408	1.834846		
	8	1.860666	1.844248	1.841458	1.844746	1.825820	1.849282	1.844410	1.834846		
	9	1.860670	1.844244	1.841462	1.844746	1.825816	1.849284	1.844408	1.834846		
	10	1.860668	1.844246	1.841456	1.844748	1.825816	1.849280	1.844410	1.834844		

		Measured Weight (g)									
	Meas #	A702	A703	A704	A705	A706	A707	A708	A709		
800 hrs	1			1.841460	1.844754	1.825810	1.849268	1.844404	1.834826		
	2			1.841456	1.844756	1.825806	1.849264	1.844406	1.834824		
	3			1.841456	1.844754	1.825808	1.849264	1.844406	1.834826		
	4			1.841458	1.844752	1.825810	1.849266	1.844408	1.834826		
	5			1.841456	1.844752	1.825810	1.849264	1.844406	1.834828		
	6			1.841458	1.844754	1.825808	1.849268	1.844406	1.834824		
	7			1.841454	1.844752	1.825808	1.849266	1.844404	1.834824		
	8			1.841458	1.844756	1.825806	1.849266	1.844406	1.834826		
	9			1.841460	1.844754	1.825808	1.849264	1.844408	1.834828		
	10			1.841458	1.844756	1.825810	1.849266	1.844408	1.834824		
1000 hrs	1					1.825810	1.849266	1.844404	1.834830		
	2					1.825806	1.849264	1.844402	1.834826		
	3					1.825808	1.849264	1.844402	1.834826		
	4					1.825810	1.849266	1.844408	1.834828		
	5					1.825810	1.849264	1.844406	1.834826		
	6					1.825808	1.849262	1.844408	1.834824		
	7					1.825810	1.849266	1.844408	1.834826		
	8					1.825806	1.849268	1.844406	1.834826		
	9					1.825808	1.849268	1.844408	1.834828		
	10					1.825810	1.849266	1.844404	1.834826		
1200 hrs	1										
	2										
	3										
	4										
	5										
	6										
	7										
	8										
	9										
	10										

Table 26: Raw Data, Expt. #3, RG-CO_2/450°C/20MPa, AFA-OC10

Project:	**SCCO2**
Grant #:	PRJ39TC
MDS:	MD24386
Expt. #:	**3**
Phase:	1 of 4
Phase Type:	Pure CO2
Temp. (°C):	450
Pressure:	2900psi
Sample ID:	**AFA-OC10**
Notes:	

Rel. Uncertainty in Meas. Mass:	Δm = ± 0.000002 g
Rel. Uncertainty in Meas. Length:	Δl = ± 0.001 mm
Rel. Uncertainty in Meas. Width:	Δw = ± 0.001 mm
Uncertainty in Meas. Area:	ΔA = ± 0.00018 cm^2

Supplier/UNS ID:	Heat # 001923 (CRADA RPT)
Metal Type:	Alumina-Forming-Austenitic
Color Designation:	Brown
Hole Diameter in Sample (mm):	3

		Sample # / Description									
	Meas #	**A102**	**A103**	**A104**	**A105**	**A106**	**A107**	**A108**	**A109**		
BARE WEIGHT (gm)	**1**	1.825548	1.799642	1.812366	1.780048	1.834716	1.803058	1.795546	1.798470		
	2	1.825542	1.799642	1.812364	1.780054	1.834718	1.803062	1.795552	1.798474		
	3	1.825544	1.799638	1.812372	1.780048	1.834718	1.803054	1.795542	1.798472		
	4	1.825542	1.799642	1.812364	1.780054	1.834712	1.803062	1.795554	1.798466		
	5	1.825540	1.799636	1.812364	1.780046	1.834714	1.803062	1.795542	1.798472		
	6	1.825546	1.799636	1.812368	1.780050	1.834714	1.803062	1.795552	1.798468		
	7	1.825540	1.799636	1.812362	1.780046	1.834718	1.803062	1.795548	1.798470		
	8	1.825544	1.799634	1.812368	1.780052	1.834714	1.803062	1.795550	1.798472		
	9	1.825544	1.799636	1.812368	1.780046	1.834716	1.803064	1.795542	1.798468		
	10	1.825542	1.799642	1.812366	1.780054	1.834716	1.803064	1.795548	1.798468		
BARE AREA (mm2)	**1_L**	12.757	12.767	12.769	12.756	12.785	12.777	12.764	12.763		
	2_L	12.759	12.765	12.768	12.757	12.785	12.776	12.763	12.761		
	3_L	12.758	12.764	12.764	12.756	12.785	12.775	12.761	12.760		
	4_W	12.637	12.667	12.679	12.665	12.648	12.656	12.663	12.655		
	5_W	12.638	12.668	12.679	12.666	12.651	12.660	12.661	12.658		
	6_W	12.639	12.671	12.673	12.667	12.649	12.661	12.660	12.662		
BARE THICKNESS (mm)	**1**	1.566	1.542	1.544	1.535	1.568	1.541	1.539	1.536		
	2	1.569	1.550	1.547	1.528	1.568	1.542	1.539	1.544		
	3	1.570	1.554	1.549	1.519	1.569	1.540	1.535	1.548		
	4	1.565	1.540	1.545	1.529	1.569	1.536	1.540	1.543		
	5	1.570	1.555	1.549	1.526	1.567	1.543	1.537	1.540		

Table 27: Raw Data, Expt. #3, RG-CO_2/450^{o}C/20MPa, AFA-OC10

		Measured Weight (g)									
	Meas #	A102	A103	A104	A105	A106	A107	A108	A109		
200 hrs	1	1.825618	1.799722	1.812426	1.780112	1.834780	1.803130	1.795612	1.798550		
	2	1.825616	1.799724	1.812424	1.780110	1.834784	1.803132	1.795614	1.798548		
	3	1.82562	1.799728	1.812426	1.780110	1.834782	1.803130	1.795616	1.798550		
	4	1.825616	1.799728	1.812428	1.780112	1.834778	1.803134	1.795614	1.798552		
	5	1.825618	1.799724	1.812428	1.780114	1.834778	1.803132	1.795612	1.798550		
	6	1.825618	1.799726	1.812424	1.780110	1.834782	1.803132	1.795612	1.798550		
	7	1.825616	1.799722	1.812426	1.780112	1.834780	1.803130	1.795610	1.798554		
	8	1.825618	1.799726	1.812424	1.780112	1.834784	1.803134	1.795612	1.798552		
	9	1.825620	1.799724	1.812424	1.780114	1.834780	1.803130	1.795612	1.798550		
	10	1.825616	1.799724	1.812422	1.780112	1.834780	1.803130	1.795614	1.798548		
400 hrs	1	1.825630	1.799754	1.812440	1.780118	1.834790	1.803148	1.795620	1.798560		
	2	1.825632	1.799750	1.812442	1.780120	1.834788	1.803148	1.795618	1.798562		
	3	1.825628	1.799756	1.812442	1.780120	1.834792	1.803150	1.795618	1.798566		
	4	1.825630	1.799754	1.812440	1.780122	1.834790	1.803150	1.795620	1.798560		
	5	1.825630	1.799752	1.812440	1.780118	1.834794	1.803146	1.795622	1.798560		
	6	1.825628	1.799750	1.812438	1.780116	1.834792	1.803144	1.795618	1.798564		
	7	1.825632	1.799754	1.812436	1.780118	1.834792	1.803148	1.795616	1.798562		
	8	1.825634	1.799752	1.812440	1.780120	1.834788	1.803150	1.795616	1.798564		
	9	1.825630	1.799750	1.812438	1.780122	1.834792	1.803148	1.795618	1.798560		
	10	1.825632	1.799750	1.812440	1.780118	1.834790	1.803150	1.795616	1.798560		
600 hrs	1	1.825656	1.799776	1.812476	1.780144	1.834820	1.803172	1.795654	1.798576		
	2	1.825656	1.799772	1.812472	1.780148	1.834822	1.803172	1.795654	1.798572		
	3	1.825654	1.799774	1.812478	1.780150	1.834826	1.803172	1.795650	1.798572		
	4	1.825654	1.799774	1.812472	1.780146	1.834824	1.803166	1.795648	1.798572		
	5	1.825656	1.799776	1.812478	1.780148	1.834828	1.803170	1.795650	1.798574		
	6	1.825658	1.799778	1.812476	1.780142	1.834828	1.803174	1.795652	1.798578		
	7	1.825656	1.799778	1.812476	1.780144	1.834826	1.803170	1.795648	1.798570		
	8	1.825656	1.799776	1.812474	1.780144	1.834824	1.803170	1.795648	1.798574		
	9	1.825658	1.799778	1.812478	1.780144	1.834824	1.803170	1.795646	1.798572		
	10	1.825658	1.799778	1.812476	1.780146	1.834826	1.803174	1.795646	1.798572		

		Measured Weight (g)									
	Meas #	A102	A103	A104	A105	A106	A107	A108	A109		
800 hrs	1			1.812482	1.780150	1.834830	1.803174	1.795644	1.798582		
	2			1.812484	1.780152	1.834832	1.803178	1.795646	1.798578		
	3			1.812480	1.780152	1.834830	1.803174	1.795644	1.798580		
	4			1.812480	1.780148	1.834828	1.803174	1.795648	1.798578		
	5			1.812480	1.780150	1.834832	1.803176	1.795648	1.798578		
	6			1.812482	1.780148	1.834830	1.803176	1.795646	1.798580		
	7			1.812480	1.780148	1.834832	1.803174	1.795648	1.798578		
	8			1.812482	1.780152	1.834830	1.803174	1.795644	1.798580		
	9			1.812482	1.780150	1.834834	1.803178	1.795646	1.798582		
	10			1.812480	1.780148	1.834830	1.803176	1.795648	1.798578		
1000 hrs	1					1.834836	1.803184	1.795652	1.798590		
	2					1.834836	1.803182	1.795652	1.798588		
	3					1.834834	1.803182	1.795648	1.798588		
	4					1.834836	1.803182	1.795650	1.798586		
	5					1.834834	1.803180	1.795650	1.798588		
	6					1.834834	1.803184	1.795650	1.798588		
	7					1.834832	1.803182	1.795648	1.798590		
	8					1.834836	1.803180	1.795650	1.798586		
	9					1.834834	1.803180	1.795652	1.798588		
	10					1.834836	1.803182	1.795650	1.798588		
1200 hrs	1										
	2										
	3										
	4										
	5										
	6										
	7										
	8										
	9										
	10										

Table 28: Raw Data, Expt. #3, RG-CO_2/450°C/20MPa, IN800H

Project:	**SCCO2**
Grant #:	PRJ39TC
MDS:	MD24386
Expt. #:	**3**
Phase:	1 of 4
Phase Type:	Pure CO2
Temp. (°C):	450
Pressure:	2900psi
Sample ID:	**IN800H**
Notes:	

Rel. Uncertainty in Meas. Mass:	Δm = ± 0.000002 g
Rel. Uncertainty in Meas. Length:	Δl = ± 0.001 mm
Rel. Uncertainty in Meas. Width:	Δw = ± 0.001 mm
Uncertainty in Meas. Area:	ΔA = ± 0.000184 cm^2

Supplier/UNS ID:	NO8810
Metal Type:	Austenitic - Superalloy
Color Designation:	Cyan
Hole Diameter in Sample (mm):	3

		Sample # / Description									
	Meas #	**I02**	**I03**	**I04**	**I05**	**I06**	**I07**	**I08**	**I09**		
BARE WEIGHT (gm)	**1**	1.992976	1.992254	1.995252	1.980230	1.981020	1.973024	1.982778	1.966720		
	2	1.992980	1.992258	1.995256	1.980234	1.981016	1.973022	1.982782	1.966718		
	3	1.992978	1.992256	1.995256	1.980234	1.981024	1.973026	1.982782	1.966720		
	4	1.992976	1.992256	1.995254	1.980232	1.981020	1.973024	1.982784	1.966722		
	5	1.992978	1.992254	1.995250	1.980230	1.981022	1.973026	1.982780	1.966724		
	6	1.992982	1.992258	1.995252	1.980234	1.981024	1.973024	1.982782	1.966722		
	7	1.992980	1.992256	1.995250	1.980232	1.981024	1.973020	1.982784	1.966724		
	8	1.992980	1.992258	1.995248	1.980228	1.981024	1.973022	1.982780	1.966720		
	9	1.992978	1.992254	1.995252	1.980232	1.981022	1.973024	1.982778	1.966722		
	10	1.992978	1.992256	1.995250	1.980230	1.981024	1.973022	1.982782	1.966722		
BARE AREA (mm2)	**1_L**	13.409	13.411	13.418	13.401	13.402	13.429	13.415	13.402		
	2_L	13.407	13.417	13.419	13.400	13.409	13.430	13.414	13.400		
	3_L	13.408	13.415	13.419	13.400	13.407	13.427	13.414	13.399		
	4_W	12.641	12.637	12.641	12.631	12.649	12.647	12.648	12.613		
	5_W	12.643	12.637	12.639	12.635	12.650	12.647	12.649	12.615		
	6_W	12.642	12.636	12.640	12.633	12.649	12.648	12.649	12.618		
BARE THICKNESS (mm)	**1**	1.558	1.563	1.560	1.556	1.562	1.543	1.543	1.537		
	2	1.565	1.560	1.560	1.556	1.558	1.544	1.546	1.540		
	3	1.563	1.555	1.558	1.554	1.551	1.541	1.545	1.541		
	4	1.559	1.561	1.556	1.550	1.563	1.544	1.541	1.538		
	5	1.565	1.558	1.561	1.558	1.554	1.541	1.544	1.540		

Table 29: Raw Data, Expt. #3, RG-CO_2/450^{o}C/20MPa, IN800H

		Measured Weight (g)									
	Meas #	I02	I03	I04	I05	I06	I07	I08	I09		
200 hrs	1	1.993016	1.992290	1.995294	1.980276	1.981058	1.973066	1.982830	1.966766		
	2	1.993014	1.992294	1.995290	1.980278	1.981062	1.973066	1.982830	1.966764		
	3	1.993014	1.992296	1.995288	1.980272	1.981060	1.973066	1.982832	1.966768		
	4	1.993016	1.992292	1.995292	1.980272	1.981060	1.973064	1.982834	1.966764		
	5	1.993016	1.992290	1.995294	1.980274	1.981062	1.973064	1.982834	1.966766		
	6	1.993016	1.992290	1.995292	1.980278	1.981062	1.973060	1.982832	1.966770		
	7	1.993014	1.992294	1.995290	1.980276	1.981058	1.973062	1.982828	1.966768		
	8	1.993018	1.992296	1.995292	1.980276	1.981058	1.973064	1.982828	1.966764		
	9	1.993018	1.992294	1.995294	1.980272	1.981060	1.973060	1.982830	1.966764		
	10	1.993016	1.992292	1.995290	1.980278	1.981060	1.973062	1.982828	1.966768		
400 hrs	1	1.993022	1.992302	1.995304	1.980284	1.981066	1.973072	1.982834	1.966776		
	2	1.993024	1.992302	1.995302	1.980284	1.981068	1.973070	1.982838	1.966774		
	3	1.993022	1.992300	1.995304	1.980286	1.981068	1.973070	1.982836	1.966778		
	4	1.993026	1.992306	1.995304	1.980284	1.981066	1.973074	1.982838	1.966778		
	5	1.993026	1.992304	1.995302	1.980282	1.981064	1.973072	1.982832	1.966774		
	6	1.993024	1.992304	1.995300	1.980286	1.981068	1.973074	1.982840	1.966776		
	7	1.993022	1.992300	1.995302	1.980280	1.981066	1.973070	1.982840	1.966778		
	8	1.993022	1.992302	1.995300	1.980284	1.981068	1.973076	1.982838	1.966774		
	9	1.993024	1.992300	1.995304	1.980286	1.981064	1.973074	1.982840	1.966774		
	10	1.993024	1.992302	1.995300	1.980284	1.981068	1.973072	1.982842	1.966776		
600 hrs	1	1.993024	1.992306	1.995300	1.980278	1.981060	1.973072	1.982838	1.966768		
	2	1.993028	1.992302	1.995300	1.980272	1.981058	1.973070	1.982832	1.966766		
	3	1.993024	1.992304	1.995302	1.980274	1.981058	1.973070	1.982834	1.966766		
	4	1.993026	1.992306	1.995302	1.980276	1.981058	1.973068	1.982834	1.966768		
	5	1.993020	1.992306	1.995300	1.980274	1.981060	1.973072	1.982834	1.966768		
	6	1.993020	1.992304	1.995298	1.980276	1.981060	1.973068	1.982838	1.966768		
	7	1.993020	1.992304	1.995302	1.980274	1.981058	1.973070	1.982832	1.966772		
	8	1.993018	1.992300	1.995300	1.980276	1.981060	1.973070	1.982832	1.966770		
	9	1.993020	1.992302	1.995304	1.980272	1.981060	1.973070	1.982832	1.966768		
	10	1.993020	1.992302	1.995300	1.980274	1.981060	1.973072	1.982832	1.966770		

		Measured Weight (g)									
	Meas #	I02	I03	I04	I05	I06	I07	I08	I09		
800 hrs	1			1.995304	1.980272	1.981058	1.973068	1.982834	1.966772		
	2			1.995304	1.980278	1.981058	1.973068	1.982838	1.966770		
	3			1.995302	1.980276	1.981056	1.973070	1.982836	1.966772		
	4			1.995304	1.980274	1.981058	1.973070	1.982832	1.966770		
	5			1.995302	1.980276	1.981060	1.973072	1.982832	1.966768		
	6			1.995302	1.980272	1.981060	1.973074	1.982834	1.966768		
	7			1.995306	1.980274	1.981058	1.973068	1.982832	1.966766		
	8			1.995304	1.980276	1.981060	1.973072	1.982836	1.966770		
	9			1.995304	1.980278	1.981054	1.973068	1.982832	1.966772		
	10			1.995306	1.980274	1.981060	1.973074	1.982832	1.966770		
1000 hrs	1					1.981058	1.973072	1.982836	1.966768		
	2					1.981058	1.973072	1.982838	1.966768		
	3					1.981060	1.973072	1.982836	1.966770		
	4					1.981060	1.973074	1.982834	1.966772		
	5					1.981060	1.973070	1.982836	1.966772		
	6					1.981058	1.973070	1.982838	1.966768		
	7					1.981060	1.973072	1.982838	1.966770		
	8					1.981058	1.973074	1.982834	1.966770		
	9					1.981058	1.973072	1.982836	1.966770		
	10					1.981062	1.973070	1.982836	1.966772		
1200 hrs	1										
	2										
	3										
	4										
	5										
	6										
	7										
	8										
	9										
	10										

Table 30: Raw Data, Expt. #4, RG-CO_2/550^{o}C/20MPa, Coupon Arrangement

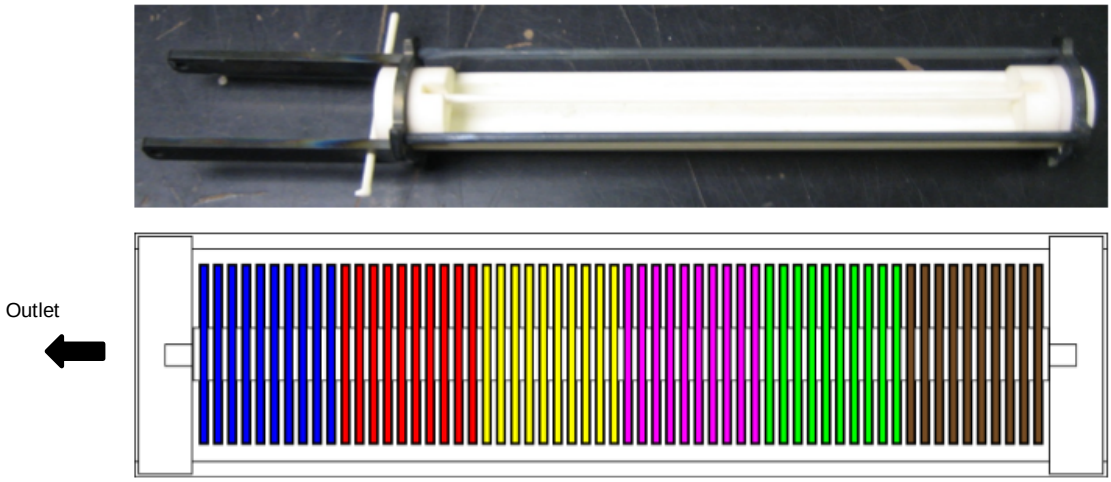

Sample	Blue	Red	Yellow	Magenta	Green	Brown
1	HCM12A H20	AFA-OC6 A616	AFA-OC7 A710	AFA-OC10 A110	347ss S16	IN800H I10
2	H21	A617	A711	A111	S17	I11
3	NF616 N20	A618	A712	A112	S18	I12
4	N21	A619	A713	A113	S19	I13
5	HCM12A H22	A620	A714	A114	S20	I14
6	H23	A621	A715	A115	S21	I15
7	NF616 N22	A622	A716	A116	S22	I16
8	N23	A623	A717	A117	S23	I17
9		A624	A718	A118	S24	I18
10		A625	A719	A119	S25	I19

Table 31: Raw Data, Expt. #4, RG-CO_2/550°C/20MPa, 347SS

Project:	**SCCO2**
Grant #:	PRJ39TC
MDS:	MD24386
Expt. #:	**4**
Phase:	1 of 4
Phase Type:	Pure CO2
Temp. (°C):	550
Pressure:	2900psi
Sample ID:	**347SS**
Notes:	

Rel. Uncertainty in Meas. Mass:	Δm = ± 0.000002 g
Rel. Uncertainty in Meas. Length:	Δl = ± 0.001 mm
Rel. Uncertainty in Meas. Width:	Δw = ± 0.001 mm
Uncertainty in Meas. Area:	ΔA = ± 0.000182 cm^2

Supplier/UNS ID:	S34700
Metal Type:	Austenitic
Color Designation:	Green
Hole Diameter in Sample (mm):	3

		Sample # / Description									
	Meas #	**S16**	**S17**	**S18**	**S19**	**S20**	**S21**	**S22**	**S23**	**S24**	**S25**
BARE WEIGHT (gm)	**1**	1.866140	1.882442	1.924338	1.892600	1.916802	1.907552	1.940288	1.929698	1.924058	1.938712
	2	1.866144	1.882442	1.924342	1.892602	1.916804	1.907554	1.940288	1.929704	1.924058	1.938712
	3	1.866144	1.882442	1.924338	1.892602	1.916804	1.907556	1.940284	1.929700	1.924060	1.938712
	4	1.866146	1.882444	1.924344	1.892598	1.916806	1.907556	1.940286	1.929702	1.924062	1.938718
	5	1.866142	1.882440	1.924342	1.892602	1.916800	1.907552	1.940288	1.929700	1.924064	1.938712
	6	1.866144	1.882444	1.924340	1.892602	1.916804	1.907554	1.940292	1.929702	1.924064	1.938716
	7	1.866146	1.882446	1.924344	1.892604	1.916804	1.907552	1.940294	1.929704	1.924058	1.938718
	8	1.866142	1.882440	1.924344	1.892606	1.916802	1.907556	1.940286	1.929708	1.924058	1.938710
	9	1.866138	1.882438	1.924340	1.892606	1.916798	1.907552	1.940284	1.929704	1.924058	1.938712
	10	1.866148	1.882444	1.924338	1.892600	1.916800	1.907554	1.940290	1.929700	1.924060	1.938712
BARE AREA (mm2)	**1_L**	13.063	13.144	13.147	13.133	13.142	13.188	13.179	13.160	13.158	13.175
	2_L	13.027	13.123	13.141	13.130	13.150	13.191	13.184	13.164	13.160	13.164
	3_L	13.018	13.095	13.142	13.134	13.153	13.183	13.185	13.184	13.165	13.160
	4_W	12.521	12.538	12.622	12.591	12.634	12.633	12.651	12.605	12.633	12.638
	5_W	12.542	12.552	12.621	12.595	12.632	12.634	12.650	12.600	12.629	12.641
	6_W	12.553	12.571	12.622	12.598	12.634	12.634	12.641	12.600	12.627	12.642
BARE THICKNESS (mm)	**1**	1.534	1.528	1.542	1.531	1.538	1.520	1.552	1.547	1.541	1.551
	2	1.526	1.532	1.559	1.541	1.548	1.540	1.560	1.563	1.557	1.570
	3	1.533	1.534	1.560	1.535	1.549	1.547	1.556	1.565	1.561	1.568
	4	1.538	1.521	1.556	1.540	1.543	1.522	1.557	1.555	1.553	1.567
	5	1.532	1.538	1.557	1.528	1.546	1.546	1.555	1.561	1.554	1.558

Table 32: Raw Data, Expt. #4, RG-CO_2/550^{o}C/20MPa, 347SS

		Measured Weight (g)									
	Meas #	S16	S17	S18	S19	S20	S21	S22	S23	S24	S25
200 hrs	1	1.866262	1.882606	1.924432	1.892694	1.916892	1.907636	1.940368	1.929820	1.924144	1.938800
	2	1.866268	1.882604	1.924436	1.892690	1.916894	1.907642	1.940368	1.929828	1.924146	1.938800
	3	1.866266	1.882608	1.924438	1.892688	1.916890	1.907636	1.940368	1.929822	1.924144	1.938806
	4	1.866270	1.882610	1.924434	1.892690	1.916892	1.907636	1.940368	1.929826	1.924144	1.938798
	5	1.866264	1.882604	1.924438	1.892686	1.916890	1.907636	1.940370	1.929822	1.924148	1.938804
	6	1.866266	1.882606	1.924434	1.892686	1.916892	1.907636	1.940374	1.929826	1.924144	1.938802
	7	1.866262	1.882612	1.924436	1.892690	1.916890	1.907634	1.940374	1.929822	1.924140	1.938802
	8	1.866268	1.882612	1.924432	1.892686	1.916896	1.907636	1.940372	1.929828	1.924144	1.938798
	9	1.866266	1.882608	1.924436	1.892690	1.916894	1.907634	1.940370	1.929822	1.924148	1.938802
	10	1.866268	1.882610	1.924432	1.892686	1.916890	1.907638	1.940374	1.929822	1.924146	1.938800
400 hrs	1			1.924460	1.892716	1.916920	1.907664	1.940394	1.929856	1.924168	1.938832
	2			1.924454	1.892712	1.916918	1.907664	1.940394	1.929852	1.924170	1.938828
	3			1.924462	1.892708	1.916918	1.907658	1.940398	1.929850	1.924168	1.938826
	4			1.924460	1.892710	1.916912	1.907660	1.940390	1.929850	1.924170	1.938824
	5			1.924458	1.892714	1.916916	1.907658	1.940398	1.929852	1.924170	1.938834
	6			1.924458	1.892712	1.916912	1.907660	1.940396	1.929848	1.924172	1.938826
	7			1.924462	1.892714	1.916916	1.907666	1.940390	1.929844	1.924168	1.938832
	8			1.924458	1.892714	1.916914	1.907666	1.940390	1.929850	1.924166	1.938826
	9			1.924462	1.892712	1.916920	1.907660	1.940390	1.929846	1.924170	1.938826
	10			1.924462	1.892714	1.916912	1.907664	1.940390	1.929852	1.924164	1.938826
600 hrs	1					1.916928	1.907674	1.940406	1.929858	1.924182	1.938840
	2					1.916928	1.907676	1.940398	1.929860	1.924186	1.938840
	3					1.916928	1.907674	1.940398	1.929856	1.924180	1.938838
	4					1.916928	1.907672	1.940400	1.929860	1.924184	1.938838
	5					1.916932	1.907672	1.940402	1.929860	1.924180	1.938838
	6					1.916930	1.907672	1.940402	1.929858	1.924178	1.938838
	7					1.916930	1.907670	1.940402	1.929856	1.924180	1.938842
	8					1.916928	1.907672	1.940402	1.929860	1.924180	1.938838
	9					1.916934	1.907672	1.940400	1.929862	1.924178	1.938838
	10					1.916934	1.907670	1.940400	1.929856	1.924184	1.938838

		Measured Weight (g)									
	Meas #	S16	S17	S18	S19	S20	S21	S22	S23	S24	S25
800 hrs	1							1.940410	1.929860	1.924186	1.938846
	2							1.940412	1.929862	1.924188	1.938846
	3							1.940406	1.929860	1.924180	1.938842
	4							1.940408	1.929862	1.924182	1.938840
	5							1.940406	1.929860	1.924188	1.938840
	6							1.940406	1.929864	1.924180	1.938838
	7							1.940406	1.929864	1.924184	1.938844
	8							1.940406	1.929864	1.924188	1.938846
	9							1.940408	1.929862	1.924184	1.938844
	10							1.940406	1.929860	1.924180	1.938840
1000 hrs	1									1.924188	1.938842
	2									1.924190	1.938854
	3									1.924188	1.938846
	4									1.924190	1.938850
	5									1.924188	1.938854
	6									1.924194	1.938850
	7									1.924194	1.938852
	8									1.924192	1.938856
	9									1.924190	1.938856
	10									1.924192	1.938850
1200 hrs	1										
	2										
	3										
	4										
	5										
	6										
	7										
	8										
	9										
	10										

Table 33: Raw Data, Expt. #4, RG-CO_2/550°C/20MPa, AFA-OC6

Project:	**SCCO2**
Grant #:	PRJ39TC
MDS:	MD24386
Expt. #:	**4**
Phase:	1 of 4
Phase Type:	Pure CO2
Temp. (°C):	550
Pressure:	2900psi
Sample ID:	**AFA-OC6**
Notes:	

Rel. Uncertainty in Meas. Mass:	Δm = ± 0.000002 g
Rel. Uncertainty in Meas. Length:	Δl = ± 0.001 mm
Rel. Uncertainty in Meas. Width:	Δw = ± 0.001 mm
Uncertainty in Meas. Area:	

Supplier/UNS ID:	Heat # 001919 (CRADA RPT)
Metal Type:	Alumina-Forming Austenitic
Color Designation:	Red
Hole Diameter in Sample (mm):	3

		Sample # / Description									
	Meas #	**A616**	**A617**	**A618**	**A619**	**A620**	**A621**	**A622**	**A623**	**A624**	**A625**
BARE WEIGHT (gm)	**1**	1.856312	1.799754	1.829854	1.855590	1.811360	1.797166	1.777076	1.807394	1.813922	1.689866
	2	1.856310	1.799756	1.829856	1.855590	1.811364	1.797164	1.777076	1.807394	1.813926	1.689868
	3	1.856312	1.799756	1.829854	1.855586	1.811368	1.797170	1.777078	1.807388	1.813922	1.689866
	4	1.856310	1.799758	1.829852	1.855592	1.811368	1.797174	1.777070	1.807396	1.813924	1.689874
	5	1.856312	1.799760	1.829850	1.855586	1.811364	1.797172	1.777074	1.807390	1.813928	1.689878
	6	1.856314	1.799756	1.829854	1.855590	1.811368	1.797166	1.777078	1.807392	1.813928	1.689870
	7	1.856312	1.799756	1.829852	1.855586	1.811366	1.797166	1.777078	1.807394	1.813924	1.689872
	8	1.856310	1.799750	1.829852	1.855590	1.811368	1.797164	1.777076	1.807390	1.813920	1.689870
	9	1.856308	1.799756	1.829858	1.855588	1.811366	1.797164	1.777074	1.807394	1.813926	1.689868
	10	1.856310	1.799754	1.829854	1.855588	1.811366	1.797164	1.777074	1.807394	1.813926	1.689870
BARE AREA (mm2)	**1_L**	12.926	12.783	12.888	12.898	12.880	12.852	12.876	12.824	12.904	12.873
	2_L	12.908	12.786	12.900	12.900	12.868	12.860	12.873	12.813	12.906	12.858
	3_L	12.857	12.727	12.890	12.902	12.840	12.855	12.869	12.815	12.903	12.822
	4_W	12.636	12.598	12.626	12.606	12.551	12.445	12.617	12.558	12.616	12.464
	5_W	12.638	12.562	12.609	12.609	12.643	12.525	12.617	12.583	12.620	12.466
	6_W	12.649	12.472	12.579	12.603	12.669	12.621	12.616	12.588	12.615	12.469
BARE THICKNESS (mm)	**1**	1.571	1.550	1.532	1.555	1.544	1.548	1.490	1.541	1.537	1.426
	2	1.576	1.563	1.558	1.561	1.552	1.553	1.520	1.544	1.545	1.479
	3	1.571	1.560	1.567	1.569	1.558	1.559	1.528	1.550	1.550	1.492
	4	1.572	1.560	1.556	1.563	1.556	1.558	1.499	1.549	1.546	1.474
	5	1.575	1.562	1.555	1.561	1.554	1.551	1.522	1.547	1.545	1.468

Table 34: Raw Data, Expt. #4, RG-CO_2/550^{o}C/20MPa, AFA-OC6

		Measured Weight (g)									
	Meas #	A616	A617	A618	A619	A620	A621	A622	A623	A624	A625
200 hrs	1	1.856536	1.799970	1.830020	1.855768	1.811524	1.797368	1.777250	1.807546	1.814104	1.690062
	2	1.856540	1.799966	1.830022	1.855768	1.811526	1.797368	1.777252	1.807542	1.814106	1.690064
	3	1.85654	1.799968	1.830018	1.855764	1.811524	1.797368	1.777250	1.807546	1.814108	1.690062
	4	1.856534	1.799970	1.830020	1.855766	1.811526	1.797372	1.777250	1.807548	1.814100	1.690058
	5	1.856538	1.799968	1.830020	1.855768	1.811526	1.797368	1.777248	1.807544	1.814102	1.690062
	6	1.856534	1.799968	1.830018	1.855764	1.811530	1.797366	1.777248	1.807542	1.814102	1.690060
	7	1.856534	1.799966	1.830018	1.855768	1.811530	1.797368	1.777250	1.807546	1.814104	1.690064
	8	1.856536	1.799970	1.830016	1.855768	1.811528	1.797370	1.777252	1.807546	1.814106	1.690064
	9	1.856536	1.799968	1.830020	1.855766	1.811526	1.797368	1.777252	1.807548	1.814102	1.690062
	10	1.856538	1.799968	1.830018	1.855764	1.811528	1.797370	1.777252	1.807546	1.814104	1.690066
400 hrs	1			1.830174	1.855948	1.811730	1.797474	1.777436	1.807728	1.814306	1.690328
	2			1.830174	1.855946	1.811728	1.797472	1.777434	1.807726	1.814310	1.690324
	3			1.830178	1.855942	1.811730	1.797476	1.777434	1.807728	1.814306	1.690326
	4			1.830176	1.855946	1.811732	1.797472	1.777436	1.807724	1.814310	1.690324
	5			1.830174	1.855944	1.811732	1.797474	1.777432	1.807726	1.814308	1.690324
	6			1.830176	1.855946	1.811734	1.797474	1.777434	1.807728	1.814308	1.690326
	7			1.830176	1.855944	1.811730	1.797476	1.777436	1.807728	1.814310	1.690322
	8			1.830178	1.855940	1.811732	1.797472	1.777434	1.807726	1.814308	1.690324
	9			1.830174	1.855942	1.811734	1.797474	1.777434	1.807728	1.814306	1.690324
	10			1.830174	1.855944	1.811734	1.797474	1.777436	1.807724	1.814308	1.690324
600 hrs	1					1.811946	1.797674	1.777680	1.807962	1.814526	1.690658
	2					1.811948	1.797668	1.777674	1.807966	1.814530	1.690660
	3					1.811942	1.797672	1.777674	1.807972	1.814526	1.690666
	4					1.811946	1.797670	1.777672	1.807964	1.814528	1.690660
	5					1.811952	1.797670	1.777674	1.807964	1.814528	1.690658
	6					1.811950	1.797672	1.777672	1.807966	1.814526	1.690662
	7					1.811948	1.797670	1.777678	1.807968	1.814528	1.690662
	8					1.811944	1.797668	1.777676	1.807968	1.814532	1.690662
	9					1.811950	1.797666	1.777676	1.807966	1.814532	1.690662
	10					1.811948	1.797668	1.777676	1.807966	1.814526	1.690660

		Measured Weight (g)									
	Meas #	A616	A617	A618	A619	A620	A621	A622	A623	A624	A625
800 hrs	1							1.777970	1.808236	1.814858	1.691014
	2							1.777970	1.808236	1.814858	1.691016
	3							1.777970	1.808236	1.814860	1.691014
	4							1.777972	1.808238	1.814858	1.691012
	5							1.777968	1.808234	1.814860	1.691012
	6							1.777972	1.808236	1.814858	1.691014
	7							1.777974	1.808234	1.814854	1.691014
	8							1.777970	1.808234	1.814858	1.691016
	9							1.777970	1.808236	1.814858	1.691014
	10							1.777974	1.808236	1.814858	1.691014
1000 hrs	1									1.815238	1.691384
	2									1.815244	1.691388
	3									1.815244	1.691386
	4									1.815244	1.691384
	5									1.815246	1.691382
	6									1.815244	1.691382
	7									1.815238	1.691384
	8									1.815242	1.691380
	9									1.815242	1.691380
	10									1.815244	1.691382
1200 hrs	1										
	2										
	3										
	4										
	5										
	6										
	7										
	8										
	9										
	10										

Table 35: Raw Data, Expt. #4, RG-CO_2/550°C/20MPa, AFA-OC7

Project:	**SCCO2**
Grant #:	PRJ39TC
MDS:	MD24386
Expt. #:	**4**
Phase:	1 of 4
Phase Type:	Pure CO2
Temp. (°C):	550
Pressure:	2900psi
Sample ID:	**AFA-OC7**
Notes:	

Rel. Uncertainty in Meas. Mass:	Δm = ± 0.000002 g
Rel. Uncertainty in Meas. Length:	Δl = ± 0.001 mm
Rel. Uncertainty in Meas. Width:	Δw = ± 0.001 mm
Uncertainty in Meas. Area:	

Supplier/UNS ID:	Heat # 001920
Metal Type:	Alumina-Forming Austenitic
Color Designation:	Yellow
Hole Diameter in Sample (mm):	3

		Sample # / Description									
	Meas #	**A710**	**A711**	**A712**	**A713**	**A714**	**A715**	**A716**	**A717**	**A718**	**A719**
BARE WEIGHT (gm)	**1**	1.834782	1.851494	1.805350	1.816360	1.813978	1.815826	1.799296	1.853808	1.709900	1.728920
	2	1.834780	1.851492	1.805350	1.816364	1.813982	1.815828	1.799296	1.853808	1.709902	1.728922
	3	1.834780	1.851494	1.805350	1.816354	1.813988	1.815826	1.799292	1.853810	1.709900	1.728918
	4	1.834782	1.851494	1.805348	1.816358	1.813984	1.815830	1.799294	1.853806	1.709904	1.728918
	5	1.834784	1.851492	1.805352	1.816354	1.813980	1.815832	1.799300	1.853808	1.709902	1.728914
	6	1.834780	1.851494	1.805354	1.816354	1.813982	1.815830	1.799296	1.853810	1.709906	1.728918
	7	1.834788	1.851492	1.805358	1.816362	1.813982	1.815828	1.799296	1.853812	1.709906	1.728916
	8	1.834780	1.851490	1.805350	1.816356	1.813984	1.815828	1.799294	1.853810	1.709906	1.728916
	9	1.834780	1.851490	1.805350	1.816354	1.813980	1.815830	1.799294	1.853812	1.709898	1.728918
	10	1.834784	1.851490	1.805350	1.816360	1.813984	1.815828	1.799294	1.853812	1.709906	1.728918
BARE AREA (mm2)	**1_L**	12.871	12.858	12.778	12.830	12.796	12.761	12.781	12.867	12.840	12.793
	2_L	12.869	12.865	12.774	12.821	12.798	12.765	12.780	12.873	12.842	12.787
	3_L	12.860	12.855	12.777	12.811	12.790	12.768	12.782	12.890	12.845	12.804
	4_W	12.672	12.671	12.608	12.658	12.615	12.640	12.605	12.655	12.569	12.675
	5_W	12.670	12.674	12.614	12.656	12.621	12.628	12.602	12.654	12.572	12.674
	6_W	12.671	12.675	12.606	12.644	12.616	12.616	12.595	12.651	12.578	12.660
BARE THICKNESS (mm)	**1**	1.537	1.560	1.522	1.520	1.529	1.540	1.522	1.559	1.423	1.440
	2	1.552	1.570	1.535	1.549	1.543	1.557	1.542	1.571	1.495	1.480
	3	1.547	1.552	1.537	1.552	1.541	1.555	1.541	1.561	1.510	1.492
	4	1.542	1.560	1.530	1.541	1.531	1.554	1.538	1.566	1.530	1.473
	5	1.549	1.561	1.533	1.540	1.543	1.545	1.536	1.559	1.400	1.469

Table 36: Raw Data, Expt. #4, RG-CO_2/550^{o}C/20MPa, AFA-OC7

		Measured Weight (g)									
	Meas #	A710	A711	A712	A713	A714	A715	A716	A717	A718	A719
200 hrs	1	1.834926	1.851674	1.805468	1.816478	1.814098	1.815946	1.799402	1.853910	1.710020	1.729026
	2	1.834928	1.851674	1.805468	1.816478	1.814100	1.815944	1.799400	1.853908	1.710018	1.729026
	3	1.834926	1.851674	1.805466	1.816474	1.814096	1.815944	1.799406	1.853908	1.710018	1.729022
	4	1.834926	1.851668	1.805466	1.816478	1.814096	1.815944	1.799404	1.853908	1.710016	1.729026
	5	1.834926	1.851674	1.805466	1.816476	1.814096	1.815944	1.799404	1.853908	1.710016	1.729024
	6	1.834924	1.851668	1.805468	1.816476	1.814096	1.815948	1.799400	1.853908	1.710016	1.729024
	7	1.834920	1.851668	1.805470	1.816476	1.814096	1.815946	1.799406	1.853904	1.710014	1.729020
	8	1.834924	1.851672	1.805466	1.816476	1.814094	1.815946	1.799406	1.853906	1.710016	1.729026
	9	1.834922	1.851668	1.805464	1.816474	1.814096	1.815942	1.799398	1.853910	1.710012	1.729020
	10	1.834924	1.851668	1.805470	1.816474	1.814094	1.815944	1.799398	1.853906	1.710016	1.729026
400 hrs	1			1.805538	1.816550	1.814168	1.815996	1.799438	1.853968	1.710078	1.729078
	2			1.805532	1.816548	1.814168	1.815994	1.799438	1.853968	1.710076	1.729078
	3			1.805538	1.816548	1.814170	1.815996	1.799436	1.853968	1.710078	1.729078
	4			1.805538	1.816550	1.814166	1.815994	1.799432	1.853964	1.710078	1.729082
	5			1.805532	1.816550	1.814168	1.815994	1.799434	1.853968	1.710080	1.729082
	6			1.805534	1.816548	1.814166	1.815992	1.799436	1.853966	1.710076	1.729078
	7			1.805534	1.816548	1.814168	1.815994	1.799436	1.853966	1.710078	1.729080
	8			1.805536	1.816552	1.814170	1.815996	1.799438	1.853962	1.710078	1.729082
	9			1.805538	1.816550	1.814166	1.815996	1.799432	1.853964	1.710076	1.729080
	10			1.805536	1.816550	1.814168	1.815996	1.799436	1.853964	1.710076	1.729082
600 hrs	1					1.814256	1.816048	1.799442	1.854002	1.710114	1.729124
	2					1.814254	1.816050	1.799442	1.854000	1.710118	1.729124
	3					1.814256	1.816048	1.799442	1.853996	1.710118	1.729120
	4					1.814254	1.816052	1.799438	1.853994	1.710114	1.729124
	5					1.814254	1.816056	1.799442	1.854000	1.710120	1.729122
	6					1.814256	1.816050	1.799442	1.853994	1.710122	1.729124
	7					1.814254	1.816052	1.799440	1.853996	1.710114	1.729124
	8					1.814256	1.816050	1.799440	1.853992	1.710114	1.729124
	9					1.814256	1.816056	1.799446	1.853996	1.710120	1.729124
	10					1.814256	1.816052	1.799442	1.853998	1.710116	1.729126

		Measured Weight (g)									
	Meas #	A710	A711	A712	A713	A714	A715	A716	A717	A718	A719
800 hrs	1							1.799472	1.854024	1.710148	1.729160
	2							1.799468	1.854018	1.710152	1.729158
	3							1.799470	1.854020	1.710150	1.729158
	4							1.799470	1.854020	1.710148	1.729156
	5							1.799472	1.854018	1.710148	1.729158
	6							1.799470	1.854018	1.710150	1.729160
	7							1.799468	1.854022	1.710152	1.729156
	8							1.799470	1.854022	1.710150	1.729156
	9							1.799472	1.854020	1.710150	1.729158
	10							1.799470	1.854022	1.710150	1.729160
1000 hrs	1									1.710194	1.729230
	2									1.710200	1.729236
	3									1.710200	1.729234
	4									1.710194	1.729240
	5									1.710204	1.729230
	6									1.710204	1.729236
	7									1.710204	1.729238
	8									1.710200	1.729234
	9									1.710200	1.729236
	10									1.710202	1.729238
1200 hrs	1										
	2										
	3										
	4										
	5										
	6										
	7										
	8										
	9										
	10										

Table 37: Raw Data, Expt. #4, RG-CO_2/550°C/20MPa, AFA-OC10

Project:	**SCCO2**
Grant #:	PRJ39TC
MDS:	MD24386
Expt. #:	**4**
Phase:	1 of 4
Phase Type:	Pure CO2
Temp. (°C):	550
Pressure:	2900psi
Sample ID:	**AFA-OC10**
Notes:	

Rel. Uncertainty in Meas. Mass:	Δm = ± 0.000002 g
Rel. Uncertainty in Meas. Length:	Δl = ± 0.001 mm
Rel. Uncertainty in Meas. Width:	Δw = ± 0.001 mm
Uncertainty in Meas. Area:	ΔA = ± 0.000179 cm^2

Supplier/UNS ID:	Heat # 001923
Metal Type:	Alumina-Forming Austenitic
Color Designation:	Magenta
Hole Diameter in Sample (mm):	3

		Sample # / Description									
	Meas #	**A110**	**A111**	**A112**	**A113**	**A114**	**A115**	**A116**	**A117**	**A118**	**A119**
BARE WEIGHT (gm)	**1**	1.811442	1.806892	1.754132	1.786232	1.789378	1.783740	1.811856	1.803970	1.756768	1.809824
	2	1.811446	1.806896	1.754134	1.786234	1.789376	1.783744	1.811856	1.803972	1.756766	1.809828
	3	1.811438	1.806894	1.754134	1.786234	1.789378	1.783740	1.811858	1.803966	1.756766	1.809826
	4	1.811442	1.806900	1.754138	1.786230	1.789374	1.783738	1.811856	1.803970	1.756774	1.809828
	5	1.811440	1.806894	1.754134	1.786234	1.789378	1.783742	1.811854	1.803966	1.756774	1.809830
	6	1.811440	1.806894	1.754136	1.786234	1.789378	1.783736	1.811858	1.803970	1.756770	1.809824
	7	1.811442	1.806896	1.754138	1.786230	1.789376	1.783742	1.811858	1.803970	1.756776	1.809824
	8	1.811440	1.806894	1.754136	1.786236	1.789378	1.783740	1.811856	1.803968	1.756774	1.809824
	9	1.811442	1.806896	1.754136	1.786232	1.789376	1.783738	1.811858	1.803968	1.756774	1.809822
	10	1.811442	1.806892	1.754138	1.786232	1.789378	1.783742	1.811858	1.803972	1.756774	1.809826
BARE AREA (mm2)	**1_L**	12.764	12.758	12.675	12.690	12.745	12.741	12.756	12.732	12.700	12.734
	2_L	12.766	12.758	12.641	12.705	12.732	12.734	12.756	12.730	12.700	12.733
	3_L	12.770	12.753	12.588	12.718	12.694	12.718	12.728	12.721	12.635	12.722
	4_W	12.667	12.662	12.520	12.520	12.546	12.517	12.566	12.534	12.373	12.552
	5_W	12.666	12.658	12.541	12.533	12.552	12.522	12.577	12.534	12.360	12.549
	6_W	12.665	12.668	12.540	12.560	12.564	12.532	12.578	12.539	12.347	12.539
BARE THICKNESS (mm)	**1**	1.548	1.532	1.527	1.554	1.540	1.542	1.547	1.560	1.520	1.558
	2	1.547	1.541	1.544	1.560	1.558	1.554	1.564	1.567	1.570	1.570
	3	1.543	1.540	1.548	1.552	1.560	1.551	1.568	1.563	1.590	1.570
	4	1.540	1.542	1.537	1.557	1.563	1.551	1.562	1.561	1.530	1.569
	5	1.542	1.536	1.541	1.548	1.535	1.546	1.561	1.563	1.589	1.567

Table 38: Raw Data, Expt. #4, RG-CO_2/550^{o}C/20MPa, AFA-OC10

		Measured Weight (g)									
	Meas #	A110	A111	A112	A113	A114	A115	A116	A117	A118	A119
200 hrs	1	1.811354	1.806972	1.754044	1.786214	1.789478	1.783586	1.811966	1.803998	1.756866	1.809924
	2	1.811362	1.806974	1.754042	1.786212	1.789484	1.783580	1.811968	1.803996	1.756872	1.809922
	3	1.81136	1.806980	1.754040	1.786210	1.789480	1.783586	1.811970	1.803994	1.756874	1.809916
	4	1.811356	1.806978	1.754044	1.786216	1.789484	1.783582	1.811964	1.803992	1.756866	1.809920
	5	1.811362	1.806974	1.754038	1.786216	1.789480	1.783580	1.811964	1.804000	1.756870	1.809918
	6	1.811362	1.806976	1.754042	1.786216	1.789486	1.783584	1.811962	1.803998	1.756870	1.809918
	7	1.811354	1.806976	1.754040	1.786216	1.789484	1.783580	1.811968	1.803994	1.756862	1.809920
	8	1.811356	1.806976	1.754042	1.786216	1.789484	1.783588	1.811968	1.803992	1.756862	1.809916
	9	1.811358	1.806978	1.754046	1.786208	1.789482	1.783584	1.811964	1.803996	1.756870	1.809920
	10	1.811360	1.806978	1.754040	1.786212	1.789486	1.783580	1.811964	1.803996	1.756870	1.809924
400 hrs	1			1.754058	1.786266	1.789528	1.783612	1.812034	1.804014	1.756878	1.809936
	2			1.754066	1.786266	1.789524	1.783612	1.812036	1.804018	1.756880	1.809930
	3			1.754064	1.786266	1.789520	1.783612	1.812026	1.804016	1.756880	1.809934
	4			1.754060	1.786260	1.789526	1.783602	1.812028	1.804016	1.756886	1.809932
	5			1.754056	1.786254	1.789520	1.783610	1.812030	1.804012	1.756882	1.809932
	6			1.754058	1.786258	1.789520	1.783612	1.812026	1.804004	1.756882	1.809934
	7			1.754062	1.786258	1.789520	1.783614	1.812030	1.804012	1.756882	1.809934
	8			1.754052	1.786252	1.789520	1.783608	1.812030	1.804010	1.756884	1.809932
	9			1.754052	1.786252	1.789516	1.783608	1.812032	1.804004	1.756880	1.809930
	10			1.754052	1.786254	1.789524	1.783608	1.812030	1.804012	1.756880	1.809932
600 hrs	1					1.789562	1.783620	1.812078	1.804018	1.756910	1.809952
	2					1.789560	1.783618	1.812078	1.804014	1.756910	1.809950
	3					1.789558	1.783622	1.812078	1.804014	1.756904	1.809950
	4					1.789564	1.783614	1.812078	1.804018	1.756906	1.809952
	5					1.789560	1.783620	1.812076	1.804016	1.756910	1.809952
	6					1.789566	1.783620	1.812074	1.804012	1.756906	1.809950
	7					1.789566	1.783616	1.812074	1.804010	1.756908	1.809948
	8					1.789560	1.783624	1.812078	1.804010	1.756906	1.809948
	9					1.789562	1.783620	1.812076	1.804010	1.756908	1.809954
	10					1.789564	1.783620	1.812074	1.804008	1.756910	1.809954

		Measured Weight (g)									
	Meas #	A110	A111	A112	A113	A114	A115	A116	A117	A118	A119
800 hrs	1							1.812066	1.804026	1.756926	1.809988
	2							1.812064	1.804026	1.756924	1.809990
	3							1.812064	1.804028	1.756926	1.809990
	4							1.812066	1.804026	1.756928	1.809986
	5							1.812066	1.804026	1.756924	1.809986
	6							1.812064	1.804024	1.756924	1.809986
	7							1.812064	1.804026	1.756926	1.809988
	8							1.812066	1.804024	1.756928	1.809988
	9							1.812068	1.804024	1.756926	1.809988
	10							1.812066	1.804026	1.756926	1.809986
1000 hrs	1									1.756956	1.810034
	2									1.756958	1.810030
	3									1.756960	1.810036
	4									1.756956	1.810032
	5									1.756966	1.810032
	6									1.756956	1.810032
	7									1.756964	1.810032
	8									1.756962	1.810034
	9									1.756960	1.810032
	10									1.756960	1.810028
1200 hrs	1										
	2										
	3										
	4										
	5										
	6										
	7										
	8										
	9										
	10										

Table 39: Raw Data, Expt. #4, RG-CO_2/550°C/20MPa, IN800H

Project:	**SCCO2**
Grant #:	PRJ39TC
MDS:	MD24386
Expt. #:	**4**
Phase:	1 of 4
Phase Type:	Pure CO2
Temp. (°C):	550
Pressure:	2900psi
Sample ID:	**IN800H**
Notes:	

Rel. Uncertainty in Meas. Mass:	Δm = ± 0.000002 g
Rel. Uncertainty in Meas. Length:	Δl = ± 0.001 mm
Rel. Uncertainty in Meas. Width:	Δw = ± 0.001 mm
Uncertainty in Meas. Area:	ΔA = ± 0.000183 cm^2

Supplier/UNS ID:	NO8810
Metal Type:	Austenitic - Superalloy
Color Designation:	Brown
Hole Diameter in Sample (mm):	3

		Sample # / Description									
	Meas #	**I10**	**I11**	**I12**	**I13**	**I14**	**I15**	**I16**	**I17**	**I18**	**I19**
BARE WEIGHT (gm)	**1**	1.978208	1.947978	1.974216	1.939696	1.935084	1.936394	1.932060	1.955006	1.876692	1.936976
	2	1.978210	1.947984	1.974212	1.939700	1.935084	1.936386	1.932066	1.955016	1.876694	1.936974
	3	1.978212	1.947978	1.974214	1.939708	1.935082	1.936390	1.932066	1.955010	1.876696	1.936974
	4	1.978214	1.947982	1.974212	1.939706	1.935084	1.936390	1.932068	1.955012	1.876698	1.936978
	5	1.978216	1.947984	1.974214	1.939702	1.935086	1.936392	1.932062	1.955014	1.876700	1.936978
	6	1.978208	1.947978	1.974216	1.939708	1.935086	1.936390	1.932066	1.955012	1.876692	1.936978
	7	1.978208	1.947980	1.974216	1.939698	1.935086	1.936386	1.932064	1.955016	1.876694	1.936982
	8	1.978210	1.947982	1.974220	1.939702	1.935080	1.936386	1.932066	1.955016	1.876694	1.936982
	9	1.978208	1.947980	1.974212	1.939702	1.935084	1.936386	1.932062	1.955010	1.876698	1.936980
	10	1.978208	1.947982	1.974210	1.939706	1.935080	1.936384	1.932062	1.955016	1.876700	1.936982
BARE AREA (mm2)	**1_L**	13.413	13.394	13.355	13.325	13.186	13.329	13.346	13.350	13.230	13.316
	2_L	13.415	13.398	13.360	13.353	13.200	13.329	13.352	13.341	13.230	13.318
	3_L	13.414	13.396	13.358	13.387	13.197	13.320	13.348	13.338	13.233	13.319
	4_W	12.652	12.648	12.601	12.580	12.612	12.580	12.478	12.605	12.337	12.526
	5_W	12.656	12.645	12.601	12.582	12.587	12.582	12.502	12.582	12.326	12.529
	6_W	12.657	12.645	12.600	12.580	12.568	12.586	12.509	12.545	12.319	12.529
BARE THICKNESS (mm)	**1**	1.543	1.516	1.528	1.503	1.525	1.499	1.509	1.521	1.504	1.512
	2	1.546	1.545	1.536	1.509	1.530	1.512	1.514	1.530	1.511	1.523
	3	1.546	1.558	1.538	1.519	1.528	1.518	1.521	1.537	1.518	1.530
	4	1.549	1.552	1.526	1.515	1.531	1.513	1.518	1.529	1.507	1.519
	5	1.540	1.535	1.535	1.517	1.526	1.516	1.519	1.532	1.516	1.524

Table 40: Raw Data, Expt. #4, RG-CO_2/550^{o}C/20MPa, IN800H

		Measured Weight (g)									
	Meas #	I10	I11	I12	I13	I14	I15	I16	I17	I18	I19
200 hrs	1	1.97831	1.948090	1.974386	1.939556	1.935216	1.936476	1.932166	1.955146	1.876824	1.937110
	2	1.978310	1.948090	1.974388	1.939558	1.935214	1.936474	1.932168	1.955148	1.876828	1.937112
	3	1.97831	1.948086	1.974388	1.939554	1.935214	1.936478	1.932164	1.955146	1.876828	1.937114
	4	1.978308	1.948088	1.974392	1.939560	1.935214	1.936480	1.932168	1.955150	1.876826	1.937110
	5	1.978312	1.948084	1.974390	1.939558	1.935216	1.936480	1.932172	1.955148	1.876830	1.937110
	6	1.978312	1.948088	1.974390	1.939556	1.935214	1.936482	1.932172	1.955144	1.876828	1.937110
	7	1.978314	1.948090	1.974390	1.939556	1.935218	1.936474	1.932170	1.955144	1.876828	1.937108
	8	1.978316	1.948090	1.974388	1.939560	1.935210	1.936476	1.932166	1.955144	1.876824	1.937114
	9	1.978308	1.948086	1.974390	1.939558	1.935214	1.936474	1.932166	1.955150	1.876830	1.937110
	10	1.978310	1.948084	1.974384	1.939558	1.935216	1.936474	1.932166	1.955146	1.876824	1.937110
400 hrs	1			1.974452	1.939588	1.935260	1.936504	1.932190	1.955198	1.876886	1.937150
	2			1.974452	1.939584	1.935252	1.936504	1.932190	1.955202	1.876884	1.937150
	3			1.974456	1.939584	1.935258	1.936494	1.932186	1.955196	1.876886	1.937154
	4			1.974452	1.939586	1.935260	1.936502	1.932192	1.955202	1.876876	1.937156
	5			1.974456	1.939588	1.935258	1.936500	1.932194	1.955200	1.876878	1.937150
	6			1.974450	1.939586	1.935250	1.936502	1.932186	1.955200	1.876888	1.937150
	7			1.974454	1.939582	1.935250	1.936504	1.932186	1.955202	1.876882	1.937152
	8			1.974454	1.939586	1.935252	1.936504	1.932190	1.955204	1.876886	1.937152
	9			1.974452	1.939588	1.935250	1.936500	1.932186	1.955200	1.876878	1.937154
	10			1.974452	1.939588	1.935254	1.936500	1.932186	1.955198	1.876876	1.937148
600 hrs	1					1.935272	1.936508	1.932200	1.955228	1.876900	1.937172
	2					1.935270	1.936512	1.932200	1.955224	1.876904	1.937170
	3					1.935270	1.936510	1.932196	1.955228	1.876900	1.937172
	4					1.935270	1.936512	1.932198	1.955224	1.876904	1.937172
	5					1.935268	1.936514	1.932200	1.955228	1.876902	1.937174
	6					1.935268	1.936512	1.932196	1.955220	1.876902	1.937176
	7					1.935272	1.936514	1.932198	1.955222	1.876900	1.937170
	8					1.935270	1.936512	1.932196	1.955226	1.876900	1.937170
	9					1.935272	1.936512	1.932196	1.955224	1.876906	1.937170
	10					1.935270	1.936510	1.932200	1.955224	1.876906	1.937170

		Measured Weight (g)									
	Meas #	I10	I11	I12	I13	I14	I15	I16	I17	I18	I19
800 hrs	1							1.932202	1.955242	1.876908	1.937178
	2							1.932208	1.955238	1.876910	1.937182
	3							1.932200	1.955240	1.876910	1.937180
	4							1.932200	1.955232	1.876914	1.937184
	5							1.932202	1.955232	1.876912	1.937182
	6							1.932204	1.955230	1.876914	1.937184
	7							1.932204	1.955240	1.876906	1.937182
	8							1.932206	1.955240	1.876910	1.937186
	9							1.932206	1.955236	1.876912	1.937186
	10							1.932208	1.955242	1.876912	1.937180
1000 hrs	1									1.876932	1.937192
	2									1.876936	1.937194
	3									1.876934	1.937194
	4									1.876930	1.937196
	5									1.876934	1.937198
	6									1.876936	1.937196
	7									1.876934	1.937200
	8									1.876938	1.937200
	9									1.876932	1.937196
	10									1.876930	1.937196
1200 hrs	1										
	2										
	3										
	4										
	5										
	6										
	7										
	8										
	9										
	10										

Table 41: Raw Data, Expt. #5, RG-CO_2/650^{o}C/20MPa, Coupon Arrangement

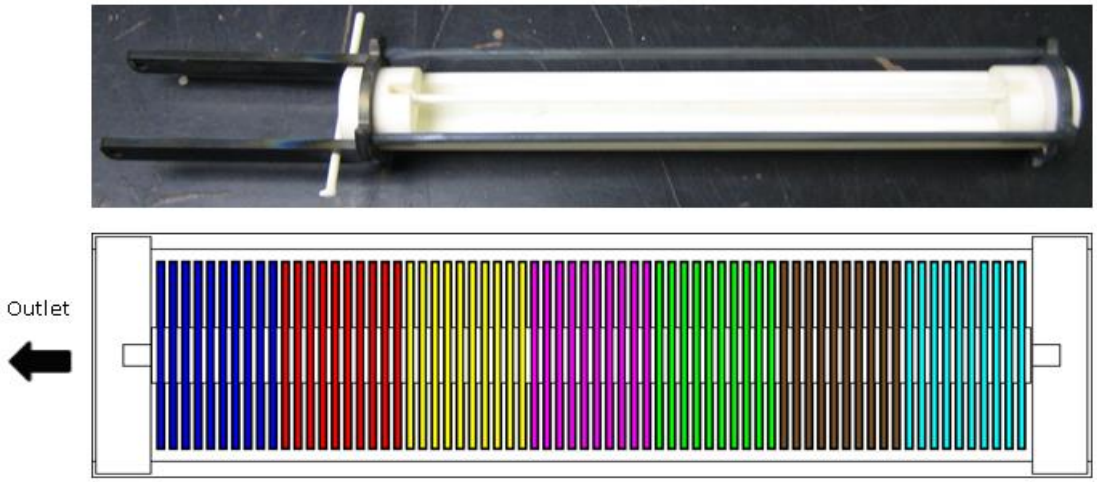

Sample	Blue	Red AFA-OC6	Yellow AFA-OC7	Magenta AFA-OC10	Green 347SS	Brown IN800H	Cyan Not Used
1	HCM12A H24	A626	A720	A120	S26	I20	
2	HCM12A H25	A627	A721	A121	S27	I21	
3	NF616 N24	A628	A722	A122	S28	I22	
4	NF616 N25	A629	A723	A123	S29	I23	
5		A630	A724	A124	S30	I24	
6		A631	A725	A125	S31	I25	
7		A632	A726	A126	S32	I26	
8		A633	A727	A127	S33	I27	
9		A634	A728	A128	S34	I28	
10		A635	A729	A129	S35	I29	

Table 42: Raw Data, Expt. #5, RG-CO_2/650°C/20MPa, 347SS

Project:	**SCCO2**
Grant #:	PRJ39TC
MDS:	MD24386
Expt. #:	**5**
Phase:	1 of 4
Phase Type:	Pure CO2
Temp. (°C):	650
Pressure:	2900psi
Sample ID:	**347SS**
Notes:	

Rel. Uncertainty in Meas. Mass:	Δm = ± 0.000002 g
Rel. Uncertainty in Meas. Length:	Δl = ± 0.001 mm
Rel. Uncertainty in Meas. Width:	Δw = ± 0.001 mm
Uncertainty in Meas. Area:	

Supplier/UNS ID:	S34700
Metal Type:	Austenitic
Color Designation:	Green
Hole Diameter in Sample (mm):	3

		Sample # / Description									
	Meas #	**S26**	**S27**	**S28**	**S29**	**S30**	**S31**	**S32**	**S33**	**S34**	**S35**
BARE WEIGHT (gm)	**1**	1.904076	1.917986	1.920220	1.919954	1.902840	1.904162	1.918242	1.913104	1.915730	1.908958
	2	1.904078	1.917988	1.920224	1.919950	1.902844	1.904156	1.918244	1.913100	1.915730	1.908960
	3	1.904076	1.917982	1.920220	1.919948	1.902842	1.904158	1.918248	1.913098	1.915738	1.908958
	4	1.904078	1.917988	1.920224	1.919948	1.902844	1.904156	1.918242	1.913098	1.915728	1.908960
	5	1.904078	1.917988	1.920222	1.919954	1.902844	1.904156	1.918240	1.913098	1.915726	1.908962
	6	1.904076	1.917988	1.920220	1.919952	1.902846	1.904160	1.918242	1.913098	1.915736	1.908958
	7	1.904074	1.917988	1.920224	1.919948	1.902840	1.904162	1.918244	1.913100	1.915736	1.908956
	8	1.904074	1.917988	1.920220	1.919948	1.902844	1.904160	1.918240	1.913102	1.915730	1.908952
	9	1.904074	1.917990	1.920224	1.919950	1.902840	1.904160	1.918242	1.913102	1.915728	1.908958
	10	1.904074	1.917988	1.920222	1.919950	1.902842	1.904162	1.918240	1.913104	1.915726	1.908962
BARE AREA (mm2)	**1_L**	13.148	13.174	13.176	13.181	13.130	13.151	13.142	13.167	13.139	13.184
	2_L	13.148	13.176	13.191	13.192	13.133	13.150	13.166	13.182	13.145	13.186
	3_L	13.143	13.171	13.193	13.192	13.134	13.148	13.170	13.178	13.153	13.189
	4_W	12.658	12.651	12.636	12.644	12.617	12.627	12.654	12.656	12.639	12.644
	5_W	12.656	12.650	12.644	12.643	12.618	12.630	12.659	12.655	12.643	12.646
	6_W	12.654	12.652	12.639	12.643	12.617	12.627	12.663	12.650	12.642	12.638
BARE THICKNESS (mm)	**1**	1.522	1.537	1.535	1.530	1.527	1.534	1.541	1.542	1.540	1.535
	2	1.540	1.547	1.552	1.545	1.550	1.553	1.557	1.557	1.561	1.546
	3	1.543	1.545	1.550	1.544	1.548	1.553	1.555	1.554	1.560	1.543
	4	1.534	1.544	1.551	1.542	1.547	1.549	1.551	1.551	1.557	1.547
	5	1.535	1.543	1.540	1.542	1.537	1.545	1.552	1.552	1.550	1.534

Table 43: Raw Data, Expt. #5, RG-CO_2/650^{o}C/20MPa, 347SS

		Measured Weight (g)									
	Meas #	S26	S27	S28	S29	S30	S31	S32	S33	S34	S35
200 hrs	1	1.904396	1.918294	1.920524	1.920234	1.903104	1.904442	1.918508	1.913370	1.915986	1.909294
	2	1.904396	1.918292	1.920522	1.920236	1.903104	1.904436	1.918506	1.913372	1.915986	1.909296
	3	1.904398	1.918302	1.920524	1.920236	1.903100	1.904430	1.918508	1.913362	1.915984	1.909288
	4	1.904392	1.918300	1.920528	1.920230	1.903110	1.904432	1.918510	1.913368	1.915982	1.909288
	5	1.904400	1.918298	1.920526	1.920230	1.903114	1.904434	1.918510	1.913364	1.915982	1.909296
	6	1.904396	1.918300	1.920530	1.920228	1.903110	1.904434	1.918508	1.913366	1.915982	1.909292
	7	1.904394	1.918298	1.920526	1.920236	1.903104	1.904436	1.918504	1.913366	1.915984	1.909292
	8	1.904396	1.918296	1.920530	1.920234	1.903108	1.904430	1.918504	1.913366	1.915988	1.909294
	9	1.904400	1.918298	1.920530	1.920234	1.903110	1.904434	1.918502	1.913364	1.915986	1.909294
	10	1.904396	1.918292	1.920532	1.920236	1.903106	1.904434	1.918512	1.913372	1.915982	1.909294
400 hrs	1			1.920582	1.920298	1.903156	1.904480	1.918564	1.913426	1.916032	1.909366
	2			1.920582	1.920296	1.903156	1.904480	1.918562	1.913428	1.916034	1.909366
	3			1.920590	1.920298	1.903158	1.904484	1.918562	1.913426	1.916032	1.909368
	4			1.920590	1.920298	1.903162	1.904486	1.918562	1.913422	1.916032	1.909368
	5			1.920582	1.920294	1.903162	1.904484	1.918560	1.913422	1.916030	1.909370
	6			1.920582	1.920296	1.903158	1.904482	1.918560	1.913426	1.916034	1.909362
	7			1.920584	1.920296	1.903154	1.904478	1.918564	1.913426	1.916034	1.909370
	8			1.920586	1.920296	1.903158	1.904484	1.918560	1.913424	1.916038	1.909372
	9			1.920586	1.920298	1.903160	1.904486	1.918564	1.913428	1.916034	1.909368
	10			1.920586	1.920296	1.903158	1.904480	1.918568	1.913428	1.916030	1.909370
600 hrs	1					1.903314	1.904614	1.918690	1.913502	1.916168	1.909852
	2					1.903310	1.904608	1.918692	1.913508	1.916164	1.909852
	3					1.903314	1.904616	1.918686	1.913496	1.916170	1.909854
	4					1.903314	1.904614	1.918690	1.913506	1.916166	1.909846
	5					1.903314	1.904608	1.918688	1.913508	1.916164	1.909846
	6					1.903320	1.904610	1.918696	1.913500	1.916170	1.909848
	7					1.903320	1.904612	1.918686	1.913504	1.916172	1.909850
	8					1.903314	1.904610	1.918690	1.913504	1.916170	1.909854
	9					1.903310	1.904612	1.918698	1.913504	1.916164	1.909856
	10					1.903320	1.904612	1.918688	1.913498	1.916166	1.909852

		Measured Weight (g)									
	Meas #	S26	S27	S28	S29	S30	S31	S32	S33	S34	S35
800 hrs	1							1.919130	1.913852	1.916470	1.910440
	2							1.919130	1.913854	1.916466	1.910440
	3							1.919132	1.913848	1.916470	1.910456
	4							1.919130	1.913848	1.916466	1.910452
	5							1.919128	1.913850	1.916464	1.910448
	6							1.919134	1.913854	1.916468	1.910446
	7							1.919132	1.913848	1.916464	1.910448
	8							1.919134	1.913844	1.916466	1.910452
	9							1.919126	1.913842	1.916466	1.910448
	10							1.919126	1.913854	1.916466	1.910452
1000 hrs	1									1.916900	1.910878
	2									1.916888	1.910882
	3									1.916890	1.910882
	4									1.916892	1.910882
	5									1.916888	1.910884
	6									1.916890	1.910886
	7									1.916886	1.910882
	8									1.916890	1.910874
	9									1.916886	1.910874
	10									1.916900	1.910874
1200 hrs	1										
	2										
	3										
	4										
	5										
	6										
	7										
	8										
	9										
	10										

Table 44: Raw Data, Expt. #5, RG-CO_2/650°C/20MPa, AFA-OC6

Project:	**SCCO2**
Grant #:	PRJ39TC
MDS:	MD24386
Expt. #:	**5**
Phase:	1 of 4
Phase Type:	Pure CO2
Temp. (°C):	650
Pressure:	2900psi
Sample ID:	**AFA-OC6**
Notes:	

Rel. Uncertainty in Meas. Mass:	Δm = ± 0.000002 g
Rel. Uncertainty in Meas. Length:	Δl = ± 0.001 mm
Rel. Uncertainty in Meas. Width:	Δw = ± 0.001 mm
Uncertainty in Meas. Area:	ΔA = ± 0.000181 cm^2

Supplier/UNS ID:	Heat # 001919
Metal Type:	Alumina-Forming Austenitic
Color Designation:	Red
Hole Diameter in Sample (mm):	3

		Sample # / Description									
	Meas #	**A626**	**A627**	**A628**	**A629**	**A630**	**A631**	**A632**	**A633**	**A634**	**A635**
BARE WEIGHT (gm)	**1**	1.804158	1.848620	1.844216	1.845394	1.845640	1.813092	1.840372	1.851586	1.821618	1.830446
	2	1.804152	1.848618	1.844212	1.845392	1.845640	1.813092	1.840372	1.851588	1.821618	1.830448
	3	1.804158	1.848620	1.844214	1.845394	1.845640	1.813094	1.840374	1.851584	1.821616	1.830448
	4	1.804156	1.848618	1.844210	1.845392	1.845646	1.813094	1.840374	1.851586	1.821612	1.830450
	5	1.804158	1.848616	1.844216	1.845392	1.845644	1.813094	1.840374	1.851584	1.821618	1.830448
	6	1.804152	1.848622	1.844212	1.845398	1.845642	1.813088	1.840374	1.851590	1.821616	1.830448
	7	1.804156	1.848618	1.844212	1.845394	1.845642	1.813090	1.840370	1.851584	1.821612	1.830448
	8	1.804156	1.848620	1.844212	1.845392	1.845640	1.813092	1.840378	1.851586	1.821614	1.830452
	9	1.804152	1.848618	1.844212	1.845396	1.845638	1.813094	1.840376	1.851584	1.821614	1.830446
	10	1.804158	1.848622	1.844212	1.845396	1.845640	1.813090	1.840372	1.851588	1.821616	1.830448
BARE AREA (mm2)	**1_L**	12.924	12.937	12.979	12.962	12.940	12.919	12.956	12.937	12.906	12.885
	2_L	12.923	12.934	12.979	12.957	12.939	12.914	12.956	12.941	12.892	12.879
	3_L	12.877	12.935	12.980	12.954	12.939	12.903	12.962	12.942	12.869	12.867
	4_W	12.632	12.634	12.670	12.633	12.652	12.626	12.613	12.649	12.658	12.657
	5_W	12.631	12.640	12.673	12.639	12.655	12.640	12.612	12.646	12.659	12.658
	6_W	12.632	12.644	12.673	12.642	12.667	12.649	12.612	12.638	12.658	12.653
BARE THICKNESS (mm)	**1**	1.535	1.554	1.564	1.559	1.551	1.526	1.558	1.560	1.544	1.555
	2	1.543	1.570	1.571	1.571	1.564	1.551	1.570	1.577	1.559	1.569
	3	1.541	1.570	1.562	1.569	1.562	1.548	1.570	1.575	1.556	1.566
	4	1.541	1.568	1.567	1.565	1.556	1.542	1.565	1.574	1.556	1.565
	5	1.538	1.562	1.560	1.565	1.563	1.539	1.568	1.573	1.554	1.560

Table 45: Raw Data, Expt. #5, RG-CO_2/650^{o}C/20MPa, AFA-OC6

		Measured Weight (g)									
	Meas #	A626	A627	A628	A629	A630	A631	A632	A633	A634	A635
200 hrs	1	1.804656	1.848988	1.844492	1.845776	1.846008	1.813428	1.840688	1.852000	1.822056	1.830820
	2	1.804660	1.848986	1.844492	1.845778	1.846008	1.813430	1.840684	1.852002	1.822048	1.830816
	3	1.80466	1.848988	1.844498	1.845780	1.846006	1.813432	1.840684	1.852004	1.822052	1.830812
	4	1.804662	1.848988	1.844496	1.845780	1.846000	1.813430	1.840682	1.851998	1.822052	1.830812
	5	1.804662	1.848992	1.844490	1.845782	1.846006	1.813430	1.840684	1.852000	1.822048	1.830818
	6	1.804662	1.848990	1.844494	1.845784	1.846008	1.813430	1.840684	1.852000	1.822054	1.830816
	7	1.804660	1.848992	1.844490	1.845782	1.846008	1.813428	1.840682	1.852004	1.822050	1.830820
	8	1.804662	1.848992	1.844498	1.845782	1.846004	1.813428	1.840680	1.852000	1.822054	1.830824
	9	1.804656	1.848994	1.844494	1.845782	1.846008	1.813430	1.840688	1.851994	1.822050	1.830822
	10	1.804662	1.848994	1.844498	1.845782	1.846008	1.813428	1.840684	1.852002	1.822052	1.830820
400 hrs	1			1.844682	1.845904	1.846158	1.813550	1.840834	1.852166	1.822224	1.830930
	2			1.844684	1.845902	1.846160	1.813554	1.840836	1.852166	1.822224	1.830934
	3			1.844682	1.845906	1.846160	1.813554	1.840834	1.852170	1.822218	1.830932
	4			1.844686	1.845902	1.846162	1.813552	1.840830	1.852168	1.822222	1.830932
	5			1.844688	1.845906	1.846158	1.813552	1.840834	1.852168	1.822224	1.830932
	6			1.844688	1.845908	1.846160	1.813552	1.840832	1.852164	1.822222	1.830934
	7			1.844686	1.845906	1.846156	1.813554	1.840834	1.852166	1.822220	1.830936
	8			1.844688	1.845910	1.846160	1.813556	1.840836	1.852168	1.822224	1.830934
	9			1.844684	1.845906	1.846154	1.813556	1.840836	1.852166	1.822222	1.830930
	10			1.844688	1.845908	1.846158	1.813554	1.840834	1.852164	1.822224	1.830932
600 hrs	1					1.850908	1.816680	1.844084	1.854218	1.823396	1.832290
	2					1.850908	1.816678	1.844082	1.854216	1.823396	1.832294
	3					1.850910	1.816686	1.844086	1.854216	1.823388	1.832290
	4					1.850910	1.816680	1.844080	1.854214	1.823388	1.832296
	5					1.850910	1.816686	1.844080	1.854212	1.823390	1.832292
	6					1.850912	1.816686	1.844088	1.854208	1.823388	1.832294
	7					1.850914	1.816680	1.844086	1.854212	1.823390	1.832296
	8					1.850908	1.816678	1.844082	1.854214	1.823386	1.832292
	9					1.850910	1.816678	1.844086	1.854212	1.823388	1.832300
	10					1.850912	1.816680	1.844086	1.854214	1.823390	1.832292

		Measured Weight (g)									
	Meas #	A626	A627	A628	A629	A630	A631	A632	A633	A634	A635
800 hrs	1							1.845034	1.854854	1.823774	1.832730
	2							1.845034	1.854858	1.823780	1.832728
	3							1.845032	1.854858	1.823770	1.832734
	4							1.845030	1.854856	1.823770	1.832734
	5							1.845032	1.854858	1.823772	1.832736
	6							1.845030	1.854858	1.823770	1.832736
	7							1.845028	1.854862	1.823774	1.832736
	8							1.845026	1.854856	1.823774	1.832738
	9							1.845028	1.854854	1.823774	1.832736
	10							1.845030	1.854858	1.823776	1.832734
1000 hrs	1									1.824118	1.833122
	2									1.824110	1.833124
	3									1.824108	1.833114
	4									1.824114	1.833114
	5									1.824122	1.833118
	6									1.824116	1.833116
	7									1.824120	1.833122
	8									1.824122	1.833130
	9									1.824116	1.833128
	10									1.824108	1.833114
1200 hrs	1										
	2										
	3										
	4										
	5										
	6										
	7										
	8										
	9										
	10										

Table 46: Raw Data, Expt. #5, RG-CO_2/650°C/20MPa, AFA-OC7

Project:	**SCCO2**
Grant #:	PRJ39TC
MDS:	MD24386
Expt. #:	**5**
Phase:	1 of 4
Phase Type:	Pure CO2
Temp. (°C):	650
Pressure:	2900psi
Sample ID:	**AFA-OC7**
Notes:	

Rel. Uncertainty in Meas. Mass:	Δm = ± 0.000002 g
Rel. Uncertainty in Meas. Length:	Δl = ± 0.001 mm
Rel. Uncertainty in Meas. Width:	Δw = ± 0.001 mm
Uncertainty in Meas. Area:	ΔA = ± 0.00018 cm^2

Supplier/UNS ID:	Heat # 001920
Metal Type:	Alumina-Forming Austenitic
Color Designation:	Yellow
Hole Diameter in Sample (mm):	3

		Sample # / Description									
	Meas #	**A720**	**A721**	**A722**	**A723**	**A724**	**A725**	**A726**	**A727**	**A728**	**A729**
BARE WEIGHT (gm)	**1**	1.796972	1.836310	1.823408	1.820662	1.836004	1.826656	1.833042	1.837836	1.846054	1.844638
	2	1.796972	1.836310	1.823412	1.820656	1.836004	1.826652	1.833050	1.837840	1.846058	1.844642
	3	1.796976	1.836314	1.823414	1.820660	1.836004	1.826650	1.833048	1.837834	1.846060	1.844642
	4	1.796970	1.836314	1.823412	1.820662	1.836002	1.826652	1.833048	1.837836	1.846056	1.844640
	5	1.796974	1.836310	1.823406	1.820658	1.836002	1.826650	1.833044	1.837838	1.846054	1.844638
	6	1.796974	1.836308	1.823412	1.820656	1.836008	1.826654	1.833044	1.837842	1.846062	1.844640
	7	1.796972	1.836308	1.823408	1.820662	1.836008	1.826650	1.833044	1.837840	1.846060	1.844638
	8	1.796974	1.836314	1.823408	1.820656	1.836002	1.826650	1.833048	1.837840	1.846054	1.844636
	9	1.796974	1.836312	1.823408	1.820658	1.836008	1.826650	1.833042	1.837836	1.846056	1.844640
	10	1.796970	1.836314	1.823412	1.820656	1.836002	1.826652	1.833046	1.837838	1.846058	1.844638
BARE AREA (mm2)	**1_L**	12.848	12.836	12.825	12.808	12.816	12.827	12.832	12.836	12.796	12.820
	2_L	12.847	12.838	12.822	12.809	12.815	12.828	12.833	12.828	12.797	12.817
	3_L	12.841	12.838	12.817	12.806	12.817	12.824	12.832	12.820	12.805	12.822
	4_W	12.622	12.651	12.650	12.548	12.644	12.605	12.628	12.673	12.625	12.652
	5_W	12.620	12.650	12.648	12.572	12.639	12.638	12.631	12.674	12.625	12.654
	6_W	12.619	12.653	12.643	12.583	12.643	12.648	12.637	12.674	12.629	12.646
BARE THICKNESS (mm)	**1**	1.523	1.545	1.528	1.539	1.543	1.539	1.539	1.539	1.557	1.558
	2	1.528	1.560	1.549	1.565	1.568	1.568	1.570	1.558	1.571	1.572
	3	1.519	1.556	1.548	1.565	1.564	1.566	1.569	1.555	1.566	1.568
	4	1.525	1.554	1.544	1.553	1.562	1.560	1.558	1.550	1.564	1.567
	5	1.518	1.552	1.540	1.559	1.557	1.555	1.558	1.554	1.566	1.561

Table 47: Raw Data, Expt. #5, RG-CO_2/650^{o}C/20MPa, AFA-OC7

		Measured Weight (g)									
	Meas #	A720	A721	A722	A723	A724	A725	A726	A727	A728	A729
200 hrs	1	1.797504	1.836476	1.823678	1.821010	1.836262	1.826998	1.833300	1.838090	1.846292	1.844878
	2	1.797500	1.836482	1.823674	1.821014	1.836260	1.827004	1.833298	1.838096	1.846288	1.844880
	3	1.797504	1.836478	1.823672	1.821004	1.836260	1.827008	1.833300	1.838092	1.846292	1.844874
	4	1.797502	1.836478	1.823676	1.821016	1.836258	1.826998	1.833292	1.838086	1.846286	1.844874
	5	1.797502	1.836480	1.823672	1.821018	1.836258	1.827006	1.833296	1.838094	1.846284	1.844870
	6	1.797498	1.836480	1.823676	1.821014	1.836262	1.827006	1.833298	1.838092	1.846292	1.844872
	7	1.797498	1.836476	1.823674	1.821016	1.836262	1.827004	1.833294	1.838094	1.846292	1.844880
	8	1.797502	1.836474	1.823674	1.821006	1.836258	1.827000	1.833296	1.838086	1.846286	1.844878
	9	1.797502	1.836478	1.823676	1.821014	1.836260	1.826998	1.833294	1.838090	1.846290	1.844878
	10	1.797504	1.836474	1.823670	1.821016	1.836256	1.826998	1.833294	1.838092	1.846290	1.844876
400 hrs	1			1.824002	1.821238	1.836410	1.827168	1.833444	1.838164	1.846382	1.844958
	2			1.823998	1.821232	1.836406	1.827164	1.833438	1.838166	1.846382	1.844954
	3			1.824000	1.821238	1.836414	1.827168	1.833440	1.838166	1.846384	1.844954
	4			1.824000	1.821232	1.836412	1.827164	1.833440	1.838166	1.846378	1.844952
	5			1.824002	1.821234	1.836412	1.827166	1.833442	1.838164	1.846380	1.844950
	6			1.824002	1.821236	1.836414	1.827168	1.833438	1.838164	1.846382	1.844954
	7			1.824000	1.821236	1.836412	1.827166	1.833440	1.838166	1.846380	1.844954
	8			1.824004	1.821234	1.836410	1.827168	1.833436	1.838164	1.846382	1.844956
	9			1.824002	1.821238	1.836406	1.827164	1.833440	1.838166	1.846380	1.844954
	10			1.824002	1.821234	1.836412	1.827168	1.833442	1.838168	1.846380	1.844950
600 hrs	1					1.837370	1.828080	1.834356	1.838916	1.847048	1.845472
	2					1.837370	1.828084	1.834354	1.838912	1.847046	1.845468
	3					1.837370	1.828084	1.834352	1.838910	1.847046	1.845468
	4					1.837370	1.828084	1.834354	1.838910	1.847046	1.845468
	5					1.837366	1.828080	1.834350	1.838908	1.847048	1.845464
	6					1.837366	1.828080	1.834350	1.838916	1.847048	1.845468
	7					1.837372	1.828076	1.834354	1.838910	1.847042	1.845470
	8					1.837370	1.828080	1.834354	1.838912	1.847048	1.845474
	9					1.837372	1.828078	1.834356	1.838908	1.847046	1.845472
	10					1.837372	1.828076	1.834354	1.838910	1.847044	1.845470

		Measured Weight (g)									
	Meas #	A720	A721	A722	A723	A724	A725	A726	A727	A728	A729
800 hrs	1							1.834816	1.839282	1.847404	1.845756
	2							1.834814	1.839284	1.847404	1.845754
	3							1.834818	1.839282	1.847404	1.845752
	4							1.834816	1.839286	1.847404	1.845752
	5							1.834808	1.839286	1.847406	1.845754
	6							1.834818	1.839282	1.847408	1.845756
	7							1.834818	1.839280	1.847404	1.845752
	8							1.834820	1.839284	1.847408	1.845750
	9							1.834810	1.839280	1.847408	1.845752
	10							1.834816	1.839286	1.847406	1.845752
1000 hrs	1									1.847676	1.845968
	2									1.847670	1.845964
	3									1.847672	1.845974
	4									1.847684	1.845964
	5									1.847676	1.845956
	6									1.847672	1.845970
	7									1.847680	1.845964
	8									1.847664	1.845960
	9									1.847682	1.845960
	10									1.847684	1.845968
1200 hrs	1										
	2										
	3										
	4										
	5										
	6										
	7										
	8										
	9										
	10										

Table 48: Raw Data, Expt. #5, RG-CO_2/650°C/20MPa, AFA-OC10

Project:	**SCCO2**
Grant #:	PRJ39TC
MDS:	MD24386
Expt. #:	**5**
Phase:	1 of 4
Phase Type:	Pure CO2
Temp. (°C):	650
Pressure:	2900psi
Sample ID:	**AFA-OC10**
Notes:	

Rel. Uncertainty in Meas. Mass:	Δm = ± 0.000002 g
Rel. Uncertainty in Meas. Length:	Δl = ± 0.001 mm
Rel. Uncertainty in Meas. Width:	Δw = ± 0.001 mm
Uncertainty in Meas. Area:	ΔA = ± 0.000179 cm^2

Supplier/UNS ID:	Heat # 001923
Metal Type:	Alumina-Forming Austenitic
Color Designation:	Magenta
Hole Diameter in Sample (mm):	3

		Sample # / Description									
	Meas #	**A120**	**A121**	**A122**	**A123**	**A124**	**A125**	**A126**	**A127**	**A128**	**A129**
BARE WEIGHT (gm)	**1**	1.746112	1.742236	1.783362	1.787412	1.795808	1.796040	1.793900	1.768478	1.773248	1.785582
	2	1.746112	1.742240	1.783362	1.787408	1.795808	1.796040	1.793894	1.768476	1.773244	1.785588
	3	1.746106	1.742240	1.783366	1.787410	1.795810	1.796038	1.793898	1.768472	1.773248	1.785584
	4	1.746110	1.742236	1.783362	1.787406	1.795810	1.796036	1.793894	1.768478	1.773248	1.785584
	5	1.746110	1.742234	1.783368	1.787408	1.795806	1.796036	1.793894	1.768476	1.773246	1.785584
	6	1.746110	1.742240	1.783368	1.787412	1.795810	1.796042	1.793896	1.768480	1.773248	1.785582
	7	1.746108	1.742236	1.783366	1.787406	1.795808	1.796042	1.793900	1.768476	1.773244	1.785586
	8	1.746106	1.742236	1.783364	1.787410	1.795812	1.796038	1.793894	1.768478	1.773246	1.785584
	9	1.746108	1.742238	1.783364	1.787406	1.795808	1.796042	1.793896	1.768478	1.773248	1.785582
	10	1.746108	1.742238	1.783364	1.787406	1.795806	1.796042	1.793896	1.768476	1.773248	1.785584
BARE AREA (mm2)	**1_L**	12.709	12.651	12.728	12.745	12.726	12.743	12.741	12.759	12.750	12.732
	2_L	12.710	12.667	12.740	12.749	12.733	12.743	12.740	12.756	12.746	12.731
	3_L	12.706	12.666	12.739	12.738	12.730	12.743	12.743	12.751	12.747	12.741
	4_W	12.451	12.401	12.602	12.610	12.620	12.621	12.605	12.636	12.603	12.591
	5_W	12.465	12.407	12.610	12.624	12.624	12.620	12.604	12.632	12.602	12.595
	6_W	12.475	12.413	12.613	12.624	12.622	12.616	12.601	12.622	12.602	12.590
BARE THICKNESS (mm)	**1**	1.527	1.535	1.532	1.532	1.533	1.538	1.537	1.507	1.524	1.529
	2	1.542	1.552	1.546	1.550	1.559	1.558	1.558	1.531	1.547	1.558
	3	1.542	1.553	1.543	1.549	1.557	1.555	1.554	1.529	1.545	1.555
	4	1.537	1.550	1.542	1.544	1.549	1.554	1.554	1.525	1.533	1.546
	5	1.536	1.545	1.536	1.549	1.550	1.546	1.546	1.522	1.542	1.547

Table 49: Raw Data, Expt. #5, RG-CO_2/650°C/20MPa, AFA-OC10

		Measured Weight (g)									
	Meas #	A120	A121	A122	A123	A124	A125	A126	A127	A128	A129
200 hrs	1	1.746624	1.742368	1.783854	1.787616	1.796136	1.796372	1.794408	1.768820	1.773640	1.785918
	2	1.746628	1.742374	1.783866	1.787616	1.796134	1.796372	1.794410	1.768818	1.773636	1.785908
	3	1.746628	1.742372	1.783862	1.787618	1.796136	1.796374	1.794414	1.768816	1.773638	1.785918
	4	1.746620	1.742374	1.783862	1.787618	1.796134	1.796366	1.794408	1.768812	1.773632	1.785912
	5	1.746620	1.742368	1.783862	1.787612	1.796138	1.796370	1.794406	1.768810	1.773632	1.785912
	6	1.746620	1.742370	1.783864	1.787614	1.796132	1.796368	1.794404	1.768812	1.773632	1.785914
	7	1.746624	1.742374	1.783864	1.787614	1.796132	1.796364	1.794406	1.768816	1.773634	1.785910
	8	1.746626	1.742374	1.783864	1.787616	1.796136	1.796372	1.794404	1.768812	1.773636	1.785910
	9	1.746622	1.742370	1.783862	1.787616	1.796136	1.796372	1.794404	1.768812	1.773630	1.785906
	10	1.746626	1.742374	1.783862	1.787616	1.796136	1.796370	1.794406	1.768812	1.773630	1.785906
400 hrs	1			1.784520	1.788348	1.797124	1.797042	1.795142	1.769882	1.774222	1.788708
	2			1.784512	1.788344	1.797128	1.797042	1.795138	1.769882	1.774228	1.788706
	3			1.784512	1.788344	1.797132	1.797042	1.795140	1.769882	1.774230	1.788708
	4			1.784512	1.788346	1.797126	1.797042	1.795142	1.769882	1.774224	1.788704
	5			1.784520	1.788346	1.797126	1.797040	1.795142	1.769884	1.774226	1.788708
	6			1.784516	1.788344	1.797122	1.797042	1.795144	1.769880	1.774226	1.788702
	7			1.784518	1.788342	1.797124	1.797044	1.795140	1.769878	1.774228	1.788704
	8			1.784516	1.788344	1.797128	1.797046	1.795138	1.769880	1.774224	1.788708
	9			1.784518	1.788342	1.797128	1.797048	1.795138	1.769878	1.774226	1.788706
	10			1.784518	1.788348	1.797126	1.797048	1.795144	1.769884	1.774222	1.788702
600 hrs	1					1.797698	1.797440	1.795506	1.770390	1.774602	1.789738
	2					1.797690	1.797446	1.795506	1.770396	1.774598	1.789748
	3					1.797698	1.797446	1.795504	1.770392	1.774600	1.789742
	4					1.797700	1.797450	1.795502	1.770390	1.774600	1.789740
	5					1.797704	1.797444	1.795502	1.770392	1.774606	1.789746
	6					1.797700	1.797450	1.795504	1.770386	1.774602	1.789740
	7					1.797698	1.797448	1.795506	1.770390	1.774604	1.789742
	8					1.797698	1.797446	1.795502	1.770388	1.774602	1.789738
	9					1.797700	1.797444	1.795500	1.770390	1.774600	1.789742
	10					1.797696	1.797446	1.795504	1.770388	1.774600	1.789742

		Measured Weight (g)									
	Meas #	A120	A121	A122	A123	A124	A125	A126	A127	A128	A129
800 hrs	1							1.795784	1.770776	1.774894	1.790462
	2							1.795784	1.770778	1.774890	1.790464
	3							1.795780	1.770780	1.774890	1.790464
	4							1.795784	1.770776	1.774888	1.790464
	5							1.795784	1.770772	1.774896	1.790462
	6							1.795782	1.770772	1.774886	1.790458
	7							1.795782	1.770780	1.774890	1.790460
	8							1.795784	1.770772	1.774890	1.790458
	9							1.795784	1.770776	1.774892	1.790458
	10							1.795786	1.770774	1.774890	1.790458
1000 hrs	1									1.775218	1.791086
	2									1.775214	1.791090
	3									1.775222	1.791084
	4									1.775220	1.791090
	5									1.775216	1.791088
	6									1.775224	1.791084
	7									1.775224	1.791090
	8									1.775222	1.791076
	9									1.775220	1.791084
	10									1.775224	1.791090
1200 hrs	1										
	2										
	3										
	4										
	5										
	6										
	7										
	8										
	9										
	10										

Table 50: Raw Data, Expt. #5, RG-CO_2/650°C/20MPa, IN800H

Project:	**SCCO2**
Grant #:	PRJ39TC
MDS:	MD24386
Expt. #:	**5**
Phase:	1 of 4
Phase Type:	Pure CO2
Temp. (°C):	650
Pressure:	2900psi
Sample ID:	**IN800H**
Notes:	

Rel. Uncertainty in Meas. Mass:	Δm = ± 0.000002 g
Rel. Uncertainty in Meas. Length:	Δl = ± 0.001 mm
Rel. Uncertainty in Meas. Width:	Δw = ± 0.001 mm
Uncertainty in Meas. Area:	ΔA = ± 0.000184 cm^2

Supplier/UNS ID:	NO8810
Metal Type:	Austenitic - Superalloy
Color Designation:	Brown
Hole Diameter in Sample (mm):	3

		Sample # / Description									
	Meas #	**I20**	**I21**	**I22**	**I23**	**I24**	**I25**	**I26**	**I27**	**I28**	**I29**
BARE WEIGHT (gm)	**1**	1.872210	1.883292	1.916614	1.946878	1.909606	1.941210	1.969402	1.953678	1.968812	1.960034
	2	1.872208	1.883298	1.916616	1.946876	1.909606	1.941206	1.969398	1.953682	1.968816	1.960030
	3	1.872210	1.883296	1.916616	1.946874	1.909600	1.941208	1.969396	1.953678	1.968810	1.960030
	4	1.872216	1.883296	1.916612	1.946880	1.909604	1.941208	1.969402	1.953682	1.968810	1.960034
	5	1.872212	1.883292	1.916610	1.946880	1.909602	1.941212	1.969400	1.953680	1.968810	1.960030
	6	1.872212	1.883292	1.916612	1.946874	1.909600	1.941208	1.969402	1.953676	1.968808	1.960032
	7	1.872212	1.883292	1.916612	1.946880	1.909602	1.941210	1.969402	1.953676	1.968808	1.960034
	8	1.872214	1.883296	1.916612	1.946872	1.909604	1.941206	1.969398	1.953682	1.968810	1.960036
	9	1.872214	1.883290	1.916612	1.946878	1.909602	1.941208	1.969400	1.953680	1.968810	1.960032
	10	1.872212	1.883292	1.916614	1.946878	1.909600	1.941208	1.969402	1.953680	1.968810	1.960030
BARE AREA (mm2)	**1_L**	13.297	13.304	13.341	13.416	13.242	13.404	13.380	13.411	13.405	13.395
	2_L	13.303	13.303	13.339	13.415	13.268	13.418	13.384	13.418	13.409	13.396
	3_L	13.306	13.284	13.338	13.404	13.270	13.405	13.386	13.414	13.412	13.387
	4_W	12.510	12.542	12.567	12.626	12.620	12.650	12.640	12.631	12.658	12.645
	5_W	12.507	12.525	12.559	12.626	12.627	12.648	12.640	12.630	12.650	12.645
	6_W	12.492	12.486	12.552	12.625	12.620	12.638	12.636	12.628	12.646	12.650
BARE THICKNESS (mm)	**1**	1.486	1.486	1.517	1.522	1.527	1.532	1.535	1.527	1.534	1.534
	2	1.512	1.510	1.527	1.539	1.545	1.553	1.554	1.543	1.550	1.547
	3	1.515	1.512	1.521	1.537	1.547	1.552	1.555	1.544	1.545	1.544
	4	1.512	1.504	1.527	1.533	1.532	1.546	1.546	1.540	1.547	1.543
	5	1.491	1.505	1.511	1.531	1.549	1.541	1.549	1.539	1.538	1.543

Table 51: Raw Data, Expt. #5, RG-CO_2/650^{o}C/20MPa, IN800H

		Measured Weight (g)									
	Meas #	I20	I21	I22	I23	I24	I25	I26	I27	I28	I29
200 hrs	1	1.872562	1.883750	1.916996	1.947360	1.910000	1.941646	1.969864	1.954004	1.969234	1.960364
	2	1.872566	1.883756	1.917000	1.947360	1.910002	1.941642	1.969864	1.954004	1.969230	1.960360
	3	1.87257	1.883748	1.916998	1.947360	1.910004	1.941640	1.969868	1.954002	1.969232	1.960364
	4	1.872560	1.883754	1.917000	1.947358	1.909998	1.941642	1.969864	1.954008	1.969232	1.960366
	5	1.872560	1.883754	1.917002	1.947358	1.910008	1.941646	1.969864	1.954010	1.969238	1.960368
	6	1.872564	1.883752	1.917004	1.947362	1.910002	1.941640	1.969868	1.954004	1.969234	1.960366
	7	1.872564	1.883754	1.917006	1.947364	1.910000	1.941636	1.969866	1.954006	1.969238	1.960362
	8	1.872564	1.883760	1.916998	1.947358	1.910008	1.941642	1.969868	1.954008	1.969234	1.960360
	9	1.872564	1.883758	1.916998	1.947362	1.910008	1.941640	1.969870	1.954006	1.969236	1.960360
	10	1.872564	1.883758	1.917000	1.947358	1.910008	1.941640	1.969872	1.954008	1.969236	1.960360
400 hrs	1			1.917076	1.947418	1.910082	1.941728	1.969926	1.954094	1.969298	1.960446
	2			1.917078	1.947418	1.910084	1.941732	1.969922	1.954096	1.969304	1.960450
	3			1.917072	1.947412	1.910082	1.941734	1.969920	1.954100	1.969300	1.960456
	4			1.917078	1.947418	1.910080	1.941734	1.969922	1.954098	1.969302	1.960448
	5			1.917074	1.947414	1.910084	1.941732	1.969930	1.954102	1.969294	1.960452
	6			1.917074	1.947418	1.910080	1.941732	1.969930	1.954098	1.969302	1.960454
	7			1.917080	1.947414	1.910080	1.941730	1.969926	1.954098	1.969302	1.960446
	8			1.917078	1.947418	1.910084	1.941732	1.969926	1.954100	1.969306	1.960454
	9			1.917074	1.947418	1.910086	1.941734	1.969926	1.954100	1.969300	1.960450
	10			1.917076	1.947418	1.910088	1.941732	1.969924	1.954100	1.969300	1.960452
600 hrs	1					1.910128	1.941778	1.969954	1.954150	1.969334	1.960486
	2					1.910132	1.941780	1.969956	1.954150	1.969326	1.960494
	3					1.910128	1.941784	1.969958	1.954160	1.969330	1.960492
	4					1.910120	1.941788	1.969954	1.954150	1.969326	1.960486
	5					1.910128	1.941786	1.969962	1.954154	1.969326	1.960486
	6					1.910130	1.941790	1.969956	1.954150	1.969328	1.960486
	7					1.910128	1.941786	1.969964	1.954148	1.969326	1.960486
	8					1.910128	1.941790	1.969954	1.954146	1.969326	1.960490
	9					1.910124	1.941788	1.969964	1.954146	1.969326	1.960492
	10					1.910122	1.941780	1.969962	1.954154	1.969332	1.960486

		Measured Weight (g)									
	Meas #	I20	I21	I22	I23	I24	I25	I26	I27	I28	I29
800 hrs	1							1.970002	1.954198	1.969360	1.960514
	2							1.970000	1.954194	1.969360	1.960528
	3							1.969998	1.954198	1.969362	1.960528
	4							1.969996	1.954192	1.969370	1.960526
	5							1.969996	1.954196	1.969358	1.960512
	6							1.970000	1.954194	1.969360	1.960524
	7							1.969998	1.954192	1.969362	1.960512
	8							1.969998	1.954188	1.969368	1.960518
	9							1.970000	1.954188	1.969362	1.960522
	10							1.970004	1.954190	1.969358	1.960524
1000 hrs	1									1.969388	1.960548
	2									1.969386	1.960548
	3									1.969386	1.960560
	4									1.969396	1.960564
	5									1.969396	1.960552
	6									1.969392	1.960566
	7									1.969394	1.960556
	8									1.969388	1.960550
	9									1.969390	1.960554
	10									1.969388	1.960552
1200 hrs	1										
	2										
	3										
	4										
	5										
	6										
	7										
	8										
	9										
	10										

Table 52: Raw Data, Expt. #6, IG-CO_2/550^{o}C/20MPa, Coupon Arrangement

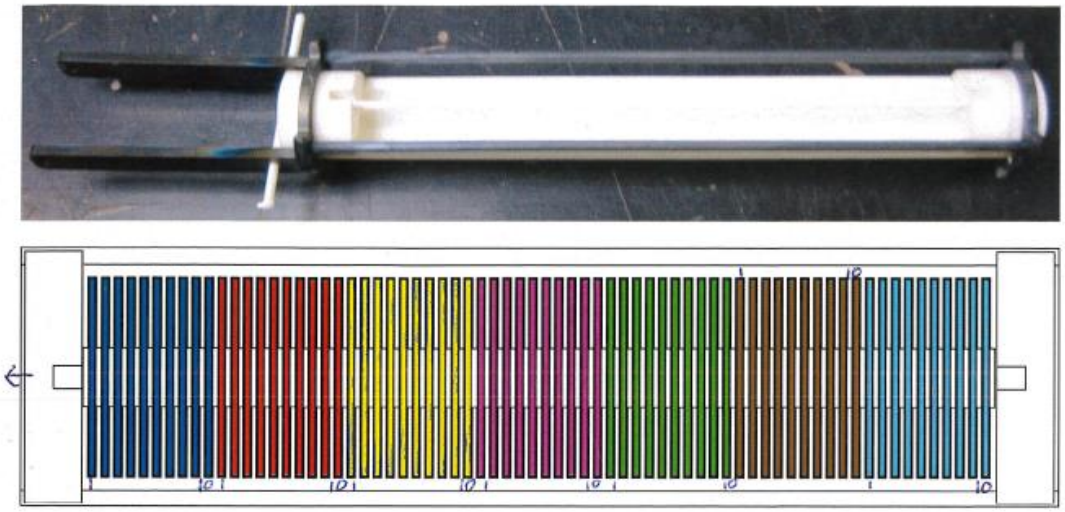

Sample	Blue HCM12A	Red NF616	Yellow 347SS	Magenta AFA-OC6	Green AFA-OC7	Brown AFA-OC10	Cyan IN800H	Orange 316/316L
1	H27	N26	S36	A636	A730	A140	I30	
2	H28	N27	S37	A637	A731	A141	I40	
3	H29	N28	S38	A638	A732	A142	I32	
4	H30	N29	S39	A639	A733	A143	I33	
5	H31	N30	S40	A640	A734	A144	I34	L1
6			S41	A641	A735	A145	I35	L2
7			S42	A642	A736	A146	I36	L3
8			S43	A643	A737	A147	I37	L4
9			S44	A644	A738	A148	I38	L5
10			S45	A645	A739	A149	I39	L6

Table 53: Raw Data, Expt. #6, IG-CO_2/550^{o}C/20MPa, HCM12A

Project:	**SCCO2**
Grant #:	PRJ39TC
MDS:	MD24386
Expt. #:	**6**
Phase:	2
Phase Type:	Industrial CO2
Temp. (^{o}C):	550
Pressure:	2900psi
Sample ID:	**HCM12A**
Notes:	

Rel. Uncertainty in Meas. Mass:	$\Delta m = \pm 0.000002$ g
Rel. Uncertainty in Meas. Length:	$\Delta l = \pm 0.001$ mm
Rel. Uncertainty in Meas. Width:	$\Delta w = \pm 0.001$ mm
Uncertainty in Meas. Area:	$\Delta A = \pm 0.000179$ cm^2

Supplier/UNS ID:	K91271
Metal Type:	Ferritic-Martensitic
Color Designation:	Blue
Hole Diameter in Sample (mm):	3

		Sample # / Description									
	Meas #	**H27**	**H28**	**H29**	**H30**	**H31**	**H32**	**H33**	**H34**	**H35**	**H36**
BARE WEIGHT (gm)	**1**	1.814370	1.831666	1.784466	1.794466	1.804712	1.824782	1.845344	1.791018	1.792564	1.810910
	2	1.814380	1.831672	1.784468	1.794468	1.804708	1.824784	1.845352	1.791022	1.792562	1.810908
	3	1.814382	1.831666	1.784468	1.794468	1.804714	1.824786	1.845352	1.791020	1.792556	1.810916
	4	1.814380	1.831670	1.784462	1.794462	1.804714	1.824786	1.845350	1.791020	1.792564	1.810910
	5	1.814374	1.831670	1.784468	1.794468	1.804716	1.824784	1.845350	1.791020	1.792562	1.810900
	6	1.814376	1.831666	1.784468	1.794468	1.804714	1.824778	1.845346	1.791020	1.792562	1.810908
	7	1.814380	1.831666	1.784462	1.794462	1.804714	1.824786	1.845350	1.791022	1.792554	1.810910
	8	1.814380	1.831672	1.784462	1.794462	1.804714	1.824786	1.845348	1.791022	1.792558	1.810906
	9	1.814382	1.831666	1.784460	1.794460	1.804708	1.824786	1.845350	1.791024	1.792556	1.810914
	10	1.814380	1.831670	1.784464	1.794464	1.804712	1.824784	1.845352	1.791016	1.792560	1.810906
BARE AREA (mm2)	**1_L**	12.716	12.703	12.690	12.703	12.699	12.671	12.686	12.626	12.699	12.710
	2_L	12.716	12.700	12.691	12.699	12.701	12.691	12.691	12.679	12.717	12.712
	3_L	12.717	12.686	12.689	12.686	12.685	12.694	12.685	12.699	12.719	12.710
	4_W	12.671	12.627	12.689	12.613	12.511	12.582	12.652	12.598	12.644	12.641
	5_W	12.669	12.642	12.689	12.633	12.598	12.590	12.678	12.609	12.647	12.644
	6_W	12.669	12.648	12.689	12.626	12.626	12.593	12.689	12.610	12.622	12.641
BARE THICKNESS (mm)	**1**	1.509	1.521	1.495	1.509	1.542	1.528	1.549	1.504	1.509	1.531
	2	1.530	1.545	1.496	1.523	1.542	1.540	1.556	1.524	1.510	1.534
	3	1.529	1.547	1.479	1.523	1.515	1.536	1.547	1.524	1.495	1.513
	4	1.492	1.541	1.469	1.482	1.511	1.533	1.550	1.531	1.505	1.529
	5	1.537	1.532	1.495	1.539	1.545	1.531	1.548	1.503	1.503	1.513

Table 54: Raw Data, Expt. #6, IG-CO_2/550^{o}C/20MPa, HCM12A

		Measured Weight (g)									
	Meas #	H27	H28	H29	H30	H31	H32	H33	H34	H35	H36
200 hrs	1	1.817462	1.833632	1.786324	1.796600	1.806386					
	2	1.817460	1.833624	1.786322	1.796600	1.806386					
	3	1.817458	1.833634	1.786334	1.796596	1.806392					
	4	1.817468	1.833628	1.786330	1.796592	1.806386					
	5	1.817468	1.833638	1.786336	1.796600	1.806394					
	6	1.817460	1.833632	1.786332	1.796600	1.806388					
	7	1.817468	1.833636	1.786340	1.796594	1.806386					
	8	1.817458	1.833638	1.786328	1.796598	1.806384					
	9	1.817468	1.833622	1.786332	1.796604	1.806386					
	10	1.817458	1.833632	1.786328	1.796596	1.806390					
400 hrs	1			1.787542	1.797732	1.807274					
	2			1.787550	1.797740	1.807264					
	3			1.787542	1.797734	1.807260					
	4			1.787548	1.797736	1.807272					
	5			1.787542	1.797742	1.807270					
	6			1.787544	1.797736	1.807272					
	7			1.787540	1.797738	1.807274					
	8			1.787542	1.797730	1.807270					
	9			1.787540	1.797728	1.807268					
	10			1.787538	1.797740	1.807276					
600 hrs	1										
	2										
	3										
	4										
	5										
	6										
	7										
	8										
	9										
	10										

		Measured Weight (g)									
	Meas #	H27	H28	H29	H30	H31	H32	H33	H34	H35	H36
800 hrs	1										
	2										
	3										
	4										
	5										
	6										
	7										
	8										
	9										
	10										
1000 hrs	1										
	2										
	3										
	4										
	5										
	6										
	7										
	8										
	9										
	10										
1200 hrs	1										
	2										
	3										
	4										
	5										
	6										
	7										
	8										
	9										
	10										

Table 55: Raw Data, Expt. #6, IG-CO_2/550°C/20MPa, NF616

Project:	**SCCO2**
Grant #:	PRJ39TC
MDS:	MD24386
Expt. #:	**6**
Phase:	2
Phase Type:	Industrial CO2
Temp. (°C):	550
Pressure:	2900psi
Sample ID:	**NF616**
Notes:	

Rel. Uncertainty in Meas. Mass:	Δm = ± 0.000002 g
Rel. Uncertainty in Meas. Length:	Δl = ± 0.001 mm
Rel. Uncertainty in Meas. Width:	Δw = ± 0.001 mm
Uncertainty in Meas. Area:	ΔA = ± 0.000178 cm^2

Supplier/UNS ID:	K91271
Metal Type:	Ferritic-Martensitic
Color Designation:	Red
Hole Diameter in Sample (mm):	3

		Sample # / Description									
	Meas #	**N26**	**N27**	**N28**	**N29**	**N30**	**N31**	**N32**	**N33**	**N34**	**N35**
BARE WEIGHT (gm)	**1**	1.764516	1.811328	1.776658	1.780604	1.803764	1.805914	1.811454	1.804234	1.775890	1.800982
	2	1.764522	1.811340	1.776662	1.780608	1.803766	1.805908	1.811452	1.804242	1.775898	1.800984
	3	1.764522	1.811328	1.776660	1.780606	1.803766	1.805908	1.811454	1.804242	1.775894	1.800982
	4	1.764524	1.811338	1.776660	1.780604	1.803762	1.805912	1.811454	1.804242	1.775894	1.800984
	5	1.764516	1.811338	1.776654	1.780604	1.803764	1.805910	1.811452	1.804242	1.775892	1.800982
	6	1.764528	1.811334	1.776656	1.780600	1.803772	1.805912	1.811458	1.804236	1.775902	1.800984
	7	1.764522	1.811340	1.776652	1.780604	1.803768	1.805912	1.811450	1.804238	1.775896	1.800986
	8	1.764520	1.811340	1.776660	1.780608	1.803764	1.805916	1.811450	1.804240	1.775896	1.800982
	9	1.764516	1.811336	1.776652	1.780606	1.803768	1.805920	1.811458	1.804240	1.775896	1.800986
	10	1.764520	1.811332	1.776660	1.780604	1.803766	1.805920	1.811450	1.804244	1.775902	1.800984
BARE AREA (mm2)	**1_L**	12.568	12.600	12.656	12.635	12.558	12.612	12.638	12.592	12.617	12.621
	2_L	12.572	12.620	12.643	12.636	12.596	12.590	12.634	12.591	12.611	12.627
	3_L	12.576	12.629	12.621	12.627	12.609	12.549	12.606	12.586	12.604	12.606
	4_W	12.541	12.592	12.364	12.457	12.579	12.583	12.545	12.568	12.383	12.551
	5_W	12.530	12.586	12.369	12.451	12.587	12.581	12.549	12.576	12.425	12.554
	6_W	12.537	12.573	12.371	12.447	12.577	12.575	12.548	12.580	12.444	12.563
BARE THICKNESS (mm)	**1**	1.560	1.578	1.576	1.578	1.579	1.585	1.587	1.574	1.586	1.586
	2	1.564	1.581	1.585	1.581	1.581	1.585	1.587	1.576	1.585	1.587
	3	1.563	1.579	1.584	1.578	1.582	1.587	1.587	1.576	1.584	1.586
	4	1.565	1.582	1.585	1.581	1.582	1.587	1.590	1.576	1.587	1.586
	5	1.546	1.568	1.579	1.571	1.577	1.582	1.581	1.573	1.577	1.578

Table 56: Raw Data, Expt. #6, IG-CO_2/550^{o}C/20MPa, NF616

		Measured Weight (g)									
	Meas #	N26	N27	N28	N29	N30	N31	N32	N33	N34	N35
200 hrs	1	1.778082	1.824550	1.789782	1.792870	1.817232					
	2	1.778090	1.824550	1.789768	1.792890	1.817240					
	3	1.778088	1.824542	1.789770	1.792882	1.817238					
	4	1.778090	1.824538	1.789774	1.792886	1.817224					
	5	1.778086	1.824536	1.789760	1.792894	1.817230					
	6	1.778084	1.824542	1.789784	1.792890	1.817228					
	7	1.778084	1.824534	1.789762	1.792886	1.817230					
	8	1.778090	1.824544	1.789756	1.792880	1.817230					
	9	1.778090	1.824534	1.789772	1.792870	1.817226					
	10	1.778092	1.824542	1.789770	1.792880	1.817226					
400 hrs	1										
	2										
	3										
	4										
	5										
	6										
	7										
	8										
	9										
	10										
600 hrs	1										
	2										
	3										
	4										
	5										
	6										
	7										
	8										
	9										
	10										

		Measured Weight (g)									
	Meas #	N26	N27	N28	N29	N30	N31	N32	N33	N34	N35
800 hrs	1										
	2										
	3										
	4										
	5										
	6										
	7										
	8										
	9										
	10										
1000 hrs	1										
	2										
	3										
	4										
	5										
	6										
	7										
	8										
	9										
	10										
1200 hrs	1										
	2										
	3										
	4										
	5										
	6										
	7										
	8										
	9										
	10										

Table 57: Raw Data, Expt. #6, IG-CO_2/550°C/20MPa, 347SS

Project:	**SCCO2**
Grant #:	PRJ39TC
MDS:	MD24386
Expt. #:	**6**
Phase:	2
Phase Type:	Industrial CO2
Temp. (°C):	550
Pressure:	2900psi
Sample ID:	**347SS**
Notes:	

Rel. Uncertainty in Meas. Mass:	Δm = ± 0.000002 g
Rel. Uncertainty in Meas. Length:	Δl = ± 0.001 mm
Rel. Uncertainty in Meas. Width:	Δw = ± 0.001 mm
Uncertainty in Meas. Area:	ΔA = ± 0.000182 cm^2

Supplier/UNS ID:	
Metal Type:	Austenitic
Color Designation:	Yellow
Hole Diameter in Sample (mm):	3

		Sample # / Description									
	Meas #	**S36**	**S37**	**S38**	**S39**	**S40**	**S41**	**S42**	**S43**	**S44**	**S45**
BARE WEIGHT (gm)	**1**	1.885434	1.885916	1.904196	1.891536	1.914592	1.902000	1.905980	1.898732	1.906838	1.906052
	2	1.885448	1.885920	1.904198	1.891538	1.914586	1.902000	1.905970	1.898738	1.906830	1.906046
	3	1.885444	1.885928	1.904192	1.891536	1.914586	1.902012	1.905972	1.898728	1.906838	1.906054
	4	1.885436	1.885920	1.904192	1.891542	1.914594	1.902008	1.905968	1.898732	1.906834	1.906054
	5	1.885448	1.885924	1.904204	1.891536	1.914590	1.902010	1.905982	1.898734	1.906840	1.906050
	6	1.885436	1.885922	1.904202	1.891528	1.914588	1.902008	1.905976	1.898730	1.906836	1.906048
	7	1.885438	1.885926	1.904198	1.891540	1.914590	1.902006	1.905978	1.898732	1.906828	1.906060
	8	1.885438	1.885918	1.904204	1.891538	1.914588	1.902014	1.905976	1.898742	1.906830	1.906062
	9	1.885434	1.885916	1.904202	1.891532	1.914592	1.902010	1.905972	1.898728	1.906834	1.906050
	10	1.885444	1.885918	1.904198	1.891540	1.914586	1.902014	1.905978	1.898738	1.906832	1.906056
BARE AREA (mm2)	**1_L**	13.110	13.114	13.139	13.011	13.152	13.098	13.160	13.076	13.128	13.122
	2_L	13.128	13.107	13.141	13.009	13.147	13.108	13.152	13.074	13.120	13.116
	3_L	13.130	13.097	13.129	12.992	13.131	13.120	13.124	13.064	13.088	13.092
	4_W	12.616	12.600	12.617	12.618	12.640	12.600	12.613	12.624	12.648	12.631
	5_W	12.624	12.598	12.617	12.623	12.628	12.612	12.612	12.610	12.643	12.623
	6_W	12.625	12.579	12.620	12.623	12.615	12.614	12.595	12.593	12.620	12.612
BARE THICKNESS (mm)	**1**	1.562	1.564	1.572	1.575	1.572	1.573	1.570	1.572	1.574	1.573
	2	1.560	1.562	1.573	1.576	1.576	1.573	1.572	1.575	1.577	1.573
	3	1.529	1.531	1.538	1.551	1.549	1.556	1.552	1.561	1.558	1.559
	4	1.541	1.560	1.559	1.569	1.566	1.566	1.567	1.569	1.573	1.567
	5	1.552	1.548	1.567	1.567	1.570	1.566	1.564	1.570	1.562	1.571

Table 58: Raw Data, Expt. #6, IG-CO_2/550^{o}C/20MPa, 347SS

		Measured Weight (g)									
	Meas #	S36	S37	S38	S39	S40	S41	S42	S43	S44	S45
200 hrs	1	1.885542	1.885988	1.904378	1.891618	1.914662	1.902116	1.906060	1.898886	1.906900	1.906124
	2	1.885534	1.885982	1.904374	1.891614	1.914656	1.902126	1.906058	1.898882	1.906902	1.906122
	3	1.885526	1.885990	1.904382	1.891616	1.914650	1.902116	1.906056	1.898870	1.906910	1.906110
	4	1.885536	1.885990	1.904376	1.891616	1.914662	1.902118	1.906050	1.898880	1.906910	1.906116
	5	1.885536	1.885986	1.904374	1.891618	1.914662	1.902110	1.906060	1.898880	1.906910	1.906120
	6	1.885530	1.885982	1.904376	1.891616	1.914652	1.902128	1.906046	1.898888	1.906910	1.906118
	7	1.885536	1.885980	1.904374	1.891618	1.914650	1.902116	1.906060	1.898882	1.906908	1.906114
	8	1.885540	1.885988	1.904374	1.891622	1.914664	1.902116	1.906062	1.898872	1.906902	1.906120
	9	1.885526	1.885990	1.904374	1.891616	1.914658	1.902126	1.906068	1.898886	1.906902	1.906118
	10	1.885534	1.885988	1.904370	1.891614	1.914650	1.902114	1.906050	1.898880	1.906902	1.906116
400 hrs	1			1.904406	1.891638	1.914670	1.902126	1.906074	1.898916	1.906920	1.906140
	2			1.904404	1.891634	1.914666	1.902128	1.906066	1.898916	1.906920	1.906140
	3			1.904414	1.891632	1.914664	1.902126	1.906080	1.898914	1.906926	1.906132
	4			1.904400	1.891634	1.914666	1.902118	1.906072	1.898914	1.906924	1.906130
	5			1.904398	1.891634	1.914664	1.902122	1.906074	1.898920	1.906918	1.906142
	6			1.904412	1.891626	1.914670	1.902118	1.906074	1.898920	1.906918	1.906140
	7			1.904412	1.891628	1.914672	1.902126	1.906070	1.898922	1.906922	1.906136
	8			1.904398	1.891636	1.914662	1.902126	1.906082	1.898918	1.906920	1.906140
	9			1.904408	1.891630	1.914670	1.902122	1.906080	1.898918	1.906922	1.906144
	10			1.904402	1.891632	1.914668	1.902120	1.906070	1.898906	1.906926	1.906134
600 hrs	1					1.914674	1.902142	1.906092	1.898930	1.906924	1.906150
	2					1.914682	1.902144	1.906086	1.898928	1.906932	1.906152
	3					1.914684	1.902138	1.906096	1.898932	1.906934	1.906154
	4					1.914680	1.902136	1.906086	1.898928	1.906932	1.906154
	5					1.914680	1.902134	1.906080	1.898938	1.906928	1.906152
	6					1.914680	1.902132	1.906086	1.898940	1.906930	1.906146
	7					1.914676	1.902138	1.906082	1.898932	1.906928	1.906154
	8					1.914684	1.902134	1.906094	1.898940	1.906928	1.906152
	9					1.914678	1.902136	1.906088	1.898934	1.906928	1.906154
	10					1.914678	1.902138	1.906088	1.898934	1.906926	1.906152

		Measured Weight (g)									
	Meas #	S36	S37	S38	S39	S40	S41	S42	S43	S44	S45
800 hrs	1							1.906106	1.898970	1.906942	1.906184
	2							1.906116	1.898970	1.906946	1.906170
	3							1.906102	1.898972	1.906950	1.906176
	4							1.906110	1.898982	1.906942	1.906168
	5							1.906116	1.898972	1.906944	1.906170
	6							1.906114	1.898982	1.906940	1.906186
	7							1.906114	1.898972	1.906948	1.906180
	8							1.906112	1.898966	1.906942	1.906168
	9							1.906102	1.898978	1.906952	1.906172
	10							1.906110	1.898964	1.906952	1.906164
1000 hrs	1									1.906958	1.906166
	2									1.906956	1.906182
	3									1.906950	1.906174
	4									1.906950	1.906180
	5									1.906960	1.906172
	6									1.906974	1.906168
	7									1.906964	1.906176
	8									1.906958	1.906170
	9									1.906960	1.906174
	10									1.906954	1.906182
1200 hrs	1										
	2										
	3										
	4										
	5										
	6										
	7										
	8										
	9										
	10										

Table 59: Raw Data, Expt. #6, IG-CO_2/550°C/20MPa, AFA-OC6

Project:	**SCCO2**
Grant #:	PRJ39TC
MDS:	MD24386
Expt. #:	**6**
Phase:	2
Phase Type:	Industrial CO2
Temp. (°C):	550
Pressure:	2900psi
Sample ID:	**AFA-OC6**

Rel. Uncertainty in Meas. Mass:	Δm = ± 0.000002 g
Rel. Uncertainty in Meas. Length:	Δl = ± 0.001 mm
Rel. Uncertainty in Meas. Width:	Δw = ± 0.001 mm
Uncertainty in Meas. Area:	ΔA = ± 0.00018 cm^2
Supplier/UNS ID:	
Metal Type:	Alumina Forming Austenitic
Color Designation:	Magenta
Hole Diameter in Sample (mm):	3

Notes: AFA = Alumina Forming Austenitic provided by Oakridge National Laboratory

		Sample # / Description									
	Meas #	**A636**	**A637**	**A638**	**A639**	**A640**	**A641**	**A642**	**A643**	**A644**	**A645**
BARE WEIGHT (gm)	**1**	1.795814	1.810142	1.805446	1.809784	1.816454	1.812938	1.817558	1.820638	1.830004	1.797296
	2	1.795816	1.810154	1.805452	1.809792	1.816454	1.812934	1.817564	1.820640	1.830006	1.797302
	3	1.795820	1.810150	1.805448	1.809786	1.816454	1.812936	1.817554	1.820634	1.830010	1.797296
	4	1.795810	1.810150	1.805452	1.809790	1.816450	1.812938	1.817560	1.820638	1.830014	1.797292
	5	1.795816	1.810150	1.805450	1.809784	1.816448	1.812938	1.817558	1.820640	1.830004	1.797300
	6	1.795820	1.810146	1.805446	1.809786	1.816448	1.812942	1.817560	1.820634	1.830010	1.797298
	7	1.795818	1.810144	1.805448	1.809788	1.816452	1.812934	1.817556	1.820634	1.830006	1.797294
	8	1.795814	1.810146	1.805452	1.809780	1.816444	1.812936	1.817560	1.820638	1.830010	1.797296
	9	1.795814	1.810144	1.805448	1.809780	1.816446	1.812936	1.817562	1.820634	1.830010	1.797302
	10	1.795814	1.810148	1.805450	1.809782	1.816448	1.812932	1.817564	1.820628	1.830014	1.797296
BARE AREA (mm2)	**1_L**	12.870	12.883	12.859	12.881	12.931	12.926	12.940	12.896	12.912	12.927
	2_L	12.900	12.905	12.858	12.846	12.950	12.913	12.938	12.917	12.945	12.921
	3_L	12.905	12.905	12.845	12.787	12.904	12.878	12.911	12.918	12.959	12.899
	4_W	12.550	12.619	12.625	12.642	12.636	12.615	12.612	12.630	12.653	12.619
	5_W	12.558	12.617	12.631	12.672	12.636	12.611	12.606	12.625	12.652	12.628
	6_W	12.553	12.597	12.629	12.677	12.591	12.591	12.606	12.615	12.652	12.627
BARE THICKNESS (mm)	**1**	1.585	1.583	1.589	1.580	1.584	1.590	1.583	1.584	1.584	1.574
	2	1.586	1.593	1.593	1.592	1.592	1.591	1.586	1.588	1.591	1.577
	3	1.556	1.570	1.556	1.571	1.559	1.565	1.558	1.560	1.553	1.529
	4	1.576	1.586	1.581	1.577	1.579	1.577	1.577	1.576	1.573	1.559
	5	1.578	1.584	1.581	1.585	1.578	1.586	1.577	1.575	1.576	1.546

Table 60: Raw Data, Expt. #6, IG-CO_2/550^{o}C/20MPa, AFA-OC6

		Measured Weight (g)									
	Meas #	A636	A637	A638	A639	A640	A641	A642	A643	A644	A645
200 hrs	1	1.79593	1.810372	1.805630	1.809858	1.816594	1.813118	1.817598	1.820768	1.830140	1.797502
	2	1.795920	1.810378	1.805632	1.809870	1.816592	1.813122	1.817590	1.820770	1.830132	1.797496
	3	1.795926	1.810370	1.805634	1.809870	1.816596	1.813126	1.817592	1.820774	1.830148	1.797496
	4	1.795918	1.810374	1.805630	1.809866	1.816594	1.813126	1.817596	1.820774	1.830132	1.797490
	5	1.795932	1.810370	1.805630	1.809872	1.816598	1.813120	1.817584	1.820774	1.830134	1.797492
	6	1.795926	1.810380	1.805634	1.809858	1.816602	1.813126	1.817598	1.820770	1.830148	1.797504
	7	1.795930	1.810364	1.805624	1.809874	1.816600	1.813128	1.817588	1.820768	1.830138	1.797494
	8	1.795920	1.810376	1.805634	1.809862	1.816608	1.813132	1.817592	1.820774	1.830146	1.797500
	9	1.795928	1.810380	1.805628	1.809874	1.816608	1.813128	1.817592	1.820774	1.830136	1.797506
	10	1.795924	1.810364	1.805634	1.809876	1.816596	1.813118	1.817586	1.820764	1.830130	1.797502
400 hrs	1			1.805684	1.809882	1.816628	1.813138	1.817614	1.820794	1.830158	1.797508
	2			1.805680	1.809882	1.816624	1.813140	1.817606	1.820788	1.830152	1.797510
	3			1.805670	1.809880	1.816622	1.813146	1.817616	1.820784	1.830156	1.797508
	4			1.805684	1.809884	1.816622	1.813148	1.817618	1.820780	1.830146	1.797510
	5			1.805684	1.809884	1.816634	1.813152	1.817610	1.820784	1.830154	1.797506
	6			1.805678	1.809874	1.816622	1.813146	1.817608	1.820788	1.830150	1.797502
	7			1.805670	1.809874	1.816628	1.813144	1.817606	1.820784	1.830146	1.797504
	8			1.805678	1.809884	1.816624	1.813150	1.817606	1.820794	1.830150	1.797508
	9			1.805678	1.809882	1.816620	1.813144	1.817614	1.820786	1.830154	1.797502
	10			1.805670	1.809870	1.816620	1.813152	1.817606	1.820784	1.830156	1.797510
600 hrs	1					1.816616	1.813154	1.817594	1.820798	1.830158	1.797520
	2					1.816610	1.813150	1.817600	1.820798	1.830156	1.797522
	3					1.816614	1.813150	1.817594	1.820796	1.830154	1.797528
	4					1.816610	1.813144	1.817594	1.820790	1.830154	1.797526
	5					1.816620	1.813150	1.817598	1.820792	1.830152	1.797526
	6					1.816612	1.813148	1.817590	1.820788	1.830152	1.797532
	7					1.816608	1.813154	1.817592	1.820802	1.830150	1.797534
	8					1.816618	1.813152	1.817602	1.820790	1.830160	1.797522
	9					1.816614	1.813152	1.817596	1.820790	1.830152	1.797530
	10					1.816616	1.813148	1.817600	1.820788	1.830158	1.797526

		Measured Weight (g)									
	Meas #	A636	A637	A638	A639	A640	A641	A642	A643	A644	A645
800 hrs	1							1.817608	1.820810	1.830168	1.797536
	2							1.817606	1.820806	1.830170	1.797558
	3							1.817620	1.820810	1.830168	1.797558
	4							1.817612	1.820808	1.830160	1.797552
	5							1.817610	1.820810	1.830158	1.797542
	6							1.817604	1.820818	1.830176	1.797560
	7							1.817604	1.820814	1.830164	1.797540
	8							1.817614	1.820814	1.830160	1.797556
	9							1.817604	1.820810	1.830164	1.797542
	10							1.817612	1.820810	1.830172	1.797558
1000 hrs	1								1.820820	1.830162	
	2								1.820822	1.830168	
	3								1.820806	1.830174	
	4								1.820806	1.830164	
	5								1.820816	1.830166	
	6								1.820820	1.830170	
	7								1.820806	1.830168	
	8								1.820806	1.830162	
	9								1.820810	1.830170	
	10								1.820812	1.830164	
1200 hrs	1										
	2										
	3										
	4										
	5										
	6										
	7										
	8										
	9										
	10										

Table 61: Raw Data, Expt. #6, IG-CO_2/550°C/20MPa, AFA-OC7

Project:	**SCCO2**
Grant #:	PRJ39TC
MDS:	MD24386
Expt. #:	**6**
Phase:	2
Phase Type:	Industrial CO2
Temp. (°C):	550
Pressure:	2900psi
Sample ID:	**AFA-OC7**
Notes:	

Rel. Uncertainty in Meas. Mass:	Δm = ± 0.000002 g
Rel. Uncertainty in Meas. Length:	Δl = ± 0.001 mm
Rel. Uncertainty in Meas. Width:	Δw = ± 0.001 mm
Uncertainty in Meas. Area:	ΔA = ± 0.00018 cm^2

Supplier/UNS ID:	
Metal Type:	Alumina Forming Austenitic
Color Designation:	Green
Hole Diameter in Sample (mm):	3

		Sample # / Description									
	Meas #	**A730**	**A731**	**A732**	**A733**	**A734**	**A735**	**A736**	**A737**	**A738**	**A739**
BARE WEIGHT (gm)	**1**	1.734642	1.777750	1.778046	1.760834	1.795342	1.762408	1.788922	1.823470	1.825202	1.842104
	2	1.734640	1.777748	1.778052	1.760834	1.795346	1.762408	1.788916	1.823468	1.825204	1.842100
	3	1.734644	1.777758	1.778044	1.760826	1.795338	1.762412	1.788924	1.823470	1.825210	1.842102
	4	1.734636	1.777746	1.778052	1.760828	1.795336	1.762408	1.788912	1.823470	1.825212	1.842110
	5	1.734642	1.777750	1.778044	1.760836	1.795342	1.762404	1.788910	1.823468	1.825208	1.842110
	6	1.734644	1.777754	1.778044	1.760832	1.795338	1.762410	1.788922	1.823466	1.825212	1.842112
	7	1.734646	1.777750	1.778046	1.760826	1.795340	1.762408	1.788918	1.823468	1.825200	1.842110
	8	1.734646	1.777752	1.778048	1.760830	1.795340	1.762406	1.788916	1.823472	1.825204	1.842104
	9	1.734642	1.777750	1.778044	1.760832	1.795336	1.762410	1.788914	1.823470	1.825204	1.842102
	10	1.734640	1.777754	1.778042	1.760828	1.795336	1.762406	1.788918	1.823460	1.825202	1.842112
BARE AREA (mm2)	**1_L**	12.809	12.811	12.763	12.765	12.802	12.799	12.835	12.814	12.825	12.866
	2_L	12.830	12.823	12.768	12.756	12.849	12.803	12.849	12.830	12.832	12.873
	3_L	12.832	12.824	12.768	12.737	12.850	12.791	12.850	12.824	12.829	12.875
	4_W	12.624	12.553	12.606	12.547	12.593	12.662	12.593	12.661	12.675	12.649
	5_W	12.633	12.610	12.617	12.569	12.629	12.657	12.629	12.657	12.671	12.658
	6_W	12.634	12.615	12.609	12.574	12.640	12.629	12.640	12.652	12.656	12.656
BARE THICKNESS (mm)	**1**	1.505	1.546	1.544	1.544	1.549	1.535	1.553	1.573	1.572	1.580
	2	1.501	1.549	1.544	1.545	1.551	1.534	1.552	1.572	1.570	1.579
	3	1.474	1.525	1.521	1.512	1.517	1.488	1.529	1.540	1.549	1.554
	4	1.501	1.535	1.536	1.519	1.540	1.529	1.549	1.564	1.561	1.564
	5	1.481	1.537	1.535	1.536	1.539	1.517	1.541	1.558	1.559	1.572

Table 62: Raw Data, Expt. #6, IG-CO_2/550^{o}C/20MPa, AFA-OC7

		Measured Weight (g)									
	Meas #	A730	A731	A732	A733	A734	A735	A736	A737	A738	A739
200 hrs	1	1.734778	1.777910	1.778160	1.760968	1.795466	1.762590	1.789080	1.823594	1.825312	1.842272
	2	1.734788	1.777910	1.778162	1.760970	1.795458	1.762590	1.789086	1.823596	1.825326	1.842276
	3	1.734786	1.777908	1.778158	1.760976	1.795470	1.762592	1.789086	1.823596	1.825328	1.842276
	4	1.734778	1.777908	1.778142	1.760964	1.795456	1.762590	1.789070	1.823600	1.825322	1.842274
	5	1.734772	1.777922	1.778162	1.760974	1.795464	1.762594	1.789086	1.823592	1.825324	1.842276
	6	1.734778	1.777912	1.778142	1.760978	1.795460	1.762596	1.789084	1.823592	1.825322	1.842274
	7	1.734786	1.777910	1.778150	1.760966	1.795468	1.762592	1.789084	1.823602	1.825314	1.842272
	8	1.734776	1.777914	1.778146	1.760972	1.795456	1.762588	1.789078	1.823588	1.825320	1.842278
	9	1.734776	1.777918	1.778142	1.760966	1.795468	1.762590	1.789072	1.823590	1.825320	1.842270
	10	1.734772	1.777916	1.778142	1.760968	1.795462	1.762590	1.789086	1.823598	1.825318	1.842274
400 hrs	1			1.778166	1.760982	1.795480	1.762604	1.789064	1.823608	1.825324	1.842298
	2			1.778162	1.760984	1.795478	1.762600	1.789058	1.823610	1.825318	1.842296
	3			1.778170	1.760984	1.795478	1.762596	1.789058	1.823610	1.825318	1.842300
	4			1.778168	1.760984	1.795480	1.762600	1.789058	1.823608	1.825324	1.842294
	5			1.778168	1.760978	1.795478	1.762600	1.789058	1.823610	1.825324	1.842306
	6			1.778168	1.760978	1.795476	1.762598	1.789064	1.823608	1.825312	1.842302
	7			1.778170	1.760976	1.795484	1.762600	1.789066	1.823614	1.825320	1.842296
	8			1.778168	1.760976	1.795478	1.762602	1.789056	1.823612	1.825312	1.842304
	9			1.778160	1.760984	1.795478	1.762602	1.789062	1.823608	1.825320	1.842302
	10			1.778168	1.760976	1.795482	1.762602	1.789060	1.823604	1.825316	1.842300
600 hrs	1					1.795492	1.762588	1.789060	1.823612	1.825306	1.842300
	2					1.795494	1.762592	1.789064	1.823614	1.825302	1.842294
	3					1.795482	1.762588	1.789070	1.823618	1.825310	1.842292
	4					1.795486	1.762590	1.789064	1.823614	1.825310	1.842300
	5					1.795496	1.762590	1.789070	1.823614	1.825304	1.842292
	6					1.795484	1.762592	1.789064	1.823620	1.825312	1.842286
	7					1.795486	1.762584	1.789064	1.823618	1.825310	1.842296
	8					1.795488	1.762592	1.789066	1.823612	1.825310	1.842300
	9					1.795488	1.762584	1.789062	1.823612	1.825300	1.842300
	10					1.795488	1.762590	1.789060	1.823620	1.825306	1.842294

		Measured Weight (g)									
	Meas #	A730	A731	A732	A733	A734	A735	A736	A737	A738	A739
800 hrs	1							1.789050	1.823636	1.825284	1.842318
	2							1.789052	1.823644	1.825280	1.842304
	3							1.789046	1.823632	1.825278	1.842310
	4							1.789046	1.823624	1.825288	1.842314
	5							1.789058	1.823630	1.825290	1.842306
	6							1.789052	1.823624	1.825292	1.842322
	7							1.789052	1.823632	1.825274	1.842310
	8							1.789046	1.823638	1.825274	1.842308
	9							1.789060	1.823624	1.825272	1.842304
	10							1.789064	1.823632	1.825272	1.842304
1000 hrs	1								1.823618		1.842296
	2								1.823632		1.842302
	3								1.823622		1.842302
	4								1.823634		1.842294
	5								1.823636		1.842288
	6								1.823618		1.842298
	7								1.823626		1.842294
	8								1.823626		1.842288
	9								1.823618		1.842290
	10								1.823620		1.842288
1200 hrs	1										
	2										
	3										
	4										
	5										
	6										
	7										
	8										
	9										
	10										

Table 63: Raw Data, Expt. #6, IG-CO_2/550°C/20MPa, AFA-OC10

Project:	**SCCO2**
Grant #:	PRJ39TC
MDS:	MD24386
Expt. #:	**6**
Phase:	2
Phase Type:	Industrial CO2
Temp. (°C):	550
Pressure:	2900psi
Sample ID:	**AFA-OC10**
Notes:	

Rel. Uncertainty in Meas. Mass:	Δm = ± 0.000002 g
Rel. Uncertainty in Meas. Length:	Δl = ± 0.001 mm
Rel. Uncertainty in Meas. Width:	Δw = ± 0.001 mm
Uncertainty in Meas. Area:	ΔA = ± 0.000179 cm^2

Supplier/UNS ID:	
Metal Type:	Alumina Forming Austenitic
Color Designation:	Brown
Hole Diameter in Sample (mm):	3

		Sample # / Description									
	Meas #	**A140**	**A141**	**A142**	**A143**	**A144**	**A145**	**A146**	**A147**	**A148**	**A149**
BARE WEIGHT (gm)	**1**	1.755098	1.751892	1.740304	1.756148	1.667722	1.746890	1.762642	1.726382	1.763102	1.766780
	2	1.755108	1.751896	1.740300	1.756150	1.667724	1.746890	1.762640	1.726386	1.763104	1.766780
	3	1.755106	1.751890	1.740298	1.756146	1.667726	1.746890	1.762636	1.726382	1.763102	1.766784
	4	1.755102	1.751892	1.740304	1.756152	1.667722	1.746892	1.762640	1.726382	1.763108	1.766782
	5	1.755108	1.751898	1.740306	1.756148	1.667726	1.746886	1.762646	1.726384	1.763102	1.766782
	6	1.755112	1.751898	1.740296	1.756150	1.667722	1.746890	1.762642	1.726386	1.763108	1.766782
	7	1.755102	1.751898	1.740296	1.756152	1.667722	1.746884	1.762636	1.726384	1.763108	1.766782
	8	1.755106	1.751894	1.740298	1.756148	1.667726	1.746886	1.762644	1.726388	1.763106	1.766778
	9	1.755106	1.751896	1.740298	1.756148	1.667720	1.746890	1.762642	1.726384	1.763102	1.766784
	10	1.755104	1.751898	1.740296	1.756148	1.667722	1.746890	1.762646	1.726384	1.763106	1.766780
BARE AREA (mm2)	**1_L**	12.701	12.659	12.715	12.660	12.709	12.649	12.683	12.639	12.685	12.715
	2_L	12.692	12.673	12.699	12.657	12.681	12.660	12.683	12.644	12.673	12.711
	3_L	12.682	12.678	12.679	12.655	12.652	12.668	12.688	12.647	12.660	12.698
	4_W	12.567	12.614	12.596	12.510	12.553	12.592	12.568	12.573	12.601	12.566
	5_W	12.571	12.614	12.603	12.531	12.570	12.595	12.567	12.569	12.604	12.569
	6_W	12.566	12.605	12.609	12.552	12.591	12.570	12.556	12.565	12.604	12.569
BARE THICKNESS (mm)	**1**	1.564	1.572	1.545	1.574	1.498	1.574	1.574	1.558	1.572	1.570
	2	1.573	1.572	1.551	1.575	1.533	1.574	1.573	1.562	1.574	1.577
	3	1.571	1.571	1.548	1.574	1.534	1.573	1.574	1.555	1.571	1.573
	4	1.572	1.574	1.550	1.577	1.536	1.575	1.577	1.562	1.575	1.579
	5	1.556	1.569	1.544	1.570	1.495	1.564	1.571	1.548	1.568	1.571

Table 64: Raw Data, Expt. #6, IG-CO_2/550^{o}C/20MPa, AFA-OC10

		Measured Weight (g)									
	Meas #	A140	A141	A142	A143	A144	A145	A146	A147	A148	A149
200 hrs	1	1.754954	1.752006	1.740130	1.756074	1.667736	1.746922	1.762594	1.726404	1.763138	1.766922
	2	1.754932	1.752000	1.740124	1.756072	1.667742	1.746920	1.762602	1.726404	1.763128	1.766916
	3	1.754926	1.752000	1.740122	1.756072	1.667742	1.746918	1.762590	1.726394	1.763134	1.766916
	4	1.754926	1.752006	1.740118	1.756068	1.667736	1.746918	1.762602	1.726386	1.763132	1.766906
	5	1.754926	1.752004	1.740120	1.756076	1.667730	1.746918	1.762598	1.726386	1.763128	1.766912
	6	1.754940	1.752004	1.740120	1.756074	1.667738	1.746916	1.762592	1.726396	1.763128	1.766916
	7	1.754928	1.752002	1.740118	1.756072	1.667736	1.746914	1.762600	1.726386	1.763138	1.766922
	8	1.754926	1.752000	1.740114	1.756076	1.667734	1.746914	1.762596	1.726384	1.763126	1.766916
	9	1.754940	1.752002	1.740114	1.756074	1.667738	1.746924	1.762596	1.726384	1.763128	1.766910
	10	1.754930	1.752000	1.740114	1.756080	1.667734	1.746918	1.762590	1.726386	1.763126	1.766912
400 hrs	1			1.739896	1.756070	1.667722	1.746964	1.762626	1.726432	1.763164	1.766852
	2			1.739894	1.756068	1.667712	1.746960	1.762632	1.726432	1.763164	1.766850
	3			1.739900	1.756068	1.667710	1.746958	1.762634	1.726430	1.763162	1.766862
	4			1.739902	1.756074	1.667710	1.746958	1.762634	1.726432	1.763156	1.766850
	5			1.739902	1.756072	1.667710	1.746964	1.762628	1.726432	1.763162	1.766862
	6			1.739896	1.756064	1.667712	1.746954	1.762632	1.726438	1.763166	1.766852
	7			1.739892	1.756064	1.667718	1.746960	1.762632	1.726430	1.763162	1.766852
	8			1.739898	1.756064	1.667704	1.746954	1.762630	1.726432	1.763166	1.766852
	9			1.739894	1.756066	1.667704	1.746956	1.762634	1.726426	1.763162	1.766852
	10			1.739890	1.756074	1.667704	1.746950	1.762634	1.726432	1.763158	1.766860
600 hrs	1					1.667612	1.747000	1.762656	1.726504	1.763214	1.766896
	2					1.667612	1.747000	1.762658	1.726504	1.763208	1.766892
	3					1.667614	1.746996	1.762660	1.726504	1.763212	1.766896
	4					1.667616	1.746998	1.762654	1.726504	1.763210	1.766884
	5					1.667612	1.746998	1.762656	1.726506	1.763212	1.766890
	6					1.667610	1.746998	1.762660	1.726510	1.763212	1.766888
	7					1.667612	1.746998	1.762660	1.726500	1.763208	1.766888
	8					1.667612	1.746998	1.762660	1.726506	1.763208	1.766892
	9					1.667612	1.746994	1.762656	1.726500	1.763210	1.766892
	10					1.667614	1.746996	1.762662	1.726504	1.763214	1.766892

		Measured Weight (g)									
	Meas #	A140	A141	A142	A143	A144	A145	A146	A147	A148	A149
800 hrs	1							1.762786	1.726630	1.763332	1.767060
	2							1.762790	1.726630	1.763354	1.767050
	3							1.762772	1.726646	1.763332	1.767062
	4							1.762776	1.726636	1.763352	1.767048
	5							1.762782	1.726628	1.763342	1.767060
	6							1.762770	1.726624	1.763346	1.767066
	7							1.762770	1.726626	1.763338	1.767048
	8							1.762774	1.726632	1.763340	1.767046
	9							1.762772	1.726634	1.763344	1.767060
	10							1.762782	1.726632	1.763334	1.767048
1000 hrs	1								1.726772		1.767188
	2								1.726786		1.767194
	3								1.726786		1.767184
	4								1.726764		1.767172
	5								1.726770		1.767184
	6								1.726768		1.767176
	7								1.726774		1.767188
	8								1.726774		1.767200
	9								1.726770		1.767186
	10								1.726784		1.767184
1200 hrs	1										
	2										
	3										
	4										
	5										
	6										
	7										
	8										
	9										
	10										

Table 65: Raw Data, Expt. #6, IG-CO_2/550°C/20MPa, IN800H

Project:	**SCCO2**
Grant #:	PRJ39TC
MDS:	MD24386
Expt. #:	**6**
Phase:	2
Phase Type:	Industrial CO2
Temp. (°C):	550
Pressure:	2900psi
Sample ID:	**IN800H**

Rel. Uncertainty in Meas. Mass:	Δm = ± 0.000002 g
Rel. Uncertainty in Meas. Length:	Δl = ± 0.001 mm
Rel. Uncertainty in Meas. Width:	Δw = ± 0.001 mm
Uncertainty in Meas. Area:	ΔA = ± 0.000182 cm^2

Operator:	Paul Roman
Polished Surface:	800 Grit Silicon Carbide
Color Designation:	Cyan
Hole Diameter in Sample (mm):	3

Notes: Incoloy® Alloy 800H from Special Metals Corporation, nickel-iron-chromium alloy

		Sample # / Description									
	Meas #	**I30**	**I40**	**I32**	**I33**	**I34**	**I35**	**I36**	**I37**	**I38**	**I39**
BARE WEIGHT (gm)	**1**	1.821524	1.912302	1.881558	1.855268	1.864560	1.838876	1.877704	1.833784	1.842200	1.825618
	2	1.821522	1.912288	1.881558	1.855270	1.864566	1.838886	1.877716	1.833782	1.842202	1.825624
	3	1.821534	1.912302	1.881558	1.855268	1.864562	1.838872	1.877714	1.833784	1.842208	1.825610
	4	1.821532	1.912284	1.881558	1.855272	1.864560	1.838874	1.877716	1.833782	1.842208	1.825616
	5	1.821526	1.912296	1.881550	1.855270	1.864568	1.838874	1.877716	1.833782	1.842206	1.825622
	6	1.821522	1.912286	1.881556	1.855278	1.864562	1.838876	1.877708	1.833780	1.842206	1.825618
	7	1.821522	1.912302	1.881562	1.855280	1.864560	1.838882	1.877706	1.833780	1.842198	1.825628
	8	1.821528	1.912292	1.881560	1.855270	1.864564	1.838882	1.877718	1.833784	1.842210	1.825616
	9	1.821524	1.912296	1.881554	1.855268	1.864562	1.838886	1.877706	1.833782	1.842206	1.825620
	10	1.821534	1.912290	1.881550	1.855274	1.864560	1.838872	1.877716	1.833774	1.842200	1.825622
BARE AREA (mm2)	**1_L**	13.218	13.347	13.292	13.138	13.224	13.147	13.219	13.234	13.205	13.141
	2_L	13.218	13.329	13.296	13.142	13.204	13.183	13.240	13.240	13.222	13.145
	3_L	13.198	13.287	13.256	13.132	13.112	13.203	13.242	13.242	13.230	13.143
	4_W	12.497	12.619	12.481	12.406	12.425	12.490	12.508	12.508	12.544	12.521
	5_W	12.531	12.631	12.577	12.411	12.423	12.508	12.510	12.510	12.522	12.483
	6_W	12.534	12.617	12.582	12.398	12.416	12.507	12.485	12.485	12.486	12.434
BARE THICKNESS (mm)	**1**	1.503	1.563	1.537	1.540	1.557	1.527	1.553	1.520	1.510	1.514
	2	1.499	1.566	1.535	1.539	1.553	1.522	1.546	1.517	1.513	1.510
	3	1.476	1.494	1.510	1.526	1.516	1.490	1.504	1.483	1.496	1.475
	4	1.485	1.557	1.521	1.531	1.540	1.507	1.530	1.504	1.503	1.494
	5	1.494	1.541	1.530	1.535	1.537	1.517	1.535	1.497	1.502	1.504

Table 66: Raw Data, Expt. #6, IG-CO_2/550^{o}C/20MPa, IN800H

		Measured Weight (g)									
	Meas #	I30	I40	I32	I33	I34	I35	I36	I37	I38	I39
200 hrs	1	1.821682	1.912368	1.881690	1.855386	1.864656	1.838972	1.877870	1.833856	1.842302	1.825708
	2	1.821668	1.912374	1.881688	1.855414	1.864652	1.838974	1.877854	1.833864	1.842314	1.825706
	3	1.821670	1.912372	1.881686	1.855386	1.864648	1.838960	1.877862	1.833860	1.842298	1.825692
	4	1.821674	1.912368	1.881684	1.855384	1.864658	1.838976	1.877848	1.833856	1.842304	1.825698
	5	1.821668	1.912372	1.881682	1.855384	1.864642	1.838972	1.877870	1.833854	1.842314	1.825698
	6	1.821674	1.912368	1.881684	1.855374	1.864652	1.838958	1.877846	1.833854	1.842302	1.825704
	7	1.821682	1.912384	1.881686	1.855376	1.864656	1.838986	1.877880	1.833856	1.842310	1.825692
	8	1.821682	1.912368	1.881690	1.855380	1.864640	1.838982	1.877872	1.833868	1.842310	1.825694
	9	1.821676	1.912368	1.881690	1.855382	1.864644	1.838974	1.877830	1.833862	1.842310	1.825696
	10	1.821664	1.912374	1.881694	1.855376	1.864648	1.838964	1.877856	1.833858	1.842308	1.825704
400 hrs	1			1.881718	1.855404	1.864676	1.839012	1.877878	1.833884	1.842336	1.825714
	2			1.881714	1.855402	1.864674	1.839006	1.877896	1.833874	1.842328	1.825726
	3			1.881724	1.855406	1.864672	1.839002	1.877888	1.833884	1.842340	1.825714
	4			1.881720	1.855404	1.864684	1.839000	1.877888	1.833880	1.842336	1.825716
	5			1.881720	1.855402	1.864676	1.839004	1.877890	1.833878	1.842326	1.825712
	6			1.881722	1.855396	1.864680	1.839004	1.877882	1.833880	1.842328	1.825716
	7			1.881718	1.855402	1.864670	1.839002	1.877884	1.833874	1.842330	1.825718
	8			1.881720	1.855398	1.864676	1.839008	1.877888	1.833872	1.842334	1.825722
	9			1.881722	1.855400	1.864670	1.839006	1.877894	1.833878	1.842338	1.825716
	10			1.881718	1.855402	1.864678	1.839006	1.877884	1.833876	1.842336	1.825724
600 hrs	1					1.864690	1.839022	1.877892	1.833886	1.842354	1.825716
	2					1.864690	1.839020	1.877898	1.833886	1.842356	1.825720
	3					1.864688	1.839022	1.877900	1.833882	1.842352	1.825724
	4					1.864690	1.839016	1.877894	1.833888	1.842354	1.825724
	5					1.864696	1.839016	1.877896	1.833888	1.842354	1.825714
	6					1.864688	1.839022	1.877900	1.833884	1.842358	1.825724
	7					1.864692	1.839024	1.877900	1.833882	1.842352	1.825724
	8					1.864686	1.839020	1.877900	1.833882	1.842360	1.825714
	9					1.864684	1.839020	1.877900	1.833884	1.842360	1.825722
	10					1.864688	1.839018	1.877890	1.833886	1.842352	1.825720

		Measured Weight (g)									
	Meas #	I30	I40	I32	I33	I34	I35	I36	I37	I38	I39
800 hrs	1							1.877924	1.833912	1.842366	1.825752
	2							1.877924	1.833920	1.842378	1.825744
	3							1.877918	1.833920	1.842378	1.825744
	4							1.877936	1.833916	1.842366	1.825742
	5							1.877922	1.833918	1.842378	1.825752
	6							1.877924	1.833922	1.842378	1.825752
	7							1.877914	1.833924	1.842370	1.825748
	8							1.877934	1.833920	1.842374	1.825760
	9							1.877922	1.833928	1.842382	1.825744
	10							1.877914	1.833922	1.842372	1.825754
1000 hrs	1								1.833932		1.825744
	2								1.833948		1.825776
	3								1.833926		1.825752
	4								1.833922		1.825752
	5								1.833922		1.825752
	6								1.833946		1.825768
	7								1.833930		1.825748
	8								1.833926		1.825768
	9								1.833928		1.825776
	10								1.833928		1.825744
1200 hrs	1										
	2										
	3										
	4										
	5										
	6										
	7										
	8										
	9										
	10										

Table 67: Raw Data, Expt. #6, IG-CO_2/550°C/20MPa, 316L

Project:	**SCCO2**
Grant #:	PRJ39TC
MDS:	MD24386
Expt. #:	**6**
Phase:	2
Phase Type:	Industrial CO2
Temp. (°C):	550
Pressure:	2900psi
Sample ID:	**316L**
Notes:	

Rel. Uncertainty in Meas. Mass:	Δm = ± 0.000002 g
Rel. Uncertainty in Meas. Length:	Δl = ± 0.001 mm
Rel. Uncertainty in Meas. Width:	Δw = ± 0.001 mm
Uncertainty in Meas. Area:	ΔA = ± 0.000178 cm^2

Supplier/UNS ID:	S31603
Metal Type:	Austenitic
Color Designation:	Orange
Hole Diameter in Sample (mm):	3

		Sample # / Description									
	Meas #	**L1**	**L2**	**L3**	**L4**	**L5**	**L6**	**L7**	**L8**	**L9**	**L10**
BARE WEIGHT (gm)	**1**	1.304420	1.332888	1.333676	1.342098	1.336316	1.349456				
	2	1.304416	1.332890	1.333668	1.342100	1.336320	1.349456				
	3	1.304418	1.332884	1.333672	1.342094	1.336326	1.349458				
	4	1.304424	1.332884	1.333676	1.342100	1.336320	1.349448				
	5	1.304422	1.332880	1.333674	1.342098	1.336316	1.349454				
	6	1.304416	1.332886	1.333666	1.342094	1.336324	1.349454				
	7	1.304418	1.332886	1.333672	1.342098	1.336326	1.349450				
	8	1.304414	1.332884	1.333672	1.342096	1.336324	1.349456				
	9	1.304414	1.332880	1.333678	1.342098	1.336316	1.349456				
	10	1.304414	1.332880	1.333670	1.342098	1.336326	1.349452				
BARE AREA (mm2)	**1_L**	12.515	12.571	12.563	12.569	12.529	12.561				
	2_L	12.541	12.578	12.563	12.566	12.527	12.558				
	3_L	12.554	12.572	12.556	12.541	12.521	12.548				
	4_W	12.569	12.605	12.570	12.573	12.586	12.545				
	5_W	12.557	12.593	12.560	12.564	12.555	12.549				
	6_W	12.542	12.560	12.548	12.577	12.510	12.538				
BARE THICKNESS (mm)	**1**	1.137	1.149	1.154	1.158	1.162	1.168				
	2	1.137	1.153	1.157	1.162	1.163	1.170				
	3	1.132	1.155	1.160	1.163	1.164	1.170				
	4	1.122	1.147	1.154	1.159	1.157	1.166				
	5	1.139	1.154	1.158	1.160	1.166	1.171				

Table 68: Raw Data, Expt. #6, IG-CO_2/550^{o}C/20MPa, 316L

		Measured Weight (g)									
	Meas #	L1	L2	L3	L4	L5	L6	L7	L8	L9	L10
200 hrs	1	1.304478	1.332946	1.333722	1.342164	1.336392	1.349520				
	2	1.304470	1.332944	1.333720	1.342152	1.336386	1.349518				
	3	1.304472	1.332940	1.333738	1.342156	1.336394	1.349510				
	4	1.304466	1.332946	1.333724	1.342156	1.336390	1.349512				
	5	1.304468	1.332956	1.333728	1.342168	1.336394	1.349522				
	6	1.304476	1.332950	1.333720	1.342158	1.336386	1.349530				
	7	1.304478	1.332942	1.333732	1.342152	1.336388	1.349524				
	8	1.304476	1.332950	1.333722	1.342158	1.336388	1.349512				
	9	1.304476	1.332956	1.333726	1.342152	1.336384	1.349530				
	10	1.304462	1.332940	1.333740	1.342152	1.336386	1.349522				
400 hrs	1		1.332948	1.333756	1.342170	1.336408	1.349550				
	2		1.332968	1.333754	1.342158	1.336418	1.349552				
	3		1.332956	1.333764	1.342154	1.336416	1.349550				
	4		1.332974	1.333754	1.342154	1.336412	1.349544				
	5		1.332950	1.333764	1.342154	1.336410	1.349548				
	6		1.332974	1.333762	1.342164	1.336406	1.349538				
	7		1.332960	1.333764	1.342174	1.336408	1.349536				
	8		1.332962	1.333756	1.342166	1.336406	1.349556				
	9		1.332970	1.333764	1.342162	1.336400	1.349552				
	10		1.332954	1.333760	1.342158	1.336424	1.349538				
600 hrs	1										
	2										
	3										
	4										
	5										
	6										
	7										
	8										
	9										
	10										

		Measured Weight (g)									
	Meas #	L1	L2	L3	L4	L5	L6	L7	L8	L9	L10
800 hrs	1										
	2										
	3										
	4										
	5										
	6										
	7										
	8										
	9										
	10										
1000 hrs	1										
	2										
	3										
	4										
	5										
	6										
	7										
	8										
	9										
	10										
1200 hrs	1										
	2										
	3										
	4										
	5										
	6										
	7										
	8										
	9										
	10										

Table 69: Raw Data, Expt. #7, RG-CO_2/650^{o}C/20MPa, Coupon Arrangement

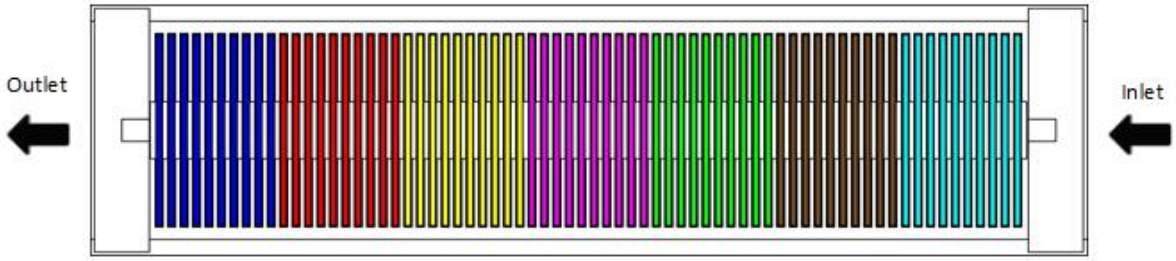

Sample	Blue 316L	Red Haynes 230	Yellow 347SS	Magenta AFA-OC6	Green IN800H	Brown	Cyan
1	L7	HAY01	S46	A646	I41		
2	L8	HAY02	S47	A647	I42		
3	L9	HAY03	S48	A648	I43		
4	L10	HAY04	S49	A649	I44		
5	L11	HAY05	S50	A650	I45		
6	L12	HAY06	S51	A651	I46		
7							
8							
9							
10							

Table 70: Raw Data, Expt. #7, IG-CO_2/650^oC/20MPa, 316L

Project:	
Contact:	
MDS:	
Expt. #:	
Phase:	
Phase Type:	Industrial CO2
Temp. (^oC):	650
Pressure (MPa):	20
Sample ID:	**316L**
Notes:	

Rel. Uncertainty in Meas. Mass:	Δm = ± 0.000002 g
Rel. Uncertainty in Meas. Length:	Δl = ± 0.001 mm
Rel. Uncertainty in Meas. Width:	Δw = ± 0.001 mm
Uncertainty in Meas. Area:	ΔA = ± 0.000176 cm^2

Supplier/UNS ID:	
Metal Type:	
Color Designation:	
Hole Diameter in Sample (mm):	3

		Sample # / Description									
	Meas #	**L7**	**L8**	**L9**	**L10**	**L11**	**L12**				
BARE WEIGHT (gm)	**1**	1.224104	1.238256	1.271206	1.286662	1.327576	1.325858				
	2	1.224102	1.238256	1.271202	1.286652	1.327578	1.325856				
	3	1.224100	1.238262	1.271204	1.286658	1.327578	1.325856				
	4	1.224102	1.238256	1.271206	1.286654	1.327578	1.325854				
	5	1.224102	1.238256	1.271206	1.286658	1.327578	1.325860				
	6	1.224096	1.238258	1.271204	1.286654	1.327580	1.325862				
	7	1.224098	1.238260	1.271206	1.286662	1.327576	1.325858				
	8	1.224098	1.238258	1.271208	1.286656	1.327576	1.325860				
	9	1.224098	1.238258	1.271204	1.286660	1.327576	1.325858				
	10	1.224100	1.238260	1.271206	1.286662	1.327574	1.325858				
BARE AREA (mm2)	**1_L**	12.478	12.474	12.501	12.478	12.482	12.451				
	2_L	12.479	12.472	12.501	12.480	12.484	12.464				
	3_L	12.470	12.467	12.499	12.468	12.478	12.468				
	4_W	12.463	12.481	12.473	12.421	12.463	12.441				
	5_W	12.461	12.481	12.480	12.422	12.445	12.442				
	6_W	12.462	12.480	12.481	12.420	12.429	12.437				
BARE THICKNESS (mm)	**1**	1.098	1.117	1.109	1.142	1.170	1.164				
	2	1.095	1.104	1.110	1.138	1.173	1.170				
	3	1.025	1.037	1.080	1.095	1.143	1.149				
	4	1.075	1.092	1.099	1.134	1.165	1.161				
	5	1.072	1.076	1.096	1.117	1.158	1.156				

Table 71: Raw Data, Expt. #7, IG-CO_2/650^{o}C/20MPa, 316L

		Measured Weight (g)									
	Meas #	L7	L8	L9	L10	L11	L12				
200 hrs	1	1.224684	1.238728	1.271626	1.287038	1.327986	1.326282				
	2	1.224682	1.238728	1.271622	1.287032	1.327986	1.326284				
	3	1.224684	1.238730	1.271618	1.287034	1.327988	1.326280				
	4	1.224680	1.238728	1.271624	1.287032	1.327990	1.326282				
	5	1.224680	1.238726	1.271622	1.287034	1.327988	1.326278				
	6	1.224680	1.238726	1.271620	1.287032	1.327992	1.326280				
	7	1.224682	1.238730	1.271620	1.287034	1.327986	1.326276				
	8	1.224674	1.238726	1.271620	1.287036	1.327988	1.326278				
	9	1.224674	1.238728	1.271620	1.287036	1.327990	1.326280				
	10	1.224680	1.238728	1.271618	1.287030	1.327990	1.326278				
400 hrs	1										
	2										
	3										
	4										
	5										
	6										
	7										
	8										
	9										
	10										
600 hrs	1										
	2										
	3										
	4										
	5										
	6										
	7										
	8										
	9										
	10										

		Measured Weight (g)									
	Meas #	L7	L8	L9	L10	L11	L12				
800 hrs	1										
	2										
	3										
	4										
	5										
	6										
	7										
	8										
	9										
	10										
1000 hrs	1										
	2										
	3										
	4										
	5										
	6										
	7										
	8										
	9										
	10										
1200 hrs	1										
	2										
	3										
	4										
	5										
	6										
	7										
	8										
	9										
	10										

Table 72: Raw Data, Expt. #7, IG-CO_2/650°C/20MPa, Haynes 230

Project:	
Contact:	
MDS:	
Expt. #:	**7**
Phase:	
Phase Type:	Industrial CO2
Temp. (°C):	650
Pressure (MPa):	20
Sample ID:	**Haynes 230**

Notes:

Rel. Uncertainty in Meas. Mass:	Δm = ± 0.000002 g
Rel. Uncertainty in Meas. Length:	Δl = ± 0.001 mm
Rel. Uncertainty in Meas. Width:	Δw = ± 0.001 mm
Uncertainty in Meas. Area:	ΔA = ± 0.000178 cm^2

Supplier/UNS ID:	
Metal Type:	
Color Designation:	
Hole Diameter in Sample (mm):	3

		Sample # / Description									
	Meas #	**HAY01**	**HAY02**	**HAY03**	**HAY04**	**HAY05**	**HAY06**				
BARE WEIGHT (gm)	**1**	2.575222	2.614884	2.647468	2.619572	2.651816	2.561152				
	2	2.575232	2.614878	2.647472	2.619576	2.651812	2.561152				
	3	2.575230	2.614886	2.647474	2.619576	2.651818	2.561150				
	4	2.575230	2.614882	2.647472	2.619576	2.651818	2.561154				
	5	2.575232	2.614886	2.647474	2.619574	2.651814	2.561154				
	6	2.575226	2.614882	2.647472	2.619576	2.651818	2.561156				
	7	2.575228	2.614878	2.647474	2.619576	2.651814	2.561158				
	8	2.575224	2.614880	2.647470	2.619576	2.651820	2.561158				
	9	2.575232	2.614882	2.647472	2.619574	2.651812	2.561152				
	10	2.575230	2.614884	2.647472	2.619574	2.651818	2.561156				
BARE AREA (mm2)	**1_L**	12.584	12.622	12.631	12.616	12.618	12.616				
	2_L	12.614	12.612	12.622	12.622	12.620	12.612				
	3_L	12.616	12.596	12.619	12.622	12.616	12.610				
	4_W	12.630	12.627	12.613	12.602	12.632	12.599				
	5_W	12.626	12.623	12.609	12.600	12.627	12.599				
	6_W	12.620	12.608	12.602	12.611	12.623	12.597				
BARE THICKNESS (mm)	**1**	1.989	2.018	2.018	2.012	2.033	1.994				
	2	1.982	2.008	2.016	2.006	2.027	1.979				
	3	1.927	1.959	1.988	1.966	1.985	1.921				
	4	1.970	1.998	2.007	1.992	2.013	1.973				
	5	1.969	1.996	2.005	1.994	2.014	1.953				

Table 73: Raw Data, Expt. #7, IG-CO_2/650^{o}C/20MPa, Haynes 230

		Measured Weight (g)									
	Meas #	HAY01	HAY02	HAY03	HAY04	HAY05	HAY06				
200 hrs	1	2.57533	2.614976	2.647546	2.619732	2.651898	2.561240				
	2	2.575324	2.614974	2.647544	2.619738	2.651898	2.561236				
	3	2.575324	2.614970	2.647548	2.619732	2.651898	2.561232				
	4	2.575332	2.614970	2.647546	2.619734	2.651894	2.561240				
	5	2.575326	2.614976	2.647544	2.619734	2.651896	2.561238				
	6	2.575322	2.614972	2.647542	2.619734	2.651892	2.561242				
	7	2.575322	2.614976	2.647546	2.619734	2.651898	2.561236				
	8	2.575320	2.614970	2.647546	2.619734	2.651896	2.561234				
	9	2.575328	2.614970	2.647544	2.619734	2.651898	2.561238				
	10	2.575326	2.614970	2.647542	2.619736	2.651898	2.561238				
400 hrs	1										
	2										
	3										
	4										
	5										
	6										
	7										
	8										
	9										
	10										
600 hrs	1										
	2										
	3										
	4										
	5										
	6										
	7										
	8										
	9										
	10										

		Measured Weight (g)									
	Meas #	HAY01	HAY02	HAY03	HAY04	HAY05	HAY06				
800 hrs	1										
	2										
	3										
	4										
	5										
	6										
	7										
	8										
	9										
	10										
1000 hrs	1										
	2										
	3										
	4										
	5										
	6										
	7										
	8										
	9										
	10										
1200 hrs	1										
	2										
	3										
	4										
	5										
	6										
	7										
	8										
	9										
	10										

Table 74: Raw Data, Expt. #7, IG-CO_2/650°C/20MPa, 347SS

Project:	
Contact:	
MDS:	
Expt. #:	**7**
Phase:	
Phase Type:	Industrial CO2
Temp. (°C):	650
Pressure (MPa):	20
Sample ID:	**347SS**
Notes:	

Rel. Uncertainty in Meas. Mass:	Δm = ± 0.000002 g
Rel. Uncertainty in Meas. Length:	Δl = ± 0.001 mm
Rel. Uncertainty in Meas. Width:	Δw = ± 0.001 mm
Uncertainty in Meas. Area:	ΔA = ± 0.000182 cm^2

Supplier/UNS ID:	
Metal Type:	
Color Designation:	
Hole Diameter in Sample (mm):	3

		Sample # / Description									
	Meas #	**S46**	**S47**	**S48**	**S49**	**S50**	**S51**				
BARE WEIGHT (gm)	**1**	1.897720	1.898866	1.902238	1.855614	1.868780	1.890170				
	2	1.897714	1.898864	1.902238	1.855620	1.868782	1.890166				
	3	1.897708	1.898870	1.902234	1.855618	1.868782	1.890170				
	4	1.897710	1.898866	1.902236	1.855624	1.868780	1.890170				
	5	1.897714	1.898868	1.902234	1.855620	1.868782	1.890168				
	6	1.897716	1.898866	1.902236	1.855622	1.868788	1.890168				
	7	1.897716	1.898866	1.902234	1.855614	1.868782	1.890168				
	8	1.897716	1.898864	1.902232	1.855616	1.868784	1.890168				
	9	1.897720	1.898866	1.902240	1.855620	1.868782	1.890170				
	10	1.897714	1.898872	1.902232	1.855616	1.868786	1.890170				
BARE AREA (mm2)	**1_L**	13.123	13.145	13.095	13.133	13.043	13.067				
	2_L	13.110	13.150	13.091	13.137	13.052	13.072				
	3_L	13.088	13.145	13.086	13.139	13.047	13.063				
	4_W	12.624	12.617	12.569	12.616	12.566	12.598				
	5_W	12.631	12.616	12.617	12.617	12.568	12.611				
	6_W	12.632	12.615	12.631	12.623	12.566	12.612				
BARE THICKNESS (mm)	**1**	1.570	1.568	1.577	1.542	1.563	1.569				
	2	1.568	1.567	1.577	1.539	1.566	1.571				
	3	1.538	1.540	1.555	1.496	1.539	1.551				
	4	1.560	1.559	1.571	1.515	1.556	1.564				
	5	1.562	1.560	1.570	1.531	1.556	1.561				

Table 75: Raw Data, Expt. #7, IG-CO_2/650^{o}C/20MPa, 347SS

		Measured Weight (g)									
	Meas #	S46	S47	S48	S49	S50	S51				
200 hrs	1	1.897888	1.899040	1.902408	1.855782	1.868978	1.890504				
	2	1.897888	1.899044	1.902406	1.855782	1.868976	1.890502				
	3	1.897886	1.899042	1.902406	1.855784	1.868976	1.890498				
	4	1.897880	1.899038	1.902406	1.855778	1.868974	1.890498				
	5	1.897882	1.899040	1.902408	1.855778	1.868978	1.890500				
	6	1.897880	1.899042	1.902408	1.855782	1.868974	1.890500				
	7	1.897890	1.899036	1.902406	1.855782	1.868978	1.890500				
	8	1.897884	1.899038	1.902404	1.855780	1.868976	1.890498				
	9	1.897884	1.899038	1.902402	1.855782	1.868970	1.890500				
	10	1.897880	1.899040	1.902402	1.855784	1.868978	1.890502				
400 hrs	1										
	2										
	3										
	4										
	5										
	6										
	7										
	8										
	9										
	10										
600 hrs	1										
	2										
	3										
	4										
	5										
	6										
	7										
	8										
	9										
	10										

		Measured Weight (g)									
	Meas #	S46	S47	S48	S49	S50	S51				
800 hrs	1										
	2										
	3										
	4										
	5										
	6										
	7										
	8										
	9										
	10										
1000 hrs	1										
	2										
	3										
	4										
	5										
	6										
	7										
	8										
	9										
	10										
1200 hrs	1										
	2										
	3										
	4										
	5										
	6										
	7										
	8										
	9										
	10										

Table 76: Raw Data, Expt. #7, IG-CO_2/650°C/20MPa, IN800H

Project:	
Contact:	
MDS:	
Expt. #:	**7**
Phase:	II
Phase Type:	Industrial CO2
Temp. (°C):	650
Pressure (MPa):	20
Sample ID:	**IN800H**
Notes:	

Rel. Uncertainty in Meas. Mass:	Δm = ± 0.000002 g
Rel. Uncertainty in Meas. Length:	Δl = ± 0.001 mm
Rel. Uncertainty in Meas. Width:	Δw = ± 0.001 mm
Uncertainty in Meas. Area:	ΔA = ± 0.00019 cm^2

Supplier/UNS ID:	
Metal Type:	
Color Designation:	
Hole Diameter in Sample (mm):	3

		Sample # / Description									
	Meas #	**I41**	**I42**	**I43**	**I44**	**I45**	**I46**				
BARE WEIGHT (gm)	**1**	1.858060	1.901326	1.906908	1.873268	1.861194	1.880800				
	2	1.858058	1.901336	1.906922	1.873270	1.861192	1.880800				
	3	1.858054	1.901330	1.906920	1.873272	1.861196	1.880796				
	4	1.858054	1.901328	1.906910	1.873270	1.861188	1.880794				
	5	1.858058	1.901338	1.906918	1.873270	1.861192	1.880800				
	6	1.858052	1.901334	1.906924	1.873272	1.861190	1.880792				
	7	1.858054	1.901336	1.906918	1.873270	1.861194	1.880792				
	8	1.858062	1.901324	1.906910	1.873270	1.861190	1.880800				
	9	1.858050	1.901330	1.906916	1.873272	1.861194	1.880796				
	10	1.858062	1.901334	1.906920	1.873270	1.861190	1.880796				
BARE AREA (mm2)	**1_L**	13.339	13.322	13.340	13.214	13.225	13.187				
	2_L	13.337	13.308	13.324	13.214	13.239	13.186				
	3_L	13.339	13.262	13.292	31.216	13.245	13.181				
	4_W	12.637	12.563	12.614	12.505	12.491	12.504				
	5_W	12.622	12.568	12.616	12.525	12.513	12.530				
	6_W	12.596	12.571	12.619	12.530	12.516	12.552				
BARE THICKNESS (mm)	**1**	1.508	1.564	1.524	1.549	1.545	1.554				
	2	1.509	1.564	1.550	1.549	1.547	1.557				
	3	1.458	1.505	1.505	1.508	1.504	1.507				
	4	1.491	1.524	1.543	1.541	1.528	1.543				
	5	1.504	1.552	1.536	1.525	1.533	1.538				

Table 77: Raw Data, Expt. #7, IG-CO_2/650^{o}C/20MPa, IN800H

		Measured Weight (g)									
	Meas #	I41	I42	I43	I44	I45	I46				
200 hrs	1	1.85842	1.901610	1.907200	1.873680	1.861510	1.881160				
	2	1.858418	1.901604	1.907206	1.873676	1.861504	1.881152				
	3	1.858418	1.901604	1.907206	1.873676	1.861504	1.881156				
	4	1.858418	1.901604	1.907206	1.873672	1.861506	1.881154				
	5	1.858418	1.901608	1.907206	1.873672	1.861504	1.881154				
	6	1.858416	1.901606	1.907208	1.873680	1.861504	1.881154				
	7	1.858416	1.901604	1.907210	1.873674	1.861504	1.881154				
	8	1.858416	1.901602	1.907206	1.873674	1.861504	1.881154				
	9	1.858416	1.901602	1.907206	1.873680	1.861502	1.881152				
	10	1.858418	1.901608	1.907210	1.873680	1.861500	1.881156				
400 hrs	1										
	2										
	3										
	4										
	5										
	6										
	7										
	8										
	9										
	10										
600 hrs	1										
	2										
	3										
	4										
	5										
	6										
	7										
	8										
	9										
	10										

		Measured Weight (g)									
	Meas #	I41	I42	I43	I44	I45	I46				
800 hrs	1										
	2										
	3										
	4										
	5										
	6										
	7										
	8										
	9										
	10										
1000 hrs	1										
	2										
	3										
	4										
	5										
	6										
	7										
	8										
	9										
	10										
1200 hrs	1										
	2										
	3										
	4										
	5										
	6										
	7										
	8										
	9										
	10										

Table 78: Raw Data, Expt. #7, IG-CO_2/650°C/20MPa, AFA-OC6

Project:	
Contact:	
MDS:	
Expt. #:	**7**
Phase:	II
Phase Type:	Industrial CO2
Temp. (°C):	650
Pressure (MPa):	20
Sample ID:	**AFA-OC6**
Notes:	

Rel. Uncertainty in Meas. Mass:	Δm = ± 0.000002 g
Rel. Uncertainty in Meas. Length:	Δl = ± 0.001 mm
Rel. Uncertainty in Meas. Width:	Δw = ± 0.001 mm
Uncertainty in Meas. Area:	ΔA = ± 0.00018 cm^2

Supplier/UNS ID:	
Metal Type:	
Color Designation:	
Hole Diameter in Sample (mm):	3

		Sample # / Description									
	Meas #	**A646**	**A647**	**A648**	**A649**	**A650**	**A651**				
BARE WEIGHT (gm)	**1**	1.740470	1.802432	1.801944	1.793168	1.794340	1.789860				
	2	1.740468	1.802432	1.801940	1.793170	1.794338	1.789862				
	3	1.740466	1.802436	1.801946	1.793168	1.794340	1.789866				
	4	1.740466	1.802434	1.801942	1.793170	1.794338	1.789862				
	5	1.740460	1.802438	1.801944	1.793166	1.794336	1.789862				
	6	1.740458	1.802432	1.801944	1.793166	1.794336	1.789864				
	7	1.740456	1.802434	1.801944	1.793170	1.794338	1.789860				
	8	1.740460	1.802434	1.801946	1.793166	1.794338	1.789866				
	9	1.740460	1.802434	1.801942	1.793164	1.794336	1.789862				
	10	1.740464	1.802432	1.801942	1.793166	1.794338	1.789866				
BARE AREA (mm2)	**1_L**	12.870	12.916	12.890	12.870	12.855	12.875				
	2_L	12.869	12.920	12.884	12.887	12.857	12.876				
	3_L	12.860	12.920	12.886	12.899	12.856	12.873				
	4_W	12.581	12.573	12.623	12.579	12.614	12.581				
	5_W	12.599	12.575	12.622	12.557	12.618	12.579				
	6_W	12.609	12.579	12.621	12.571	12.618	12.579				
BARE THICKNESS (mm)	**1**	1.554	1.574	1.570	1.574	1.576	1.571				
	2	1.553	1.577	1.572	1.579	1.579	1.576				
	3	1.470	1.551	1.542	1.548	1.548	1.547				
	4	1.536	1.565	1.546	1.566	1.565	1.560				
	5	1.529	1.564	1.569	1.568	1.564	1.565				

Table 79: Raw Data, Expt. #7, IG-CO_2/650^{o}C/20MPa, AFA-OC6

		Measured Weight (g)									
	Meas #	A646	A647	A648	A649	A650	A651				
200 hrs	1	1.740546	1.802296	1.802138	1.793118	1.794468	1.789914				
	2	1.740538	1.802288	1.802138	1.793120	1.794470	1.789918				
	3	1.740536	1.802292	1.802138	1.793116	1.794470	1.789916				
	4	1.740530	1.802292	1.802136	1.793116	1.794468	1.789918				
	5	1.740546	1.802296	1.802138	1.793118	1.794470	1.789916				
	6	1.740546	1.802290	1.802136	1.793116	1.794468	1.789912				
	7	1.740544	1.802292	1.802136	1.793118	1.794466	1.789910				
	8	1.740544	1.802292	1.802136	1.793120	1.794466	1.789916				
	9	1.740524	1.802292	1.802134	1.793118	1.794456	1.789910				
	10	1.740530	1.802290	1.802134	1.793118	1.794456	1.789910				
400 hrs	1										
	2										
	3										
	4										
	5										
	6										
	7										
	8										
	9										
	10										
600 hrs	1										
	2										
	3										
	4										
	5										
	6										
	7										
	8										
	9										
	10										

		Measured Weight (g)									
	Meas #	A646	A647	A648	A649	A650	A651				
800 hrs	1										
	2										
	3										
	4										
	5										
	6										
	7										
	8										
	9										
	10										
1000 hrs	1										
	2										
	3										
	4										
	5										
	6										
	7										
	8										
	9										
	10										
1200 hrs	1										
	2										
	3										
	4										
	5										
	6										
	7										
	8										
	9										
	10										

Table 80: Raw Data, Expt. #8, BDG-CO_2/650^{o}C/20MPa, Coupon Arrangement

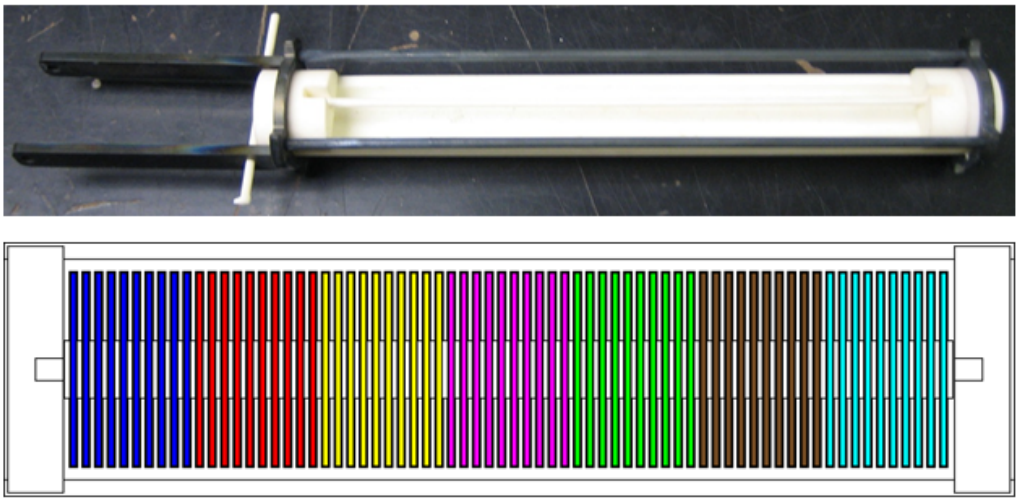

Sample	Blue IN740H	Red 316L	Yellow Haynes 230	Magenta 347SS	Green AFA-OC6	Brown IN800H	Cyan
1	Y01	L13	HAY07	S52	A652	I47	
2	Y02	L14	HAY08	S53	A653	I48	
3	Y03	L15	HAY09	S54	A654	I49	
4	Y04	L16	HAY10	S55	A655	I50	
5	Y05	L17	HAY11	S56	A656	I51	
6	Y06	L18	HAY12	S57	A657	I52	
7							
8							
9							
10							

Table 81: Raw Data, Expt. #8, BDG-CO_2/650^{o}C/20MPa, IN740H

Project:	
Contact:	
MDS:	
Expt. #:	**8**
Phase:	II
Phase Type:	Bone Dry CO2
Temp. (^{o}C):	650
Pressure (MPa):	20
Sample ID:	**IN740**
Notes:	

Rel. Uncertainty in Meas. Mass:	Δm = ± 0.000002 g
Rel. Uncertainty in Meas. Length:	Δl = ± 0.001 mm
Rel. Uncertainty in Meas. Width:	Δw = ± 0.001 mm
Uncertainty in Meas. Area:	ΔA = ± 0.000176 cm^2

Supplier/UNS ID:	
Metal Type:	
Color Designation:	
Hole Diameter in Sample (mm):	3

		Sample # / Description									
	Meas #	**Y01**	**Y02**	**Y03**	**Y04**	**Y05**	**Y06**				
BARE WEIGHT (gm)	**1**	1.127380	1.131032	1.158898	1.086204	1.140158	1.156448				
	2	1.127380	1.131028	1.158896	1.086198	1.140158	1.156452				
	3	1.127380	1.131028	1.158894	1.086198	1.140154	1.156448				
	4	1.127378	1.131026	1.158900	1.086200	1.140154	1.156448				
	5	1.127378	1.131030	1.158894	1.086204	1.140154	1.156448				
	6	1.127372	1.131030	1.158894	1.086194	1.140158	1.156446				
	7	1.127372	1.131026	1.158894	1.086196	1.140158	1.156450				
	8	1.127380	1.131026	1.158892	1.086198	1.140164	1.156448				
	9	1.127372	1.131028	1.158894	1.086202	1.140164	1.156448				
	10	1.127380	1.131026	1.158898	1.086200	1.140156	1.156450				
BARE AREA (mm2)	**1_L**	12.494	12.565	12.564	12.537	12.496	12.532				
	2_L	12.540	12.509	12.552	12.517	12.494	12.532				
	3_L	12.553	12.472	12.547	12.517	12.492	12.579				
	4_W	12.246	12.300	12.495	12.074	12.409	12.484				
	5_W	12.244	12.217	12.527	12.012	12.491	12.490				
	6_W	12.240	12.150	12.542	11.987	12.520	12.490				
BARE THICKNESS (mm)	**1**	0.952	0.975	0.950	0.962	0.948	0.976				
	2	0.962	0.980	0.961	0.963	0.957	0.981				
	3	0.940	0.955	0.959	0.903	0.952	0.922				
	4	0.955	0.973	0.958	0.938	0.958	0.957				
	5	0.960	0.965	0.959	0.957	0.946	0.971				

Table 82: Raw Data, Expt. #8, BDG-CO_2/650^{o}C/20MPa, IN740H

		Measured Weight (g)									
	Meas #	Y01	Y02	Y03	Y04	Y05	Y06				
200 hrs	1	1.127420	1.131092	1.158944	1.086266	1.140214	1.156506				
	2	1.127422	1.131090	1.158950	1.086264	1.140218	1.156502				
	3	1.127426	1.131090	1.158942	1.086260	1.140210	1.156504				
	4	1.127426	1.131086	1.158952	1.086260	1.140218	1.156502				
	5	1.127430	1.131092	1.158942	1.086262	1.140216	1.156506				
	6	1.127430	1.131092	1.158948	1.086264	1.140214	1.156498				
	7	1.127430	1.131088	1.158942	1.086260	1.140214	1.156502				
	8	1.127426	1.131088	1.158944	1.086262	1.140218	1.156500				
	9	1.127422	1.131092	1.158946	1.086262	1.140212	1.156506				
	10	1.127420	1.131094	1.158942	1.086256	1.140208	1.156502				
400 hrs	1										
	2										
	3										
	4										
	5										
	6										
	7										
	8										
	9										
	10										
600 hrs	1										
	2										
	3										
	4										
	5										
	6										
	7										
	8										
	9										
	10										

		Measured Weight (g)									
	Meas #	Y01	Y02	Y03	Y04	Y05	Y06				
800 hrs	1										
	2										
	3										
	4										
	5										
	6										
	7										
	8										
	9										
	10										
1000 hrs	1										
	2										
	3										
	4										
	5										
	6										
	7										
	8										
	9										
	10										
1200 hrs	1										
	2										
	3										
	4										
	5										
	6										
	7										
	8										
	9										
	10										

Table 83: Raw Data, Expt. #8, BDG-CO_2/650°C/20MPa, IN800H

Project:	
Contact:	
MDS:	
Expt. #:	**8**
Phase:	II
Phase Type:	Bone Dry CO2
Temp. (°C):	650
Pressure (MPa):	20
Sample ID:	**IN800H**

Notes:

Rel. Uncertainty in Meas. Mass:	Δm = ± 0.000002 g
Rel. Uncertainty in Meas. Length:	Δl = ± 0.001 mm
Rel. Uncertainty in Meas. Width:	Δw = ± 0.001 mm
Uncertainty in Meas. Area:	ΔA = ± 0.000183 cm^2

Supplier/UNS ID:	
Metal Type:	
Color Designation:	
Hole Diameter in Sample (mm):	3

		Sample # / Description									
	Meas #	**I47**	**I48**	**I49**	**I50**	**I51**	**I52**				
BARE WEIGHT (gm)	**1**	1.817526	1.881522	1.892374	1.891702	1.912794	1.911818				
	2	1.817528	1.881520	1.892374	1.891700	1.912792	1.911818				
	3	1.817526	1.881522	1.892376	1.891706	1.912790	1.911814				
	4	1.817526	1.881524	1.892374	1.891708	1.912790	1.911814				
	5	1.817522	1.881522	1.892376	1.891704	1.912786	1.911810				
	6	1.817526	1.881518	1.892376	1.891700	1.912788	1.911812				
	7	1.817520	1.881520	1.892380	1.891700	1.912796	1.911814				
	8	1.817520	1.881522	1.892376	1.891700	1.912786	1.911814				
	9	1.817526	1.881526	1.892372	1.891702	1.912784	1.911818				
	10	1.817522	1.881522	1.892374	1.891700	1.912788	1.911816				
BARE AREA (mm2)	**1_L**	13.332	13.318	13.315	13.267	13.333	13.324				
	2_L	13.321	13.314	13.341	13.258	13.330	13.348				
	3_L	13.279	13.309	13.358	13.252	13.331	13.357				
	4_W	12.587	12.580	12.543	12.583	12.600	12.560				
	5_W	12.591	12.565	12.556	12.576	12.590	12.572				
	6_W	12.594	12.545	12.565	12.565	12.584	12.583				
BARE THICKNESS (mm)	**1**	1.486	1.535	1.548	1.550	1.547	1.549				
	2	1.490	1.539	1.549	1.553	1.552	1.549				
	3	1.416	1.482	1.489	1.493	1.511	1.505				
	4	1.483	1.527	1.535	1.539	1.545	1.535				
	5	1.453	1.520	1.524	1.533	1.519	1.535				

Table 84: Raw Data, Expt. #8, BDG-CO_2/650^{o}C/20MPa, IN800H

		Measured Weight (g)									
	Meas #	I47	I48	I49	I50	I51	I52				
200 hrs	1	1.817642	1.881900	1.892704	1.892026	1.913180	1.912164				
	2	1.817632	1.881906	1.892702	1.892026	1.913176	1.912162				
	3	1.817636	1.881906	1.892706	1.892020	1.913176	1.912168				
	4	1.817640	1.881906	1.892704	1.892020	1.913178	1.912160				
	5	1.817632	1.881902	1.892706	1.892022	1.913182	1.912158				
	6	1.817640	1.881910	1.892706	1.892022	1.913174	1.912168				
	7	1.817632	1.881908	1.892706	1.892020	1.913176	1.912162				
	8	1.817634	1.881900	1.892708	1.892020	1.913178	1.912168				
	9	1.817634	1.881908	1.892704	1.892020	1.913182	1.912158				
	10	1.817636	1.881902	1.892710	1.892018	1.913174	1.912160				
400 hrs	1										
	2										
	3										
	4										
	5										
	6										
	7										
	8										
	9										
	10										
600 hrs	1										
	2										
	3										
	4										
	5										
	6										
	7										
	8										
	9										
	10										

		Measured Weight (g)									
	Meas #	I47	I48	I49	I50	I51	I52				
800 hrs	1										
	2										
	3										
	4										
	5										
	6										
	7										
	8										
	9										
	10										
1000 hrs	1										
	2										
	3										
	4										
	5										
	6										
	7										
	8										
	9										
	10										
1200 hrs	1										
	2										
	3										
	4										
	5										
	6										
	7										
	8										
	9										
	10										

Table 85: Raw Data, Expt. #8, BDG-CO_2/650^oC/20MPa, 316L

Project:	
Contact:	
MDS:	
Expt. #:	**8**
Phase:	II
Phase Type:	Bone Dry CO2
Temp. (^oC):	650
Pressure (MPa):	20
Sample ID:	**316L**
Notes:	

Rel. Uncertainty in Meas. Mass:	Δm = ± 0.000002 g
Rel. Uncertainty in Meas. Length:	Δl = ± 0.001 mm
Rel. Uncertainty in Meas. Width:	Δw = ± 0.001 mm
Uncertainty in Meas. Area:	ΔA = ± 0.000176 cm^2
Supplier/UNS ID:	
Metal Type:	
Color Designation:	
Hole Diameter in Sample (mm):	3

		Sample # / Description									
	Meas #	**L13**	**L14**	**L15**	**L16**	**L17**	**L18**				
BARE WEIGHT (gm)	**1**	1.232218	1.271142	1.287848	1.321032	1.322912	1.295306				
	2	1.232216	1.271144	1.287848	1.321032	1.322910	1.295306				
	3	1.232216	1.271140	1.287846	1.321028	1.322910	1.295304				
	4	1.232216	1.271140	1.287842	1.321030	1.322906	1.295304				
	5	1.232216	1.271140	1.287840	1.321026	1.322900	1.295308				
	6	1.232220	1.271140	1.287840	1.321026	1.322908	1.295308				
	7	1.232218	1.271142	1.287840	1.321030	1.322908	1.295306				
	8	1.232216	1.271140	1.287844	1.321028	1.322904	1.295310				
	9	1.232216	1.271140	1.287848	1.321032	1.322906	1.295308				
	10	1.232216	1.271140	1.287848	1.321034	1.322906	1.295306				
BARE AREA (mm2)	**1_L**	12.452	12.474	12.483	12.532	12.516	12.493				
	2_L	12.456	12.479	12.445	12.540	12.546	12.470				
	3_L	12.454	12.481	12.411	12.548	12.564	12.462				
	4_W	12.479	12.442	12.465	12.499	12.477	12.406				
	5_W	12.481	12.445	12.462	12.495	12.453	12.402				
	6_W	12.480	12.446	12.452	12.493	12.445	12.400				
BARE THICKNESS (mm)	**1**	1.118	1.124	1.130	1.151	1.154	1.141				
	2	1.103	1.124	1.134	1.153	1.159	1.146				
	3	1.034	1.082	1.113	1.118	1.131	1.116				
	4	1.092	1.112	1.129	1.137	1.148	1.137				
	5	1.073	1.108	1.122	1.142	1.148	1.134				

Table 86: Raw Data, Expt. #8, BDG-CO_2/650^{o}C/20MPa, 316L

		Measured Weight (g)									
	Meas #	L13	L14	L15	L16	L17	L18				
200 hrs	1	1.233598	1.272378	1.288914	1.322004	1.324102	1.296438				
	2	1.233596	1.272376	1.288914	1.322000	1.324108	1.296436				
	3	1.233598	1.272386	1.288918	1.322000	1.324108	1.296440				
	4	1.233598	1.272380	1.288916	1.322000	1.324098	1.296438				
	5	1.233606	1.272376	1.288918	1.321996	1.324104	1.296436				
	6	1.233604	1.272384	1.288910	1.321994	1.324108	1.296440				
	7	1.233602	1.272380	1.288914	1.321998	1.324104	1.296436				
	8	1.233602	1.272376	1.288916	1.322000	1.324100	1.296434				
	9	1.233598	1.272380	1.288908	1.322000	1.324102	1.296436				
	10	1.233606	1.272382	1.288914	1.322000	1.324104	1.296436				
400 hrs	1										
	2										
	3										
	4										
	5										
	6										
	7										
	8										
	9										
	10										
600 hrs	1										
	2										
	3										
	4										
	5										
	6										
	7										
	8										
	9										
	10										

		Measured Weight (g)									
	Meas #	L13	L14	L15	L16	L17	L18				
800 hrs	1										
	2										
	3										
	4										
	5										
	6										
	7										
	8										
	9										
	10										
1000 hrs	1										
	2										
	3										
	4										
	5										
	6										
	7										
	8										
	9										
	10										
1200 hrs	1										
	2										
	3										
	4										
	5										
	6										
	7										
	8										
	9										
	10										

Table 87: Raw Data, Expt. #8, BDG-CO_2/650°C/20MPa, Haynes 230

Project:	
Contact:	
MDS:	
Expt. #:	**8**
Phase:	II
Phase Type:	Bone Dry CO2
Temp. (°C):	650
Pressure (MPa):	20
Sample ID:	**Haynes 230**

Notes:

Rel. Uncertainty in Meas. Mass:	Δm = ± 0.000002 g
Rel. Uncertainty in Meas. Length:	Δl = ± 0.001 mm
Rel. Uncertainty in Meas. Width:	Δw = ± 0.001 mm
Uncertainty in Meas. Area:	ΔA = ± 0.000178 cm^2

Supplier/UNS ID:	
Metal Type:	
Color Designation:	
Hole Diameter in Sample (mm):	3

		Sample # / Description									
	Meas #	**HAY07**	**HAY08**	**HAY09**	**HAY10**	**HAY11**	**HAY12**				
BARE WEIGHT (gm)	**1**	2.603196	2.591636	2.607654	2.571584	2.629992	2.628586				
	2	2.603200	2.591632	2.607658	2.571584	2.629990	2.628588				
	3	2.603196	2.591630	2.607656	2.571582	2.629996	2.628584				
	4	2.603198	2.591634	2.607658	2.571582	2.629990	2.628586				
	5	2.603196	2.591634	2.607662	2.571584	2.629996	2.628584				
	6	2.603198	2.591630	2.607662	2.571580	2.629994	2.628590				
	7	2.603198	2.591628	2.607662	2.571588	2.629996	2.628592				
	8	2.603200	2.591630	2.607660	2.571584	2.629990	2.628586				
	9	2.603196	2.591634	2.607658	2.571586	2.630000	2.628588				
	10	2.603196	2.591636	2.607656	2.571582	2.629994	2.628586				
BARE AREA (mm2)	**1_L**	12.601	12.633	12.584	12.592	12.594	12.605				
	2_L	12.602	12.635	12.603	12.591	12.592	12.599				
	3_L	12.608	12.628	12.611	12.587	12.592	12.601				
	4_W	12.623	12.561	12.600	12.535	12.542	12.513				
	5_W	12.626	12.560	12.612	12.516	12.544	12.513				
	6_W	12.624	12.554	12.613	12.496	12.541	12.513				
BARE THICKNESS (mm)	**1**	2.003	2.002	2.002	1.997	2.034	2.023				
	2	1.997	1.990	1.997	1.991	2.034	2.028				
	3	1.957	1.946	1.968	1.954	1.977	1.985				
	4	1.989	1.976	1.992	1.980	2.023	2.013				
	5	1.980	1.979	1.985	1.979	2.004	2.001				

Table 88: Raw Data, Expt. #8, BDG-CO_2/650^{o}C/20MPa, Haynes 230

		Measured Weight (g)									
	Meas #	HAY07	HAY08	HAY09	HAY10	HAY11	HAY12				
200 hrs	1	2.603290	2.591748	2.607782	2.571684	2.630102	2.628738				
	2	2.603286	2.591740	2.607780	2.571684	2.630102	2.628736				
	3	2.603284	2.591742	2.607784	2.571682	2.630106	2.628740				
	4	2.603286	2.591742	2.607784	2.571678	2.630098	2.628732				
	5	2.603282	2.591740	2.607780	2.571686	2.630106	2.628736				
	6	2.603280	2.591740	2.607774	2.571680	2.630100	2.628734				
	7	2.603280	2.591746	2.607778	2.571676	2.630102	2.628732				
	8	2.603282	2.591744	2.607776	2.571676	2.630100	2.628738				
	9	2.603286	2.591746	2.607778	2.571680	2.630102	2.628734				
	10	2.603282	2.591740	2.607778	2.571680	2.630104	2.628736				
400 hrs	1										
	2										
	3										
	4										
	5										
	6										
	7										
	8										
	9										
	10										
600 hrs	1										
	2										
	3										
	4										
	5										
	6										
	7										
	8										
	9										
	10										

		Measured Weight (g)									
	Meas #	HAY07	HAY08	HAY09	HAY10	HAY11	HAY12				
800 hrs	1										
	2										
	3										
	4										
	5										
	6										
	7										
	8										
	9										
	10										
1000 hrs	1										
	2										
	3										
	4										
	5										
	6										
	7										
	8										
	9										
	10										
1200 hrs	1										
	2										
	3										
	4										
	5										
	6										
	7										
	8										
	9										
	10										

Table 89: Raw Data, Expt. #8, BDG-CO_2/650°C/20MPa, AFA-OC6

Project:	
Contact:	
MDS:	
Expt. #:	**8**
Phase:	II
Phase Type:	Bone Dry CO2
Temp. (°C):	650
Pressure (MPa):	20
Sample ID:	**AFA-OC6**
Notes:	

Rel. Uncertainty in Meas. Mass:	Δm = ± 0.000002 g
Rel. Uncertainty in Meas. Length:	Δl = ± 0.001 mm
Rel. Uncertainty in Meas. Width:	Δw = ± 0.001 mm
Uncertainty in Meas. Area:	ΔA = ± 0.00018 cm^2

Supplier/UNS ID:	
Metal Type:	
Color Designation:	
Hole Diameter in Sample (mm):	3

		Sample # / Description									
	Meas #	**A652**	**A653**	**A654**	**A655**	**A656**	**A657**				
BARE WEIGHT (gm)	**1**	1.737622	1.772050	1.789914	1.785938	1.797540	1.791600				
	2	1.737620	1.772058	1.789912	1.785938	1.797534	1.791588				
	3	1.737624	1.772052	1.789914	1.785944	1.797534	1.791594				
	4	1.737620	1.772050	1.789906	1.785944	1.797532	1.791594				
	5	1.737622	1.772050	1.789912	1.785940	1.797536	1.791594				
	6	1.737624	1.772054	1.789908	1.785938	1.797540	1.791596				
	7	1.737624	1.772050	1.789910	1.785942	1.797532	1.791596				
	8	1.737626	1.772056	1.789906	1.785942	1.797532	1.791594				
	9	1.737626	1.772050	1.789906	1.785938	1.797532	1.791590				
	10	1.737620	1.772050	1.789906	1.785940	1.797536	1.791596				
BARE AREA (mm2)	**1_L**	12.894	12.901	12.883	12.891	12.906	12.878				
	2_L	12.893	12.913	12.854	12.888	12.906	12.877				
	3_L	12.892	12.919	12.838	12.887	12.904	12.875				
	4_W	12.559	12.571	12.597	12.538	12.556	12.532				
	5_W	12.558	12.571	12.599	12.560	12.574	12.543				
	6_W	12.561	12.570	12.595	12.591	12.588	12.544				
BARE THICKNESS (mm)	**1**	1.543	1.560	1.566	1.565	1.568	1.570				
	2	1.541	1.561	1.568	1.568	1.573	1.577				
	3	1.469	1.517	1.543	1.539	1.544	1.543				
	4	1.529	1.549	1.558	1.557	1.563	1.564				
	5	1.512	1.546	1.558	1.557	1.558	1.564				

Table 90: Raw Data, Expt. #8, BDG-CO_2/650^{o}C/20MPa, AFA-OC6

		Measured Weight (g)									
	Meas #	A652	A653	A654	A655	A656	A657				
200 hrs	1	1.737612	1.772194	1.790160	1.785956	1.797604	1.791792				
	2	1.737614	1.772194	1.790162	1.785952	1.797606	1.791790				
	3	1.737614	1.772192	1.790160	1.785952	1.797610	1.791794				
	4	1.737618	1.772194	1.790156	1.785952	1.797604	1.791790				
	5	1.737608	1.772196	1.790160	1.785954	1.797612	1.791790				
	6	1.737614	1.772192	1.790160	1.785958	1.797610	1.791794				
	7	1.737614	1.772194	1.790160	1.785950	1.797608	1.791790				
	8	1.737618	1.772186	1.790158	1.785952	1.797602	1.791792				
	9	1.737614	1.772186	1.790156	1.785952	1.797608	1.791792				
	10	1.737616	1.772186	1.790160	1.785954	1.797602	1.791790				
400 hrs	1										
	2										
	3										
	4										
	5										
	6										
	7										
	8										
	9										
	10										
600 hrs	1										
	2										
	3										
	4										
	5										
	6										
	7										
	8										
	9										
	10										

		Measured Weight (g)									
	Meas #	A652	A653	A654	A655	A656	A657				
800 hrs	1										
	2										
	3										
	4										
	5										
	6										
	7										
	8										
	9										
	10										
1000 hrs	1										
	2										
	3										
	4										
	5										
	6										
	7										
	8										
	9										
	10										
1200 hrs	1										
	2										
	3										
	4										
	5										
	6										
	7										
	8										
	9										
	10										

Table 91: Raw Data, Expt. #8, BDG-CO_2/650°C/20MPa, 347SS

Project:	
Contact:	
MDS:	
Expt. #:	**8**
Phase:	II
Phase Type:	Bone Dry CO2
Temp. (°C):	650
Pressure (MPa):	20
Sample ID:	**347SS**

Notes:

Rel. Uncertainty in Meas. Mass:	Δm = ± 0.000002 g
Rel. Uncertainty in Meas. Length:	Δl = ± 0.001 mm
Rel. Uncertainty in Meas. Width:	Δw = ± 0.001 mm
Uncertainty in Meas. Area:	ΔA = ± 0.000182 cm^2

Supplier/UNS ID:	
Metal Type:	
Color Designation:	
Hole Diameter in Sample (mm):	3

		Sample # / Description									
	Meas #	**S52**	**S53**	**S54**	**S55**	**S56**	**S57**				
BARE WEIGHT (gm)	**1**	1.802552	1.856070	1.844400	1.874468	1.879122	1.879420				
	2	1.802556	1.856070	1.844404	1.874466	1.879114	1.879416				
	3	1.802556	1.856072	1.844404	1.874466	1.879120	1.879416				
	4	1.802560	1.856072	1.844400	1.874466	1.879116	1.879420				
	5	1.802558	1.856074	1.844402	1.874464	1.879122	1.879416				
	6	1.802556	1.856072	1.844396	1.874464	1.879116	1.879420				
	7	1.802554	1.856074	1.844402	1.874460	1.879118	1.879418				
	8	1.802556	1.856072	1.844404	1.874460	1.879116	1.879418				
	9	1.802560	1.856068	1.844402	1.874468	1.879114	1.879416				
	10	1.802558	1.856074	1.844402	1.874464	1.879118	1.879416				
BARE AREA (mm2)	**1_L**	13.053	13.091	13.155	13.090	13.091	13.060				
	2_L	13.065	13.104	13.130	13.118	13.103	13.060				
	3_L	13.076	13.111	13.115	13.129	13.101	13.059				
	4_W	12.598	12.570	12.582	12.579	12.591	12.581				
	5_W	12.596	12.599	12.577	12.593	12.591	12.602				
	6_W	12.595	12.605	12.573	12.585	12.590	12.615				
BARE THICKNESS (mm)	**1**	1.510	1.546	1.540	1.556	1.559	1.560				
	2	1.512	1.550	1.544	1.562	1.566	1.568				
	3	1.449	1.506	1.484	1.525	1.530	1.539				
	4	1.495	1.538	1.535	1.545	1.552	1.558				
	5	1.484	1.529	1.509	1.549	1.548	1.555				

Table 92: Raw Data, Expt. #8, BDG-CO_2/650^{o}C/20MPa, 347SS

		Measured Weight (g)									
	Meas #	S52	S53	S54	S55	S56	S57				
200 hrs	1	1.802856	1.856368	1.844694	1.874798	1.879374	1.879730				
	2	1.802854	1.856366	1.844688	1.874792	1.879376	1.879722				
	3	1.802856	1.856370	1.844692	1.874796	1.879384	1.879728				
	4	1.802852	1.856374	1.844686	1.874796	1.879380	1.879722				
	5	1.802856	1.856368	1.844694	1.874794	1.879382	1.879732				
	6	1.802858	1.856370	1.844686	1.874794	1.879382	1.879732				
	7	1.802852	1.856368	1.844688	1.874796	1.879382	1.879724				
	8	1.802852	1.856370	1.844688	1.874796	1.879382	1.879732				
	9	1.802856	1.856370	1.844688	1.874790	1.879380	1.879730				
	10	1.802852	1.856368	1.844692	1.874798	1.879380	1.879722				
400 hrs	1										
	2										
	3										
	4										
	5										
	6										
	7										
	8										
	9										
	10										
600 hrs	1										
	2										
	3										
	4										
	5										
	6										
	7										
	8										
	9										
	10										

		Measured Weight (g)									
	Meas #	S52	S53	S54	S55	S56	S57				
800 hrs	1										
	2										
	3										
	4										
	5										
	6										
	7										
	8										
	9										
	10										
1000 hrs	1										
	2										
	3										
	4										
	5										
	6										
	7										
	8										
	9										
	10										
1200 hrs	1										
	2										
	3										
	4										
	5										
	6										
	7										
	8										
	9										
	10										

Table 93: Raw Data, Expt. #9, RG-CO_2/550^{o}C/20MPa, Coupon Arrangement

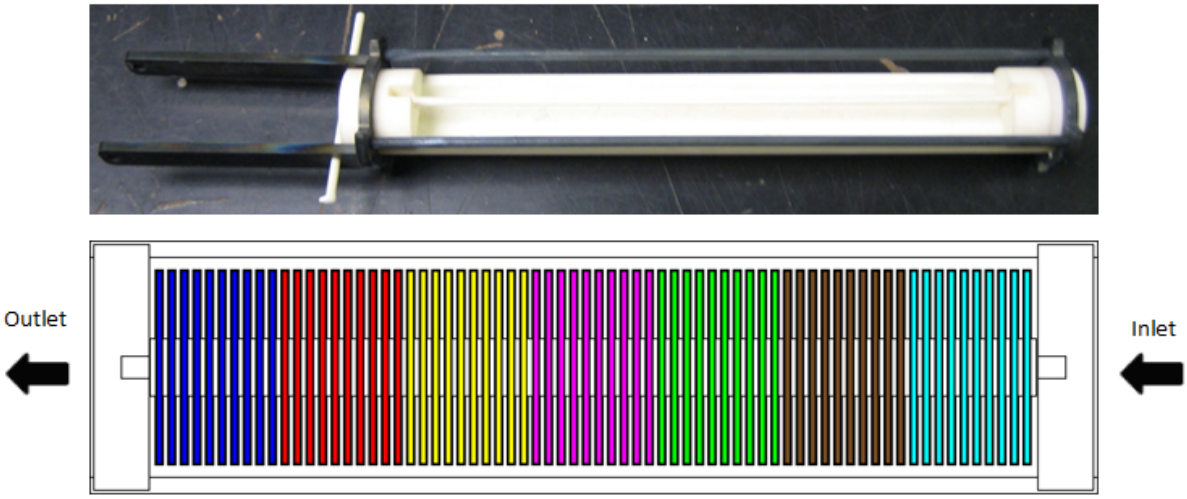

Sample	Blue **Al-Coat**	Red **Al-Coat**	Yellow **Y-Coat**	Magenta **Y-Coat**	Green **Peened**	Brown **Peened**	Cyan
1	H32	N31	H42	N44	H52	N57	
2	H33	N32	H43	N45	H53	N58	
3	H34	N33	H44	N46	H54	N59	
4	H35	N34	H45	N47	H55	N60	
5	H36	N35	H46	N48	H56	N61	
6	H37	N36	H47	N49	H57	N62	
7	H38	N37	H48	N50	H58	N63	
8	H39	N38	H49	N51	H59	N64	
9	H40	N39	H50	N52	H60	N65	
10	H41	N40	H51	N53	H61	N66	

Table 94: Raw Data, Expt. #9, RG-CO_2/550°C/20MPa, HCM12A Al-Coated

Project:	**SCCO2**
Contact:	PRJ39TC
MDS:	24386
Expt. #:	**7**
Phase:	**Aluminum Coated**
Phase Type:	Research CO2
Temp. (°C):	550
Pressure (MPa):	20
Sample ID:	**HCM12A**
Notes:	Bare weight is meas weight of samples after coating

Rel. Uncertainty in Meas. Mass:	Δm = ± 0.000002 g
Rel. Uncertainty in Meas. Length:	Δl = ± 0.001 mm
Rel. Uncertainty in Meas. Width:	Δw = ± 0.001 mm
Uncertainty in Meas. Area:	ΔA = ± 0.000179 cm^2

Supplier/UNS ID:	
Metal Type:	
Color Designation:	
Hole Diameter in Sample (mm):	3

		Sample # / Description									
	Meas #	**H32**	**H33**	**H34**	**H35**	**H36**	**H37**	**H38**	**H39**	**H40**	**H41**
COATED WEIGHT (gm)	**1**	1.825242	1.845860	1.791540	1.793060	1.811400	1.819174	1.800782	1.824968	1.835884	1.845392
	2	1.825240	1.845860	1.791542	1.793062	1.811398	1.819172	1.800778	1.824962	1.835882	1.845394
	3	1.825242	1.845864	1.791546	1.793062	1.811402	1.819182	1.800776	1.824960	1.835882	1.845400
	4	1.825244	1.845854	1.791540	1.793054	1.811398	1.819180	1.800776	1.824970	1.835884	1.845400
	5	1.825242	1.845862	1.791542	1.793060	1.811396	1.819180	1.800780	1.824972	1.835880	1.845400
	6	1.825238	1.845866	1.791542	1.793060	1.811400	1.819176	1.800774	1.824962	1.835878	1.845390
	7	1.825232	1.845864	1.791550	1.793062	1.811398	1.819176	1.800782	1.824966	1.835882	1.845398
	8	1.825240	1.845866	1.791544	1.793066	1.811396	1.819174	1.800780	1.824970	1.835886	1.845394
	9	1.825240	1.845864	1.791548	1.793062	1.811402	1.819186	1.800776	1.824964	1.835882	1.845390
	10	1.825234	1.845864	1.791542	1.793056	1.811398	1.819178	1.800776	1.824972	1.835876	1.845394
BARE AREA (mm2)	**1_L**	12.671	12.686	12.626	12.699	12.710	12.687	12.701	12.682	12.689	12.721
	2_L	12.691	12.691	12.679	12.717	12.712	12.685	12.713	12.683	12.688	12.713
	3_L	12.694	12.685	12.699	12.719	12.710	12.678	12.713	12.681	12.686	12.708
	4_W	12.582	12.652	12.598	12.644	12.641	12.666	12.659	12.643	12.694	12.652
	5_W	12.590	12.678	12.609	12.647	12.644	12.677	12.654	12.644	12.687	12.654
	6_W	12.593	12.689	12.610	12.622	12.641	12.679	12.646	12.646	12.677	12.656
BARE THICKNESS (mm)	**1**	1.528	1.549	1.504	1.509	1.531	1.563	1.542	1.566	1.572	1.575
	2	1.540	1.556	1.524	1.510	1.534	1.566	1.546	1.571	1.577	1.579
	3	1.536	1.547	1.524	1.495	1.513	1.498	1.502	1.526	1.532	1.547
	4	1.533	1.550	1.531	1.505	1.529	1.556	1.540	1.556	1.566	1.571
	5	1.531	1.548	1.503	1.503	1.513	1.550	1.526	1.557	1.556	1.564

Table 95: Raw Data, Expt. #9, RG-CO_2/550^{o}C/20MPa, HCM12A Al-Coated

		Measured Weight (g)									
	Meas #	H32	H33	H34	H35	H36	H37	H38	H39	H40	H41
200 hrs	1	1.825944	1.846460	1.792176	1.793936	1.812288	1.819712	1.801460	1.825604	1.836486	1.846034
	2	1.825946	1.846456	1.792178	1.793936	1.812284	1.819722	1.801458	1.825596	1.836488	1.846024
	3	1.82594	1.846464	1.792170	1.793932	1.812284	1.819714	1.801452	1.825600	1.836494	1.846032
	4	1.825942	1.846462	1.792182	1.793936	1.812286	1.819716	1.801456	1.825602	1.836490	1.846034
	5	1.825942	1.846456	1.792178	1.793934	1.812282	1.819716	1.801460	1.825596	1.836494	1.846032
	6	1.825936	1.846466	1.792180	1.793932	1.812284	1.819714	1.801456	1.825598	1.836486	1.846034
	7	1.825942	1.846462	1.792178	1.793936	1.812288	1.819722	1.801454	1.825606	1.836484	1.846028
	8	1.825938	1.846464	1.792178	1.793938	1.812286	1.819720	1.801458	1.825600	1.836486	1.846032
	9	1.825940	1.846456	1.792178	1.793934	1.812280	1.819714	1.801460	1.825600	1.836488	1.846032
	10	1.825938	1.846460	1.792180	1.793936	1.812282	1.819718	1.801456	1.825600	1.836488	1.846034
400 hrs	1			1.792452	1.794212	1.812606	1.819948	1.801704	1.825850	1.836712	1.846302
	2			1.792454	1.794218	1.812604	1.819952	1.801706	1.825860	1.836714	1.846294
	3			1.792454	1.794216	1.812604	1.819950	1.801710	1.825860	1.836720	1.846292
	4			1.792456	1.794214	1.812602	1.819946	1.801714	1.825858	1.836712	1.846292
	5			1.792454	1.794216	1.812602	1.819956	1.801706	1.825860	1.836722	1.846298
	6			1.792450	1.794216	1.812602	1.819956	1.801704	1.825852	1.836712	1.846300
	7			1.792446	1.794218	1.812602	1.819956	1.801714	1.825854	1.836712	1.846298
	8			1.792456	1.794216	1.812610	1.819950	1.801708	1.825858	1.836714	1.846302
	9			1.792456	1.794220	1.812604	1.819948	1.801710	1.825860	1.836716	1.846298
	10			1.792454	1.794218	1.812602	1.819952	1.801714	1.825856	1.836712	1.846300
600 hrs	1							1.801944	1.826094	1.836922	1.846526
	2							1.801936	1.826098	1.836924	1.846530
	3							1.801942	1.826096	1.836922	1.846530
	4							1.801938	1.826100	1.836930	1.846526
	5							1.801944	1.826096	1.836928	1.846532
	6							1.801938	1.826096	1.836930	1.846524
	7							1.801936	1.826098	1.836932	1.846534
	8							1.801940	1.826100	1.836932	1.846532
	9							1.801938	1.826104	1.836926	1.846530
	10							1.801934	1.826098	1.836930	1.846526

		Measured Weight (g)									
	Meas #	H32	H33	H34	H35	H36	H37	H38	H39	H40	H41
800 hrs	1							1.802164	1.826340	1.837138	1.846766
	2							1.802174	1.826340	1.837130	1.846766
	3							1.802172	1.826338	1.837132	1.846768
	4							1.802174	1.826342	1.837134	1.846762
	5							1.802174	1.826342	1.837136	1.846766
	6							1.802166	1.826338	1.837136	1.846768
	7							1.802164	1.826338	1.837134	1.846768
	8							1.802164	1.826336	1.837132	1.846766
	9							1.802166	1.826336	1.837134	1.846768
	10							1.802172	1.826340	1.837134	1.846766
1000 hrs	1							1.802342	1.826538	1.837306	1.846964
	2							1.802352	1.826540	1.837308	1.846960
	3							1.802350	1.826538	1.837300	1.846960
	4							1.802352	1.826538	1.837302	1.846962
	5							1.802348	1.826532	1.837302	1.846968
	6							1.802350	1.826538	1.837302	1.846966
	7							1.802344	1.826540	1.837304	1.846964
	8							1.802352	1.826534	1.837302	1.846962
	9							1.802342	1.826532	1.837300	1.846964
	10							1.802344	1.826542	1.837302	1.846960
1200 hrs	1										
	2										
	3										
	4										
	5										
	6										
	7										
	8										
	9										
	10										

Table 96: Raw Data, Expt. #9, RG-CO_2/550°C/20MPa, NF616 Al-Coated

Project:	**SCCO2**
Contact:	PRJ39TC
MDS:	24386
Expt. #:	**7**
Phase:	**Al-Coated**
Phase Type:	Research CO2
Temp. (°C):	550
Pressure (MPa):	20
Sample ID:	**NF616**
Notes:	Bare weight is meas weight of samples after coating

Rel. Uncertainty in Meas. Mass:	Δm = ± 0.000002 g
Rel. Uncertainty in Meas. Length:	Δl = ± 0.001 mm
Rel. Uncertainty in Meas. Width:	Δw = ± 0.001 mm
Uncertainty in Meas. Area:	ΔA = ± 0.000178 cm^2

Supplier/UNS ID:	
Metal Type:	
Color Designation:	
Hole Diameter in Sample (mm):	3

		Sample # / Description									
	Meas #	**N31**	**N32**	**N33**	**N34**	**N35**	**N36**	**N37**	**N38**	**N39**	**N40**
COATED WEIGHT (gm)	**1**	1.721224	1.770414	1.764326	1.743092	1.775974	1.798992	1.822726	1.818224	1.820570	1.836138
	2	1.721226	1.770410	1.764326	1.743090	1.775986	1.798990	1.822724	1.818226	1.820568	1.836136
	3	1.721222	1.770406	1.764324	1.743092	1.775982	1.798988	1.822724	1.818226	1.820570	1.836138
	4	1.721220	1.770408	1.764324	1.743092	1.775982	1.798984	1.822726	1.818224	1.820574	1.836142
	5	1.721220	1.770410	1.764326	1.743088	1.775984	1.798986	1.822728	1.818220	1.820572	1.836140
	6	1.721226	1.770414	1.764328	1.743082	1.775986	1.798992	1.822720	1.818218	1.820576	1.836146
	7	1.721218	1.770408	1.764328	1.743084	1.775984	1.798992	1.822720	1.818224	1.820574	1.836146
	8	1.721220	1.770410	1.764330	1.743090	1.775986	1.798994	1.822718	1.818224	1.820572	1.836146
	9	1.721218	1.770406	1.764332	1.743088	1.775986	1.798996	1.822728	1.818222	1.820568	1.836144
	10	1.721218	1.770408	1.764328	1.743090	1.775984	1.798984	1.822728	1.818222	1.820570	1.836142
BARE AREA (mm2)	**1_L**	12.501	12.592	12.479	12.570	12.574	12.652	12.648	12.652	12.651	12.653
	2_L	12.464	12.585	12.493	12.546	12.561	12.646	12.644	12.644	12.651	12.651
	3_L	12.420	12.544	12.495	12.539	12.541	12.629	12.637	12.620	12.648	12.645
	4_W	12.514	12.455	12.528	12.309	12.488	12.636	12.654	12.613	12.629	12.634
	5_W	12.505	12.461	12.515	12.327	12.517	12.637	12.662	12.629	12.627	12.627
	6_W	12.484	12.451	12.497	12.337	12.524	12.634	12.660	12.632	12.614	12.618
BARE THICKNESS (mm)	**1**	1.556	1.577	1.565	1.578	1.578	1.561	1.569	1.574	1.577	1.584
	2	1.551	1.578	1.565	1.578	1.576	1.560	1.573	1.577	1.576	1.587
	3	1.510	1.550	1.556	1.558	1.561	1.512	1.540	1.549	1.530	1.556
	4	1.535	1.569	1.561	1.573	1.571	1.548	1.558	1.574	1.551	1.571
	5	1.550	1.575	1.562	1.575	1.576	1.547	1.565	1.547	1.574	1.581

Table 97: Raw Data, Expt. #9, RG-CO_2/550^{o}C/20MPa, NF616 Al-Coated

		Measured Weight (g)									
	Meas #	N31	N32	N33	N34	N35	N36	N37	N38	N39	N40
200 hrs	1	1.724476	1.772772	1.766742	1.745710	1.778130	1.801918	1.825904	1.821476	1.824036	1.839876
	2	1.724486	1.772772	1.766748	1.745716	1.778138	1.801922	1.825902	1.821474	1.824036	1.839876
	3	1.724482	1.772762	1.766748	1.745706	1.778140	1.801922	1.825902	1.821472	1.824038	1.839878
	4	1.724486	1.772768	1.766746	1.745716	1.778140	1.801922	1.825904	1.821476	1.824038	1.839876
	5	1.724478	1.772764	1.766746	1.745706	1.778134	1.801926	1.825896	1.821478	1.824034	1.839878
	6	1.724476	1.772766	1.766740	1.745706	1.778132	1.801928	1.825896	1.821474	1.824040	1.839878
	7	1.724476	1.772762	1.766738	1.745710	1.778130	1.801928	1.825902	1.821474	1.824040	1.839886
	8	1.724484	1.772764	1.766738	1.745714	1.778134	1.801926	1.825894	1.821470	1.824036	1.839882
	9	1.724486	1.772762	1.766738	1.745708	1.778132	1.801928	1.825904	1.821472	1.824030	1.839878
	10	1.724484	1.772764	1.766748	1.745706	1.778132	1.801928	1.825902	1.821476	1.824036	1.839880
400 hrs	1			1.768092	1.747258	1.779408	1.803534	1.827638	1.823270	1.825968	1.841926
	2			1.768102	1.747266	1.779398	1.803528	1.827640	1.823270	1.825968	1.841930
	3			1.768092	1.747260	1.779406	1.803526	1.827648	1.823272	1.825966	1.841934
	4			1.768102	1.747266	1.779404	1.803526	1.827640	1.823276	1.825966	1.841924
	5			1.768094	1.747268	1.779398	1.803524	1.827646	1.823278	1.825972	1.841926
	6			1.768098	1.747260	1.779400	1.803524	1.827638	1.823268	1.825970	1.841924
	7			1.768100	1.747258	1.779408	1.803534	1.827640	1.823278	1.825968	1.841924
	8			1.768096	1.747268	1.779398	1.803526	1.827638	1.823268	1.825964	1.841928
	9			1.768098	1.747258	1.779406	1.803524	1.827642	1.823268	1.825964	1.841930
	10			1.768094	1.747260	1.779408	1.803526	1.827640	1.823270	1.825966	1.841928
600 hrs	1							1.829488	1.825130	1.827936	1.844068
	2							1.829494	1.825132	1.827930	1.844070
	3							1.829494	1.825128	1.827936	1.844068
	4							1.829492	1.825134	1.827932	1.844068
	5							1.829492	1.825126	1.827930	1.844072
	6							1.829490	1.825128	1.827930	1.844072
	7							1.829488	1.825130	1.827932	1.844066
	8							1.829490	1.825132	1.827934	1.844064
	9							1.829488	1.825132	1.827936	1.844074
	10							1.829488	1.825128	1.827932	1.844074

		Measured Weight (g)									
	Meas #	N31	N32	N33	N34	N35	N36	N37	N38	N39	N40
800 hrs	1							1.831372	1.826980	1.829938	1.846258
	2							1.831378	1.826984	1.829936	1.846254
	3							1.831378	1.826984	1.829932	1.846258
	4							1.831376	1.826982	1.829942	1.846254
	5							1.831376	1.826980	1.829940	1.846252
	6							1.831372	1.826988	1.829936	1.846256
	7							1.831372	1.826982	1.829938	1.846258
	8							1.831374	1.826980	1.829940	1.846258
	9							1.831374	1.826984	1.829936	1.846252
	10							1.831372	1.826980	1.829938	1.846254
1000 hrs	1							1.833318	1.828784	1.831922	1.848512
	2							1.833314	1.828782	1.831928	1.848512
	3							1.833318	1.828774	1.831924	1.848514
	4							1.833314	1.828778	1.831920	1.848518
	5							1.833314	1.828774	1.831926	1.848516
	6							1.833314	1.828774	1.831922	1.848512
	7							1.833316	1.828778	1.831922	1.848514
	8							1.833314	1.828780	1.831920	1.848516
	9							1.833320	1.828774	1.831922	1.848512
	10							1.833318	1.828774	1.831924	1.848514
1200 hrs	1										
	2										
	3										
	4										
	5										
	6										
	7										
	8										
	9										
	10										

Table 98: Raw Data, Expt. #9, RG-CO_2/550°C/20MPa, HCM12A Y-Coated

Project:	**SCCO2**
Contact:	PRJ39TC
MDS:	24386
Expt. #:	**7**
Phase:	**Y-Coated**
Phase Type:	Research CO2
Temp. (°C):	550
Pressure (MPa):	20
Sample ID:	**HCM12A**
Notes:	Bare weight is meas weight of samples after coating

Rel. Uncertainty in Meas. Mass:	Δm = ± 0.000002 g
Rel. Uncertainty in Meas. Length:	Δl = ± 0.001 mm
Rel. Uncertainty in Meas. Width:	Δw = ± 0.001 mm
Uncertainty in Meas. Area:	ΔA = ± 0.000178 cm^2

Supplier/UNS ID:	
Metal Type:	
Color Designation:	
Hole Diameter in Sample (mm):	3

		Sample # / Description									
	Meas #	**H42**	**H43**	**H44**	**H45**	**H46**	**H47**	**H48**	**H49**	**H50**	**H51**
COATED WEIGHT (gm)	**1**	1.666864	1.761748	1.759558	1.788938	1.781780	1.782118	1.788328	1.794786	1.797204	1.801020
	2	1.666862	1.761748	1.759556	1.788946	1.781782	1.782122	1.788334	1.794778	1.797212	1.801026
	3	1.666862	1.761742	1.759556	1.788938	1.781774	1.782118	1.788328	1.794782	1.797216	1.801016
	4	1.666858	1.761752	1.759560	1.788940	1.781780	1.782126	1.788330	1.794786	1.797212	1.801016
	5	1.666862	1.761738	1.759570	1.788948	1.781774	1.782122	1.788324	1.794782	1.797216	1.801012
	6	1.666864	1.761750	1.759560	1.788938	1.781776	1.782118	1.788326	1.794788	1.797212	1.801014
	7	1.666860	1.761742	1.759568	1.788938	1.781778	1.782126	1.788332	1.794784	1.797214	1.801016
	8	1.666860	1.761750	1.759562	1.788944	1.781780	1.782120	1.788324	1.794776	1.797210	1.801016
	9	1.666860	1.761740	1.759558	1.788944	1.781780	1.782126	1.788328	1.794778	1.797216	1.801022
	10	1.666862	1.761746	1.759558	1.788948	1.781776	1.782126	1.788328	1.794786	1.797206	1.801014
BARE AREA (mm2)	**1_L**	12.544	12.588	12.598	12.624	12.598	12.570	12.653	12.646	12.656	12.599
	2_L	12.528	12.585	12.605	12.612	12.597	12.570	12.650	12.642	12.652	12.594
	3_L	12.510	12.584	12.622	12.607	12.590	12.562	12.650	12.640	12.648	12.591
	4_W	12.476	12.531	12.574	12.585	12.641	12.610	12.591	12.590	12.565	12.606
	5_W	12.483	12.525	12.563	12.575	12.632	12.628	12.576	12.585	12.565	12.600
	6_W	12.487	12.519	12.557	12.565	12.632	12.636	12.568	12.570	12.563	12.594
BARE THICKNESS (mm)	**1**	1.510	1.550	1.541	1.558	1.546	1.552	1.555	1.560	1.556	1.563
	2	1.504	1.550	1.542	1.560	1.550	1.554	1.558	1.563	1.560	1.567
	3	1.408	1.500	1.495	1.521	1.504	1.514	1.525	1.531	1.541	1.544
	4	1.485	1.530	1.530	1.550	1.543	1.549	1.548	1.552	1.551	1.561
	5	1.468	1.530	1.523	1.545	1.529	1.534	1.541	1.548	1.555	1.559

Table 99: Raw Data, Expt. #9, RG-CO_2/550°C/20MPa, HCM12A Y-Coated

		Measured Weight (g)									
	Meas #	H42	H43	H44	H45	H46	H47	H48	H49	H50	H51
200 hrs	1	1.667266	1.762128	1.759962	1.789372	1.782180	1.782524	1.788778	1.795182	1.797570	1.801472
	2	1.667264	1.762122	1.759962	1.789368	1.782172	1.782524	1.788778	1.795176	1.797568	1.801472
	3	1.667258	1.762122	1.759960	1.789362	1.782176	1.782516	1.788782	1.795182	1.797566	1.801468
	4	1.667266	1.762118	1.759966	1.789364	1.782178	1.782518	1.788776	1.795182	1.797576	1.801470
	5	1.667264	1.762126	1.759962	1.789366	1.782178	1.782516	1.788784	1.795172	1.797576	1.801470
	6	1.667268	1.762120	1.759958	1.789366	1.782178	1.782516	1.788776	1.795182	1.797574	1.801472
	7	1.667262	1.762118	1.759966	1.789368	1.782180	1.782522	1.788784	1.795174	1.797574	1.801470
	8	1.667264	1.762124	1.759956	1.789368	1.782182	1.782520	1.788774	1.795182	1.797566	1.801462
	9	1.667266	1.762120	1.759956	1.789362	1.782182	1.782516	1.788774	1.795174	1.797564	1.801468
	10	1.667262	1.762122	1.759964	1.789364	1.782174	1.782522	1.788778	1.795178	1.797566	1.801470
400 hrs	1					1.782336	1.782680	1.788920	1.795338		
	2					1.782342	1.782676	1.788918	1.795336		
	3					1.782338	1.782676	1.788918	1.795342		
	4					1.782342	1.782682	1.788924	1.795338		
	5					1.782332	1.782676	1.788922	1.795340		
	6					1.782334	1.782672	1.788926	1.795336		
	7					1.782336	1.782672	1.788916	1.795338		
	8					1.782332	1.782672	1.788916	1.795336		
	9					1.782336	1.782676	1.788920	1.795334		
	10					1.782338	1.782674	1.788918	1.795332		
600 hrs	1					1.782482	1.782818	1.789082			
	2					1.782482	1.782818	1.789078			
	3					1.782480	1.782818	1.789076			
	4					1.782482	1.782816	1.789080			
	5					1.782480	1.782818	1.789078			
	6					1.782480	1.782822	1.789078			
	7					1.782480	1.782818	1.789082			
	8					1.782480	1.782818	1.789076			
	9					1.782476	1.782822	1.789076			
	10					1.782478	1.782822	1.789078			

		Measured Weight (g)									
	Meas #	H42	H43	H44	H45	H46	H47	H48	H49	H50	H51
800 hrs	1					1.782644	1.782974	1.789254	1.795526		
	2					1.782644	1.782972	1.789258	1.795520		
	3					1.782642	1.782972	1.789250	1.795522		
	4					1.782644	1.782968	1.789252	1.795526		
	5					1.782646	1.782970	1.789252	1.795526		
	6					1.782642	1.782972	1.789250	1.795524		
	7					1.782644	1.782968	1.789250	1.795524		
	8					1.782642	1.782970	1.789256	1.795518		
	9					1.782642	1.782972	1.789250	1.795520		
	10					1.782644	1.782976	1.789252	1.795524		
1000 hrs	1					1.782818	1.783118	1.789430	1.795712		
	2					1.782826	1.783120	1.789432	1.795710		
	3					1.782826	1.783116	1.789430	1.795704		
	4					1.782828	1.783114	1.789430	1.795712		
	5					1.782818	1.783120	1.789432	1.795706		
	6					1.782826	1.783118	1.789430	1.795708		
	7					1.782822	1.783116	1.789436	1.795708		
	8					1.782824	1.783116	1.789434	1.795710		
	9					1.782826	1.783120	1.789430	1.795704		
	10					1.782828	1.783118	1.789432	1.795708		
1200 hrs	1										
	2										
	3										
	4										
	5										
	6										
	7										
	8										
	9										
	10										

Table 100: Raw Data, Expt. #9, RG-CO_2/550°C/20MPa, NF616 Y-Coated

Project:	**SCCO2**
Contact:	PRJ39TC
MDS:	24386
Expt. #:	**7**
Phase:	**Y-Coated**
Phase Type:	Research CO2
Temp. (°C):	550
Pressure (MPa):	20
Sample ID:	**NF616**
Notes:	Bare weight is meas weight of samples after coating

Rel. Uncertainty in Meas. Mass:	Δm = ± 0.000002 g
Rel. Uncertainty in Meas. Length:	Δl = ± 0.001 mm
Rel. Uncertainty in Meas. Width:	Δw = ± 0.001 mm
Uncertainty in Meas. Area:	ΔA = ± 0.000179 cm^2

Supplier/UNS ID:	
Metal Type:	
Color Designation:	
Hole Diameter in Sample (mm):	3

		Sample # / Description									
	Meas #	**N44**	**N45**	**N46**	**N47**	**N48**	**N49**	**N50**	**N51**	**N52**	**N53**
BARE WEIGHT (gm)	**1**	1.789584	1.811770	1.793678	1.806584	1.766808	1.791582	1.822936	1.772092	1.821846	1.808552
	2	1.789588	1.811768	1.793672	1.806586	1.766804	1.791582	1.822934	1.772096	1.821848	1.808554
	3	1.789586	1.811766	1.793682	1.806584	1.766812	1.791574	1.822932	1.772098	1.821842	1.808548
	4	1.789582	1.811768	1.793674	1.806590	1.766810	1.791578	1.822934	1.772090	1.821852	1.808548
	5	1.789586	1.811766	1.793676	1.806580	1.766806	1.791574	1.822932	1.772092	1.821842	1.808550
	6	1.789582	1.811766	1.793682	1.806586	1.766802	1.791572	1.822928	1.772090	1.821846	1.808556
	7	1.789586	1.811760	1.793672	1.806586	1.766802	1.791576	1.822930	1.772100	1.821844	1.808550
	8	1.789582	1.811764	1.793680	1.806588	1.766812	1.791576	1.822932	1.772098	1.821844	1.808556
	9	1.789582	1.811770	1.793676	1.806586	1.766806	1.791576	1.822926	1.772100	1.821852	1.808554
	10	1.789580	1.811766	1.793676	1.806580	1.766804	1.791574	1.822930	1.772098	1.821850	1.808552
BARE AREA (mm2)	**1_L**	12.655	12.658	12.646	12.637	12.644	12.661	12.668	12.621	12.629	12.632
	2_L	12.676	12.657	12.657	12.637	12.648	12.659	12.674	12.624	12.627	12.613
	3_L	12.676	12.642	12.658	12.638	12.650	12.650	12.674	12.622	12.621	12.624
	4_W	12.633	12.627	12.655	12.614	12.639	12.639	12.618	12.639	12.646	12.673
	5_W	12.634	12.620	12.650	12.608	12.630	12.634	12.620	12.634	12.648	12.673
	6_W	12.630	12.615	12.640	12.591	12.615	12.622	12.614	12.616	12.649	12.669
BARE THICKNESS (mm)	**1**	1.561	1.566	1.558	1.567	1.538	1.559	1.580	1.548	1.574	1.567
	2	1.563	1.572	1.560	1.569	1.541	1.559	1.578	1.533	1.575	1.552
	3	1.509	1.544	1.511	1.533	1.506	1.496	1.535	1.522	1.560	1.559
	4	1.559	1.537	1.547	1.563	1.540	1.543	1.569	1.539	1.564	1.566
	5	1.529	1.569	1.529	1.549	1.501	1.547	1.562	1.544	1.573	1.562

Table 101: Raw Data, Expt. #9, RG-CO_2/550°C/20MPa, NF616 Y-Coated

		Measured Weight (g)									
	Meas #	N44	N45	N46	N47	N48	N49	N50	N51	N52	N53
200 hrs	1	1.790086	1.812286	1.794164	1.807072	1.767338	1.792064	1.823410	1.772614	1.822376	1.809074
	2	1.790084	1.812294	1.794158	1.807072	1.767336	1.792060	1.823408	1.772614	1.822372	1.809074
	3	1.790090	1.812284	1.794164	1.807068	1.767336	1.792064	1.823404	1.772624	1.822376	1.809072
	4	1.790090	1.812288	1.794158	1.807068	1.767336	1.792058	1.823406	1.772614	1.822382	1.809066
	5	1.790082	1.812290	1.794166	1.807072	1.767344	1.792054	1.823412	1.772616	1.822372	1.809064
	6	1.790086	1.812286	1.794158	1.807078	1.767336	1.792062	1.823402	1.772614	1.822380	1.809068
	7	1.790090	1.812284	1.794168	1.807076	1.767336	1.792062	1.823408	1.772614	1.822382	1.809066
	8	1.790090	1.812286	1.794166	1.807074	1.767334	1.792064	1.823402	1.772614	1.822372	1.809072
	9	1.790092	1.812288	1.794158	1.807072	1.767340	1.792062	1.823412	1.772616	1.822372	1.809068
	10	1.790090	1.812286	1.794160	1.807076	1.767336	1.792064	1.823408	1.772614	1.822374	1.809070
400 hrs	1			1.794372	1.807304	1.767572	1.792262	1.823604	1.772872	1.822646	1.809300
	2			1.794372	1.807300	1.767562	1.792256	1.823600	1.772870	1.822656	1.809302
	3			1.794374	1.807294	1.767564	1.792264	1.823604	1.772872	1.822648	1.809304
	4			1.794378	1.807302	1.767566	1.792256	1.823600	1.772866	1.822656	1.809294
	5			1.794368	1.807298	1.767562	1.792258	1.823598	1.772872	1.822646	1.809296
	6			1.794378	1.807302	1.767570	1.792256	1.823602	1.772868	1.822646	1.809298
	7			1.794372	1.807304	1.767572	1.792262	1.823608	1.772862	1.822646	1.809304
	8			1.794374	1.807294	1.767562	1.792262	1.823600	1.772866	1.822656	1.809296
	9			1.794368	1.807300	1.767564	1.792260	1.823600	1.772868	1.822648	1.809304
	10			1.794376	1.807298	1.767568	1.792262	1.823602	1.772872	1.822648	1.809300
600 hrs	1					1.767820	1.792486	1.823840	1.773172		
	2					1.767820	1.792482	1.823840	1.773174		
	3					1.767816	1.792484	1.823838	1.773166		
	4					1.767816	1.792484	1.823842	1.773176		
	5					1.767818	1.792486	1.823836	1.773168		
	6					1.767818	1.792490	1.823834	1.773168		
	7					1.767820	1.792486	1.823834	1.773166		
	8					1.767818	1.792488	1.823836	1.773168		
	9					1.767820	1.792484	1.823834	1.773166		
	10					1.767818	1.792482	1.823842	1.773170		

		Measured Weight (g)									
	Meas #	N44	N45	N46	N47	N48	N49	N50	N51	N52	N53
800 hrs	1					1.768244	1.792846	1.824190	1.773632		
	2					1.768248	1.792846	1.824186	1.773632		
	3					1.768246	1.792848	1.824188	1.773638		
	4					1.768244	1.792846	1.824184	1.773634		
	5					1.768248	1.792844	1.824186	1.773634		
	6					1.768246	1.792844	1.824182	1.773632		
	7					1.768250	1.792846	1.824184	1.773632		
	8					1.768250	1.792846	1.824182	1.773634		
	9					1.768244	1.792842	1.824184	1.773636		
	10					1.768246	1.792844	1.824186	1.773634		
1000 hrs	1					1.768744	1.793272	1.824580	1.774160		
	2					1.768746	1.793274	1.824578	1.774160		
	3					1.768748	1.793270	1.824572	1.774158		
	4					1.768754	1.793274	1.824574	1.774158		
	5					1.768748	1.793272	1.824576	1.774154		
	6					1.768752	1.793272	1.824578	1.774156		
	7					1.768750	1.793272	1.824572	1.774158		
	8					1.768754	1.793274	1.824574	1.774160		
	9					1.768754	1.793272	1.824580	1.774158		
	10					1.768748	1.793270	1.824576	1.774156		
1200 hrs	1										
	2										
	3										
	4										
	5										
	6										
	7										
	8										
	9										
	10										

Table 102: Raw Data, Expt. #9, RG-CO_2/550°C/20MPa, HCM12A Shot Peened

Project:	**SCCO2**
Contact:	PRJ39TC
MDS:	24386
Expt. #:	**7**
Phase:	**Shot Peened**
Phase Type:	Research CO2
Temp. (°C):	550
Pressure (MPa):	20
Sample ID:	**HCM12A**

Rel. Uncertainty in Meas. Mass:	Δm = ± 0.000002 g
Rel. Uncertainty in Meas. Length:	Δl = ± 0.001 mm
Rel. Uncertainty in Meas. Width:	Δw = ± 0.001 mm
Uncertainty in Meas. Area:	ΔA = ± 0.000178 cm^2

Pressure:	60 psi
Time:	6 secs
Both Sides?	Yes
Hole Diameter in Sample (mm):	3

Notes: Bare weight is meas weight of samples after peening; Ervin AMACAST ES-300 SS Shot

		Sample # / Description									
	Meas #	**H52**	**H53**	**H54**	**H55**	**H56**	**H57**	**H58**	**H59**	**H60**	**H61**
BARE WEIGHT (gm)	**1**	1.754422	1.748470	1.757928	1.792338	1.800320	1.825638	1.835708	1.828378	1.814376	1.834442
	2	1.754422	1.748464	1.757932	1.792336	1.800330	1.825648	1.835710	1.828368	1.814380	1.834446
	3	1.754422	1.748470	1.757932	1.792338	1.800326	1.825638	1.835716	1.828370	1.814380	1.834448
	4	1.754426	1.748468	1.757934	1.792340	1.800332	1.825644	1.835706	1.828368	1.814374	1.834450
	5	1.754430	1.748464	1.757932	1.792346	1.800328	1.825638	1.835710	1.828374	1.814376	1.834444
	6	1.754422	1.748468	1.757928	1.792340	1.800324	1.825648	1.835716	1.828374	1.814372	1.834444
	7	1.754422	1.748474	1.757930	1.792340	1.800320	1.825648	1.835706	1.828376	1.814382	1.834440
	8	1.754432	1.748464	1.757924	1.792336	1.800330	1.825648	1.835714	1.828376	1.814376	1.834440
	9	1.754432	1.748468	1.757930	1.792342	1.800330	1.825640	1.835710	1.828370	1.814374	1.834446
	10	1.754422	1.748472	1.757928	1.792346	1.800328	1.825648	1.835706	1.828370	1.814380	1.834444
BARE AREA (mm2)	**1_L**	12.584	12.557	12.546	12.614	12.530	12.646	12.711	12.654	12.672	12.608
	2_L	12.587	12.571	12.548	12.619	12.545	12.634	12.725	12.666	12.683	12.602
	3_L	12.601	12.581	12.545	12.622	12.545	12.647	12.711	12.549	12.683	12.579
	4_W	12.614	12.505	12.563	12.662	12.646	12.692	12.632	12.673	12.564	12.702
	5_W	12.625	12.510	12.593	12.672	12.611	12.694	12.631	12.703	12.567	12.688
	6_W	12.609	12.530	12.570	12.675	12.628	12.720	12.635	12.713	12.538	12.698
BARE THICKNESS (mm)	**1**	1.561	1.569	1.561	1.576	1.580	1.574	1.565	1.560	1.562	1.572
	2	1.565	1.564	1.561	1.580	1.584	1.575	1.568	1.553	1.558	1.571
	3	1.554	1.537	1.555	1.565	1.584	1.569	1.563	1.540	1.561	1.566
	4	1.553	1.553	1.558	1.575	1.582	1.567	1.560	1.549	1.561	1.569
	5	1.562	1.556	1.556	1.581	1.578	1.569	1.568	1.549	1.557	1.558

Table 103: Raw Data, Expt. #9, RG-CO_2/550^{o}C/20MPa, HCM12A Shot Peened

		Measured Weight (g)									
	Meas #	H52	H53	H54	H55	H56	H57	H58	H59	H60	H61
200 hrs	1	1.754948	1.749028	1.758534	1.792920	1.800990	1.826226	1.836402	1.829064	1.814956	1.835070
	2	1.754946	1.749026	1.758536	1.792922	1.800982	1.826216	1.836404	1.829070	1.814952	1.835062
	3	1.754946	1.749026	1.758530	1.792920	1.800980	1.826222	1.836406	1.829074	1.814958	1.835064
	4	1.754946	1.749028	1.758536	1.792916	1.800980	1.826220	1.836406	1.829064	1.814960	1.835068
	5	1.754944	1.749028	1.758530	1.792924	1.800984	1.826216	1.836402	1.829068	1.814960	1.835068
	6	1.754944	1.749034	1.758530	1.792922	1.800990	1.826224	1.836410	1.829070	1.814956	1.835060
	7	1.754940	1.749028	1.758534	1.792920	1.800980	1.826216	1.836410	1.829064	1.814962	1.835068
	8	1.754940	1.749032	1.758536	1.792920	1.800982	1.826216	1.836406	1.829068	1.814962	1.835070
	9	1.754938	1.749034	1.758530	1.792918	1.800980	1.826220	1.836408	1.829064	1.814960	1.835068
	10	1.754944	1.749030	1.758532	1.792920	1.800988	1.826222	1.836410	1.829072	1.814958	1.835064
400 hrs	1			1.758680	1.793034	1.801110	1.826346	1.836588	1.829224	1.815092	1.835172
	2			1.758684	1.793036	1.801116	1.826346	1.836582	1.829230	1.815102	1.835170
	3			1.758688	1.793028	1.801112	1.826354	1.836580	1.829226	1.815096	1.835168
	4			1.758684	1.793032	1.801106	1.826354	1.836588	1.829228	1.815096	1.835170
	5			1.758688	1.793032	1.801114	1.826348	1.836586	1.829226	1.815098	1.835172
	6			1.758680	1.793030	1.801106	1.826352	1.836584	1.829230	1.815096	1.835174
	7			1.758690	1.793030	1.801116	1.826346	1.836582	1.829226	1.815096	1.835170
	8			1.758688	1.793032	1.801106	1.826350	1.836578	1.829232	1.815100	1.835172
	9			1.758688	1.793038	1.801114	1.826348	1.836582	1.829228	1.815098	1.835178
	10			1.758690	1.793038	1.801110	1.826352	1.836588	1.829232	1.815096	1.835178
600 hrs	1					1.801234	1.826468	1.836736	1.829370		
	2					1.801238	1.826470	1.836734	1.829366		
	3					1.801242	1.826464	1.836736	1.829368		
	4					1.801236	1.826468	1.836742	1.829368		
	5					1.801236	1.826464	1.836736	1.829364		
	6					1.801240	1.826464	1.836740	1.829364		
	7					1.801244	1.826466	1.836736	1.829370		
	8					1.801236	1.826464	1.836734	1.829362		
	9					1.801234	1.826466	1.836736	1.829366		
	10					1.801244	1.826470	1.836736	1.829368		

		Measured Weight (g)									
	Meas #	H52	H53	H54	H55	H56	H57	H58	H59	H60	H61
800 hrs	1					1.801340	1.826562	1.836874	1.829496		
	2					1.801342	1.826560	1.836868	1.829494		
	3					1.801346	1.826560	1.836870	1.829490		
	4					1.801346	1.826558	1.836870	1.829494		
	5					1.801342	1.826560	1.836868	1.829490		
	6					1.801340	1.826560	1.836864	1.829490		
	7					1.801340	1.826556	1.836866	1.829492		
	8					1.801340	1.826558	1.836866	1.829490		
	9					1.801336	1.826556	1.836868	1.829490		
	10					1.801338	1.826560	1.836870	1.829492		
1000 hrs	1					1.801416	1.826616	1.836962	1.829586		
	2					1.801416	1.826620	1.836962	1.829580		
	3					1.801410	1.826622	1.836960	1.829582		
	4					1.801412	1.826616	1.836962	1.829586		
	5					1.801410	1.826618	1.836958	1.829586		
	6					1.801408	1.826624	1.836960	1.829580		
	7					1.801408	1.826616	1.836954	1.829580		
	8					1.801410	1.826620	1.836960	1.829586		
	9					1.801408	1.826620	1.836962	1.829578		
	10					1.801412	1.826622	1.836954	1.829580		
1200 hrs	1										
	2										
	3										
	4										
	5										
	6										
	7										
	8										
	9										
	10										

Table 104: Raw Data, Expt. #9, RG-CO_2/550°C/20MPa, NF616 Shot Peened

Project:	**SCCO2**
Contact:	PRJ39TC
MDS:	24386
Expt. #:	**7**
Phase:	**Shot Peened**
Phase Type:	Research CO2
Temp. (°C):	550
Pressure (MPa):	20
Sample ID:	**NF616**
Notes:	Bare weight is meas weight of samples after peening

Rel. Uncertainty in Meas. Mass:	Δm = ± 0.000002 g
Rel. Uncertainty in Meas. Length:	Δl = ± 0.001 mm
Rel. Uncertainty in Meas. Width:	Δw = ± 0.001 mm
Uncertainty in Meas. Area:	ΔA = ± 0.000178 cm^2

Supplier/UNS ID:	
Metal Type:	
Color Designation:	
Hole Diameter in Sample (mm):	3

		Sample # / Description									
	Meas #						**N62**	**N63**	**N65**	**N66**	**N67**
BARE WEIGHT (gm)	**1**						1.787062	1.771886	1.781804	1.778558	1.739888
	2						1.787068	1.771880	1.781806	1.778556	1.739884
	3						1.787062	1.771886	1.781800	1.778566	1.739890
	4						1.787062	1.771880	1.781802	1.778560	1.739892
	5						1.787070	1.771888	1.781800	1.778566	1.739892
	6						1.787070	1.771886	1.781810	1.778566	1.739892
	7						1.787068	1.771880	1.781804	1.778556	1.739888
	8						1.787070	1.771878	1.781800	1.778556	1.739886
	9						1.787072	1.771884	1.781806	1.778560	1.739888
	10						1.787072	1.771882	1.781808	1.778566	1.739886
BARE AREA (mm2)	**1_L**	.					12.596	12.600	12.627	12.578	12.604
	2_L						12.612	12.593	12.643	12.567	12.612
	3_L						12.598	12.584	12.640	12.546	12.602
	4_W						12.643	12.611	12.632	12.621	12.585
	5_W						12.650	12.639	12.627	12.609	12.598
	6_W						12.653	12.650	12.583	12.570	12.583
BARE THICKNESS (mm)	**1**						1.507	1.537	1.543	1.555	1.522
	2						1.520	1.538	1.544	1.558	1.524
	3						1.518	1.538	1.523	1.552	1.515
	4						1.527	1.539	1.544	1.558	1.521
	5						1.525	1.537	1.534	1.556	1.522

Table 105: Raw Data, Experiment #9, RG-CO_2/550^{o}C/20MPa, NF616 Shot Peened

		Measured Weight (g)									
	Meas #						N62	N63	N65	N66	N67
200 hrs	1						1.791492	1.776060	1.786526	1.781598	1.743950
	2						1.791492	1.776052	1.786534	1.781604	1.743954
	3						1.791490	1.776050	1.786536	1.781606	1.743958
	4						1.791490	1.776052	1.786528	1.781604	1.743960
	5						1.791492	1.776058	1.786530	1.781600	1.743950
	6						1.791496	1.776058	1.786532	1.781604	1.743956
	7						1.791490	1.776054	1.786530	1.781606	1.743954
	8						1.791490	1.776060	1.786534	1.781606	1.743954
	9						1.791492	1.776052	1.786528	1.781604	1.743950
	10						1.791498	1.776054	1.786526	1.781608	1.743952
400 hrs	1						1.793838	1.778260	1.788710	1.783288	1.746056
	2						1.793844	1.778254	1.788708	1.783284	1.746056
	3						1.793842	1.778254	1.788714	1.783280	1.746056
	4						1.793838	1.778258	1.788712	1.783288	1.746052
	5						1.793844	1.778258	1.788718	1.783288	1.746056
	6						1.793838	1.778258	1.788716	1.783288	1.746056
	7						1.793840	1.778256	1.788710	1.783284	1.746056
	8						1.793840	1.778256	1.788712	1.783290	1.746052
	9						1.793844	1.778260	1.788714	1.783290	1.746054
	10						1.793840	1.778254	1.788712	1.783288	1.746054
600 hrs	1						1.796470	1.780624	1.790988	1.785172	
	2						1.796466	1.780626	1.790984	1.785172	
	3						1.796466	1.780628	1.790984	1.785170	
	4						1.796466	1.780626	1.790982	1.785174	
	5						1.796464	1.780626	1.790980	1.785170	
	6						1.796468	1.780624	1.790984	1.785172	
	7						1.796466	1.780624	1.790990	1.785172	
	8						1.796468	1.780622	1.790984	1.785174	
	9						1.796466	1.780626	1.790982	1.785174	
	10						1.796470	1.780624	1.790988	1.785170	

		Measured Weight (g)									
	Meas #						N62	N63	N65	N66	N67
800 hrs	1						1.798954	1.782898	1.793038	1.787028	
	2						1.798956	1.782894	1.793040	1.787032	
	3						1.798956	1.782894	1.793040	1.787028	
	4						1.798958	1.782892	1.793038	1.787028	
	5						1.798960	1.782894	1.793036	1.787030	
	6						1.798954	1.782894	1.793036	1.787028	
	7						1.798956	1.782894	1.793038	1.787030	
	8						1.798954	1.782900	1.793036	1.787030	
	9						1.798950	1.782902	1.793036	1.787028	
	10						1.798954	1.782894	1.793036	1.787028	
1000 hrs	1						1.801390	1.785050	1.795016	1.788822	
	2						1.801386	1.785054	1.795012	1.788828	
	3						1.801388	1.785056	1.795010	1.788828	
	4						1.801388	1.785050	1.795012	1.788822	
	5						1.801384	1.785052	1.795016	1.788828	
	6						1.801386	1.785054	1.795014	1.788832	
	7						1.801388	1.785052	1.795012	1.788830	
	8						1.801386	1.785054	1.795012	1.788828	
	9						1.801386	1.785050	1.795010	1.788824	
	10						1.801388	1.785052	1.795014	1.788822	
1200 hrs	1										
	2										
	3										
	4										
	5										
	6										
	7										
	8										
	9										
	10										